CASL-U-2014-0116-000

Power uprates
and plant life extension

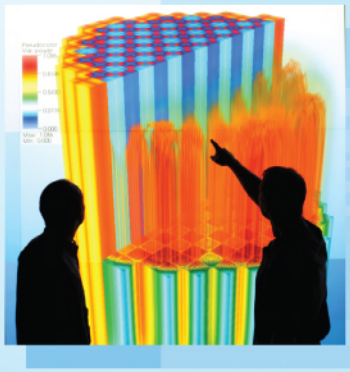

Engineering design
and analysis

Science-enabling
high performance
computing

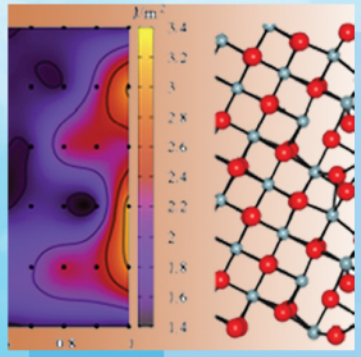

Fundamental science

Plant operational data

Consortium for Advanced Simulation of LWRs

2014 CASL Round Table Presentations

Doug Kothe
Oak Ridge National Laboratory

July 16-18, 2014

U.S. DEPARTMENT OF ENERGY | Nuclear Energy

2014 CASL Round Table Virtual Meeting Schedule (Draft)

July 14-16, 2014
The meeting will be held in Doug Burns' Vidyo Room
All Times are EDT

Monday, July 14		Tuesday, July 15		Wednesday, July 16	
SESSION 1: Challenge Problems Chair: Zeses Karoutas		**SESSION 4: MPO** Chair: Chris Stanek		**SESSION 7: Management** Chair: Doug Burns	
10:30 – 11:00	CRUD Challenge Problem Update: Jeff Secker (WEC)	**10:30 – 11:00**	Development of Zirconium Oxidation and Hydride Modeling for Peregrine: Bilge Yildiz (MIT)	**10:30 – 11:30**	CASL Phase 2 Proposal Summary: Rose Montgomery (ORNL)
11:00 – 11:30	GTRF Challenge Problem Update: Brian Wirth (UTK)	**11:00 – 11:30**	Thermodynamic Modeling of B-Phases in CRUD – The Failed Search for Bonacordite: Don Brenner (NCSU)	**11:30 – 12:00**	CASL Awards: Doug Kothe (ORNL)
11:30 – 12:00	DNB Challenge Problem Update: Yixing Sung (WEC)	**11:30 – 12:00**	Modeling Dislocations in UO2 for Improved Fuel Mechanical Behavior Models for Peregrine: Sam Murphy (Imperial College)		
--- BREAK ---					
SESSION 2: Challenge Problems Chair: Zeses Karoutas		**SESSION 5: RTM** Chair: Bill Martin		**SESSION 8: AMA** Chair: Steve Hess	
1:00 – 1:30	PCI Challenge Problem Update: Robert Montgomery (PNNL)	**1:00 – 1:30**	Deterministic Transport Methods – Status and Plans: Ben Collins (UMich)	**1:00 – 1:30**	AP-1000 Initial Core Zero Power Physics Test Benchmarks Using VERA: Jeff Secker (WEC)
1:30 – 2:00	RIA Challenge Problem Update: Gregg Swindlehurst (GSN)	**1:30 – 2:00**	Monte Carlo Methods – Status and Plans: Tom Evans (ORNL)	**1:30 – 1:50**	Comparison of Peregrine to Falcon Fuel Performance Models: Brenden Mervin (EPRI)
2:00 – 2:30	LOCA Challenge Problem Update: Gregg Swindlehurst (GSN)	**2:00 – 2:30**	Cross Section Development – Status and Plans: Kang Seog Kim	**1:50 – 2:10**	Lower Plenum Flow Anomaly Modeling Using VERA: Bill Bird (TVA)
				2:10 – 2:30	Modeling an iPWR SMR Reactor Core Using VERA-CS: Kelly Kenner (UTK/TVA)
--- BREAK ---					

2014 CASL Round Table Virtual Meeting Schedule (Draft)

July 14-16, 2014

The meeting will be held in Doug Burns' Vidyo Room

All Times are EDT

Monday, July 14		Tuesday, July 15		Wednesday, July 16	
SESSION 3: PHI Chair: Jess Gehin		**SESSION 6: VUQ** Chair: Vince Mousseau		**SESSION 9: THM** Chair: Yixing Sung	
3:00 – 3:30	Tiamat – Coupling VERA-CS and Peregrine: Roger Pawlowski (SNL)	**3:00 – 3:30**	DAKOTA Users Manual: Brian Williams (LANL)	**3:00 – 3:30**	ITM/DNS and Experimental Capabilities in THM: Igor Bolotnov (NCSU)
3:30 – 4:00	CTF Validation Plans and Activities: Bob Salko (PSU)	**3:30 – 4:00**	DAKOTA Capabilities Update: Brian Adams (SNL)	**3:30 – 4:00**	New Capabilities in Hydra-TH: Mark Christon (LANL)
4:00 – 4:30	VERA-CS Validation Plans and Activities: Andrew Godfrey (ORNL)	**4:00 – 4:30**	CASL VUQ Plans: Vince Mousseau (SNL)	**4:00 – 4:30**	Advances in Multiphase Closure Modelling: Emilio Baglietto (MIT)

Crud Challenge Problem Status

J. Secker
Westinghouse Electric Co., LLC

CASL Roundtable

July 14, 2014

Outline

- Introduction
- Seabrook 5x5 COBRA/MAMBA
- Seabrook 5x5 STAR-CCM+/MAMBA
- POR9 Plans/Status
- Conclusions

Seabrook Cycle 5 Crud Failures

For POR7, a 5x5 rod array from Seabrook Cycle 5 was modeled with both COBRA/MAMBA and STAR-CCM+/MAMBA

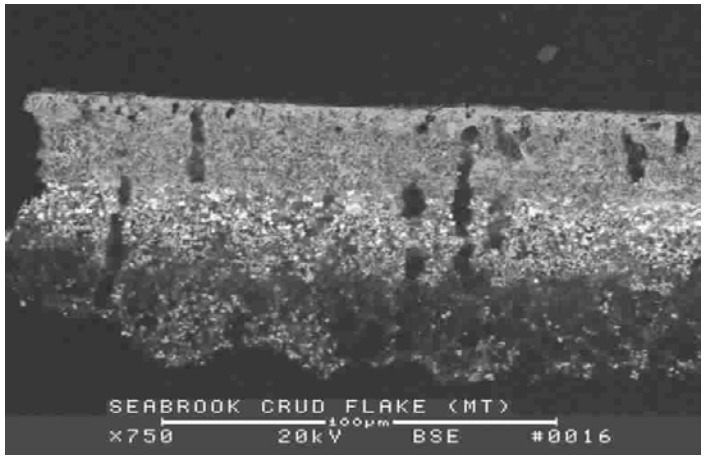

(a)

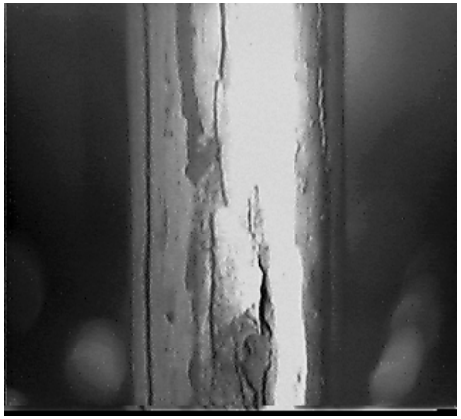

(b)

(c)

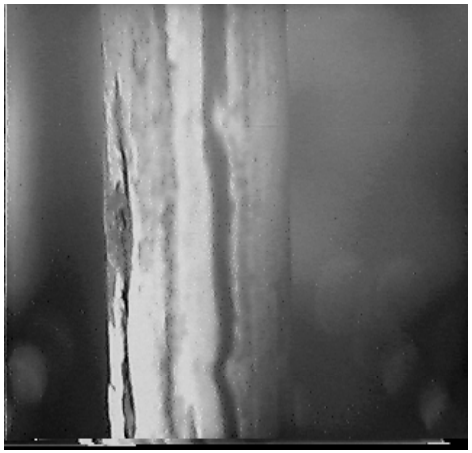

(d)

Seabrook Cycle 5 had moderate CIPS, but had CILC failures
A total of 5 rods failed in 4 assemblies about 260 days into the cycle

Seabrook Cycle 5 Assemblies and Rods

SEABROOK UNIT 1, CYCLE 5
REFERENCE CORE LOADING PATTERN

	R	P	N	M	L	K	J	H	G	F	E	D	C	B	A	
					E45 C-11	F11 K-9	F26 D-7	E41 H-14	F13 M-7	F33 F-9	E48 N-11					1
			E65 N-10	F10 K-11	G25 FEED	G33 FEED	G34 FEED	F51 D-13	G35 FEED	G36 FEED	G26 FEED	F34 F-11	E68 C-10			2
		E70 F-3	G37 FEED	G38 FEED	G61 FEED	F40 E-2	F59 K-2	G01 FEED	F70 F-2	F38 L-2	G62 FEED	G39 FEED	G40 FEED	E53 K-3		3
		F20 E-6	G41 FEED	F45 C-13	F60 B-7	E01 R-6	G73 FEED	F03 G-8	G74 FEED	E07 A-6	F72 P-7	F44 N-13	G42 FEED	F22 L-6		4
	E49 E-13	G27 FEED	G63 FEED	F63 J-14	F53 N-4	G02 FEED	E75 G-1	G64 FEED	E56 J-1	G03 FEED	F52 D-3	F57 G-14	G65 FEED	G28 FEED	E43 L-13	5
	F19 G-6	G43 FEED	F48 P-11	E03 K-1	G04 FEED	F27 E-4	G05 FEED	F30 M-11	G06 FEED	F08 D-11	G07 FEED	E08 F-1	F39 B-11	G44 FEED	F23 J-6	6
	F29 J-12	G45 FEED	F71 P-6	G75 FEED	E62 R-9	G08 FEED	E61 H-15	G09 FEED	E73 R-8	G10 FEED	E54 A-9	G76 FEED	F58 B-6	G46 FEED	F18 G-12	7
90°	E51 B-8	F54 C-4	G11 FEED	F01 H-7	G66 FEED	F32 E-12	G12 FEED	A04 D-10	G13 FEED	F07 L-4	G67 FEED	F04 H-9	G14 FEED	F55 N-12	E46 P-8	8
	F14 J-4	G47 FEED	F65 P-10	G77 FEED	E74 R-7	G15 FEED	E72 A-8	G16 FEED	E63 H-1	G17 FEED	E76 A-7	G78 FEED	F66 B-10	G48 FEED	F17 G-4	9
	F24 G-10	G49 FEED	F47 P-5	E04 K-15	G18 FEED	F28 M-5	G19 FEED	F09 D-5	G20 FEED	F15 L-12	G21 FEED	E02 F-15	F37 B-5	G50 FEED	F36 J-10	10
	E44 E-3	G29 FEED	G68 FEED	F62 J-2	F56 M-13	G22 FEED	E58 G-15	G69 FEED	E57 J-15	G23 FEED	F49 C-12	F64 G-2	G70 FEED	G30 FEED	E39 L-3	11
		F21 E-10	G51 FEED	F46 C-3	F68 B-9	E06 R-10	G79 FEED	F02 J-8	G80 FEED	E05 A-10	F67 P-9	F41 N-3	G52 FEED	F25 L-10		12
		E67 F-13	G53 FEED	G54 FEED	G71 FEED	F43 E-14	F61 K-14	G24 FEED	F69 F-14	F42 L-14	G72 FEED	G55 FEED	G56 FEED	E66 K-13		13
* from Cycle 1			E60 N-6	F06 K-5	G31 FEED	G57 FEED	G58 FEED	F50 M-3	G59 FEED	G60 FEED	G32 FEED	F35 F-5	E55 C-6			14
Y YY Assembly Identifier Z-ZZ Previous Cycle Location					E52 C-5	F16 K-7	F31 D-9	E50 H-2	F12 M-9	F05 F-7	E38 N-5					15

0°

E REGION 5 (4.403 w/o)

F REGION 6 (3.608 w/o)

G REGION 7 (4.802 w/o)

Fuel Assembly Orientation

• Reference Hole
○ Core Pin Hole
/ Holdown Bar

NOTE: Figures are Top View

			17	16	15	14	13	12	11	10	9	8	7	6	5	4	3	2	1	rod					
		Ycorner									Face 1														
rod		Y	1	2	3	4	5	6	7	8	9	10	11	12	13	14	15	16	17						
1		A																				17			
2		B																				16			
3		C																				15			
4		D																				14			
5		E																				13			
6		F																				12			
7	F	G									70										F	11		Failed Rod	
8	a	H																			a	10		Crud Visuals	
9	c	I																			c	9		Cladding Oxide Thickness	
10	e	J																			e	8			
11	4	K																			2	7			
12		L																				6			
13		M																				5			
14		N																				4			
15		O																				3			
16		P																				2			
17		Q																				1			
		O																				rod			
		Reference Hole									Face 3														
		roc	1	2	3	4	5	6	7	8	9	10	11	12	13	14	15	16	17						

Rod Locations can be designated by Face #, Rod #
or by rod coordinates (A-Q, 1-17)

Assemblies with failures were some of the highest powered assemblies/rods throughout the cycle

COBRA-TF/MAMBA-2D Coupling

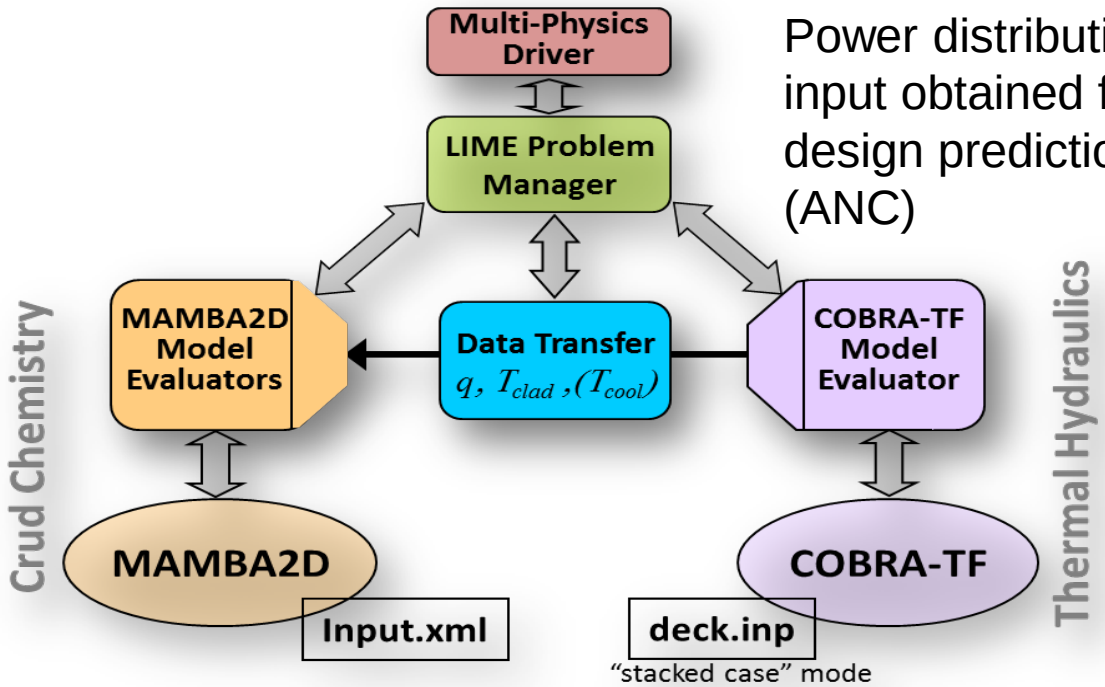

Power distribution input obtained from design predictions (ANC)

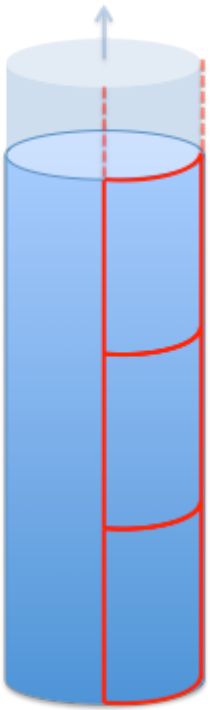

Illustration of a MAMBA2D surface mesh on a single rod

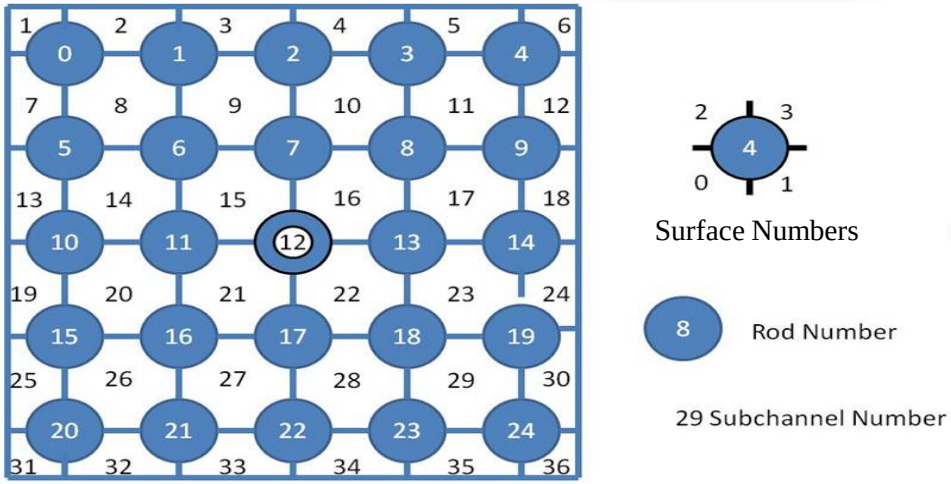

Predicted Crud and Boron Distribution – 5x5

	7	8	9	10	11
D	9.9	9.6	10.7	9.6	10.0
E	9.8	10.0	10.2	10.0	9.9
F	10.9	10.2	2.2	10.2	11.0
G	10.1	10.2	10.4	10.2	10.0
H	10.4	10.1	11.3	10.1	10.4

Seabrook Assembly G70 Rods D7-H11 predicted crud mass (grams)

	7	8	9	10	11
D	106.3	102.1	116.3	102.2	107.3
E	105.0	106.8	108.8	107.3	105.5
F	119.0	109.5	8.2	109.4	119.5
G	107.9	110.2	112.7	110.1	107.3
H	112.7	108.9	123.8	108.6	111.9

Seabrook Assembly G70 Rods D7-H11 predicted boron mass (milligrams) deposited in crud

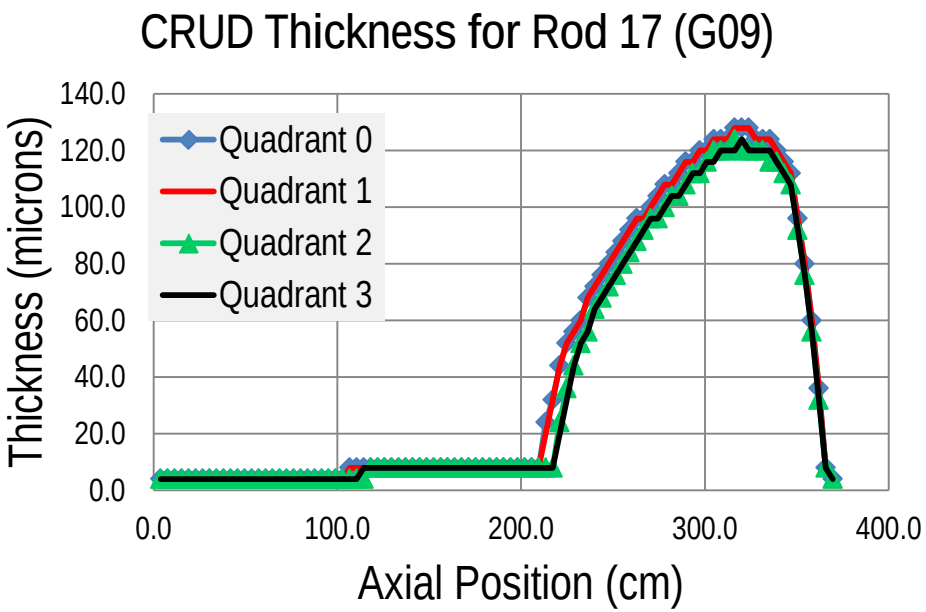

Eddy current liftoff measurements for G70 rod G09 (no cleaning prior to measurement)

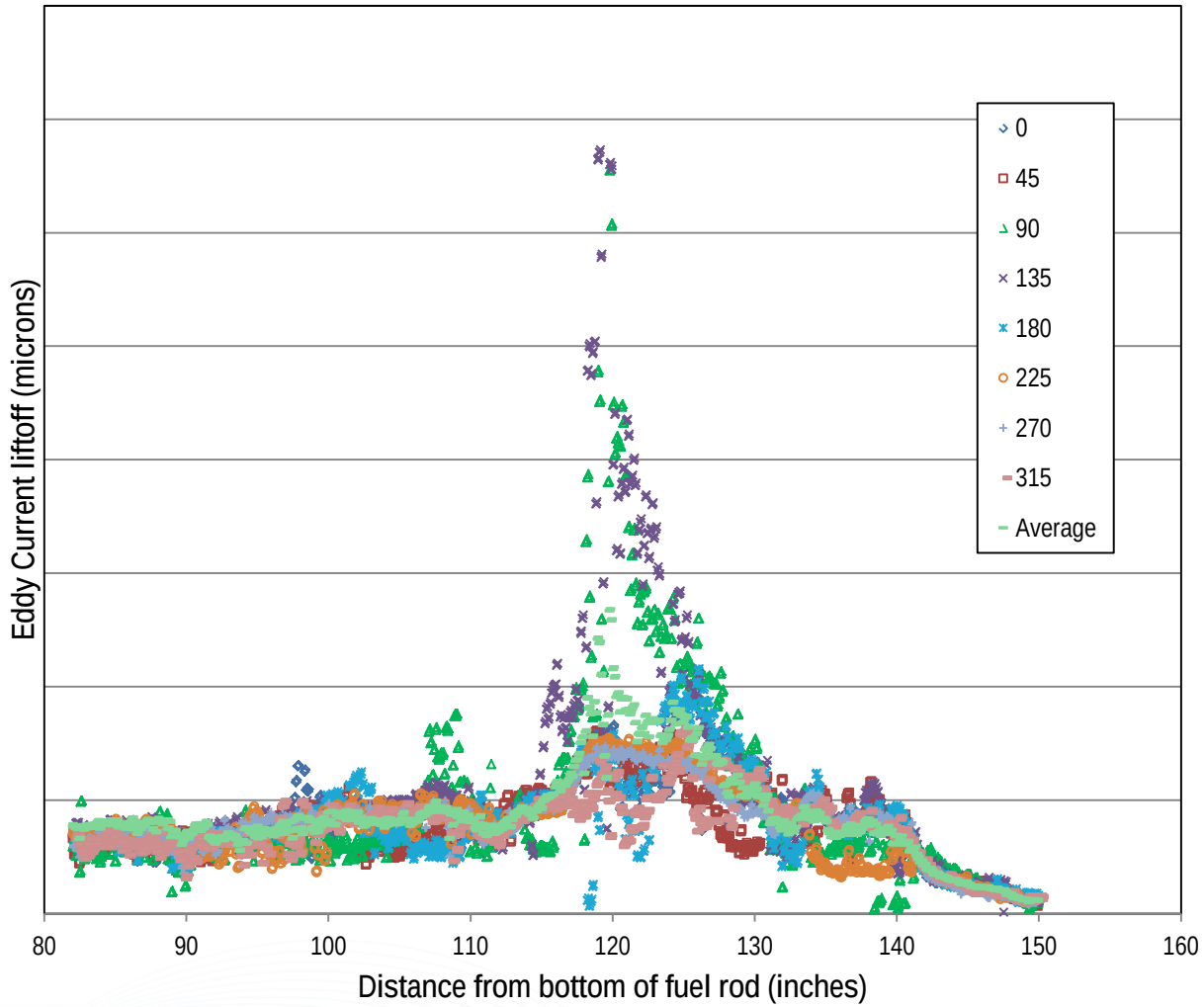

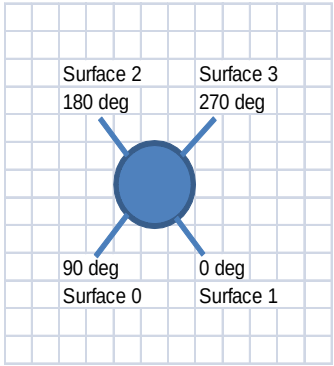

Max crud plus oxide thickness occurs at 90, 135 degrees

Corresponds to MAMBA surface 0, which also had max predicted crud thickness

Comparison to BOA predictions

Code	BOA 3.1	MAMBA 2D 5x5
G70 Total Assembly Crud Mass	1.076 lbm, 488.2 grams	
G70 5x5 Rod Crud Mass	44.4 grams	198 grams
G70 Total Assembly Boron Mass	0.026 lbm, 11.7 grams	
G70 5x5 Rod Boron Mass	1.1 grams	2.65 grams
G70 Maximum Crud Thickness	42 microns	124 microns

Significant differences in boiling area because of grid forced convection enhancement models in VIPRE/BOA

Seabrook COBRA-TF/MAMBA Conclusions

- COBRA-TF and MAMBA-2D successfully coupled under VERA to produce a multi-physics crud model
  - VERAIn used for all model inputs
- Model successfully applied to Seabrook Cycle 5 modeling a 5x5 rod array from one of the assemblies with CILC failures
- Predicted axial location of crud generally consistent with observations
  - Predicted crud 220-360 cm
  - Observed crud 200-350 cm
- Quarter rod surface with maximum predicted crud thickness also corresponds to rod locations with highest measured crud+oxide
- Problem run on 64 cores, 100 MAMBA cases, (25 rods x 4 surfaces/rod), run time 1 hour 40 minutes
- Milestone L1:CASL.P7.05 completed
  - CASL report CASL-I-2013-0191-00

Simulation of Seabrook 1 Cycle 5 CRUD formation using coupled STAR-CCM+ and MAMBA3D

CASL's high-fidelity CRUD simulation capability using STAR-CCM+ and MAMBA3D has been used to simulation the formation of CRUD in Cycle 5 at the Seabrook 1 PWR

- 5-rod by 5-rod array for which qualitative and quantitative data is available was selected for analysis
- First high-fidelity, two-way coupled CFD/CRUD simulation of an industrial relevant plant cycle
- Input power provided by industry simulations
- Showed that <u>both</u> axial and azimuthal thermal hydraulic effects dramatically affect CRUD deposition patterns
- Showed that azimuthal power variations have very little impact on CRUD deposition patterns
- Axial and azimuthal CRUD deposition patterns were consistent with plant data

STAR-CCM+
5x5 spacer grid

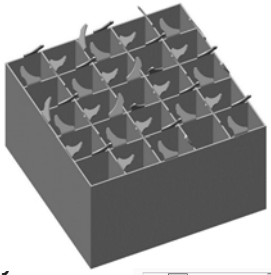

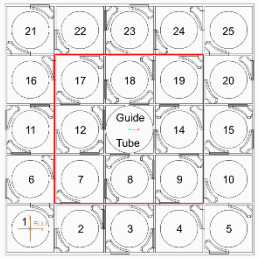

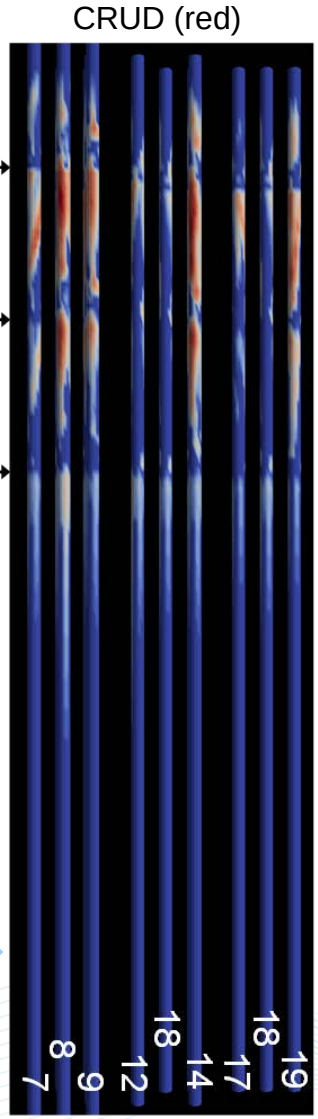

view

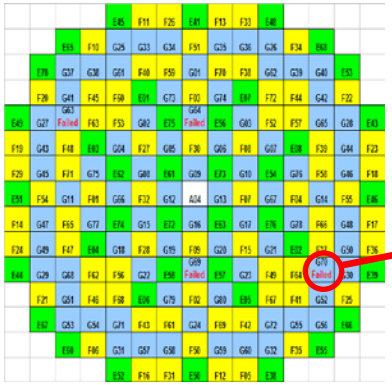

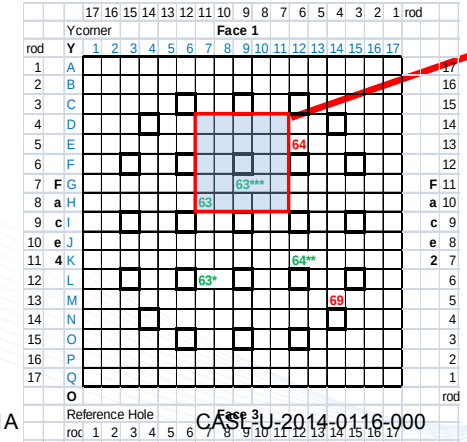

Seabrook cycle 5 ANC axial power profile and coupled time stepping approach

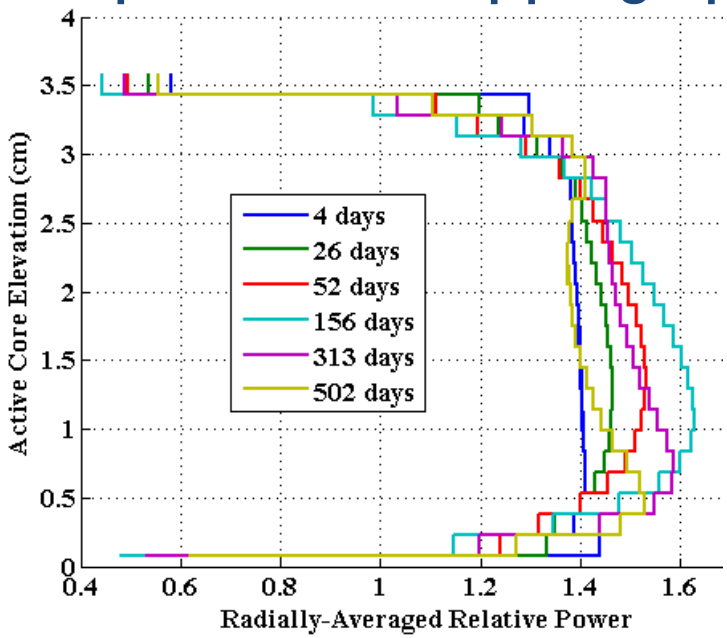

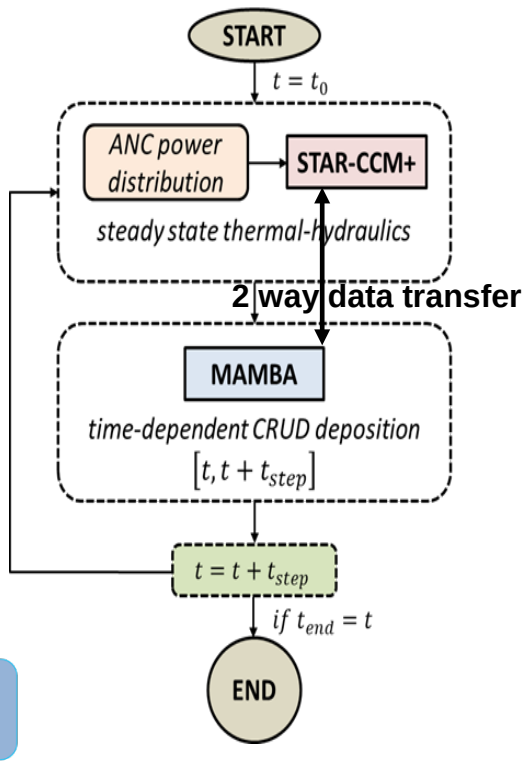

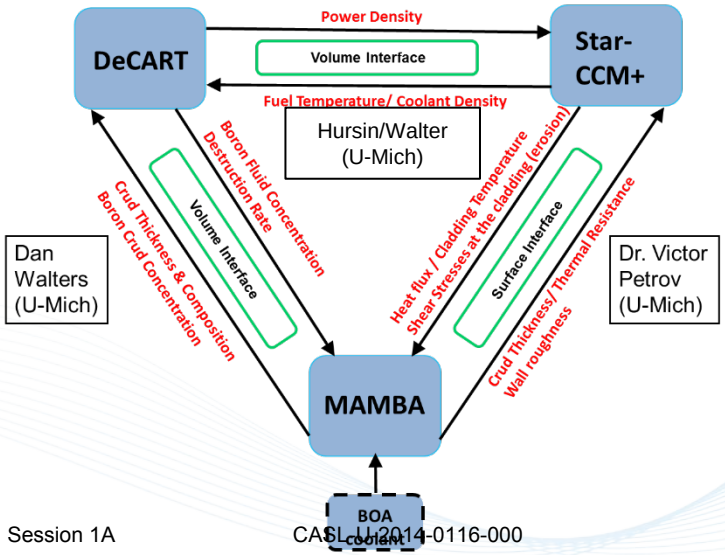

STAR-CCM+ computed surface cladding temperature and turblent kinetic energy

Cladding Temperature at 502 days

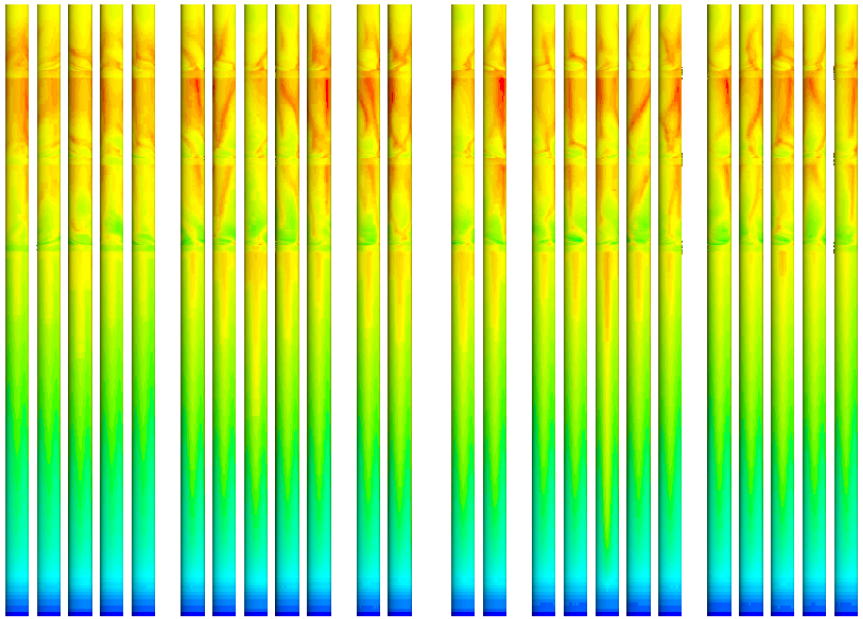

Turbulent kinetic energy at 502 days

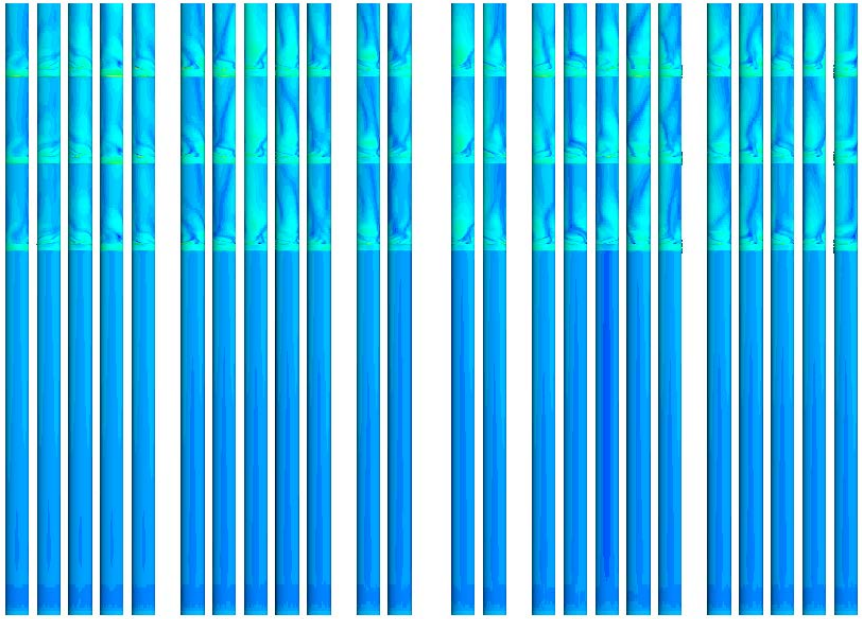

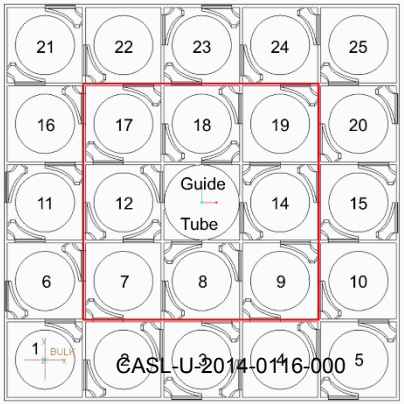

5

4

3

2

1 row

MAMBA computed crud thickness at 502 days

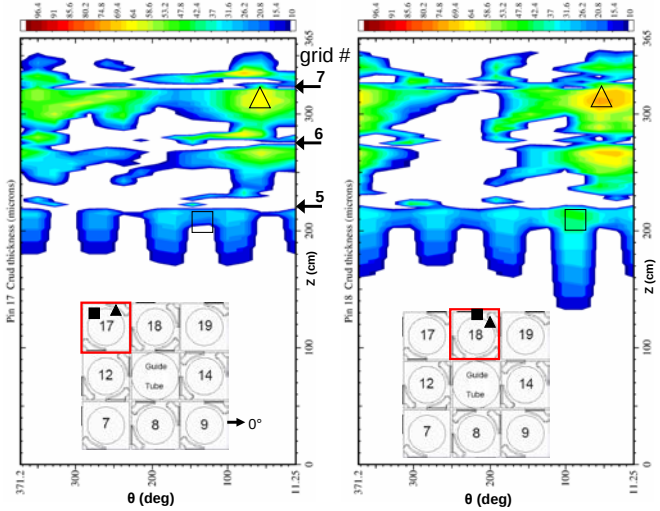

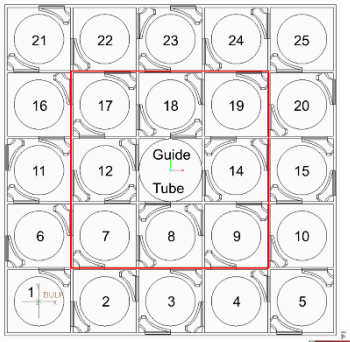

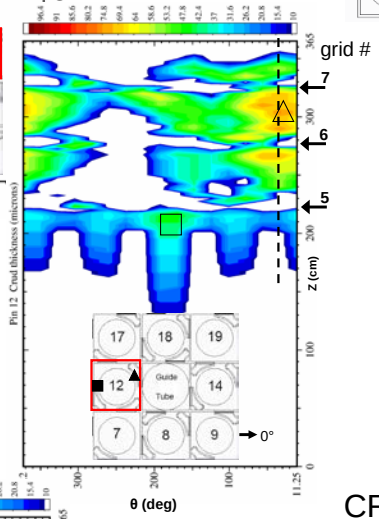

Guide Tube Here

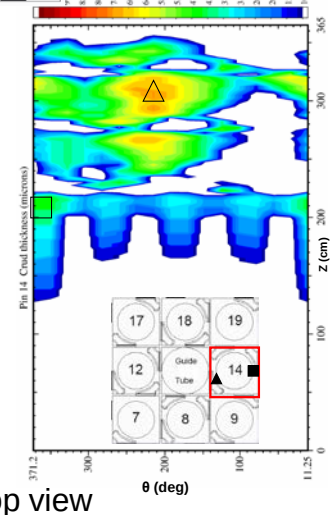

1D profile slice on next slide

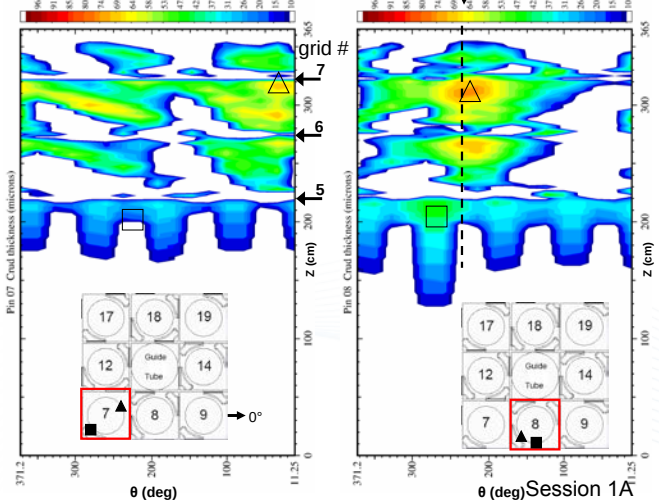

CRUD (red)

3D Top view

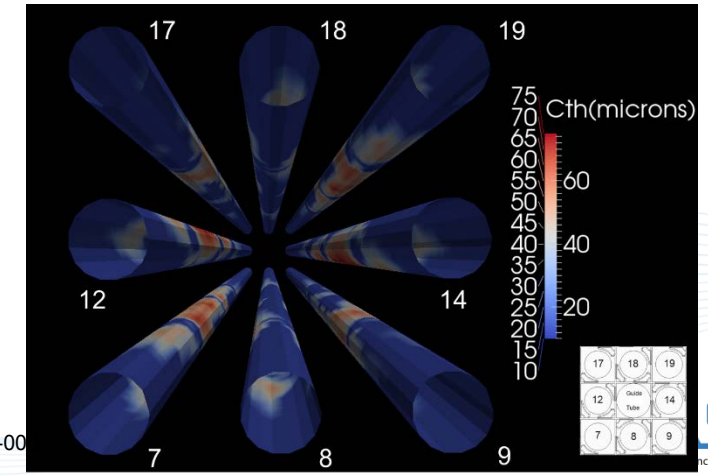

Profile view of crud layer for pin 8 at 502 days

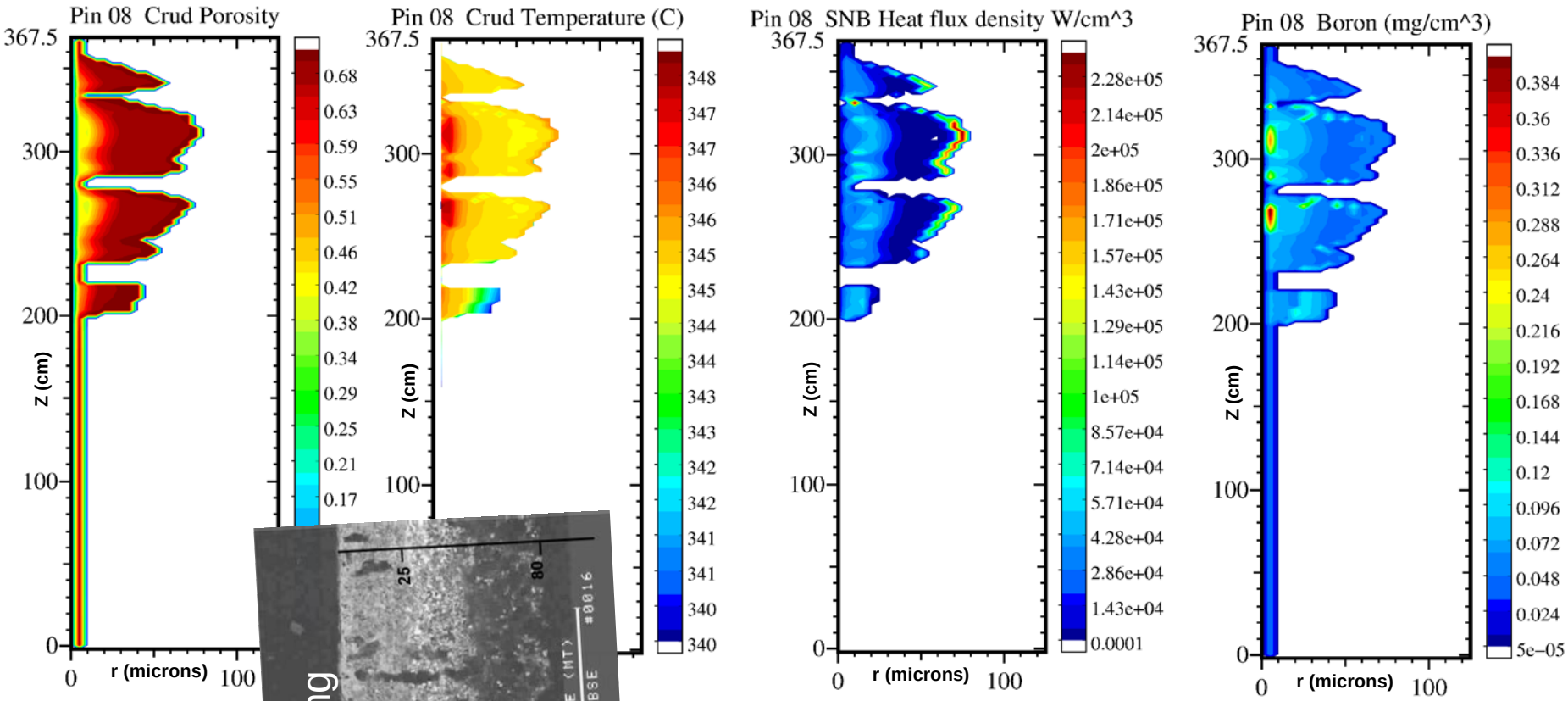

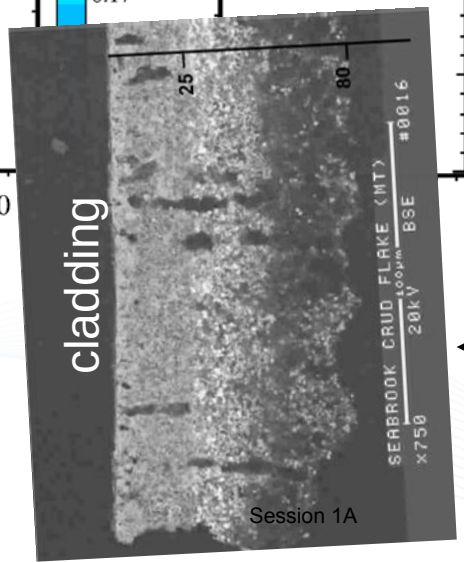

Actual Seabrook crud flake (80 microns thick)

DeCart computed azimuthal power variations

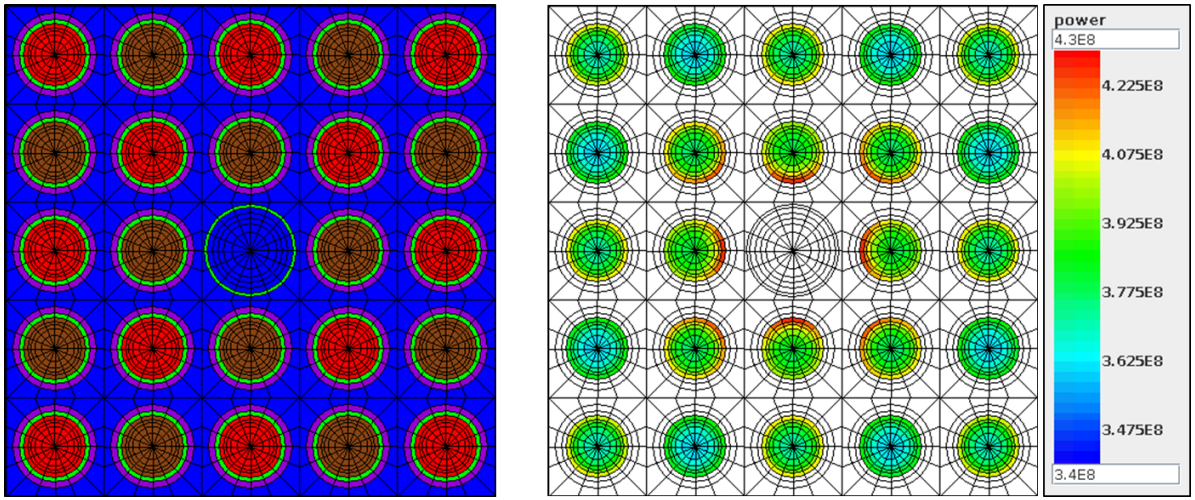

5 % variations <u>did not</u> affect crud

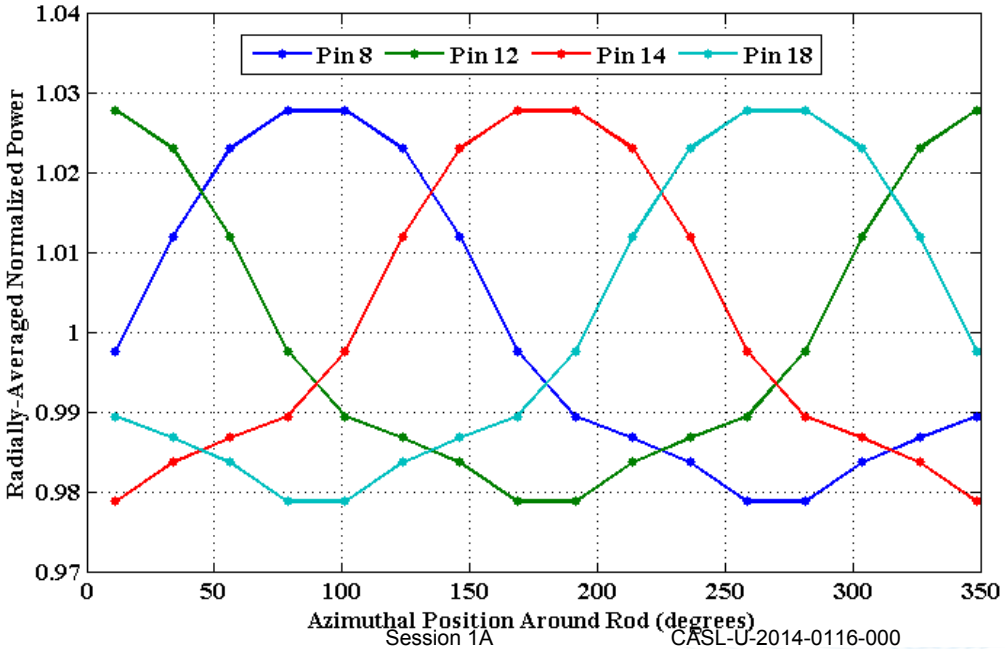

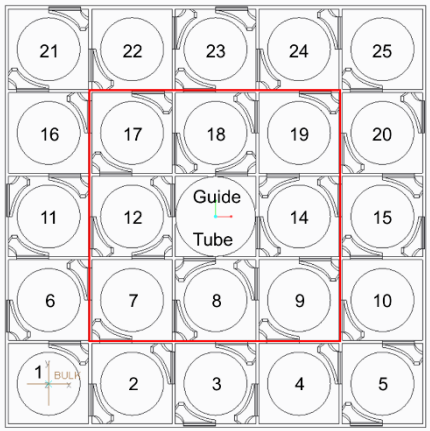

Comparisons with Seabrook Cycle 5 oxide data

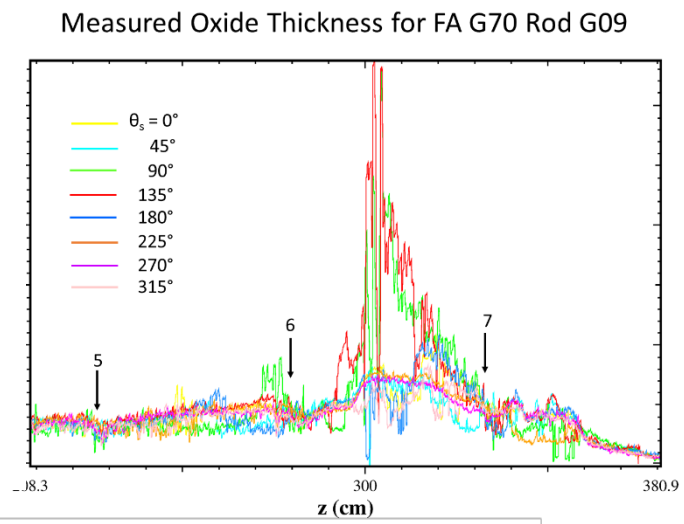

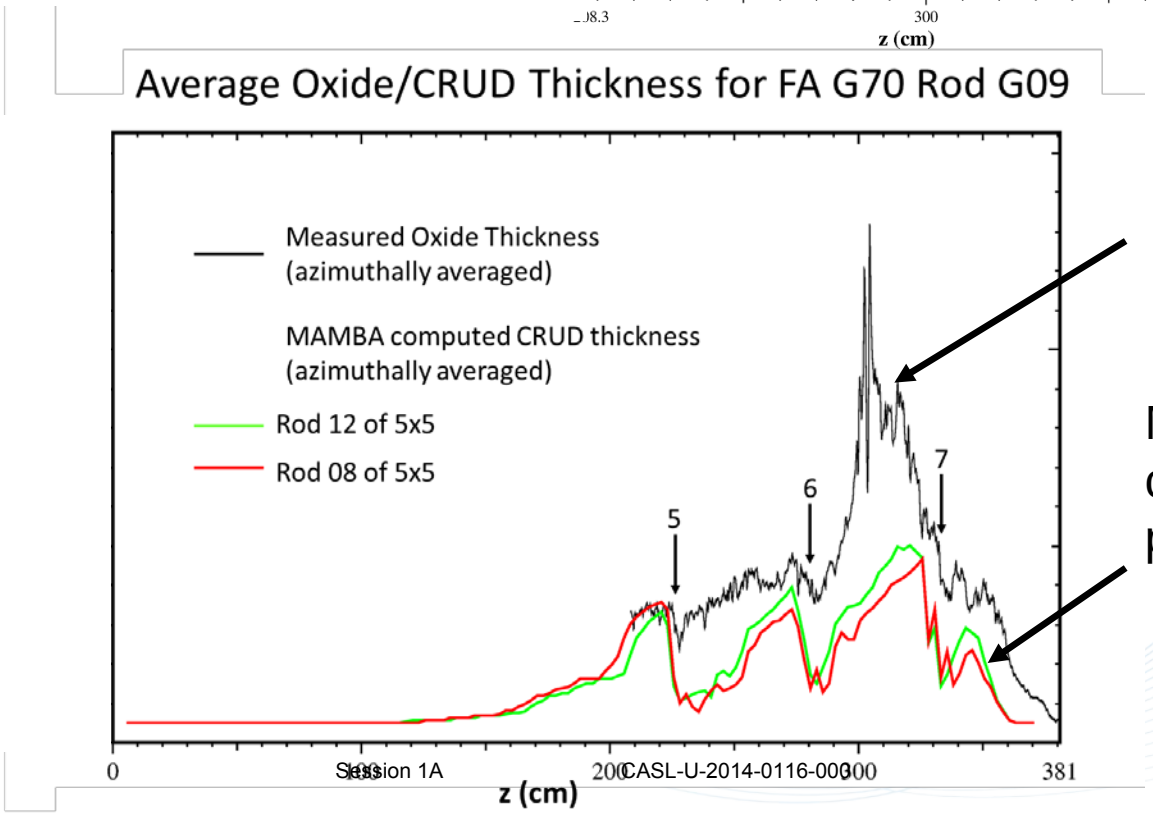

Average of azimuthal data plotted in black

MAMBA computed crud thickness plotted in color

Comparisons with Seabrook Cycle 5 oxide data

MAMBA computed crud thickness (pin 12)

Measured oxide data FA G70 pin G09

MAMBA computed crud thickness (pin 8)

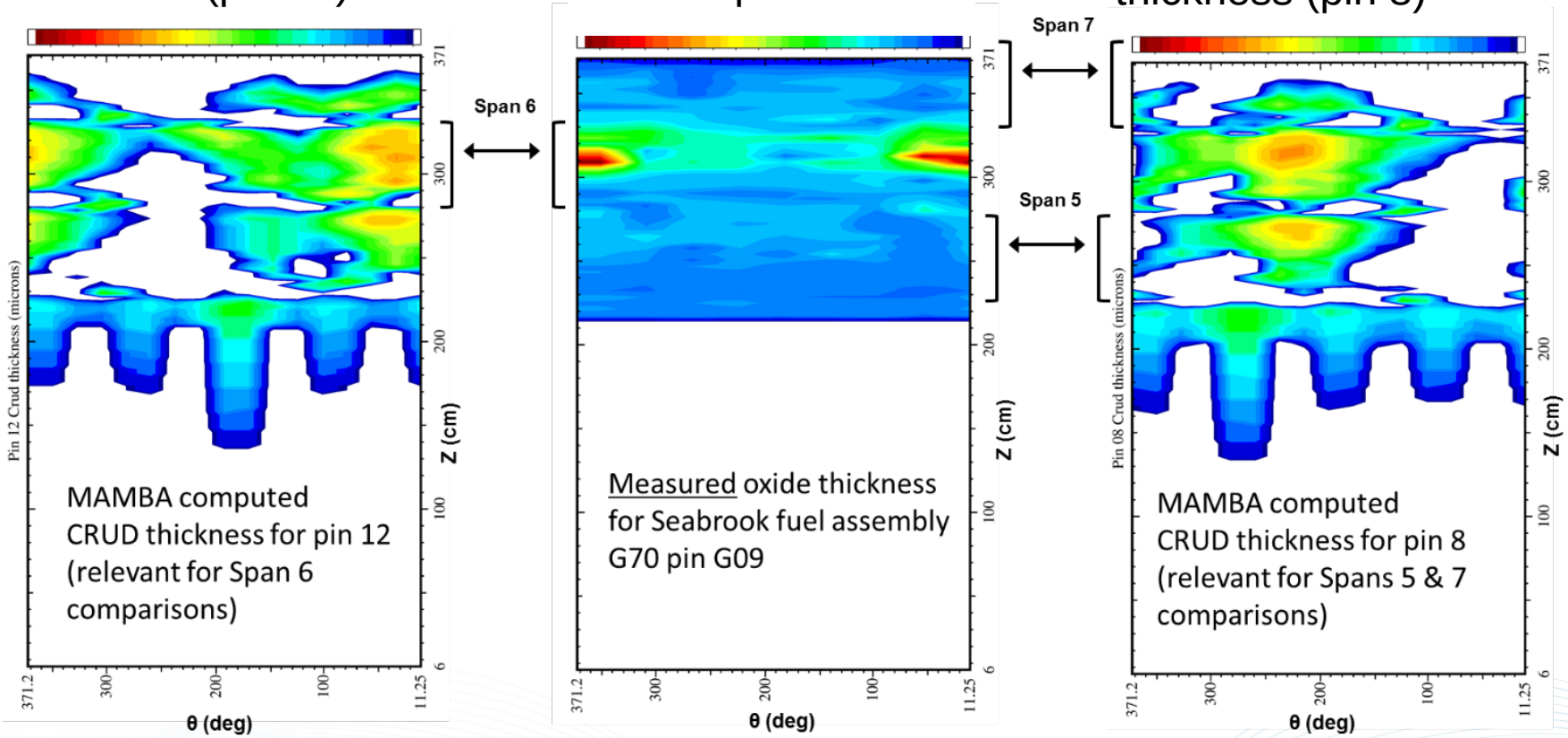

Comparisons with Seabrook Cycle 5 oxide data

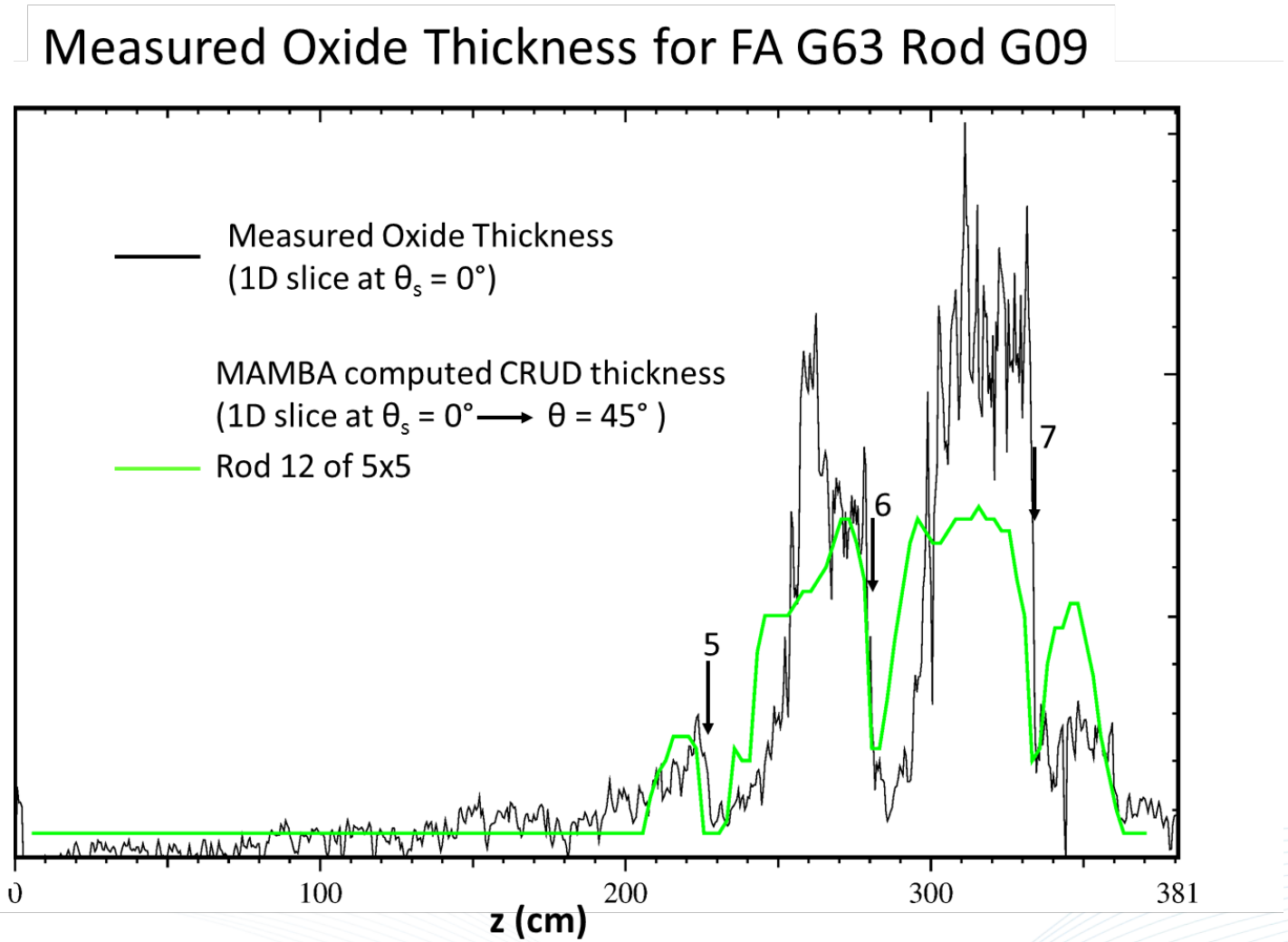

STAR-CCM+/MAMBA Summary / Ongoing Work

- First coupled MAMBA / STAR-CCM+ simulation of Seabrook cycle 5 predicted crud surface distributions that are consistent with measured oxide data

- MAMBA "1D" subgrid module development and interface with HYDRA in progress (MPO-crud L2):

  Plan:

  (a) An initial demonstration Hydra / MAMBA simulation (3x3) early summer

  (b) An initial Hydra / MAMBA simulation of Seabrook cycle 5 (5x5)

  Status: Behind Schedule

- Implement new (non-proprietary) thermodynamic models, improved boric acid chemistry, erosion, microstructure, thermal conductivity / boiling models

POR9 Crud Milestones

- L3:THM.CFD.P9.11, Trac 932, 9/30/2014
  - Change software approach – put MAMBA into HYDRA and COBRA-TF as a library/subroutine rather than coupling to MAMBA
  - 1D MAMBA version
- L3:PHI.VCS.P9.01, Trac 972, 9/30/2014
  - Add MAMBA surrogate model into COBRA based on HYDRA lessons learned
- L3:AMA.APP.P9.01, Trac 909, 9/30/2014
  - Stretch goal: Model full core CIPS with COBRA/MAMBA
  - Stretch goal: Repeat Seabrook 5x5 analysis with HYDRA/MAMBA
- L2:MPO.P9.02, Trac 915, DOE reportable, 9/30/2014
  - Demonstrate coupled CFD/Crud for a portion of an assembly
- Current status
  - HYDRA/MAMBA update underway
  - May not be able to run full length 5x5 problem – revert to 3x3 for single grid span
  - COBRA update may just add temporary surrogate model rather than actual MAMBA
  - L3 AMA stretch goals unlikely to be met
  - L2 not as specifically defined, general enough that 3x3 single span will meet milestone

Phase 1 Crud Status

- Industry Codes Coupled – ANC/VIPRE/BOA
  - Watts Bar Cycles 1-3
  - Vogtle 1 Cycles 11-14
  - Error recently discovered in linked code crud shuffling between cycles, fix underway
- CASL Crud / Chemistry Code created – MAMBA, MAMBA-BDM
- COBRA/MAMBA initial linkage
  - Seabrook 5x5 rod array
- STAR-CCM+/MAMBA linkage
  - Single rod
  - 4x4
  - Seabrook 5x5 rod array
- Struggling to complete HYDRA/MAMBA linkage
  - Also affects COBRA-TF/MAMBA linkage
- No coupled, full core Transport Neutronics / Sub-channel T-H / Crud-Chemistry for CIPS modeling yet
- No coupled Transport Neutronics / CASL CFD / Crud-Chemistry for fuel assembly sub-region for CILC modeling yet

DNB Challenge Problem (CP) Update

CP Product Integrator
Yixing Sung
Westinghouse

2014 CASL Round Table Virtual Meeting
July 14-16, 2014

Outline

- DNB CP Overview
  - CP Description
  - CASL Path Forward
  - Deliverables in Phase I
- Summary of VERA Applications
  - COBRA-TF (CTF) subchannel code
  - Hydra-TH Computational Fluid Dynamics (CFD) code
  - Initial UQ Study using DAKOTA

Departure from Nucleate Boiling (DNB) CP

- DNB also referred to as Critical Heat Flux (CHF)
- Local clad surface dryout causes dramatic reduction in heat transfer during transients (e.g., overpower and loss of coolant flow)
- One of safety and regulatory acceptance criteria for PWR (DNB) and BWR (dryout)
- CASL objectives and path forward defined in Charter and Implementation Plan
  - Focus on PWR (DNB) in the first 5 years (Phase I)

Boiling Curve

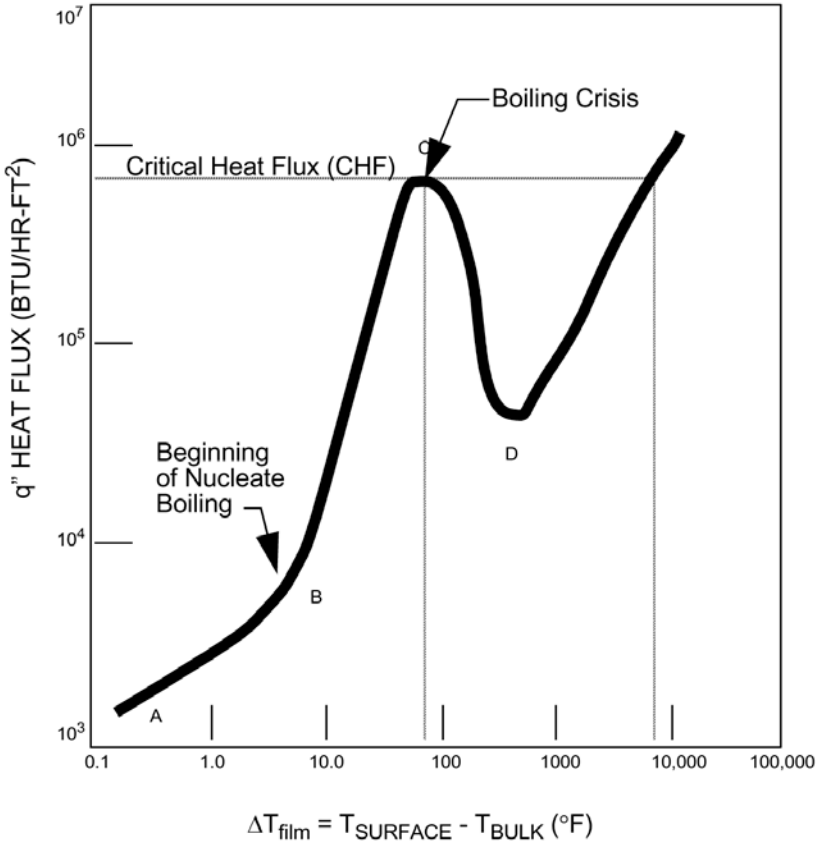

Current Industry Practice & CASL Focus (Highlighted)

Fuel Hardware Design

Plant Design Conditions

Small Scale Testing (5x5 bundle) → Subchannel Code Predictions → DNB Correlation → Licensing Approval → Safety Analysis Application

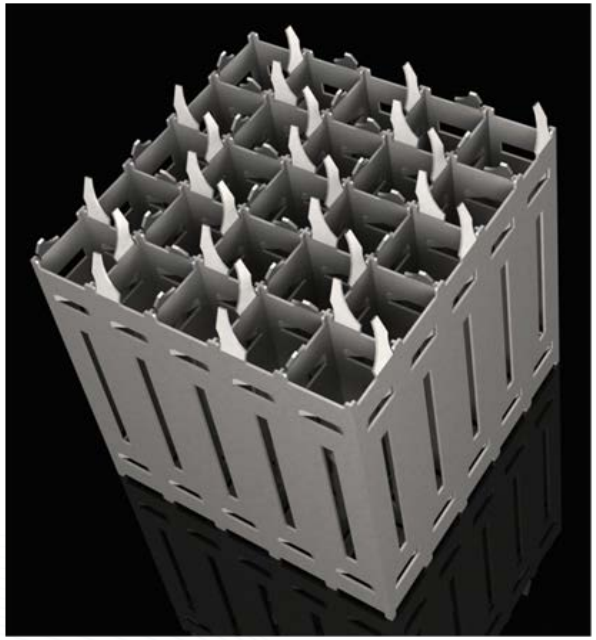

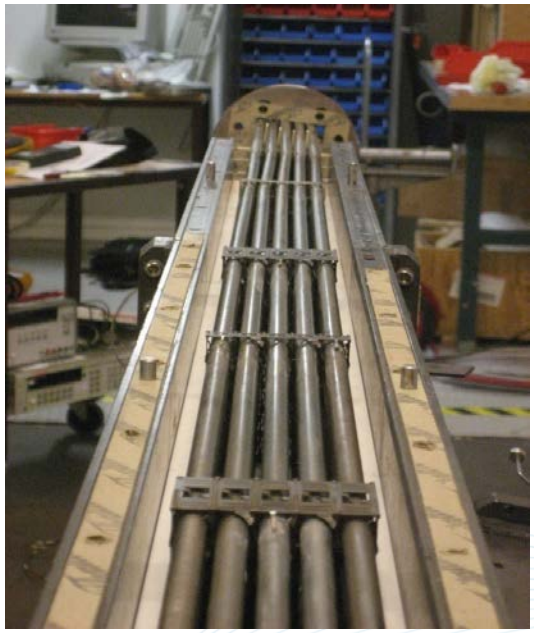

Desired Path Forward – Address Modeling & Simulation (M&S) Needs for Industry

- Fuel hardware design improvement
  - Higher fidelity of M&S capabilities (multi-phase) to predict fluid and fuel surface conditions and effects of fuel design features (e.g., grid spacer)
  - Applications of advanced data assimilation and uncertainty quantification methods on test design, data collection and analysis

- Safety margin quantification in accident analysis
  - Multi-scale and multi-physics M&S capabilities
  - Technical basis for DNB-related fuel failure (e.g., DNB during Reactivity Insertion Accident (RIA))
  - Control and optimization of fuel cladding surface morphology and properties during reactor operation

CASL DNB CP Deliverables

Enhanced computational performance of VERA/COBRA-TF (CTF) subchannel code via improved solver with parallelization

Developed initial Hydra-TH modeling of subchannel turbulent mixing in rod bundles with grid spacers, compared CTF predictions with rod bundle test data, and developed CTF subchannel models of fuel assembly and reactor core

Yr1 Yr2 Yr3 Yr4 Yr5

Developed Hydra-TH M-CFD code utilizing fully-implicit, parallel solver and closure relationships developed using experimental data and DNS

Collected rod bundle DNB and mixing test data, provided reference solutions of industry T/H codes, applied CTF to predict thermal-hydraulic behaviors and rod responses during RIA transient

Complete CTF full core modeling and simulation of DNB limiting events, Hydra-TH simulation of rod bundle mixing tests, 2-phase CFD simulation using industry code, and UQ of turbulent mixing model

Summary of CASL VERA Applications to DNB CP

- Current applications based on VERA T/H codes
  - COBRA-TF (CTF) subchannel code
  - Hydra-TH CFD code
- VUQ DAKOTA coupling with CTF for data and uncertainty analysis
- Model development and calculations on different computer platforms
  - Current industry capability (~500 cores at Westinghouse)
  - High power computing (HPC) (>4000 cores at LANL and ORNL)

NSRR (Japan) RIA Test Cases –CTF Analysis

- Onset of DNB, indicated by the Minimum DNB ratio (DNBR)

$$MDNBR = \frac{q''_{CHF}}{q''_{actual}} \leq 1.0$$

Input

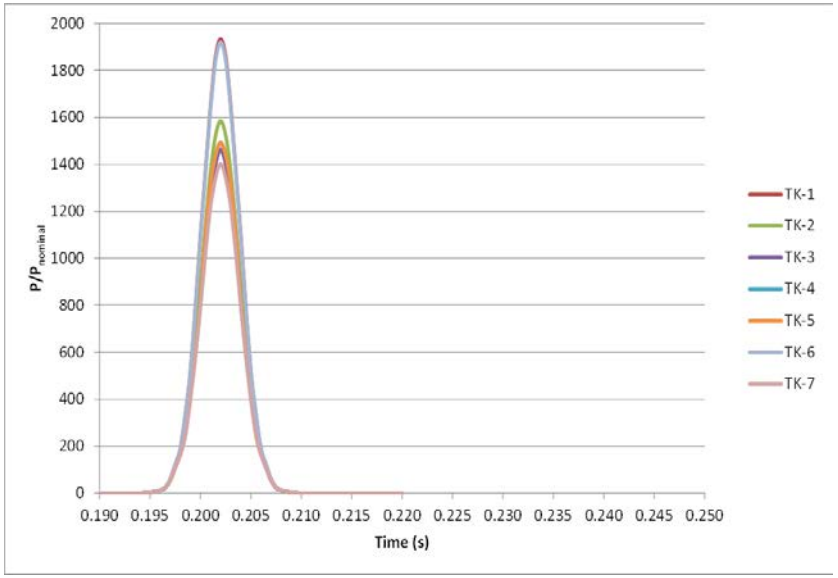

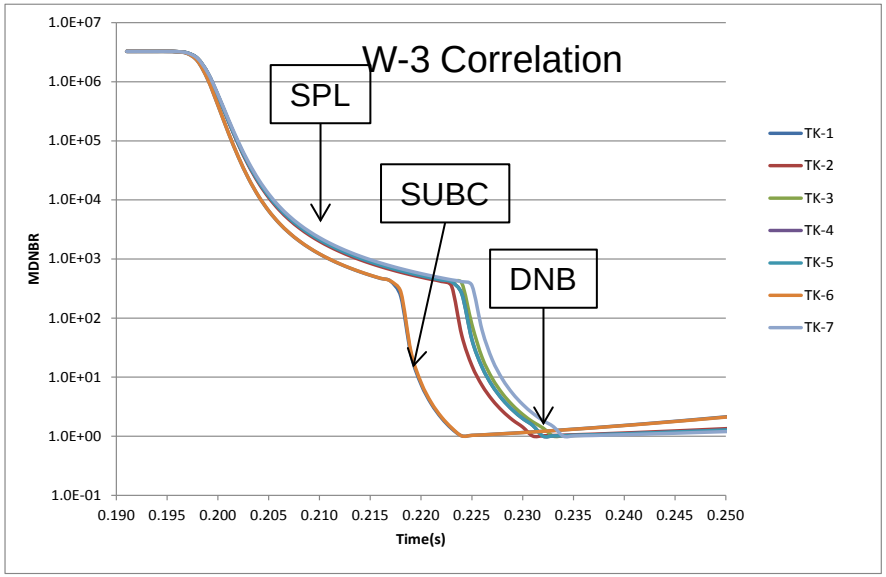

- Pulse duration ~16 ms initiated at zero power
- TK-1 and TK-6 have the highest peak (~x2000)
- Variable time step size: DTMAX=1.E-05, DTMIN=1.E-07 s
- Cladding failures reported in TK-2 and TK-7
- DNB occurrence in every case, including cases without cladding failure

CTF Modeling of PWR Fuel Assembly

- Applications of CTF Pre-Processor & Post-Processor

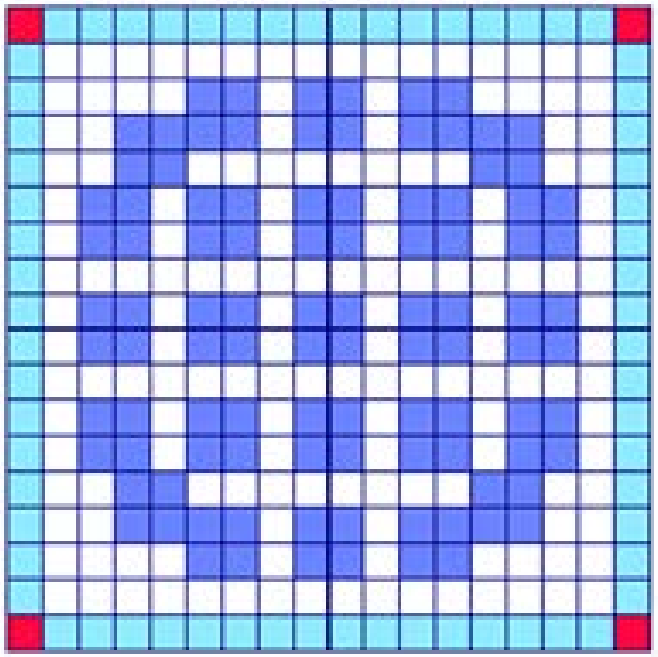

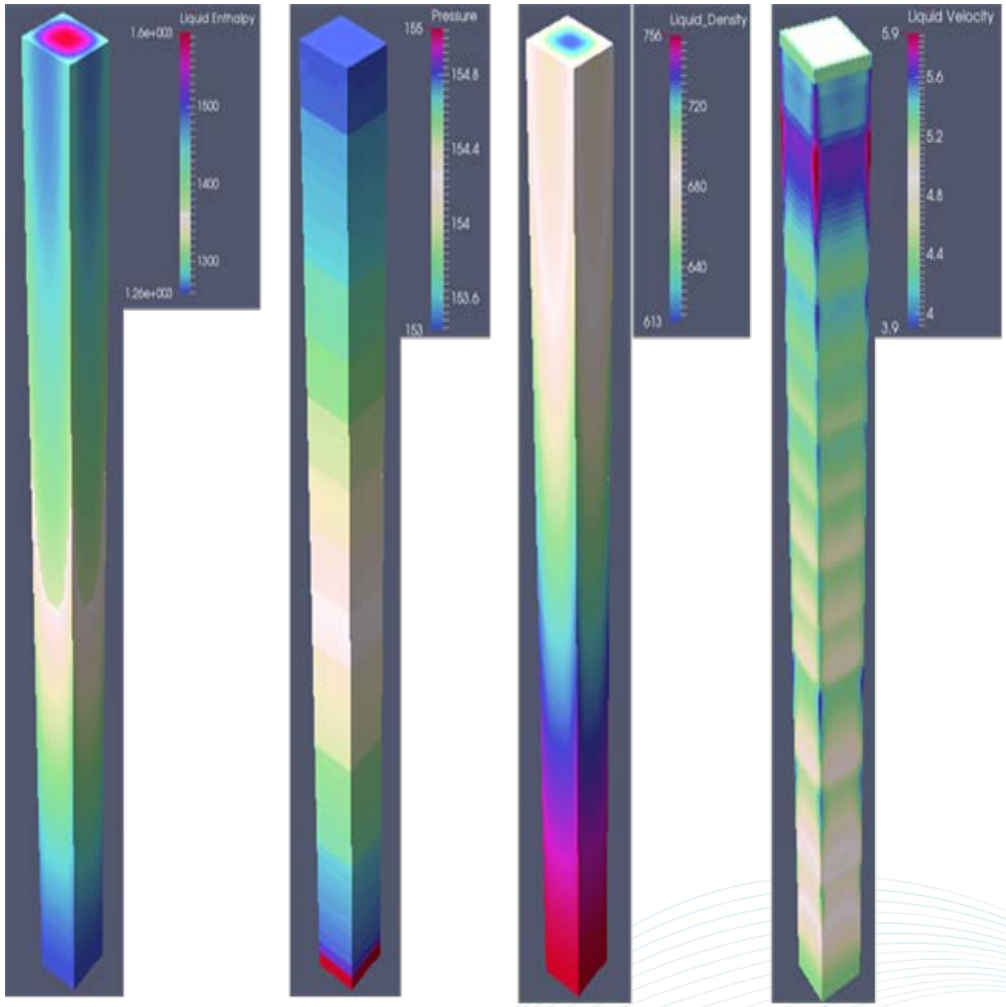

Ongoing CTF Modeling & Simulations

- Quarter core subchannel modeling
  - Steady state DNBR
  - Complete loss of coolant flow transient DNBR

- Full Core subchannel modeling (no coupling)
  - Steady state steamline break without offsite power (low flow) DNBR
  - RIA initiated at hot full power
  - Calculations being performed on HPC machine at ORNL

Hydra-TH CFD Modeling and Simulation

- 3x3 rod bundle simulation on industry machine

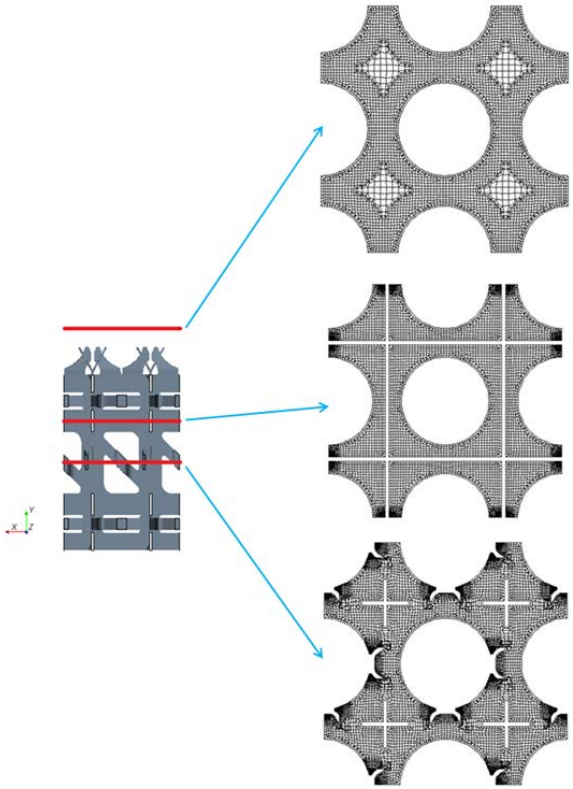

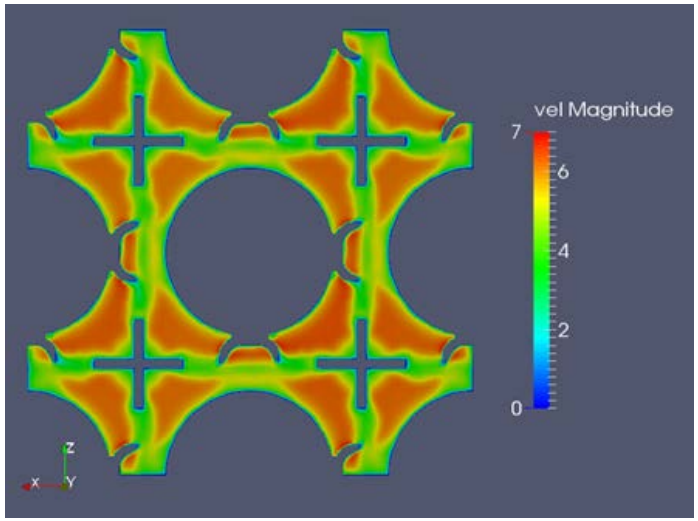

Hydra-TH

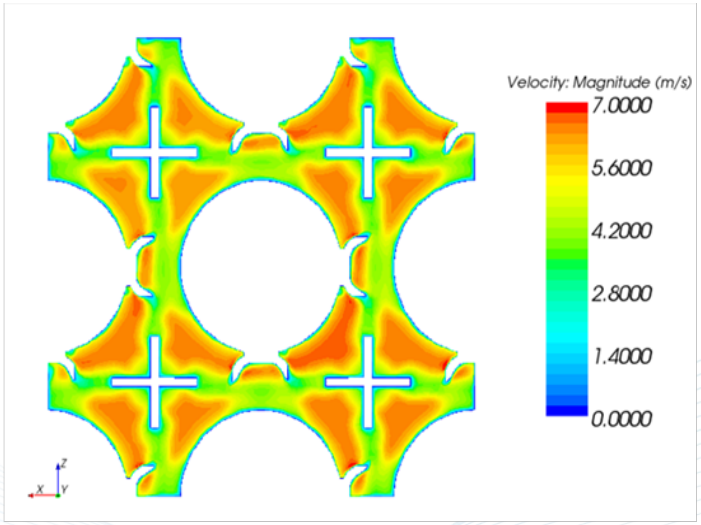

STAR-CCM+

Ongoing Hydra-TH Modeling & Simulations

- 5x5 rod bundle turbulent mixing
  - One-span modeling for code, model and computer system checks
  - Full length model for comparison with test data

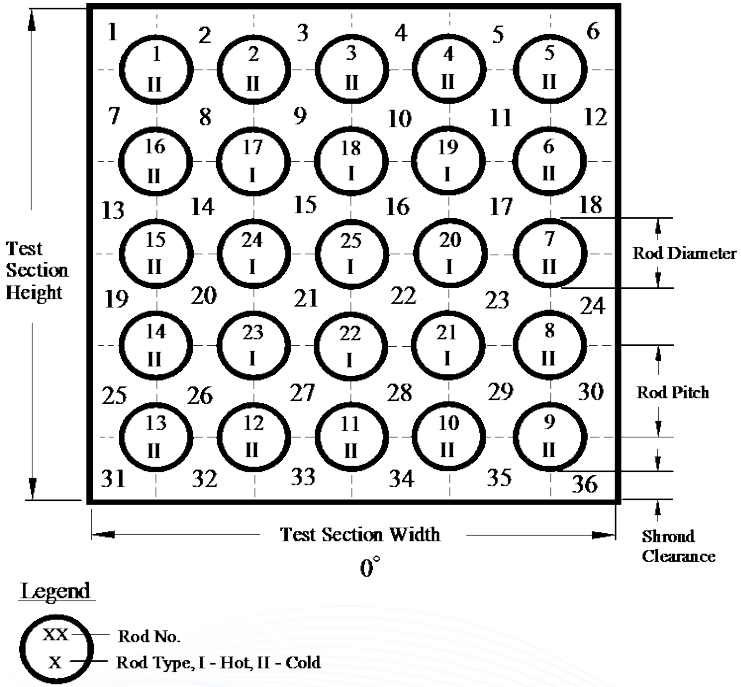

Subchannel

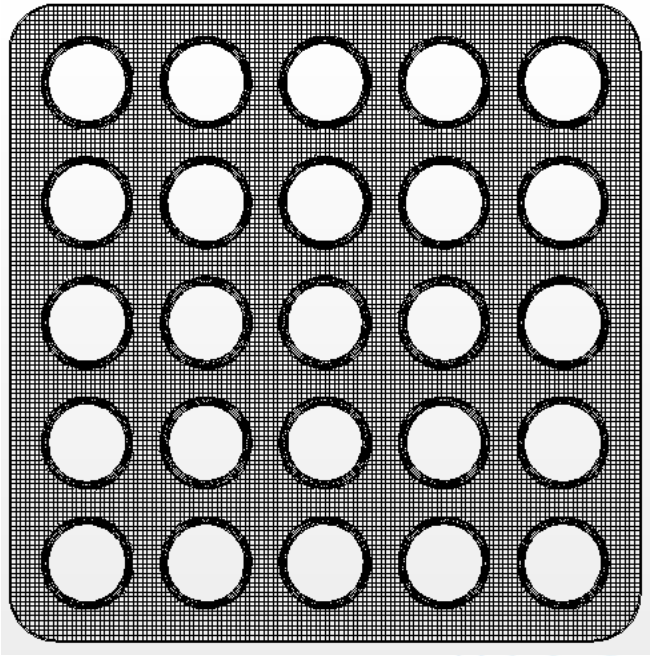

CFD

Ongoing UQ Study of CTF Turbulent Mixing Model

The turbulent mixing in subchannels was modeled using the following empirical correlation:

$$\Delta Q = -w' \times \Delta h \times \Delta X \qquad (5\text{-}1)$$

where ΔQ = energy exchange due turbulent mixing (W or Btu/hr)
w' = lateral turbulent flow per unit length (kg/s/m or lbm/hr-ft)
Δh = enthalpy difference between two subchannels (J/kg or Btu/lbm)
ΔX = axial nodal length (m or ft)

$$w' = ABETA \times G_{AVG} \times S \qquad (5\text{-}2)$$

where $ABETA$ = empirical coefficient,
G_{AVG} = average axial mass flow in the connected channels (kg/s/m^2 or lbm/s/ft^2)
S = rod-to-rod gap width (m or ft)

- Initial CTF/DAKOTA sensitivity study and calibration of turbulent mixing coefficient (ABETA) with test data

DNB Challenge Problem – Summary

- Work in good progress in accordance with Charter and Implementation Plan
- Current modeling and simulations based on VERA T/H subchannel and CFD codes for PWR
- VUQ study initiated with CTF/DAKOTA code system
- CASL milestone reports provide additional information on DNB CP-related accomplishments

Grid To Rod Fretting (GTRF) Challenge Problem Update

Brian Wirth
University of Tennessee, Knoxville

2014 CASL Round Table Meeting
July 14-16, 2014

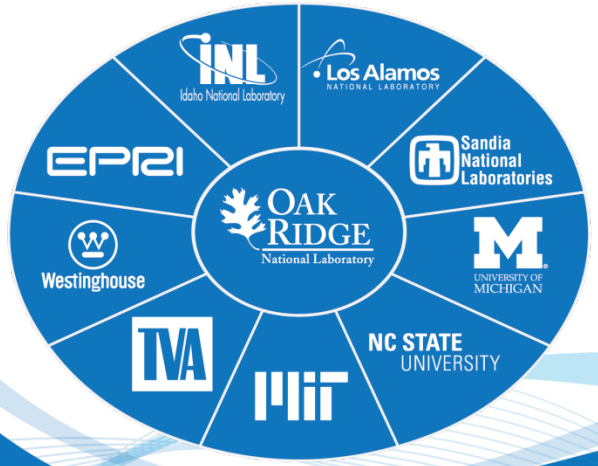

GTRF Challenge Problem Review

- Challenge Problem Description
- Evolution of Effort on GTRF to focus on Engineering Wear model development & pragmatic structural mechanics assessments
- Update on Fretting wear testing capability & engineering wear model
- Conclusions

Grid-to-rod fretting failure (GTRF)

- Clad failure that occurs as a consequence of high cycle vibrational contact between spacer grid (spring, dimple) and fuel rod
- Leading cause of PWR fuel leakers (reliability & performance issue)
- Power uprates and increasing fuel burnup could exacerbate GTRF failures
- Important components of GTRF:

  - Development of gap between spacer grid and clad (due to thermal expansion, thermal/irradiation creep, spring relaxation, oxidation stress & growth);
  - Flow induced vibration;
  - Contact and abrasion/wear; and
  - Full length rod vibration and wear depth

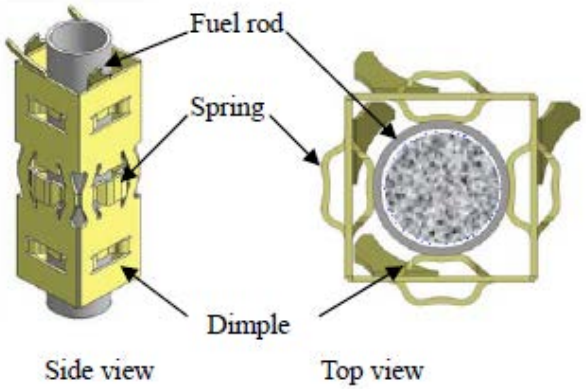

Evolution of GTRF activities --- January 2012 approach

WEC VITRAN Methodology*

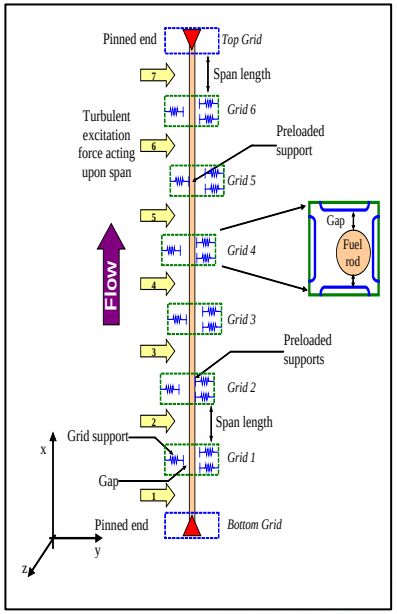

- Point contact at wear site
- 1D model
- PSD excitation force and 1D flow correlation

CFD to Determine Excitation Force on Fuel Rod

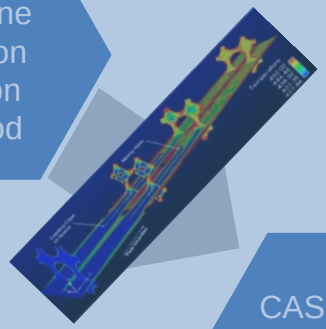

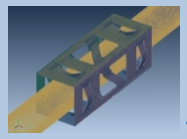

3D Structural Finite Element Analysis

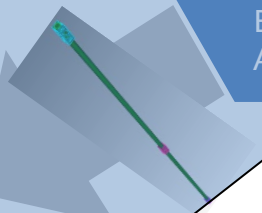

CASL/VERA Development of GTRF Capabilities

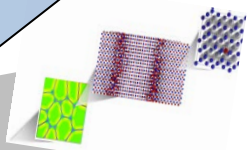

GTRF Wear Mechanisms
Time varying material degradation, contact conditions

Constitutive Models:
Capturing thermal creep, irradiation creep and growth, and hydriding

- Single crystal and polycrystal modeling of creep and dislocation mechanisms in irradiation environment
- Molecular statics, molecular dynamics, and accelerated molecular dynamics modeling of clad microstructure involving interaction of both interstitials and vacancies with edge dislocations
- Pair potential development to simulate chemistry and mechanical response

Integrate with Validation and Uncertainty Quantification

* Lu, Karoutas and Sham, *JOM* **63** (2011) 53-58

CASL Approach to GTRF – Jan 2013

TEAM: Dave Parks, Ken Kamrin, Michael Demkowicz, Sam Sham, Peter Blau Michael Thouless, Wei Lu,

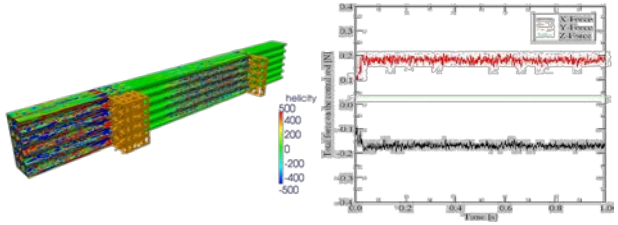

CFD Pressure Load History (Hydra-TH & limited fluid-structure interaction sims)

Structural mechanics

Wear model

Consisting of incubation, oxide and substrate controlled stages in the wear history.

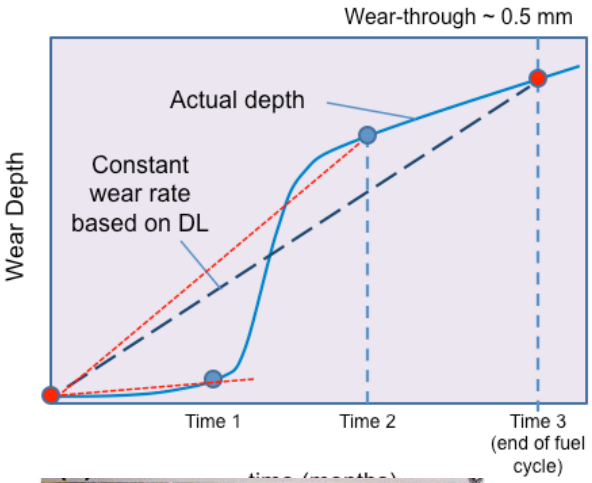

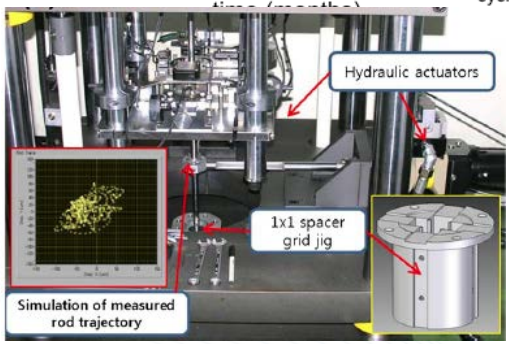

ORNL controlled fretting wear measurements

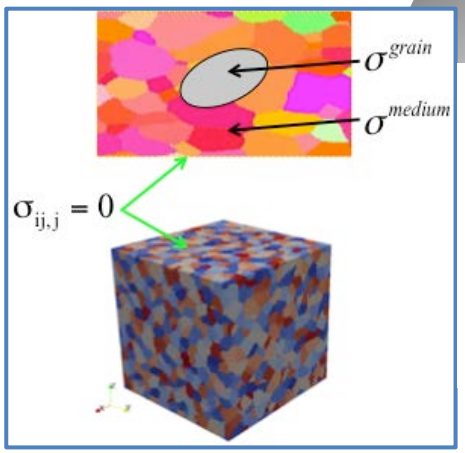

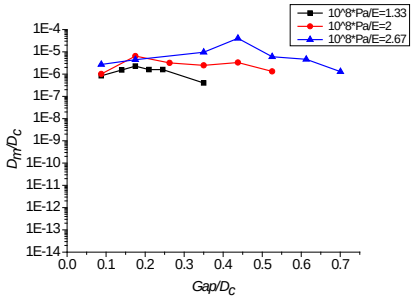

Grid-rod gap evolution, mechanical property evolution & parameteric studies of gap size/rod stiffness on wear shapes

Engineering Wear Model development*

Factors like Normal Force, Frequency and Amplitude of Sliding Contact Affect GTRF

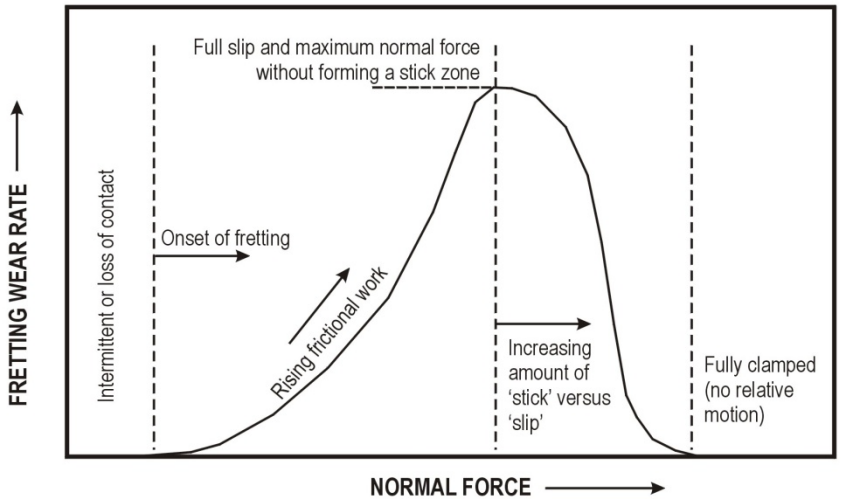

If normal force is either too high or two low, fretting is reduced or stopped.

High frequencies of impact and large oscillation amplitudes increase the wear rate.

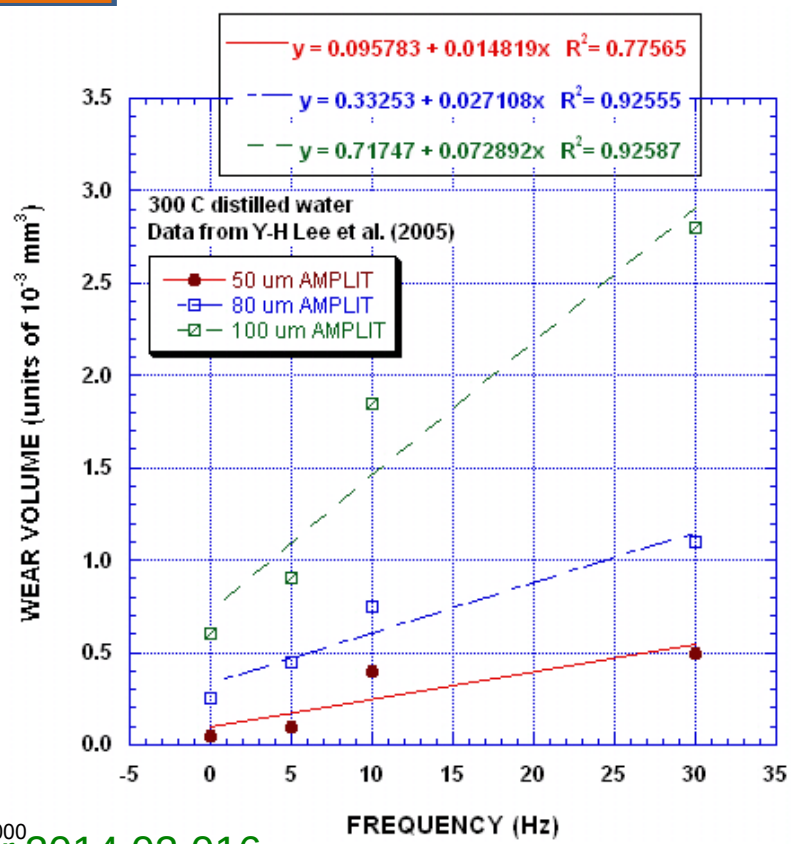

* P.J. Blau, *Wear* (2014) http:..dx.doi.org/10.1016/j.wear.2014.02.016

Engineering Wear Model development

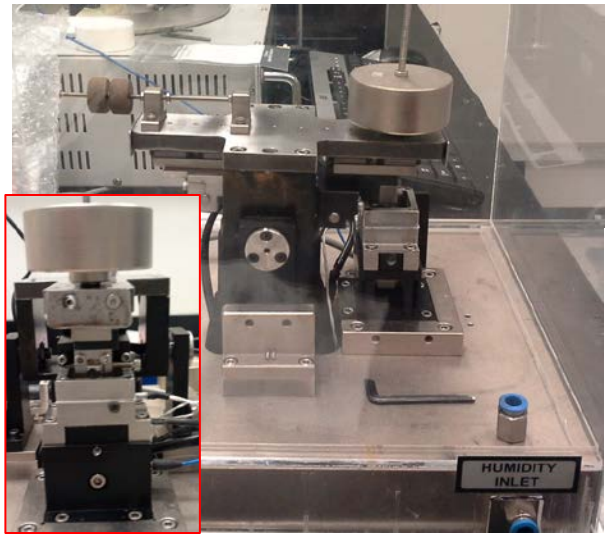

TR282 fretting wear testing at ORNL suitable for friction/wear testing under water conditions, ball on disk or tube on tube – provide laboratory data for engineering wear model validation

Use lab tests to evaluate effects of water flow rate & temperature, and to verify the model, which will then be 'trained' against literature/ field data

$$ZrO_2\ thick. = K_{waterflow} \frac{\mu_{ZrO2}\, P_{rec}\, (2X_{rec})\, f_{rec}\, T_1}{A_1} \left(\frac{V_{w\text{-}lab\text{-}ZrO2}}{\mu'_{ZrO2}\, P_{lab}\, (2X_{lab})\, f_{lab}\, t_1} \right)$$

$$Z_t = K_{waterflow} \frac{\mu_{Zr}\, P_{rec}\, (2X_{rec})\, f_{rec}\, (t\text{-}T_1)}{A_t} \left(\frac{V_{w\text{-}lab\text{-}Zr}}{\mu'_{Zr}\, P_{lab}\, (2X_{lab})\, f_{lab}\, t_2} \right)$$

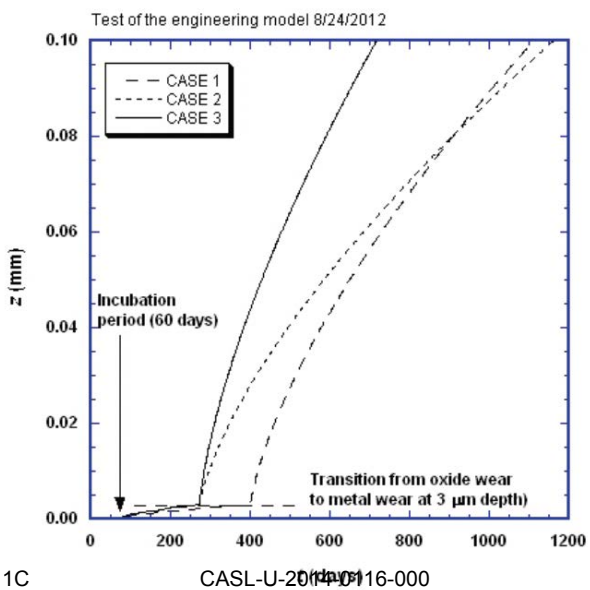

(μ) Friction coefficient

(P_{rec}) Normal force during time t

(X_{eff}) amplitude of oscillation

(f) oscillation frequency

Fretting wear test – facility & measurements

Oak Ridge National Laboratory, FY14.CASL.005 – L2.MPO.P9.01

- Commercial sliding tribometer modified into a fretting machine, with contact loads in range from 0.1 to 0.5 N, 25 Hz and 0.2 mm amplitude in water --- generating data relevant to GTRF phenomena & benchmarking Engineering Wear model

- Zirconium alloy tubes and grid strap provided by Westinghouse, and heat treated to pre-oxidize – thus, specimens measured in as-received versus pre-oxidized conditions

- Initial measurements showed significant reduction (~15X) of the wear volume in the pre-oxidized specimens

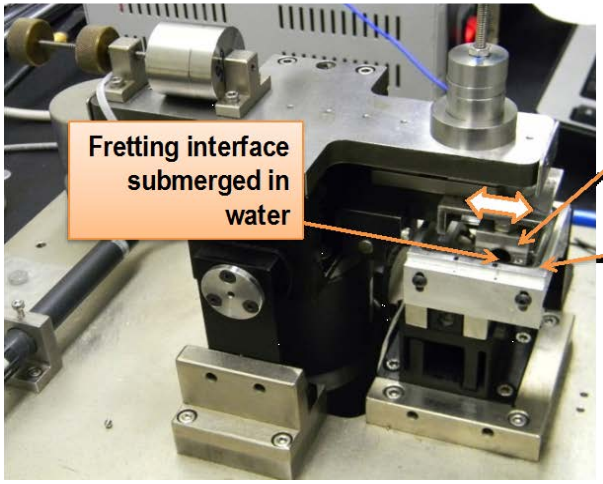

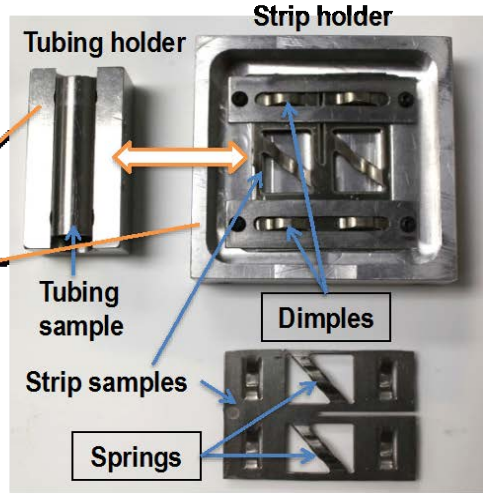

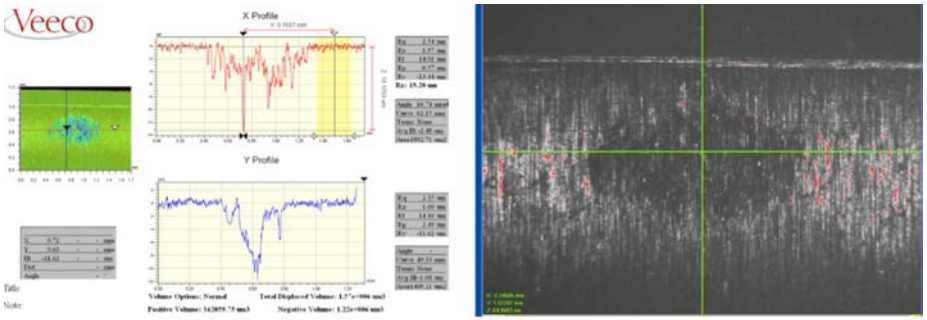

(a) As-received

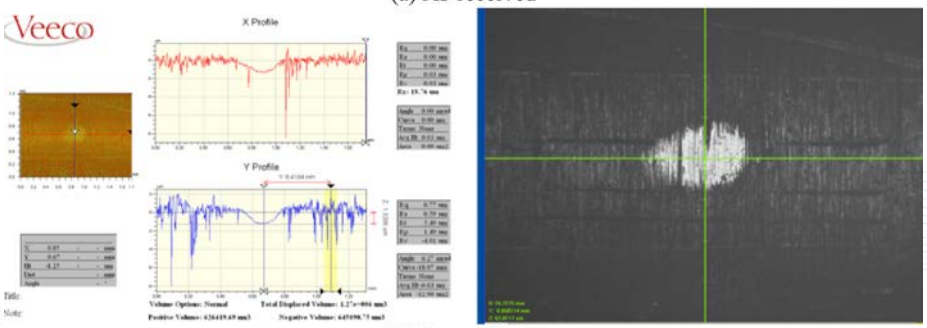

(b) Pre-oxidized

GTRF fretting bench testing – background

- Workrate = N (normal load)*2A (oscillation amplitude)*f (oscillation frequency)
- Normal load
  - VITRAN: spring impact force: 0.05 N (mean) and 0.175 N (peak)
  - VITRAN: dimple impact force up to 10 times of spring impact force
- Oscillation amplitude:
  - 0.01-0.03 mm (field experience)
- Oscillation frequency:
  - 20-30 Hz (field experience)
- VIPER test parameters

	Load (N)	Amplitude (mm)	Frequency (Hz)	Workrate (mW)	Duration (h)	Work (mWh)
Spring	0.1	0.01	25	0.05	500	25
Dimple	0.2	0.02	25	0.2	500	100

- AECL CANFRET test parameters (impact + sliding)

	Load (N)	Amplitude (mm)	Frequency (Hz)	Workrate (mW)
Spring	1	0.02	6.25	0.125
Dimple	4	0.01	6.25	0.25

Fretting test matrix

- Bench test results are expected to provide initial validation and training of the Engineering Wear Model by correlating with VIPER and AECL data with distinguished wear rates for materials 'as-received' and 'pre-oxidized'.

In water at RT*		Load** at each contact (N)	Amplitude (mm)	Frequency (Hz)	Workrate (mW)	Duration (h)	Work*** (mWh)
Tube against 2 springs	As-received	0.1 (0.2 total)	0.2	25	1	25	25
		0.5 (1 total)	0.2	25	5	5	25
	Pre-oxidized	0.1 (0.2 total)	0.2	25	1	25	25
		0.5 (1 total)	0.2	25	5	5	25
Tube against 2 dimples	As-received	0.5 (1 total)	0.2	25	5	20	100
		2.5 (5 total)	0.2	25	25	4	100
	Pre-oxidized	0.5 (1 total)	0.2	25	5	20	100
		2.5 (5 total)	0.2	25	25	4	100

**Interface submerged in distilled water at room temperature*

***Load – assuming load evenly divided between two contact points*

****Work – matching VIPER's 500-hr test*

- *Friction force trace to be monitored to calculate the impact frequency (due to machine vibration)*
- *2 repeats for each data point (additional 1-2 repeats warranted if data scatter)*

Tube against dimples – as received

Wear scar on tube (as received)
0.5 N, 0.2 mm, 25 Hz, 20 hrs

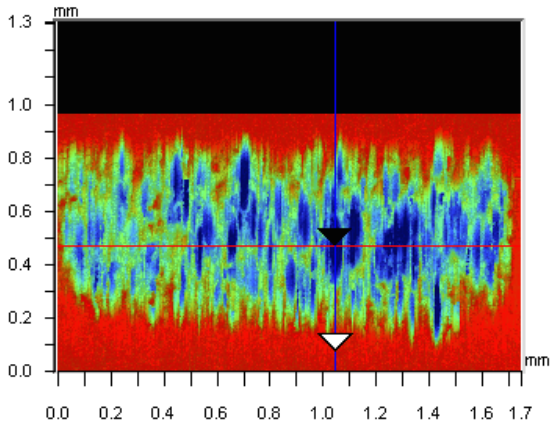

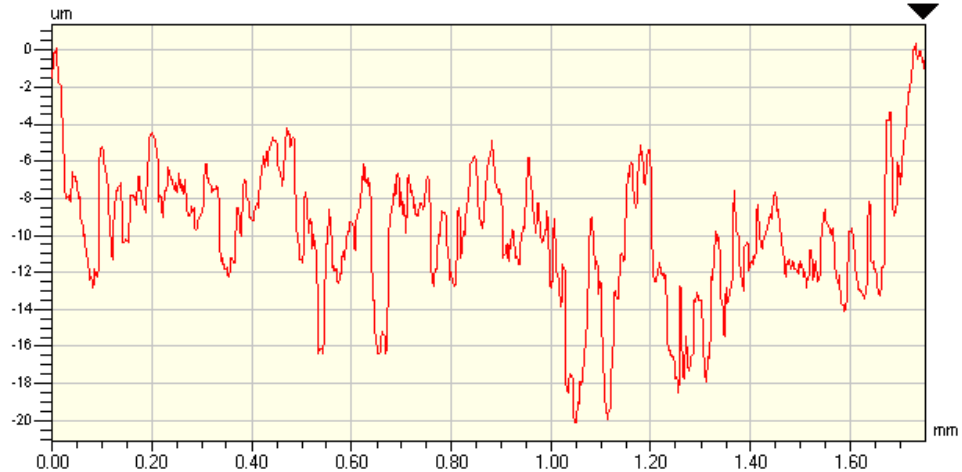

Y Profile

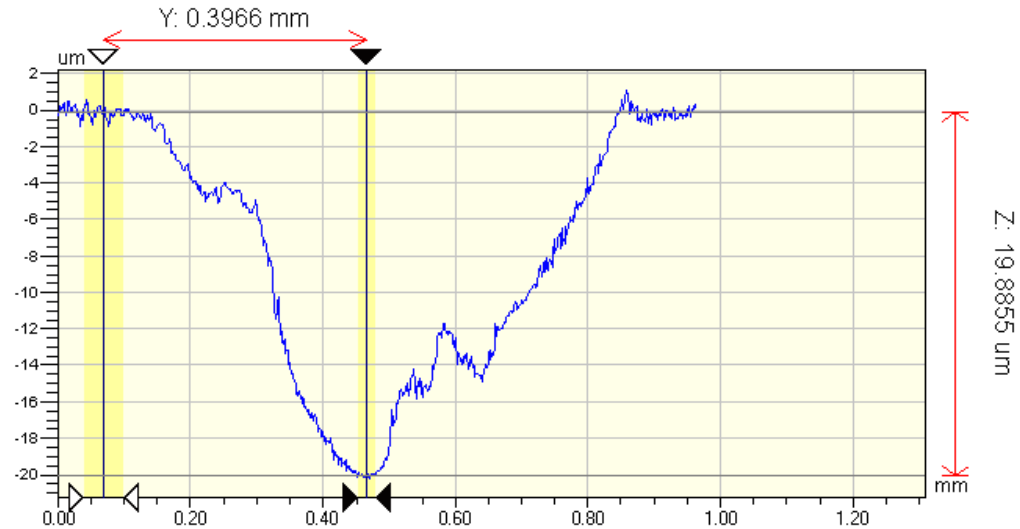

X	1.05	-	-	mm
Y	0.47	-	-	mm
Ht	-20.03	-	-	um
Dist			-	mm
Angle			-	°

Title:

Note:

Volume Options: Normal **Total Displaced Volume: 8.84e+006 um3**

Positive Volume: 71557.82 um3 **Negative Volume: 8.77e+006 um3**

Tube against dimples – Pre-oxidized

Wear scar on tube (pre-oxidized) – much smaller!
0.5 N, 0.2 mm, 25 Hz, 20 hrs

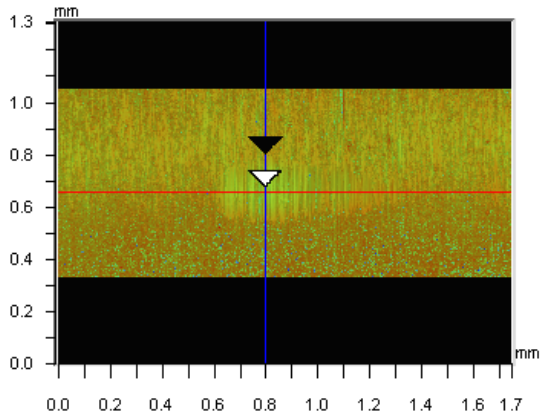

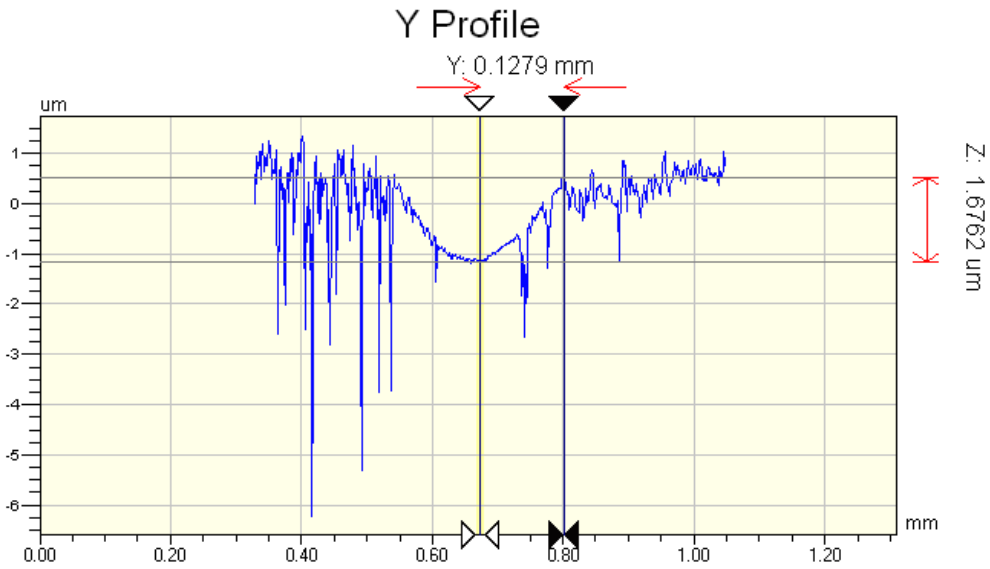

X	0.80	-	-	mm
Y	0.65	-	-	mm
Ht	-1.10	-	-	um
Dist			-	mm
Angle			-	°

itle:

ote:

Volume Options: Normal **Total Displaced Volume: 637049.75 um3**

Positive Volume: 308347.06 um3 **Negative Volume: 328702.72 um3**

Wear results comparison

- The wear depth and wear coefficient results obtained in ORNL bench fretting tests are in the same order of magnitude as the literature data!
- Reasonable to good repeatability.
- Pre-oxidation reduces the wear depth by 10X and wear coefficient by 23X!

0.5 N, 0.2 mm, 25 Hz, 20 hrs Workrate: 5 mW		Work* (mWh)	Max wear depth (μm)			Wear volume ($x10^{-3}$ mm^3)			Wear coefficient ($x10^{-15}$ Pa^{-1})		
			Left	Right	AVE	Left	Right	AVE	Left	Right	AVE
As-received	Test 1	100	18.2	16.4	17.3	8.5	4.5	6.5	2.3	1.3	1.8
	Test 2		23.0	19.9	21.5	11.5	8.8	10.1	3.2	2.4	2.8
	AVE				19.4			8.3			2.3
Pre-oxidized	Test 1	100	**	2.1	2.1	**	0.4	0.4		0.1	0.1
	Test 2		1.7	1.6	1.6	0.3	0.3	0.3	0.1	0.1	0.1
	AVE				1.9			0.3			0.1
Wear reduction					90%			96%			96%

**Work – matching VIPER's 500-hr test*

***Left scar not found on the tube, possibly due to misalignment*

Providing a first-principles assessment of wear & investigating fluid structure interactions

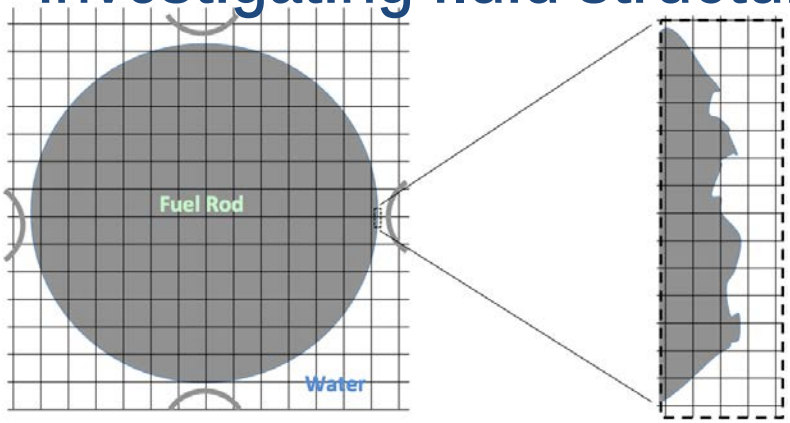

Discrete element modeling to evaluate Surface roughness, third bodies (asperities) & complex loading (contact load, slip amplitude & impact) affects on fretting wear

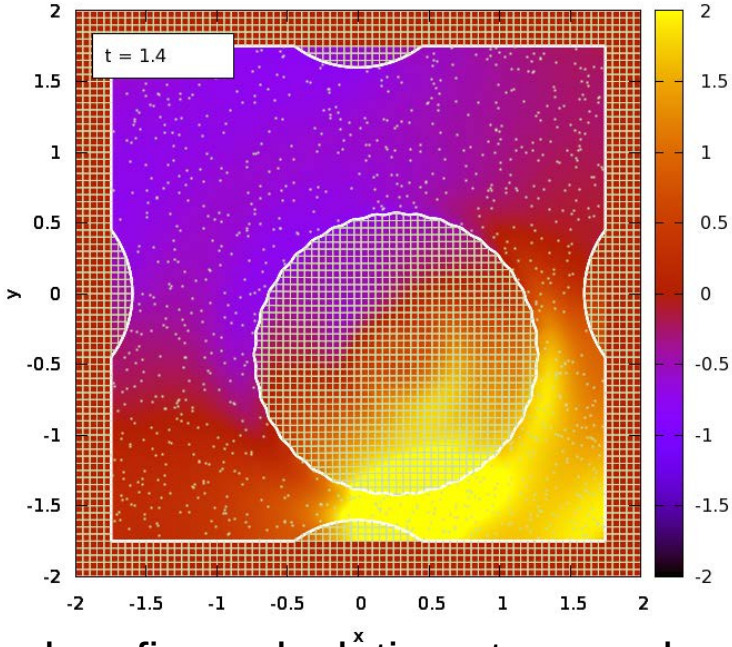

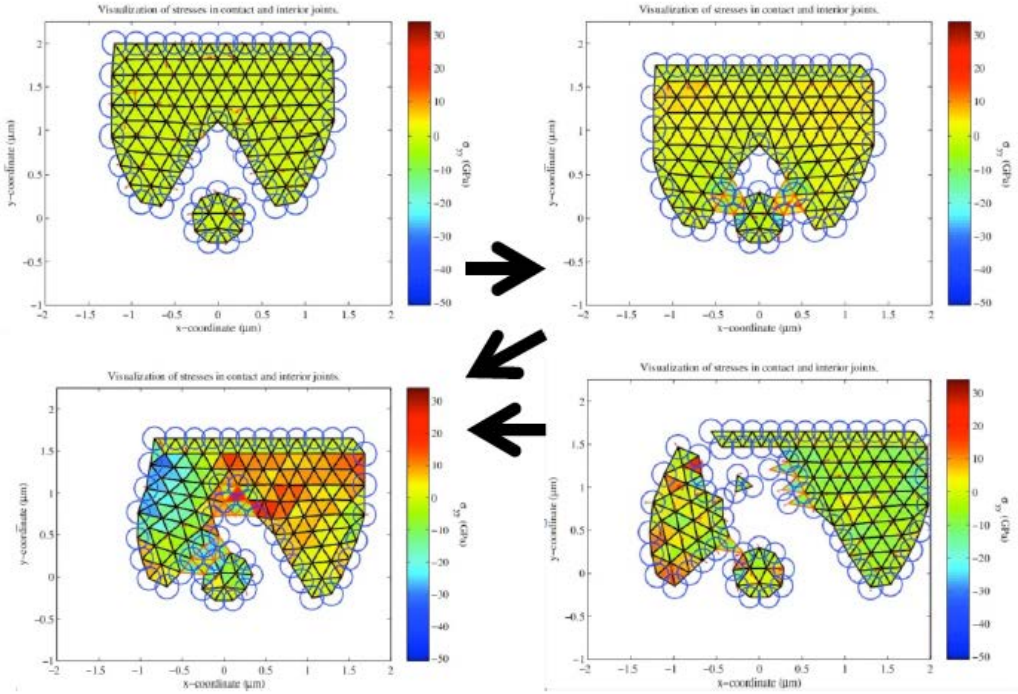

Intensely refine calculations to speedup calculations of induced pressures on rod

Parametric variation of key assumptions within GTRF using 3D single cell grid (e.g., creep mechanisms*, rod stiffness & gap size)

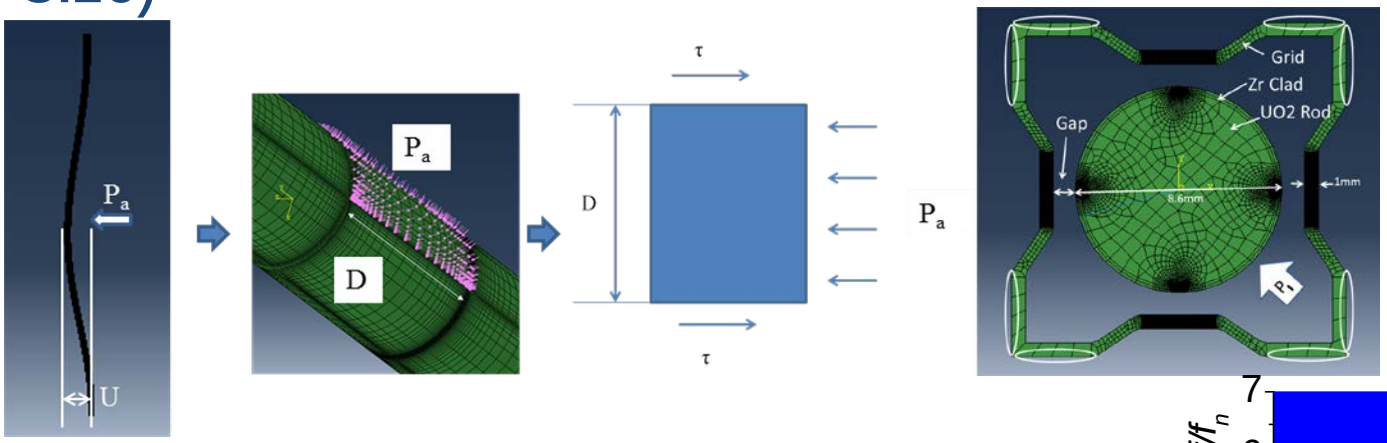

- Rod stiffness, gap & load frequency affects vibration and wear
- The wear rate reaches a peak value at a certain gap.
- Moving towards 'wear map' showing the overall dependence on grid-to-rod gap and load frequency

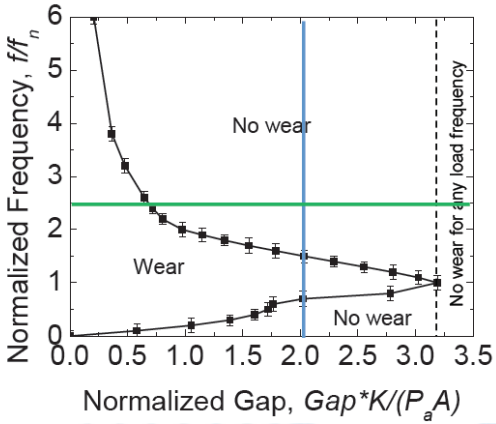

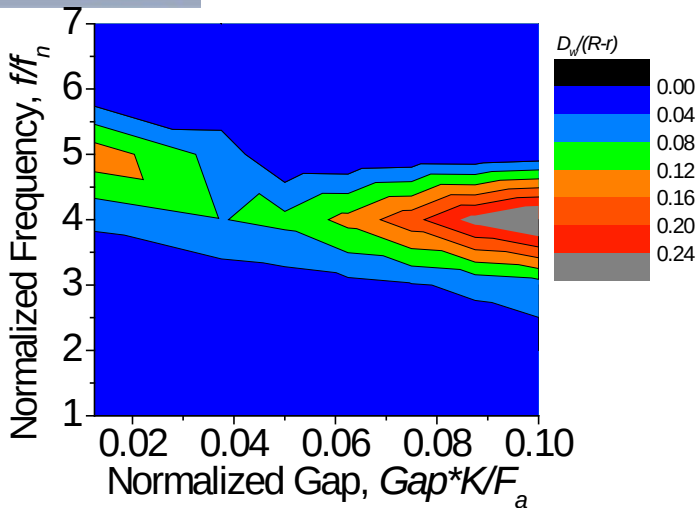

* Wang, Hu, Lu and Thouless, *JNM* **4333** (2013) 188-198

Summary

- FY14 saw transition of GTRF approach within MPO, shift away from full-scale, coupled fluid-structure interactions activities to emphasize engineering wear model development and laboratory data to refine that model, in addition to smaller-scale, University activities to provide base physics and pragmatic evaluation of FSI and structural mechanics activities

- Phase 1 success within CASL on GTRF is engineering wear model + these pragmatic structural mechanics assessments (e.g., creep models in ABAQUS, influence of gap)

- Path forward: Phase 2 work will focus on wrapping up a validated engineering wear model plus limited structural mechanics assessments (e.g., gap development effects)

Pellet-Cladding Interaction (PCI) Challenge Problem Update

Robert Montgomery (Presented by Brian Wirth UTK)
Pacific Northwest National Laboratory

2014 CASL Round Table Meeting
July 14-16, 2014

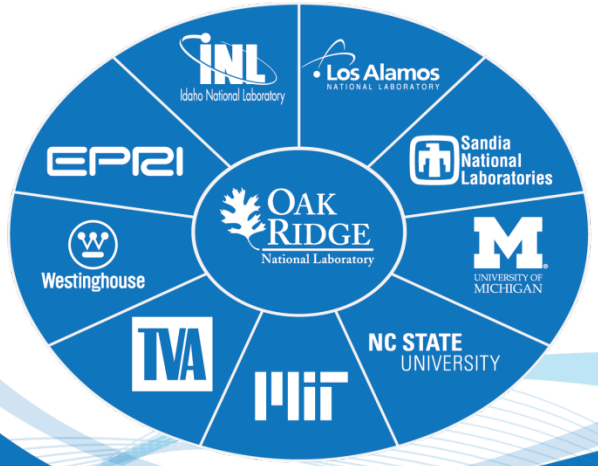

U.S. DEPARTMENT OF ENERGY
Nuclear Energy

CASL
Consortium for Advanced Simulation of LWRs

PCI Challenge Problem Review

- Challenge Problem Description
- Current Industry Practice
- Desired Industry Path Forward
- What is Success?
- Development of Capabilities and Status

PCI: Why it is important?

- PCI failure potential limits reactor performance associated with power uprates, higher burnup, fuel rod manufacturing quality and operating flexibility during power changes
- Requires new 3D multi-physics simulation capability to reduce uncertainties in assessing PCI failure conditions during normal operation and in the presence of anomalies

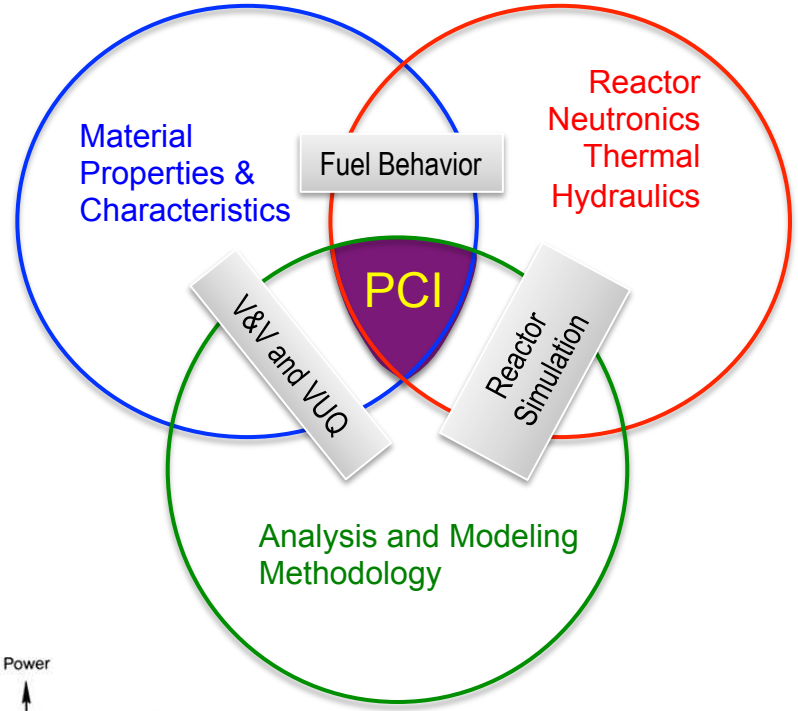

PCI is possible in many rods and assemblies

PCI is controlled by local effects

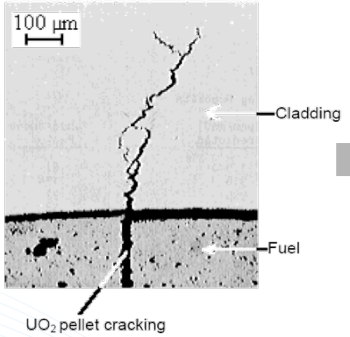

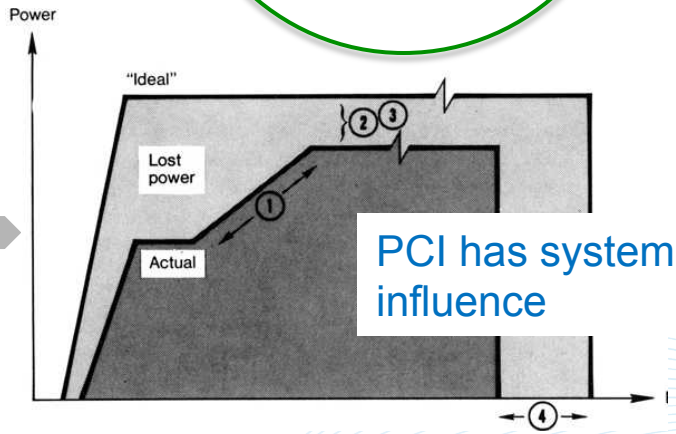

PCI has system wide influence

3D fuel performance model is critical to assess complex, coupled physics and irregular geometries responsible for PCI fuel failures

Current Industry Practices for Mitigating PCI Failures

- Power ramp rate restrictions during restart following a refueling outage or mid-cycle power maneuver
- Limitations on extent of low power operation with return to full power
- Restrictions on core loading patterns to minimize power peaking
- Fuel design changes to address key mechanisms of SCC
- EPRI PCI Guidelines from “Zero by 10” initiative outlines PCI Risk Assessment Procedure (PRAP)

Costs associated with lost power generation, fuel development, and process

Current Industry Practices for Modeling PCI

- State of the art modeling approaches have focused on
  - 1.5D or 2D methods that consider the coupled thermal/ mechanical behavior
  - EPRI Falcon code represents one of the most widely used PCI analysis capabilities (2-D FEM based)
  - Others include RODEX4, PAD/ANSYS, CYRANO3, etc.
- PCI modeling requires unique capabilities to capture local pellet-cladding interfacial forces
  - Discrete modeling of pellet cracks –> local stress concentrations
  - Failure criterion based on Stress Corrosion Cracking (SCC) or empirically derived stress from ramp test data

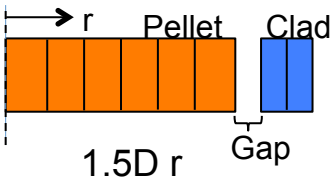

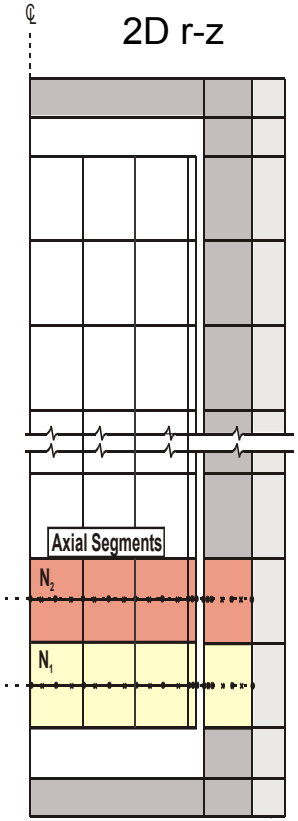

- Based on V&V using Ramp Test Data
  - Diametral and axial strains/displacements
  - Failure or no-failure
  - Fission product release and distributions in pellet

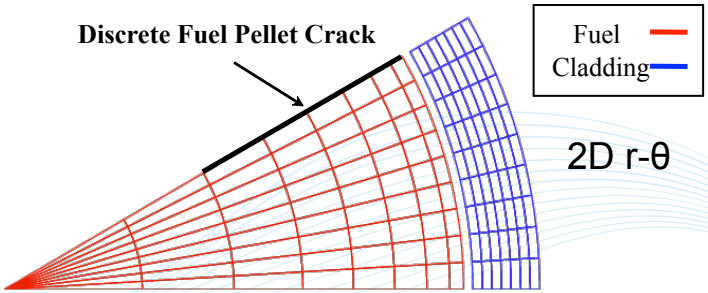

Desired Industry Path Forward

- Increase confidence in PCI failure potential assessments
  - Account for uncertainties in fuel performance parameters using improved mechanistic material models
  - Improve representation of non-uniform (non axi-symmetric) effects not included in current modeling approaches
  - Take advantage of improved neutronics simulations to reduce power uncertainties
  - Reduce empiricism in current methods used to assess cladding failure
- Improve core-wide PCI failure assessment process

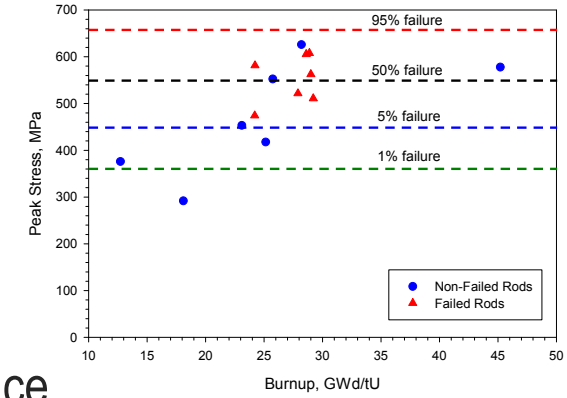

Figure 12. Stress-Based Failure Probability Levels

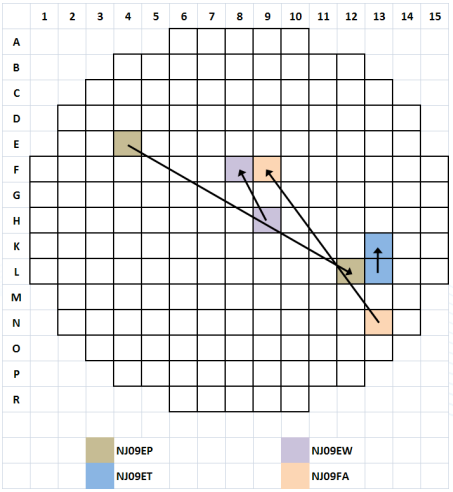

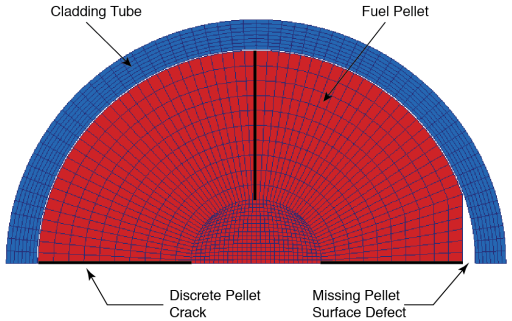

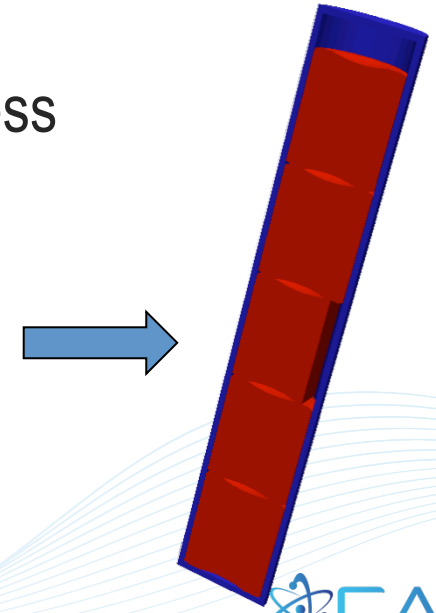

Measures of Success

- Minimal: Use coupled neutronics/thermal-hydraulics/fuel performance to calculate axi-symmetric cladding stress distribution throughout the core.
  - Compare to empirical failure threshold stress (e.g. XEDOR/Powerplex)

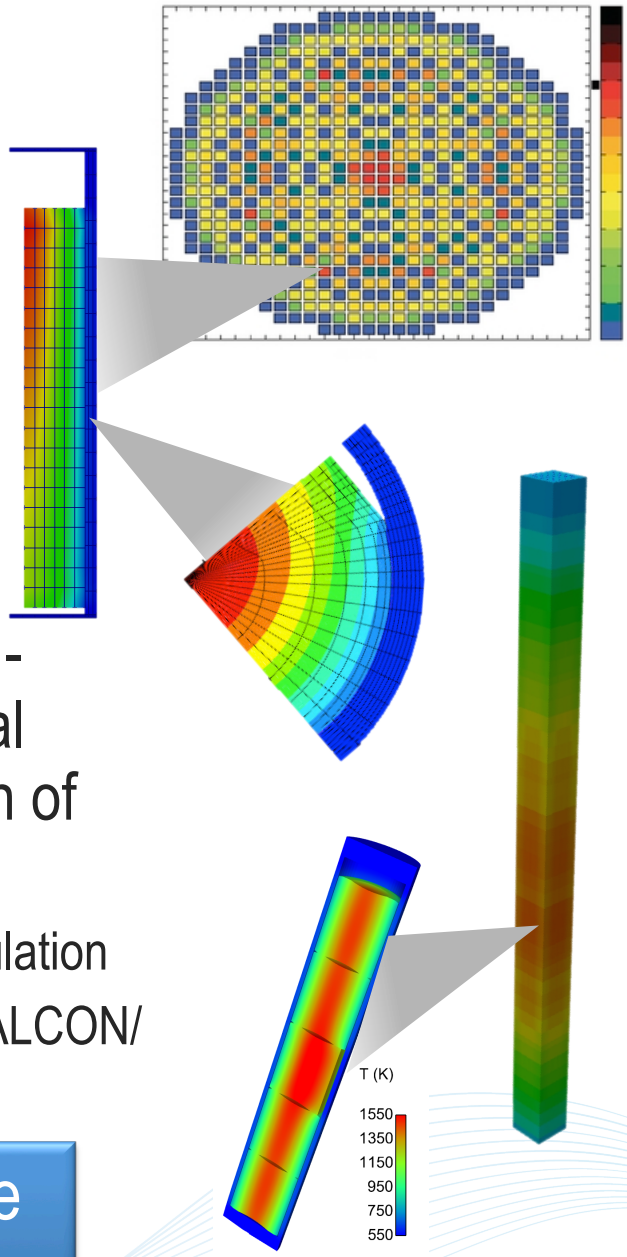

- Acceptable: Use coupled neutronics/thermal-hydraulics/fuel performance to calculate local cladding stress concentrations in core region of interest
  - Requires separate 3-D local region standalone calculation
  - Compare to empirical failure threshold stress (e.g FALCON/ SIMULATE)

Goal: Methodology for PCI Failure Probability Assessment

Measures of Success (con't)

- Ultimate End Game:
  - Reliably calculate PCI failure potential for specific core loading patterns and operating strategies
  - Define impact of material defects and material properties/ characteristics on PCI failure potential
  - Define impact of plant operating strategy and fuel design on PCI failure potential

Atomistic simulation for defect behavior, including mobility and interaction with dislocations

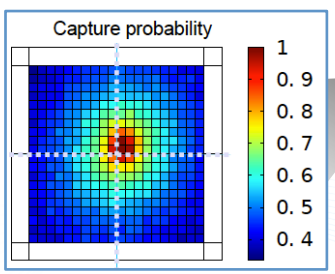

Visco Plastic Self Consistent (VPSC) model, which accounts for crystallographic mechanisms, interactions between grains and coupling between growth and creep (radiation and thermal)

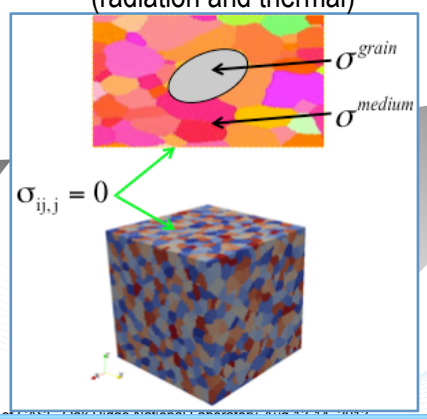

PEREGRINE engineering scale fuel performance

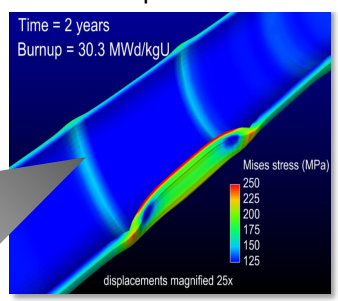

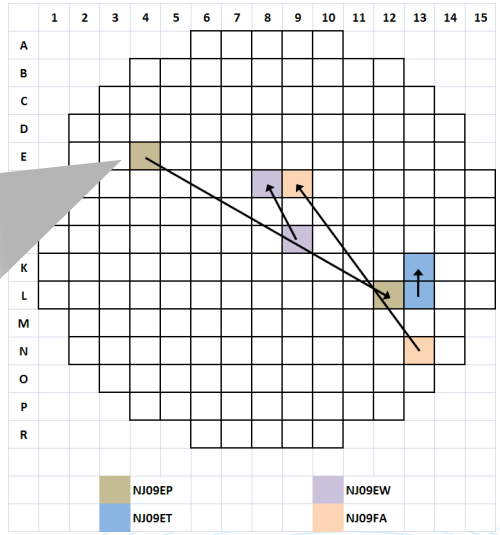

Challenge will be sufficient validation

PCI M&S Capabilities Required

- Core-wide neutronics for local fission density and neutron flux that considers depletion, time dependent effects, and local reactivity perturbations (control rod movement)
- Subchannel thermal hydraulics for clad to coolant heat transfer conditions
- Full core fuel rod behavior modeling using reduced dimension (2-D) representation – performance indicator
- Local effects fuel rod simulation accounting for non-uniformities, improved mechanistic material and behavior models

Reactor Simulation

Fuel Behavior

V&V and VUQ

Core-wide to local effects bridging

PCI Challenge Problem – Current Activities

MPO PCI Efforts/Focus

- Develop Peregrine to calculate fuel rod conditions during operation for full-length rods
- Mechanistic model development for corrosion and hydriding, cladding fracture, and cladding creep/growth/plastic deformation
- Develop 3-D local effects (few pellets) modeling methods to evaluate environmental conditions leading to PCI failure

VERA-CS Efforts/Focus

- Couple Peregrine fuel rod model (2-D) to core simulator (core-wide power/ TH calculations) to calculate performance indicator throughout entire core
- Develop method to couple full-length fuel rod model to local effects stress and failure potential simulation (3-D effects)

V&V and VUQ

- Benchmark and calibration of material/behavior models
- Validation of individual domain codes and coupled system

2-D Finite Element Models for PCI Analysis

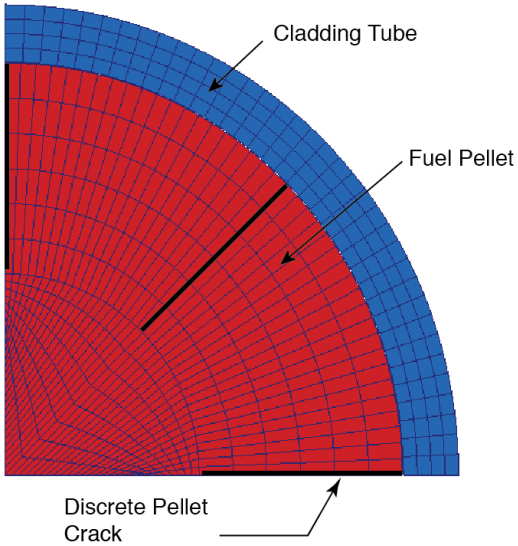

3 Crack Model for Classical PCI

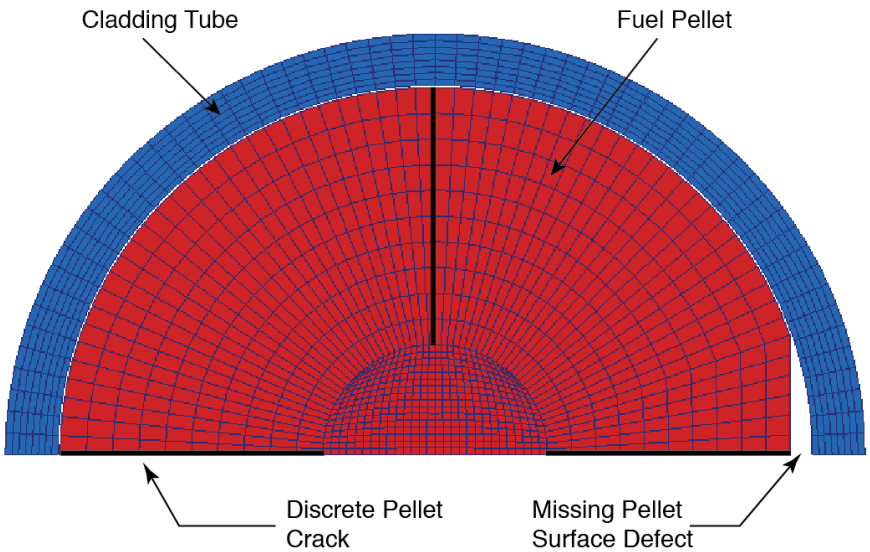

MPS Defect Model for non-Classical PCI

3-D Finite Element Models for PCI Analysis

Single Pellet Model with Discrete Cracks

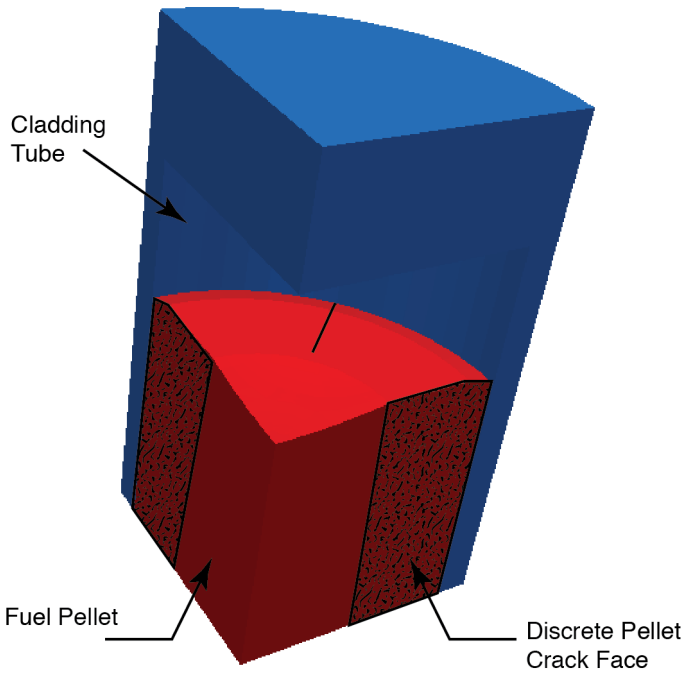

5 Pellet Model with Discrete Cracks and MPS Defect

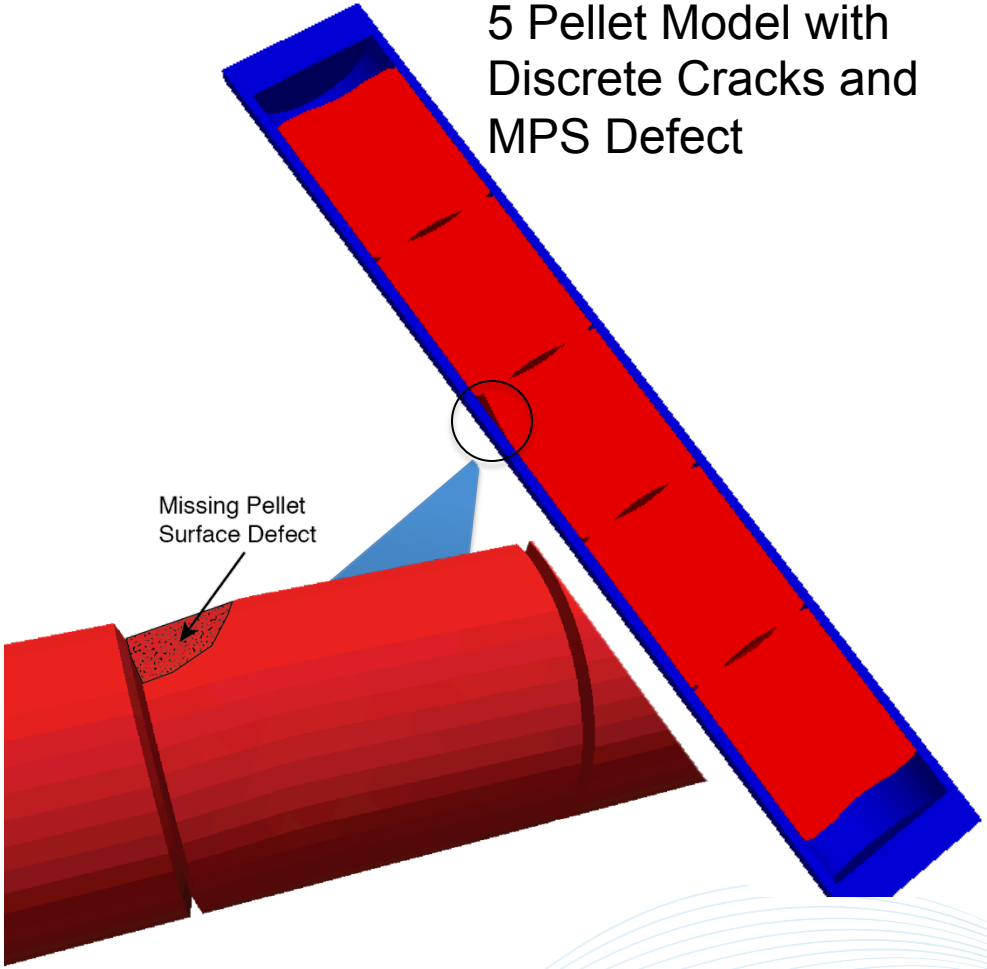

Cladding Stress History During Power Ramp for Classical PCI Conditions

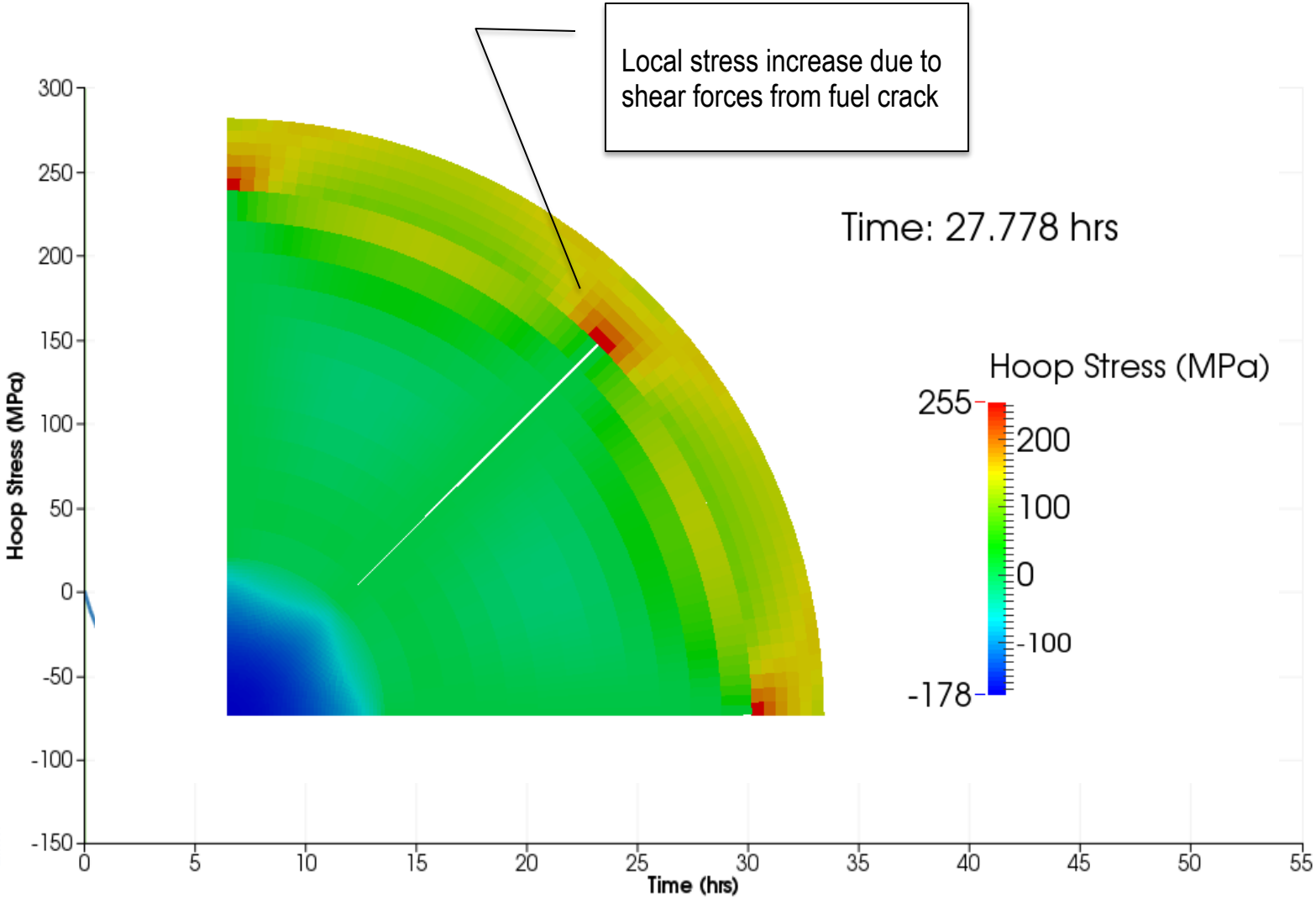

Effect of MPS Defect on Temperature Distribution

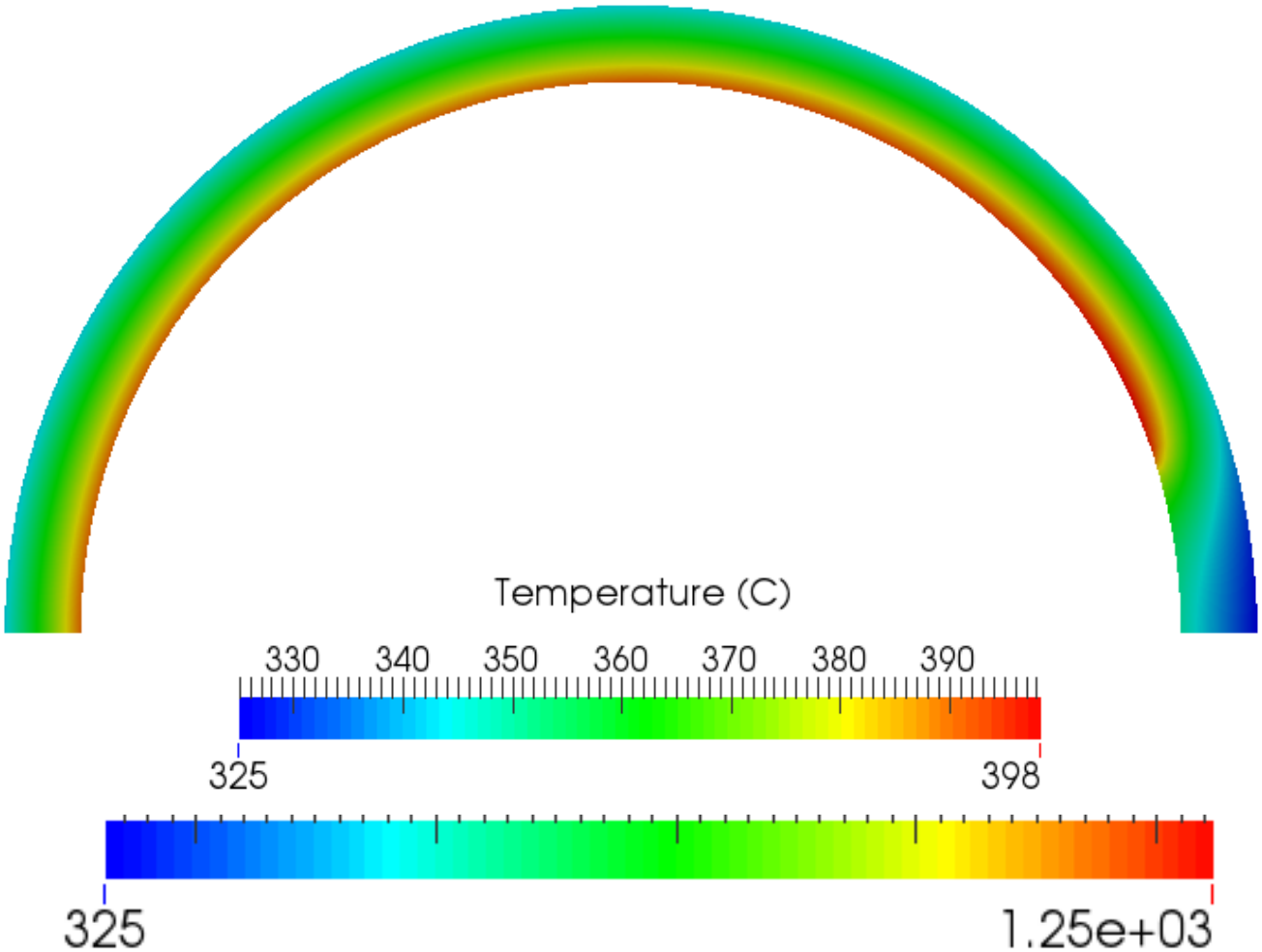

Effect of MPS Defect on Cladding Hoop Stress Response

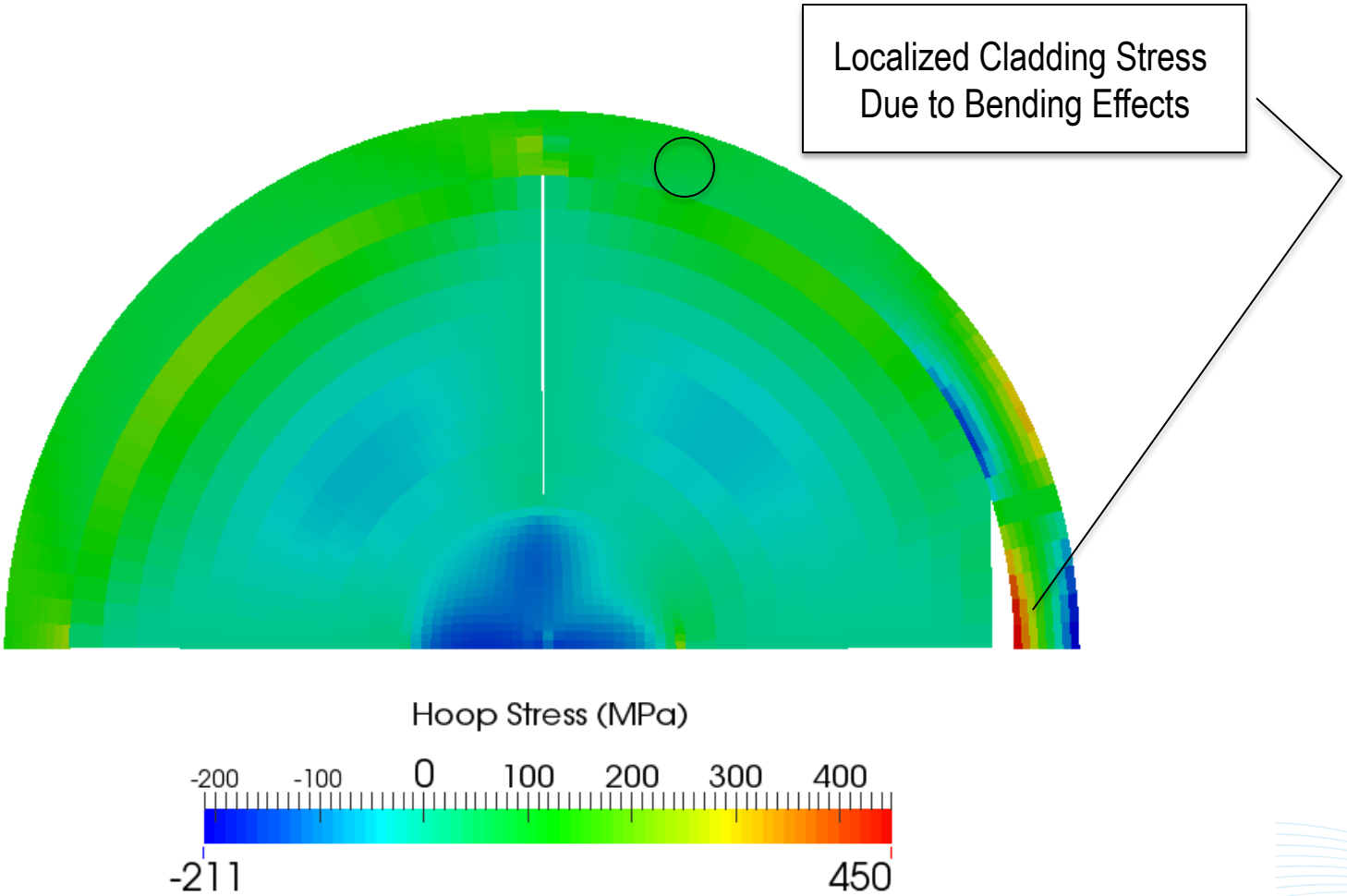

105 mil (2.6 mm) MPS Defect

Recent Results – Geometry Effects
2-D and 3-D modeling

Crack Depth Impact on PCI Cladding Stress

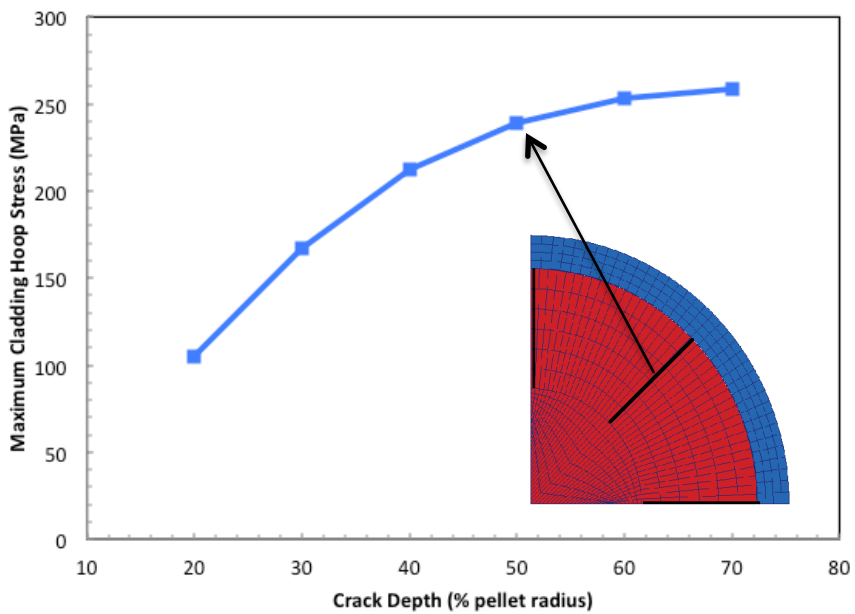

MPS Defect Width Effect on Cladding Stress

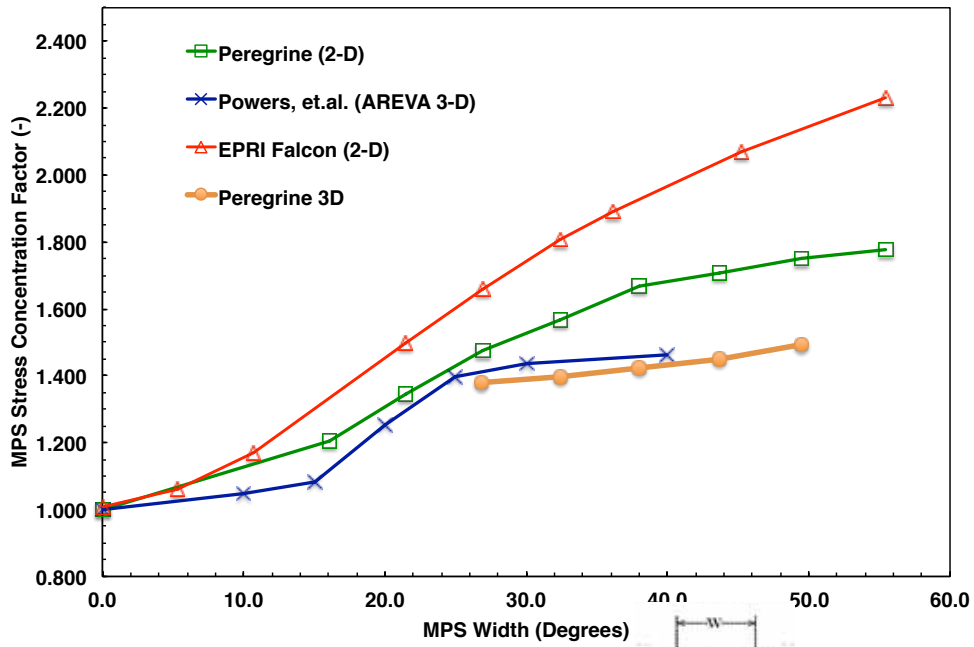

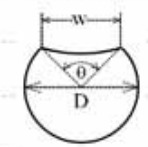

$$\theta = 2\sin^{-1}\left(\frac{w}{D}\right)$$

Versatile Geometric Modeling Allows for Local Effects Considerations

Planned Accomplishments in FY14

- Axisymmetric core-wide stress calculation
  - Coupled neutronics (pin resolved powers), thermal-hydraulics and fuel performance with depletion and xenon effects
- Local stress calculation
  - 3-D cracked pellet simulation with mechanistic cladding creep and fission product interaction
- Integrated methodology
  - Core wide to pellet scale simulation with local effects considerations

Aggressive Schedule to Achieve Impact

Supplemental Material

Single Fuel Rod Modeling Capability
Peregrine Code

Problem Setup ★
- Power Density
- Burnup Distribution
- Fast/Thermal Flux Dist.
- Thermal B/C
- Mechanical B/C

Material Properties (e.g.)
- Specific Heat
- Density
- Conductivity
- Elastic/Plastic Behavior
- Creep Rate

Behavior Models (e.g.)
- Swelling/Densification/Cracking
- Irradiation Creep/Growth
- Grain Growth
- Fission Gas Release
- Corrosion

Physics Solution ★
- Thermal Transport
- Mechanical Forces
- Chemical Transport

Global Parameters Integration ★
- Rod Pressure
- Fission Gas Composition
- Linear Power

Result Output ★
- Write global variables
- Shift Internal State Variables

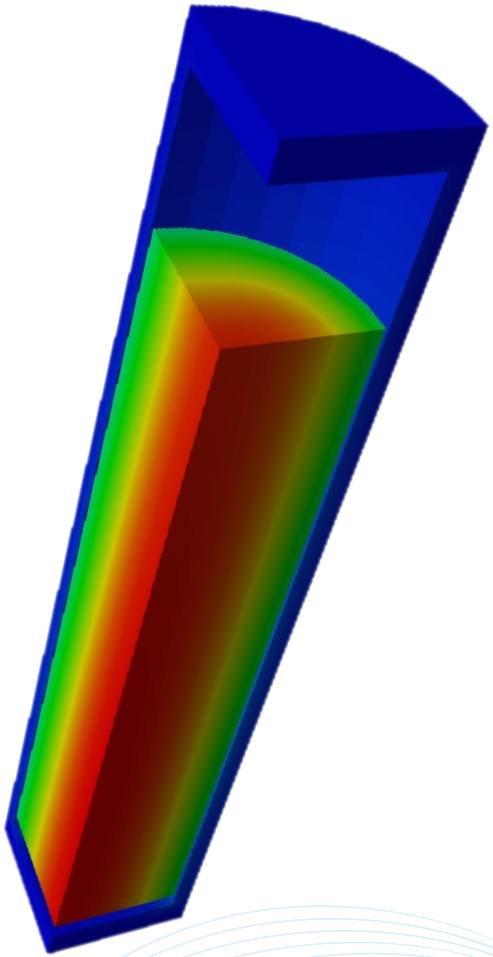

★ - Elements provided by MOOSE/ELK/FOX systems (INL)

Peregrine: Validation and Benchmark Evaluation of Integrated Fuel Performance Modeling Using Test Reactor Data and Falcon

Objective and Approach

- Evaluate Peregrine to calculate the thermal, mechanical, and irradiation behavior of UO_2/Zr-alloy fuel rods
- Fuel temperature, cladding displacements, and fission gas release measurements from 14 fuel rods used in assessment
- Compare to Falcon results to understand performance of material and behavior models

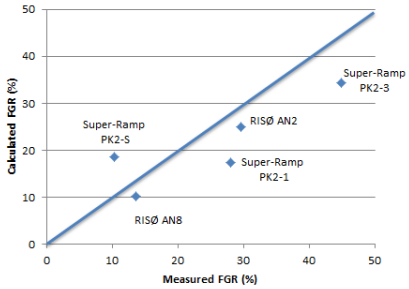

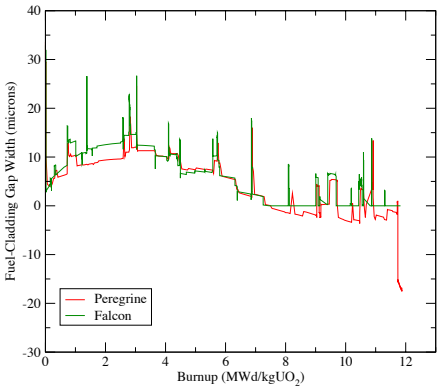

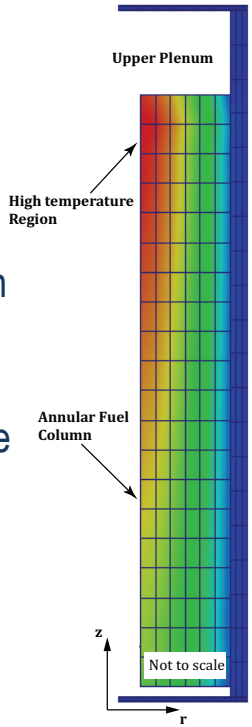

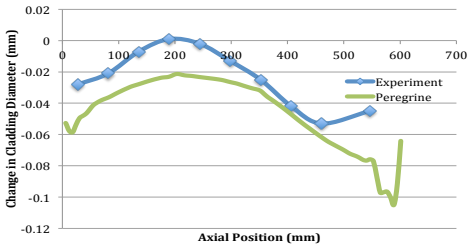

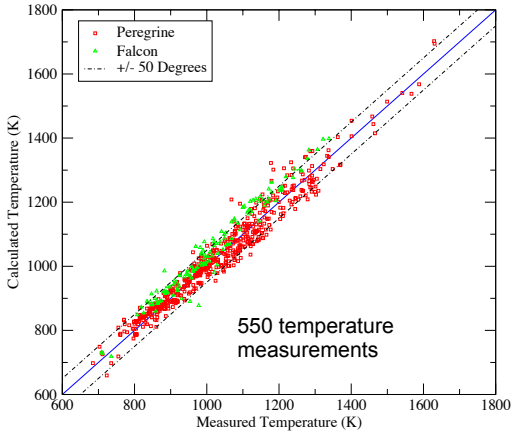

Assessment

- Peregrine is on par with industry standard codes (e.g. FALCON) up to 75 GWd/tU
- Reliably calculates fuel temperatures, cladding deformations, and fission gas release as function of environmental conditions
- Versatile framework to evaluate critical parameters and improved modeling approaches

Path Forward

- Enhanced mechanistic models for UO_2 thermal conductivity, Zircaloy creep and growth, pellet cracking and fragment relocation.
- Use lower length scale modeling to inform fission gas release kinetics
- Expand to 3-D and local effects modeling

Peregrine Interface with other MPO (blue) and Virtual Reactor Activities

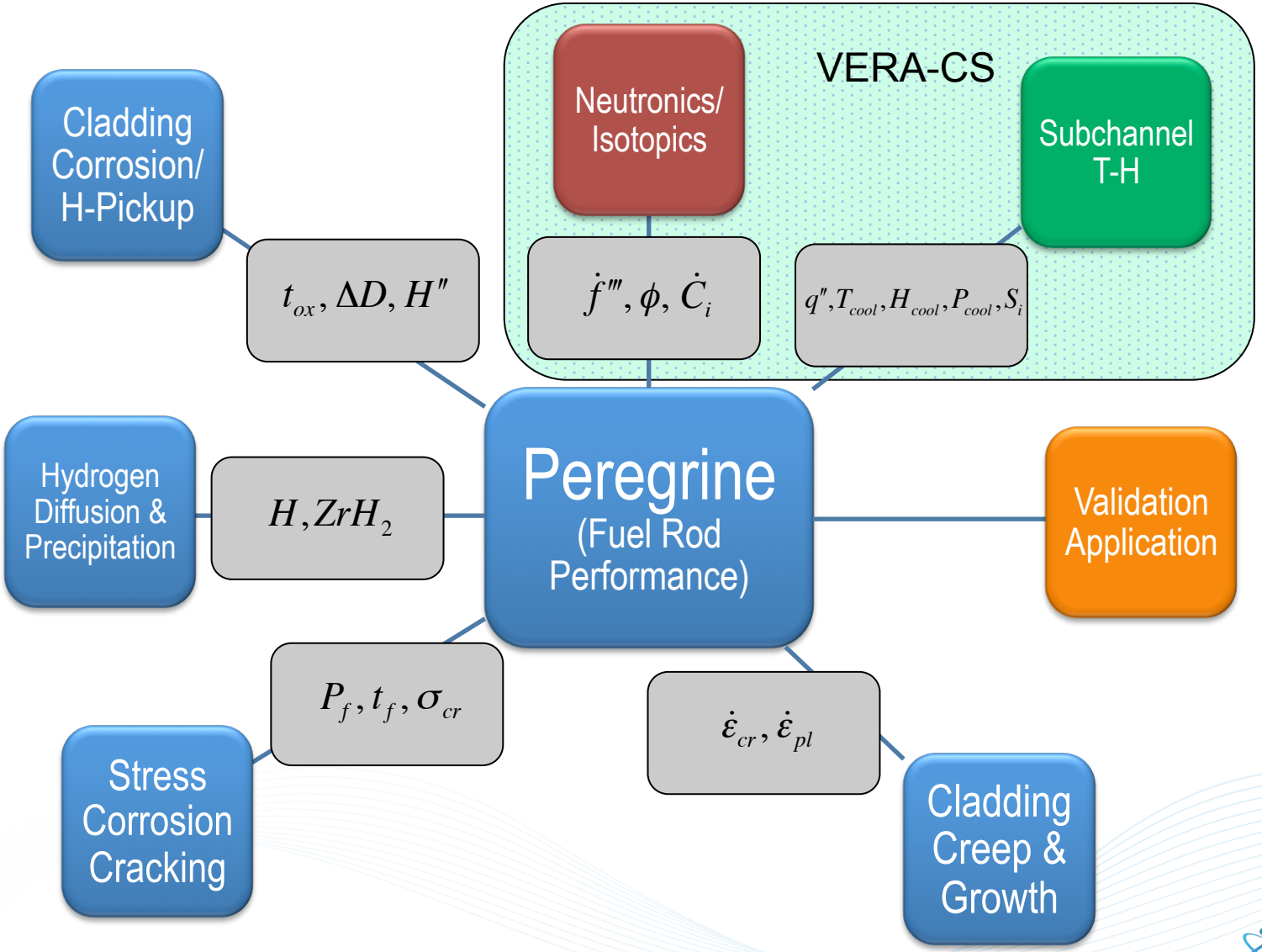

Multiscale/Multiphysics Approach to Zr Clad Creep and Growth – LANL/ORNL

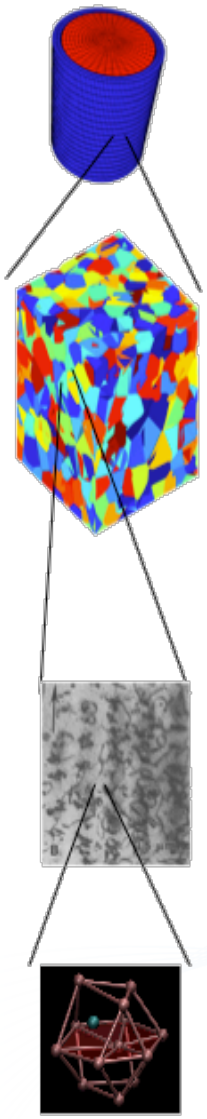

F.E. Code (PEREGRINE)

MACRO

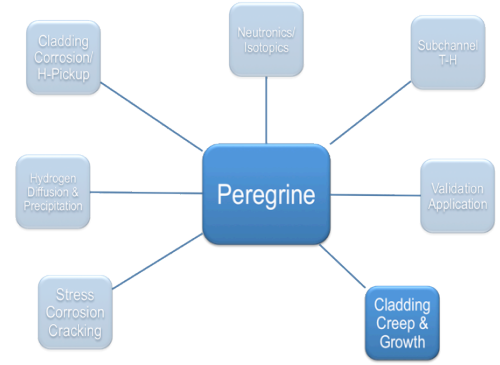

Constitutive response from
Visco Plastic Self Consistent (VPSC)
polycrystal plasticity model for irradiation growth & creep

POLYCRYSTAL

Moving beyond the empirical material models used today

SINGLE CRYSTAL PHYSICAL LAW

Model for irradiation growth based on nucleation & evolution of dislocation loops

Model for thermal & irradiation creep based on dislocation climb & glide

STATE OF THE ART ATOMISTIC CALCULATIONS

SINGLE CRYSTAL

Interfaces to couple Peregrine with Neutronics and Thermal-Hydraulics (VERA-CS)

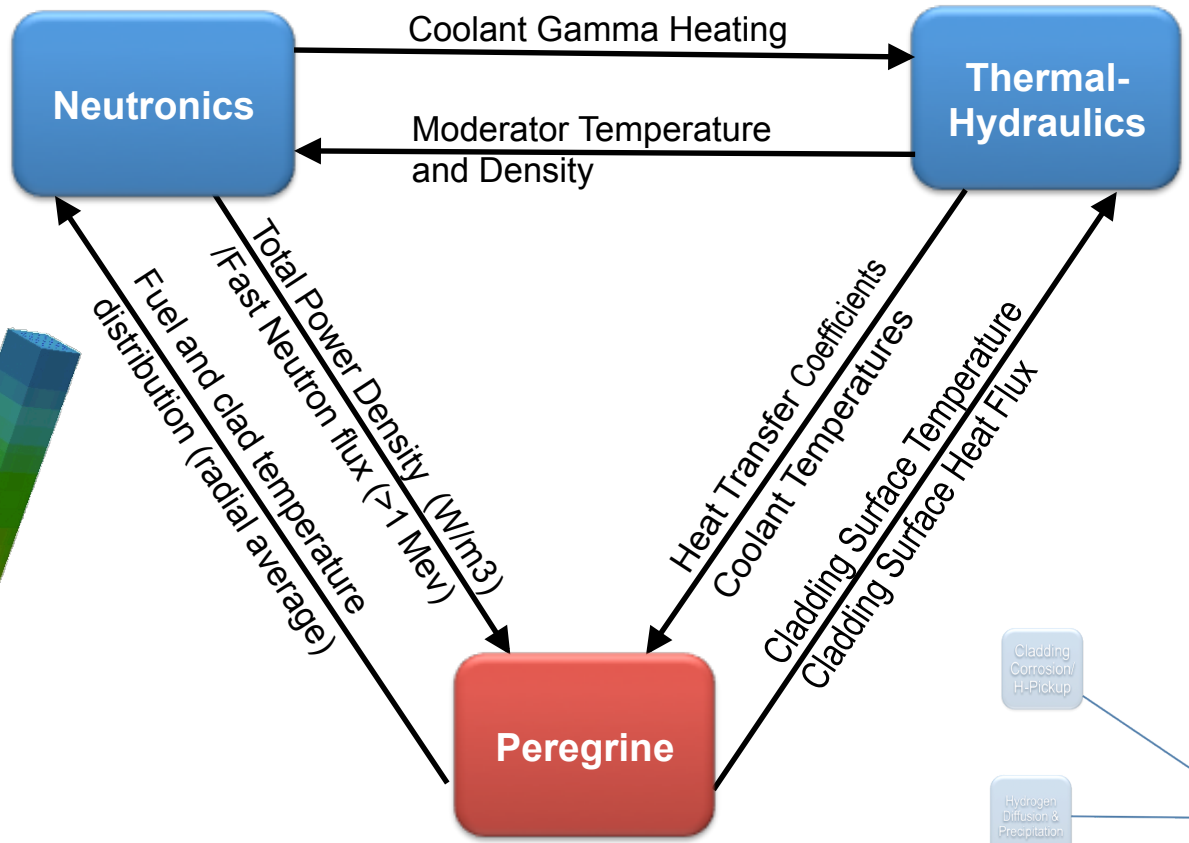

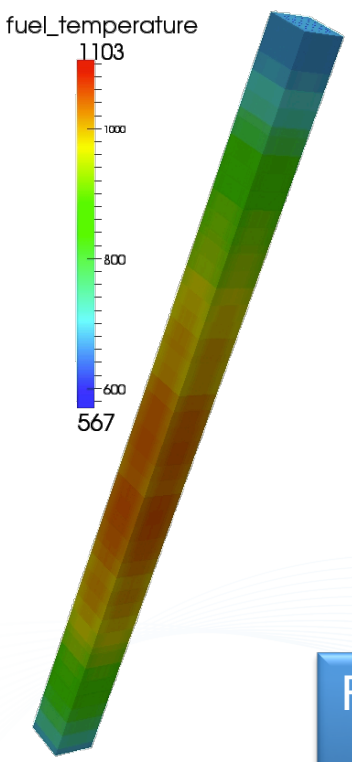

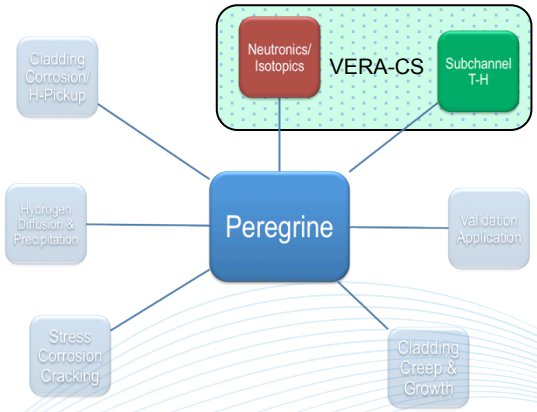

First Steps to Assembly and Core-Wide Fuel Performance Calculations

Overview of PCI/SCC Failure Process

- State of pellet and cladding interaction is a complex function of the prior irradiation history
  - Role of Pellet
    - Densification => opens gap; Relocation/pellet cracking, Thermal expansion, Swelling => closes gap
  - Role of Cladding
    - Thermal/irradiation creep => closes gap or induces plastic strain
  - Role of fission products
    - Production/release/decay => availability of reactive species for SCC
- Leads to processes of <u>conditioning</u> (able to withstand power change with minimal change in stress) or <u>deconditioning</u> (power change will induce large increase in stress)
  - Defined by residual (or cold) pellet-cladding gap (larger -> conditioned, smaller-> deconditioned)

RIA Challenge Problem Status

G. Swindlehurst
GS Nuclear Consulting., LLC

CASL Roundtable

July 14, 2014

RIA CP – Presentation Topics

- Introduction
- Planning
  - Charter
  - Implementation Plan
- Challenges
- Current Status
- Summary

RIA CP – Introduction (1 of 3)

- RIA fuel rod tests at CABRI (France) and NSRR (Japan) raised issues about the effect of high burnup on fuel behavior
- NRC issued SRP 4.2 Appendix B interim criteria
- Expect NRC will issue final criteria in the next year or so
- Nuclear Safety Issues
  - Cladding Integrity (radiological / challenge to core coolability)
  - Core Coolability (potential for fuel and pressure boundary damage)
- Current industry plan is to avoid need to develop RIA core coolability analysis methodology by demonstrating cladding integrity is maintained
  - No cladding failure due to PCMI (Δcal/gm) during power excursion
  - No cladding failure following post-DNB overheating

RIA CP – Introduction (2 of 3)

FIGURE B-1: PWR PCMI Fuel Cladding Failure Criteria

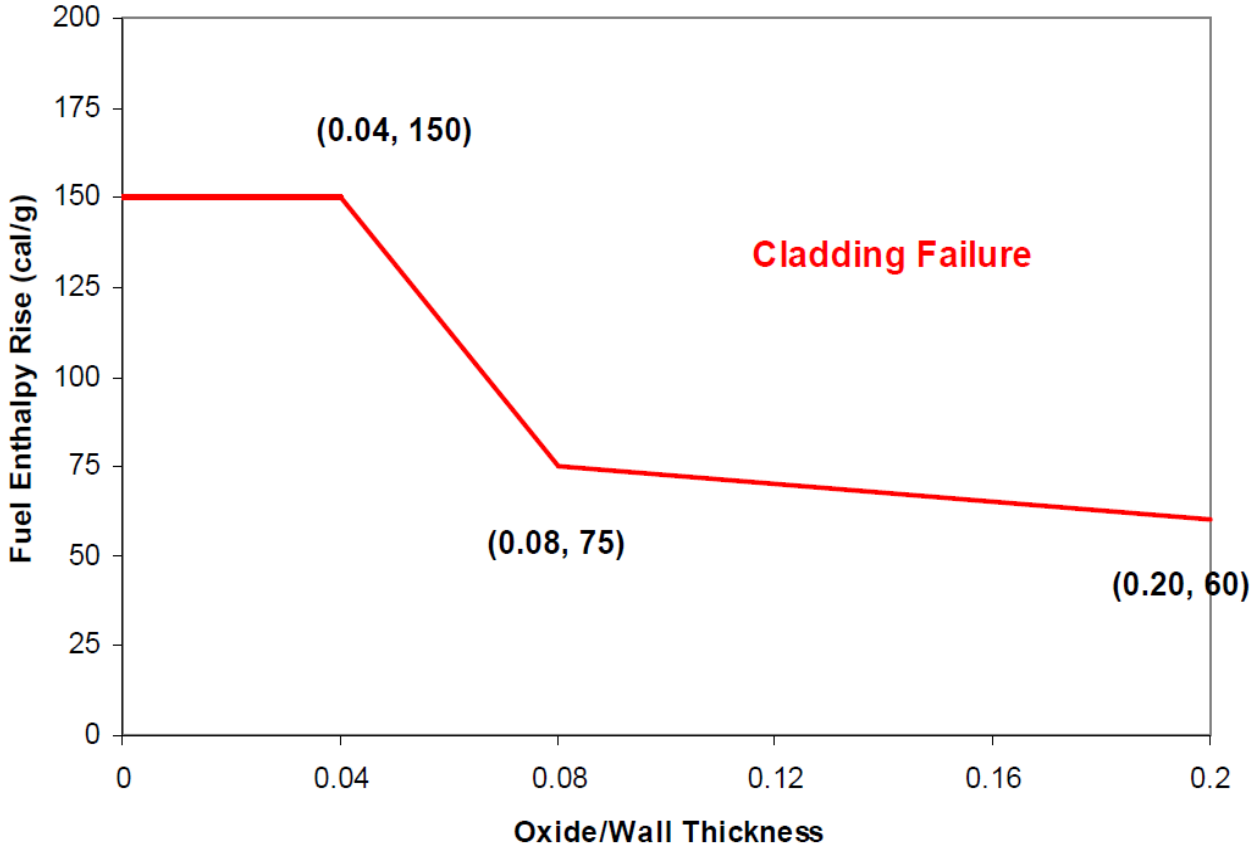

RIA CP – Introduction (3 of 3) [from May 2014 NRC presentation at AREVA]

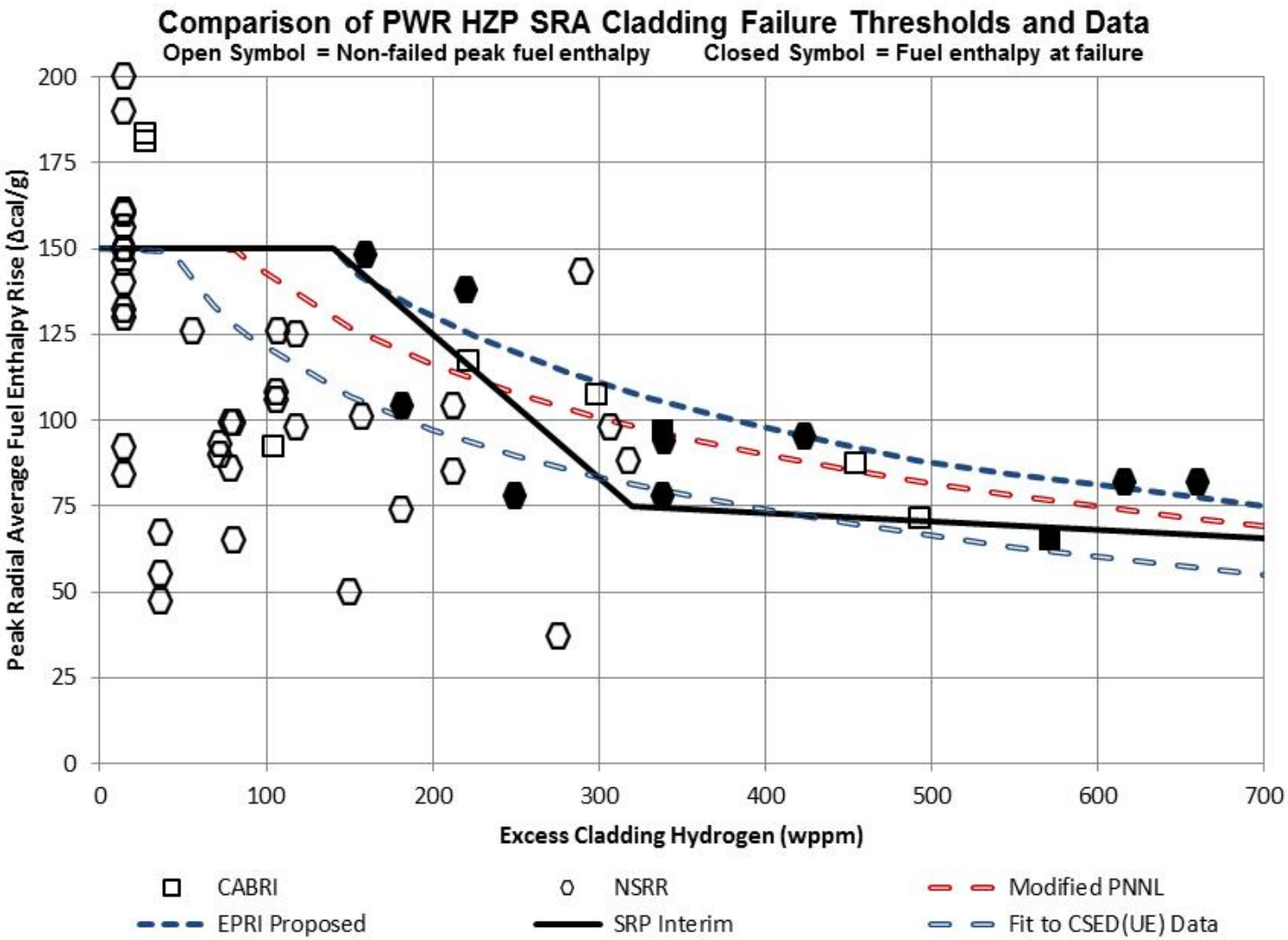

RIA CP – Planning (1 of 3)

- RIA Charter
  - PWR rod ejection characterization and regulatory background
  - Overview of current analysis methods and codes
  - What is needed for CASL to advance the RIA simulation capability
  - Why it is needed
- RIA Implementation Plan
  - Specification of capabilities needed for each CASL code
  - Descriptions of stand-alone and coupling approaches
  - Benchmarking activities
  - Demonstration analysis activities
  - Comparison to WEC licensed methodology results
  - Schedule and resource loading (future)

RIA CP – Planning (2 of 3)

- Benchmarking Activities
  - MPACT: SPERT reactor dropped rod tests
  - Peregrine: Transient fuel rod phenomena
  - Peregrine: CABRI and NSRR RIA tests
- CASL-VERA: Stand-alone and then coupled modeling with focus on fuel behavior
  - MPACT: Transient neutronics
  - Peregrine: Fuel rod thermal-mechanical
  - COBRA-TF: Subchannel thermal-hydraulics
  - RELAP5-3D: System thermal-hydraulics

RIA CP – Planning (3 of 3)

VERA RIA Coupling

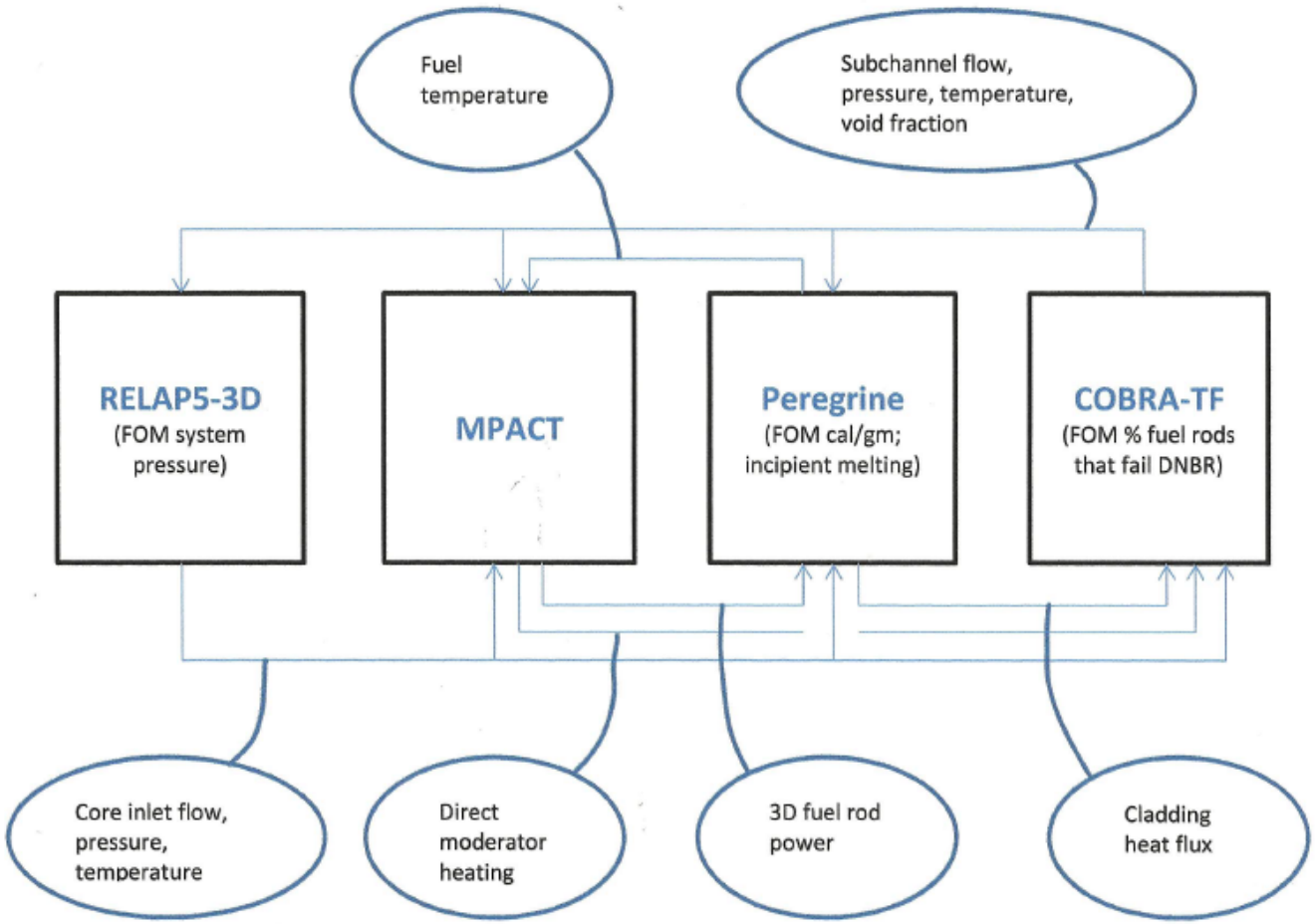

RIA CP - Challenges

- PWR rod ejection requires 3D full-core simulation, but very local phenomena of interest
- Coupled approach to capture physics
- PCMI failure scenario
- DNB overheating failure scenario
- Future CABRI water-loop RIA tests
- Very computer resource intensive

RIA CP – Current Status

- Planning complete except for scheduling and resource loading
- CASL codes are recently becoming ready for RIA
- MPACT SPERT dropped rod test benchmark analysis scheduled for completion by end of PoR-9
- Peregrine capabilities are approaching readiness for RIA modeling

RIA CP – Summary

- CASL value added
  - Higher-fidelity transient neutronics capability (pin resolved)
  - Higher-fidelity transient fuel rod thermal-mechanical capability
  - Tightly-coupled simulation to capture the physics
  - Industry can use insights from CASL-VERA higher-fidelity modeling to reduce conservatism in production codes used for licensing
- New RIA regulatory requirements related to high burnup effects
  - Industry needs improved analytical capability to offset margin loss
- Unique analytical capabilities to evaluate emerging issues from CABRI water-loop RIA testing (start in late 2015?)

LOCA Challenge Problem Status

G. Swindlehurst
GS Nuclear Consulting., LLC

CASL Roundtable

July 14, 2014

LOCA CP – Presentation Topics

- Introduction
- Planning
  - Charter
  - Implementation Plan
- Challenges
- Current Status
- Summary

LOCA CP – Introduction (1 of 3)

- LOCA remains a significant technical challenge and regulatory issue for the industry
- NRC LOCA research program at ANL (RIL-0801 and NUREG/CR-6967) raised issues about the effect of high burnup on cladding embrittlement behavior
- NRC proposed LOCA rule (50.46c) currently in the public comment period
- Issues with fuel vendor LOCA evaluation models (e.g. thermal conductivity degradation)
- Legacy issues (e.g. GSI-191 PWR post-LOCA debris impact on long-term core cooling; boric acid precipitation)
- Emerging issues (e.g. fuel fragmentation, relocation, and dispersal)

LOCA CP – Introduction (2 of 3)

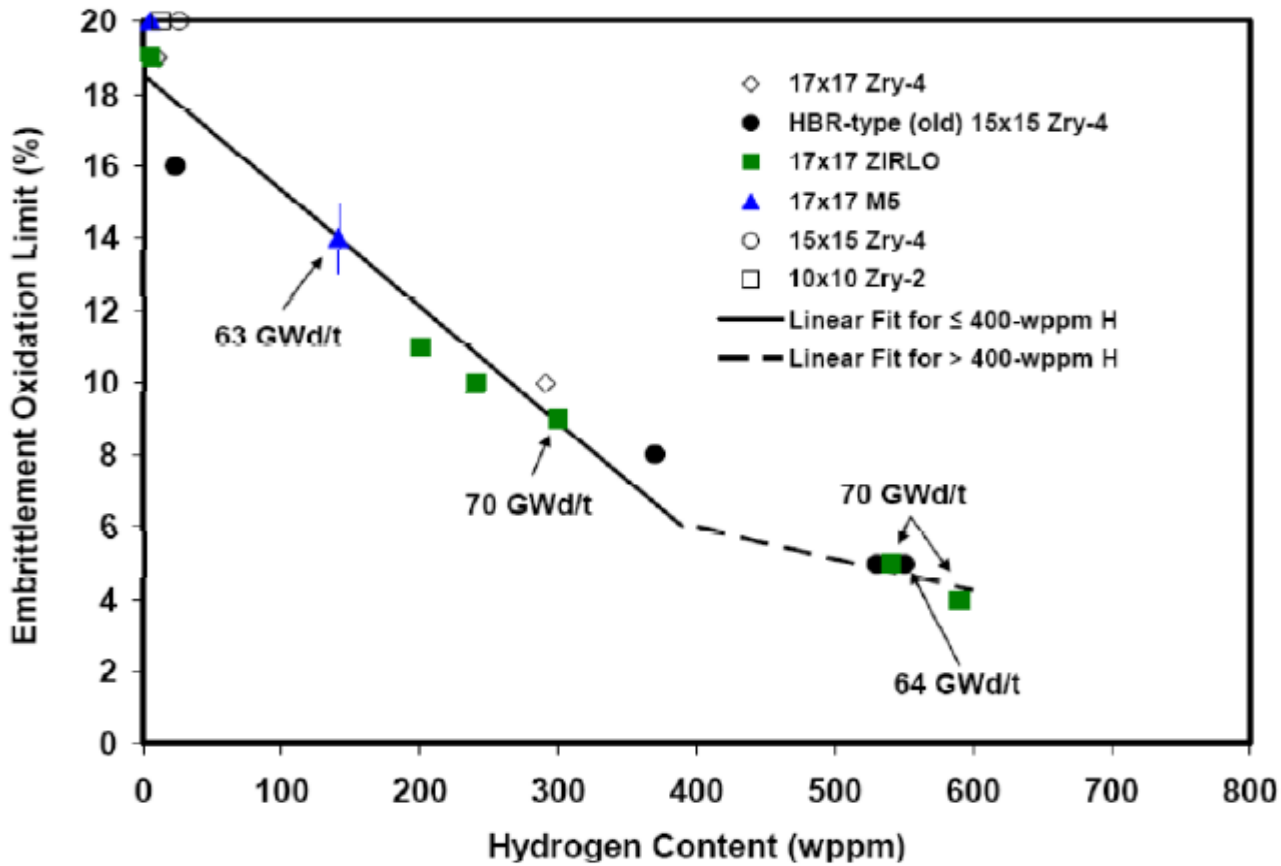

ANL LOCA testing program results showing cladding embrittlement oxidation limit due to pre-existing hydrogen pickup [DG-1263]

LOCA CP – Introduction (3 of 3)

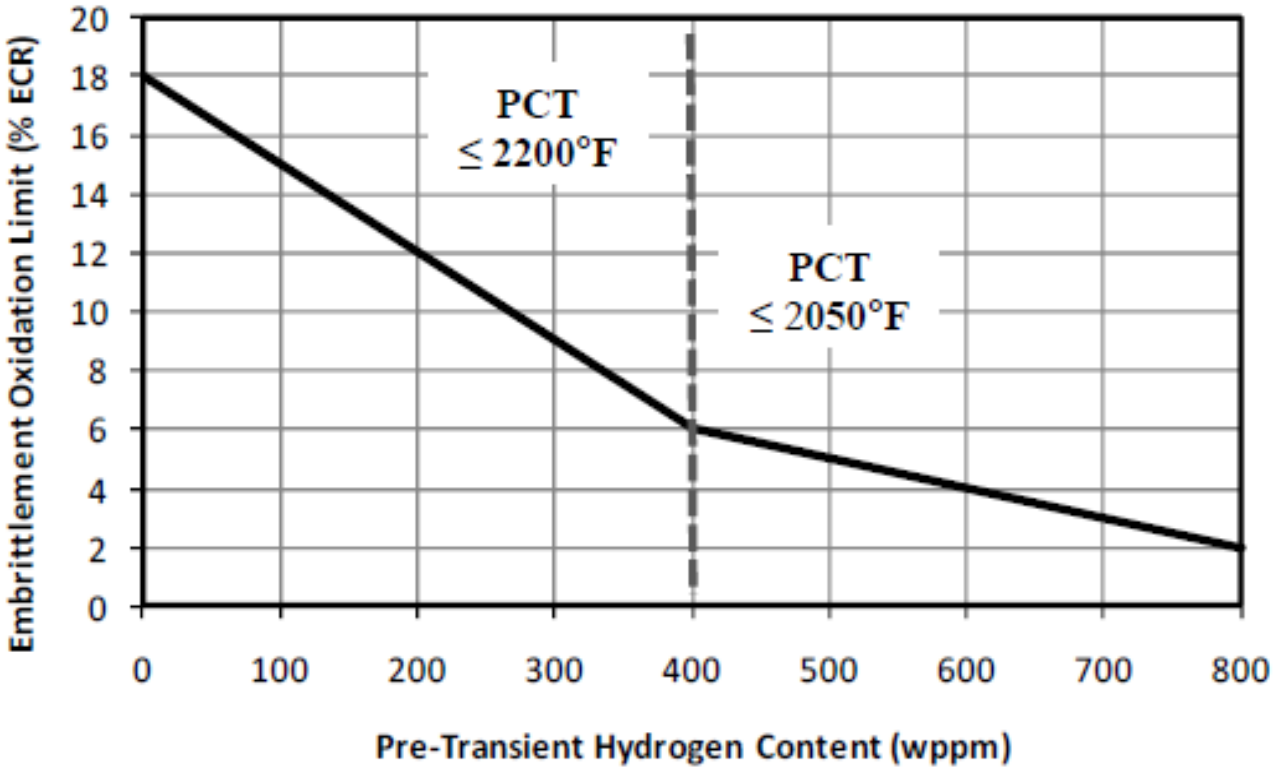

NRC's acceptable analytical limit to replace 10 CFR 50.46 cladding embrittlement limit of 17% ECR [DG-1263]

LOCA CP – Planning (1 of 2)

- LOCA Charter
  - PWR LOCA characterization and regulatory background
  - Current and emerging LOCA regulatory issues
  - What is needed for CASL to advance the LOCA simulation capability
  - Why it is needed
- LOCA Implementation Plan
  - Specification of capabilities needed for each CASL code
    - Focus is on fuel rod behavior
  - Extensive Peregrine benchmarking activities
  - LBLOCA and SBLOCA fuel rod demonstration analysis activities
  - Schedule and resource loading (future)

LOCA CP – Planning (2 of 2)

Peregrine Fuel Rod LOCA Benchmarking Activities (initial LOCA CP Implementation Plan list)

- Post-DNB PBF Test PCM-2
- Post-DNB TREAT Tests FRF-1 and FRF-2
- ORNL THTF Blowdown Tests
- PSU RBHT Reflood Tests
- FLECHT-SEASET Reflood Tests
- ANL Cladding Embrittlement Tests
- NUREG-0630 Swelling and Rupture Tests
- ANL Swelling and Rupture Tests
- Halden Swelling and Rupture Tests
- Studsvik Swelling and Rupture Tests
- Halden Fragmentation and Relocation Tests
- Studsvik Fragmentation and Relocation Tests

LOCA CP – Challenges (1 of 3)

- Develop higher-fidelity LOCA fuel rod simulation capabilities to provide industry a tool to study current and emerging LOCA issues
  - Cladding embrittlement issues on current and future claddings
  - Recover margin lost as a result of 50.46c rulemaking (e.g. cladding ID oxidation; pre-charged hydrogen specimens)
- Cladding integrity during post-LOCA long-term cooling
  - NRC is proposing a second peak cladding temperature limit
  - Many technical issues have not been fully explored
- Ballooning and blockage models are based on testing of unirradiated cladding
- Fragmentation, relocation, and dispersal
  - NRC still in “discovery” / not in proposed 50.46c rule

LOCA CP – Challenges (2 of 3)

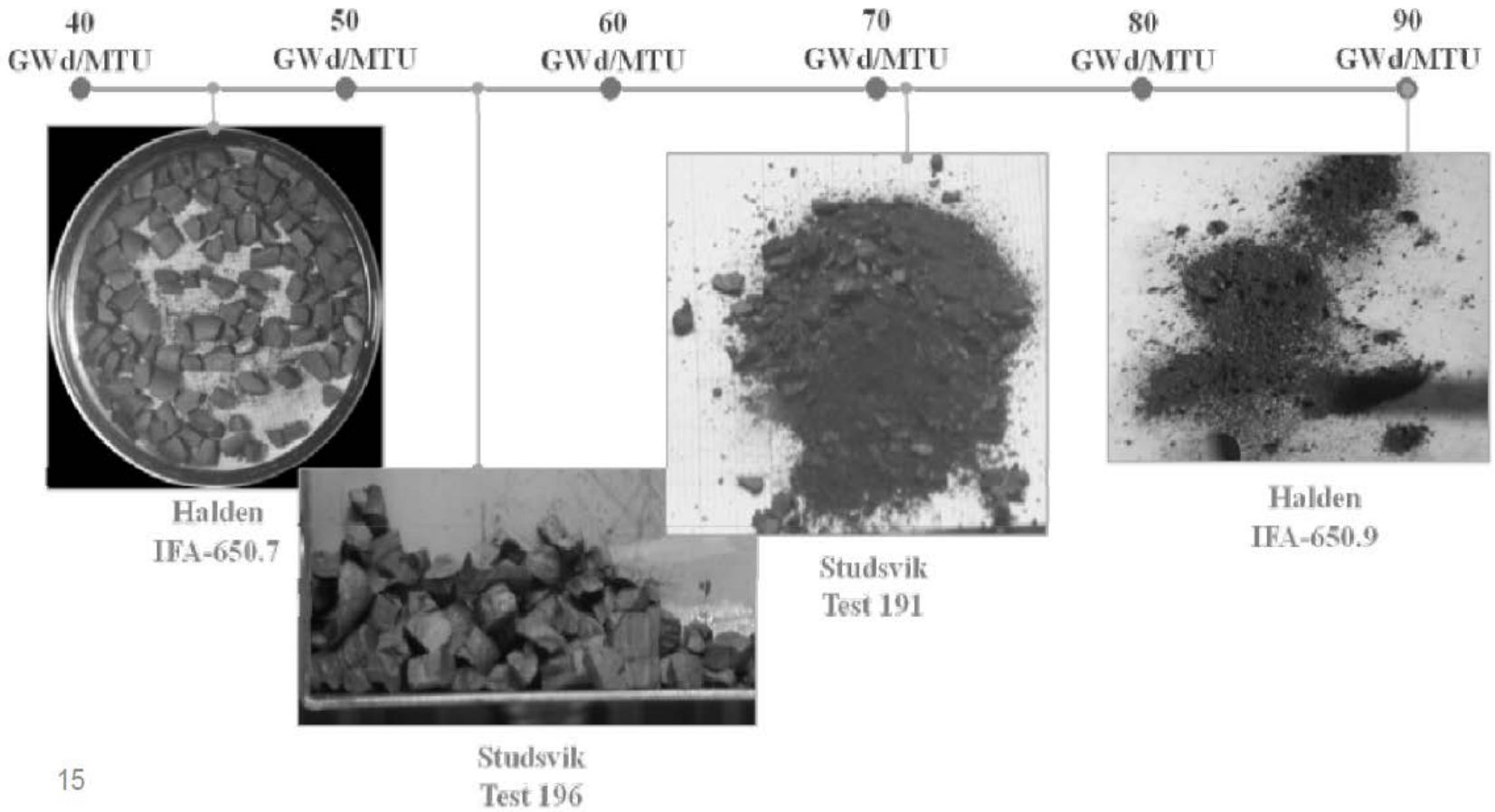

Post-LOCA fuel fragmentation vs. burnup [NRC presentation at 3/13/2014 public meeting]

LOCA CP – Challenges (3 of 3)

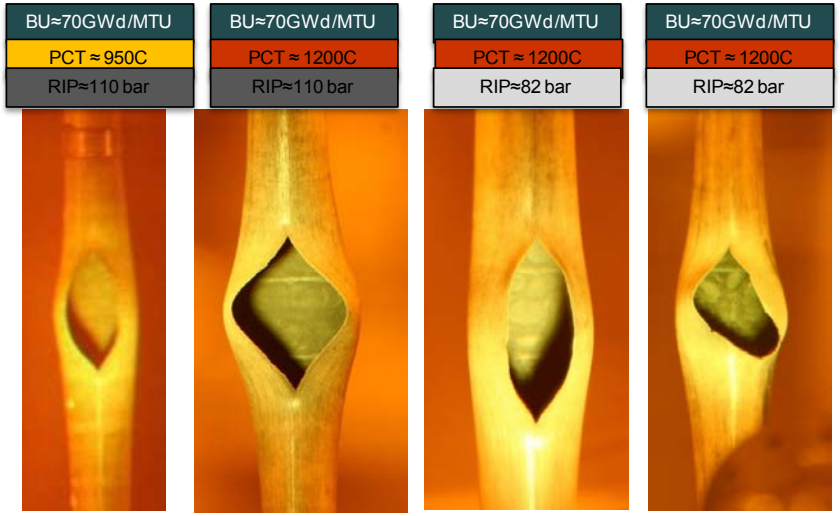

Rupture opening in Studsvik LOCA tests 189, 191, 192, and 193 (left to right), showing the absence of fuel in the rupture plane.

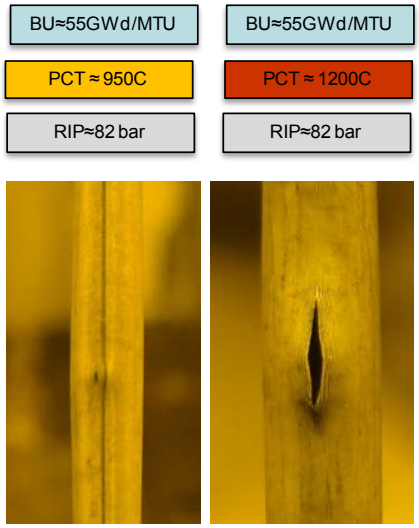

Rupture opening in Studsvik LOCA tests 196 and 198 (left to right)

Post-LOCA cladding rupture opening from Studsvik tests suggesting a burnup threshold [NUREG-2121]

LOCA CP – Current Status

- Planning complete except for scheduling and resource loading
- Peregrine code is recently becoming ready for LOCA modeling
- Preliminary Peregrine fuel rod model LOCA analysis demonstration using WEC WCOBRA/TRAC boundary conditions is scheduled for completion by end of PoR-9

LOCA CP – Summary

- CASL value added
  - Peregrine will provide a higher-fidelity LOCA transient fuel rod thermal-mechanical analysis capability
  - Industry can use insights from Peregrine modeling to reduce conservatism in vendor production codes used for licensing
  - Peregrine could be used to respond to emerging issues resulting from international testing
  - Peregrine simulation capabilities could replace very expensive LOCA-related testing, in particular testing of irradiated fuel and cladding
  - Improved analytical capabilities could be used to minimize the impact of proposed regulatory changes so that power uprates, reload design optimization, and fuel design innovation are not constrained

L2 PHI.P9.01: Challenge Problem Coupling

Roger Pawlowski
SNL

Roscoe Bartlett, Kevin Clarno, Bob Salko, and Stuart Slattery
ORNL

Scott Palmtag
Core Physics Inc.

Derek Gaston, Cody Permann, Jason Hales and Rich Williamson
INL

CASL Roundtable
July 14-16, 2014

SAND2014-15722PE

Executive Summary

- Goal: Transition Tiamat from a demonstration capability to a research and production quality code
  - Prepare code for L1 PCI demonstration simulations due at the end of August

- Accomplishments
  - An improved initialization/ramping phase was implemented to provide robust startup of the reactor code.
  - The data transfer methods were modified to improve robustness of the global solution methods.
  - Energy is now conserved in the data transfers between codes.
  - A Gauss-Seidel-based Picard iteration option has ben added to the original Gauss-Jacobi method.
  - A sub-cycling capability was added to the MOOSE transient MultiApp to allow for fixed-point iteration within a time step.
  - A new inline mesh generation capability was added to CASL_MOOSE that generated a smeared pellet mesh that is aligned with the VERA coupling transfer boundaries.
  - The MOOSE update/build process for VERA has been streamlined and improved.
  - A more rigorous set of unit and system tests have been implemented.
  - A new driver layer has been implemented with significant enhancements for user flexibility.

Coupled VERA-CS Capability for Pellet-Clad Interaction (PCI) Challenge Problem

- Core Simulator with improved model fidelity
- Extend basic Problem 6 capability
  - Replace COBRA-TF fuel rod model with MOOSE-based Peregrine fuel performance capability
- 2D R-Z Peregrine model for every rod
- *Original Results documented in Milestone L2:VRI.P7.02 (7/31/2013).*
- Follow on Milestones this year:
  - L3: PHI.CMD.P8.02 (2/28/2014) “MOOSE development”
  - L2: PHI.P9.01 (6/30/2014) “PHI Development”
  - L1: CASL.P9.03 (8/31/2014) “Deployment”

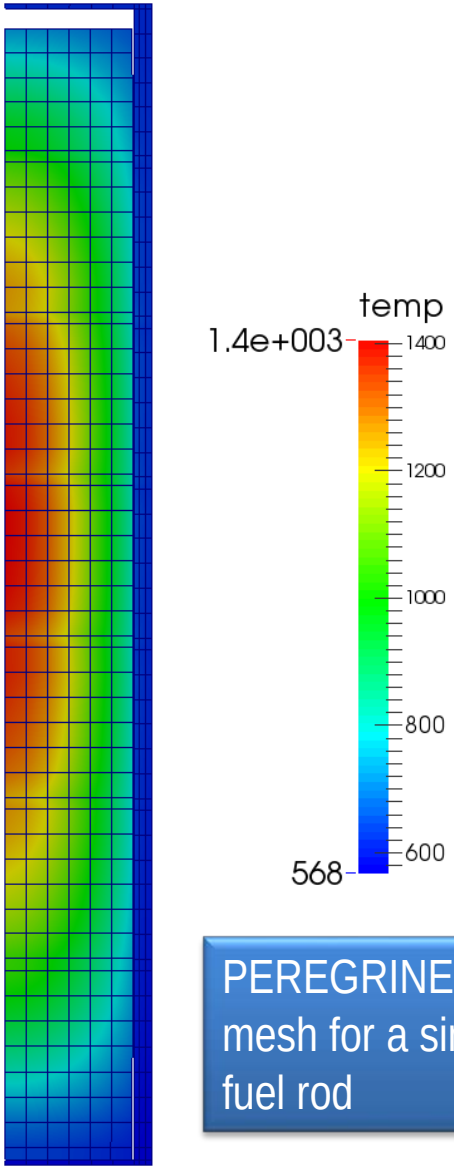

PEREGRINE r-z mesh for a single fuel rod

CTF + Insilico + Peregrine Coupled Driver

- Named “Tiamat”, multi-headed dragon (Babylonian)
  - easy to add new “heads” provided the apps meet integration criteria
- Solved using Picard iteration between components (details later)
- All applications are run in their own MPI process space
  - Can overlap codes on MPI processes if desired
  - Separation reduces collisions (globals/threading/memory) and improves algorithms performance
- Data Transfers are handled through DTK with MPI sub-communicators

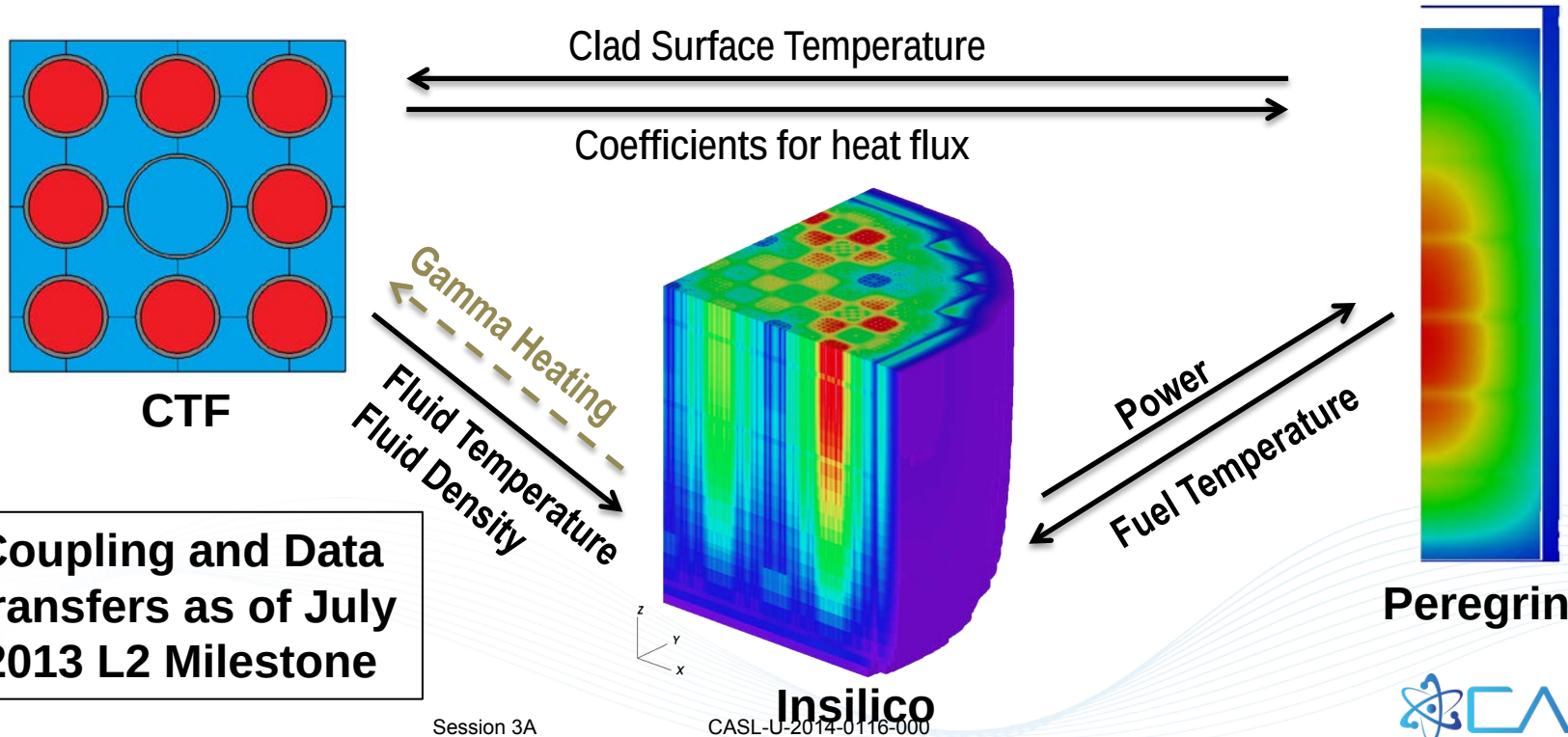

Coupling and Data Transfers as of July 2013 L2 Milestone

VERA 2015

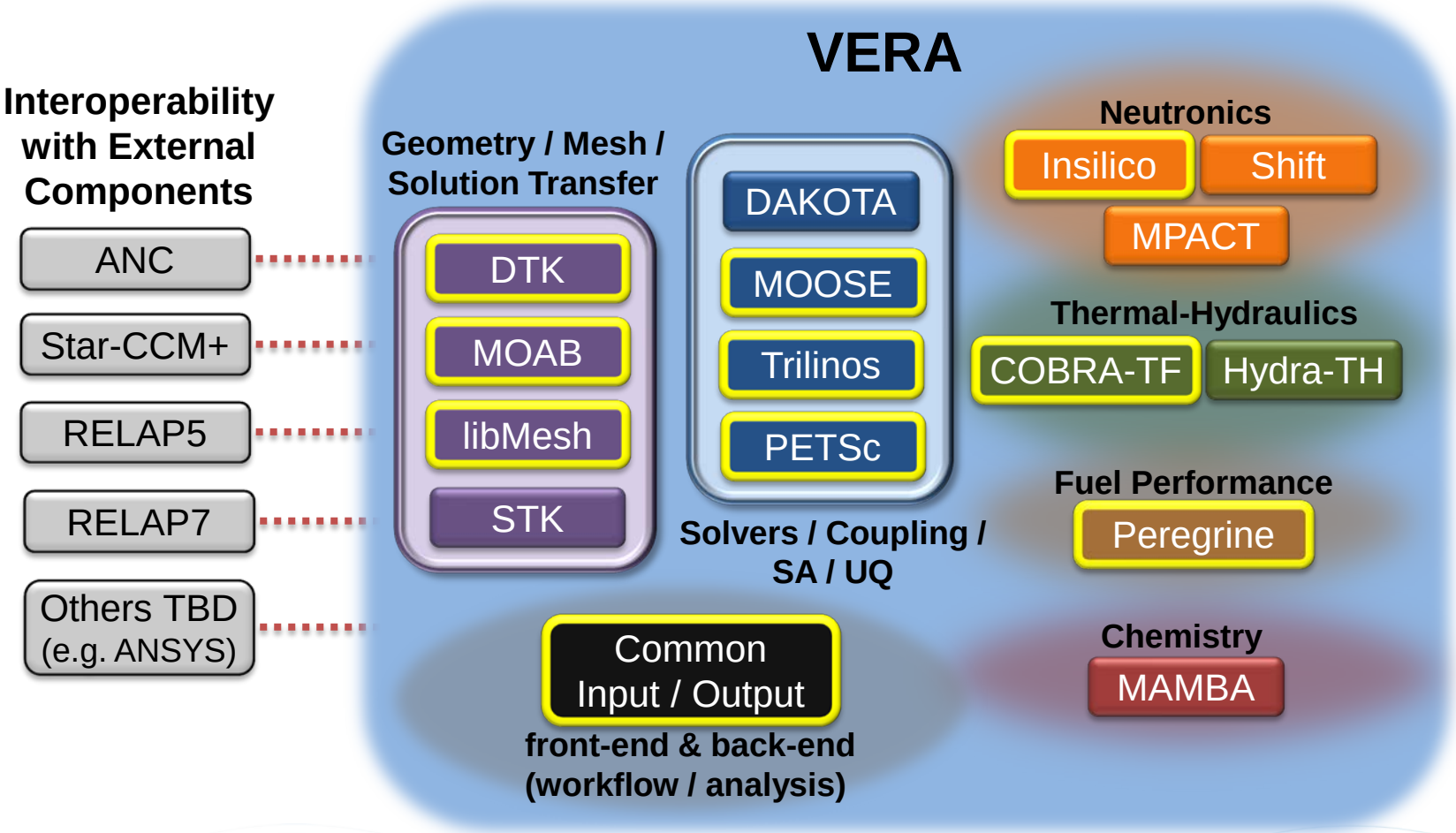

Components currently used in Tiamat outlined in yellow

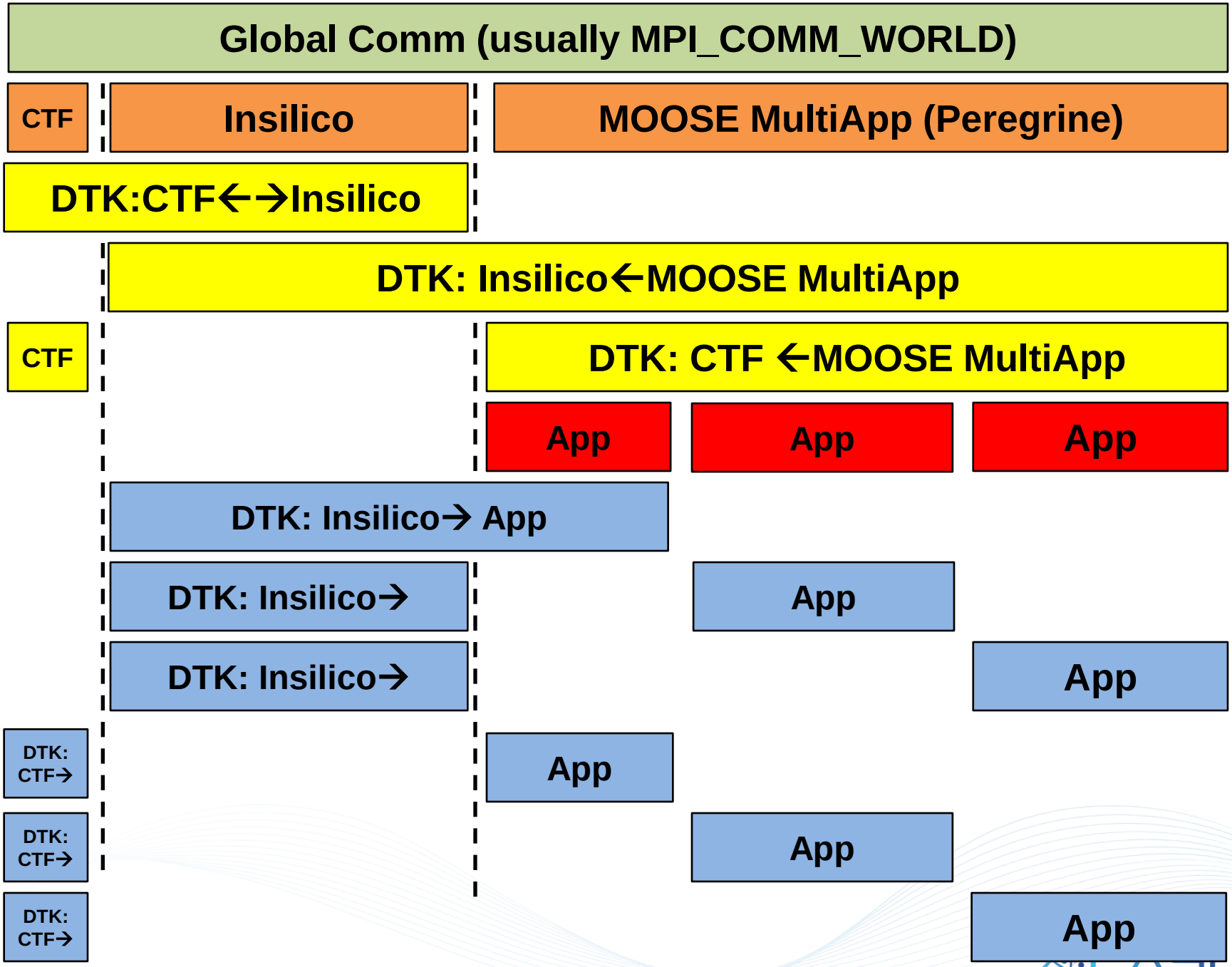
Global Comm (usually MPI_COMM_WORLD)
CTF
Insilico
MOOSE MultiApp (Peregrine)
DTK:CTF←→Insilico
DTK: Insilico←MOOSE MultiApp
CTF
DTK: CTF ←MOOSE MultiApp
App
App
App
DTK: Insilico→ App
DTK: Insilico→
App
DTK: Insilico→
App
DTK: CTF→
App
DTK: CTF→
App
DTK: CTF→
App

Solution Methods

- We fixed-point iteration treating the codes as a "black box".
  - Set parameters
  - Call Solve
  - Evaluate responses

$f_p(x_p, z_p) = 0$	Peregrine
$f_c(x_c, z_c) = 0$	CTF
$f_i(x_i, z_i) = 0$	Insilico
$z_{p,c} = r_{p,c}(x_c)$	Clad Temp
$z_{p,i} = r_{p,i}(x_i)$	Power
$z_{c,p} = r_{c,p}(x_p)$	Clad Heat Flux
$z_{i,p} = r_{i,p}(x_p)$	Fuel Temp
$z_{i,c} = r_{i,c}(x_c)$	Fluid Temp/density

Algorithm GS: Block Gauss-Seidel

GIVEN x_p^0, x_c^0, x_i^0.
FOR $k = 0, 1, \ldots$ (UNTIL CONVERGED) DO:
  $k = k+1$
  TRANSFER TO p:
    $z_{p,c}^k = r_{p,c}(x_c^{k-1})$
    $z_{p,i}^k = r_{p,i}(x_i^{k-1})$
  SOLVE $f_p(x_p^k, r_{p,c}(x_c^{k-1}), r_{p,i}(x_i^{k-1})) = 0$ FOR x_p^k
  TRANSFER TO c:
    $z_{c,p}^k = r_{c,p}(x_p^k)$
  SOLVE $f_c(x_c^k, r_{c,p}(x_p^k)) = 0$ FOR x_c^k
  TRANSFER TO i:
    $z_{i,c}^k = r_{i,c}(x_c^k)$
    $z_{i,p}^k = r_{i,p}(x_p^k)$
  SOLVE $f_i(x_p^k, r_{i,c}(x_c^k), r_{i,p}(x_p^k)) = 0$ FOR x_i^k

- Jacobi and Gauss-Seidel options available.
- Algorithm GS is solved at each time step at HFP and results in subcycling all codes to converged state within each time step!

Computing initial guess is not trivial!

Development of Robust Ramping Strategy

- For core simulator, wish to solve for hot full power (HFP) state.
- Peregrine is a transient code
  - Needs time history for depletion and structural evolution
- CTF and Insilico are run to “steady-state” in each “solve”
- In PoR 7 L2, ramping was VERY unstable.
  - Simulation was difficult to converge
  - Sensitive to both local and global tolerances
- A critical insight was to reverse the coupling between CTF and Peregrine
  - Natural BC on Peregrine outer clad was more difficult to solve
- Toggling of CTF conduction solve was important
  - Enabled for pre-ramp “Estimated HFP”
  - Disabled for Time step subcycling (replaced with Peregrine model)
- Significantly more stable (failures in ramping no longer occur)

Robust Ramping Strategy

1. Estimate state at hot, full power (HFP)
   - Perform several iterations of CTF+Insilico
   - Estimate of clad surface temperature for each pin at each axial node
   - Estimate of power distribution for each pin and axial node.
2. Model transition from cold zero power (CZP) to hot, zero-power (HZP)
   - Peregrine transient for 100 seconds
   - Linear ramp of clad surface temperature from 20 to 293 C
   - Power in every pin is zero.
3. Model transition from HZP to estimated HFP
   - Peregrine transient for 1.7e5 seconds
   - Linear ramp of clad surface temperature from 293 C to estimated value
   - Linear ramp of power distribution from zero to the estimated distribution at full power
4. Model reactor state at HFP conditions with CTF+Insilico+Peregrine
   - Subcycle all three codes using a fixed-point iteration scheme.
   - Converge Insilico with pin temperatures from Peregrine and coolant conditions from CTF
   - Converge CTF to steady-state with a Peregrine heat flux using a series of time-steps
   - Model a single time-step in Peregrine at each coupled iteration using power from Insilico and clad surface temperature from CTF

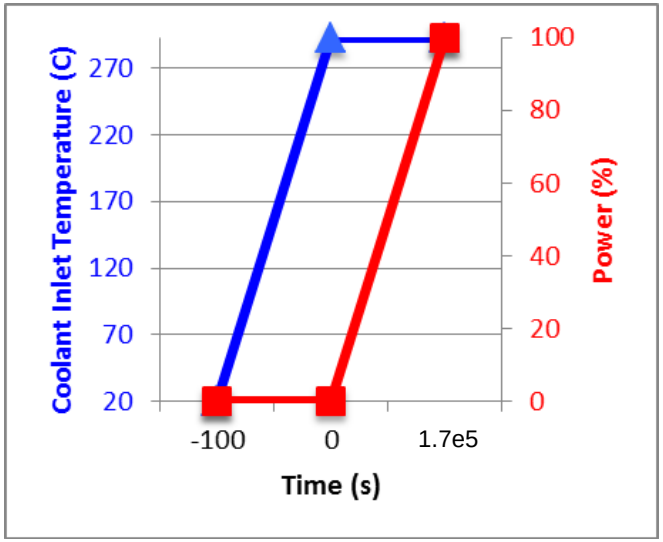

NOTE:
- We could avoid steps 1, 2 and 3 by using fixed-point iteration (step 4) within each time step for the complete transient simulation from CZP to HFP.
- Significantly increased runtimes for no gain and not pursued here.

Current Data Transfers

Fixed-point Solves

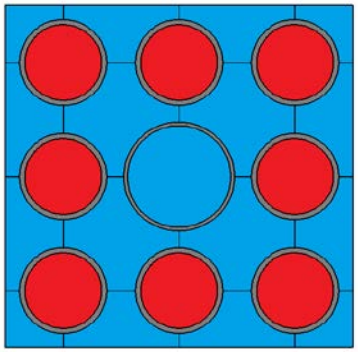

CTF

Clad heat flux

Clad Surface Temperature

Gamma Heating

Fluid Temperature
Fluid Density

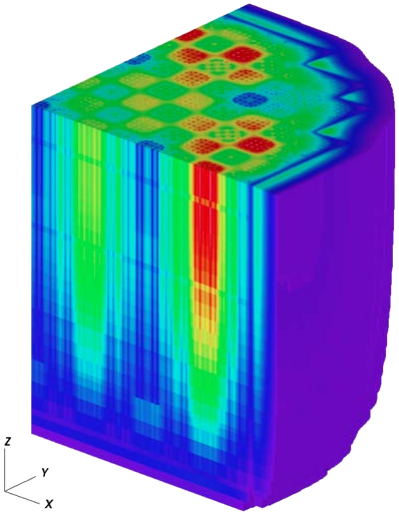

Insilico

Power

Fuel Temperature

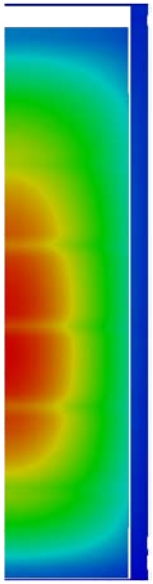

Peregrine

Estimate HFP
(Pre ramp initialization)

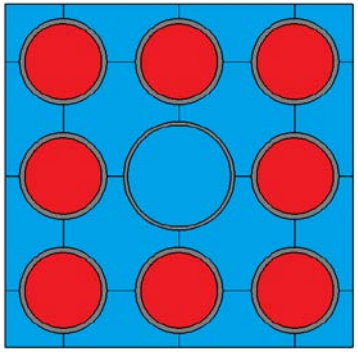

CTF

Power

Fluid Temperature
Fluid Density
Fuel Temperature

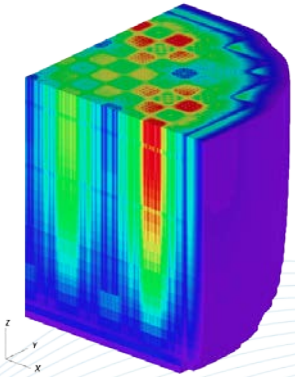

Insilico

Data Transfers

- Currently have 5 data transfers (do not support gamma heating yet)
  - MOOSE →Insilico: Average temperature from mesh to control volume
    - Aligned mesh means allows for integration of average Temp for mesh
    - Not a conserved quantity
  - CTF → MOOSE: Clad temperature to finite element basis points
    - Not a conserved quantity
  - CTF → Insilico: Fluid temperature and density from CTF control volume to Insilico/XSProc control volume
    - Aligned control volumes
    - Not conserved quantities
  - Insilico → MOOSE: Power from control volume to FE basis points
    - Power is a conserved
  - MOOSE → CTF: Average heat flux from mesh surface to control volume
    - Heat flux is a conserved quantity
- Extra transfer for Estimated HFP
  - Insilico→CTF : Power from control volume to control volume
    - Conservative by construction

Insilico→Peregine: Power Data Transfer

- Transfer requires alignment of MOOSE mesh finite elements with coupling mesh (axial edit bounds)
- Graphic below is very coarse. Use 3 inch intervals in real simulation.

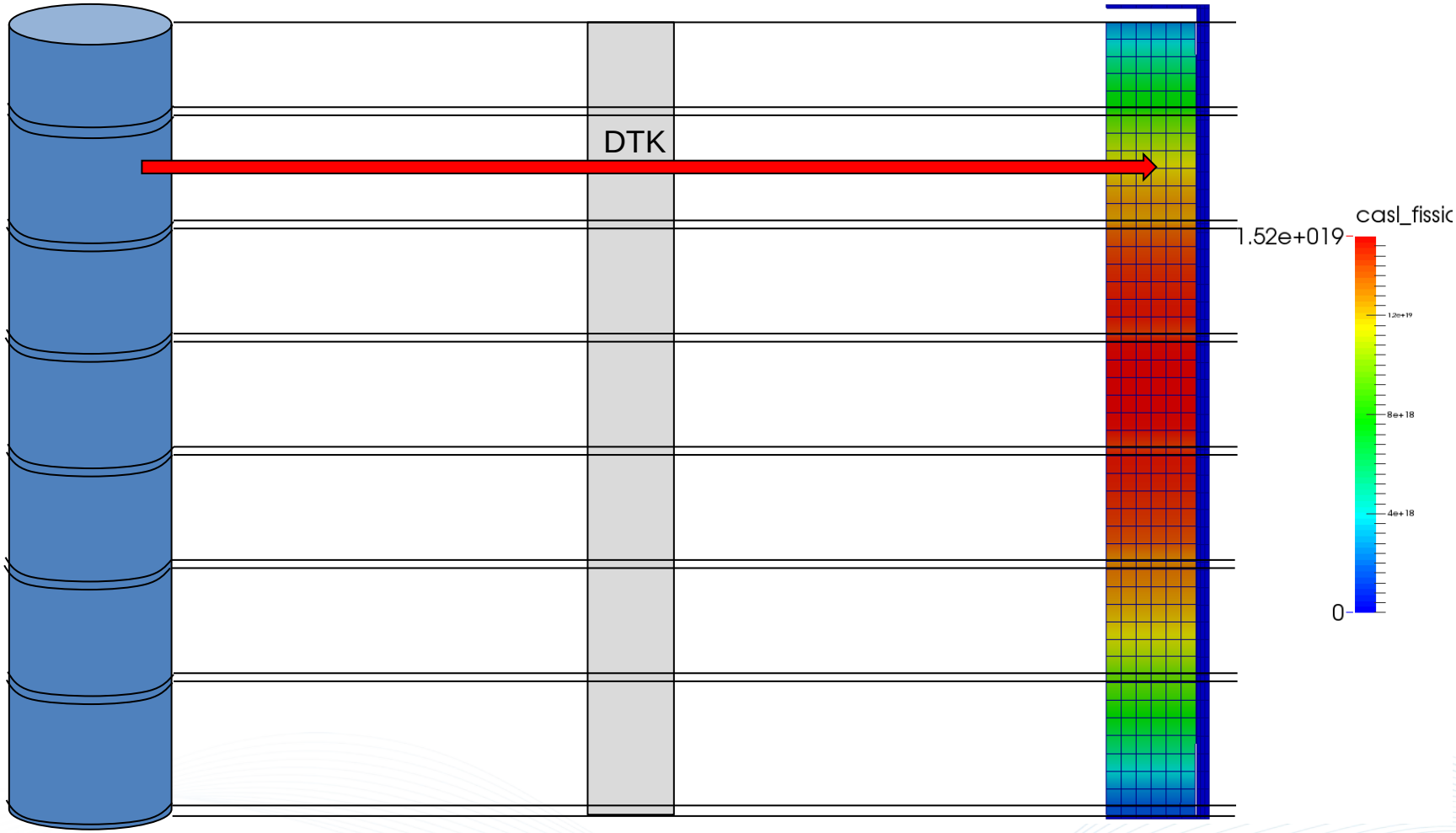

Insilico (XSProc)

Coupling Mesh Coordinates

Smeared Pellet Mesh (MOOSE Coordinates)

Conservation Issue

- For now, we enforce conservation at the PIN level!
- Currently must map power to finite element basis points in MOOSE (not quadrature points)
- Forces decision: what value to use on edit bound boundary? determined by DTK search during setup.
- Will show impact of this in results section
- Future work:
  - To enforce conservation at edit bound level, push power directly to quadrature points.
  - Could be significant amount of work
    - MOOSE DTK adapters
    - Fox Kernels
    - Possibly MOOSE assembly
  - DTK transfers are serialized at the pin level for “to Peregrine” transfers
    - Need to investigate scalability

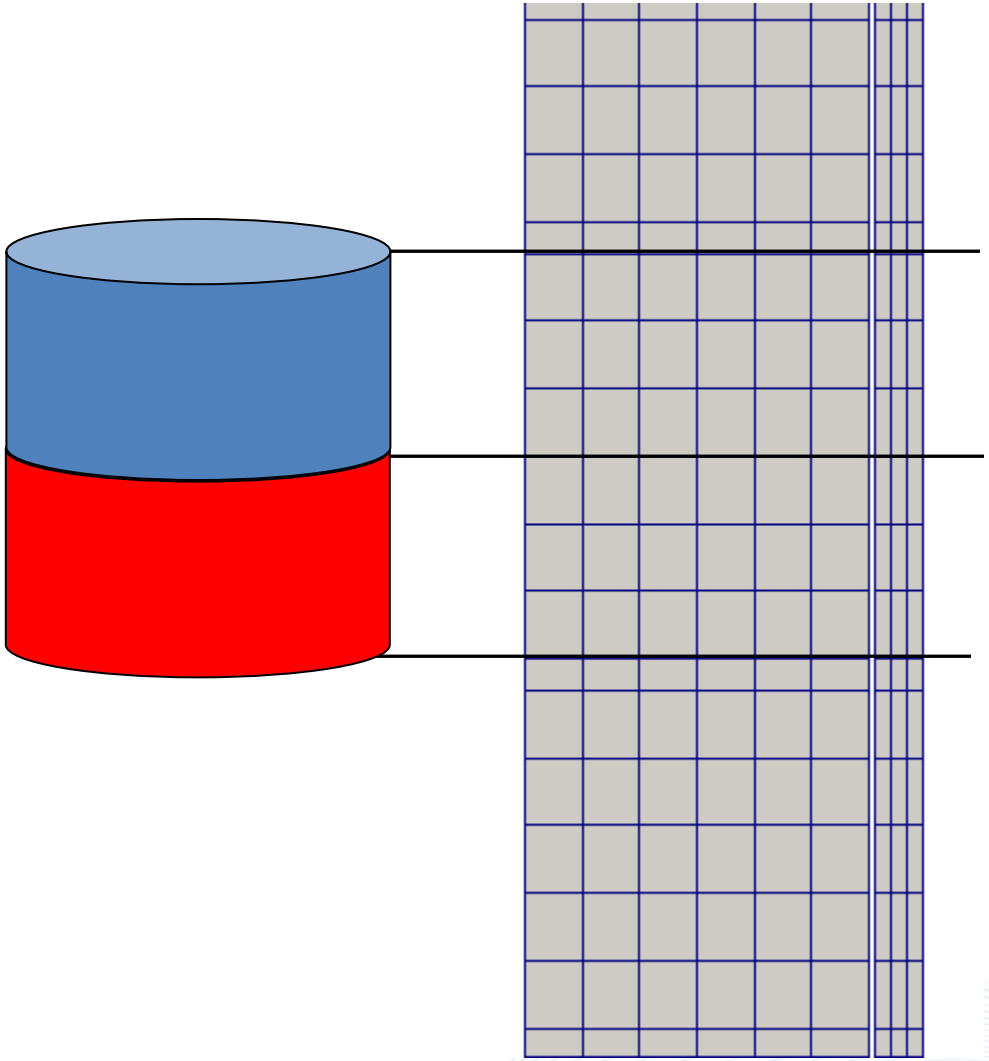

Conservation Algorithm

- Conservation of power for each pin is output to screen during run for each data transfer
- Procedure is:

1. Use DTK to transfer point-wise power values to the finite element basis points for each rod/application in the MOOSE MultiApp.
2. Use a MOOSE custom target user object to integrate the total power in each rod (i.e. each MOOSE application in the MultiApp).
3. Perform a second data transfer to pull all pin powers for each axial edit bound region associated with each locally-owned fuel rod to the Peregrine application MPI process space.
4. Compute the scaling factor for each rod and apply the factor to the power transferred in step 1.
5. Use the MOOSE custom target user object to re-integrate the total power to verify that the scaling has enforced conservation.

Example output is shown below a very coarse mesh for process 57 on fixed-point iteration 3 for fuel pin App number 258:

```
p=57, Peregrine  | Iter=3, app=258, Insilico pin power=64348.8 W, MOOSE
transferred power=64133.2 W, scaling factor=1.00336, MOOSE conserved
power=64348.8 W
```

2 DTK transfers per pin!

Peregrine→CTF: Heat Flux Data Transfer

- Conservative by construction over axial edit bounds
- Alignment of element boundaries with axial edit bounds is critical!

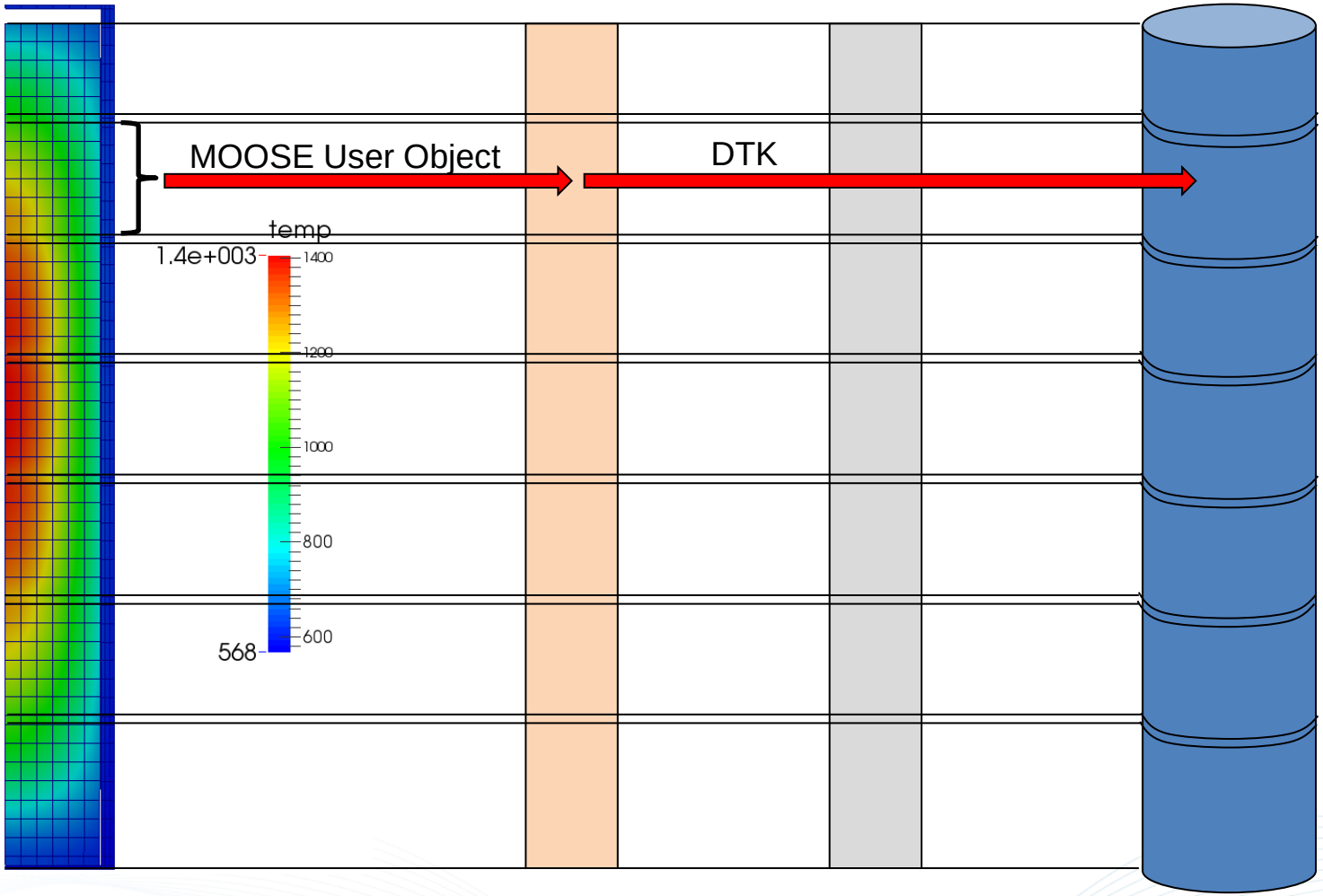

Smeared Pellet Mesh (MOOSE Coordinates)

MOOSE LayeredSideFluxAverage (MOOSE DTK Position Coordinates)

Coupling Mesh Coordinates

CTF Cell

Results: 17x17 WEC Assembly
(AMA progression problem 6)

Prob. #6

- Based on Watts Barr Unit 1 Cycle 1
- Assembly Layout:
  - 264 fuel rods
  - 24 guide tubes
  - 1 instrument tube

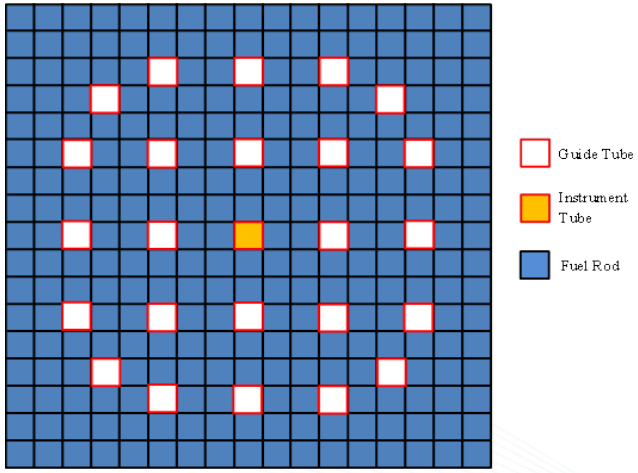

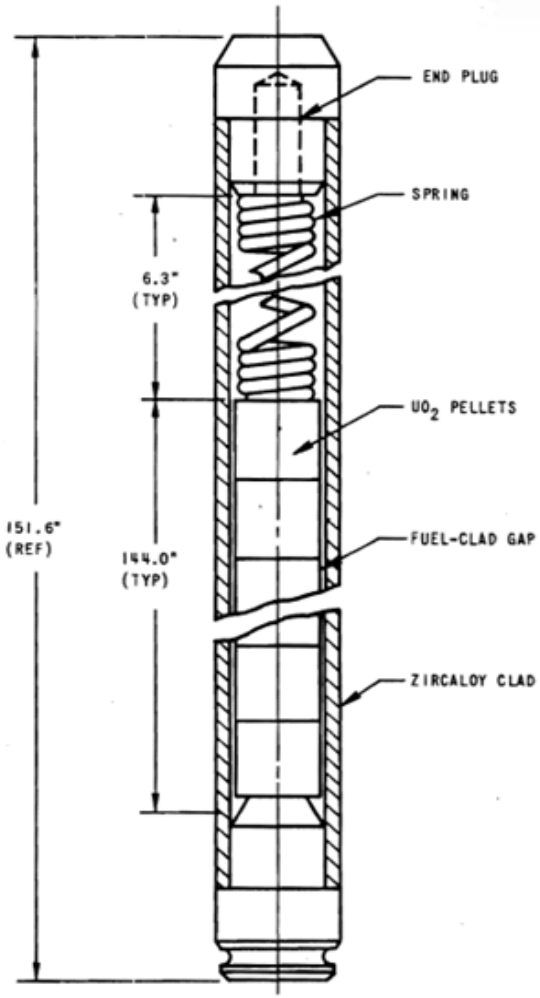

Figure from Watts Bar Unit 2 Final Safety Analysis Report (FSAR), Amendment 93, Section 4, ML091400651, April 30, 2009.
Figure 4.2-3

Peregrine Fields for Fuel Pin #100 (Exodus File Output)

Prob. #6

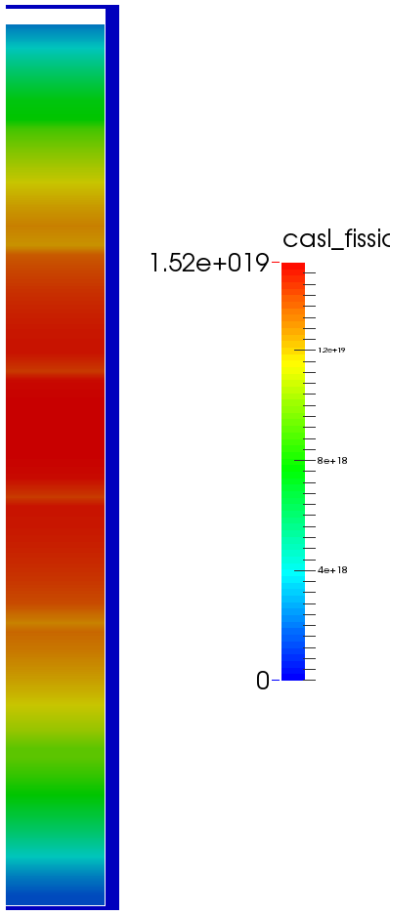

Transferred Fission Rate from Insilico

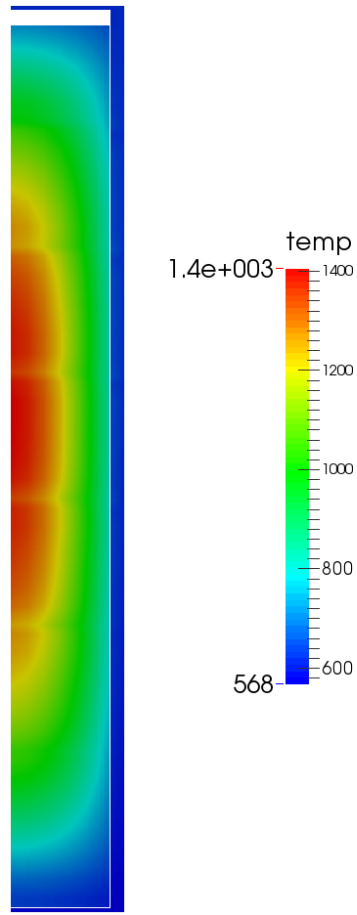

Peregrine Fuel Temperature (K)

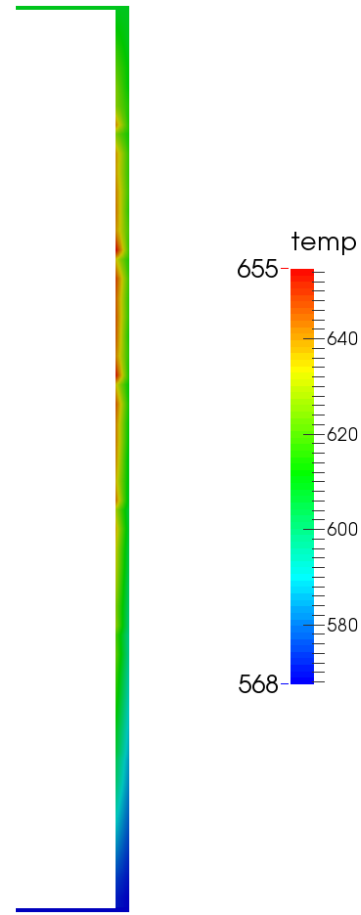

Peregrine Clad Fuel Temperature (K)

CTF Fields (VTK File Output)

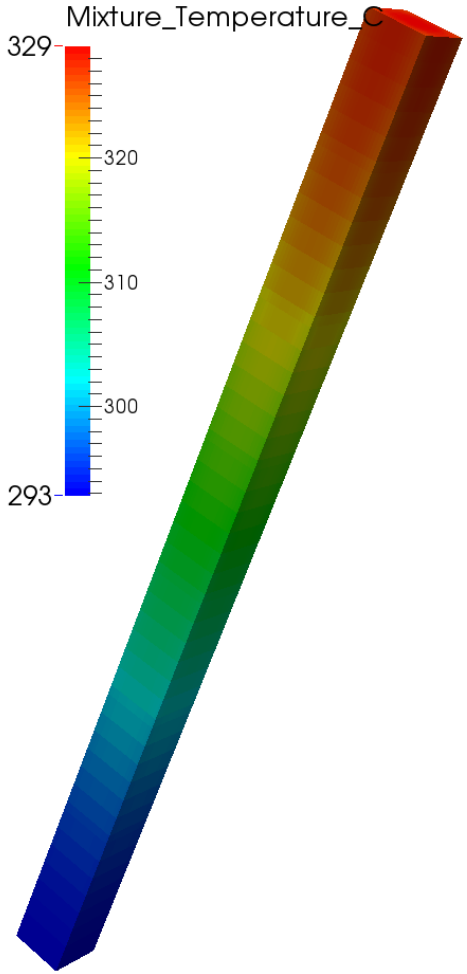

CTF Mixture Temperature (C)

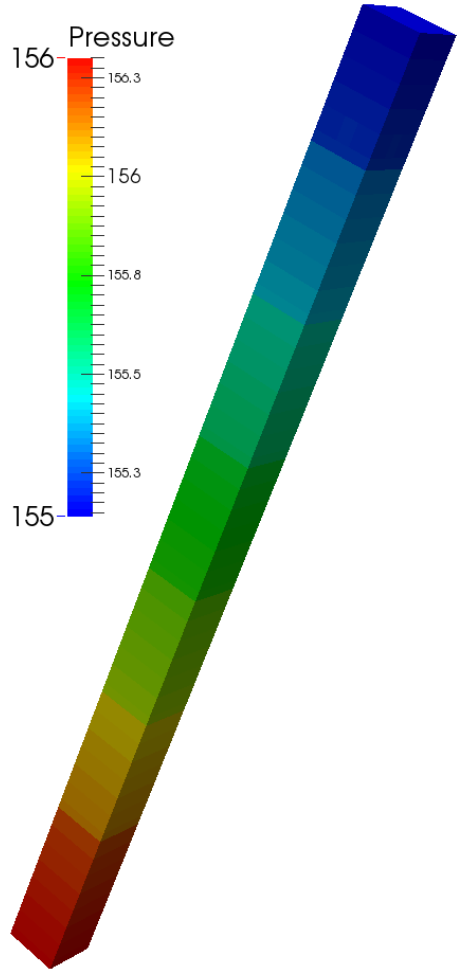

CTF Fluid Pressure

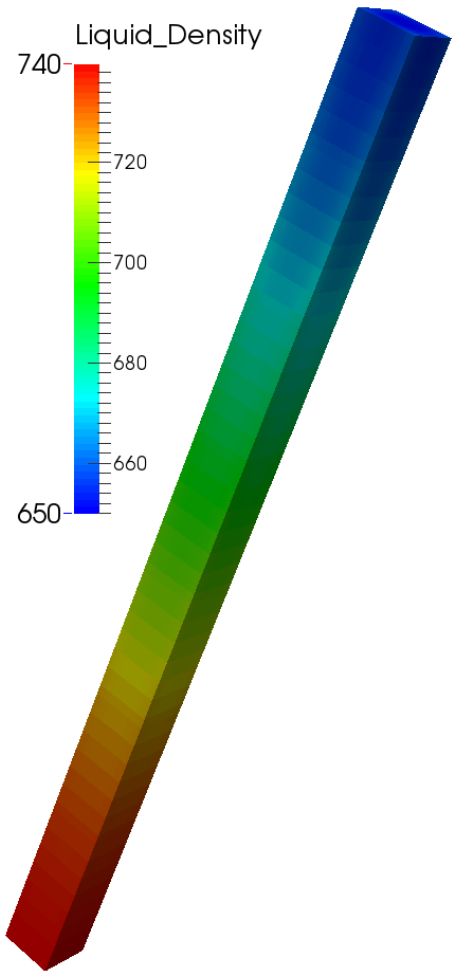

CTF Liquid Density

Comparison To CTF+Insilico

- A comparison of CTF+Insilico with Tiamat provides a reasonable benchmark for timings and predicted QoI.
- The CTF pin heat transfer model is very different from Peregrine
  - CTF used with a fixed gap-heat transfer coefficient (major effect on fuel temperature), and does not account for change to the gap thickness.
  - Differences wrt thermal conductivity models of the fuel and cladding
  - One future project planned in CASL will be to improve the models used in CTF through comparisons with Peregrine.

Timings (S)	Tiamat	CTF/Ins
Num Cores	60	49
Total time	12580	3833
Object Construction Time	470	-
Solve Time (Incl Init/Ramp)	12110	-
Initilaization/Ramping	4392	-
Num fixed-point Iterations	8	8

	keff	Avg. Fuel Temp (C)	Peak Power (W/cm)
Tiamat	1.188519	662	252
CTF	1.188964	570	266

Comparison: Average Axial Fuel Temperature

- Average values for each axial edit bound region
- Temperature is higher in Tiamat
- Likely due to the gap heat transfer coefficient that was arbitrarily chosen in CTF for VERA.

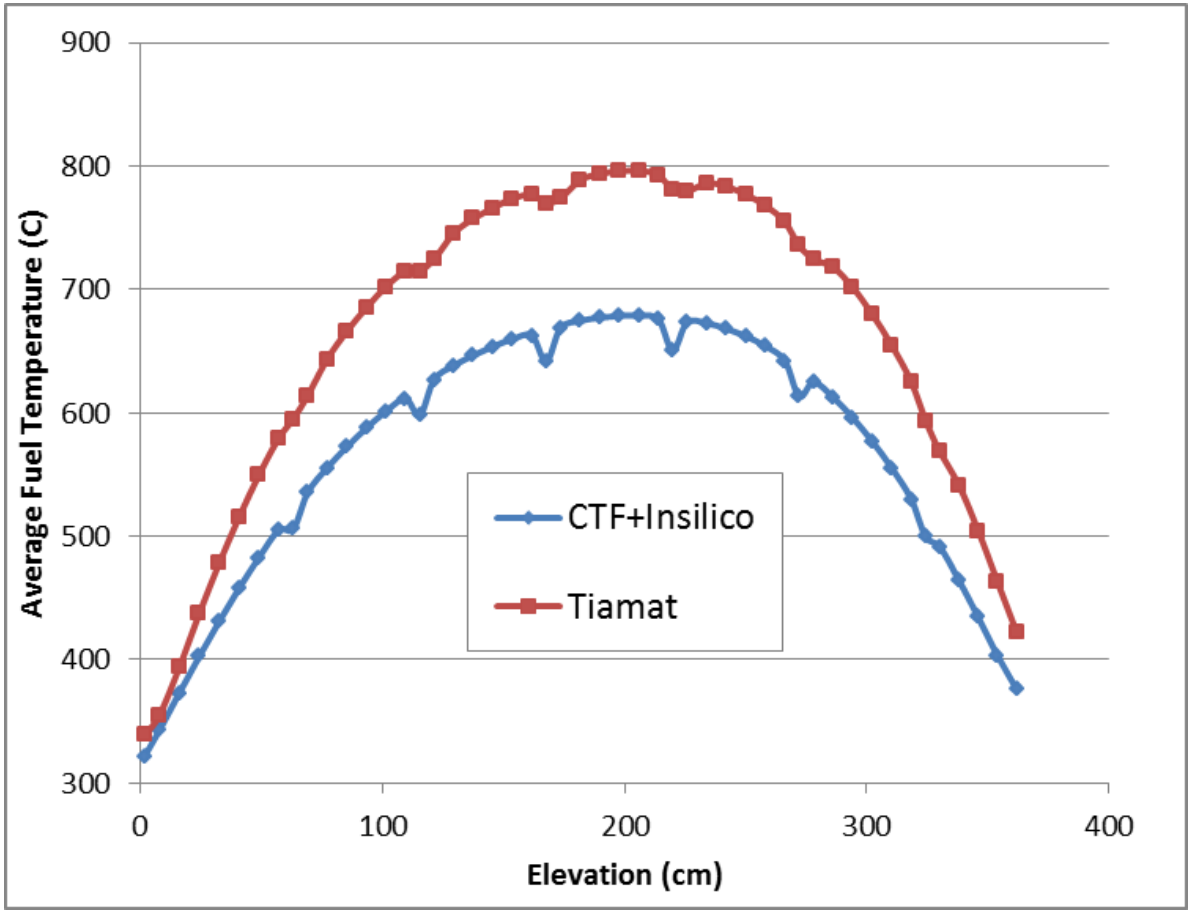

Note:
- CTF+Insilico sharply resolves spacer grid depressions
- Tiamat smears this over two edit bound regions due to mapping to nodal basis points instead of quadrature points (future work planned to correct)

Comparison: Linear Power Rate

- Averaged values for each axial edit bound region are plotted
  - Peak power computed from maximum power over individual pin edit bound regions
- Increased temperatures in Tiamat affects the power as expected:
  - Distribution is flattened (in terms of peak power) and shifted to right
  - Peak power is reduced and the eigenvalue (keff) is reduced by 45 pcm (% milli-k), which is approximately 0.8 pcm/F
  - The flattened power distribution is due to the increased fuel temperature
  - The flattened power distribution alters the coolant density distribution, which results in the shift of the power to the right

	keff	Avg. Fuel Temp (C)	Peak Power (W/cm)
Tiamat	1.188519	662	252
CTF	1.188964	570	266

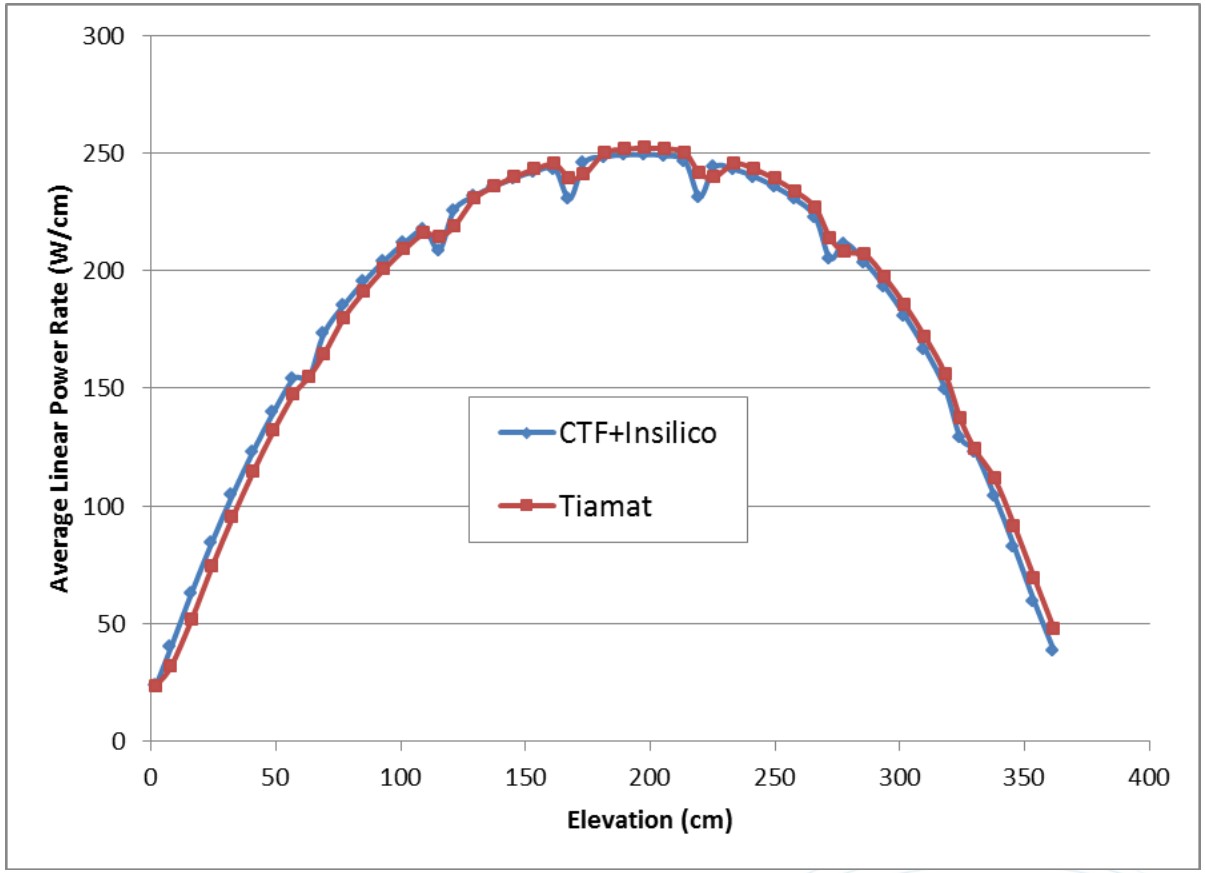

Convergence of the Picard Iteration

- Convergence statistics output to screen and summary file
- This output shows the quantity of interest (QoI) values and the difference of the values between iterations for the convergence metrics.
- Global Convergence requires change in QoI between fixed-point iterations is less than specified amount:
  - keff < 2 pcm (Insilico)
  - total power < 5e-5 (Insilico)
  - clad temperature < 0.5 C (CTF)
  - coolant temperature < 0.5 C (CTF)

Case: p6a_spn8g

Iter	keff	keff diff (pcm)	Power diff	Cool Max T (C)	Clad Max T (C)	Cool diff (C)	Clad diff (C)
1	1.1898021	63.465577	0.24886931	324.78731	342.44971	3.7667081	30.242601
2	1.1892533	46.153879	0.19859106	327.32669	343.62091	2.5393833	1.1712015
3	1.1887158	45.214341	0.08754653	328.39586	345.75582	1.0691648	2.1349105
4	1.1886283	7.3617736	0.035123985	328.75212	345.77666	0.35625995	0.020839199
5	1.1885553	6.1411602	0.013399296	328.93251	345.91934	0.1803889	0.14268329
6	1.1885331	1.8695316	0.004787669	328.96704	345.90031	0.034535571	0.019035699
7	1.1885225	0.88603707	0.0016933955	328.99245	345.91207	0.025405842	0.011767485
8	1.1885193	0.27014407	6.1244532e-06	328.99344	345.9055	0.00098790761	0.0065690492

Solve Status: CONVERGED!

Local vs Global Convergence

- Global vs Local Convergence
  - Global: Convergence of the coupled simulation
  - Local: Convergence of a single solve in an individual application
  - Global convergence is strongly affected by local convergence tolerances!
- Local CTF
  - CTF does not locally converge if the "balance" tolerances are set at or below 1.0e-5.
  - The issue has to do with the solution algorithm and boundary conditions for the multiphase equations.
  - This is currently being addressed in PHI Kanban ticket #3372. Currently the balance equations use a tolerance of 1e-3 to 1e-4 and seem to be sufficient.
- Local Insilico
  - For the SPn equations, eigensolver tolerance is main control parameter
  - For global convergence, a value of 1.0e-6 or tighter is typically needed
- Local Peregrine
  - Equations solved by Jacobian-Free Newton-Krylov
    - Nonlinear Absolute tolerance
    - Nonlinear Relative tolerance
    - GMRES linear solve tolerance
  - In clad_solid_mechanics block, an internal point-wise nonlinear solve occurs
  - Discretization Error: Both spatial and temporal error can affect convergence
  - If MultiApp local pin failures are occurring, tightening up the inner solid mechanics nonlinear solve and the GMRES linear solver tolerance usually helps. Refining the finite element mesh and cutting the ramping time step can also help in certain situations.

```
global_energy_balance    0.0001 !%
global_mass_balance      0.0001 !%
fluid_energy_storage     0.005  !%
solid_energy_storage     0.005  !%
mass_storage             0.005  !%
```

```
tolerance     1e-6
init_tolerance 1e-6
```

```
Executioner
  l_tol = 8e-3
  nl_rel_tol = 1e-4
  nl_abs_tol = 1e-10

clad_solid_mech
  absolute_tolerance = 1e-12
  relative_tolerance = 1e-3

ny_p = 48
nx_c = 3
ny_c = 48
nx_p = 6

dtmax = 1.e+6
```

Example of Peregrine Spatial Discretization Error

Peregrine Heat Flux

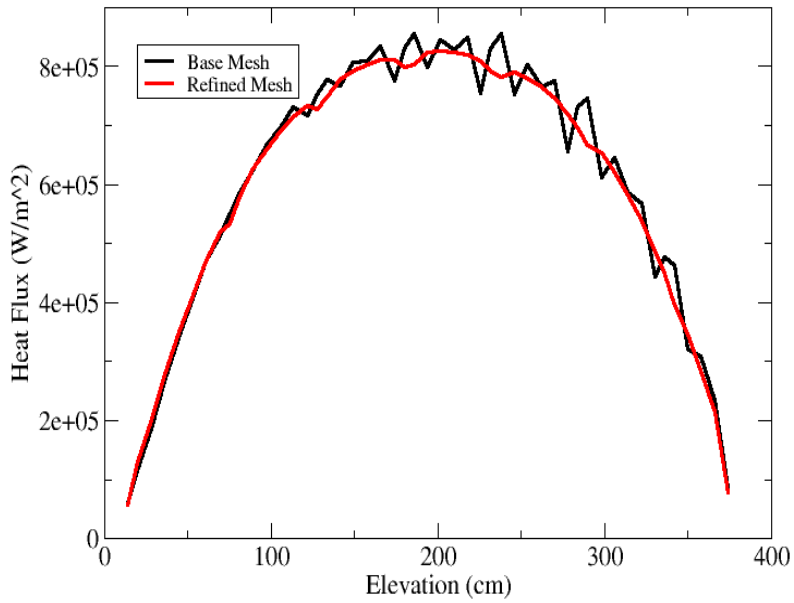

CTF Clad Temperature

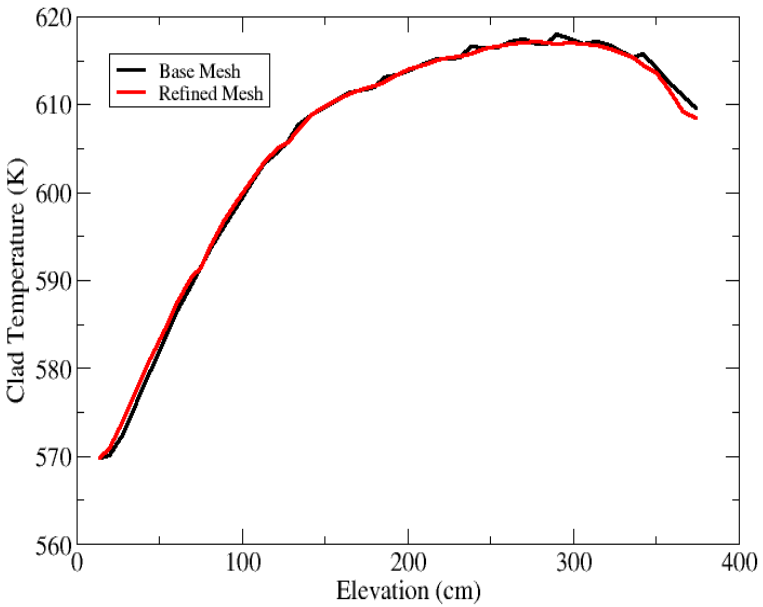

- Approximately one level of refinement in Peregrine mesh
- Spacer grid indentations are shown on refined mesh
- Significant affect on accuracy of integrated heat flux
- Does not significantly affect QoI:
  - Keff coarse mesh: 1.2025111
  - Keff refined mesh: 1.2025031

Timings

Timings (S)	Tiamat	CTF/Ins
Num Cores	60	49
Total time	12580	3833
Object Construction Time	470	-
Solve Time (Incl Init/Ramp)	12110	-
Initilaization/Ramping	4392	-
Num fixed-point Iterations	8	8

Application	Num Cores	Solve Time (s)	Num Solves	Avg/Solve (s)
CTF	1	2303	9	256
Insilico	36	2372	9	264
Peregrine	23	6883	20	344

Transfer	SetupTime (s)			Transfers (s)				
	Min	Mean	Max	Number	Min	Mean	Max	Mean/Trans
CTF to Insilico	1.716	7.081	200	9	0.2094	0.2218	0.23	0.02465
Insilico to Peregrine	41.18	41.18	41.18	19	26.96	437.9	535.1	23.05
Perregrine to Insilico	0.09383	0.09431	0.09482	8	0.0566	0.05926	0.064	0.007408
CTF to Peregrine	210.4	210.4	201.4	19	0.6898	17.01	319.9	0.8954
Peregrine to CTF	0.4274	0.4277	0.4291	8	0.046	0.05495	0.067	0.006869

- Insilico used 8 group library (primarily for unit testing). Will use larger for L1 runs.
- Coarse Peregrine mesh - may be adequate
- The overall time spent in data transfers (setup+transfer) is approximately 1100 seconds. This suggests that we are doing an efficient job of transferring data.
- The setup time for "CTF to Insilico" stands out because the max is much larger than the average. Each of the 36 Insilico processes require approximately 1.7 seconds and the single CTF processor, which must communicate with all 36 takes 200 seconds.
- Two data transfers are significantly longer than the others. These are data transfers that push values into Peregrine. The reason for this is that when data is pushed into Peregrine, a single data transfer is not used, but one data transfer is set up for each fuel rod separately. Each App transfer inserts a communication barrier between the other App transfers, so this serialized computation is costly. The reverse situation where Peregrine is the source for data only requires a single data transfer for all pins. This is a possible area for future improvement.
- NOTE: DTK efficiency was significantly improved this FY, but not reflected in numbers above. May have a dramatic drop in data transfer runtimes

Generalization of Tiamat Driver and Coupling Library

- Generalized Tiamat Driver for multiple couplings
  - Eventual integration of MPACT
- LIME lacked flexibility to support Tiamat coupling requirements
- L3 milestone in PoR3 outlined the design of a “LIME 2”
- Implemented this year as a new package called PIKE (Physics Integration KErnels)
  - 2000 lines of c++ (~1 week of effort)
  - Awaiting DOE copyright for eventual release in Trilinos
- Converted Tiamat to use this package
  - Simplified model interfaces
  - Explicit separation of global and local convergence
  - User defined convergence test hierarchy
  - Local pin convergence checking
  - Unified control via observers
    - Unit testing, output summary, initialization
  - Timing control
- Takes about < 1 hour to convert from LIME to PIKE
  - Written with backwards compatibility in mind

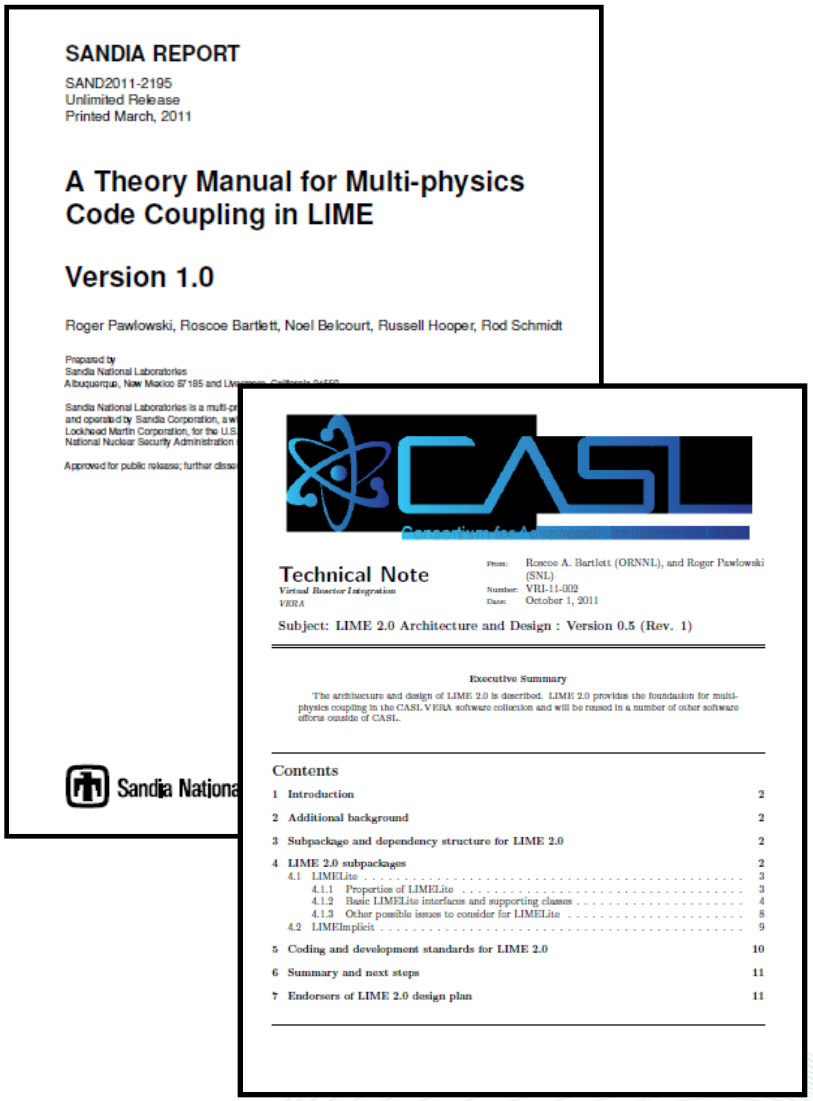

SANDIA REPORT

SAND2011-2195
Unlimited Release
Printed March, 2011

A Theory Manual for Multi-physics Code Coupling in LIME

Version 1.0

Roger Pawlowski, Roscoe Bartlett, Noel Belcourt, Russell Hooper, Rod Schmidt

Prepared by
Sandia National Laboratories
Albuquerque, New Mexico 87185 and Livermore, California 94550

Sandia National Laboratories is a multi-pr
and operated by Sandia Corporation, a w
Lockheed Martin Corporation, for the U.S.
National Nuclear Security Administration

Approved for public release; further disse

Sandia Nationa

Technical Note
Virtual Reactor Integration
VERA

From: Roscoe A. Bartlett (ORNNL), and Roger Pawlowski (SNL)
Number: VRI-11-002
Date: October 1, 2011

Subject: LIME 2.0 Architecture and Design : Version 0.5 (Rev. 1)

Executive Summary

The architecture and design of LIME 2.0 is described. LIME 2.0 provides the foundation for multi-physics coupling in the CASL VERA software collection and will be reused in a number of other software efforts outside of CASL.

Contents

1 Introduction 2
2 Additional background 2
3 Subpackage and dependency structure for LIME 2.0 2
4 LIME 2.0 subpackages 2
4.1 LIMELite 3
4.1.1 Properties of LIMELite 3
4.1.2 Basic LIMELite interfaces and supporting classes 4
4.1.3 Other possible issues to consider for LIMELite 8
4.2 LIMEImplicit 9
5 Coding and development standards for LIME 2.0 10
6 Summary and next steps 11
7 Endorsers of LIME 2.0 design plan 11

Drive Problem from VERA Input File

- Previously a single moose input file and position file was used.
  - Manually synced to VERA input
- A new standalone parser developed to translate vera input file into peregrine input files
  - Critical for users: ~10 geometry parameters (some repeated) in each moose file in different sections!
  - Nontrivial calculations based on geometry are done to put in "moose form"
  - Tracking file to tie fuel pin to moose multiapp global index
- Runtime generation of filenames vector

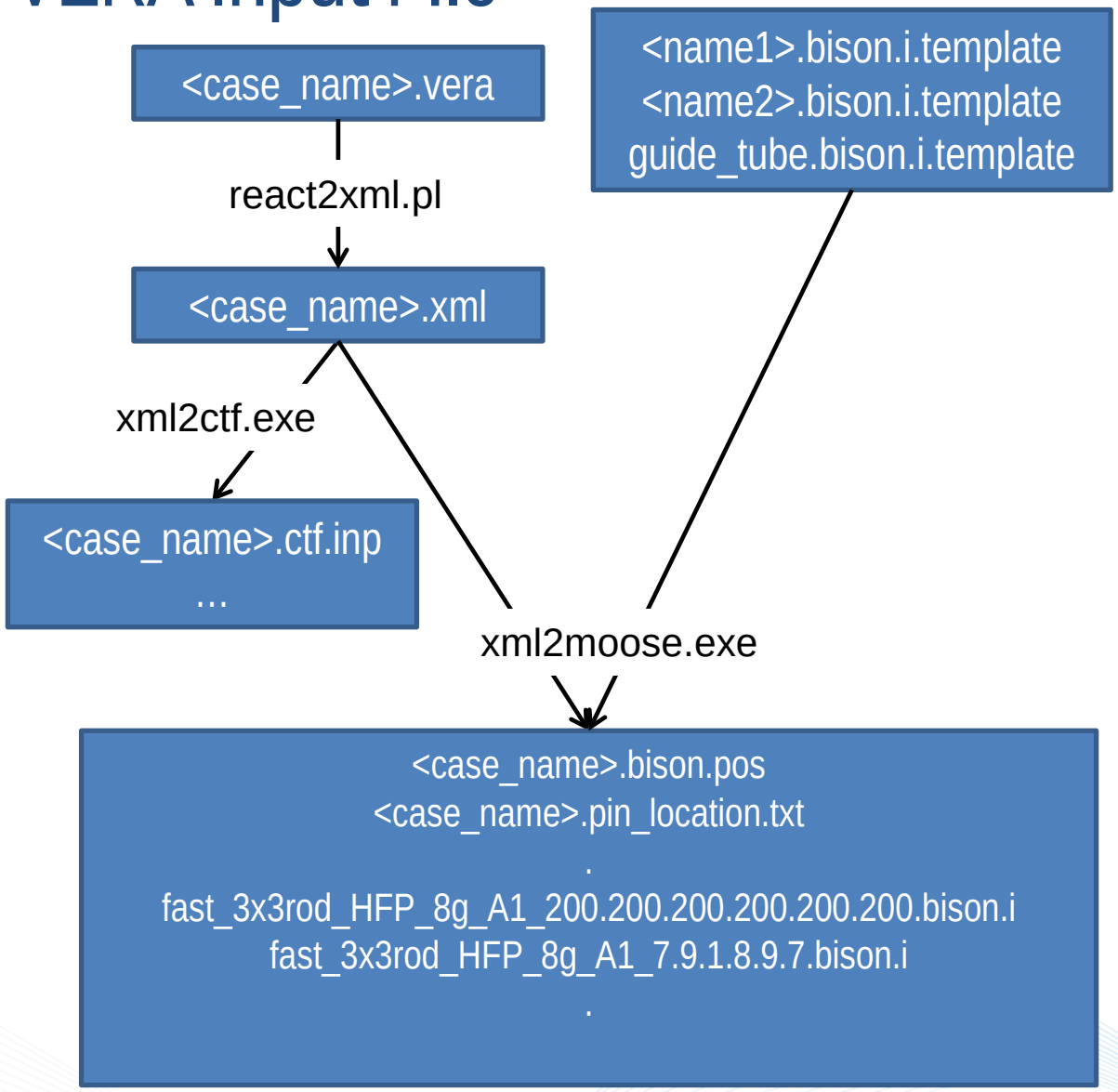

A look at “xml2moose.exe”

- Peregrine input is 650+ lines long.
- We override approximately 35 parameters if encountered in input file.
- If peregrine needs a parameter, then it forces user to supply it in <case_name>.vera input file!
- Keys associated to functors: can replace lines or entire blocks of code.
  - Extensible by users: can register new functors

```
[Mesh]
  type = CASLSmearedPelletMesh
  displacements = 'disp_x disp_y'
  clad_mesh_density = customize
  clad_thickness = 0.00057 #  <<VERA MODIFIED>>
  pellet_mesh_density = customize
  pellet_outer_radius = 0.004096 #  <<VERA MODIFIED>>
  clad_bot_gap_height = 0.00152 #  <<VERA MODIFIED>>
  pellet_quantity = 1 #  <<VERA MODIFIED>>
  pellet_height = 3.6576 #  <<VERA MODIFIED>>
  clad_gap_width = 8.4e-05 #  <<VERA MODIFIED>>
  plenum_fuel_ratio = 0.0437445 #  <<VERA MODIFIED>>
  ny_p = 48 # number of axial elements in the fuel
  nx_c = 3 # number of elements in the clad thickness
  ny_c = 48 # number of elements in the axially in the clad
  nx_p = 6 # number of radial elements in the fuel
  intervals = '0.03866 0.08211 0.08211 0.08211 0.08212
0.08211 0.08211 0.08211 0.0381 0.08065 0.08065 0.08065
0.08065 0.08065 0.08065 0.0381 0.08065 0.08065 0.08065
0.08065 0.08065 0.08065 0.0381 0.08065 0.08065 0.08065
0.08065 0.08065 0.08065 0.0381 0.08065 0.08065 0.08065
0.08065 0.08065 0.08065 0.0381 0.08065 0.08065 0.08065
0.08065 0.08065 0.08065 0.0381 0.079212 0.079212 0.079212
0.079212 0.079212' #  <<VERA MODIFIED>>
[]
.
.
.
```

```
p.AddKey("pellet_outer_radius", casl_moose::replaceLine<double>(pin.coldPelletRadius * cmToM, "[Mesh]"));

p.AddKey("pellet_height",
         casl_moose::replaceLine<double>((pin.activeFuelTop - pin.activeFuelBottom) * cmToM,
         "[Mesh]"));
```

Improved Build/Integration Process

- Background
  - MOOSE is the only code with separate build system in VERA: Will NOT support TRIBITS/Cmake
  - MOOSE is changing rapidly!
- Updated MOOSE repo used by CASL ~8 times this year
  - Can't automate due to two-factor authentication for INL firewall
  - Every update required manual interaction to fix
- Build Issues Resolved:
  - MOOSE does in-source builds that caused collisions with checkin test script
    - Now the configure process mirrors the entire moose source code into the build directory (sym links → rsync)
  - Parallel build level support
  - Optimized/debug and shared/static support
  - Compile time check for hypre support in petsc
- Improved Integration/Updating Strategy
  - Previously pulling from git clone of svn repo, then applying patches: very time consuming, merge errors caused real headaches, rebasing caused collisions, repo from new clone not possible (different hash), …
  - Completely revamped how we create and manage the moose clone:
    - Snapshot SVN repo via rsync into CASL MOOSEExt git repository
    - Manage 2 git branches: "inl_clean_svn" and "master"
    - Update clean branch and merge into master that contains CASL patches

Summary

- Significant Improvements:
  - Generalization of driver and coupling library
  - Robust ramping strategy
  - Subcycling of codes within a time step
  - Data transfers conserve energy
  - Drive coupled problem from VERA input file
  - Robust code update strategy
  - Robust build mechanism
  - Improved testing

- L1 due August 30th: Working with Rob Montgomery (MPO) to apply to multi-assembly test problem for PCI challenge problem.

Future Work

- Enhance data transfers within MOOSE to allow for data (specifically the power) to be defined at quadrature points rather than mesh nodes; this will allow for conservation at the axial edit bound regions.
- Remove the per Application serialization bottleneck for data transferred to MOOSE.
- Perform a scaling study with more processors and a variation in the distribution of processors per application.
- Perform the full core reactor simulation and evaluate the memory requirements.
- Parallelization of CTF. The CTF parallel capability is limited to a single assembly per process, which may not be enough. Increased parallelization will also decrease the data transfer bottleneck because all CTF transfers must now talk to a single process per assembly.
- Integrate true 3D surface transfers in MOOSE and utilize 3D fuels models.
- Integrate MPACT into Tiamat so that we can switch out Insilico.
- Make MOOSE an optional dependency of Tiamat so that we can replace the independent cobra_mpact and cobra_denovo packages.
- Use Tiamat to develop improved reduced order models for CTF conduction solves, such as gap heat transfer models.
- Improve the solution of the multiphase equations in CTF such that tighter tolerances can be achieved.

Introduction
The Experiments
Conclusion

CTF Validation Plans and Activities

Bob Salko—salkork@ornl.gov

THE OAK RIDGE NATIONAL LABORATORY

07/15/2014
Oak Ridge, Tennessee

Outline

1 Introduction

2 The Experiments

3 Conclusion

Introduction

Introduction
The Experiments
Conclusion

- CTF Documentation includes:
  - User Manual
  - Theory Manual
  - Style Guide
- Major gap is Validation/Verification Manual
- Milestone L3.PHI.VCS.P9.02 seeks to remedy Validation portion of this gap (by August 29)
- Collaborative effort between PSU and ORNL:
  - Taylor Blyth, Chris Dances, and Jeff Magedanz

Introduction

Introduction
The Experiments
Conclusion

- Document organized by major effects tested:
  - Pressure drop
  - Void/quality content
  - Turbulent-mixing
  - Void drift
  - Departure from Nucleate Boiling (DNB)
  - Single-phase heat transfer
  - Subcooled boiling heat transfer

Introduction

Introduction
The Experiments
Conclusion

Current status

- Document outline and structure completed in LaTeX
- Experiments selected
- CTF models created

Need to compile results in document

The Experiments
Overview

Introduction
The Experiments
Conclusion

- Nuclear Power Engineering Corporation of Japan (NUPEC) PSBT/BFBT rod-bundle experiments
- Combustion Engineering (CE) 5x5 subcooled boiling tests
- General Electric (GE) 3x3 two-phase experiments
- 36-rod Marviken assembly test section (FRIGG)
- Harwell high-pressure two-phase heat transfer loop (DNB)
- Pacific Northwest National Lab (PNNL) 2x6 natural convection experiments

The Experiments
PSBT

Item	Data		
Assembly	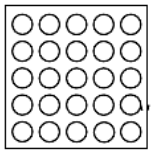 B5	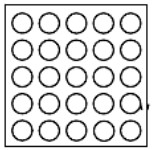 B6	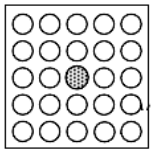 B7
Rods array	5×5	5×5	5×5
Number of heated rods	25	25	24
Number of thimble rods	0	0	1
Heated rod outer diameter (mm)	9.50	9.50	9.50
Thimble rod outer diameter (mm)	-	-	12.24
Heated rods pitch (mm)	12.60	12.60	12.60
Axial heated length (mm)	3658	3658	3658
Flow channel inner width (mm)	64.9	64.9	64.9
Radial power shape	A	A	B
Axial power shape	Uniform	Cosine	Cosine
Number of MV spacers	7	7	7
Number of NMV spacers	2	2	2
Number of simple spacers	8	8	8
MV spacer location (mm)	471, 925, 1378, 1832, 2285, 2739, 3247		
NMV spacer location (mm)	2.5, 3755		
Simple spacer location (mm)	237, 698, 1151, 1605, 2059, 2512, 2993, 3501		

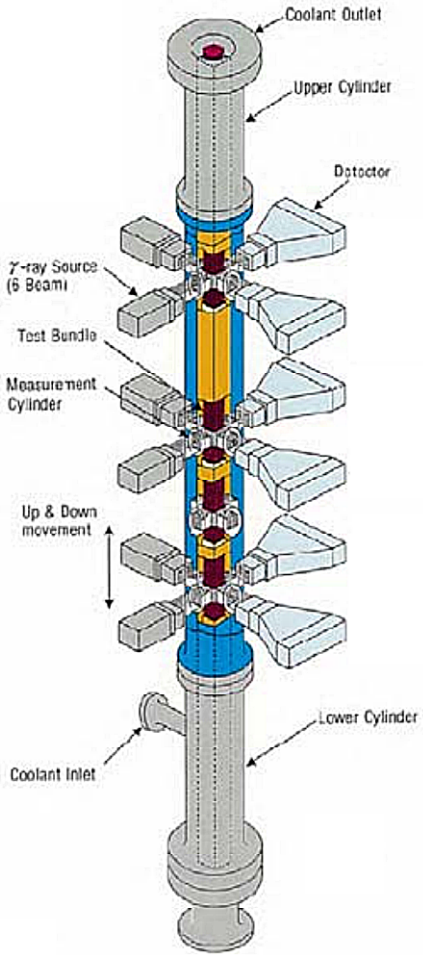

The Experiments
PSBT

Introduction
The Experiments
Conclusion

Using Chen

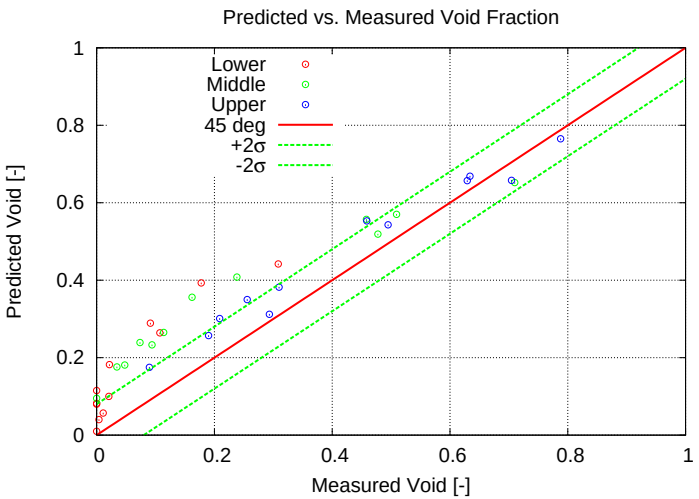

Using Thom

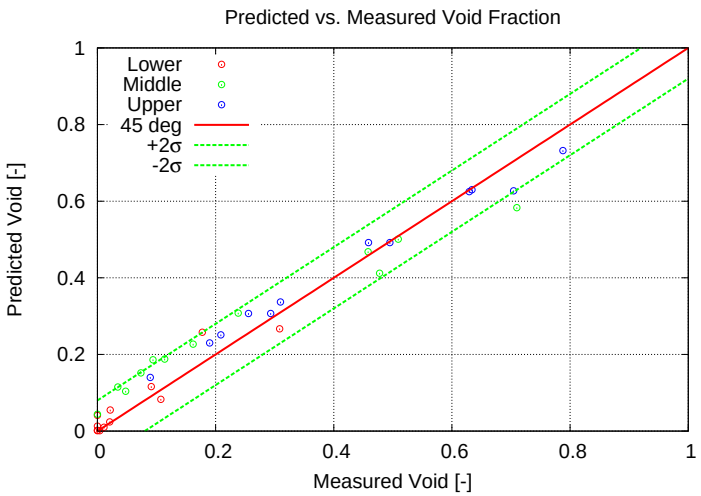

The Experiments
BFBT

Assembly	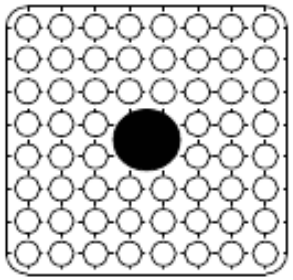 C2A	
Boundary conditions	Pressure (MPa) Flow rate (t/h)	0.2, 1, 7.2 10 15 20 25 30 35 40 45 55 60 65 70
Data	Pressure drop along with axial heated length Corresponding boundary conditions	
No. of cases	Data supplied cases Exercise cases	36 10
Concerned issues	Single-phase pressure drop from bottom to top of heated length	

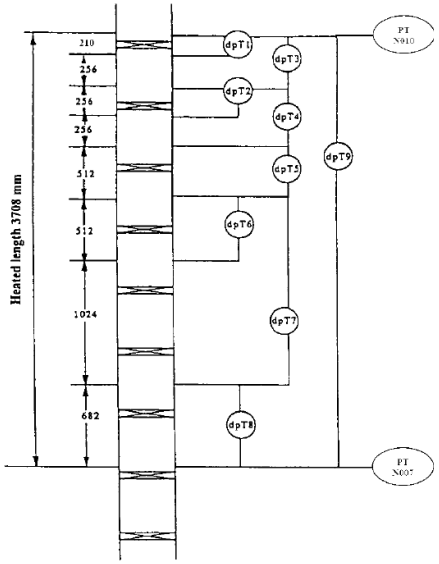

Introduction
The Experiments
Conclusion

Single-phase pressure drop

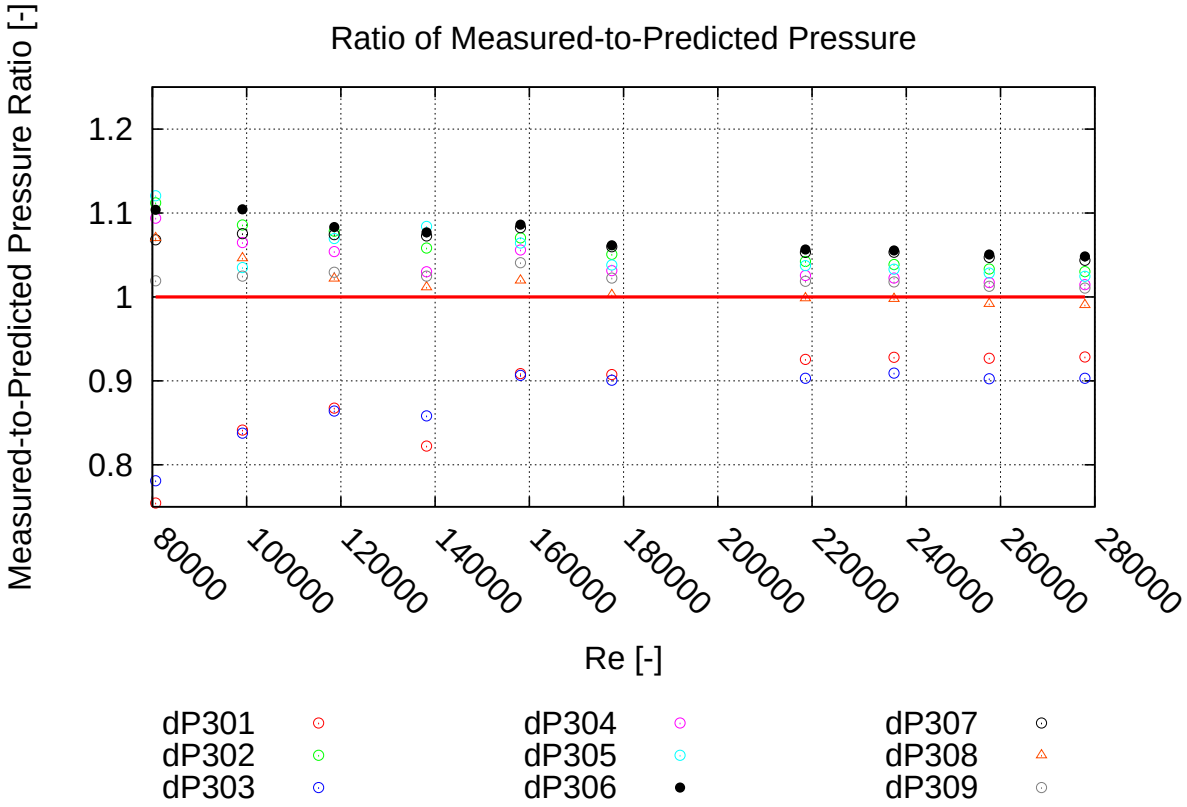

Introduction
The Experiments
Conclusion

Two-phase pressure drop

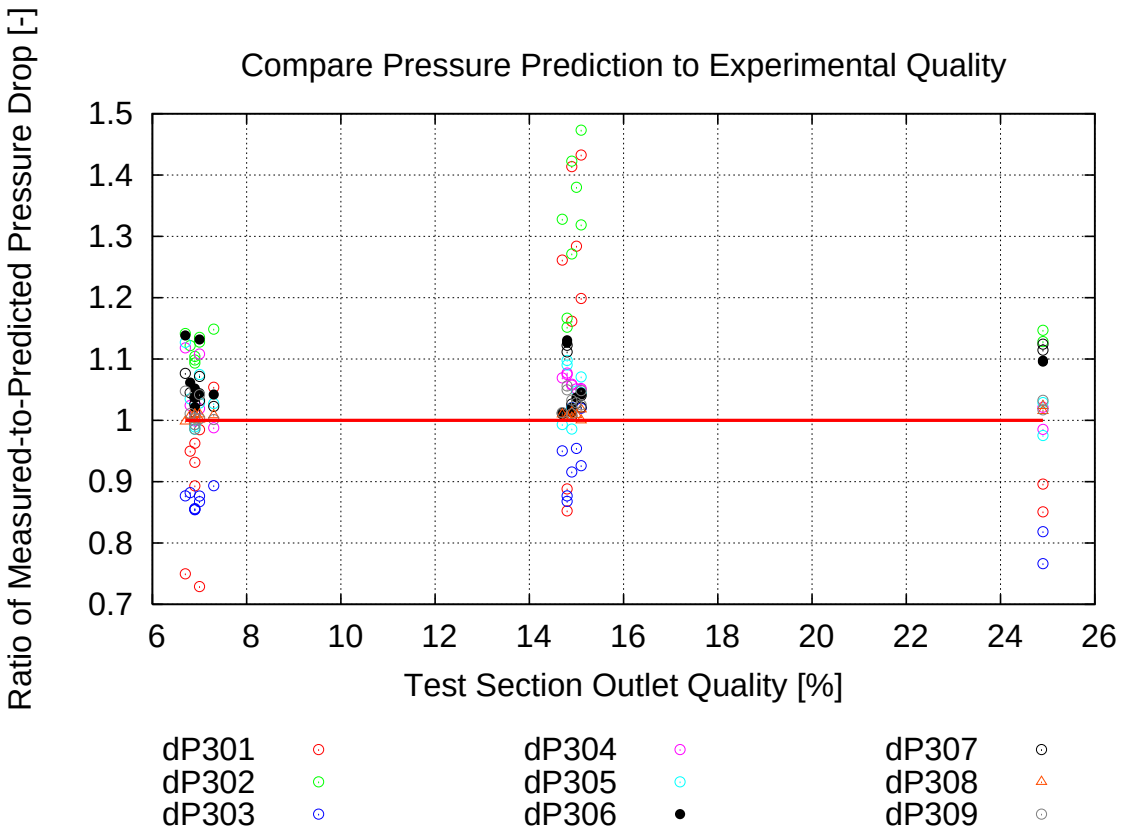

The Experiments
CE 5x5

Introduction

The Experiments

Conclusion

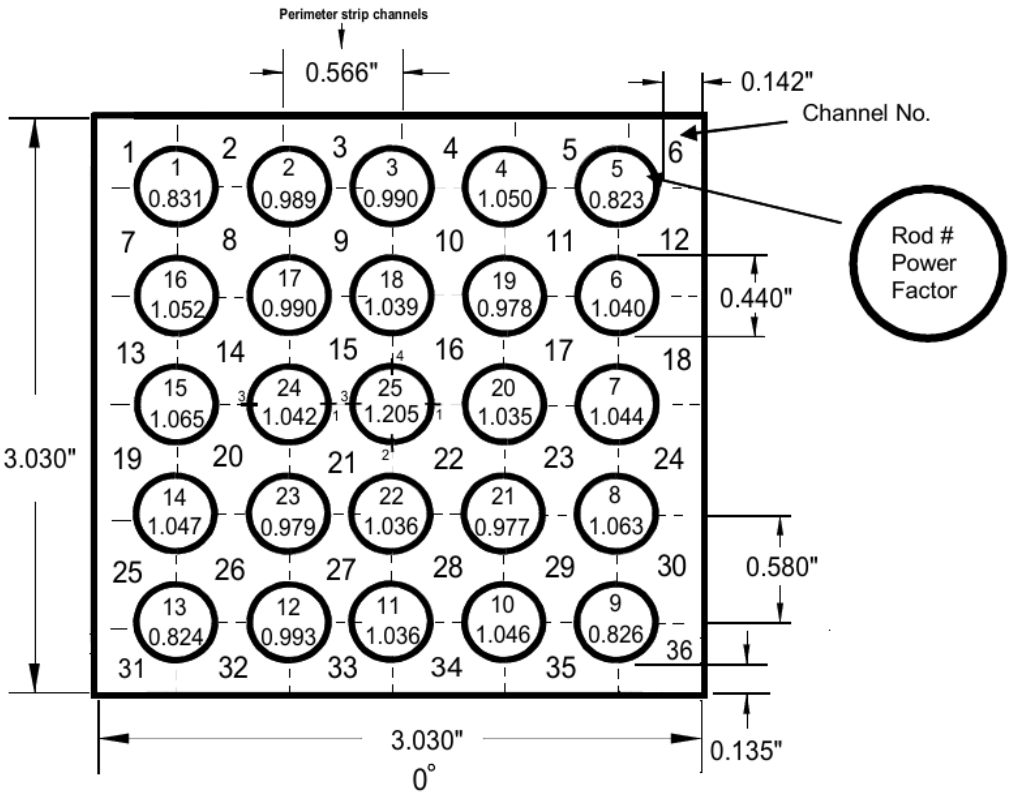

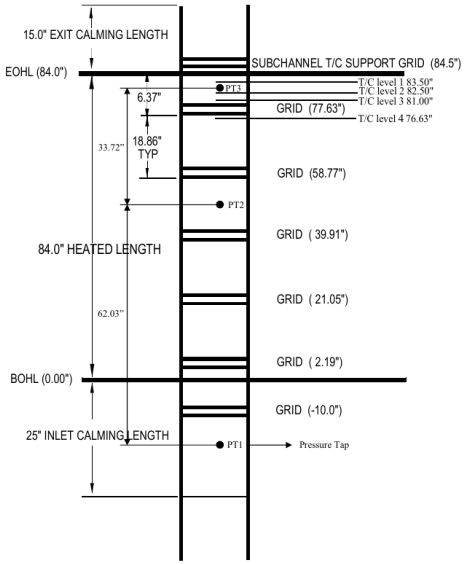

The Experiments
CE 5x5

Introduction
The Experiments
Conclusion

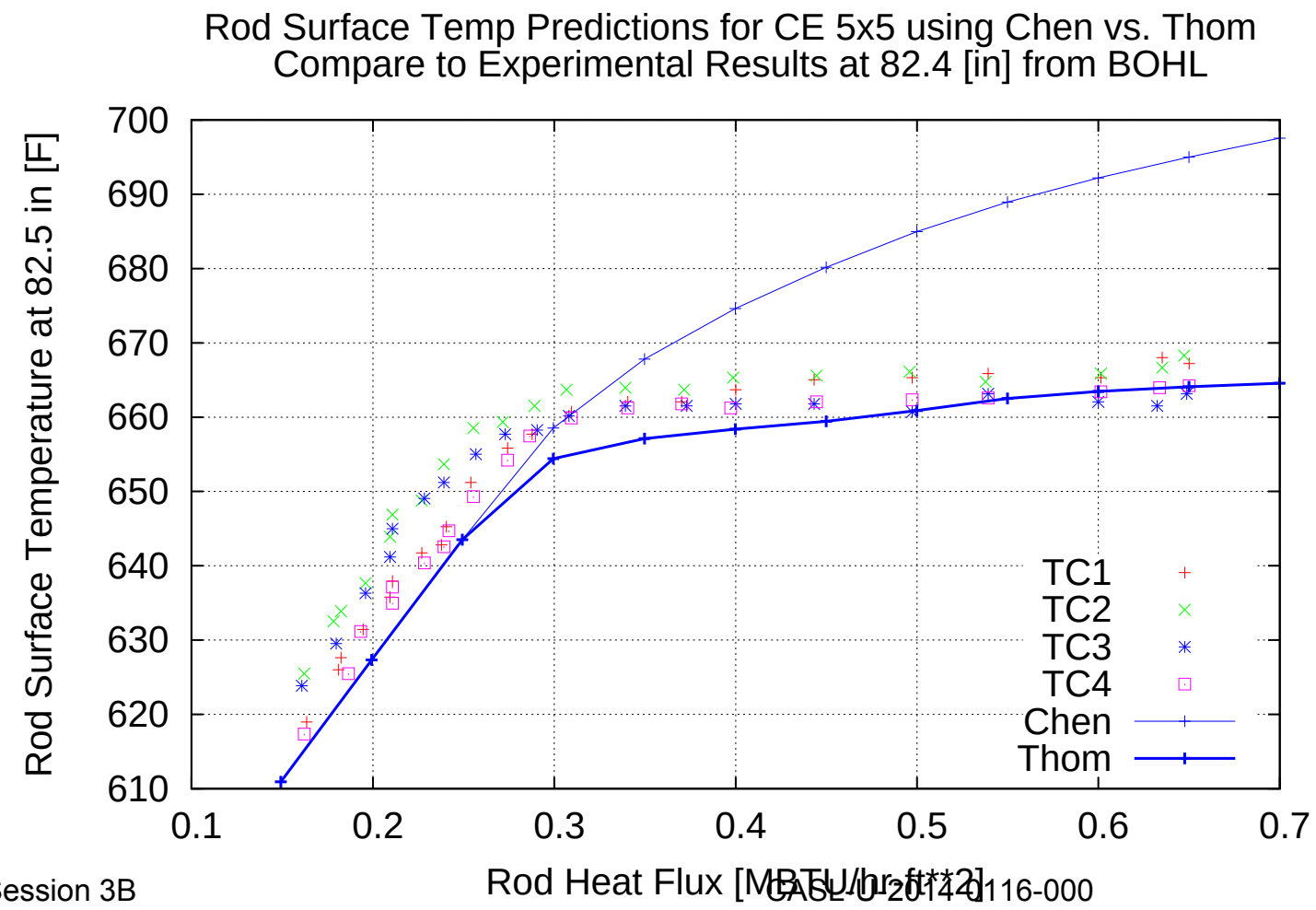

The Experiments
CE 5x5

Introduction
The Experiments
Conclusion

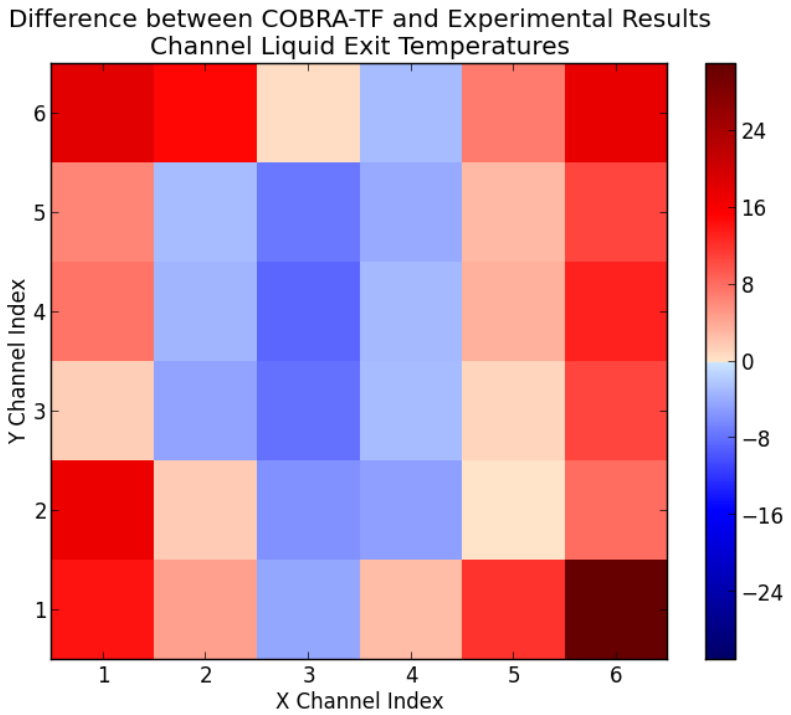

The Experiments
GE 3x3

Introduction
The Experiments
Conclusion

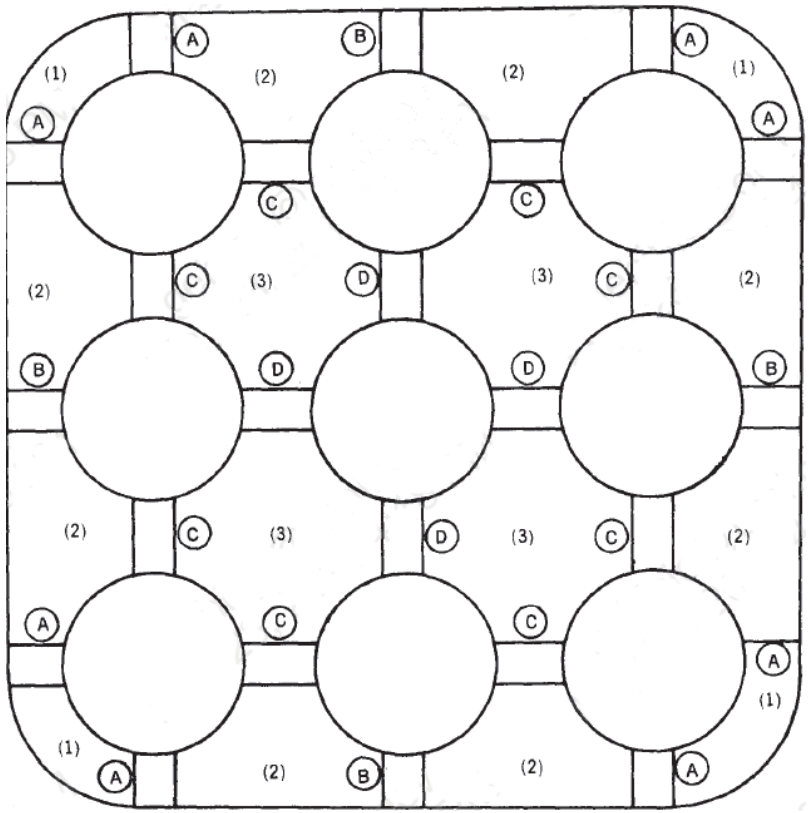

The Experiments
GE 3x3

Introduction
The Experiments
Conclusion

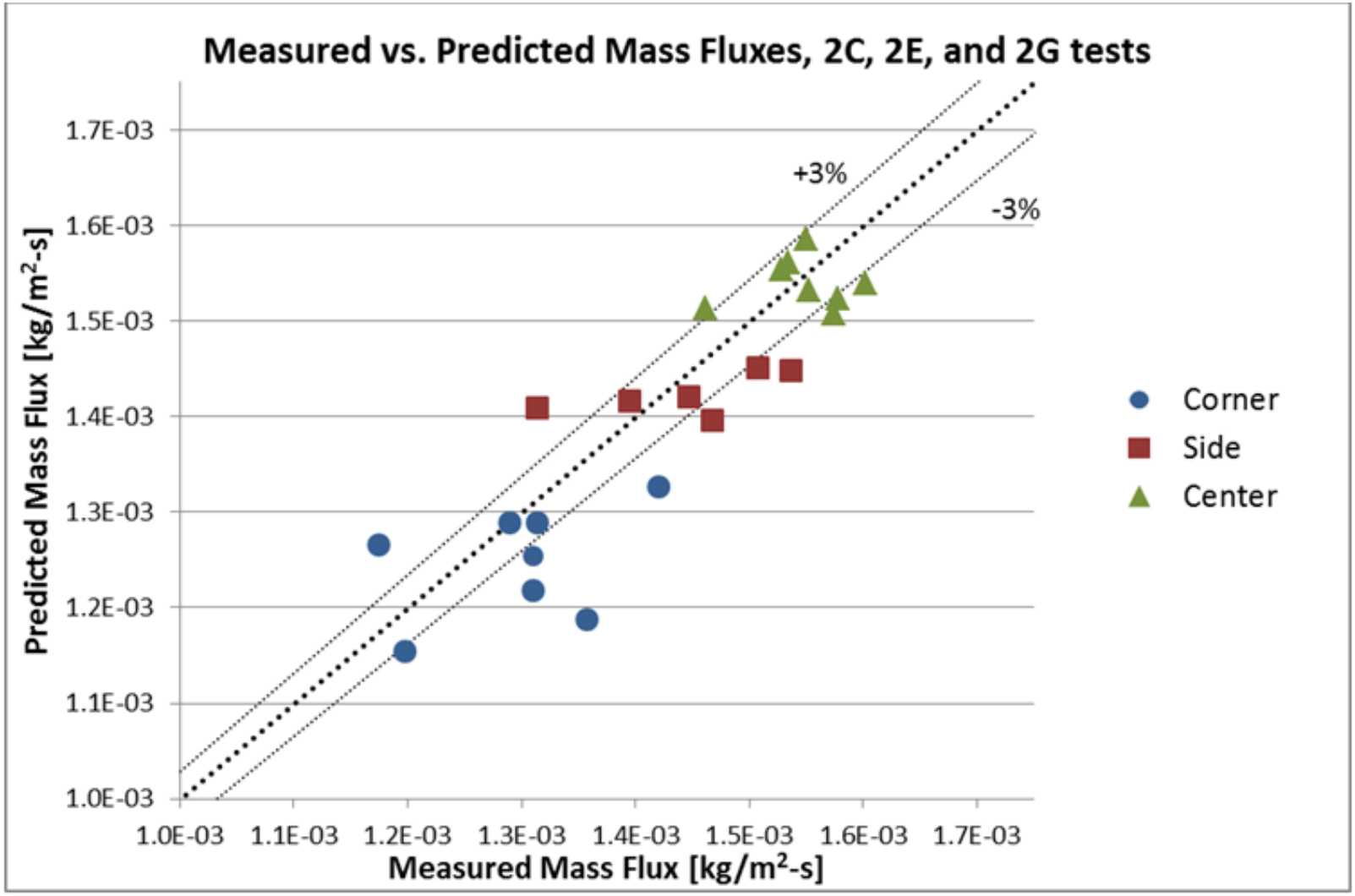

The Experiments
FRIGG

Introduction

The Experiments

Conclusion

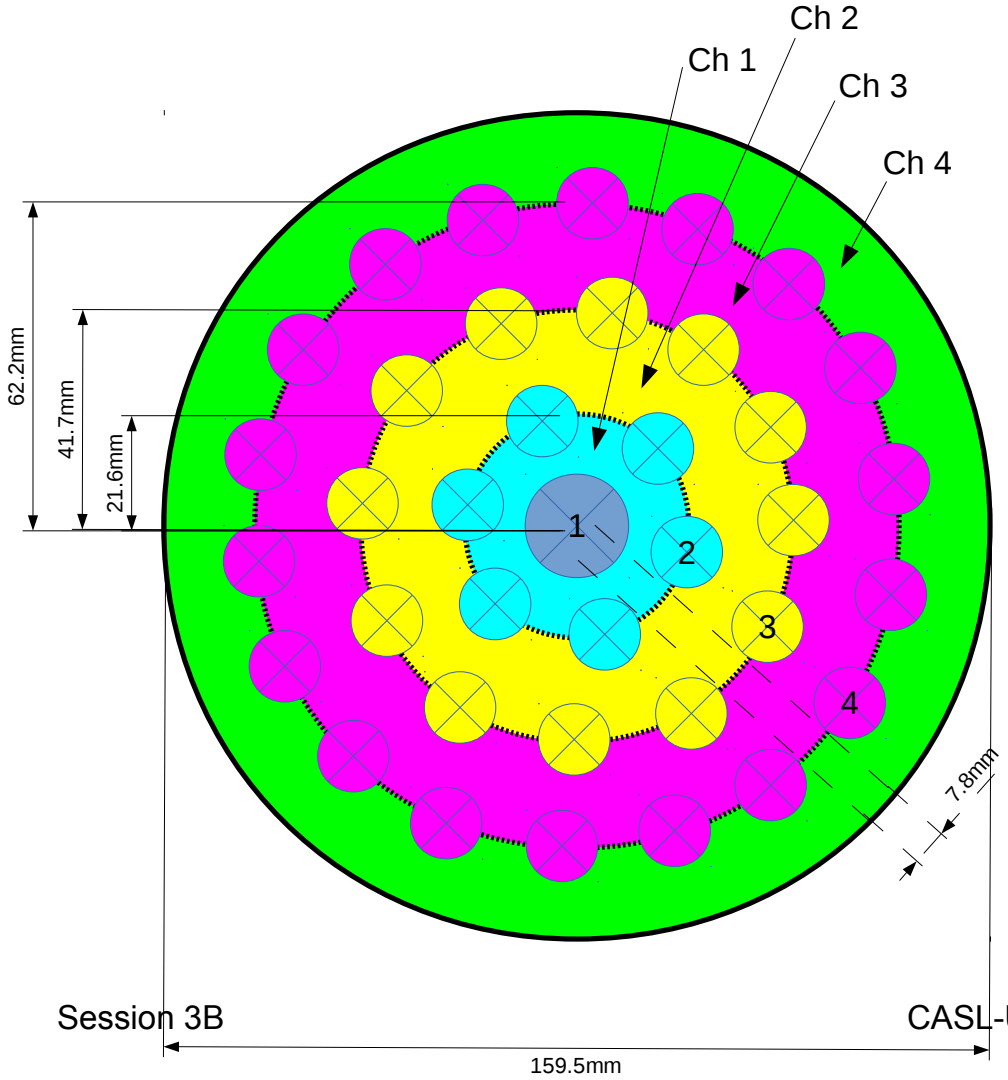

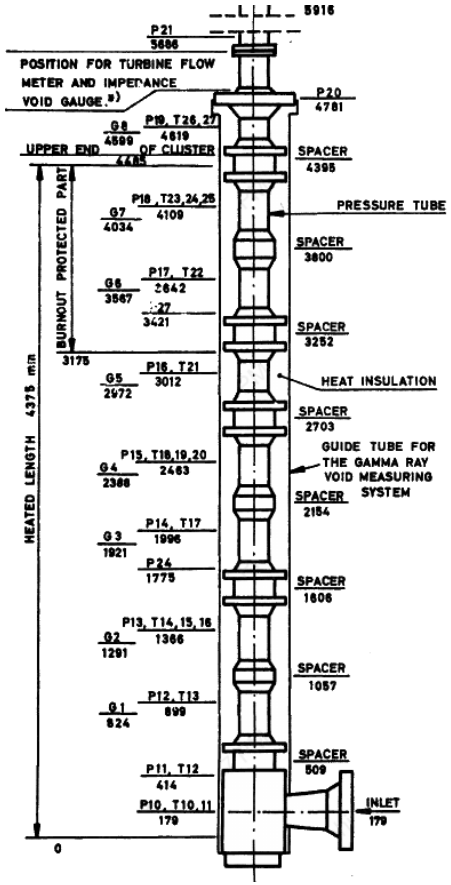

The Experiments
FRIGG

Introduction
The Experiments
Conclusion

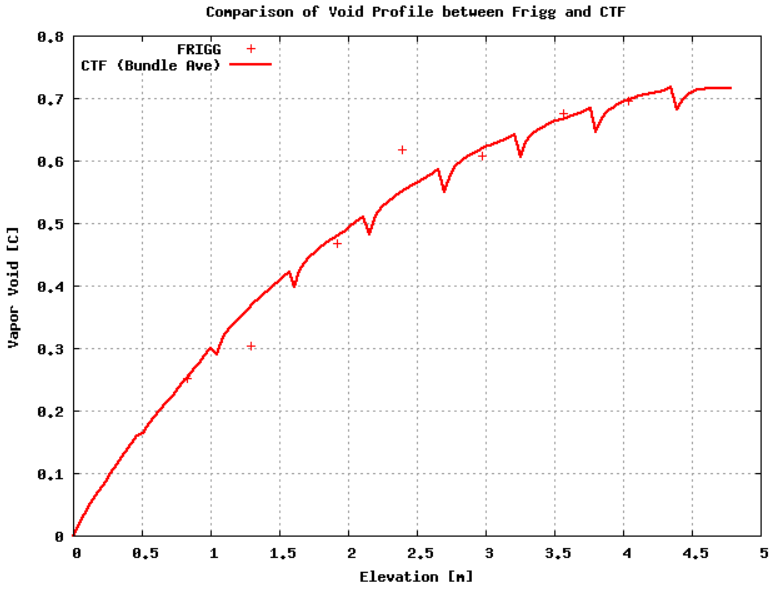

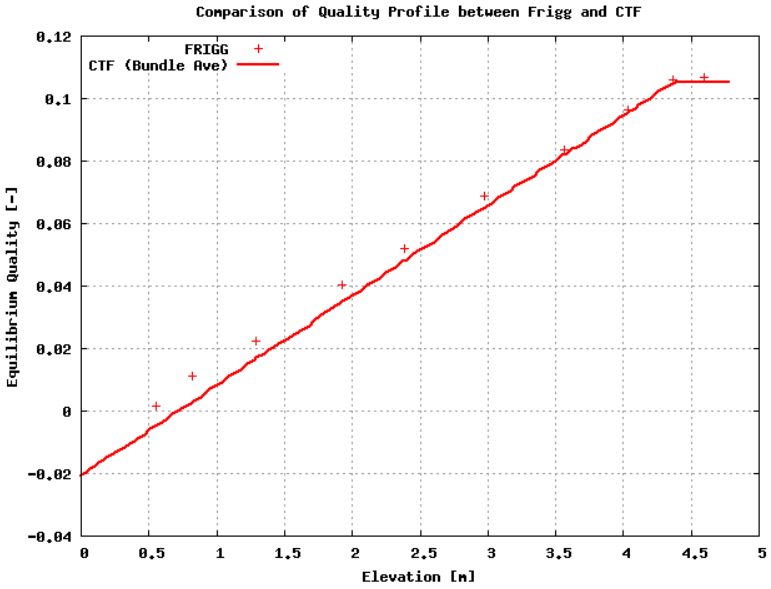

The Experiments
FRIGG

Introduction
The Experiments
Conclusion

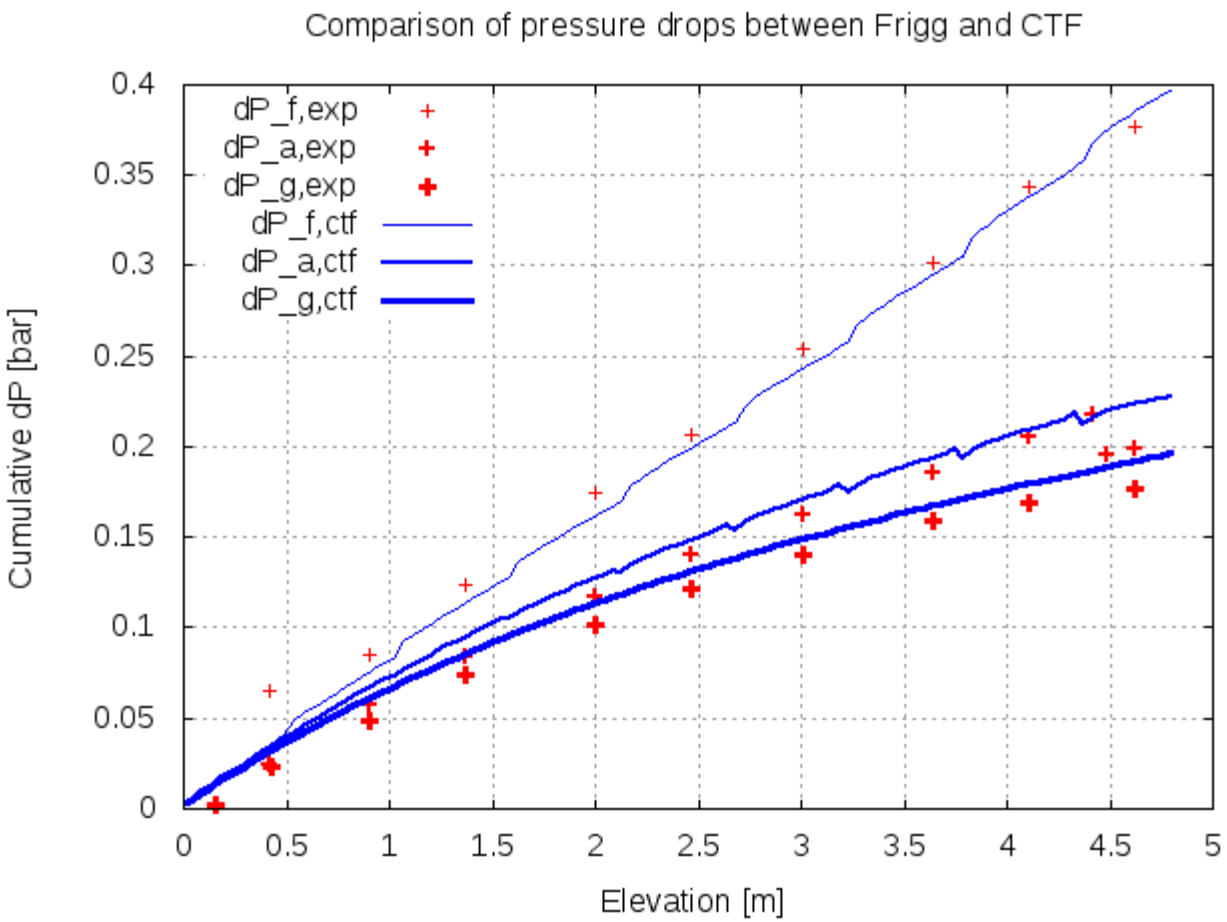

The Experiments
Harwell Tube

Introduction
The Experiments
Conclusion

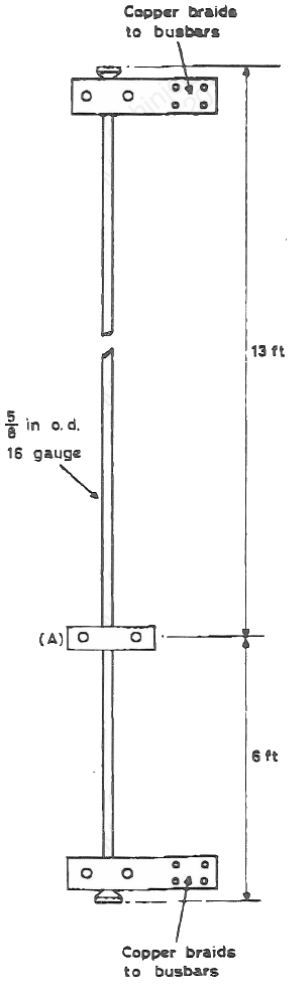

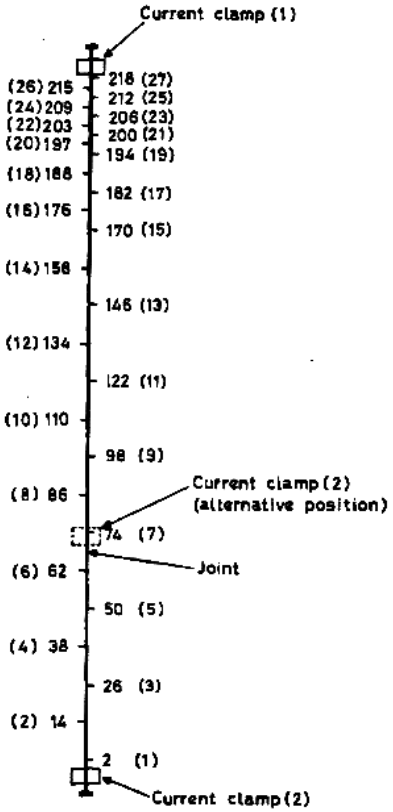

The Experiments
Harwell Tube

Introduction
The Experiments
Conclusion

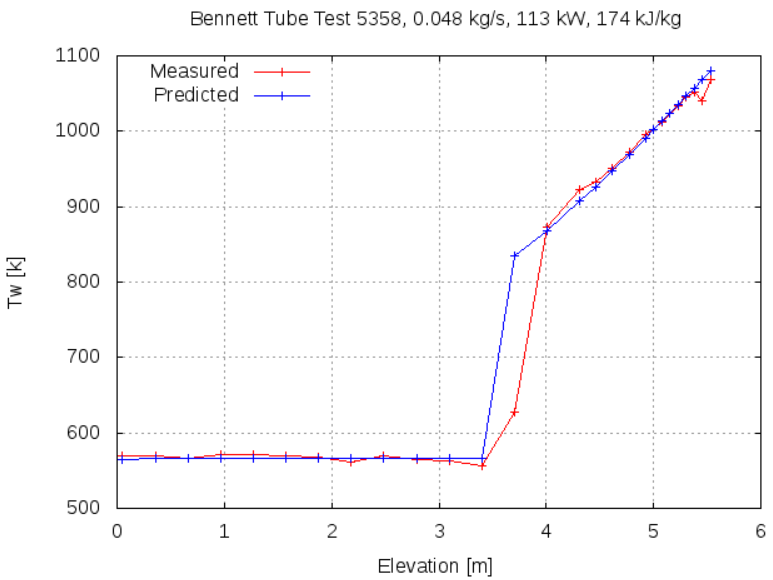

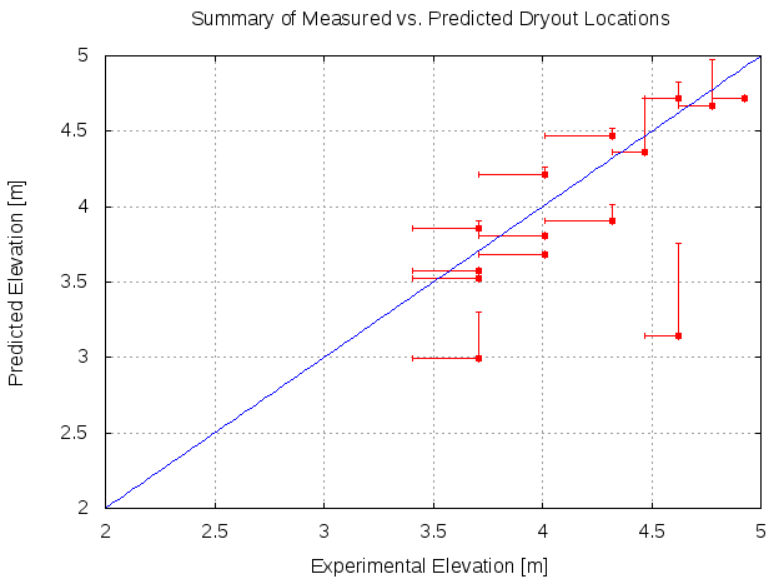

The Experiments
PNNL 2x6

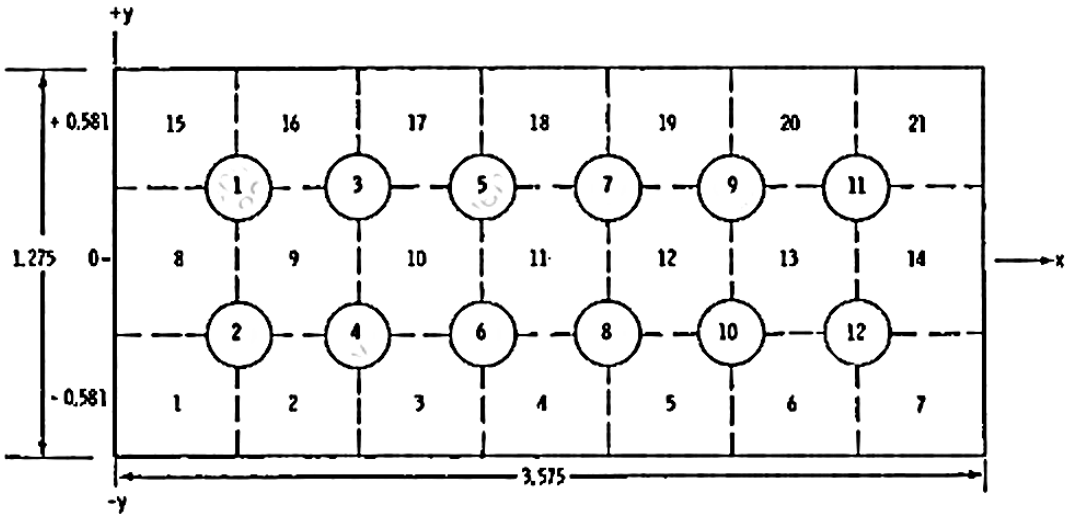

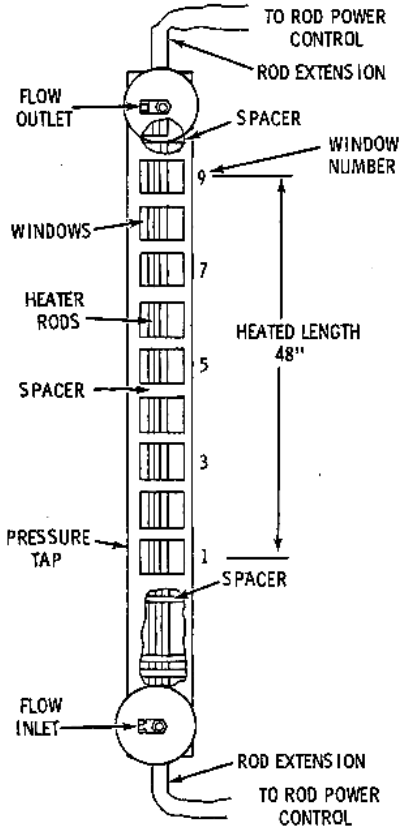

The Experiments
PNNL 2x6

Introduction
The Experiments
Conclusion

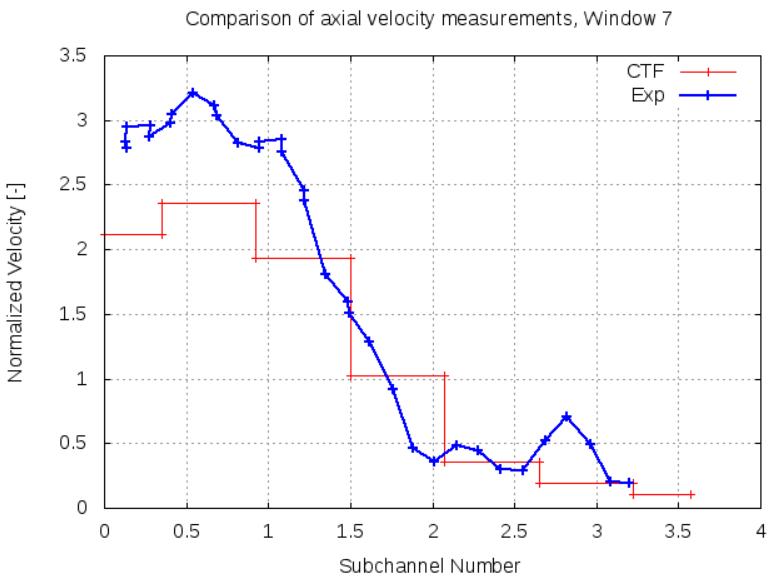

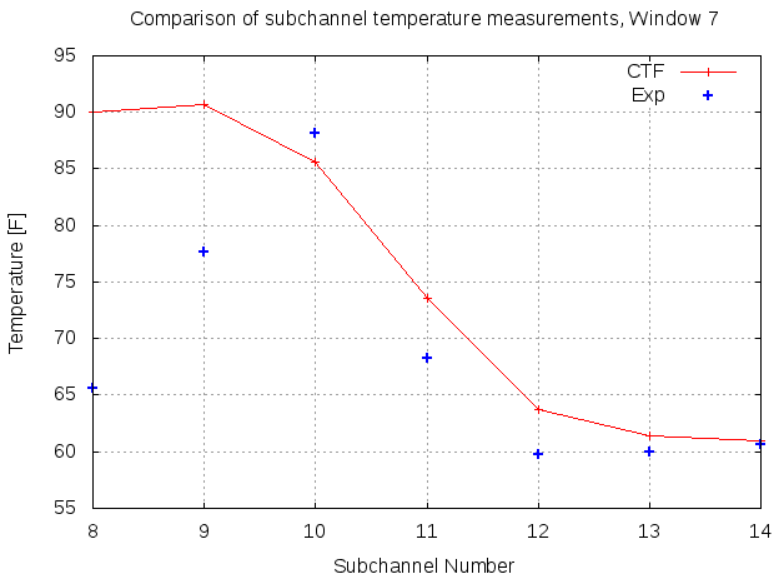

Conclusion

Introduction
The Experiments
Conclusion

- Modeled a broad range of experiments with CTF
- Began summarizing these results into validation document
- This milestone will be completed by finishing results summary in document
- Future tasks:
  - More quantitative analysis of results
  - Expand on document with code and solution verification

VERA-CS Validation Plans and Activities

Andrew Godfrey, ORNL

2014 CASL Round Table Virtual Meeting
July 14, 2014

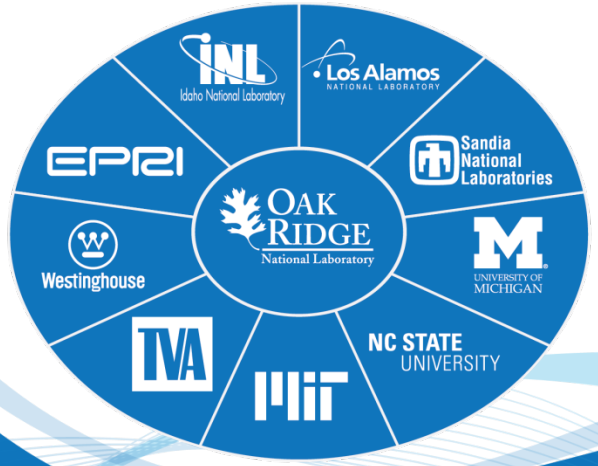

Milestones

- March 29, 2012: L3:AMA.VAL.P4.01 – Hongbin Zhang
  - "*Review of Experiments for CASL Neutronics Validation*", CASL-U-2012-0039-000, March 29, 2012.

- August 29, 2014: L3:PHI.VCS.P9.04 – Godfrey
  - Core Simulator Validation Plan
  - Contributors: Gehin, Palmtag, Wieselquist
  - Likely to be changed to September 30th due to other emerging work

- More to come…

Pure planning until VERA-CS is ready

Validation Plan Goal

- Frequent code changes
- Limited availability of benchmark data
- Funding typically supports development but not validation
- M&S supports education and research, not safety-related activities

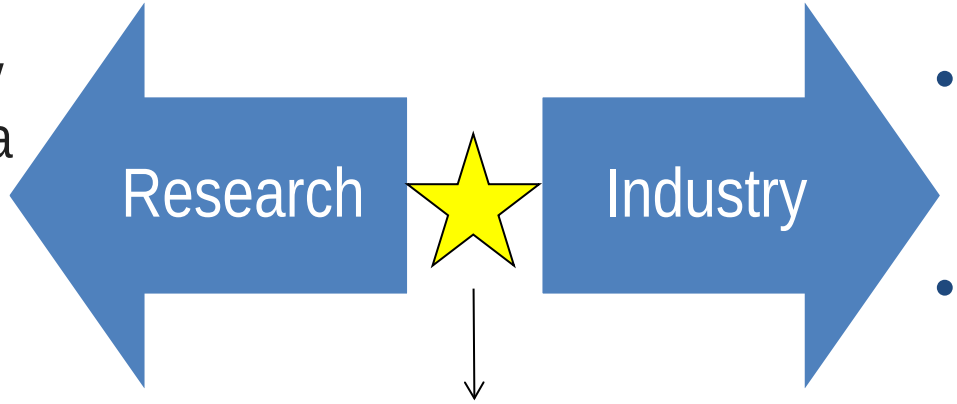

VERA-CS

- Establish confidence in code capabilities and accuracy
- Ensure flexibility for many reactor/fuel design types
- Demonstrate value and encourage investment from industrial users

- Static code versions
- Access to large volume of benchmark data
- Extensive validation and benchmarking
- M&S supports plant/fuel design, operation, and licensing

Balance is needed to ensure Industrial impact

VERA-CS Validation Vision

- Benchmarking and Validation of *integrated* product
- Consistent with industry core simulator (ANC, SIM-3, etc.) methods and activities (but on a smaller scale)
- Utilize all components from input to output (when possible)
- Produce documentation for consumption by end users with licensing-grade quality (but not directly for licensing)
- Primary focus on operating reactors with supplementation from experiments and continuous-energy Monte Carlo methods
- Required to establish credibility with nuclear power industry for nearly any advanced VERA application (i.e. Challenge problems)

Integrated VERA-CS validation is in addition to validation of components

Nuclear Power Plant Operating Data

- Watts Bar Unit 1
  - Cycles 1 & 2
  - Prioritize recent cycles (6?-13)
- Watts Bar Unit 2 startup – 2016
- BEAVRS Cycles 1 & 2
  - Limited data

- Additional TVA plants (Sequoyah?)
- WEC customers/partners?
- Industry Council sites?
  - Duke, Dominion, Exelon, Areva
- Other plant/fuel types?
  - B&W 15x15, CE 14x14, 16x16, gad, etc.

- Actual data is fairly coarse:
  - BOC physics tests (temperature coefficients, control bank worths)
  - Core average reactivity vs. power and exposure
  - Average fuel assembly powers for 1/3rd of the core about every month
  - Flux maps provide very detailed axial shapes in instrument tube
  - No rod level data

Will need increased cooperation with industry

Critical Experiment Data

- Provides rod level powers at cold conditions for small reactor-like geometries
- Will require 3D and/or 2D+axial buckling capability
- Geometries may not be supported by the common input
- Does not validate T/H capabilities, neutronics feedback, or depletion
- Measurement uncertainty can be significant, and population size can be small

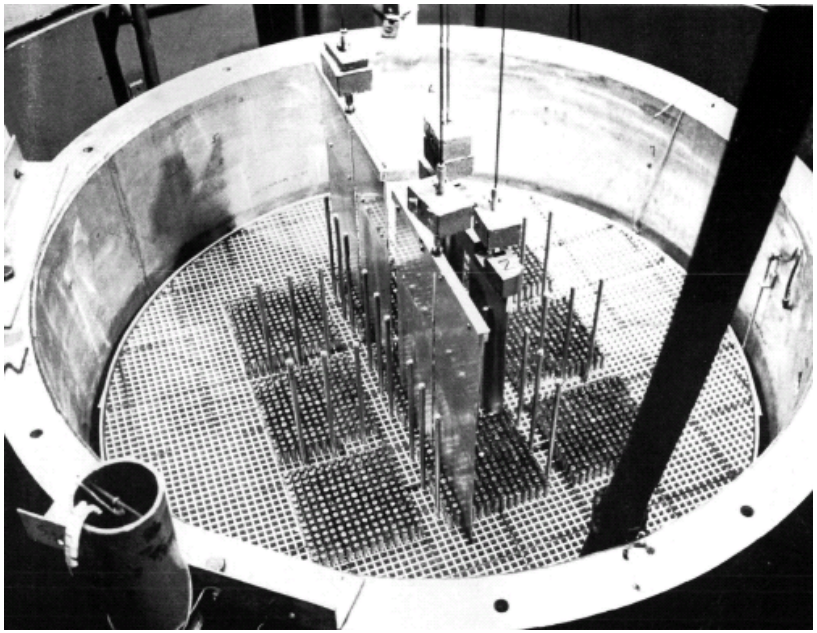

- Example Experiments
  - B&W, Kritz, Strawbridge-Barry, Venus, Dimple, Saxton, etc.
  - NEA IRPhEP and ICSBEP handbooks

Criticals have limited value but are standard procedure for establishing pin power uncertainties

B&W 1484 Criticals w/MPACT - Collins (Preliminary)

- Core 1 and 2 use same pin geometry in different configurations
- Different coolant boron concentration
- Minor issues with axial buckling and scattering treatments

	Core 1	Core 2	Difference
P0	1.10278	1.04317	5961
TCP0	Unstable	Unstable	--
P1	0.99900	1.00174	-274
P2	1.00168	1.00253	-85
P3	1.00150	1.00243	-93

- Will Gurecky (Univ. of Texas-Austin) is developing common input models for 1484 and 1810 and documenting issues

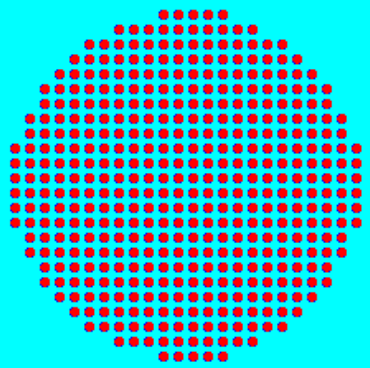

Core 1

Core 2

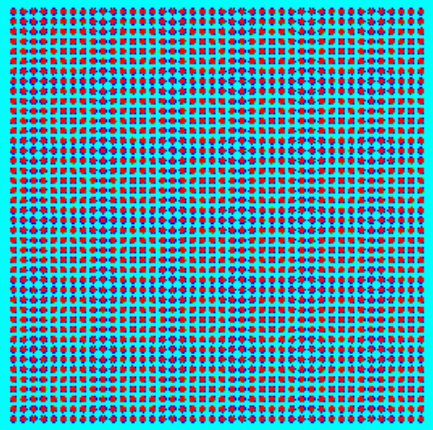

Shift and OpenMC results - Pandya

B&W1810 core 13 XY slice

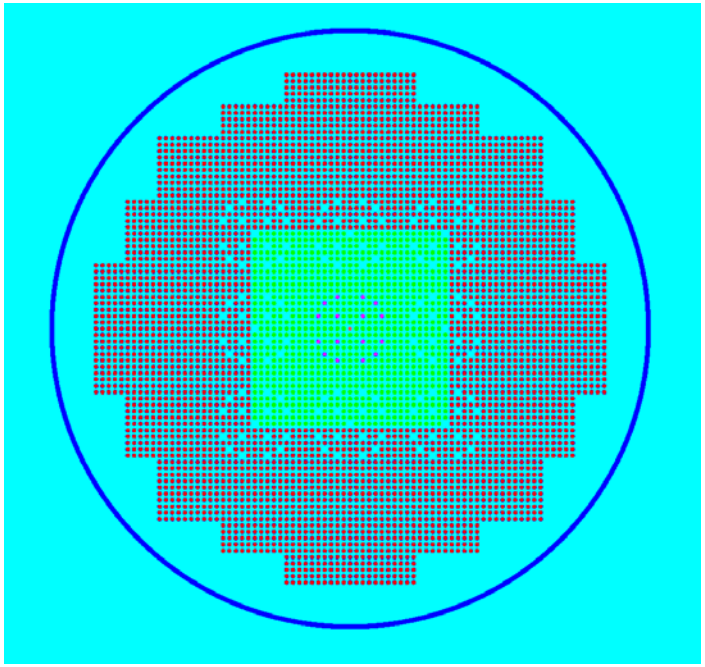

- Shift - ORNL
  - Using RTK geometry run through **python** frontend
  - Run on Remus using 64 processors
  - Did not model top grid plate
  - No vessel for B&W1484 cores
  - Using AMPX processed ENDFVII.0 data
- OpenMC - MIT
  - Run on MIT machine using 128 processors
  - Using NJOY processed ENDFVII.0 data

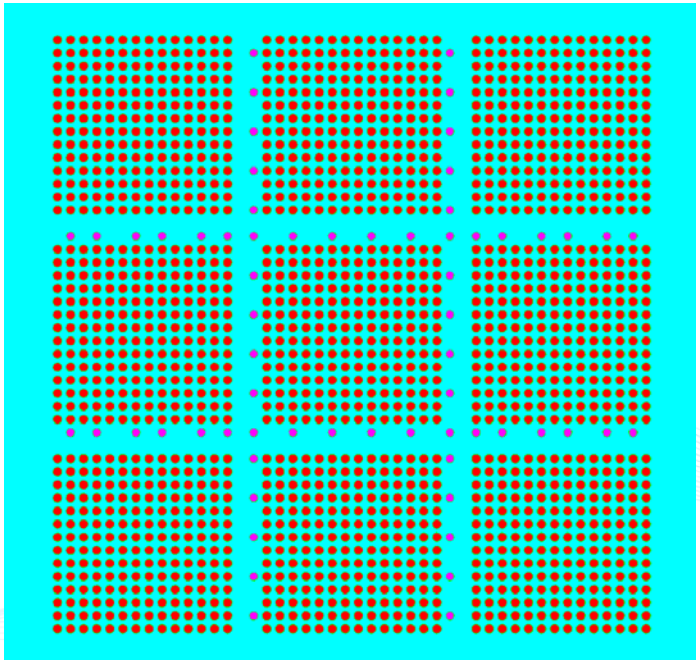

B&W1484 core 5 XY slice

B&W1810 Reactivity Comparisons - Pandya

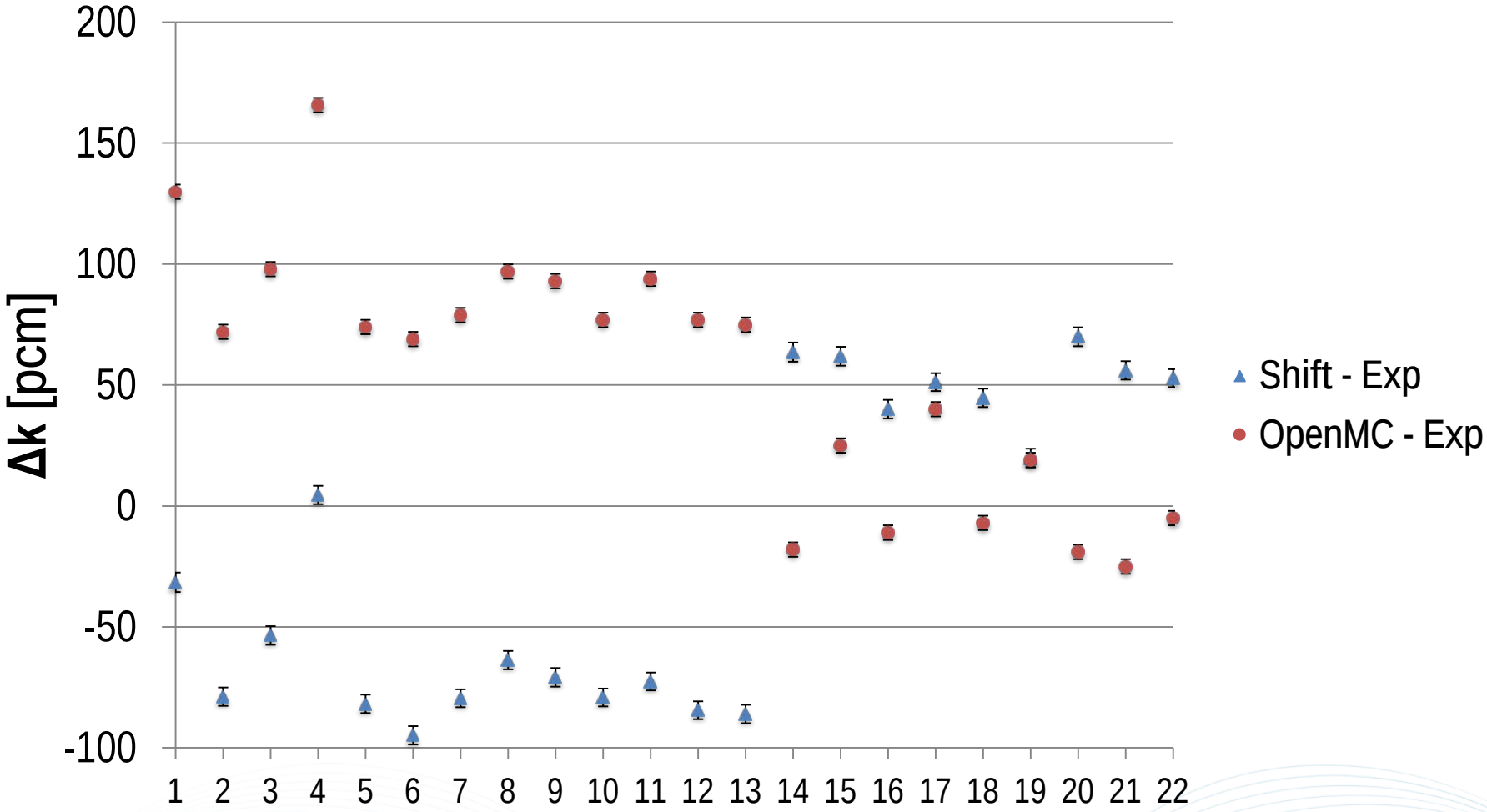

B&W1810 Core III pin power comparison - Pandya

- Core III relative power difference with OpenMC
- 2.46 wt % fuel
- Max: 2.0%
- Most: < 1.5%

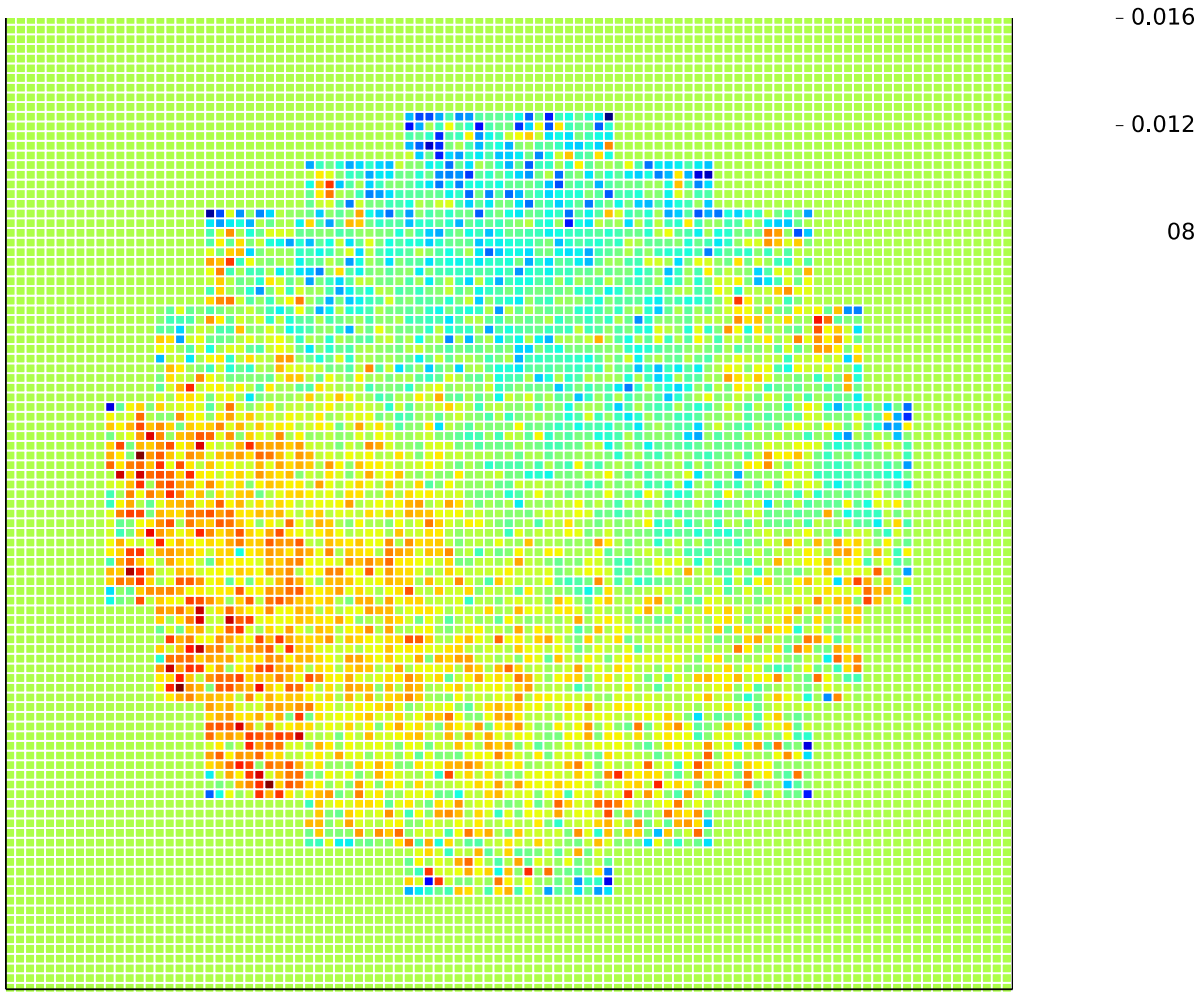

Isotopics Data

- Limited post-irradiation data is available publicly
- Difficult to get operating history for measured rods/assemblies
- Working with the ORIGEN/SCALE team, top three possibilities for comparison to PIE data following actual plant operation
  - Calvert Cliffs
  - Malibu
  - TMI-1
- Five MOX LTA rods from Catawba brought to ORNL for examination
  - Would require Duke, Westinghouse, Areva, and ORNL joint collaboration

Plan still being developed

CE Monte Carlo Used to Fill the Gaps

- Not validation, but most rigorous and computationally expensive neutronics method
- Can provide a high-fidelity reference for pin (and sub-pin) power distributions for reactor operating conditions
- Latest methods have on-the-fly doppler broadening and thermal scattering interpolation for operating conditions
- Latest methods can deplete small problems in continuous-energy and track thousands of isotopes
- Will eventually have capability to get isotopic distribution from MPACT for transport calculation
- However, this is still active research….

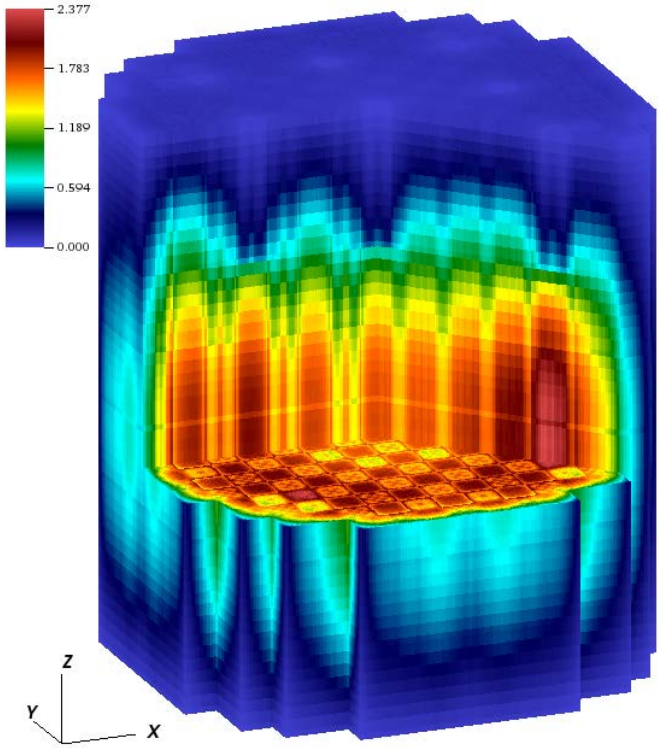

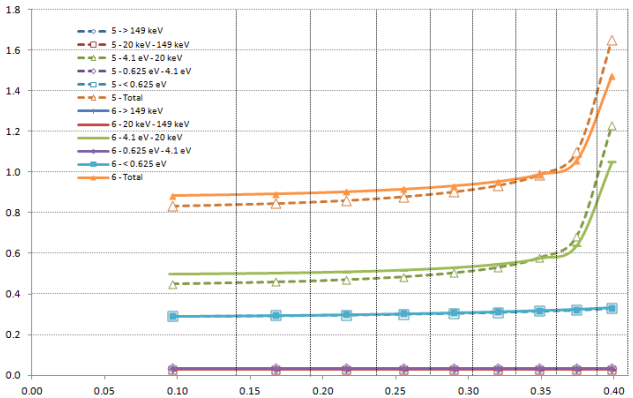

More rigorous than Industry practice

Summary

- VERA-CS Validation is an integrated product activity
  - Focus on MPACT+CTF
  - Repeatable for other codes/combinations if desired
- Plan will be a long term, living document
- Focused on operating power reactors
  - Will need more data and collaboration with Industry
- Critical experiments
  - B&W criticals in progress
- PIE data comparisons – coordination with ORIGEN team
- Will supplement measured data with continuous-energy Monte Carlo (KENO, MCNP, Shift, MC21) results when useful
  - Pin-by-pin power distributions at operating or depleted conditions
  - Sub-pin power distributions and continuous-energy depletion

Questions / Comments / Feedback

godfreyat@ornl.gov

Consortium for Advanced Simulation of LWRs

Development of Zirconium Oxidation and Hydride Modeling for Peregrine:

- Zr Alloy Corrosion/Oxidation
- Hydrogen Pickup
- Hydride Precipitation

Bilge Yildiz, Mike Short (MIT), Anton Van der Ven (UM/UCSB),
Katsuyo Thornton, Gary Was, Wei Lu, Michael Thouless (UM),
Dane Morgan, Izabela Szlufarska (UW),
Rob Montgomery, Dion Sunderland (PNNL)

2014 CASL Roundtable Virtual Meeting

July 15, 2014

Zr-H-O Team

- PNNL
  - Robert Montgomery <Robert.Montgomery@pnnl.gov>
  - Dion Sunderland <dion.sunderland@pnnl.gov>
- MIT
  - Bilge Yildiz <byildiz@mit.edu>
    - Mostafa Youssef <myoussef@mit.edu>
    - Ming Yang <yangm@mit.edu>
  - Mike Short <hereiam@mit.edu>
    - Andrew Dykhuis <adykhuis@mit.edu>
- U Michigan
  - Anton Van der Ven (now UCSB) <avdv@engineering.ucsb.edu>
  - Katsuyo Thornton <kthorn@umich.edu>
    - Andrea Jokisaari <anmida@umich.edu>
  - Michael Thouless <thouless@umich.edu>
    - Wei Lu <weilu@umich.edu>
    - Hai Wang wanghai1208@gmail.com
  - Gary Was <gsw@umich.edu>
    - Peng Wang <wpf@umich.edu>
- U Wisconsin
  - Dane Morgan ddmorgan@engr.wisc.edu, Izabela Szlufarska <szlufarska@wisc.edu>
    - Ming-Jie Zheng <mzheng@cae.wisc.edu>

MPO Zr-H-O Framework – Problem View

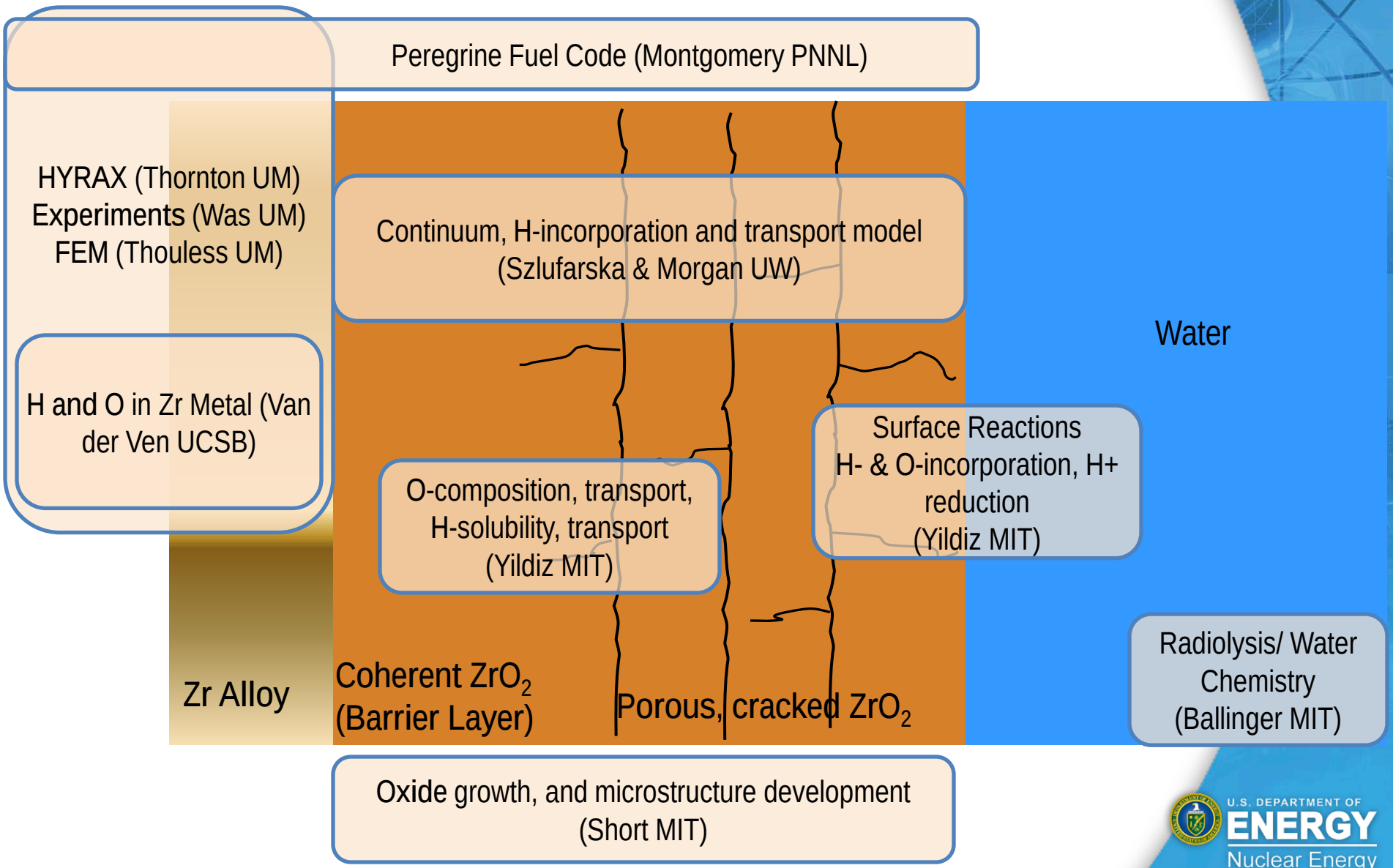

MPO Zr-H-O Framework – Flow Chart

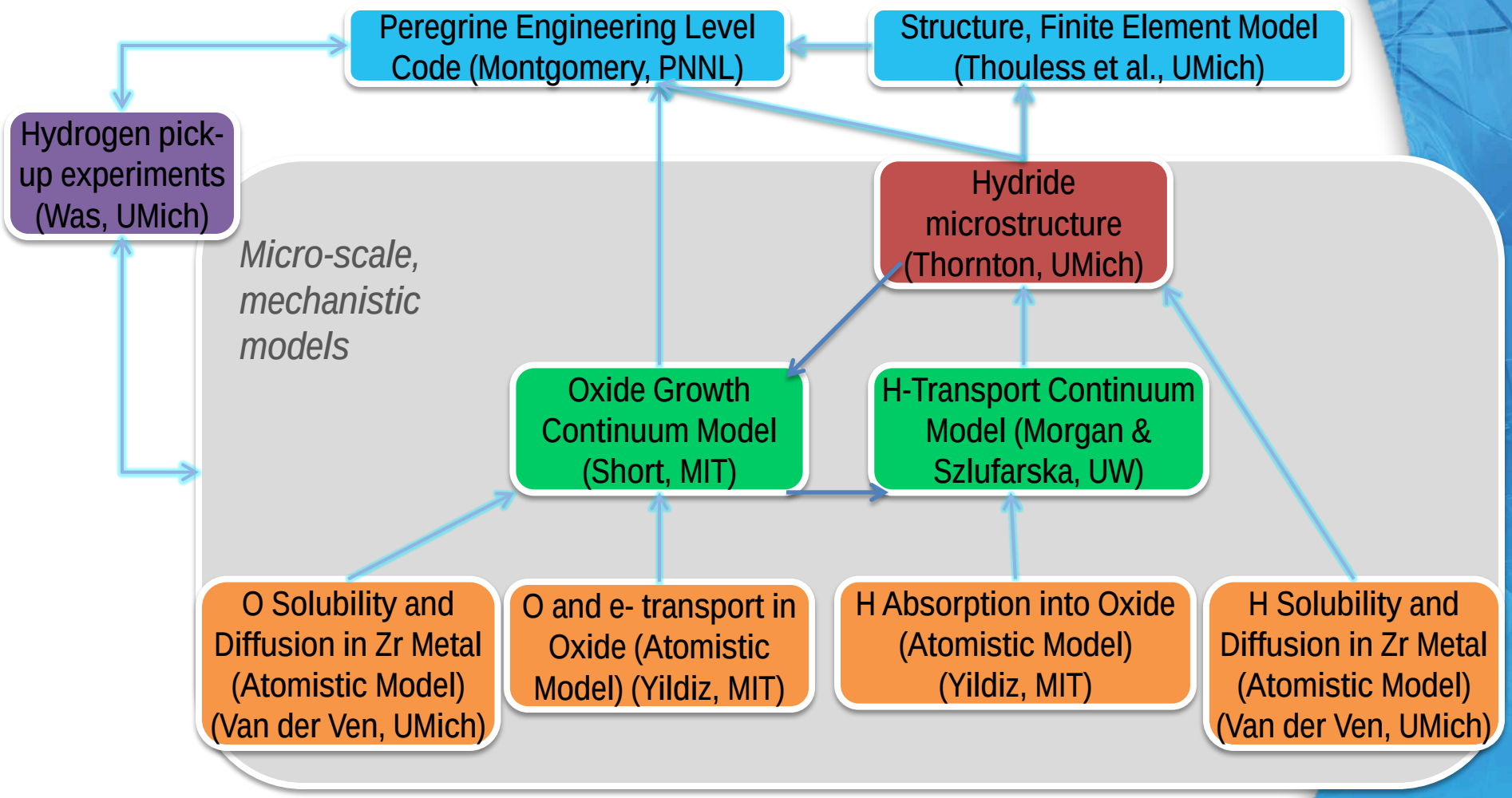

Roadmap to multiscale modeling of corrosion and hydriding of cladding

Macroscale

Engineering Scale Code (Peregrine)
Calculate impact on temperature of thermal resistance from corrosion/crud layer, on stress distribution due to metal loss/volume changes, on mechanical properties of hydrogen content/distribution.
Peregrine Interface: interrogate model/table of corrosion layer thickness provided by corrosion model as function of metal-oxide temperature, coolant chemistry, etc, oxide layer integrity, etc. Interrogate model/table for hydrogen content and distribution.

Mesoscale

Meso/Macro scale model for corrosion layer growth that includes effect of local temperature, material chemistry and microstructure, irradiation damage, and coolant chemistry

Meso/Macro scale model for hydrogen diffusion and hydride precipitation that includes effect of local temperature, material chemistry and microstructure, irradiation damage, and stress distribution

Oxygen transport through realistic microstructure

Oxide growth and microstructure development kinetics

Hydrogen transport through realistic oxide microstructure

Hydrogen diffusion and precipitation in Zr microstructure, chemistry, and stress

Microscale

Oxygen and hydrogen diffusivity

Diffusivity of vacancies & interstitials in ZrO_2 (MD calculation based on atomistic potentials)

Evolution of defects (clusters, loops) in ZrO_2 with irradiation dose and interaction with dislocations

Surface Reactivity at oxide-water interface (hydrogen, oxygen, and impurity)

Oxide structure (monoclinic & tetragonal), porosity structure, and grain structure

Clad microstructure evolution dislocation density, grain boundary orientations, etc. (Clad group)

Atomistic modeling of O and H incorporation into and transport in *Zr-oxide*

Mostafa Youssef and Bilge Yildiz, MIT

Objective: Predict oxygen diffusivity, hydrogen solubility, hydrogen transport, surface reaction kinetics in ZrO_2 calculated from first principles; and provide these thermodynamic and kinetic parameters as input to meso/macro scale models at UW and MIT.

The key point we will build up to in this presentation (MIT part): The 'valley' of hydrogen absorption on the electron chemical potential space of the Zr-oxide

M. Youssef and B. Yildiz (in review, 2014)

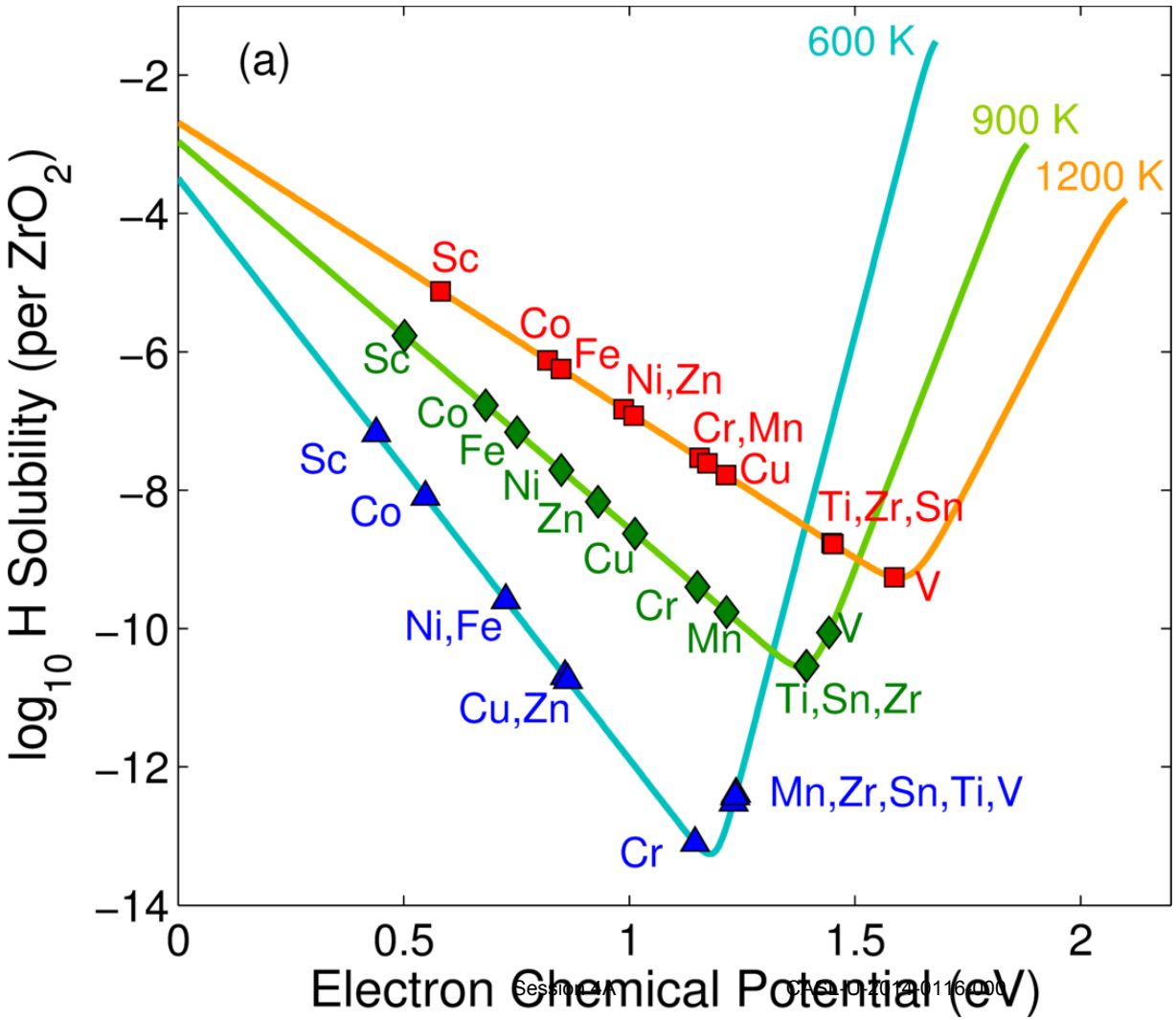

- We uncovered the ***electron chemical potential*** (or, equivalently the Fermi level, E_F) as the ***descriptor*** of the absorption of hydrogen into ZrO2.
- Higher E_F also accelerates H-reduction and H_2 gas evolution on the surface. ***Good!***
- **Provides a physics-based guide for Zr-alloy design to minimize H-pick-up.**
- **Provides H-solubility values for the hydrogen-pick-up model of UW-Madison team.**

Objective: Develop and provide atomistic and quantitative models as input to continuum level corrosion and hydrogen pickup models

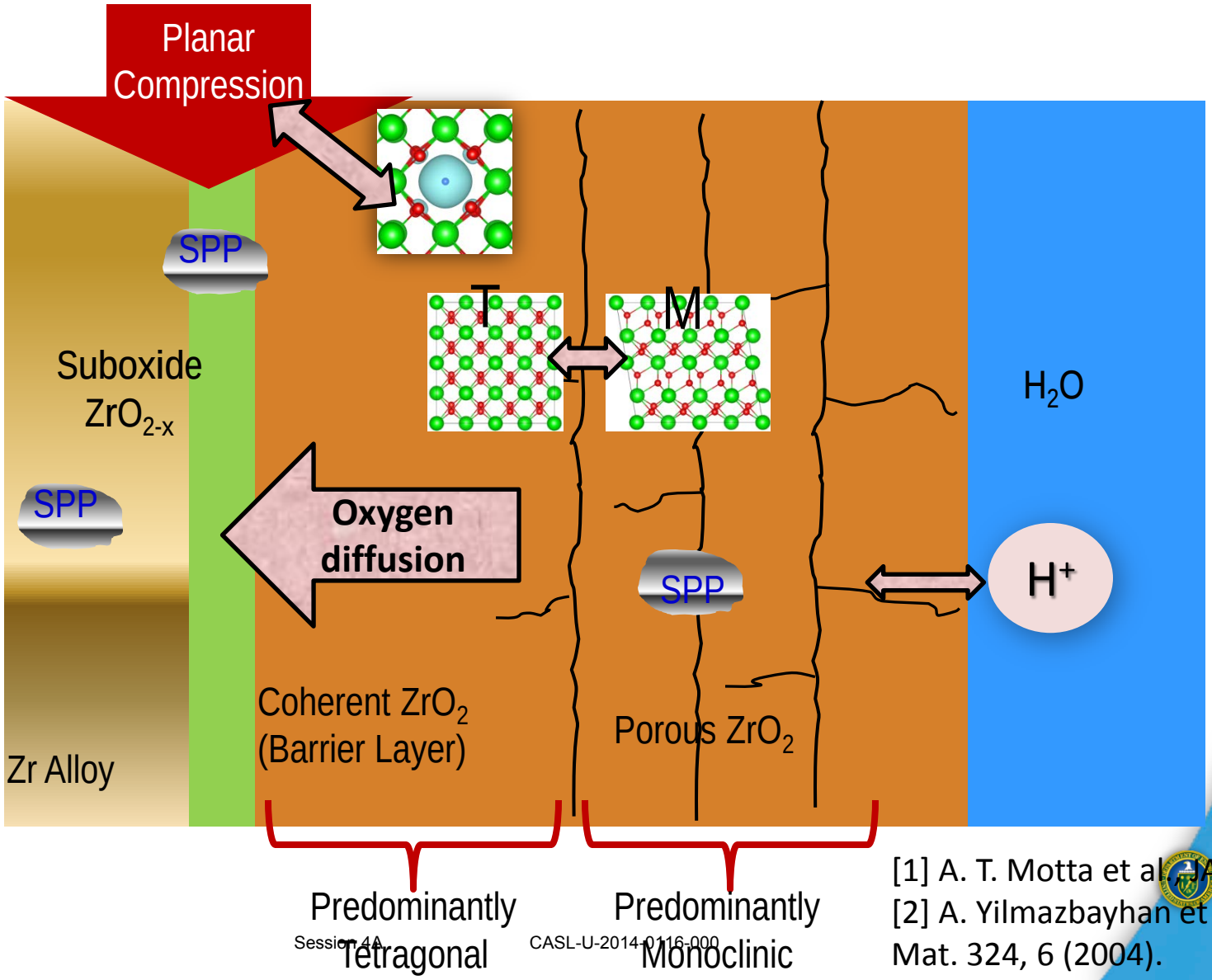

[1] A. T. Motta et al., JAI 5 (2008).
[2] A. Yilmazbayhan et al., J. Nucl. Mat. 324, 6 (2004).

Mechanisms and kinetic parameters are needed to model corrosion and hydrogen pick-up kinetics

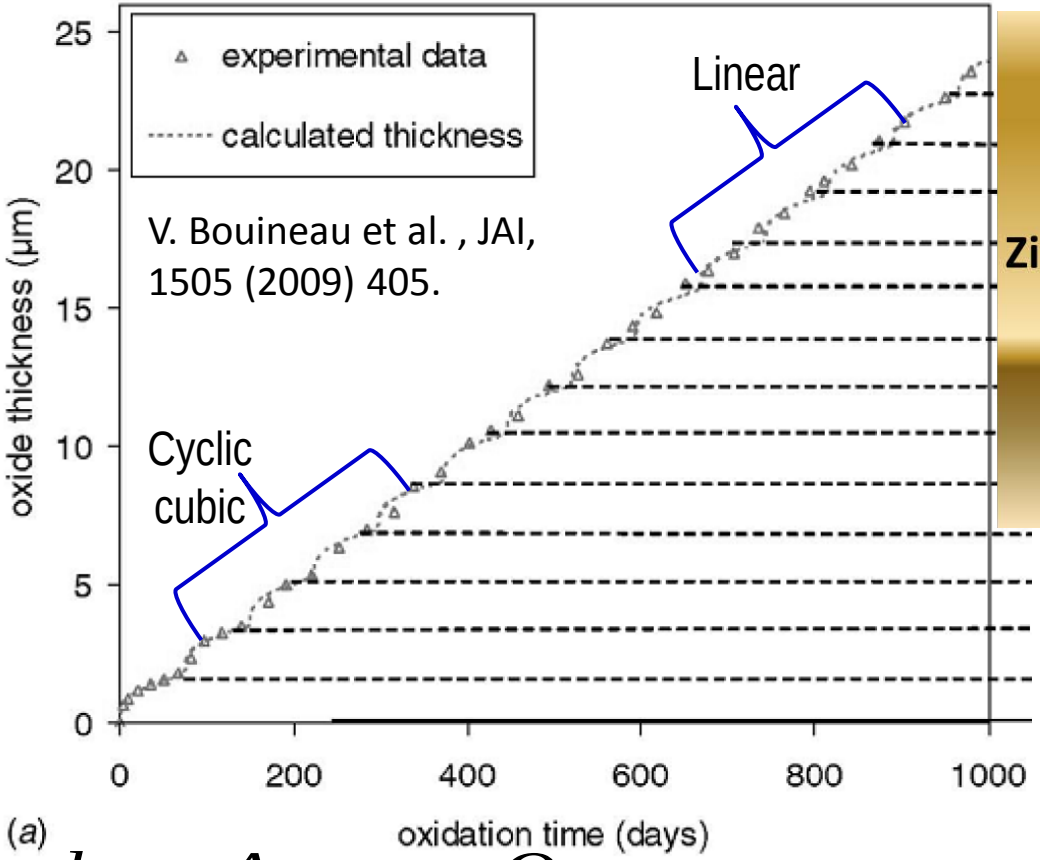

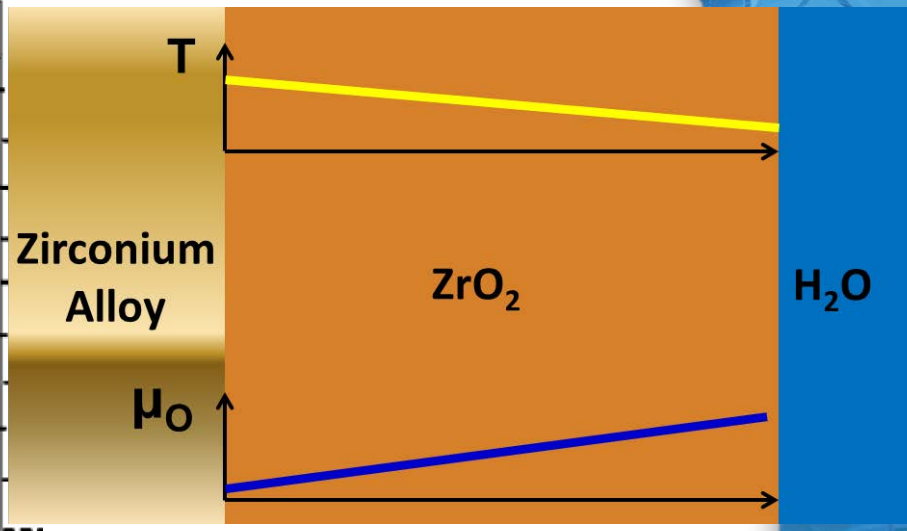

Self-diffusion (T, μ_O)
→ modeling corrosion kinetics

$$\frac{ds}{dt} = \frac{A}{s^2}\exp\left(\frac{-Q_1}{RT_1}\right) : s < 2micron$$

FRAPCON 3

$$\frac{ds}{dt} = \{C_0 + U(M\Phi)^p\}\exp\left(\frac{-Q_2}{RT_1}\right) : s > 2micron$$

Approach based on equilibria of point defects

Corrosion of zirconium alloys

H-pickup of Zirconium alloys

Density Functional Theory

Statistical Thermodynamics

Dilute Charged Defect Equilibria in a Metal Oxide

Oxygen Self-diffusion in ZrO_2

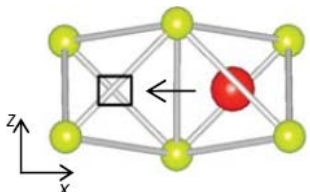

Hydrogen solubility

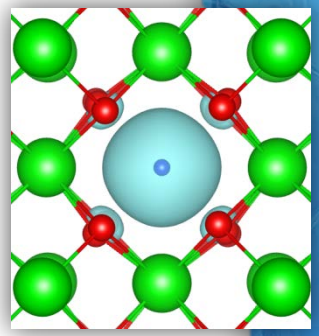

Kröger-Vink Diagram for tetragonal ZrO_2

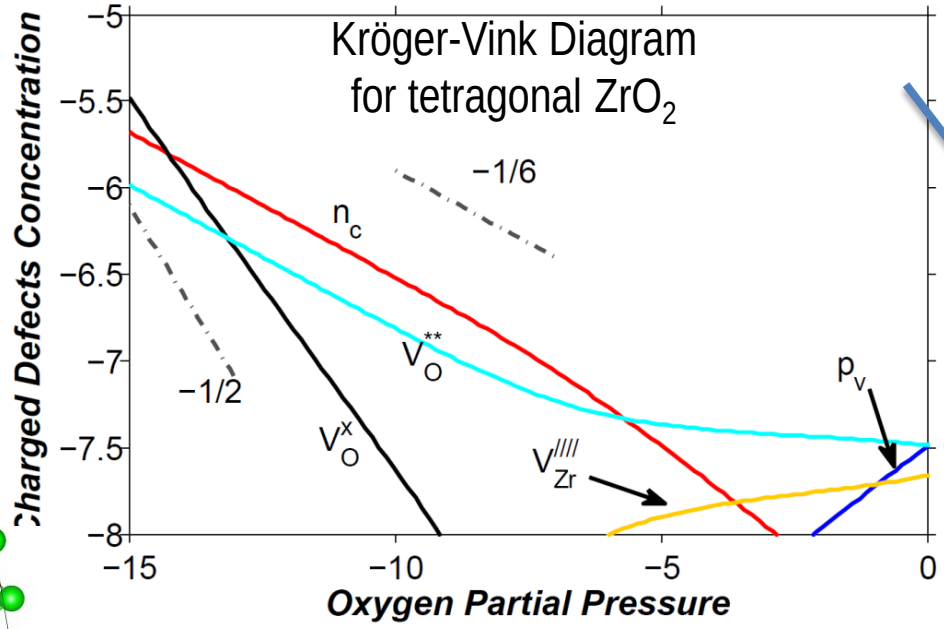

Tetragonal-Monoclinic transition

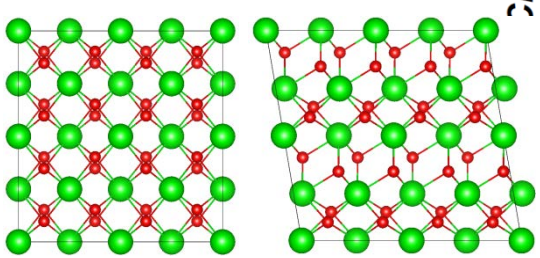

Interplay between stress and H

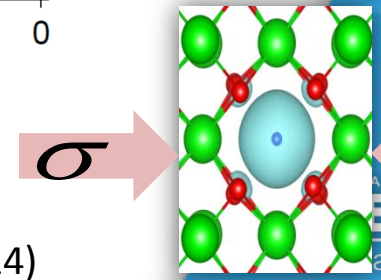

M. Youssef and B. Yildiz

Phys. Rev. B (2012 and 2014) and *PCCP* (2014)

+ one in review, and one in preparation

Corrosion of zirconium alloys

Equilibria of point defects

Oxygen Self-diffusion in ZrO_2

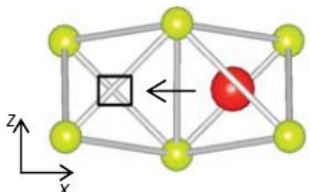

$D_O(T,P_{O2})$ =
Defect Concentration
x **Mobility**

Density Functional Theory

Statistical Thermodynamics

Dilute Charged Defect Equilibria in a Metal Oxide

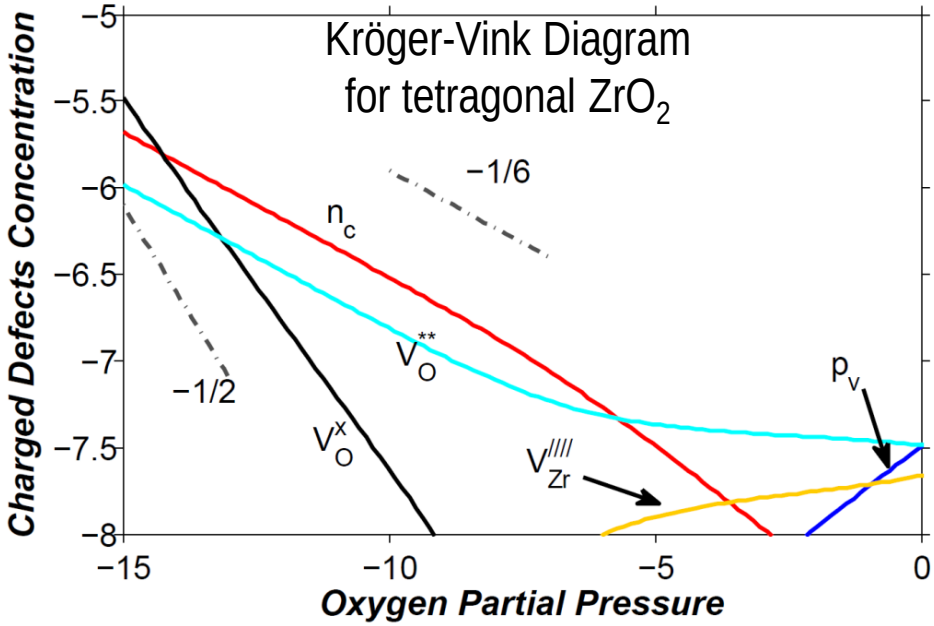

Oxygen diffusion (T, PO_2) = concentration x migration

Provides input for the oxidation model, HOGNOSE (Short)

Kröger-Vink diagram

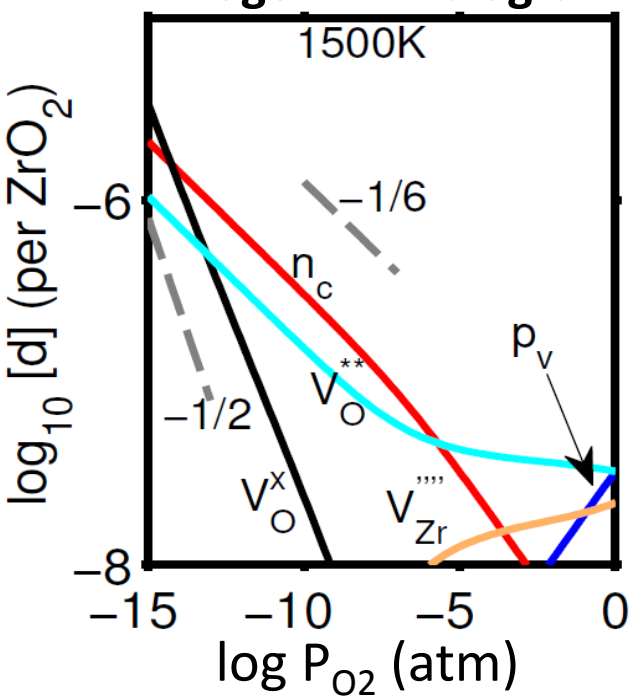

Random Walk Diffusion Theory

Oxygen diffusion coefficient (T, PO_2)

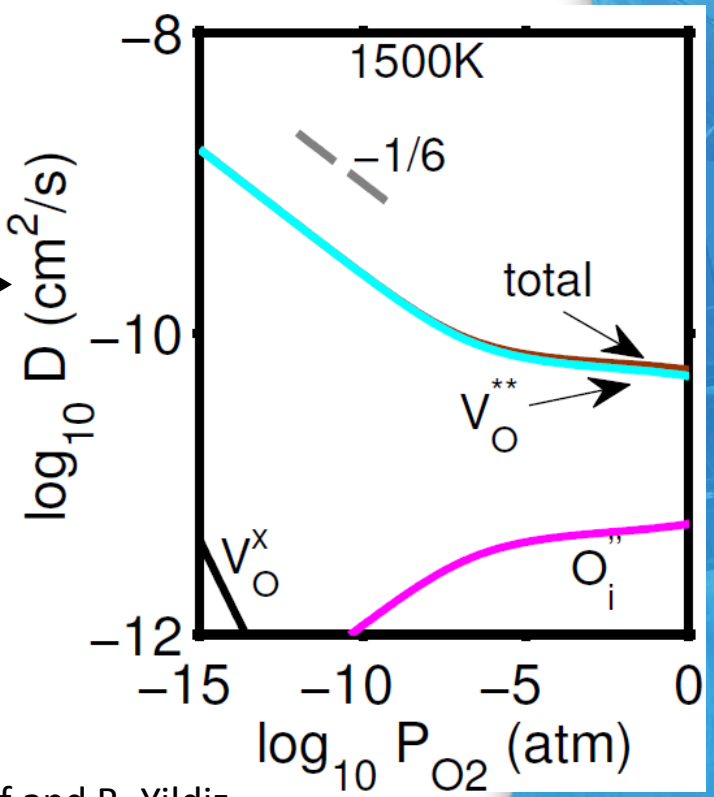

	<100>	<001>
$V_O^{\bullet\bullet}$	0.37	0.58
V_O^x	1.48	1.24

Migration barriers (eV) calculated using CI-NEB method

M. Youssef and B. Yildiz
Phys. Rev. B (2012 and 2014)

Validating the overall oxygen self-diffusivity

Experiments:
Park and Olander,
J. Electrochem. Soc. (1991)

Impurities explain the small difference from the experimental data.

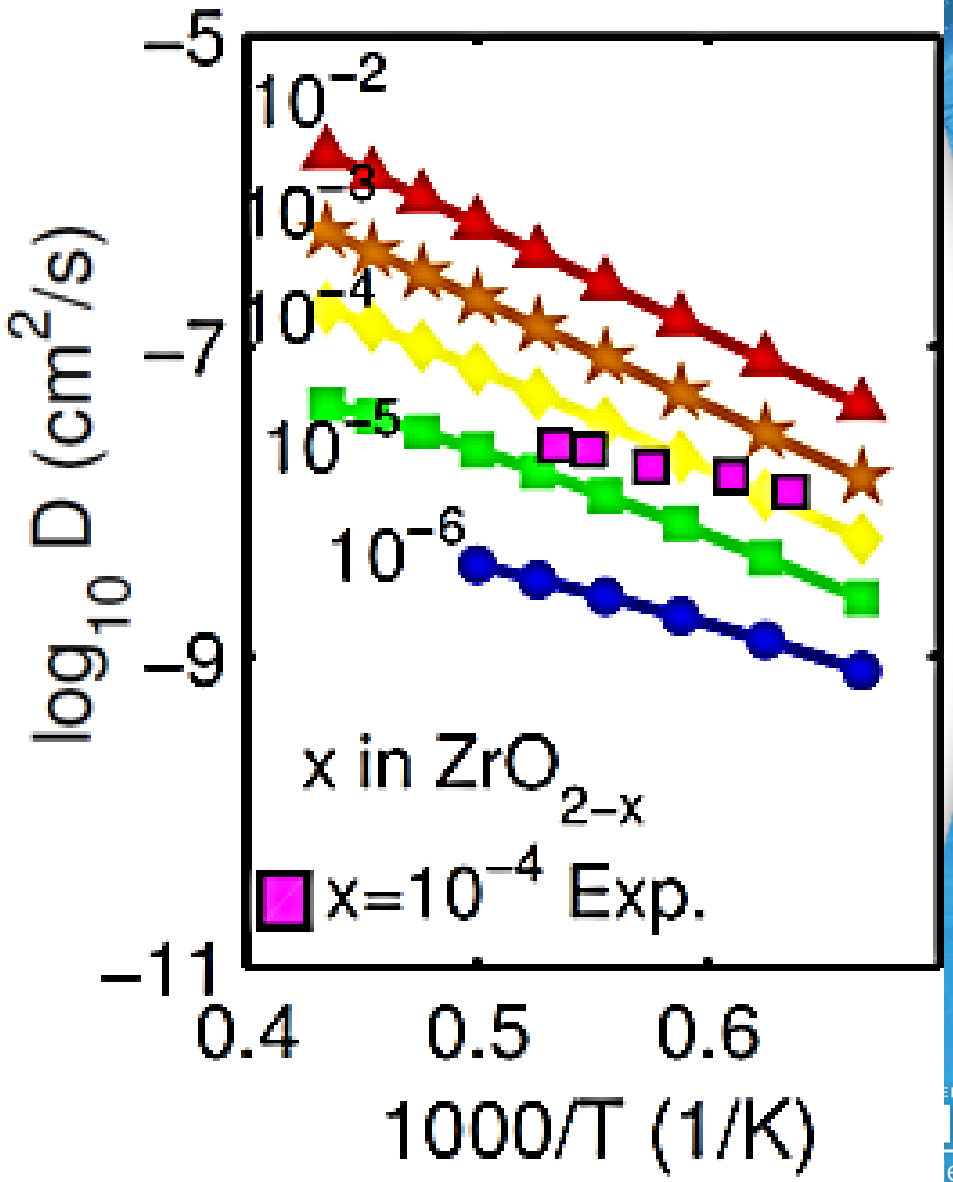

M. Youssef and B. Yildiz
Phys. Rev. B (2012 and 2014)

Objective: Develop and provide atomistic and quantitative models as input to continuum level corrosion and hydrogen pickup models

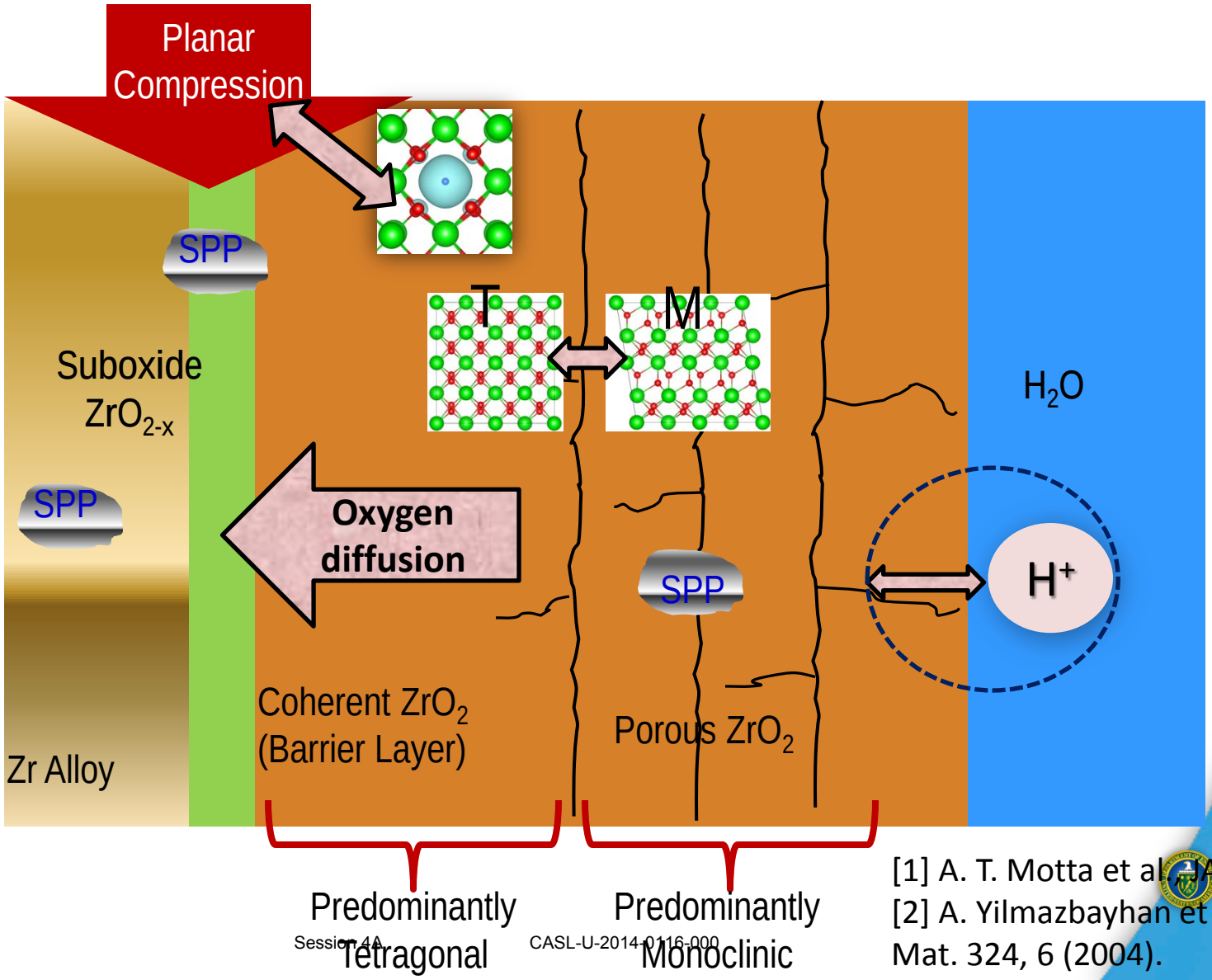

[1] A. T. Motta et al., JAI 5 (2008).
[2] A. Yilmazbayhan et al., J. Nucl. Mat. 324, 6 (2004).

Equilibria of point defects

H-pickup of Zirconium alloys

Density Functional Theory

Statistical Thermodynamics

Dilute Charged Defect Equilibria in a Metal Oxide

Hydrogen solubility

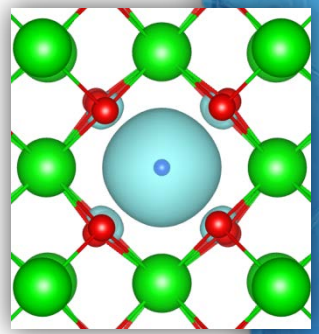

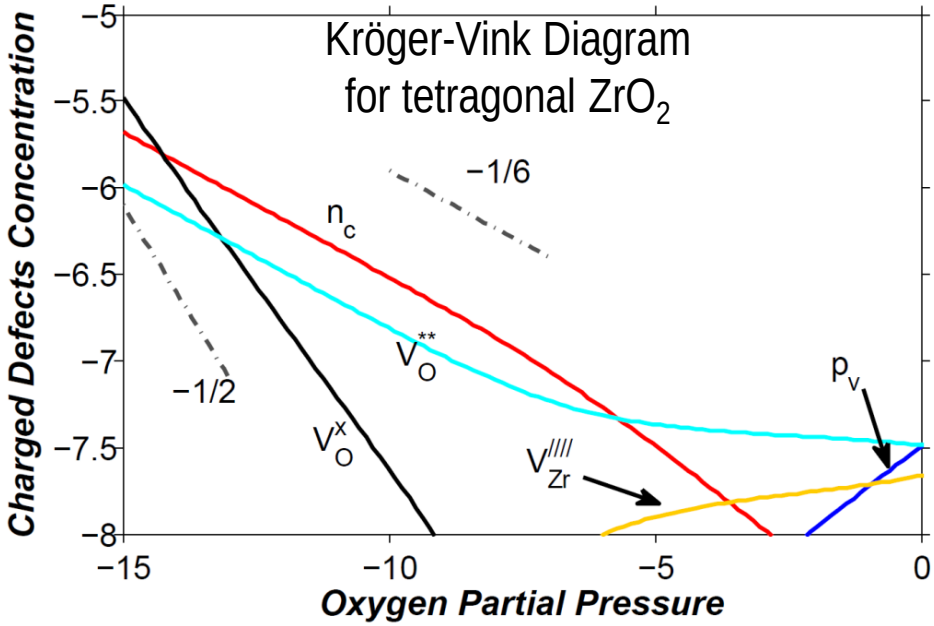

U.S. DEPARTMENT OF ENERGY
Nuclear Energy

Volcano of H-pickup (from 1960) can be explained by the chemical potential of electrons (in 2014)

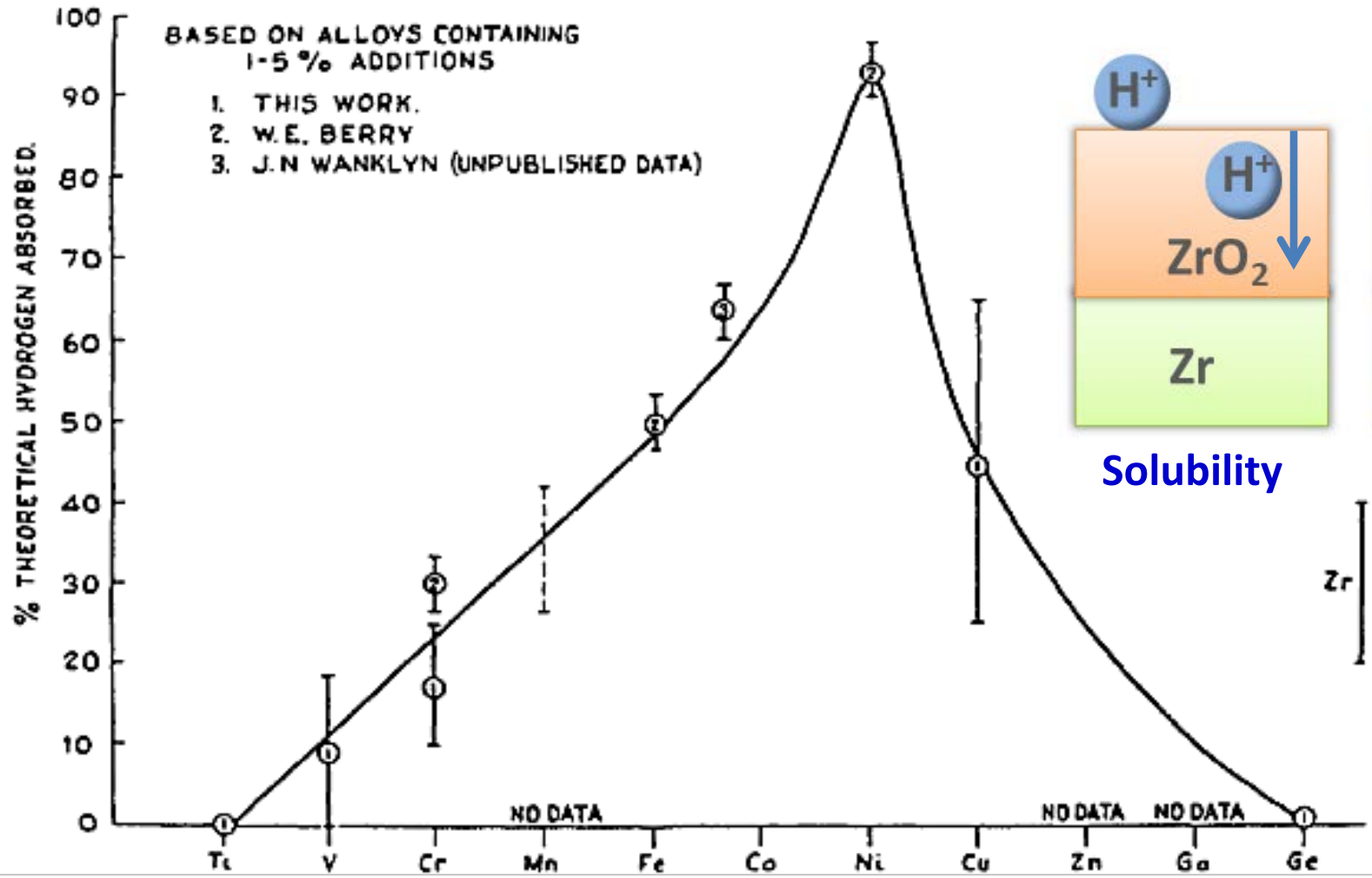

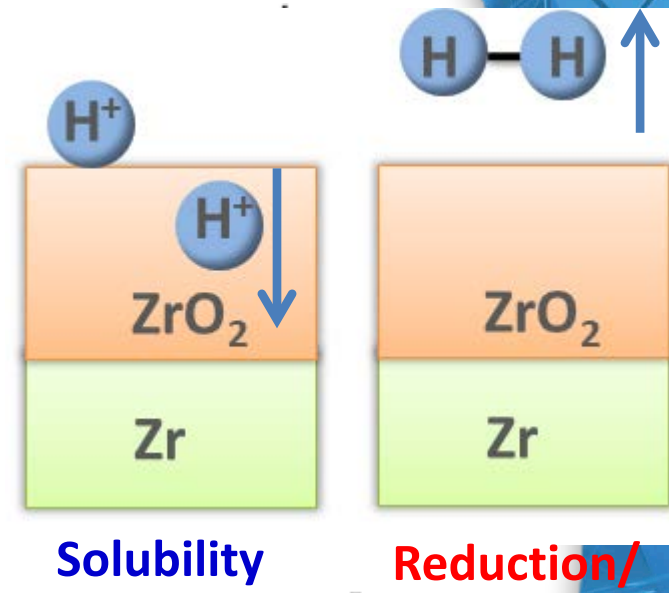

B. Cox, M. J. Davies, A. D. Dent, The Oxidation and Corrosion of Zirconium alloys, Part X., Hydrogen Absorption during Oxidation in Steam and Aqueous Solutions, HARWELL, AERE-M621 (1960).

Approach based on defect equilibria in co-doped monoclinic ZrO_2 (M-ZrO_2)

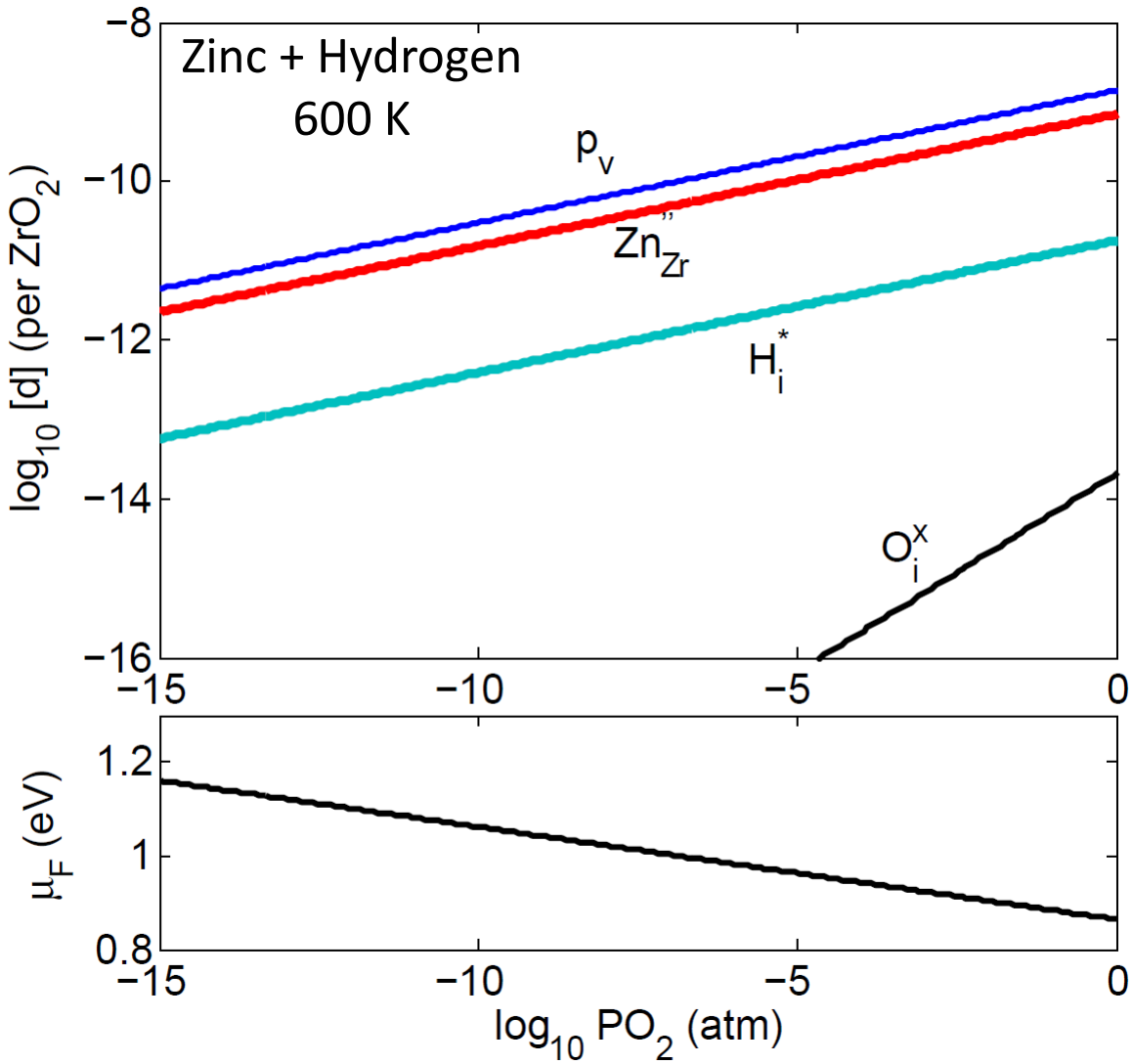

Extract the **solubility** of hydrogen

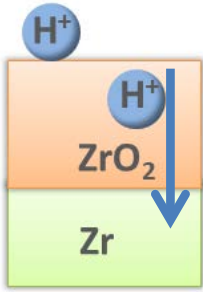

Extract μ_F (e^- chemical potential) (**reduction/evolution**)

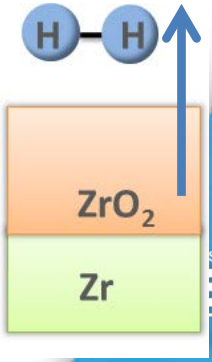

M. Youssef and B. Yildiz, in review (2014)

The 'predicted' volcano of hydrogen solubility in M-ZrO_2

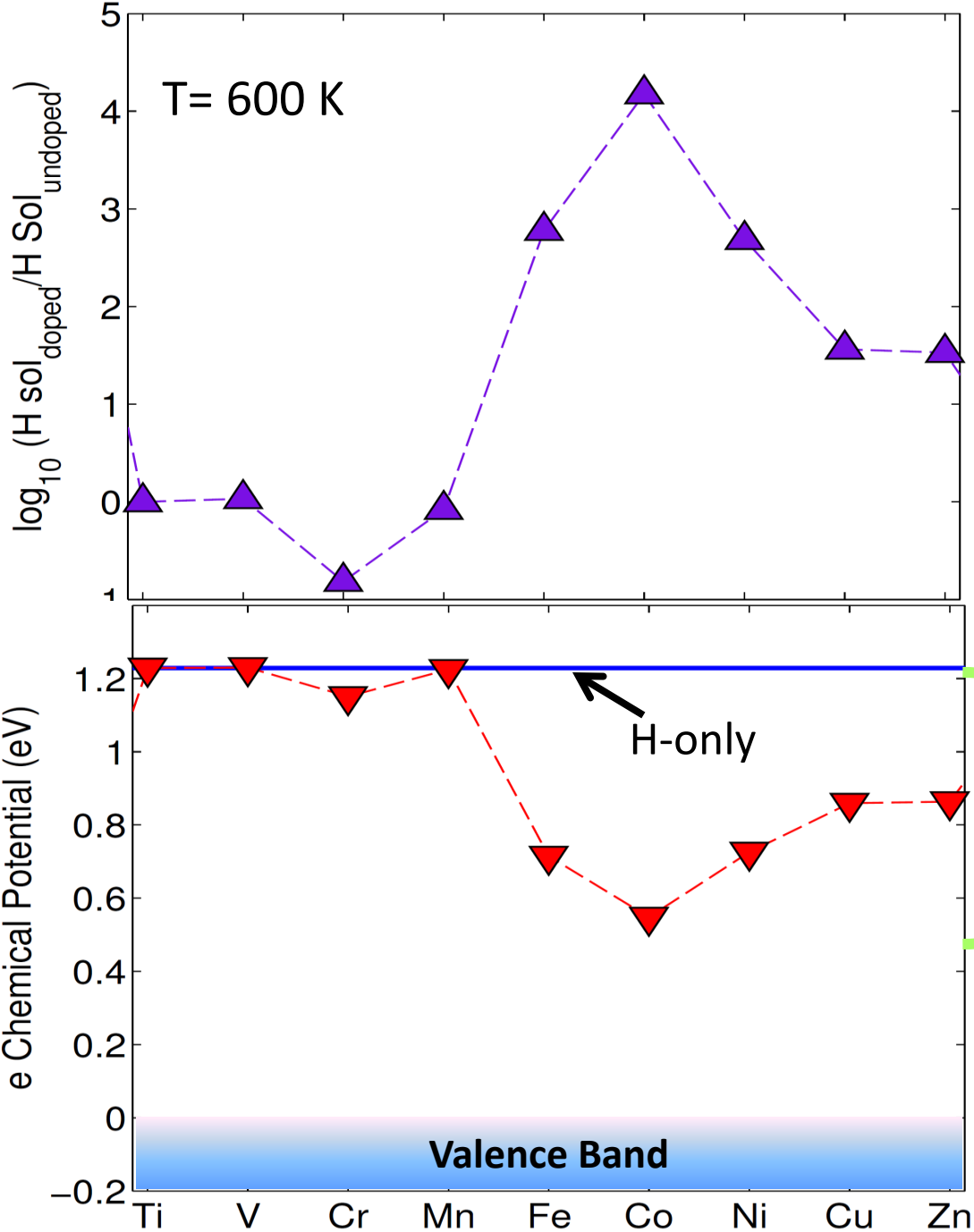

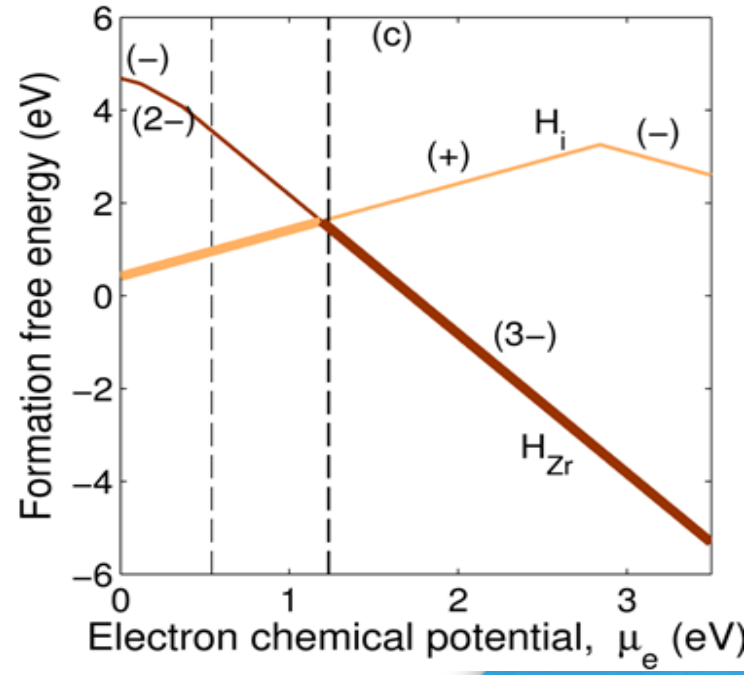

M. Youssef and B. Yildiz, in review (2014)

The *valley* of hydrogen solubility in M-ZrO_2.

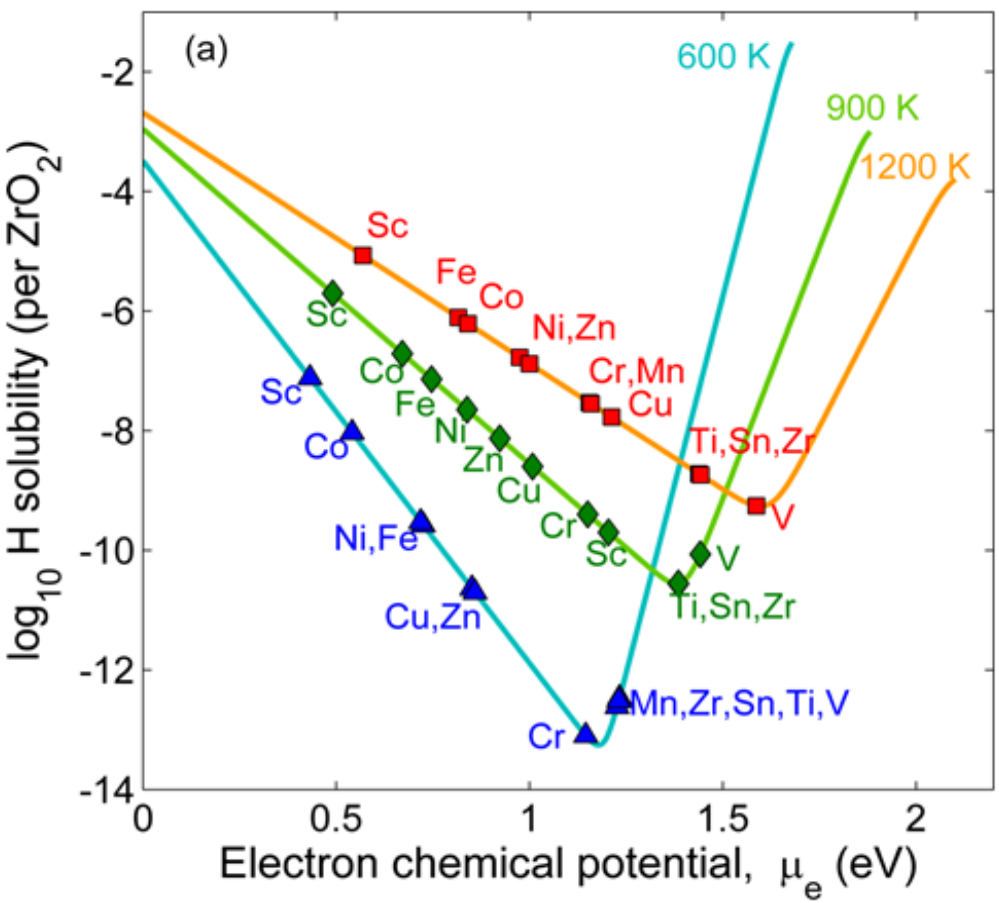

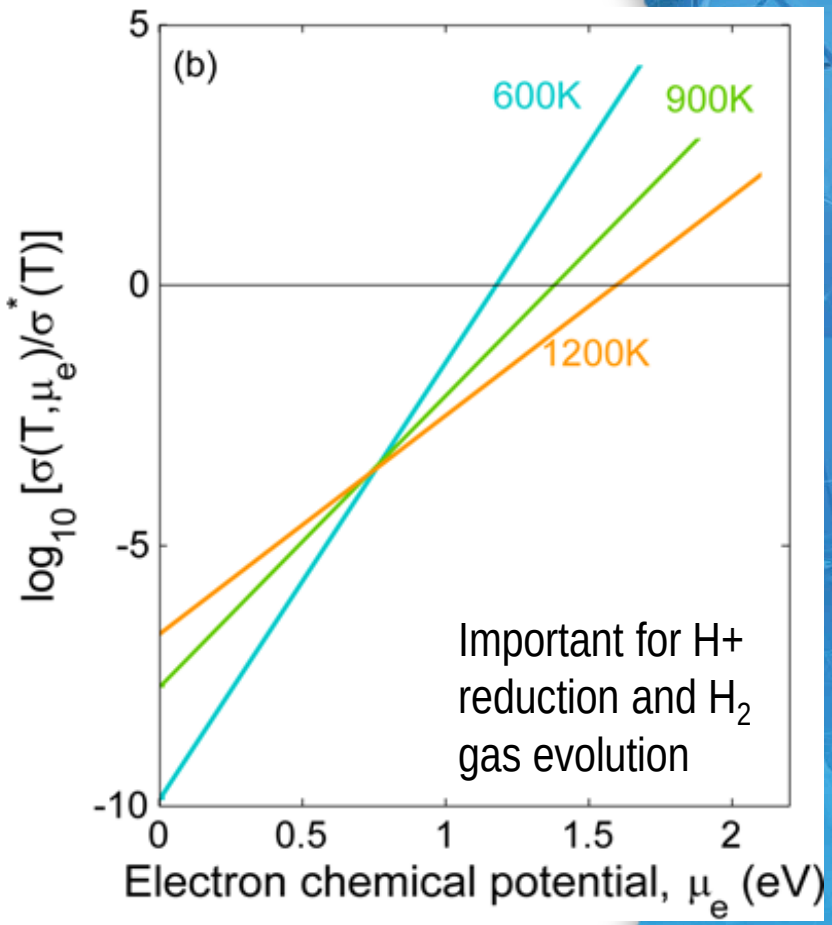

(a) The calculated solubility of hydrogen in monoclinic ZrO_2 as a function of the electron chemical potential 600 K, 900 K and 1200 K.

(b) The ratio of the electronic conductivity doped to pure in M-ZrO_2

M. Youssef and B. Yildiz, in review (2014)

Design strategies on the valley of H-solubility in ZrO_2

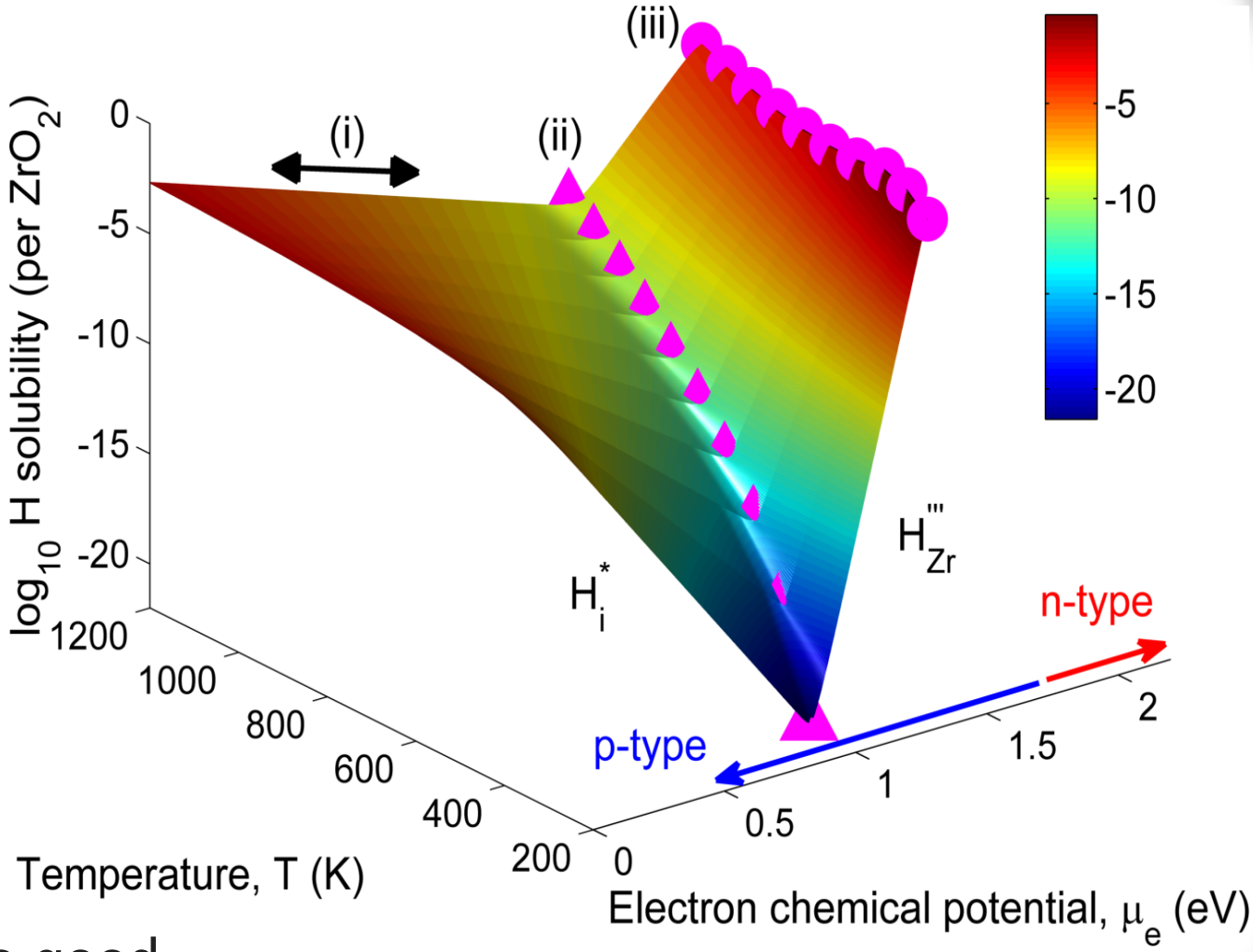

M. Youssef and B. Yildiz, in review (2014)

- (i) → No good
- (ii)→ Minimize hydrogen solubility (good)
- (iii)→Maximize H^+ reduction and $H_{2(g)}$ evolution (good)

Future Work: Corrosion and H-pickup processes investigated at the atomistic level, as input to mesoscale models:

- Effect of stress and extended defects (including grain boundaries, precipitate phase boundaries) on O-diffusion and H-pickup in ZrO_2.
- Fracture criteria for ZrO_2 based on stress, phases, and Li content
- Surface reactions at water/ZrO_2 interface (source term for corrosion and H-pickup)
- Guiding input from experiments of G. Was (UM).
- Provide quantitative input to the continuum level H-pick up model of Morgan & Szlufarska at UW-Madison and mesoscale oxidation / corrosion model of M. Short at MIT.

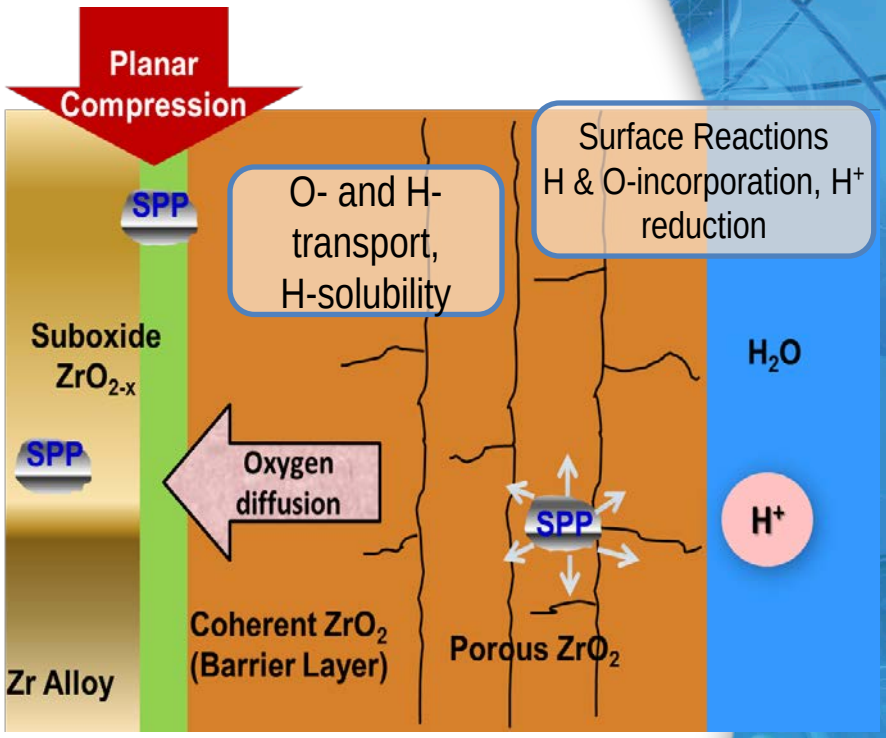

Predicting thermodynamic, kinetic and mechanical constitutive relations relevant to Zr cladding corrosion

To predict the thermodynamic, kinetic and mechanical properties in the Zr-H-O ternary.

John Thomas, Brian Puchala
Department of Materials Science and Engineering
University of Michigan

Anton Van der Ven
Materials Department
University of California Santa Barbara

CASL Energy Innovation Hub, DOE DE-AC05-00OR22725

Calculated Zr-O phase diagram

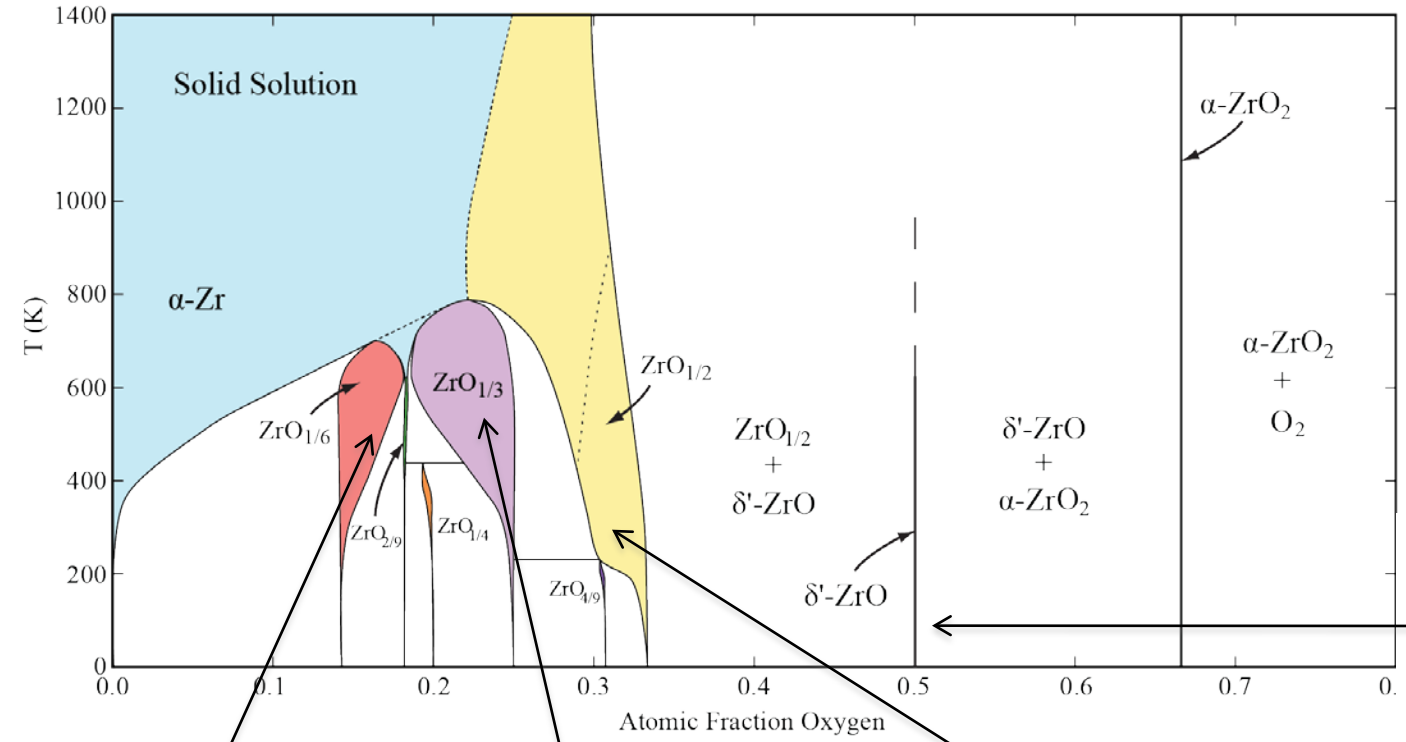

ZrO

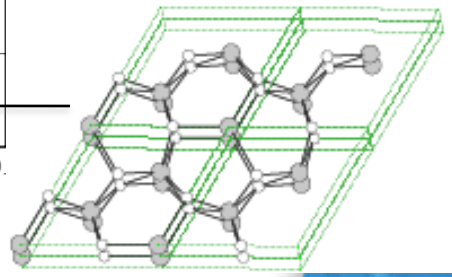

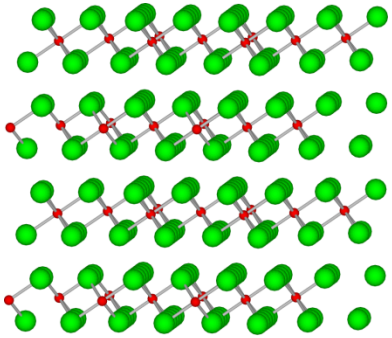

$ZrO_{1/6}$

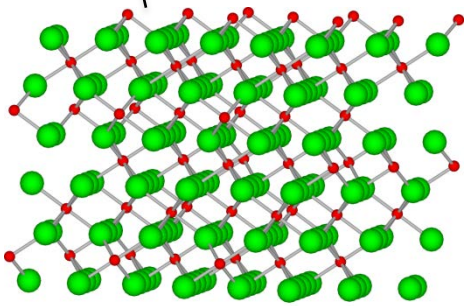

$ZrO_{1/3}$

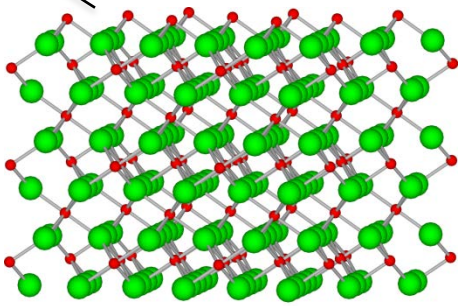

$ZrO_{1/2}$

B. Puchala, A. Van der Ven, Physical Review B, 88, 094108 (2013).

Ongoing work

-Predict chemo-mechanical free energy of ZrH_2 with first-principles statistical mechanics (free energies as a function of composition and strain to predict coherent and metastable hydride stability) → as input to HYRAX of UM (Thornton)

-Calculate oxygen diffusion coefficients in ZrO_x as a function of oxygen concentration → as input to HOGNOSE of MIT (Short)

Continuum Level Model for H-Pickup

Highlights from University of Wisconsin - Madison

Izabela Szlufarska, Dane Morgan
Postdoc: Ming-Jie Zheng

Research objective and approach

Research objective: develop a continuum model for H-pickup

Staged approach: Start from simplest possible physics and add in new processes in stages, as needed to explain data

Goal: Full Model of H-pickup

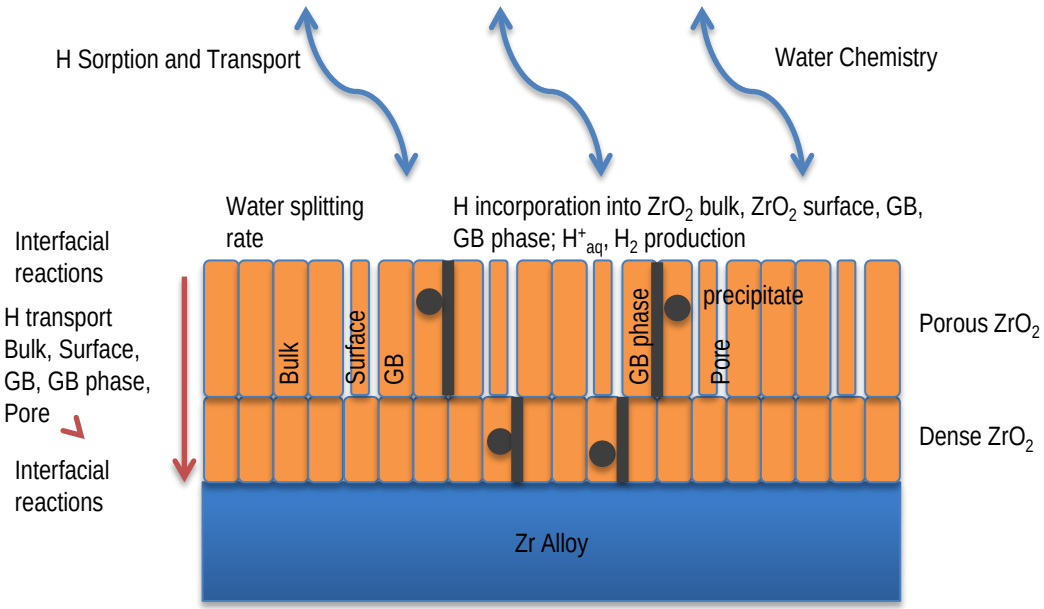

Stage 1: Double-layered Bulk Oxide Transport Model

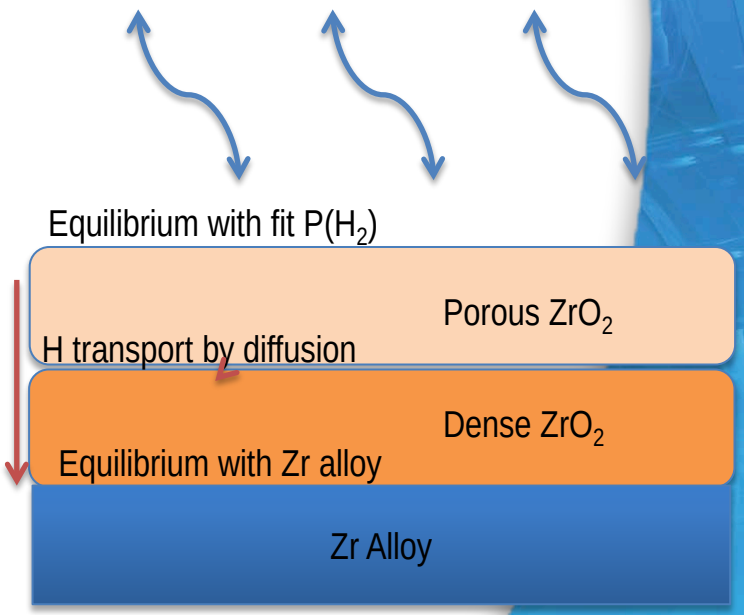

Calculated vs. Experimental Hydrogen Pickup Fraction (f_H) in Steam-Corroded Zr Alloys at 673K

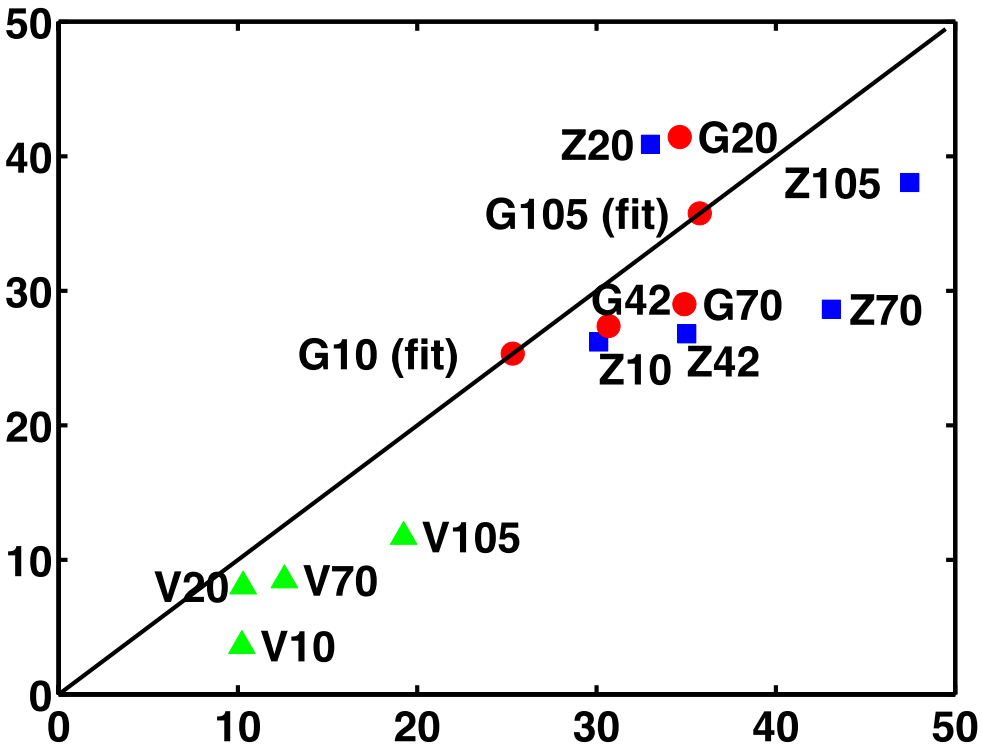

- Stage 1 bulk oxide transport limited model with all values from experiment except single fitted pH_2 at oxide surface.
- Successful prediction indicates hydrogen pickup is rate-limited by hydrogen diffusion in bulk ZrO_2.

Experimental data from [1] K. Une, et Al., Journal of ASTM International 8, JAI102950 (2011).

Calculated vs. Experimental Hydrogen Pickup Fraction (fH) in LiOH-water-corroded Zr Alloys at 563K

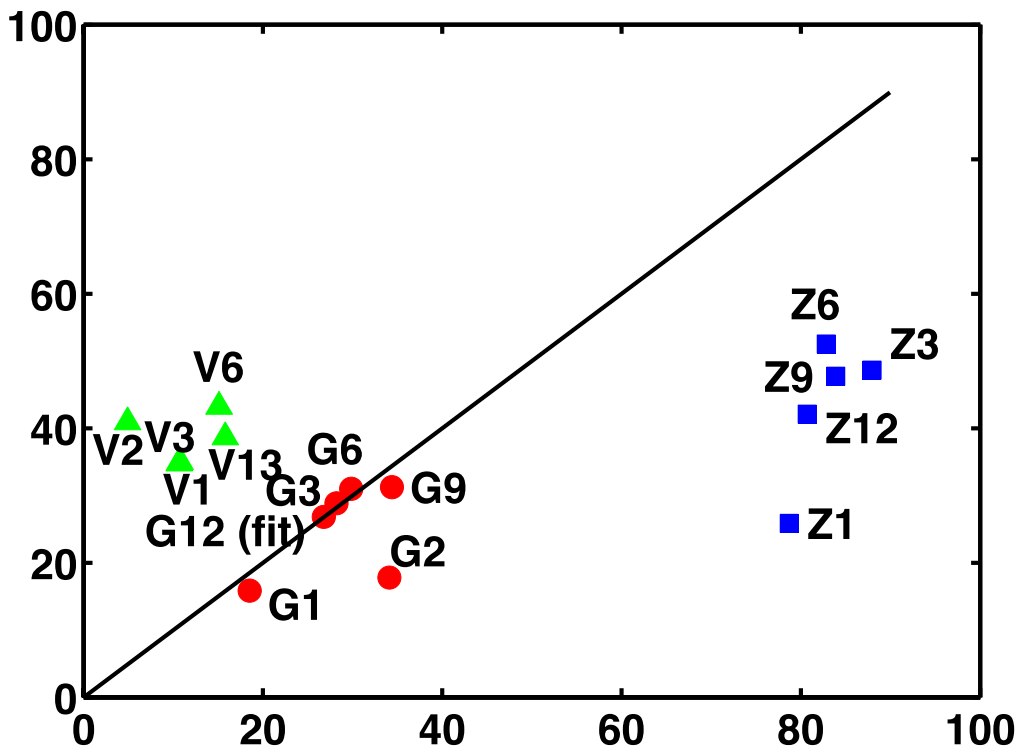

- Stage 1 bulk oxide transport limited model fails to predict fH in Zr alloys under the LiOH-water-corroded conditions due to lack of dense oxide.
- Unsuccessful prediction indicates that, as expected, under LiOH-water conditions hydrogen pickup is NOT rate-limited by hydrogen diffusion in bulk ZrO_2 – was proposed to be reaction-controlled [1].

Experimental data from [1] K. Une, et Al., Journal of ASTM International 8, JAI102950 (2011).

Accomplishments Summary and Future Work

- Constructed basic hydrogen bulk transport model through oxides
  - Double-layered oxide model under steam-corroded conditions
    - provides accurate prediction for 3 zircaloys
  - Single-layered oxide model under LiOH-water-corroded conditions
    - fails to predict corrosion in LiOH-water-corroded conditions due to lack of dense oxide
- Future work is to add in effects in stages
  - Short circuit diffusion paths (degraded grain boundaries)
  - Surface reaction rates
  - Alloying elements effects
  - LiOH concentration coupling to mechanism
  - Oxide transition effects
- Modeling will build on experimental data from Was (UM) and atomistic modeling from Yildiz (MIT), and provide input for hydride precipitation modeling by Thornton (UM).

Hyrax: Simulation Tool for Hydride Precipitation and Microstructure Evolution

A. M. Jokisaari, K. Thornton, University of Michigan

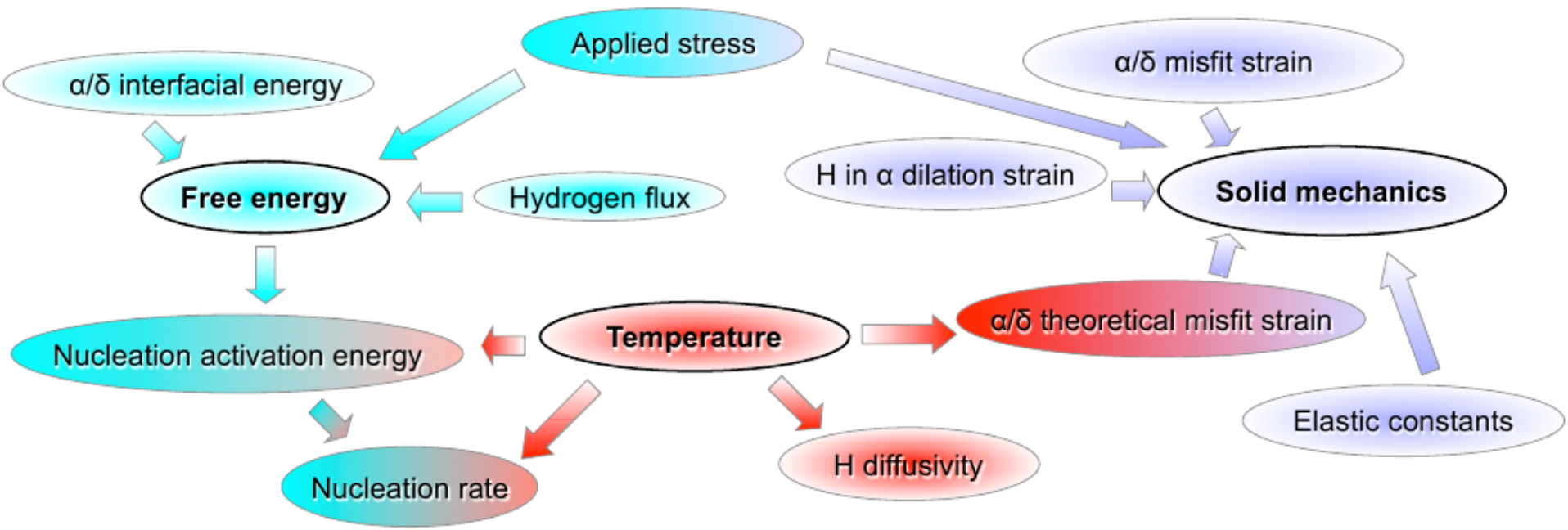

→ Incorporate the atomic-scale simulation results from Hyrax into a finite-element model to study stress distributions caused by hydride formation and dissolution at the continuum scale; by M. D. Thouless, W. Lu, H. Wang at University of Michigan, Ann Arbor

CASL-U-2014-0116-000

Research Objectives and Key Results

- Physics-based mesoscale modeling of δ-hydride precipitation and growth in single-crystal α-zirconium
  - MOOSE-based phase field modeling framework
  - Incorporates classical nucleation theory, heat conduction, hydride/zirconium misfit strain (solid mechanics)
- Reproduced experimentally observed hysteresis of the hydrogen terminal solid solubility of hcp-Zr solid solution upon heating and cooling
- Studied the effect of applied stress on hydride composition, phase fraction, and transformation kinetics
- Documented the sensitivity of hydride nucleation rate on applied stress, temperature, supersaturation, and hydride/zirconium interfacial energy

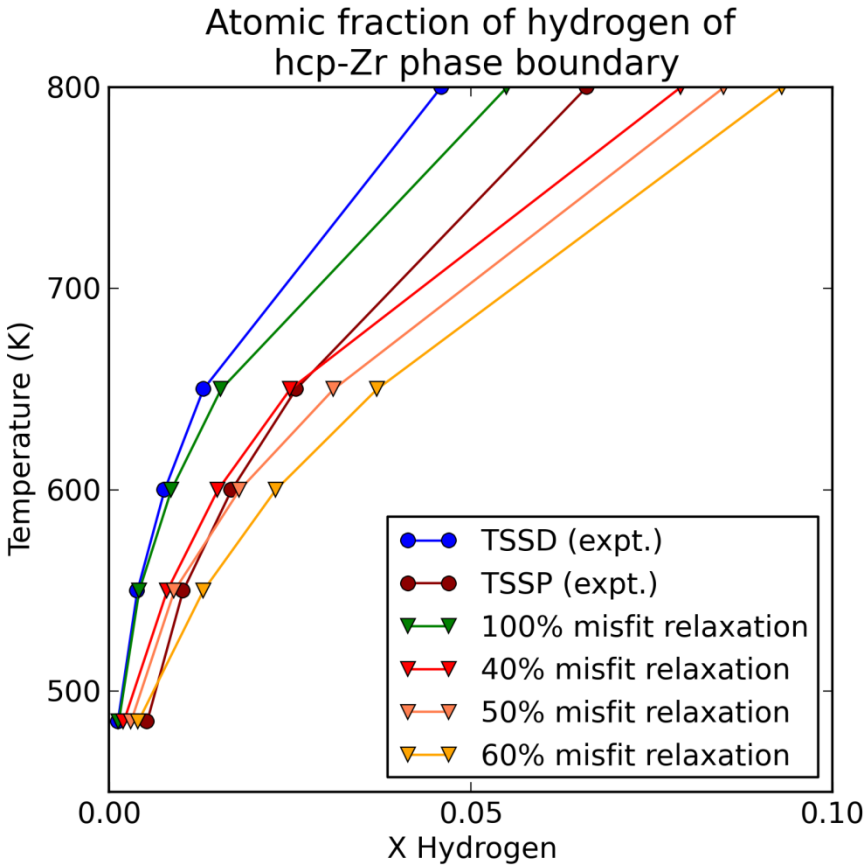

Experimental results from K.B. Colas et al., Acta Materialia 58 (2010) 6575-6583

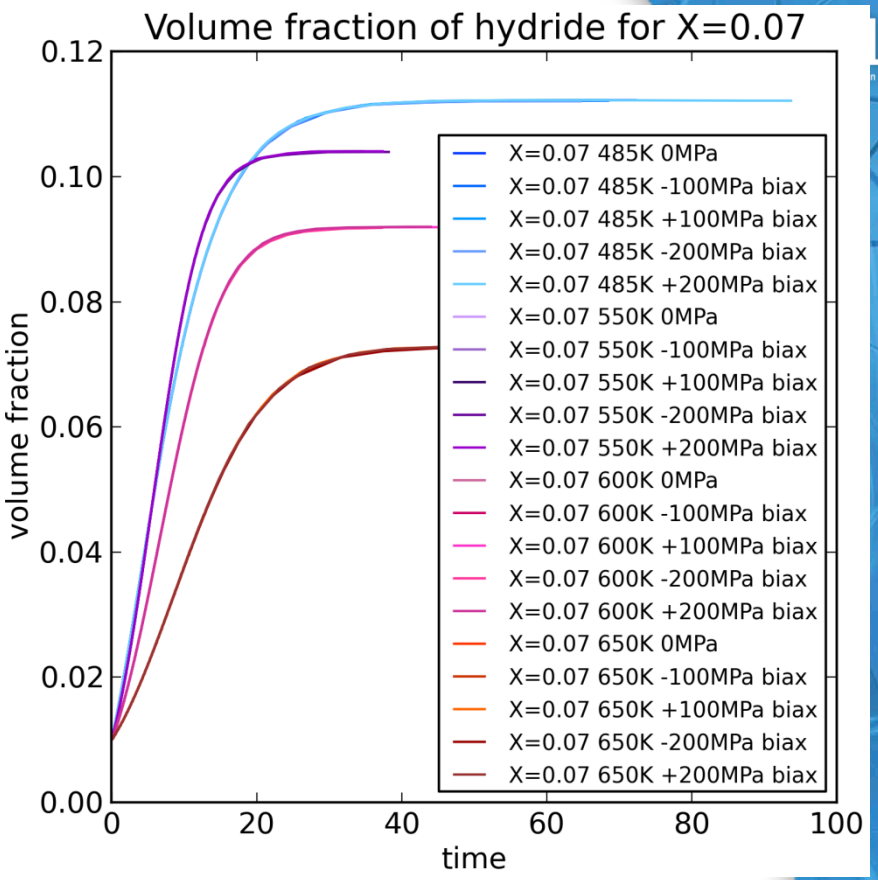

- Our model, along with its parameterization, reproduce experimentally observed hydrogen terminal solid solubility (TSS) hysteresis
- Hydride volume fraction, phase composition, and transformation kinetics can be passed to macroscale models, such as cladding creep models
- Potential next steps: study hydride reorientation phenomenon and effect of hydrogen flux and temperature gradients on resulting microstructure

Uncovering the Origin of Linear-Cubic Zircaloy Oxidation

A. Dykhuis and M. Short (MIT)

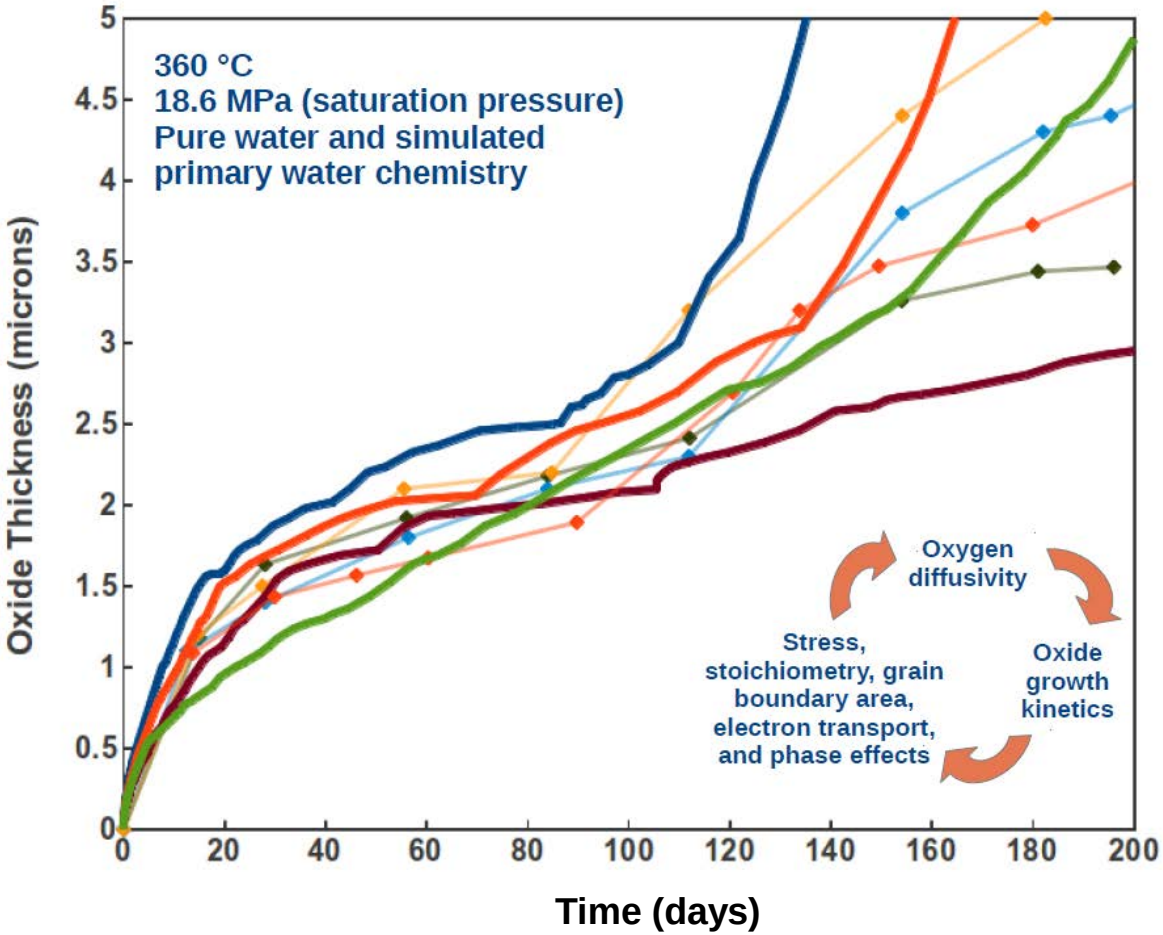

- Zircaloys exhibit breakaway corrosion
  - Temperature can exaggerate this
- Using mechanistic parameters to fit breakaway oxidation model (HOGNOSE) to literature data
  - Oxide/metal stress
  - Oxide stoichiometry
  - Composition-dependent diffusivity

Thick lines – Simulation
Thin lines – Experimental Data

Uncovering the Origin of Linear-Cubic Zircaloy Oxidation

A. Dykhuis and M. Short

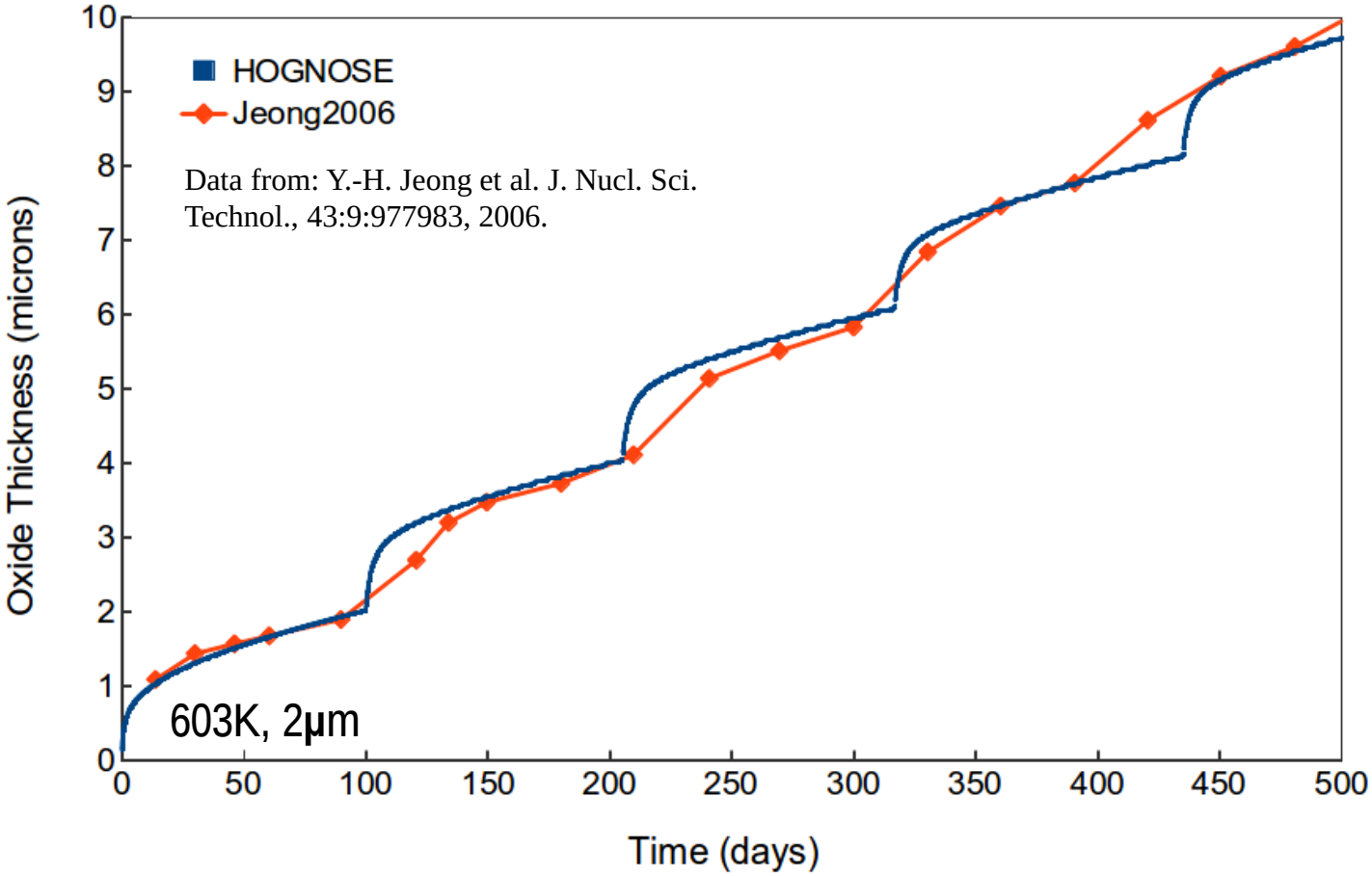

- **Oxide thickness increases with temperature (all simulations 400 days)**
- **More transitions occur with increasing temperature**
- **With only 3-5 fitting parameters, HOGNOSE matches literature data**
- **Integrated with MOOSE MultiApp, ready for Peregrine integration!**

Experiments on oxidation and hydrogen pickup under irradiation

Gary Was and Peng Wang (University of Michigan)

Objective

- Determine hydrogen content (pickup fraction) during corrosion in simulated PWR with/without proton irradiation.

Key findings

- Identification of hydride formation following irradiation in PWR primary water.
- Significant increase in oxidation rate with irradiation (e.g. oxide on the irradiated sample is 5-10x thicker than the unirradiated case)

Future Work

- Fully characterize the oxides formed w/ or w/o irradiation (oxide morphology, phase, interfacial chemical composition, etc.)
- Determine hydrogen content using Vacuum Hot Extraction (VHE)

Irradiation of Zr-4 to a dose of 0.14 dpa in 320°C water containing 3 ppm H_2 over a 24 hr period (image on left) resulted in an oxide that was 5-10x that of the unirradiated case (image on right).

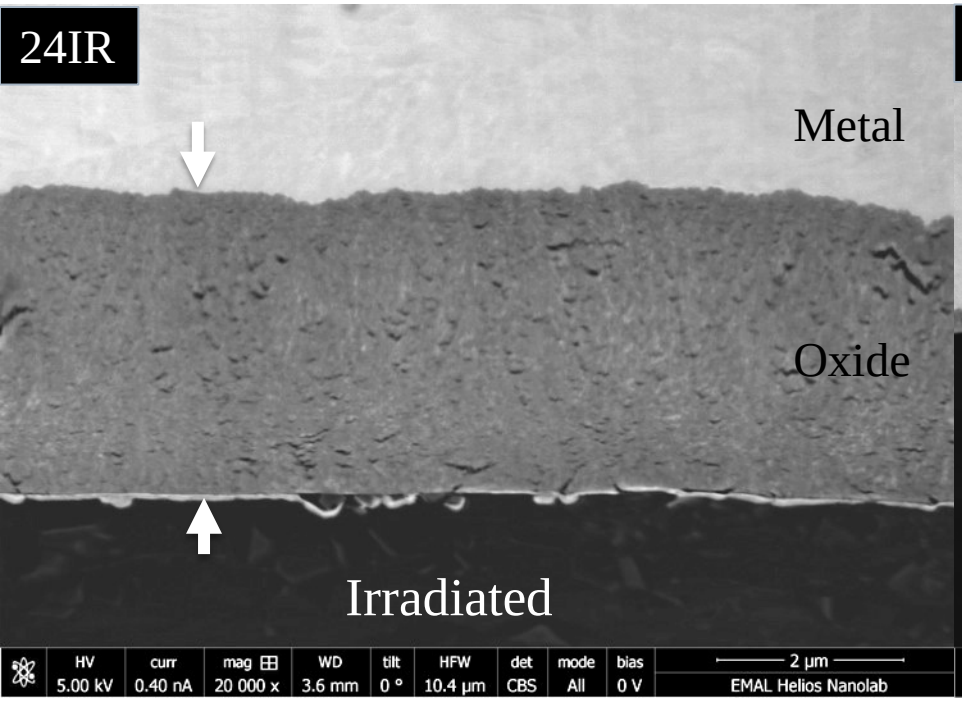

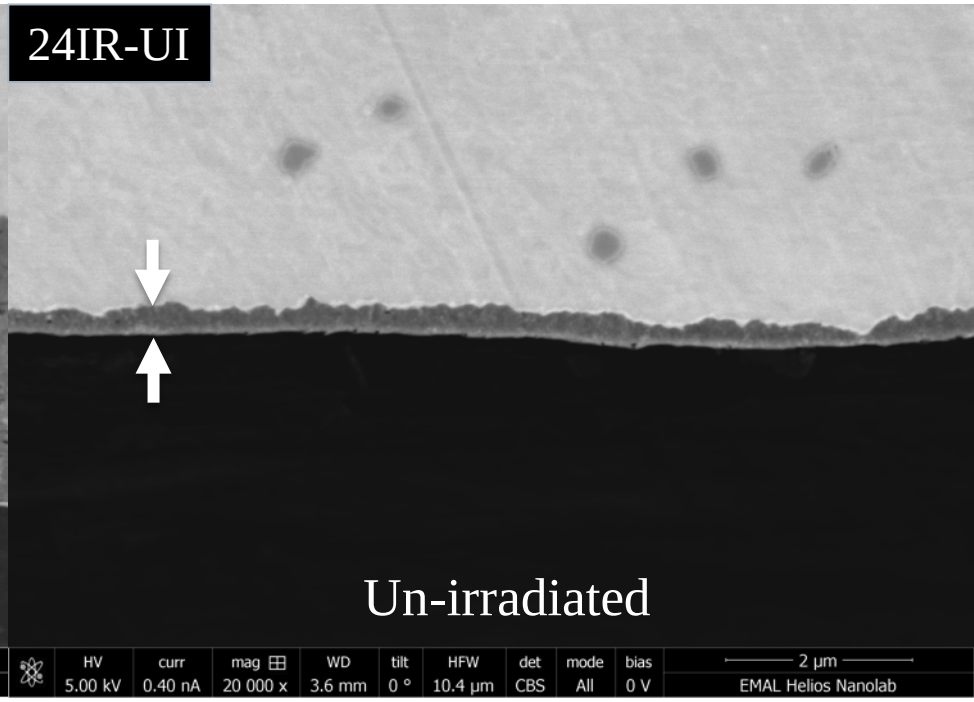

MPO Zr-H-O Framework

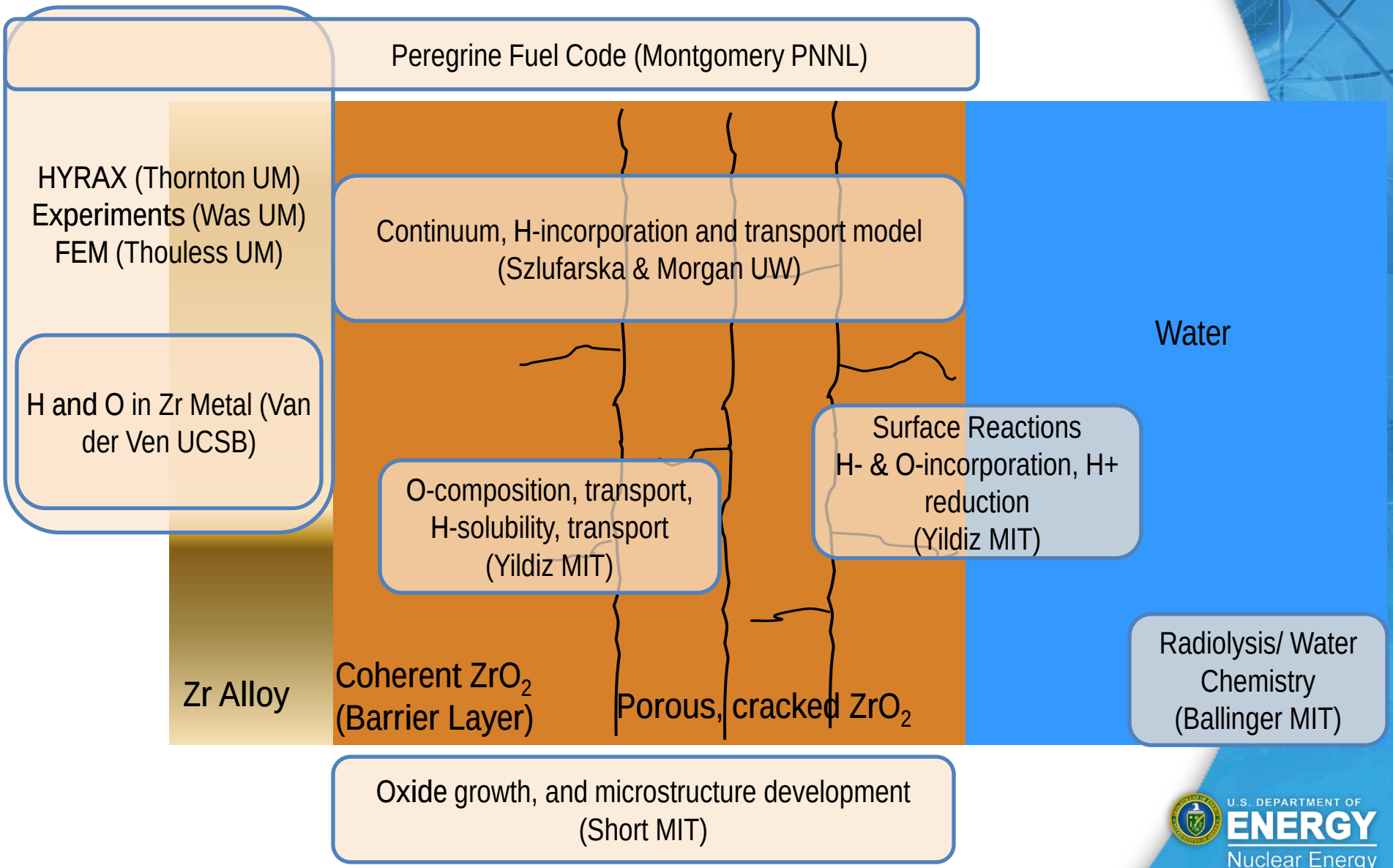

BACK UP SLIDES

Summary of Accomplishments in Phase-I (by Yildiz, MIT)

Clad corrosion and H-pickup

- Computed oxygen diffusivity and hydrogen solubility in ZrO_2 calculated from first principles. Both provided as input to continuum models at UW and MIT.

[1] M. Youssef, B. Yildiz, Phys. Rev. B 86, 144109 (2012)

[2] M. Youssef, B. Yildiz, Phys. Rev. B 89, 024105 (2014)

[3] M. Youssef, B. Yildiz, Phys. Chem. Chem. Phys. 16, 1354 (2014)

- Discovered physics-based design criteria to minimize H-pickup in Zr-alloys through ZrO_2.

[4] M. Youssef, B. Yildiz, in review (2014)

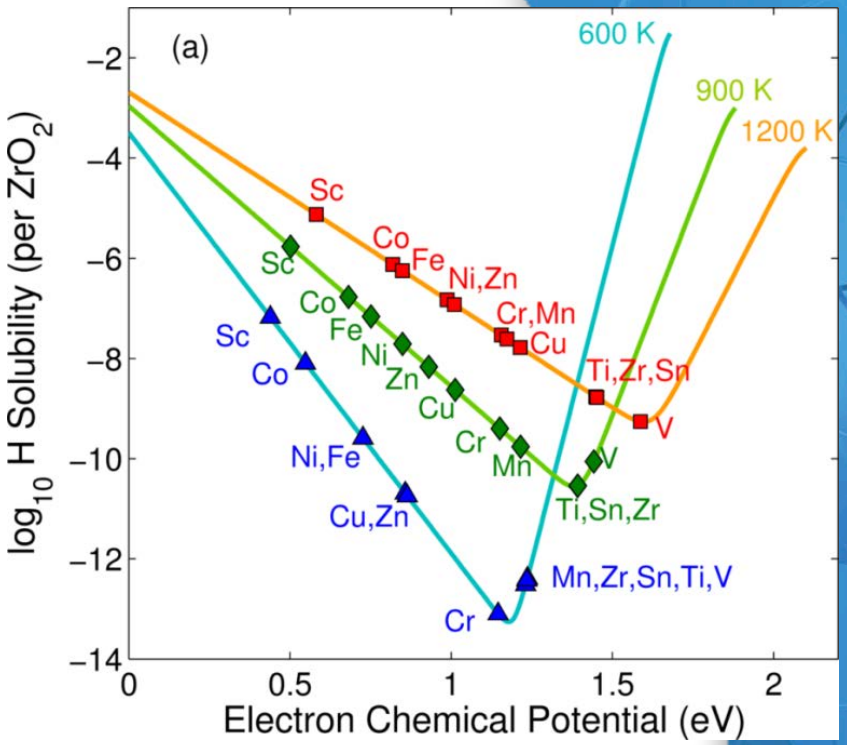

Clad creep and growth

- Combining atomistic simulations and constitutive relations to predict dislocation-defect interactions in temperature-strain rate space. Provided input to LANL's VPSC model.

[1] Y. Fan, A. Kushima, B. Yildiz, Phys. Rev. B 81, 104102 (2010)

[2] Y. Fan, A. Kushima, S. Yip, B. Yildiz, Phys. Rev. Lett. 106, 125501 (2011)

[3] Y. Fan, Y. Osetsky, S. Yip, B. Yildiz, Phys. Rev. Lett. 109, 135503 (2012)

[4] Y. Fan, Y. Osetsky, S. Yip, B. Yildiz, Proc. Nat. Acad. Sci. 110, 17756 (2013)

[5] Y. Fan, B. Yildiz, S. Yip, Soft Mat. 9, 9511 (2013)

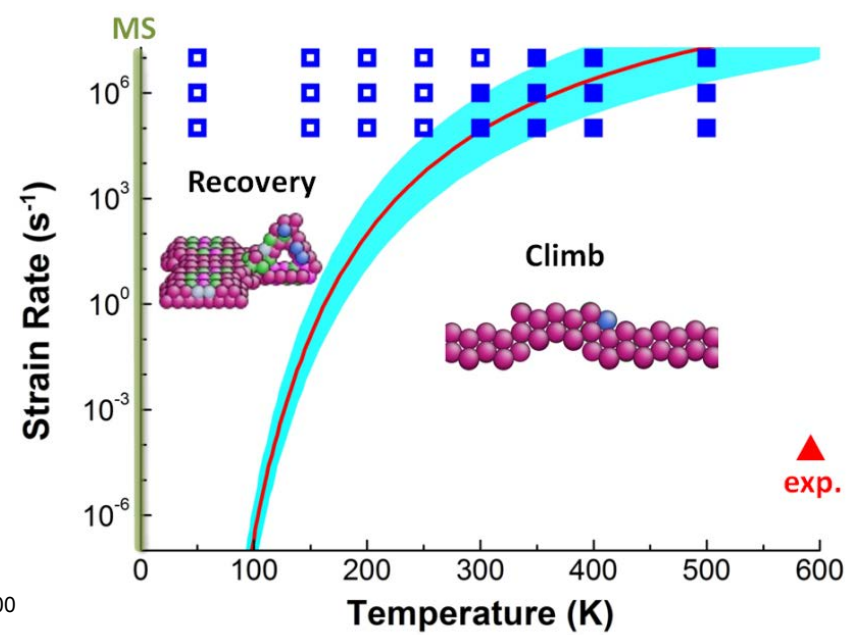

Summary of the simulation framework
(Youssef and Yildiz, MIT)

Charge Neutrality Condition

$$\sum_{d}\sum_{q} q[d^{q}] + p_{v} - n_{c} = 0$$

Point Defects Free Holes Free Electrons

0 K formation energies using Density Functional Theory

Sample finite T excitation using Density Functional Theory (phonons – band electronic entropy)

Apply charge neutrality and construct Kröger-Vink diagram

[1] Vienna Ab initio Simulation Package (VASP)
[2] A. Van de Walle, G. Ceder, Rev. Mod. Phys. (2002)
[3] N. Ashcroft, N. Mermin, *solid state physics*, (1976)
[4]F. Kröger, H. Vink, Sol. Stat. Phys., (1956)

Developed an anharmonic lattice dynamical effective Hamiltonian to predict the high temperature properties of cubic ZrH_2

Axial-Axial Response

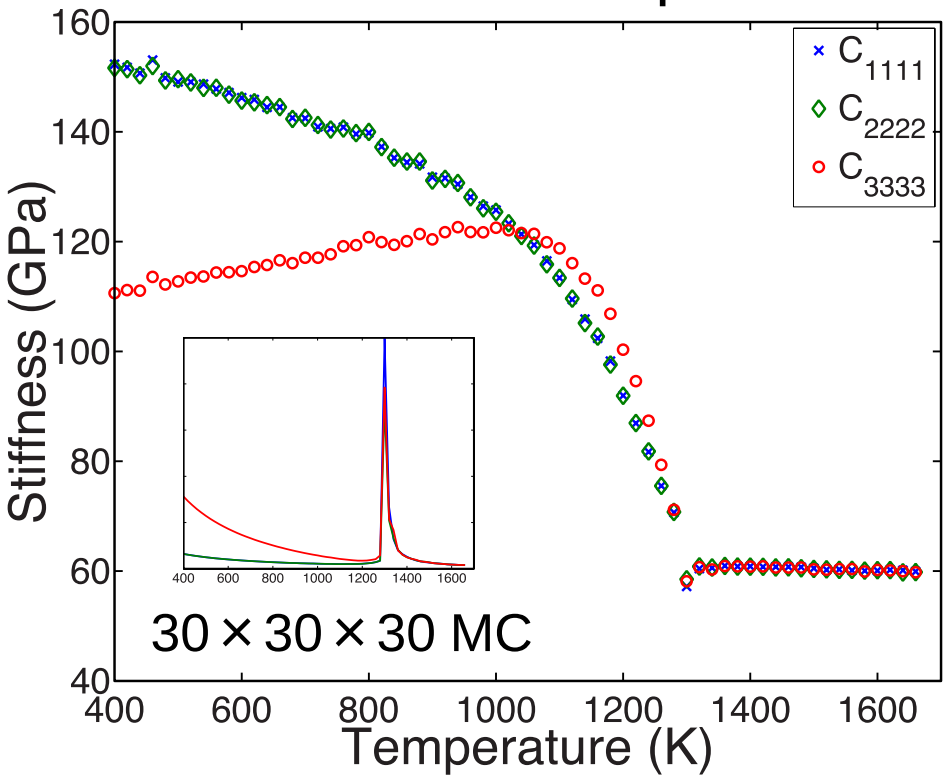

Axial-Transverse Response

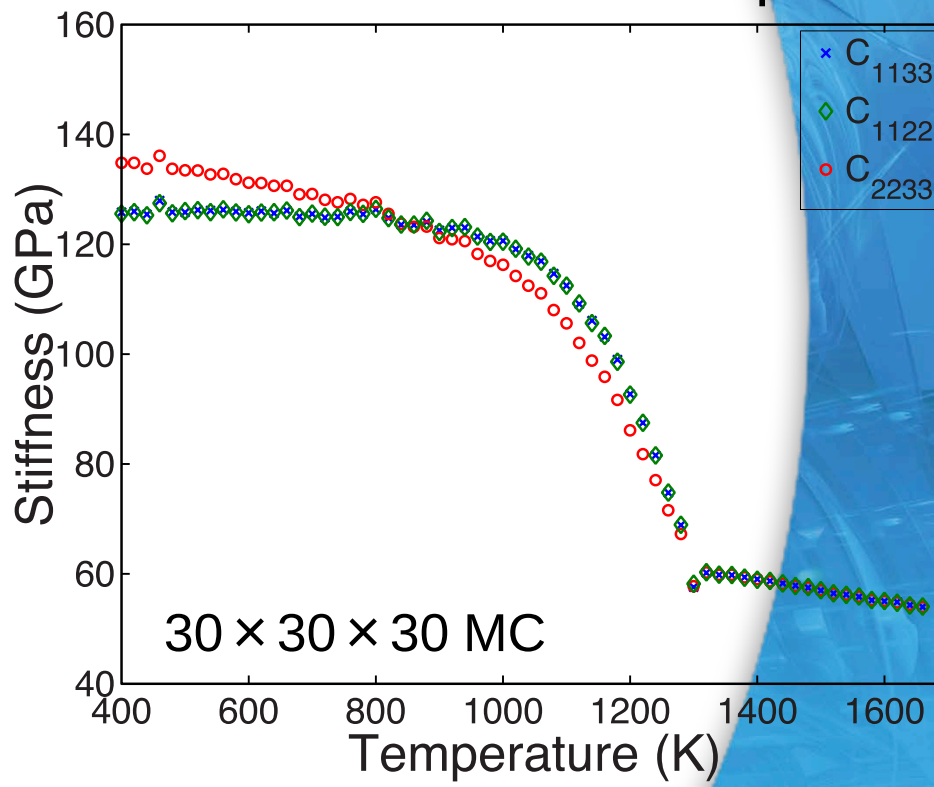

Eulerian Stiffness Tensor

$$\sigma_{ij} = C_{ijkl}\varepsilon_{kl}$$

J. C. Thomas, A. Van der Ven, Physical Review B, 88, 214111 (2013).
J. C. Thomas, A. Van der Ven, to be submitted (2014).

What's Next for HOGNOSE?

A. Dykhuis and M. Short

- **Solution of micron-scale CILC underneath a mm-scale CRUD flake**

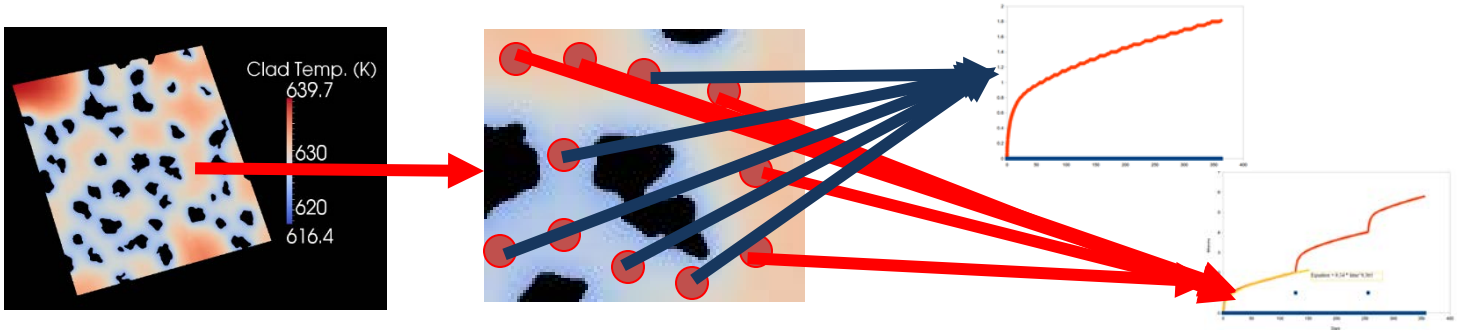

- **Integration of HOGNOSE with BISON/PEREGRINE**

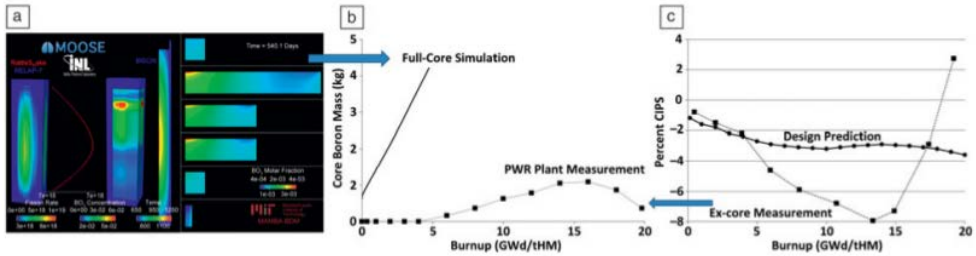

- **Validation of HOGNOSE data using experiments (lab & synchrotron)**

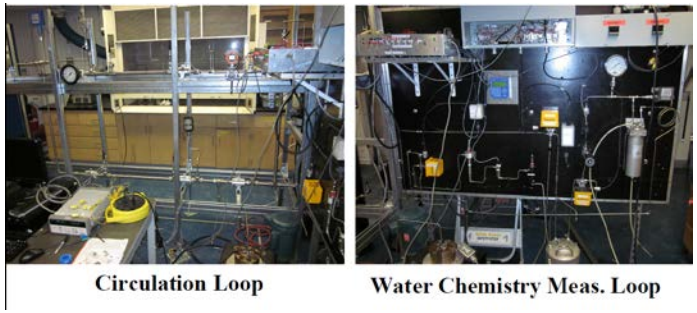

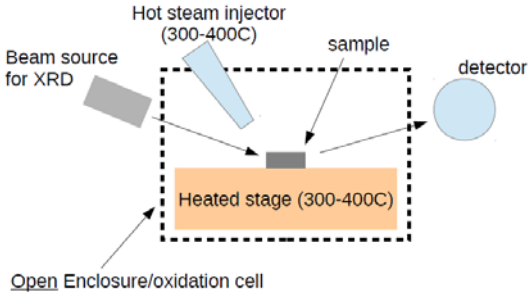

- **Integration of solid mechanics (stresses) into HOGNOSE**

Hydride formation and dissolution simulation: a connection between atomic-scale simulation and continuum-scale simulation

M. D. Thouless, W. Lu, H. Wang, A. Jokisaari and K. Thornton, *University of Michigan, Ann Arbor*

Objective

Incorporate the atomic-scale simulation results from Hyrax into a finite-element model to study stress distributions caused by hydride formation and dissolution at the continuum scale

Finite-element model includes:

- Average texture
- Hydrogen diffusion
- Temperature gradients
- Thermal expansion
- Mechanism-based constitutive models of Zircaloy-4

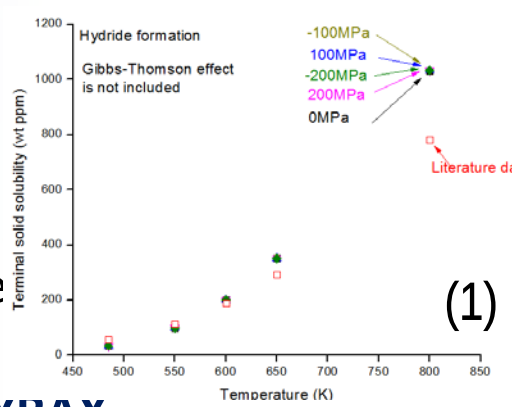

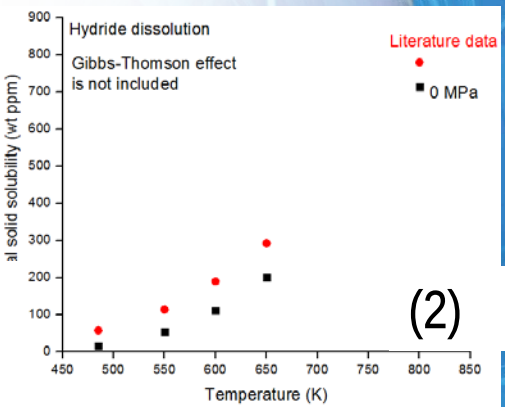

Atomic-scale simulations from HYRAX

1. Solubility limit of H in alpha-zir[illegible] stresses for *hydride formation*
2. Solubility limit of H in alpha-zir[illegible] stresses for *hydride dissolution*
3. Value of *x* in the chemical form[illegible] temperatures and biaixal stres[illegible]
4. Incorporates hysteresis betwee[illegible]

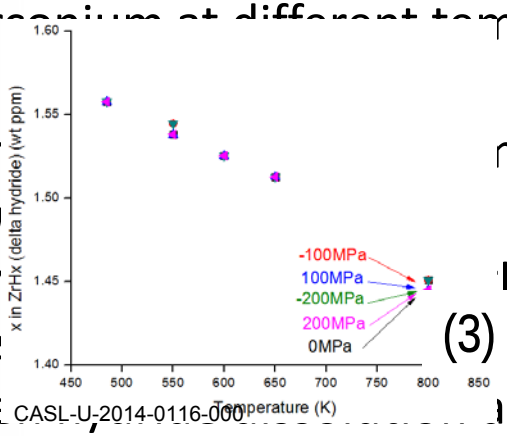

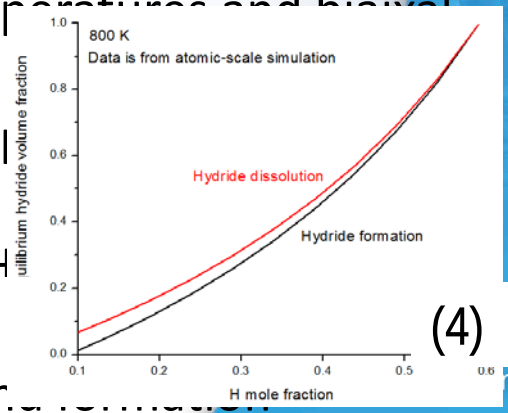

Finite-element simulation

- Proof-of-concept with different texture, varying flux, temperatures, and constraints to induce stresses, along with creep mechanisms
- Analysis proceeds by calculating H concentration in every element and use interpolated results from HYDRAX to calculate hyride concentration
- Anisotropic volume expansion from hyrides give stresses
- Stresses are relaxed by creep mechanisms

Finite-element model

- Duration of the simulation is 1×10^5 s
- Hydrogen fluxes (ppm m/s): 0: $(0 < t < 1\times10^4\ \text{s})$, 5×10^{-5}: $(1\times10^4\ \text{s} < t < 3\times10^4\ \text{s})$
  0: $(3\times10^4\ \text{s} < t < 4\times10^4\ \text{s})$, -8×10^{-6}: $(4\times10^4\ \text{s} < t < 1\times10^5\ \text{s})$

Hydride formation and dissolution

von Mises stress distribution units [kPa]

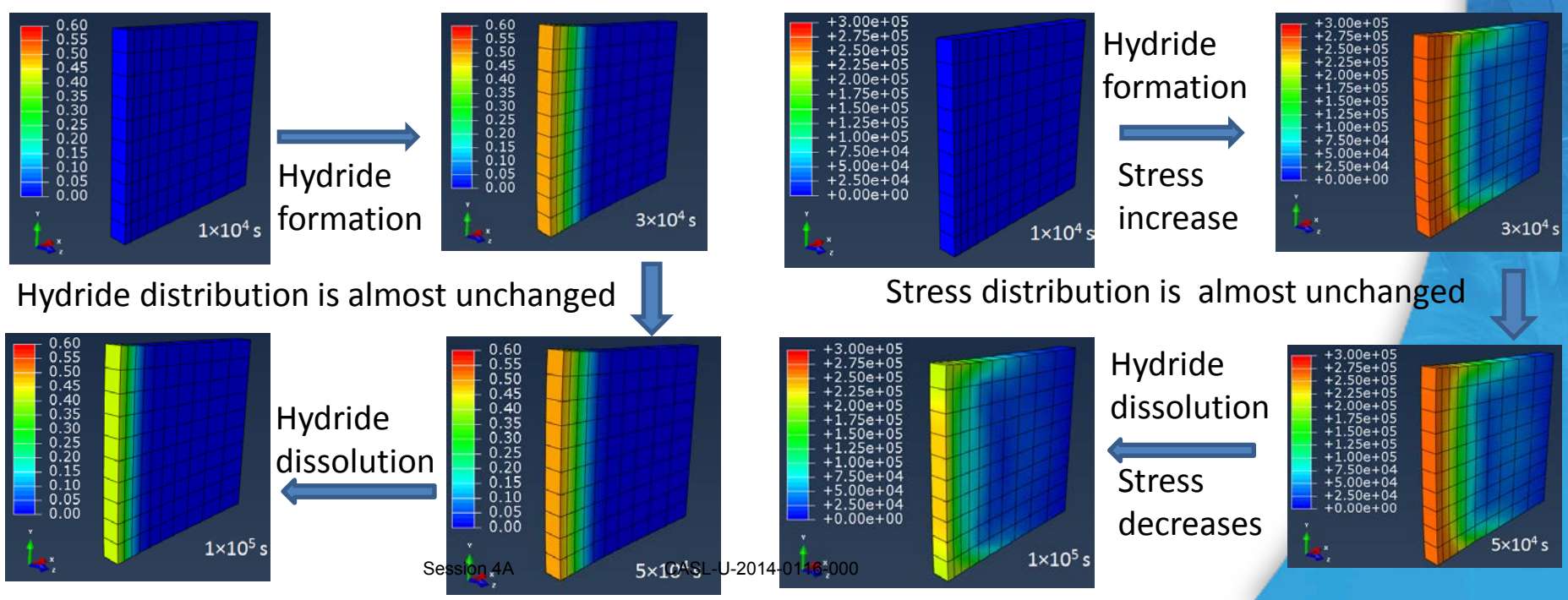

Exposure of unirradiated samples of Zr-4 in 320°C water containing 3 ppm H_2 resulted in oxide thickness values that are in good agreement with the MATPRO out-of-pile database. Proton irradiation results in significant increases in oxide thickness that are well above the MAPTRO in-pile database. Scaling the oxidation rate with the damage rates yields an equivalent neutron damage rate of 4 x 10^{-8} dpa/s, which is very reasonable for PWR fuel cladding, implying that proton irradiation is driving the enhanced oxidation rate.

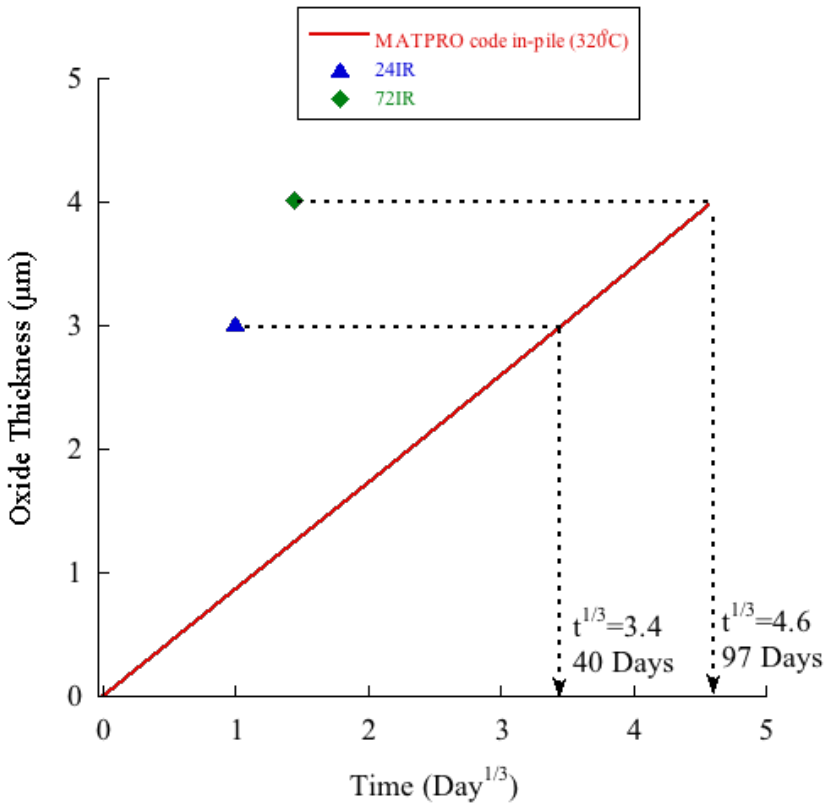

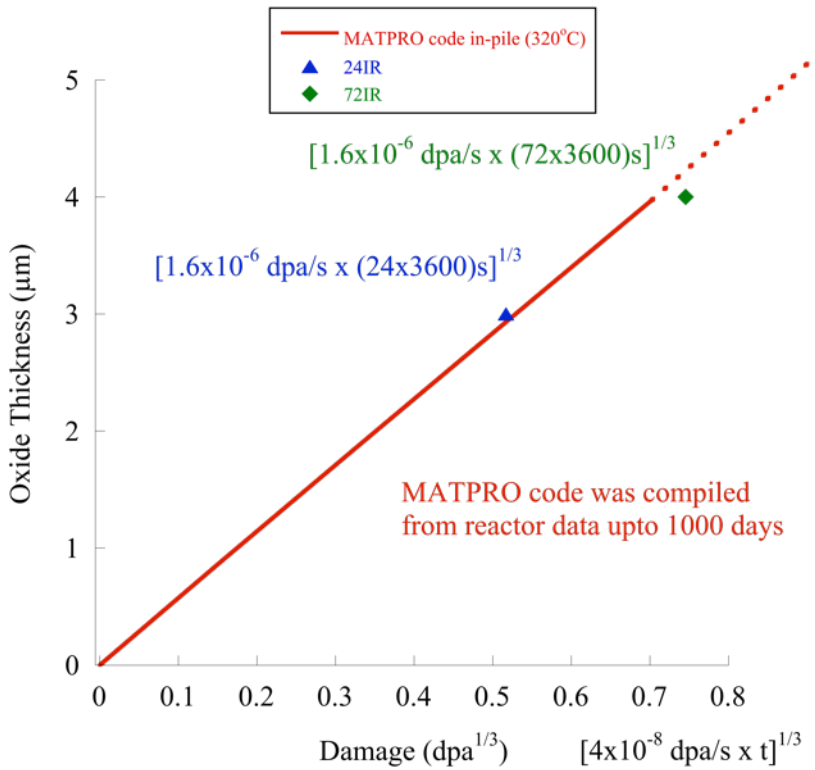

Porosities/cracks distributed through out the irradiated oxide film (Zry-4, 320°C, 24hr, 3.2MeV p-Irrad., 0.14 dpa), FIB liftout TEM lamella

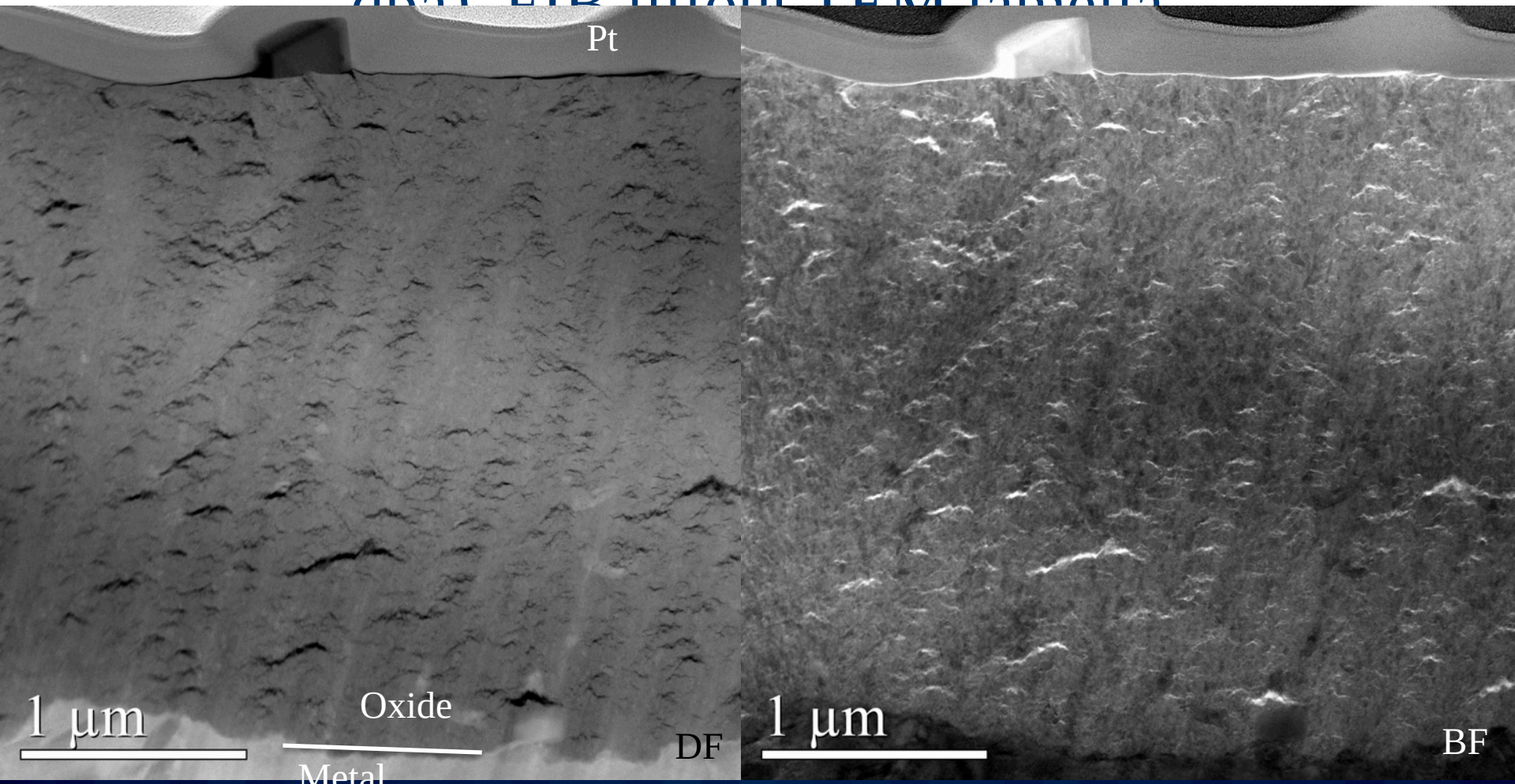

Thermodynamic Modeling of Boron Phases in CRUD: The ~~Failed~~ Continuing Search for Bonaccordite*

* Plus a couple of other things

C.J. O'Brien, B.K. Kendrick, D. Shin,
D.A. Andersson, C.R. Stanek,
T.M. Besmann, D.W. Brenner

Roundtable Discussion, July 15, 2014

CRUD-Induced Power Shift

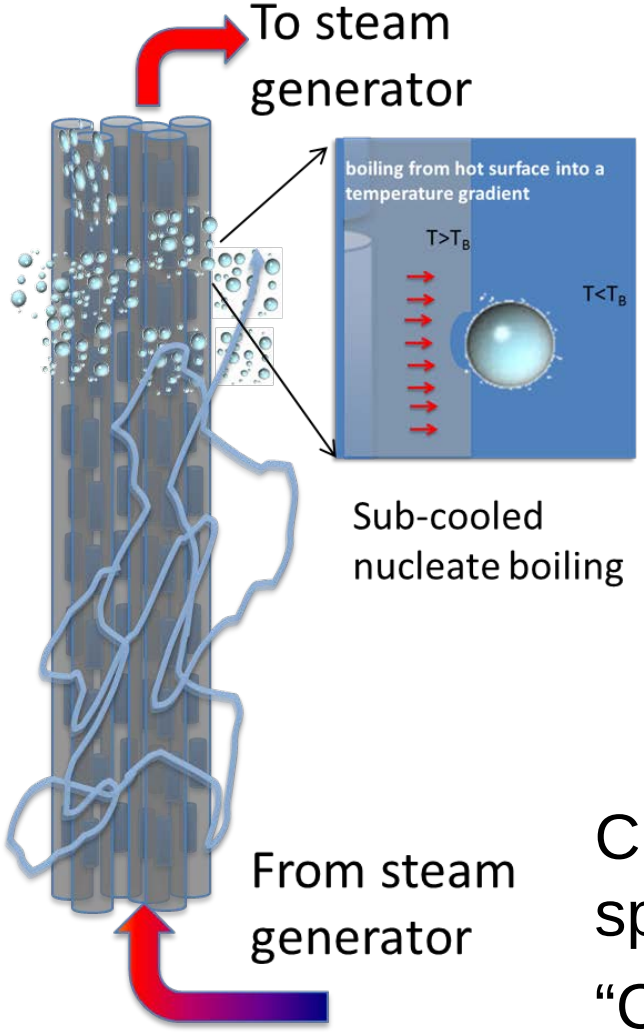

- Metal oxide scale (CRUD) forms at boiling sites
- Porous oxide with boiling chimneys
- Capillary forces pull coolant into CRUD
- Boiling in CRUD/steam loss through chimneys condenses other compounds

From Mike Short

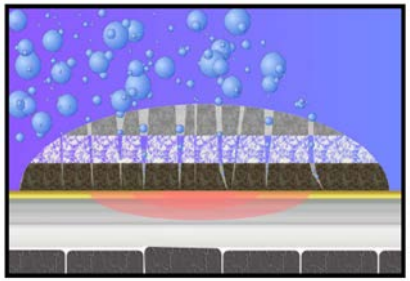

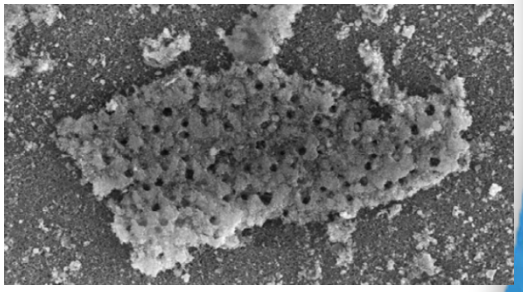

CRUD promotes formation of B-containing species that reduce neutron flux - "CRUD-Induced Power Shift (CIPS)"

Bonaccordite

Presence of Bonaccordite in CRUD has been associated with severe CIPS

$Ni_2Fe^{3+}(BO_3)O_2$

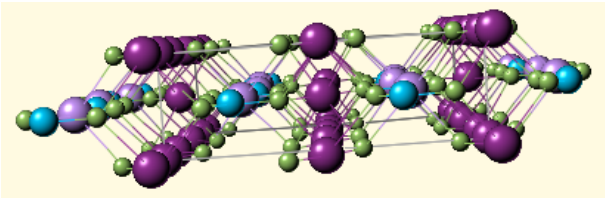

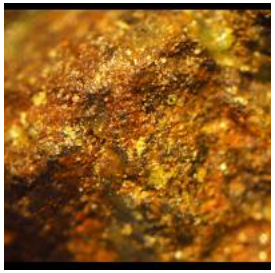

- Ludwigite group of boron containing minerals of form $M_2^{+2}M^{+3}O_2BO_3$.
- Very rare - only naturally found in Bon Accord region of South Africa
- Made via hydrothermal synthesis in supercritical water by Sawicki in presence of Ni, Fe and Boron acid/oxide.
- Presence of Li appears to promote Bonaccordite formation.

Thermochemical data not available for Bonaccordite despite apparent importance in CRUD/CIPS

MPO Modeling Hierarchy

MAMBA chemical kinetics to search for Bonaccordite formation conditions in CRUD

CALPHAD model to find solubility

First principles predictions of Bonaccordite thermodynamics

First Principles Based Thermodynamics

- Use experiment for ΔG(T,P) values
- Reference everything to first principles energies

Solve system of equations for unknown ECPs:

$$\Delta_f G^0_{\mathrm{Fe_2O_3}}(T) = E_{\mathrm{Fe_2O_3}}(0\,\mathrm{K}) - 2\mu^0_{\mathrm{Fe}}(T) - \frac{3}{2}\mu^0_{\mathrm{O_2}}(T)$$

$$\Delta_f G^0_{\mathrm{FeO(OH)}}(T) = E_{\mathrm{FeO(OH)}}(0\,\mathrm{K}) - \mu^0_{\mathrm{Fe}}(T) - \mu^0_{\mathrm{O_2}}(T) - \frac{1}{2}\mu^0_{\mathrm{H_2}}(T)$$

$$\Delta_f G^0_{\mathrm{Fe_3O_4}}(T) = E_{\mathrm{Fe_3O_4}}(0\,\mathrm{K}) - 3\mu^0_{\mathrm{Fe}}(T) - 2\mu^0_{\mathrm{O_2}}(T)$$

$$\Delta_f G^0_{\mathrm{NiO}}(T) = E_{\mathrm{NiO}}(0\,\mathrm{K}) - \mu^0_{\mathrm{Ni}}(T) - \frac{1}{2}\mu^0_{\mathrm{O_2}}(T)$$

$$\Delta_f G^0_{\mathrm{ZnO}}(T) = E_{\mathrm{ZnO}}(0\,\mathrm{K}) - \mu^0_{\mathrm{Zn}}(T) - \frac{1}{2}\mu^0_{\mathrm{O_2}}(T)$$

$$\underbrace{\Delta_f G^0_{\mathrm{Co_3O_4}}(T)}_{\text{From database}} = \underbrace{E_{\mathrm{Co_3O_4}}(0\,\mathrm{K})}_{\text{First-Principles}} \underbrace{- 3\mu^0_{\mathrm{Co}}(T) - 2\mu^0_{\mathrm{O_2}}(T)}_{\text{ECPs}}$$

6 equations and 6 unknowns at each T (effective chemical potentials of Fe, O_2, H_2, Ni, Zn, Co)

Adding Solvation Chemistry

- Free energies of formation of aqueous species can be incorporated into the scheme
- We use SUPCRT92 database that includes high temperature and pressure data for aqueous ions calculated using the Helgeson-Kirkham-Flowers equation of state:

$$
\begin{aligned}
(\Delta_f G_{\mathrm{H_2O}}(T,P))_g &= (\mu_{\mathrm{H_2O}}(T,P))_g - \frac{1}{2}\mu^0_{\mathrm{O_2}}(T) - \mu^0_{\mathrm{H_2}}(T) \\
(\Delta_f G_{\mathrm{H_2O}}(T,P))_l &= (\mu_{\mathrm{H_2O}}(T,P))_l - \frac{1}{2}\mu^0_{\mathrm{O_2}}(T) - \mu^0_{\mathrm{H_2}}(T) \\
(\Delta_f G_{\mathrm{Ni^{+2}}}(T,P))_{aq} &= (\mu_{\mathrm{Ni^{+2}}}(T,P))_{aq} - \mu^0_{\mathrm{Ni}}(T) - \mu^0_{\mathrm{H_2}}(T) + 2\left(\mu^0_{\mathrm{H^+}}(T,P)\right)_{aq} \\
(\Delta_f G_{\mathrm{Fe^{+2}}}(T,P))_{aq} &= (\mu_{\mathrm{Fe^{+2}}}(T,P))_{aq} - \mu^0_{\mathrm{Fe}}(T) - \mu^0_{\mathrm{H_2}}(T) + 2\left(\mu^0_{\mathrm{H^+}}(T,P)\right)_{aq} \\
(\Delta_f G_{\mathrm{Fe^{+3}}}(T,P))_{aq} &= (\mu_{\mathrm{Fe^{+3}}}(T,P))_{aq} - \mu^0_{\mathrm{Fe}}(T) - \frac{3}{2}\mu^0_{\mathrm{H_2}}(T) + 3\left(\mu^0_{\mathrm{H^+}}(T,P)\right)_{aq} \\
\underbrace{(\Delta_f G_{\mathrm{Zn^{+2}}}(T,P))_{aq}}_{\text{From database}} &= \underbrace{(\mu_{\mathrm{Zn^{+2}}}(T,P))_{aq}}_{\text{Unknown}} - \underbrace{\mu^0_{\mathrm{Zn}}(T) - \mu^0_{\mathrm{H_2}}(T) + 2\left(\mu^0_{\mathrm{H^+}}(T,P)\right)_{aq}}_{\text{ECPs from DFT training set}}
\end{aligned}
$$

Validation

Can the effective chemical potentials derived from binary oxides be extended to ternary oxides?

$$\Delta_f G^0_{\mathrm{NiFe_2O_4}}(T) = E_{\mathrm{NiFe_2O_4}}(0\,\mathrm{K}) - \mu^0_{\mathrm{Ni}}(T) - 2\mu^0_{\mathrm{Fe}}(T) - 2\mu^0_{\mathrm{O_2}}(T)$$

$$\Delta_f G^0_{\mathrm{CoFe_2O_4}}(T) = E_{\mathrm{CoFe_2O_4}}(0\,\mathrm{K}) - \mu^0_{\mathrm{Co}}(T) - 2\mu^0_{\mathrm{Fe}}(T) - 2\mu^0_{\mathrm{O_2}}(T)$$

$$\Delta_f G^0_{\mathrm{ZnFe_2O_4}}(T) = E_{\mathrm{ZnFe_2O_4}}(0\,\mathrm{K}) - \mu^0_{\mathrm{Zn}}(T) - 2\mu^0_{\mathrm{Fe}}(T) - 2\mu^0_{\mathrm{O_2}}(T)$$

Least-squares fit ECPs to binary oxides *and* ferrites

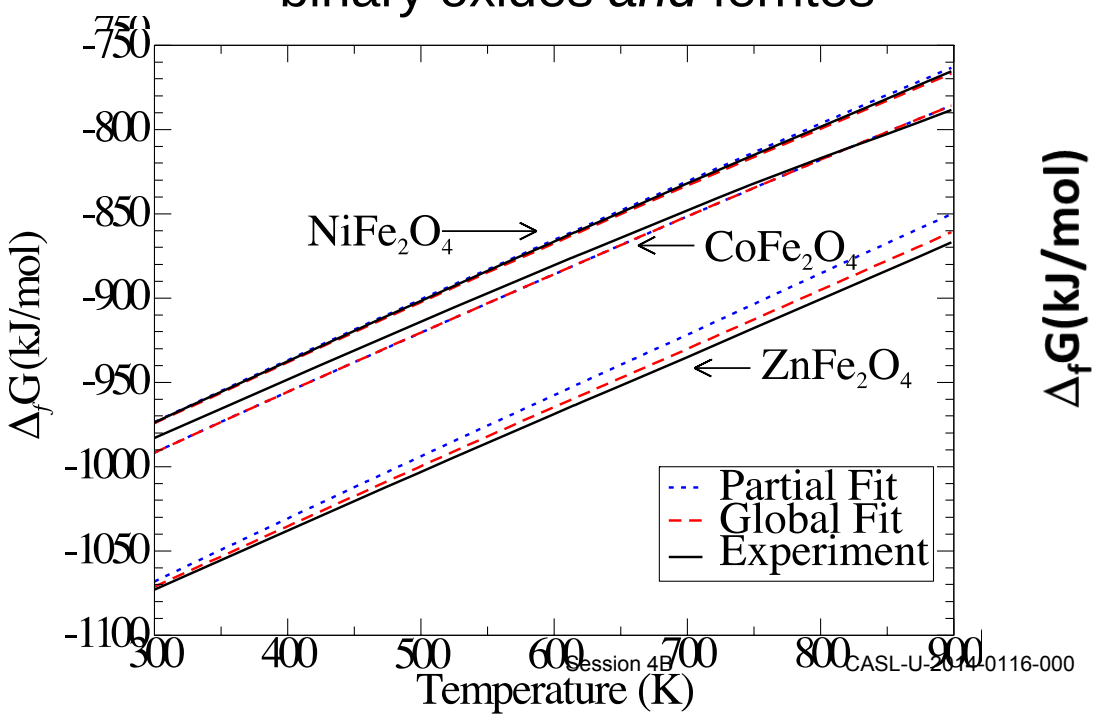

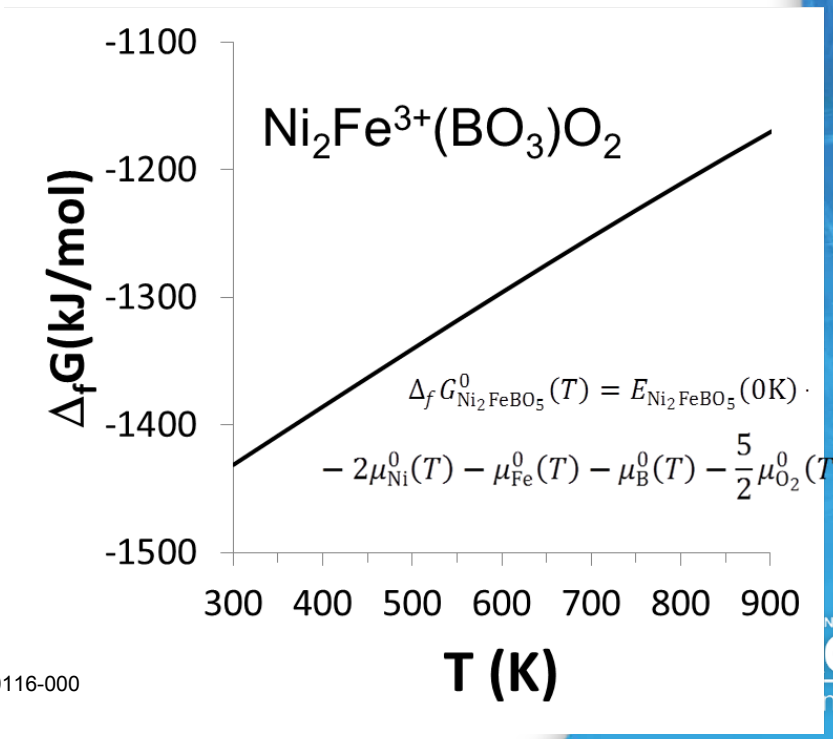

CALPHAD

Dongwon Shin
Ted Besmann

- CALculation of PHAse Diagram
- Used to calculate solubility of CRUD constituents & Bonaccordite
- Implemented in Thermo-Calc via AQS2 database
- Comparing to known solubilities provides some validation

Solubilities at 155 bar
(experiment at 207.9 bar)

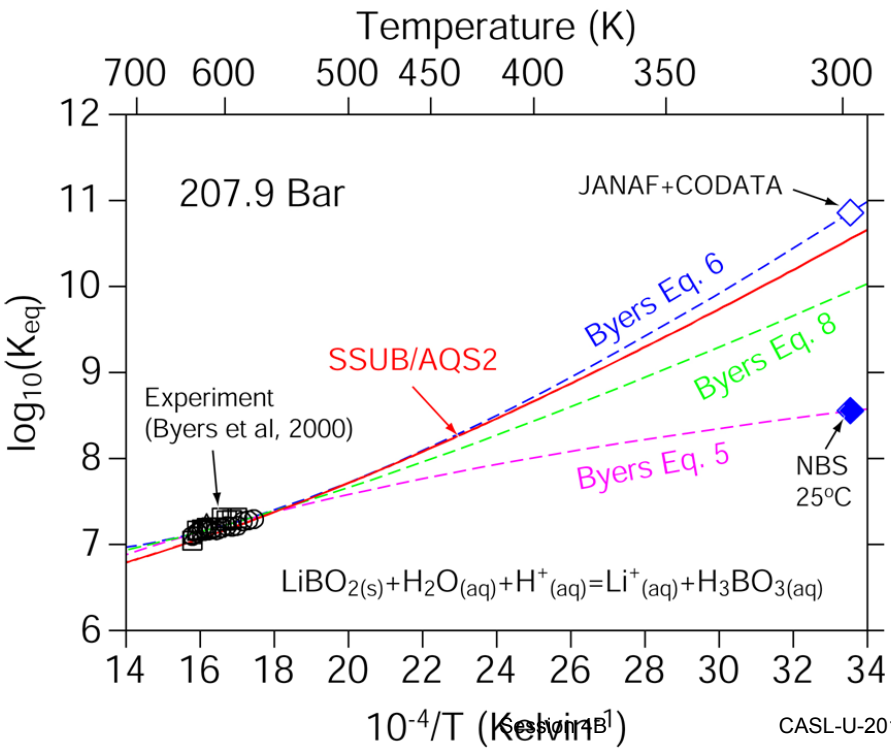

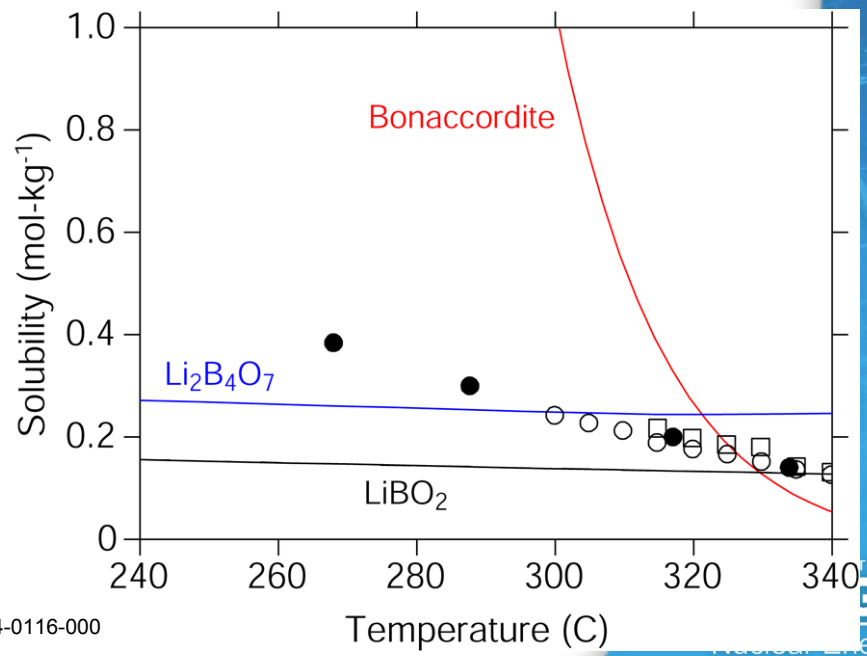

MAMBA Calculations

MAMBA Computed Solubilities for PWR Conditions
(based on the SSUB/AQS2 computed equilibrium constants)

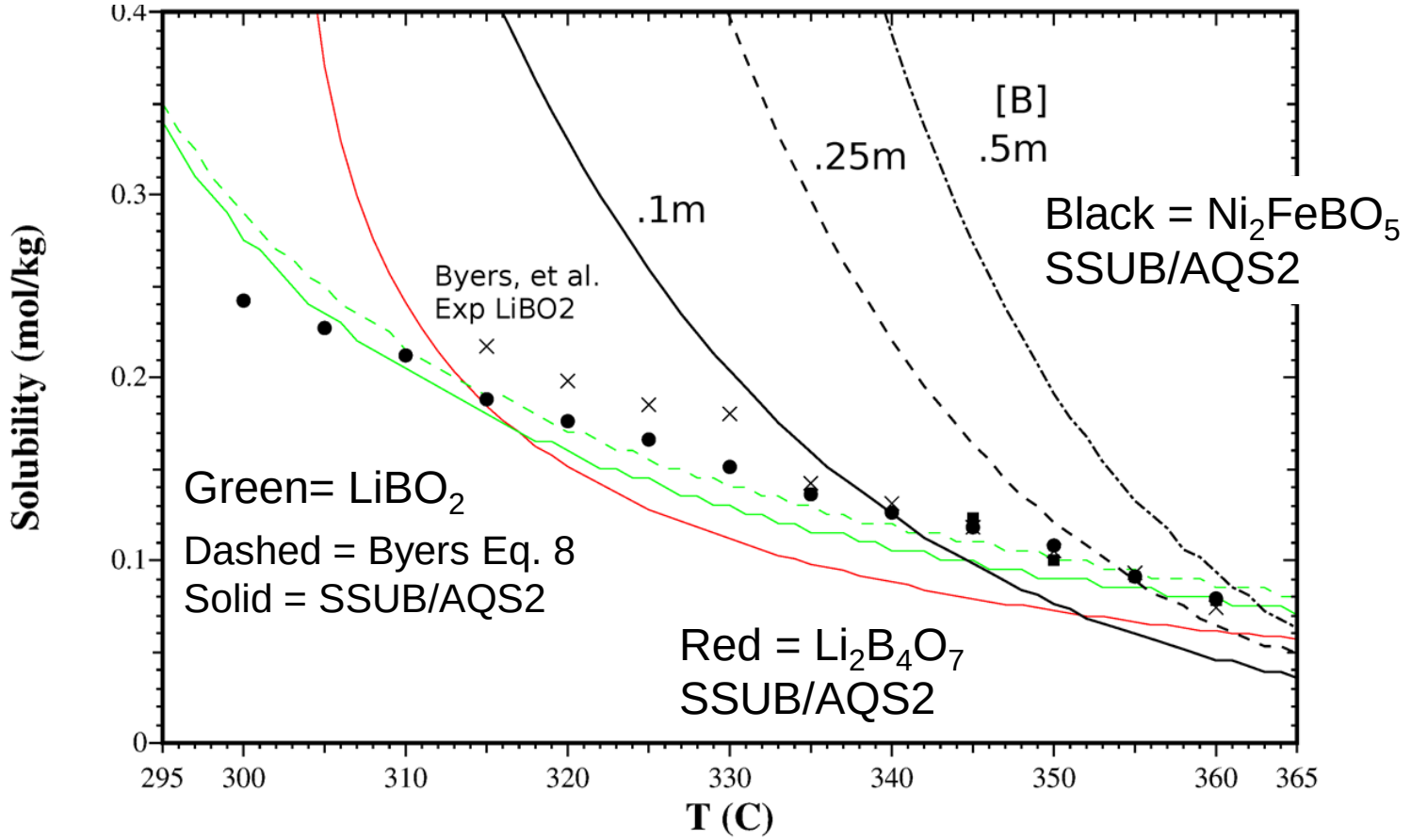

MAMBA Calculations

Thermodynamic correlations + MAMBA transport / boiling models determine precipitation threshold and boron uptake in CRUD

Current MAMBA crud / thermo models predict precipitation of $Li_2B_4O_7$ but <u>not</u> $LiBO_2$ or Ni_2FeBO_5

Crud porosity at 450 days
(profile view of crud layer)

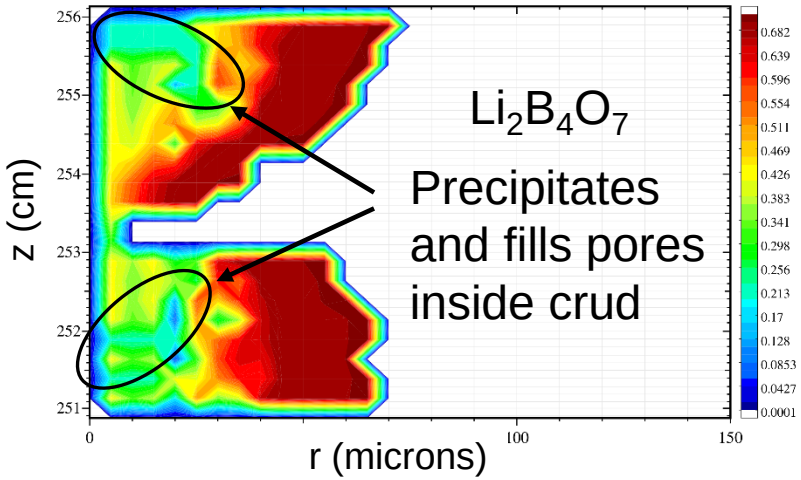

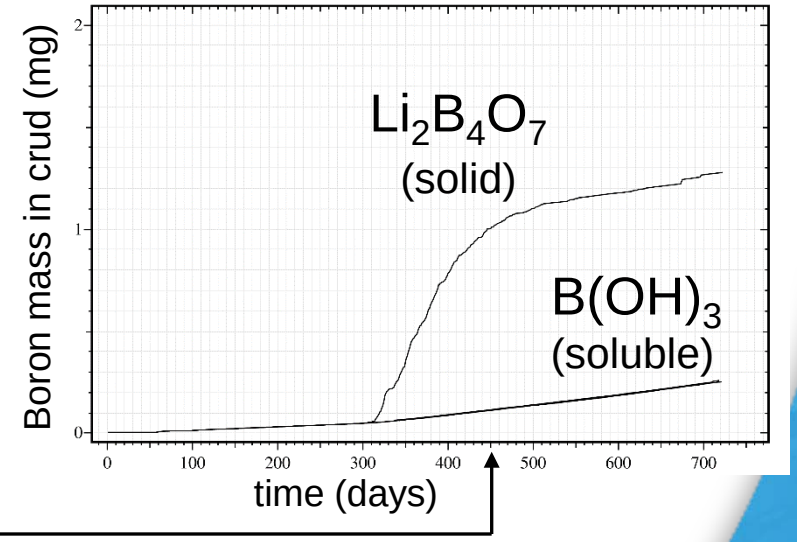

Where's the Bonaccordite?

Possible reasons for not observing Bonaccordite in calculations:

- First principles predictions are not accurate enough
  - Hubbard + spin parameters (U')
  - Magnetic spin states
  - Non-stoichiometries
  - More consistent data set for chemical potentials
- Conditions are missing in the MAMBA calculations
  - Super critical water
  - ^{10}B → Li capture and micro-chemistry

Related Project – Nickel Ferrite Clusters

New model for CRUD nucleation – <u>Nickel Ferrite Particles</u>

- First principles thermodynamics predict: **+ΔG** for forming bulk nickel ferrite, **-ΔG** for forming (111) surfaces @ PWR conditions

$$\gamma(T,P) = \frac{1}{2A}\left\{G_{\text{slab}} - \Gamma_{\text{Fe}}\mu_{\text{Fe}^{+2}} - \Gamma_{\text{Ni}}\mu_{\text{Ni}^{+2}} - \Gamma_{\text{NiFe}_2\text{O}_4}g_{\text{NiFe}_2\text{O}_4} - n_{\text{H}_2}\mu_{\text{H}_2\text{O}} - [\Gamma_{\text{Fe}} + \Gamma_{\text{Ni}}] \cdot \left(\left(\Delta_f G_{\text{H}_2}\right)_{aq} - \left(\mu_{\text{H}_2}\right)_{aq} + 2\mu_{\text{H}^+}\right)\right\}$$

155 bar, pH = 7.2, $[Ni^{2+}] = 1.66 \times 10^{-14}$
$[Fe^{2+}] = 4.17 \times 10^{-13}$ mol/kg

- $\Gamma_{\text{Fe}} = \Gamma_{\text{Ni}} = 0$, $\Gamma_{\text{NiFe2O4}} = 1$ for stoichiometric surface
- Reduces to traditional surface energy
- Non-stoichiometric surface energy depend on environment

{111} surfaces have very negative surface energies in PWR coolant conditions

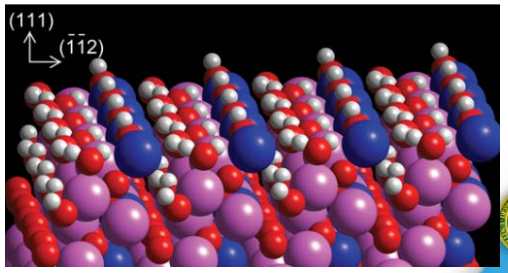

Related Project – Nickel Ferrite Clusters

New model for CRUD nucleation – <u>Nickel Ferrite Particles</u>

- Stabilizes ~60 nm octahedral clusters in PWR coolant.
- Too small for filters, too big for demineralizers
- Octahedral shape consistent with CRUD morphology

CRUD nucleated from thermodynamically stable nickel ferrite particles?

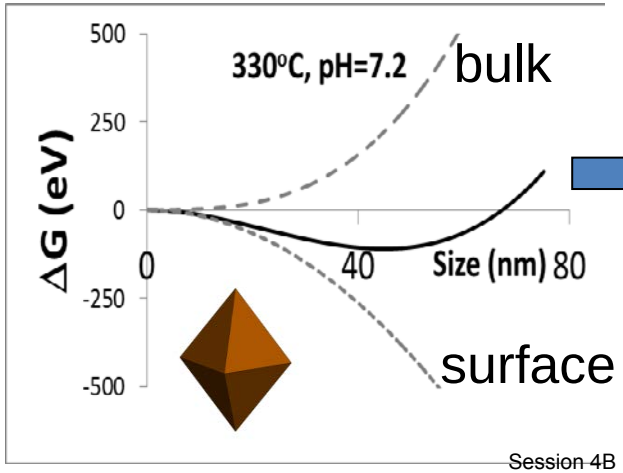

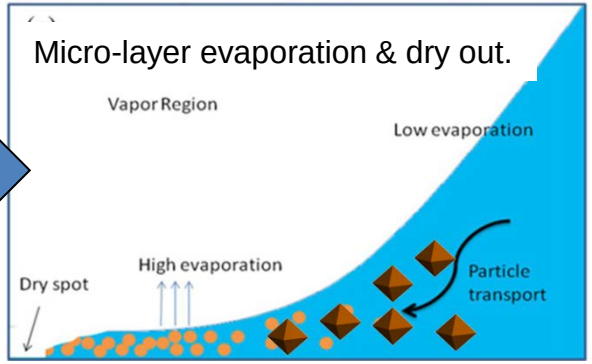

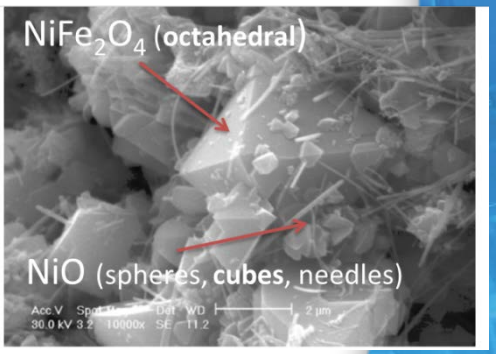

New Project – Stability of Porous CRUD

Particle Assembled /Confined Expansion (PACE) model

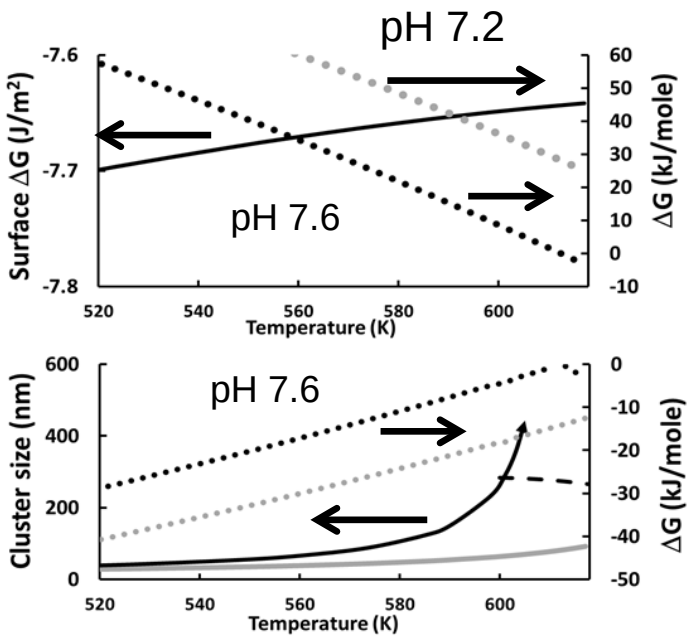

Bonding along <100> directions eliminates {100} planes

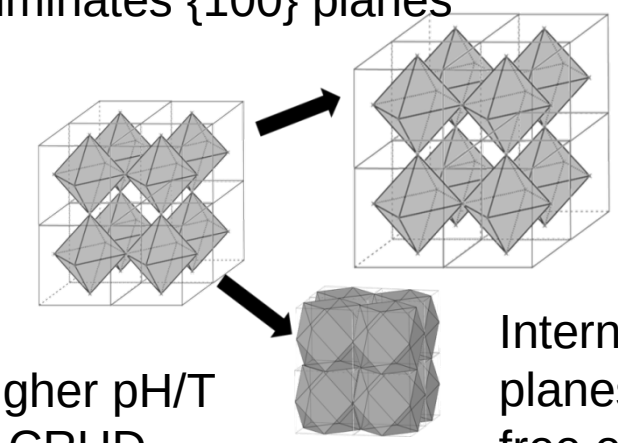

Higher pH/T in CRUD

Internal {111} planes lower free energy

- Higher T & pH in CRUD drives larger particle sizes
- When ΔG for bulk goes negative, particle size gets infinite

- Confined particles fill out instead of enlarge
- Leads to porous CRUD structure

New Project – Stability of Porous CRUD

Particle Assembled/Confined Expansion (PACE) model

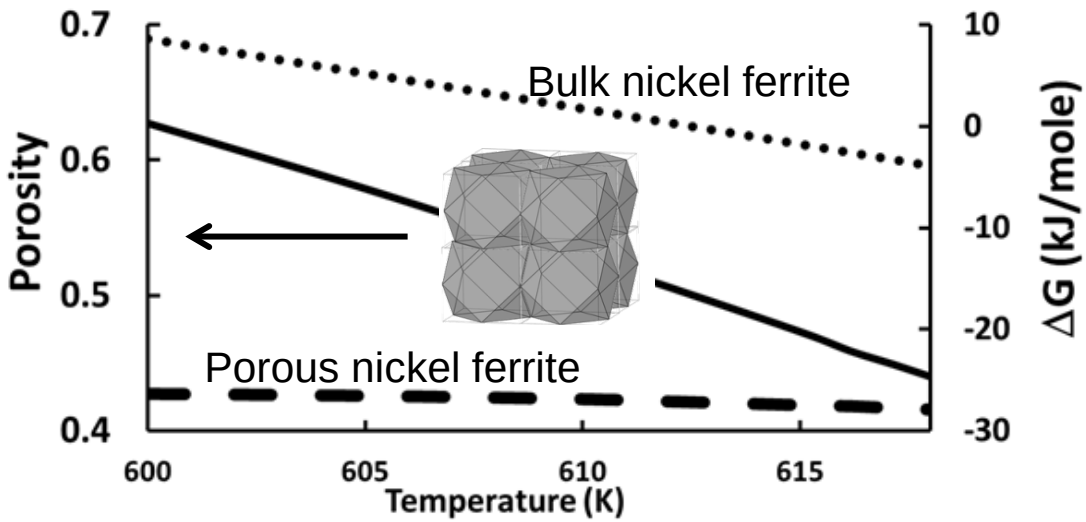

- Models predicts decreasing porosity with increasing T
- Porous nickel ferrite (CRUD) has negative ΔG even where bulk ΔG is positive.

- Explains porosity variations observed in CRUD
- Consistent with CRUD particulate microstructure
- Explains high concentration of nickel ferrite observed in CRUD
- Explains stability of porous structure

Nickel ferrite models need experimental validation!

Chris O'Brien, now at postdoc at SNL

Dongwon Shin, Ted Besmann, ORNL

Brian Kendrick, David Andersson, Chris Stanek, LANL

Don Brenner, Zsolt Rak, Eric Buchholz, NCSU

Imperial College London

Dislocations and creep in UO_2

Samuel T. Murphy, Paul Fossati and Robin. W. Grimes

Centre for Nuclear Engineering

Dislocations in UO_2

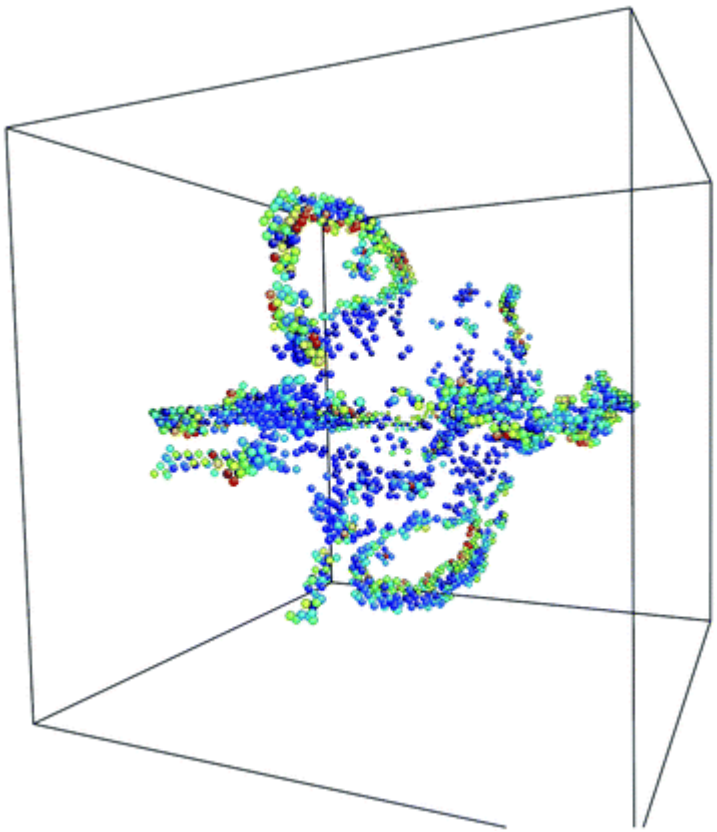

MD simulation showing the evolution of a thermal spike in UO_2 (Devanathan *et al.* EES 3 (2010) 1406).

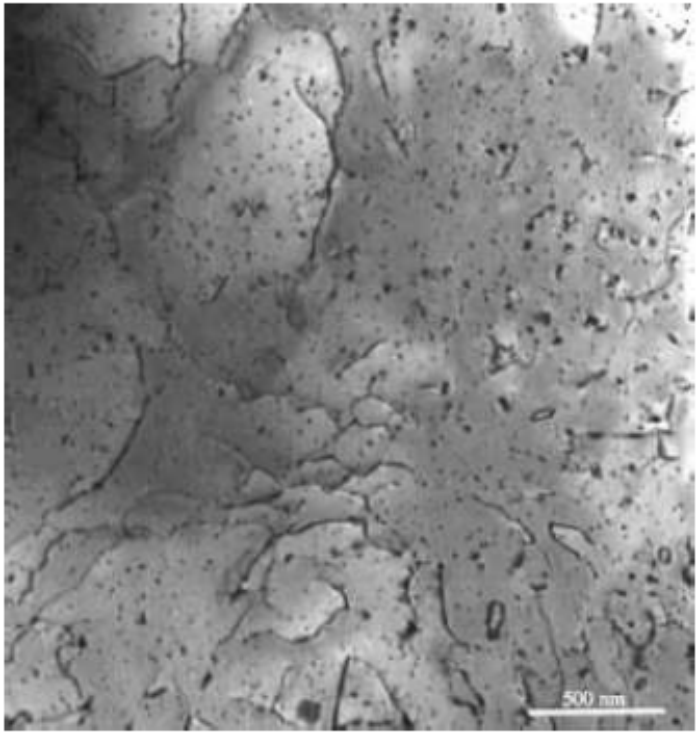

Micrograph showing dislocations in nuclear fuel (image courtesy of EDF energy).

Dislocations in UO_2

- The presence of these dislocations can lead to a significant change in the fuel's properties, such as:
  - creep rate
  - thermal conductivity
  - fission product behaviour
- Accelerated Xe diffusion along dislocations has been proposed to explain the unexpectedly high fission gas release during a transient at high temperatures.
- Dislocations piling up against bubbles and precipitates in the rim of the fuel pellet has been suggested as the mechanism responsible for the formation of the high burn-up structure (HBS).

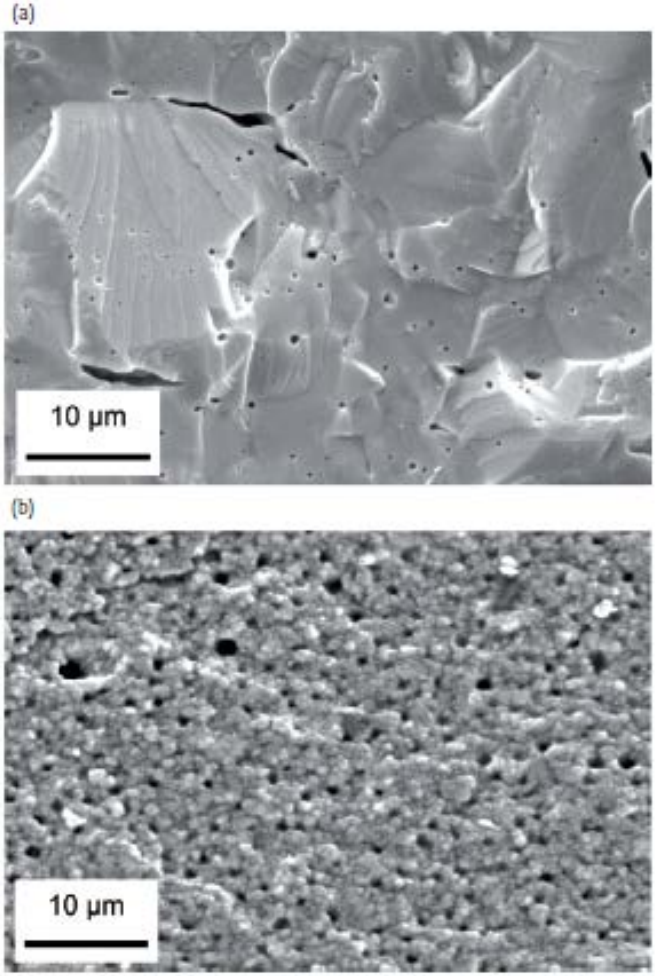

(a) Unirradiated UO_2 and (b) fuel with local burn-up of 75 GWd/tHM showing typical HBS morphology Rondinella and Wiss (Mater. Today 13 (2010) 24).

Methodology

- Due to the large strain fields surrounding dislocations it is necessary to use a large number of atoms so DFT impractical, therefore molecular dynamics.
- Employ empirical pair potentials with the potential parameters taken from.
  - U-O and O-O from Morelon *et al.* (Phil. Mag. 83 (2003) 2533)
  - Xe-U and Xe-O from Chartier *et al.* (Phys. Rev. B 81 (2010) 174111)
  - Xe-Xe from Tang and Toennies (J. Chem. Phys. 118 (2003) 4976).
- Dynamics simulations employed a timestep of 1 fs.
- Simulation cells seeded with random arrangements of Xe on Schottly trivacancy defects.
- Xe diffusivity is calculated by determining the mean squared displacement (msd), i.e.

$$D = \lim_{t \to \infty} \frac{1}{2d} \frac{\left[r_i(t) - r_i(t_0) \right]^2}{t}$$

- Simulations employed the LAMMPS simulation package.

Simulation methodologies

	Xe diffusion	Dislocation pinning
Supercell size	280 Å x 280 Å x 100 Å	200 Å x 200 Å x 100 Å
Number of atoms	550,000	300,000
Number of dislocations	4	2
Xe concentration	1.5%	0-2%
Temperature range	2300 – 3200 K	1500 K
Simulation outline	1. Energy minimise 2. Equilibrate using NPT for 10 ps. 3. Collect data for up to 350 ps.	1. Energy minimise 2. Equilibrate using NPT for 10 ps. 3. Collect data for up to 350 ps.

Imperial College London

Strain fields surrounding a {100}<110> edge dislocation

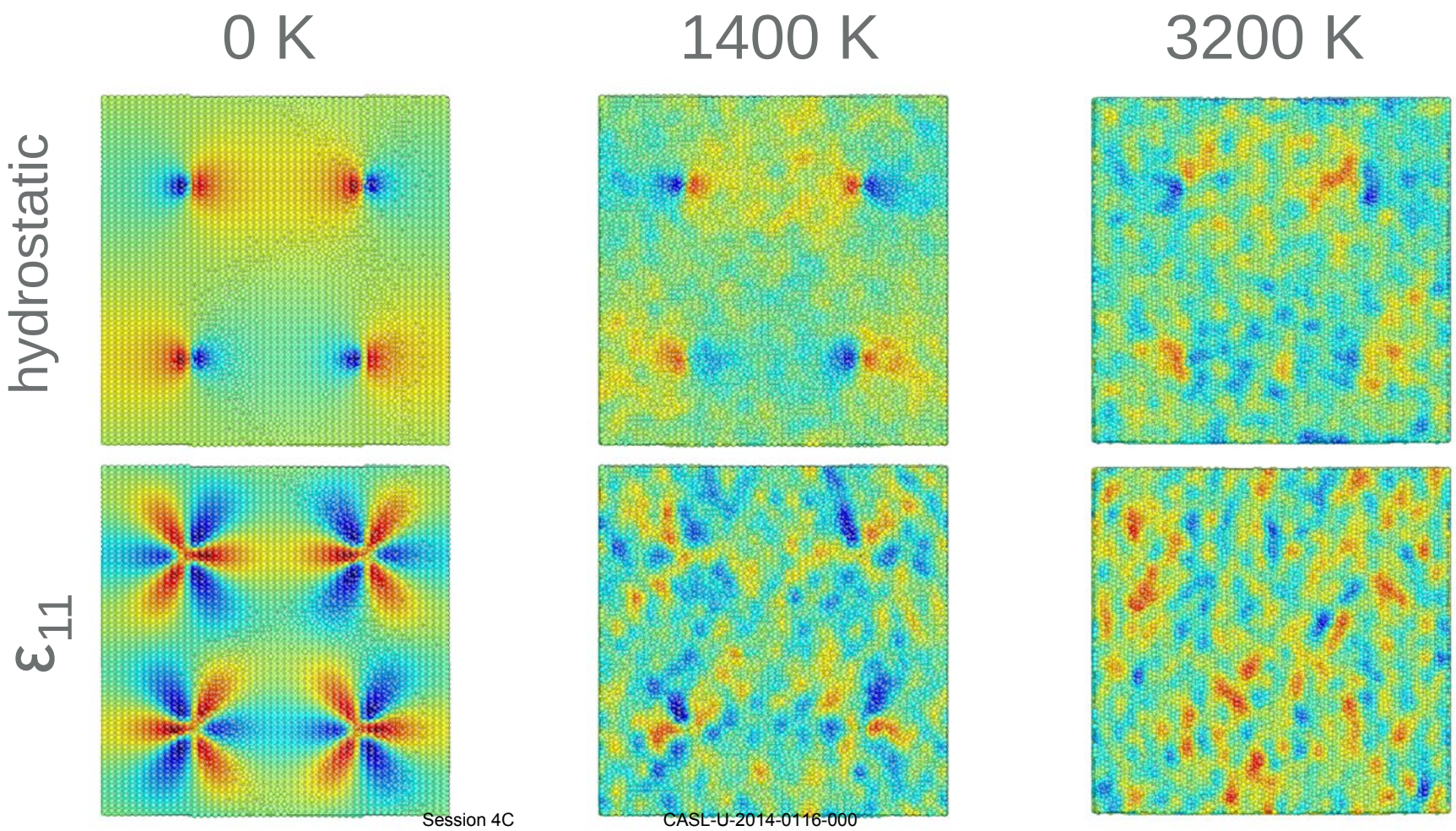

A potential problem…

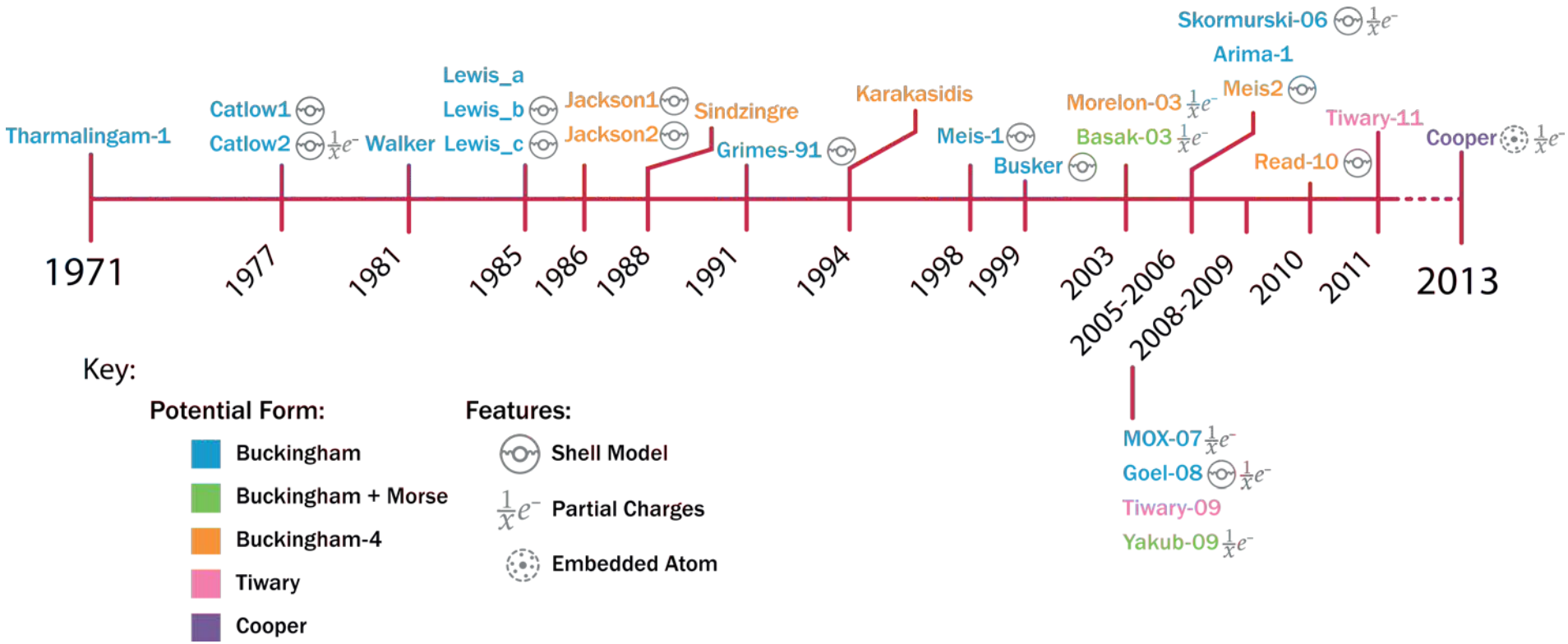

Comparison of interatomic potentials

- Compare dislocation stabilities via the line energy:

$$E(r) = E_d(r) - E_p(r) \cong E_d(r) - \sum_{j=U,O} N_j \langle E_j \rangle$$

- Partial charge potentials have lower line energies due to reduced electrostatic interactions.

Line energies for the {100}<110> dislocation in UO_2.

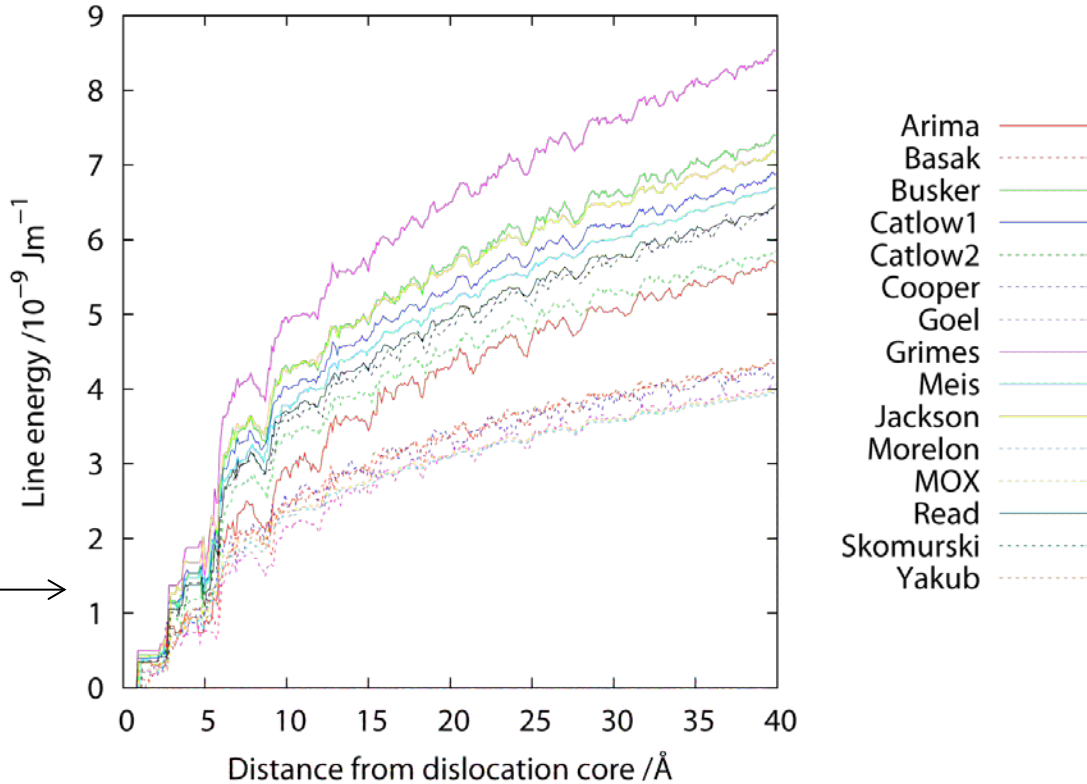

Murphy *et al.* Prog. Nucl. Energy 72 (2014) 27

Comparison of interatomic potentials

Line energies ($x10^{-9}$ Jm^{-1}) at 40 Å from the dislocation line.

Potential	{100}⟨110⟩	{110}⟨110⟩	{111}⟨110⟩	Screw
Arima	5.691	6.763	6.123	**5.358**
Basak	4.328	5.422	5.234	**4.081**
Busker	7.389	9.006	7.985	**6.835**
Catlow1	6.874	7.913	7.307	**5.823**
Catlow2	5.846	7.107	6.332	**5.412**
Cooper	4.121	5.66	4.91	**3.784**
Goel	4.062	4.876	4.492	**4.05**
Grimes	8.522	10.239	8.968	**7.474**
Jackson	7.16	8.077	7.341	**5.879**
Meis	6.691	7.63	6.939	**5.586**
Morelon	3.944	4.344	4.001	**3.099**
MOX07	3.984	4.475	4.085	**3.276**
Read	6.473	7.405	6.741	**6.473**
Skormurski	6.431	7.266	6.553	**5.462**
Yakub	4.367	5.581	4.922	**4.1**

Comparison of interatomic potentials

Line energies ($x10^{-9}$ Jm^{-1}) at 40 Å from the dislocation line.

Potential	{100}⟨110⟩	{110}⟨110⟩	{111}⟨110⟩	Screw
Arima	5.691	6.763	6.123	**5.358**
Basak	4.328	5.422	5.234	**4.081**
Busker	7.389	9.006	7.985	**6.835**
Catlow1	6.874	7.913	7.307	**5.823**
Goel	4.062	4.876	4.492	**4.05**
Grimes	8.522	10.239	8.968	**7.474**
Jackson	7.16	8.077	7.341	**5.879**
Meis	6.691	7.63	6.939	**5.586**
Morelon	3.944	4.344	4.001	**3.099**
MOX07	3.984	4.475	4.085	**3.276**
Read	6.473	7.405	6.741	**6.473**
Skormurski	6.431	7.266	6.553	**5.462**
Yakub	4.367	5.581	4.922	**4.1**

Screw < {100}<110> < {111}<110> < {110}<110>

Comparison of interatomic potentials

Arima {110}<110>

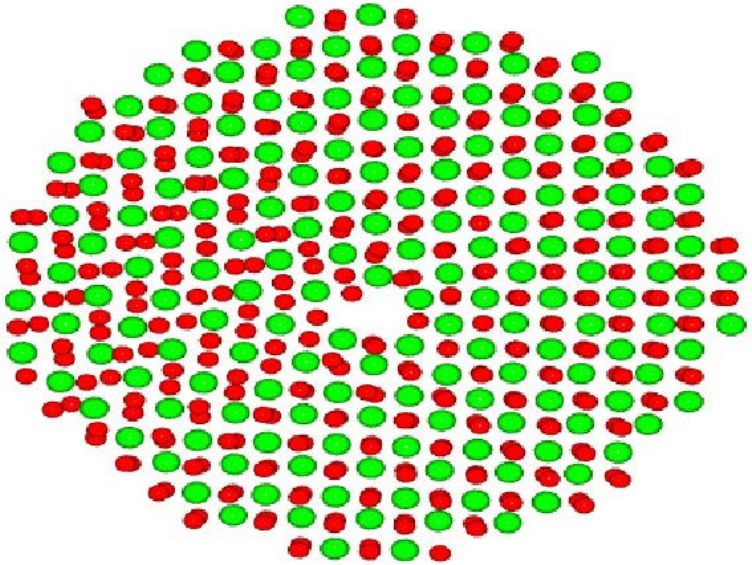

Basak {110}<110>

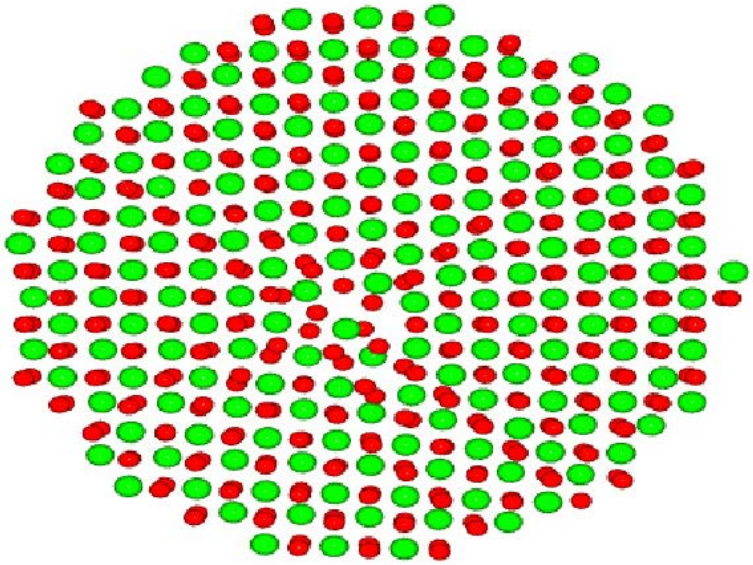

Comparison of interatomic potentials - Xe

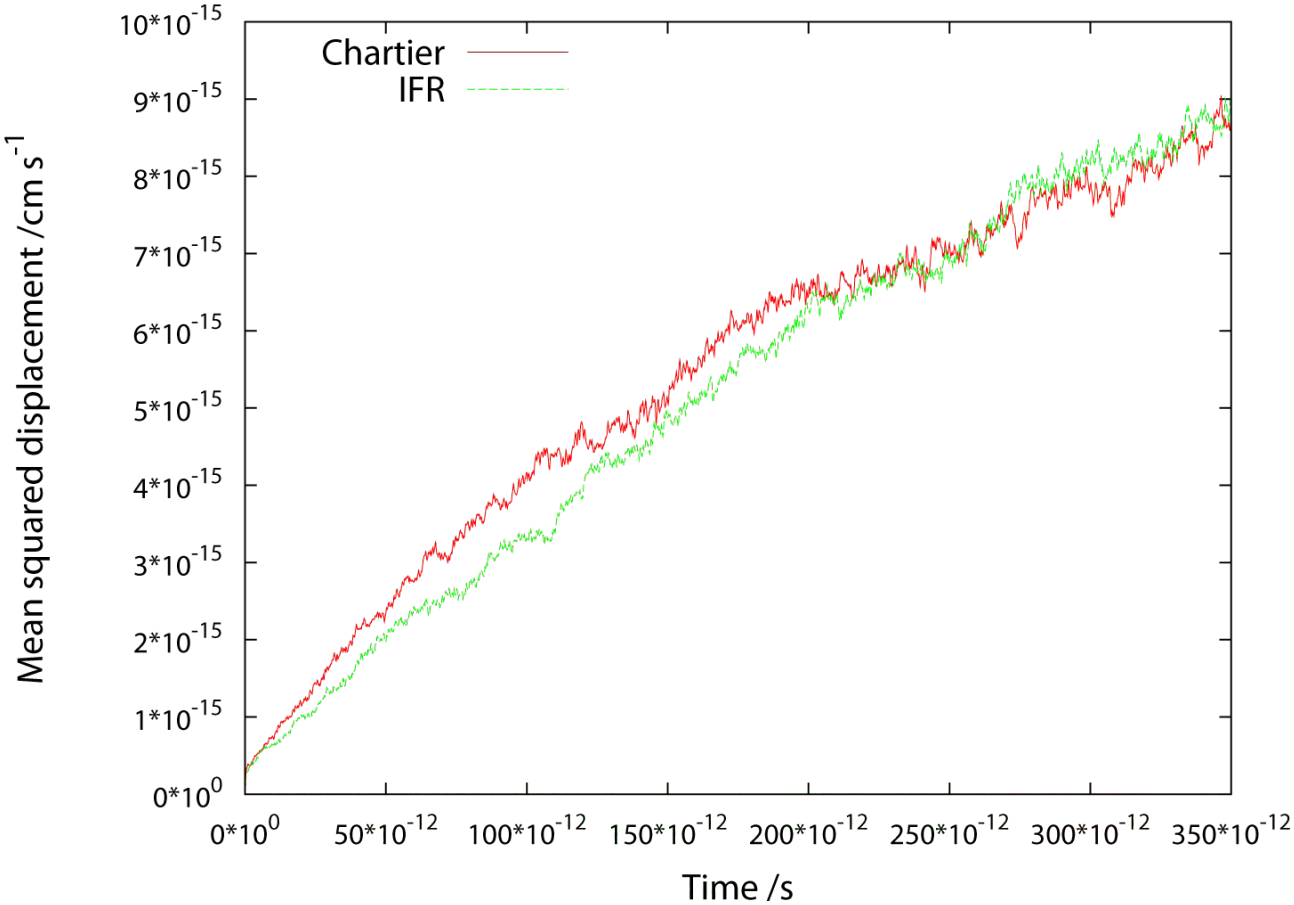

Comparison of the average Xe msd around 12 {100}<110> using the potentials of Chartier *et al.* and the IFR potential of Thompson *et al.* (these simulations also contained an excess of Schottky tri vacancies)

The effect of dislocations on Xe

Pipe diffusion of intrinsic O^{2-} and U^{4+}

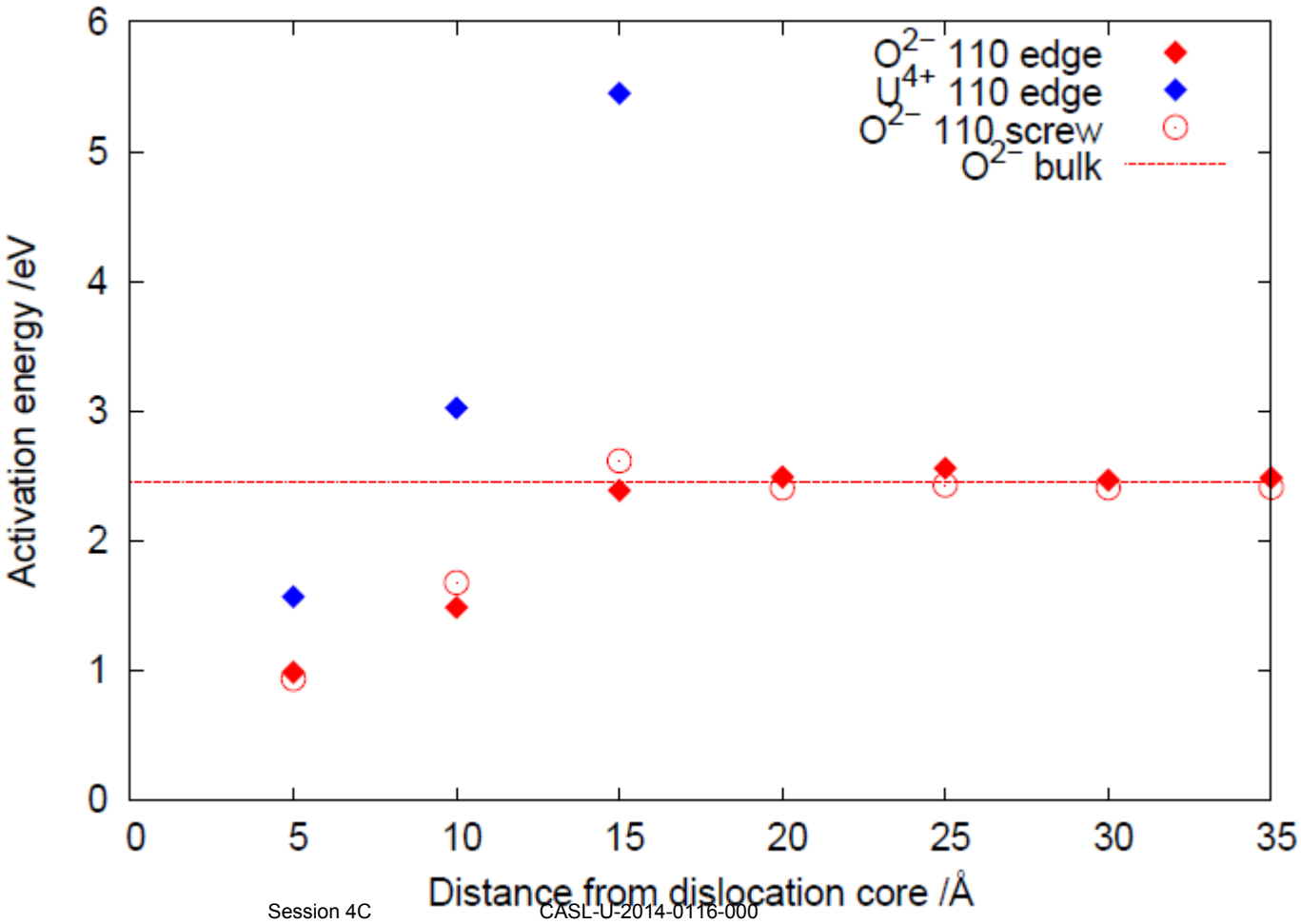

Murphy *et al.* J. Nucl. Mater. 447 (2014) 143

Influence of core structure on O^{2-} diffusivity

Arrhenius plots for oxygen diffusion within 20 Å of the dislocation core for our dislocations compared to bulk UO_2.

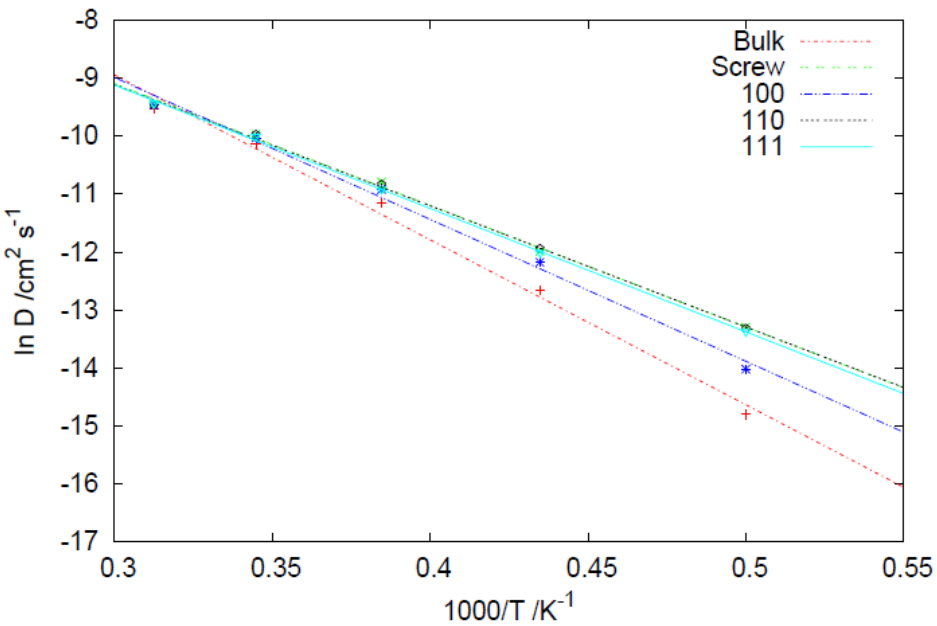

Activation energies for oxygen diffusion along dislocations compared to pristine UO_2.

System	E_a /eV
Pristine	2.45
{110}<110>	1.74
{100}<110>	2.17
{111}<110>	1.66
Screw	1.75

Dislocations provide a pathway for enhanced diffusion. This is strongly influenced by the dislocation core structure.

Xe diffusion close to the core of the dislocation

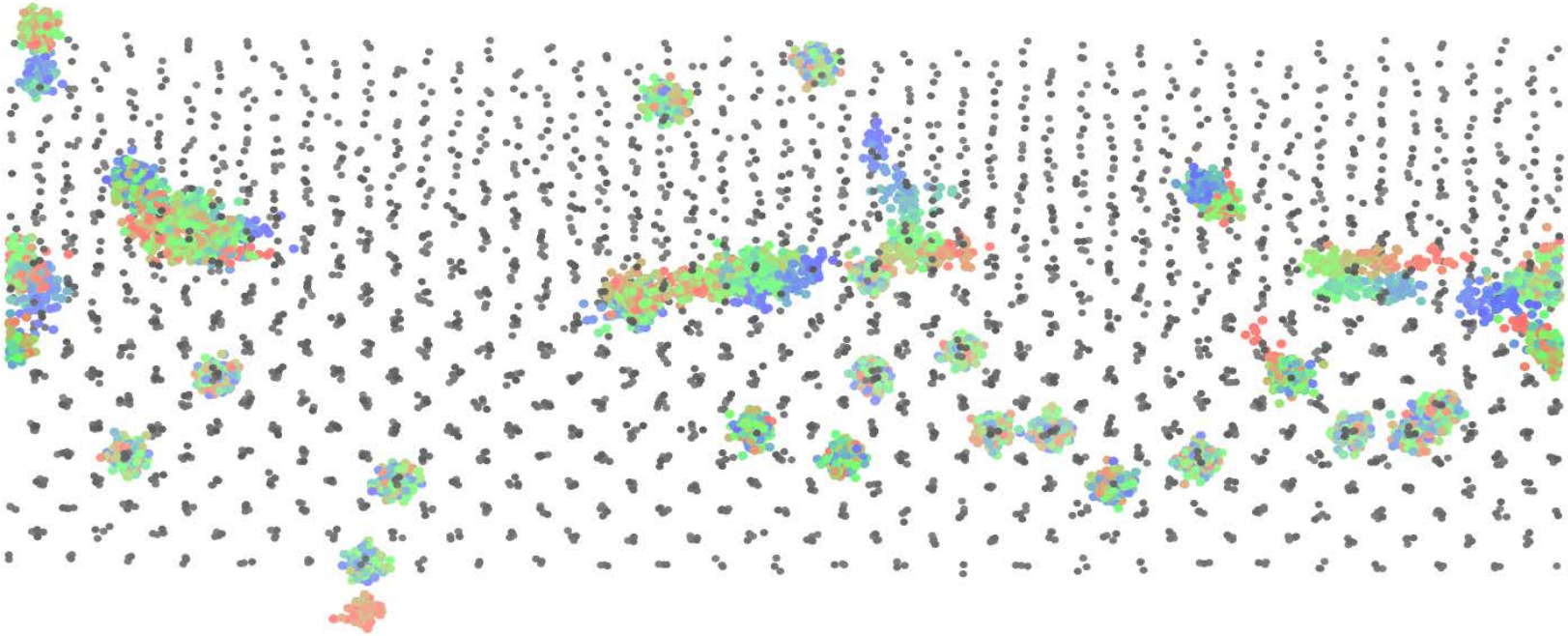

Xe diffusion close to the dislocation core. Grey speheres represent positons of the uranium ions in the final timestep. The Xe are plotted as a superposition of all positions at every timestep coloured from blue to red in time.

Xe diffusion around dislocations

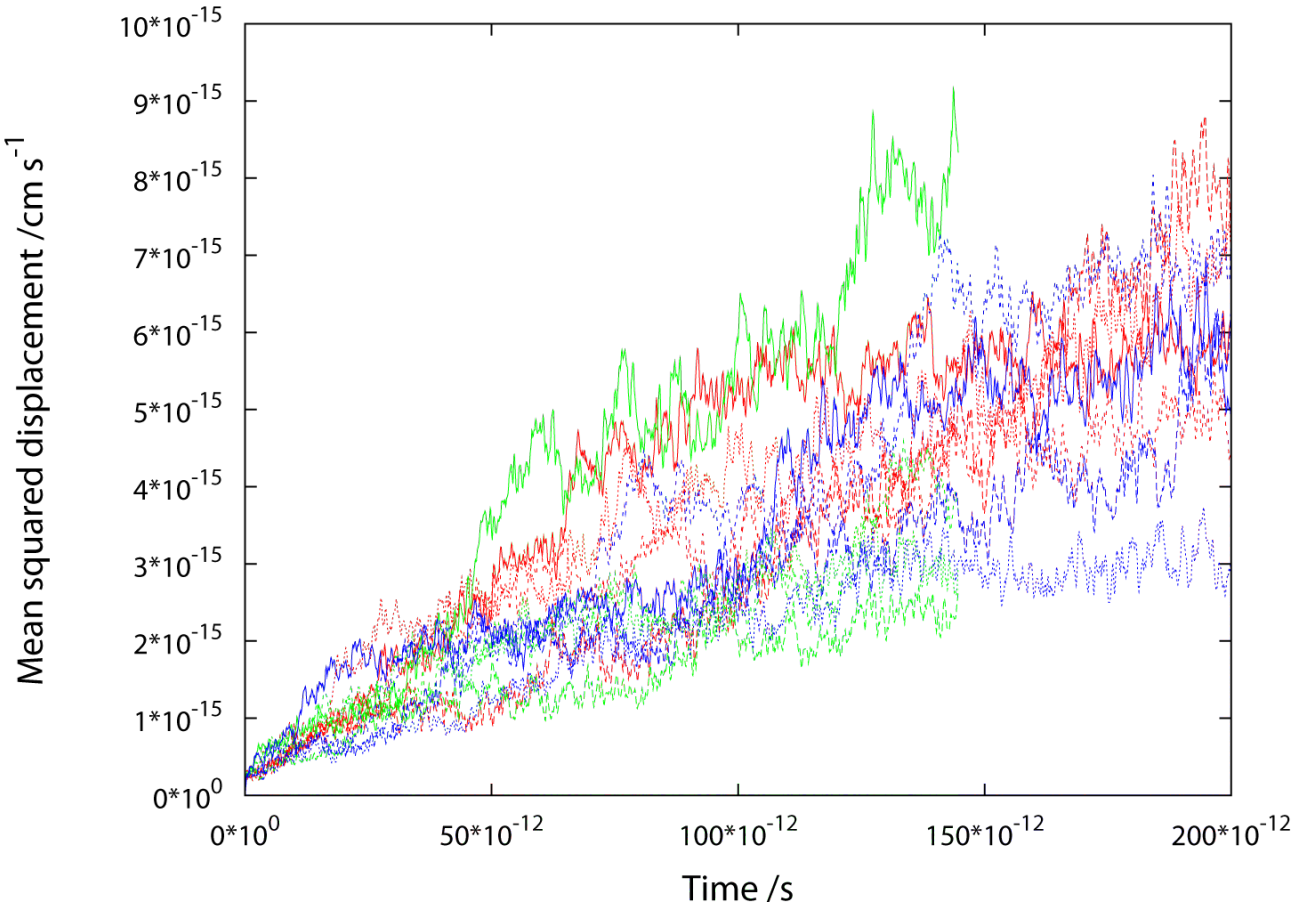

Mean squared displacement of Xe around 12 {100}<110> dislocations at 3200 K.

Xe diffusion around dislocations

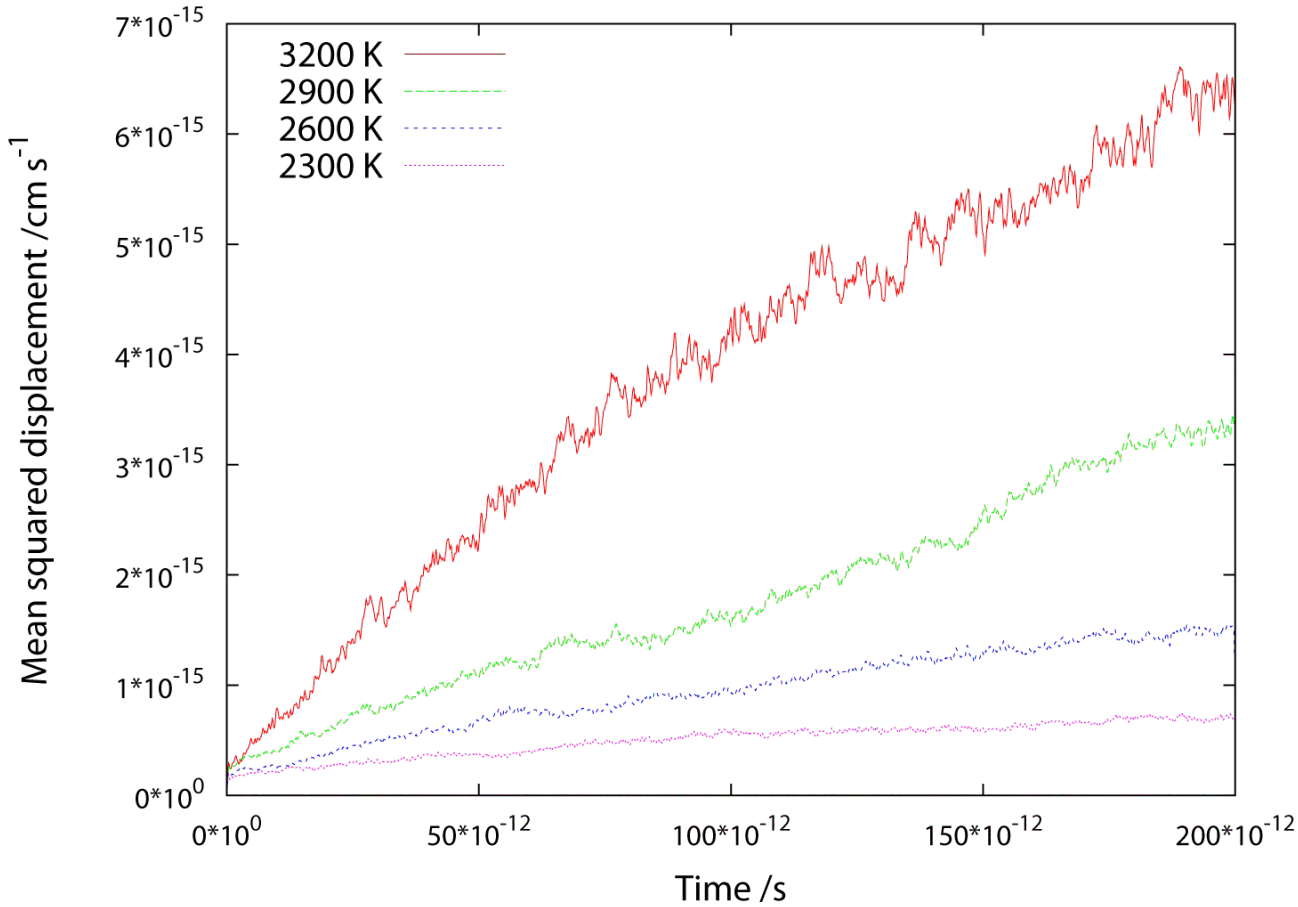

Averaged mean squared displacements around a {100}<110> dislocation at a range of temperatures.

Xe diffusion around dislocations

Arrhenius plots for xenon diffusion within 20 Å of the dislocation core for our dislocation compared to bulk UO_2 and a Schottky excess.

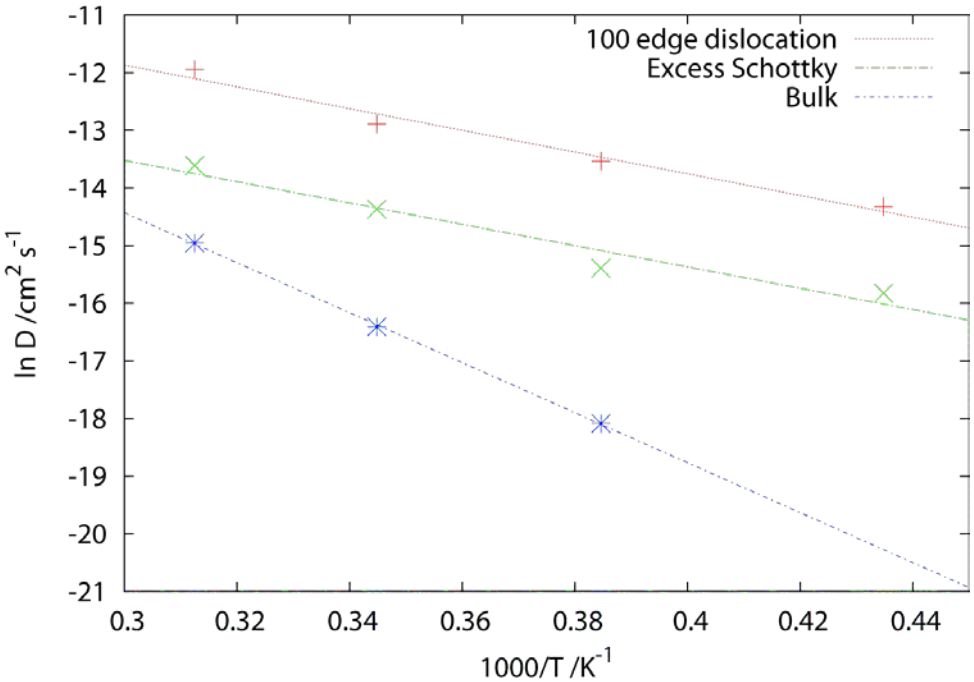

System	E_a /eV	D_0 /cm^2 s^{-1}
Bulk	3.64	0.24
Dislocation	1.62	0.0020
Excess Schottky	1.58	0.00035

Govers and Verweft predict an activation energies for Xe in the bulk of 2.89 eV and 0.5 eV near a grain boundary.

Xe mobility is dramatically enhanced near a dislocation, but.....

Govers and Verweft. J. Nucl. Mater. 438 (2013) 134

Xe diffusion around dislocations

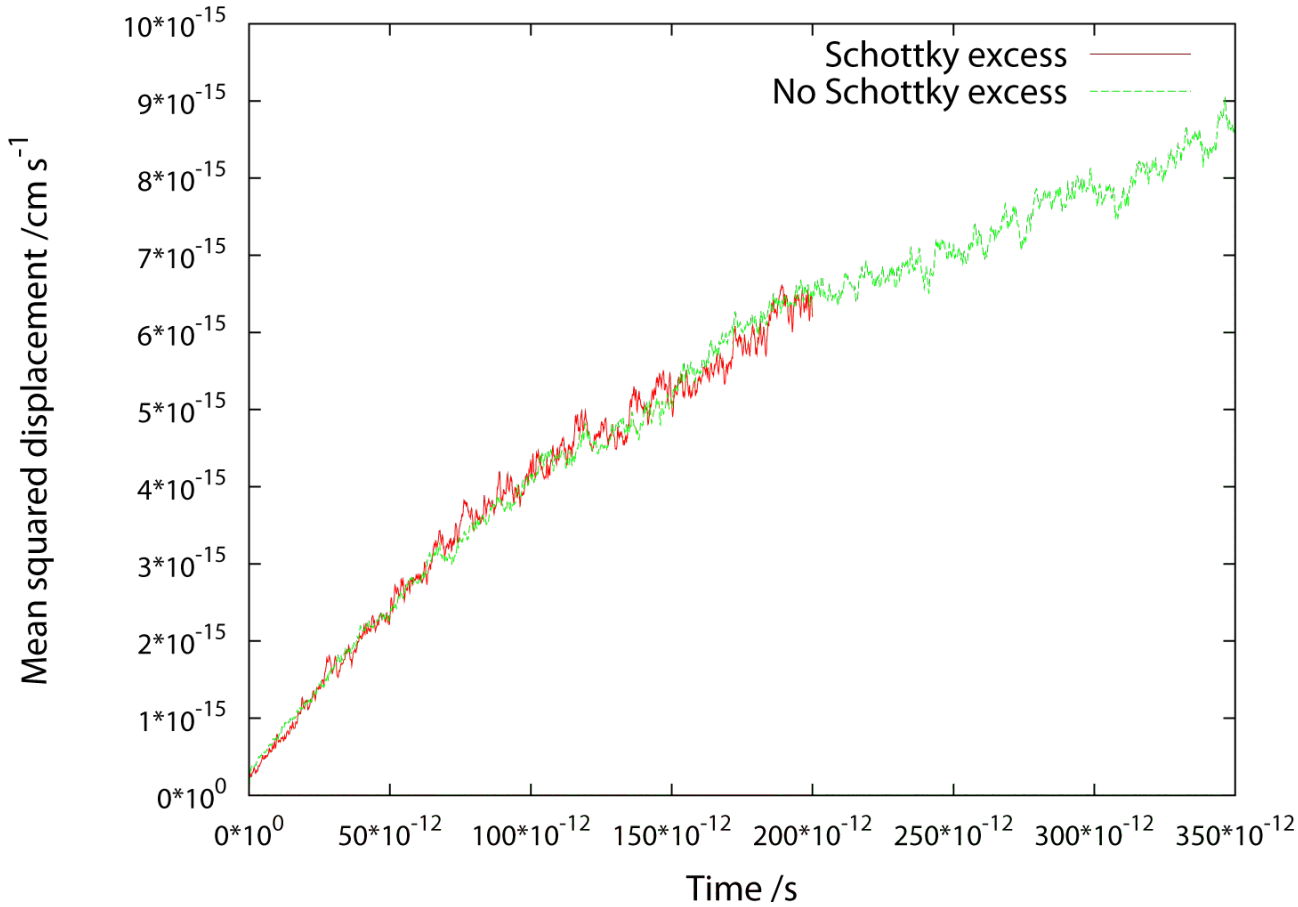

Averaged MSD for Xe around a {100}<100> both with and without a Schottky excess.

Xe clustering around dislocations

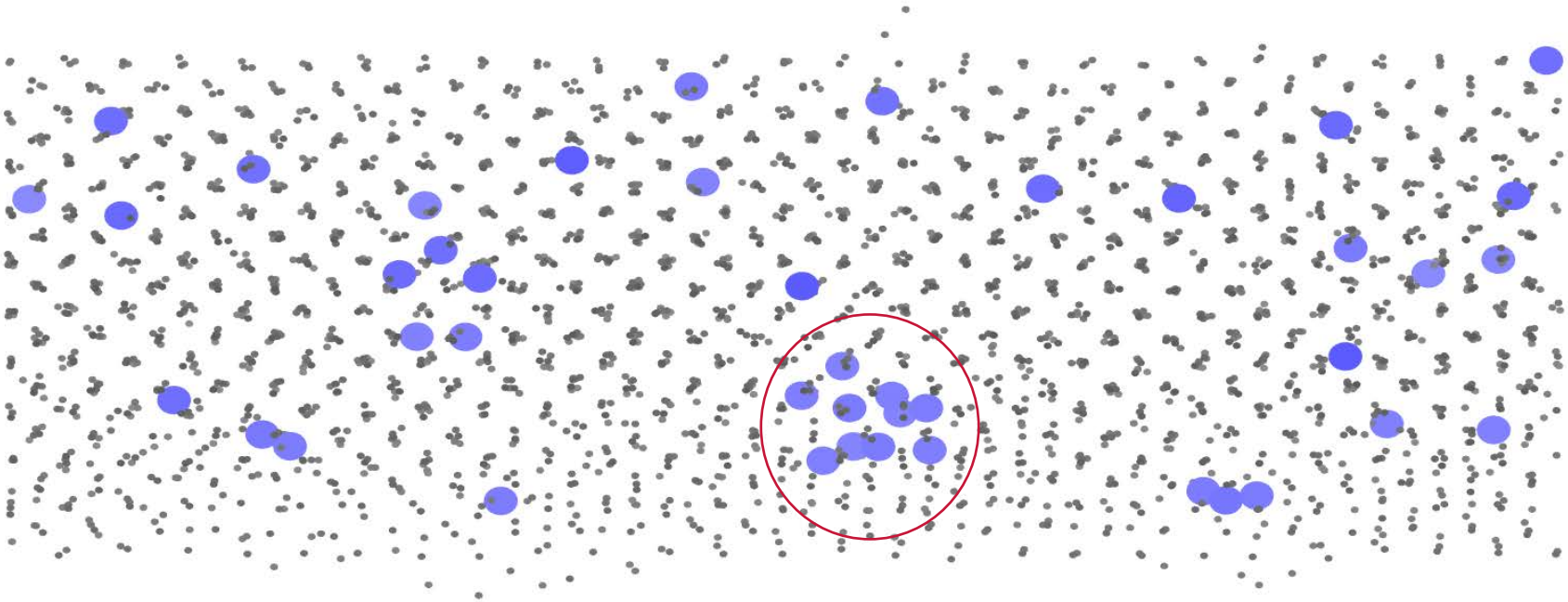

Final uranium (grey) and Xenon (blue) positions after 360 ps at 3200 K.
Clearly visible is the small cluster containing 10 Xe atoms.

The effect of Xe on dislocations

Dislocation glide in UO_2

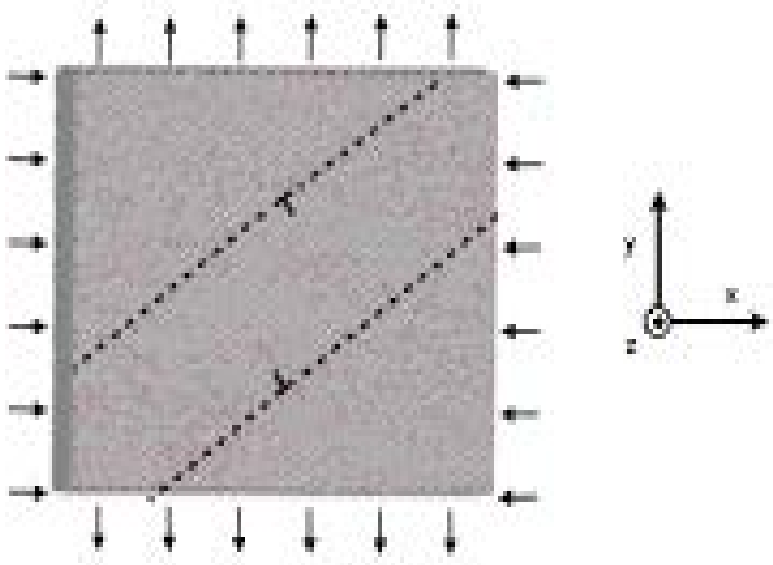

- **Burgers vector**: <110>
  Known from experiments
- **Favoured glide plane**: {100}
  Easy glide
- **Distance between dislocations**: 10 nm
  Could be better; fine for small displacements
- **Constant strainrate**: ~10^8 s^{-1}
  Not much effect at that point; not “realistic” anyway

Fossati *et al.* J. Nucl. Mater 443 (2013) 359

Dislocation glide in UO_2

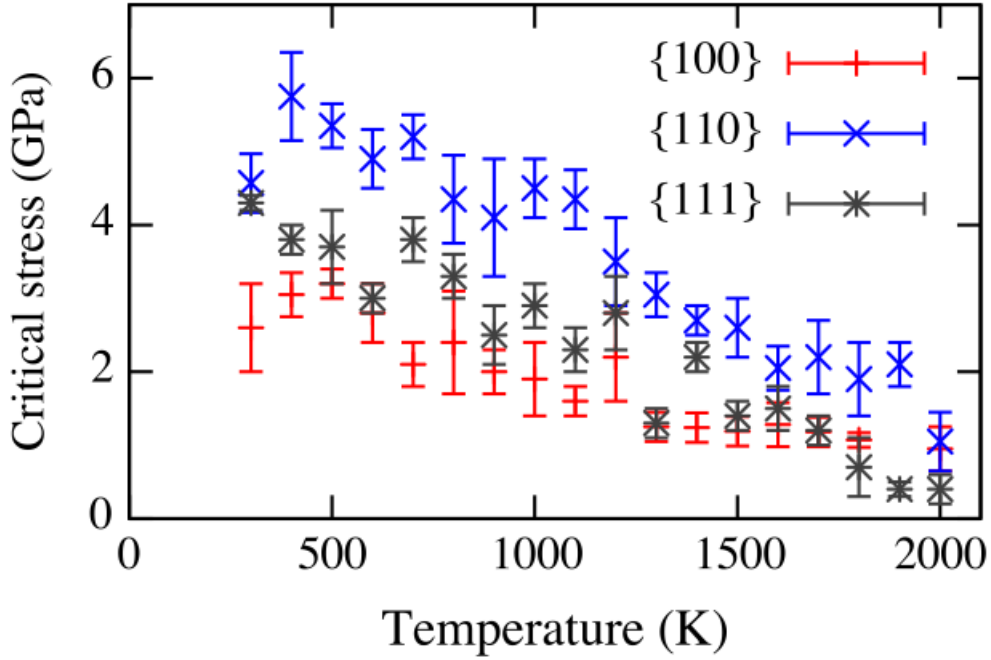

- **Plasticity significant starting from 1400 K**
- **Easiest glide system**
  - » lower temperatures: <110>{100}
  - » higher temperatures: {100} and {111}
- **CRSS at 1500 K: ~ 1 GPa**

Xe pinning of dislocations

Xe pinning of dislocations

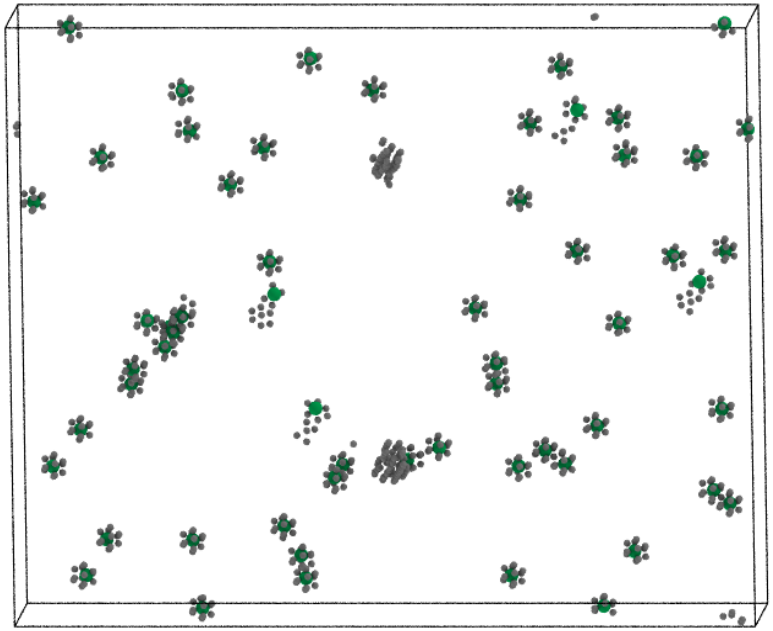

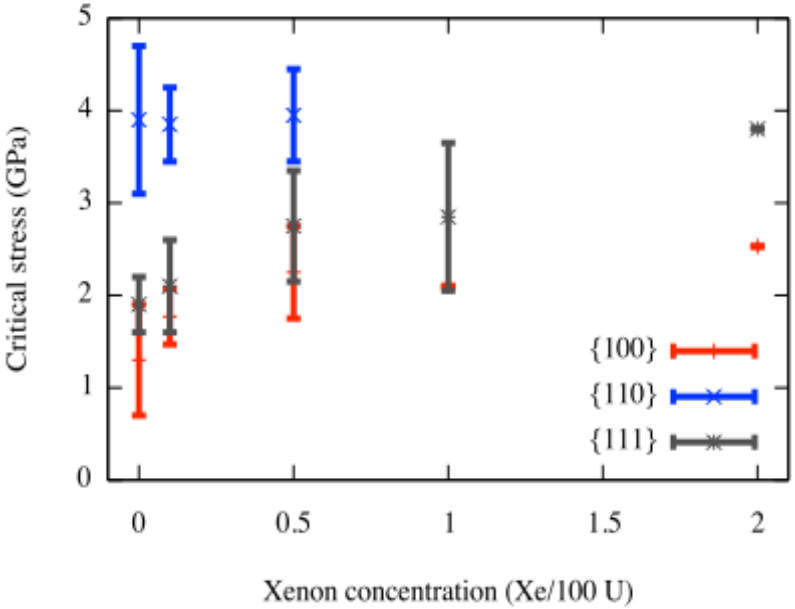

- Critical stress increases with Xe concentration…
  …except for {110}
- Saturation at ~ 1-2 Xe/100 U (about 2-3 GPa)
- {110} stress higher than that anyway

Xe pinning of dislocations

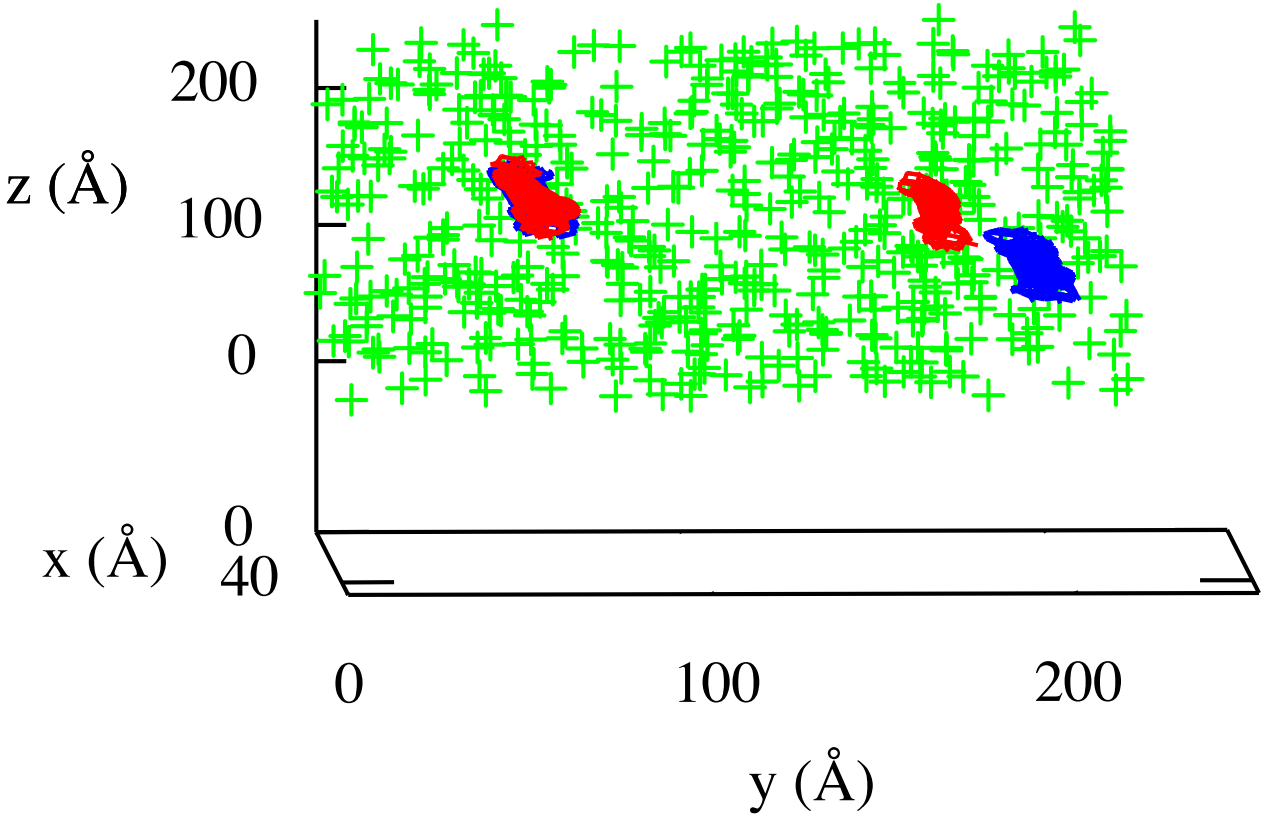

Conclusions

- A number of empirical pair potentials predict the same ordering for the energies of the dislocations studied here.
- The simulations predict the dominance of the {100} and {111} slip systems in good agreement with experiment.
- Isolated Xe is shown to migrate rapidly along the dislocations, however, clustering leads to a significant reduction in the diffusivity.
- Individual atoms have a small pinning effect on the dislocations, however, larger Xe clusters can pin dislocations, even at very high sheer stresses.
- Xe atoms are not swept along with the dislocation.
- Overall, Xe atoms/clusters can slow dislocations down and even stop them completely, once pinned other Xe atoms will diffuse along the dislocation to increase cluster/bubble size which can then pin more dislocations.

Imperial College London

Thank you for your attention

Any questions?

Consortium for Advanced Simulation of LWRs

Samuel.murphy05@imperial.ac.uk

Centre for Nuclear Engineering

Creating dislocations in fully periodic supercells

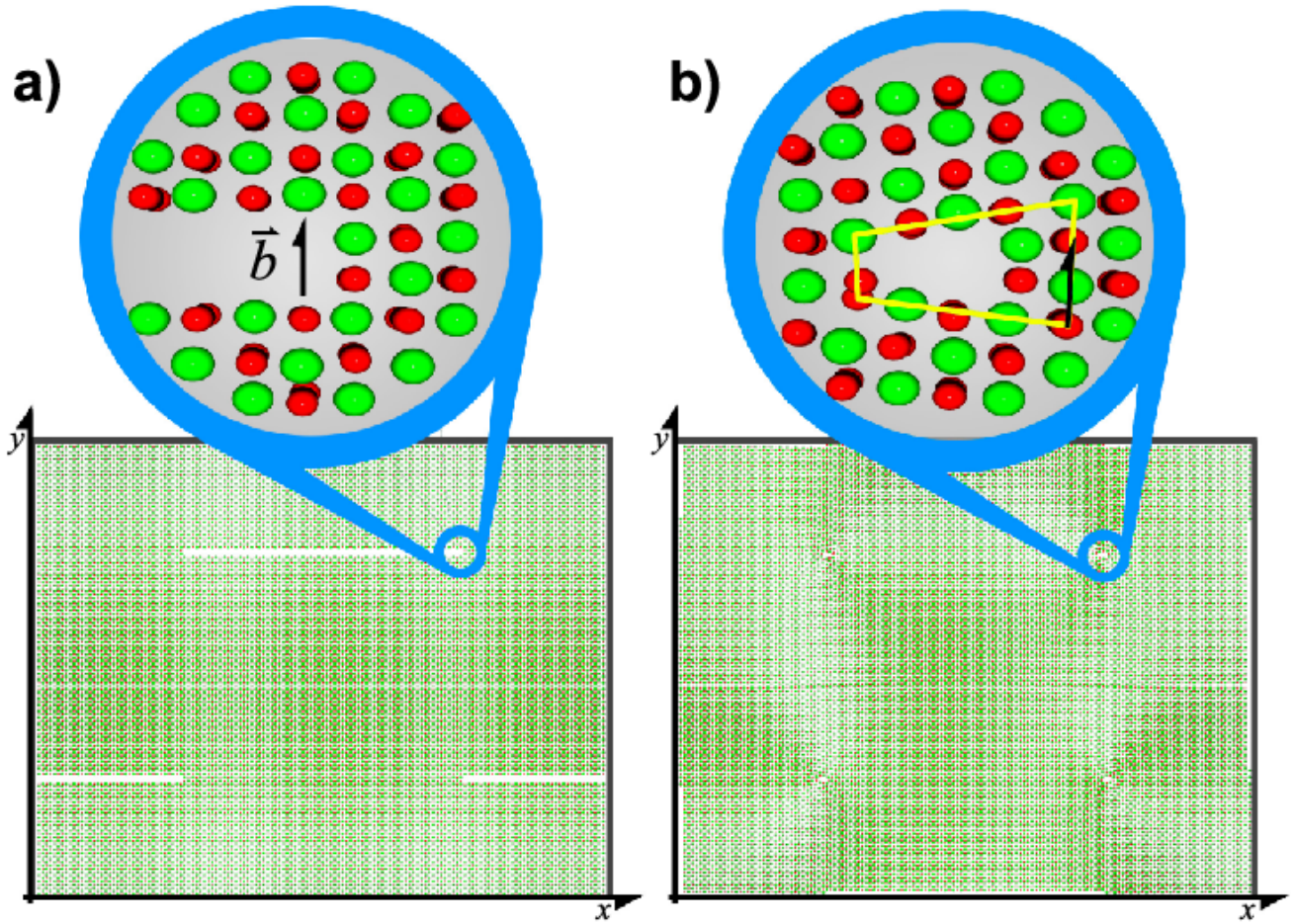

Xenon segregation to dislocations

edge

screw

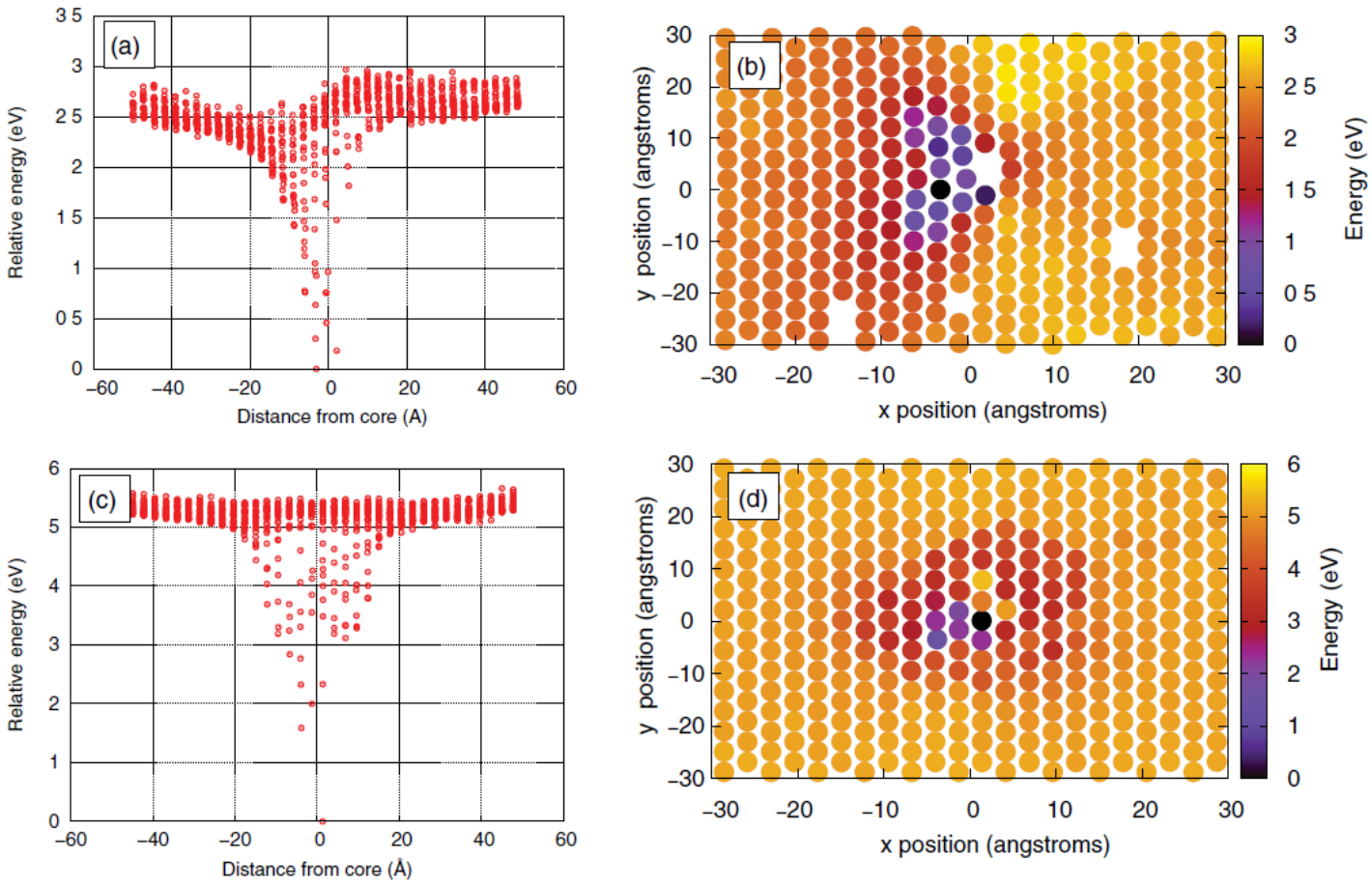

Nerikar *et al.* Phys. Rev. B 84 (2011) 174105

Radiation Transport Methods (RTM)
Deterministic Transport

Benjamin Collins, ORNL
Bill Martin, RTM Lead, Michigan
Tom Evans, RTM Deputy Lead, ORNL

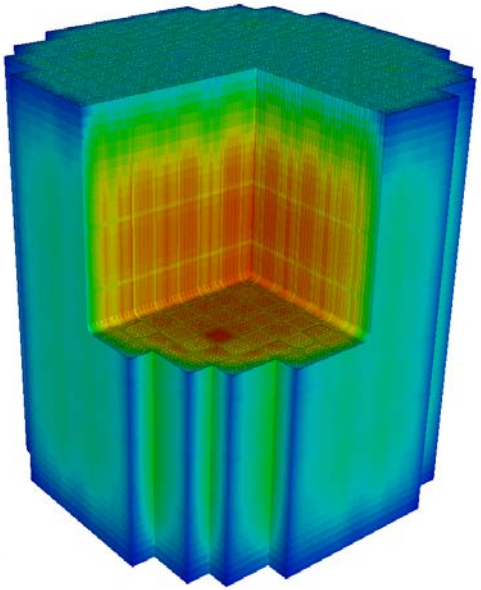

RTM projects

- Pin-resolved transport (PRT)
  - MPACT development including coupling and depletion (UM + ORNL)
  - Insilico development (ORNL)
  - Improved 2D/1D axial model (UM)
  - 2D/3D method (UM + ORNL)
  - Advanced pincell homogenization (NCSU)
- Monte Carlo / Hybrid (MCH)
  - Shift development (ORNL)
  - Monte Carlo methods: OTF Doppler, data decomposition (ORNL + MIT + UM)
  - Hybrid methods: FW-CADIS, FMC, CMFD, and fission matrix (ORNL + MIT + UM)
- Supporting Methodologies (SUP
  - Transient capability (UM)
  - Advanced coupling strategies (NCSU)
  - XS/Depletion (UM + ORNL)
  - ESSM (UM + ORNL)

MPACT Development

- Completed 2D/1D solver and resolved accuracy issues
- Completed initial coupling to COBRA-TF for single assembly and full core capability
- Added capability to deplete 2D full core
- Performed initial transient demonstration
- Integrated the ORIGIN API for depletion using SCALE

RTM:P6.01 – Application of MPACT 2D/1D to AMA Benchmark 5

Collins,Stimpson, Kochunas,Downar RTM

- 2D/1D capability developed
  - Radial MOC solver with explicit geometry and P2 scattering treatment
  - 1D axial diffusion solver with NEM
  - Dynamic under-relaxation scheme
- Verification and Validation
  - Single assembly comparisons to Monte Carlo
  - Control rod cluster comparisons to Monte Carlo
  - Comparison to measured critical conditions for full core

Watts Bar 1 Cycle 1 ZPPT Results - Godfrey

Criticality (pcm)

	KENO-VI†	Shift‡	MPACT
Initial	-67	-33	-144
ARO	-25	11	-98
D	-149	-113	-234
C	-153	-127	-255
B	-121	-85	-228
A	-177	-153	-275
SD	-160	-129	-267
SC	-159	-130	-262
SB	-125	-88	-222
SA	-155	-123	-267
Average	-129	-97	-225

†KENO σ <= 1 pcm
‡Shift σ <= 6 pcm

Bank Worth Differences

Bank	Measured (pcm)	KENO-VI	Shift	MPACT
D	1342	3.3 ± 0.1%	3.4 ± 0.6%	3.6%
C	951	3.5 ± 0.1%	3.9 ± 0.9%	4.2%
B	879	-0.5 ± 0.2%	-0.8 ± 0.9%	1.2%
A	843	6.4 ± 0.2%	6.9 ± 1.0%	5.7%
SD	480	4.0 ± 0.4%	3.6 ± 1.7%	3.8%
SC	480	3.9 ± 0.4%	3.9 ± 1.7%	2.9%
SB	1056	1.0 ± 0.2%	1.1 ± 0.8%	1.4%
SA	435	2.6 ± 0.4%	1.3 ± 1.9%	3.9%
Total	6467	2.9 ± 0.1%	2.9 ± 0.4%	3.3%

*Meshes moved to match control rod tip

Bank D Integral Worth

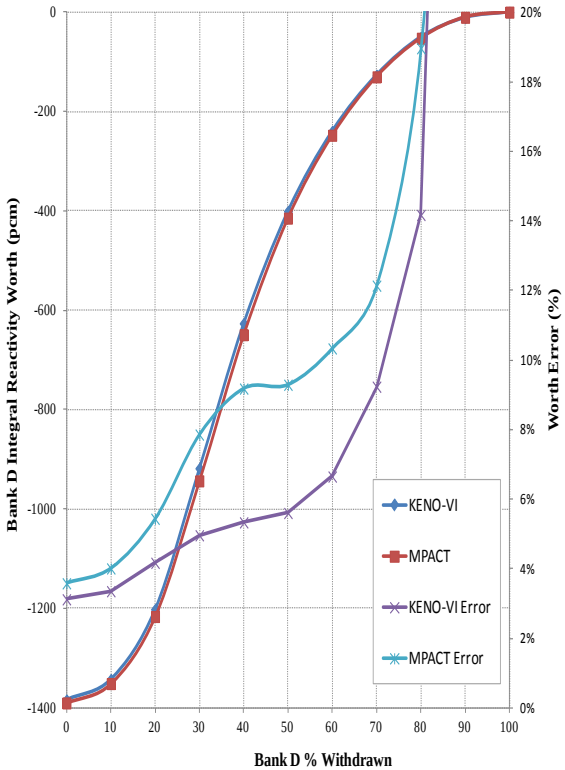

Reactivity Coefficients

	Measured	KENO-VI	Shift	MPACT
Differential Boron Worth (pcm/ppm)	-10.77	0.56 ± 0.02	0.55 ± 0.07	0.61
Isothermal Temperature Coefficient (pcm/F)	-2.17	-1.01 ± 0.04	--	-1.55

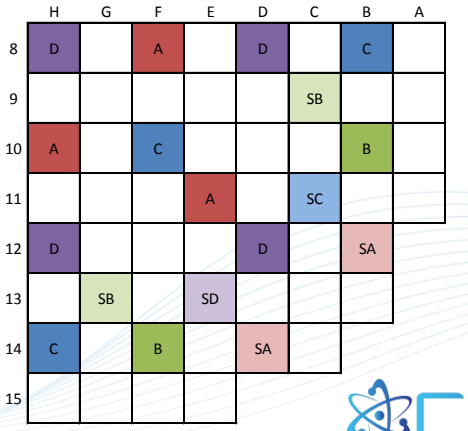

*Doppler unscatter in KENO-VI worth an additional -66 pcm

RTM.P8.01 – Demonstration of Advanced Pin-Resolved Depletion with MPACT

Collins,Zhu,Kochunas,Downar RTM

- Develop Code Features
  - Point Depletion based on ORIGEN Methodology
  - Predictor-Corrector Time Stepping Methodology
  - Addition of critical boron search for core follow calculation
- Verify Solution
  - Comparisons to computation benchmark does well for HELIOS library
  - Comparisons to experimental benchmark does well for both cross-section libraries
  - 2D core depletion agrees well compared to WEC methods

Validation – Takahama 3 Assay Data

- Experimental data taken from NEA's Spent Fuel Isotopic Composition Database
- Data is compared for 2 different fuel pins
  - The first is irradiated for 2 cycles and 5 data points are analyzed
  - The second is irradiated for 3 cycles and 6 data points are analyzed

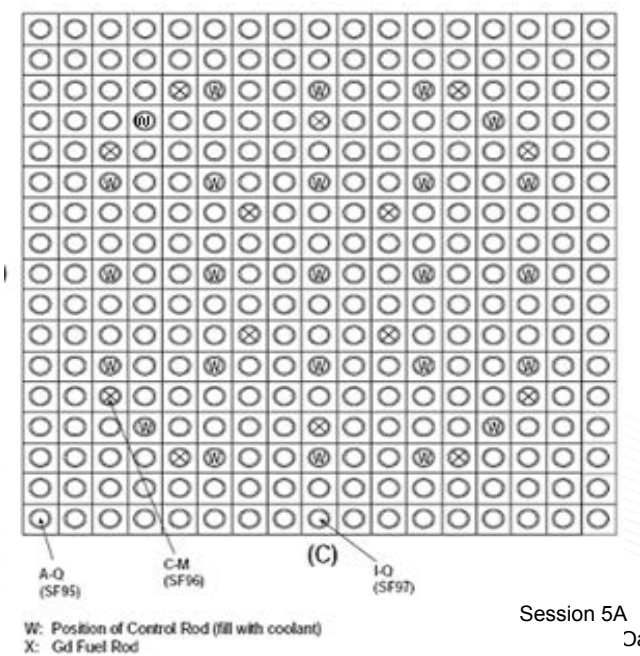

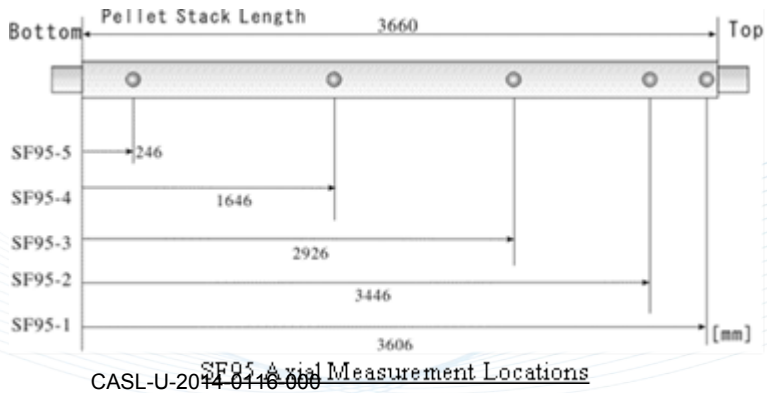

Takahama 3 – SF95

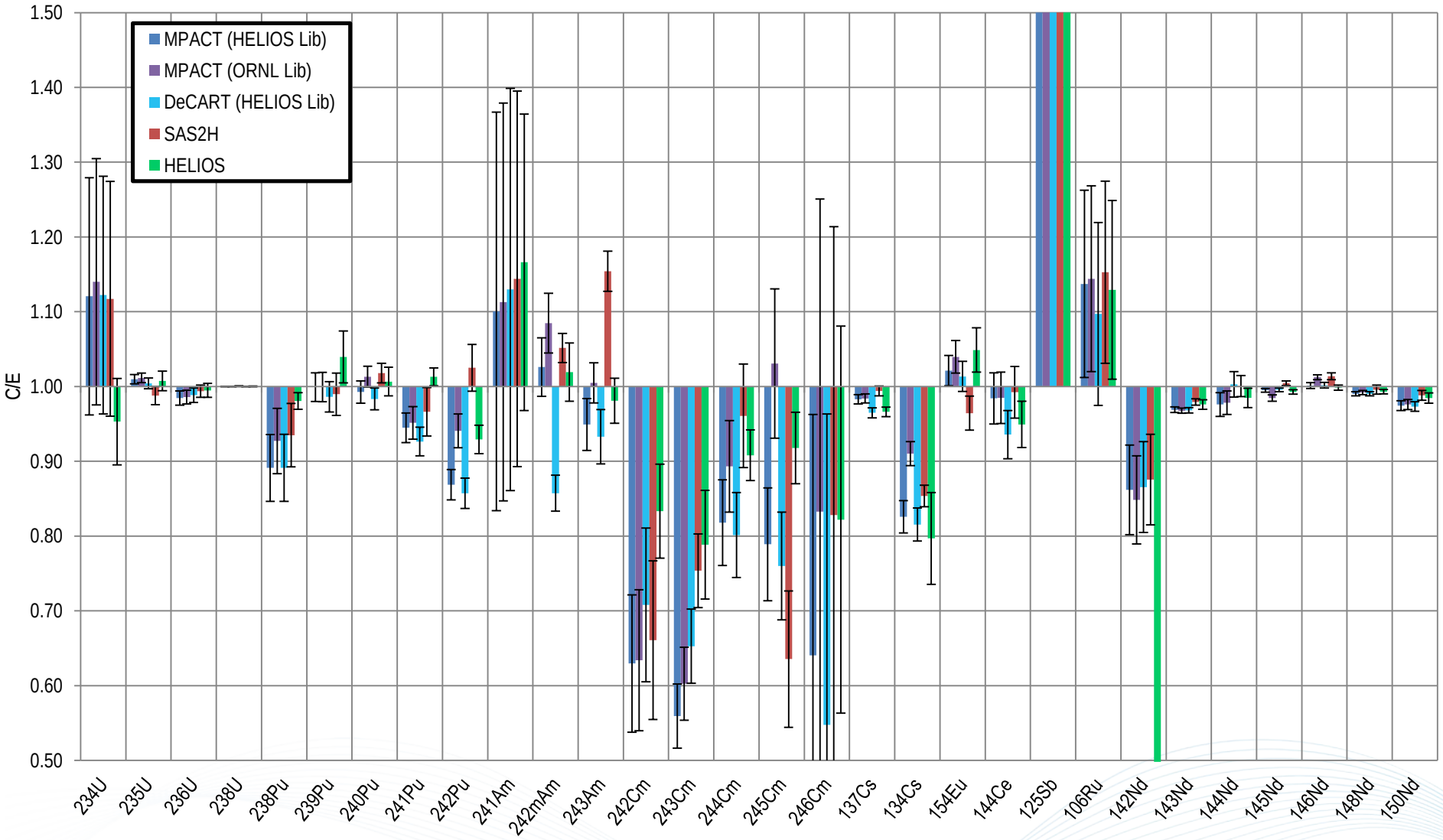

2D Core Depletion

- 2D slice of Watts Bar Core was used at approximate core average temperature and density
- Boron search was used to make reactor critical

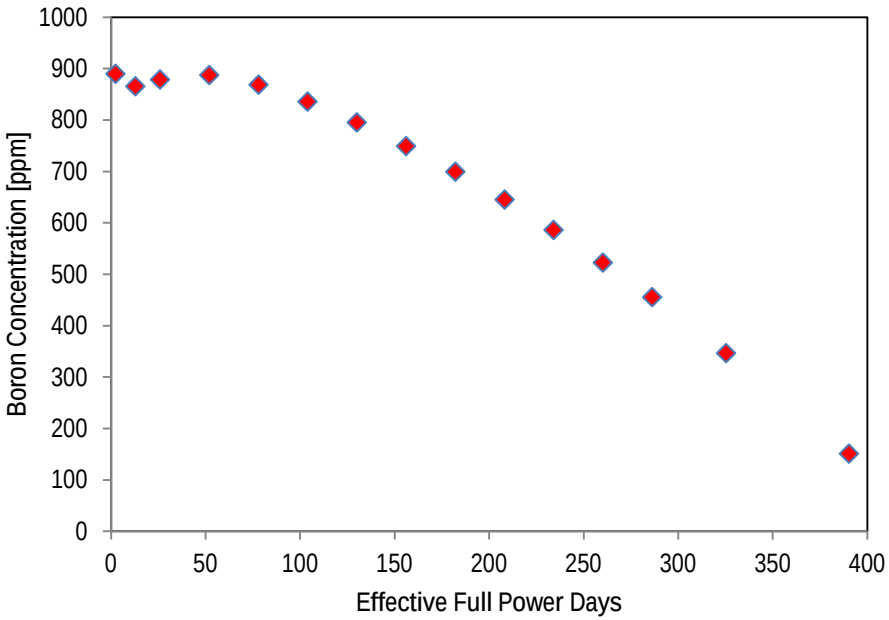

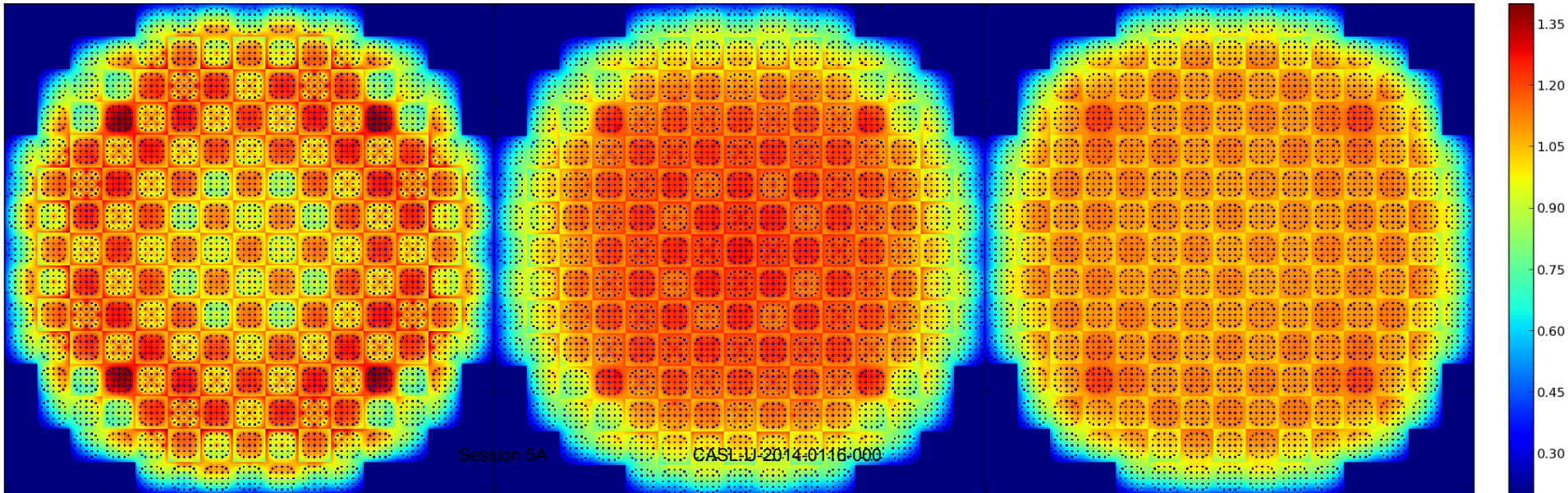

RTM.SUP.P9.03 ORIGEN Integration into MPACT

Kochunas,Wieselquist,Zhu,Kim

- In reactor applications, depletion of the fuel is a necessary capability.
  - ORIGEN has a long history of being applied to depletion problems and is extensively validated.
  - MPACT has an existing depletion capability, but does not have a large validation base.
- By integrating ORIGEN into MPACT we provide a better validated depletion capability.
  - ORIGEN also has additional capability to compute decay heat and gamma sources.
- Initial verification compared to 2 benchmarks
  - Takahama-3 spent fuel isotopics
  - JAERI benchmark on Reactor Physics analysis of next generation LWR fuels.

Selected Results of MPACT+ORIGEN Initial verification

- Takahama-3 benchmark has PIE data and numerical results.
  - Fuel operated for 3 cycles in Takahama PWR reactor.
- ORIGEN results are consistent with other codes compared to experimentally measured values.
- Comparison to experimentally measured values are generally in good agreement.
  - Poor agreement is seen for some fission products (Sb-125) and higher actinides (Cm).consistently by all codes.

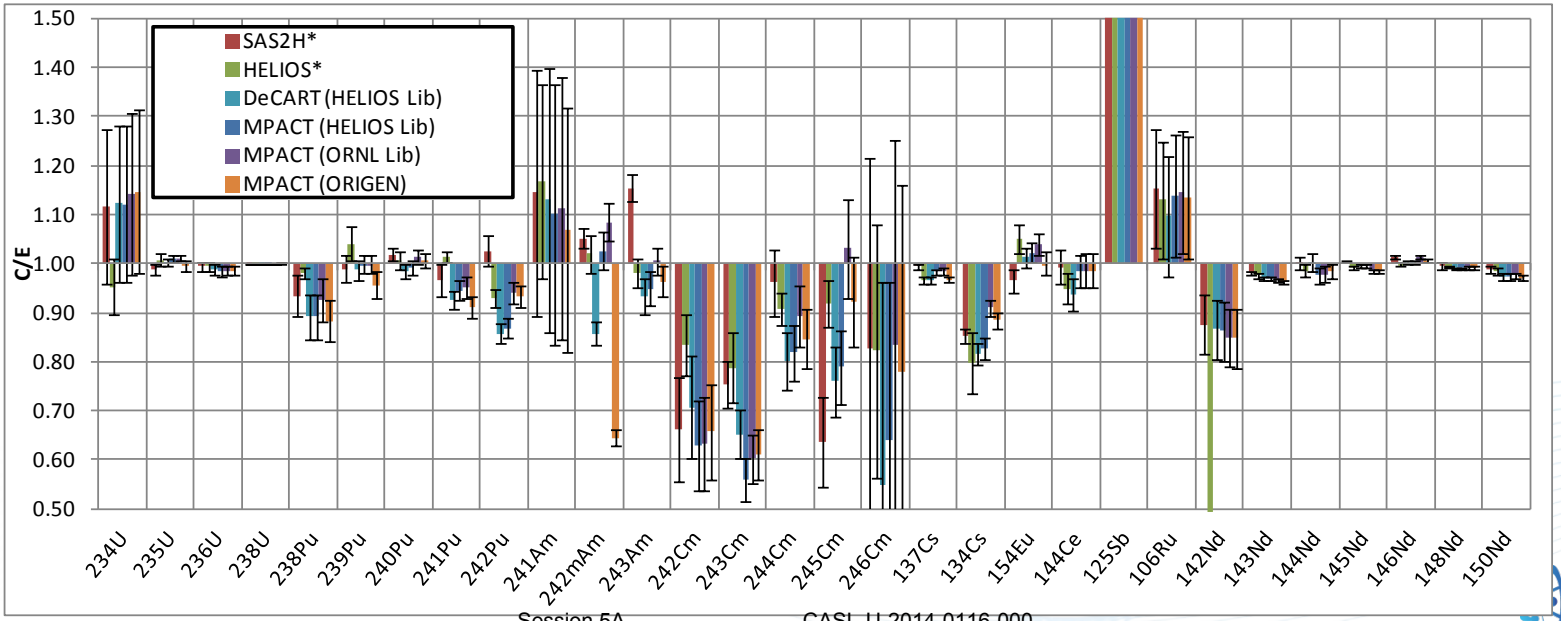

VRI:PSS.P7.03 Hot Full Power Assembly
RTM:PRT.P7.05 Hot Full Power Core

Kochunas,Jabaay,Clarno,Collins,Downar

- Development of coupling interface to COBRA-TF
  - Development of DTK interface for MPACT
  - Development of LIME driver to control coupled iteration
  - Development of solution transfer routines

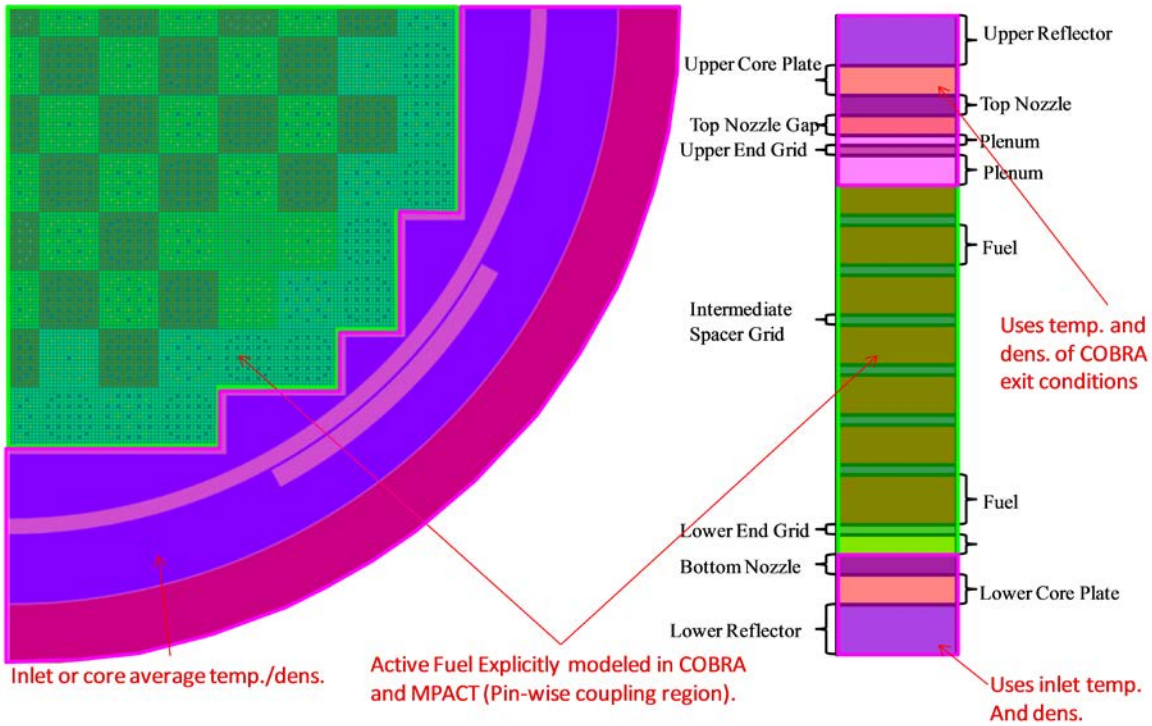

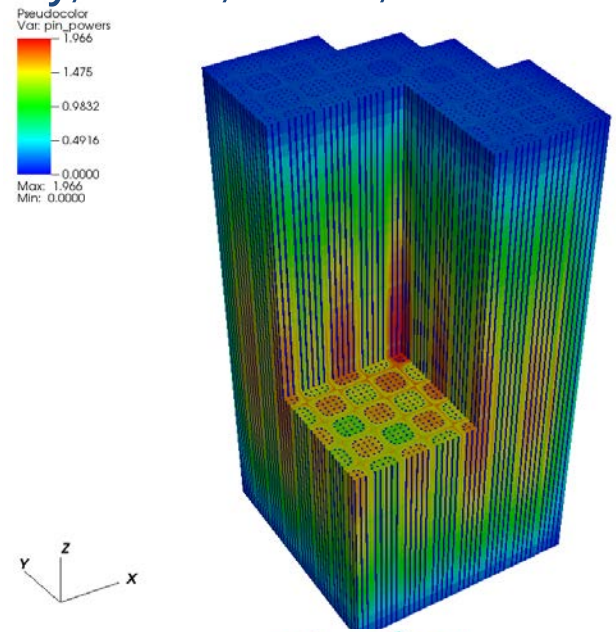

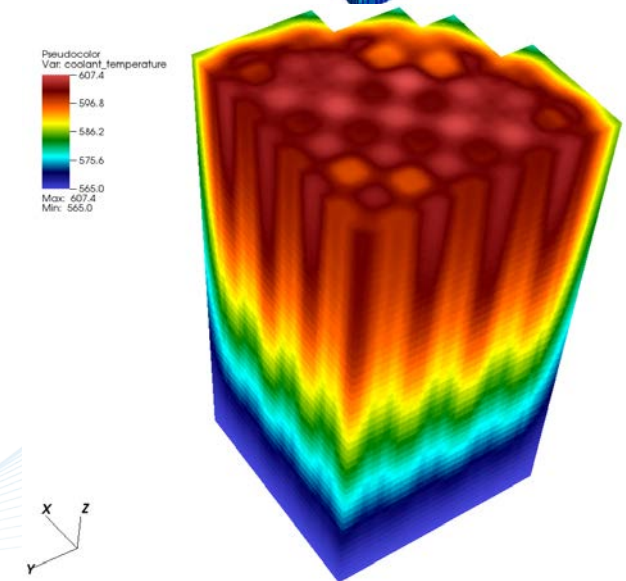

RTM.PRT.P9.01 – Demonstration of Reactor Startup Flux Maps with MPACT

Collins, Zhu,Jabaay,Graham,Downar

- Simulate hour long time steps
  - Track important isotopes such as Xe during startup
  - Semi-predictor-corrector scheme
- Determine Incore Detector Response
- Move control rods between states

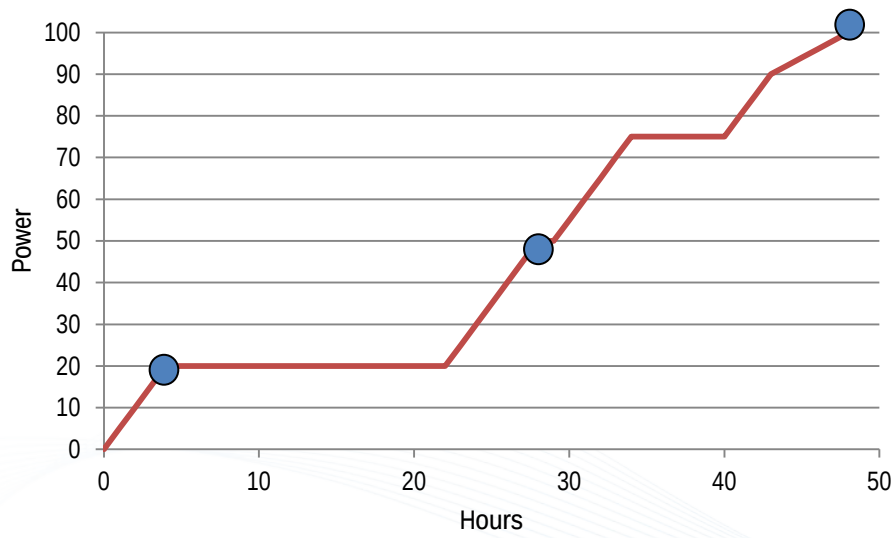

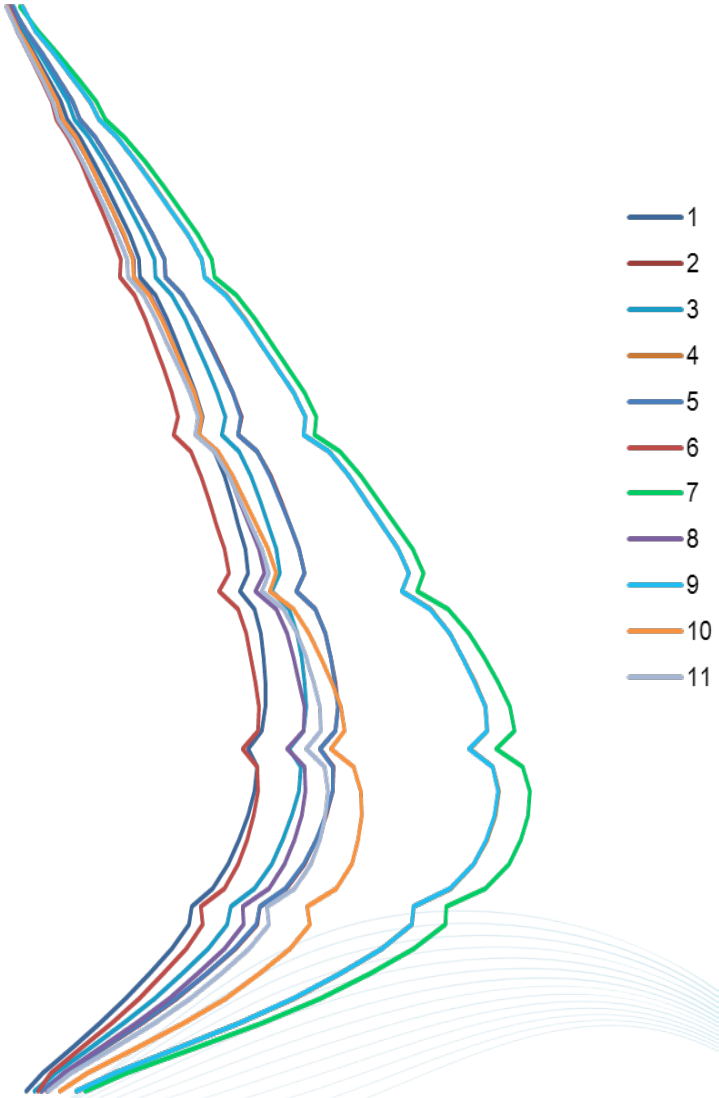

Insilico Development –Efficient Solvers for the SPN Equations Hamilton,Evans

- The k-eigenvalue problem can be written as the generalized eigenvalue problem:

$$\mathbf{A}\mathbf{u} = \frac{1}{k}\mathbf{B}\mathbf{u} \qquad \mathbf{A}^{-1}\mathbf{B}\mathbf{u} = k\mathbf{u}$$

	Solver Type	
Linear System Matrix	**Fixed Point**	**Subspace**
$\mathbf{M} \approx \mathbf{A}$	–	Davidson
$\mathbf{A}$	Power Iteration	Arnoldi
$\mathbf{A} - \mu\mathbf{B}$	Shifted Power Iteration	Shift-and-Invert Arnoldi
$\mathbf{A} - \lambda^{(m)}\mathbf{B}$	Rayleigh Quotient It.	Jacobi-Davidson

Convergence for Watts Bar

Eigensolver	Preconditioner	Eigenvalue Iterations	Total Linear Iterations	Solve (min.)
PI	AMG	523	10572	353.1
	MGE	523	4919	851.5
Shifted PI	AMG	16	2647	161.5
	MGE	16	1319	224.7
RQI	AMG	3	765	125.6
	MGE	3	435	103.1
Arnoldi	AMG	43	2118	85.4
	MGE	43	901	109.0
Davidson	AMG	201	–	8.5
	MGE	76	–	10.1

Improvements to Stability and Accuracy of 2D/1D

Kelley,Stimpson,Larsen,Collins,Downar

- Addition of SP_N and S_N axial solvers
- Stabilized iterations through under-relaxation

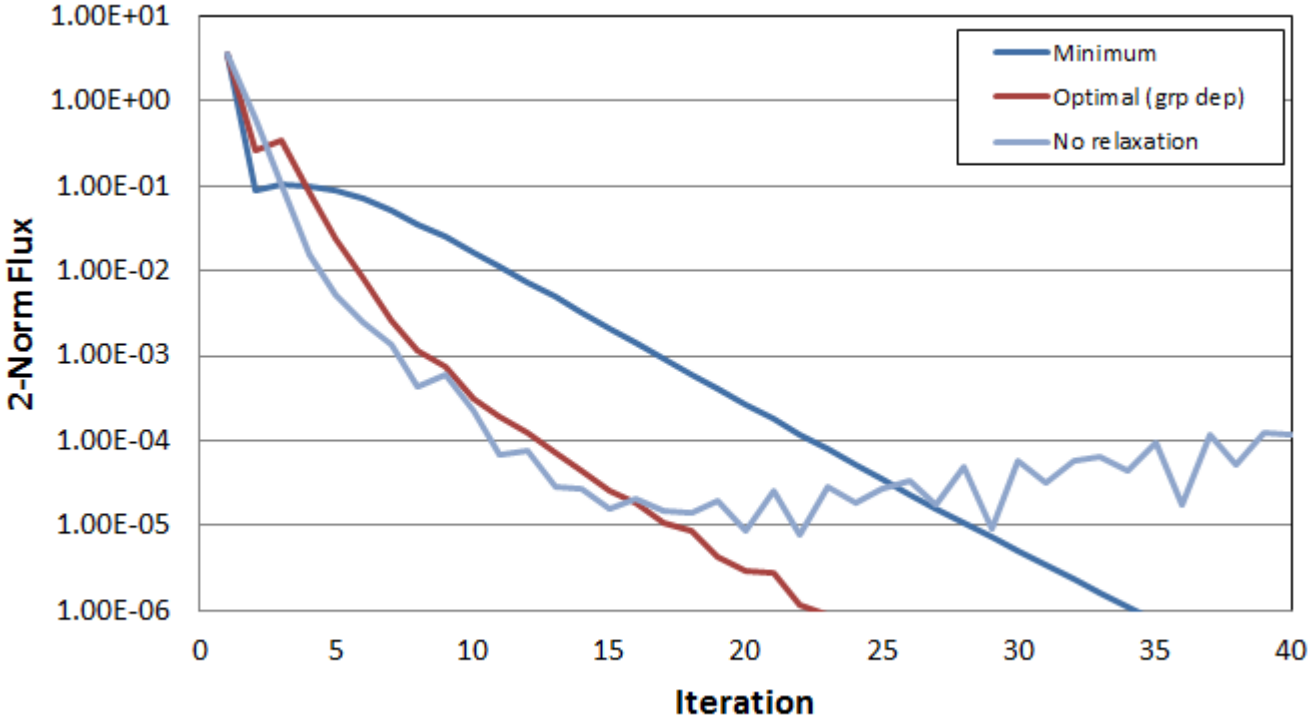

RTM.SUP.P8.02 Development of Transient Methods in MPACT

Young,Xu,Graham,Collins,Downar

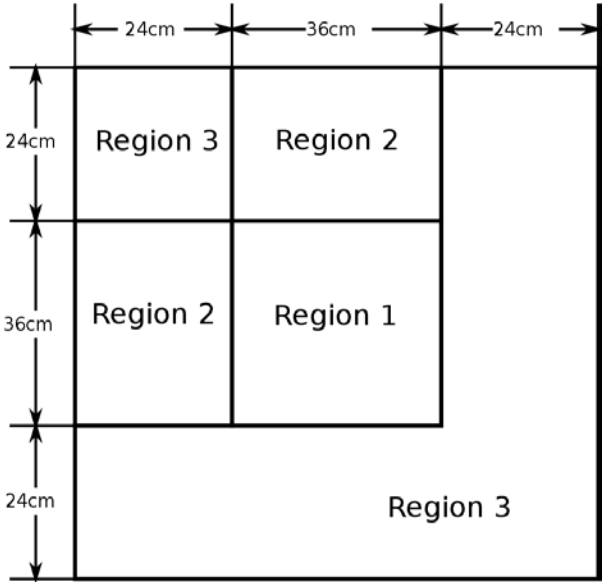

Time (sec)	Perturbation
0.0 -> 0.2	Ramp: 1 -> 4
0.2	Step: 5
0.2 -> 0.4	Ramp: 5 -> 6
0.4	Step: 1

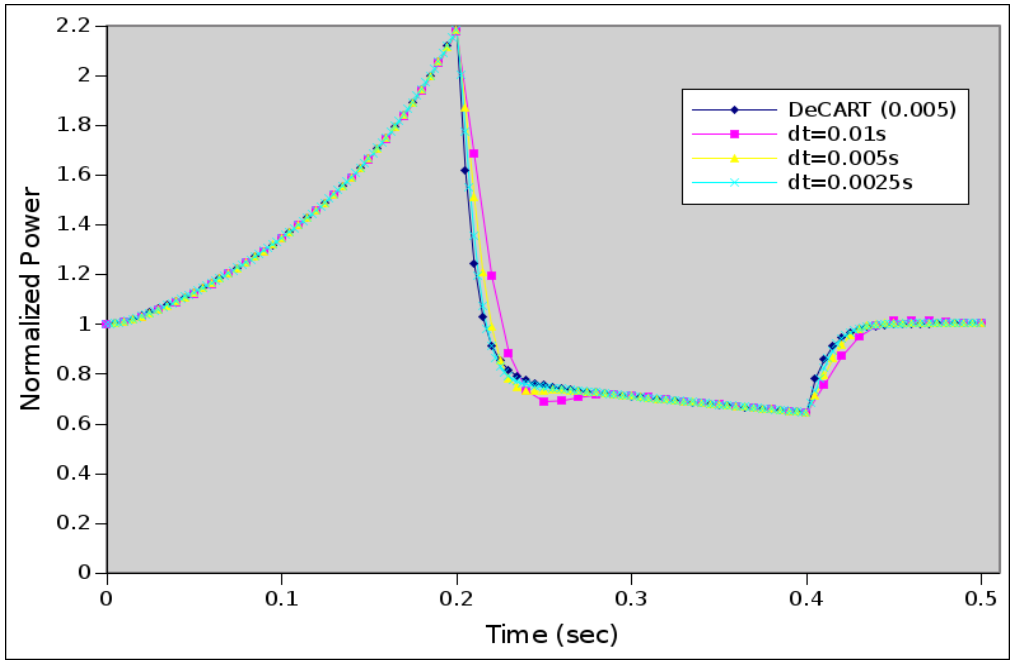

MPACT Discretization

- 0.03 cm,
- 4 azimuthal
- 2 polar angles

MPACT Transient Validation: SPERT E-Core

- SPERT III
- Construction: 1955-58
- Reactor Power Excursion Test
- Typical PWR Design
- Full Range of CZP/HZP/HFP Tests

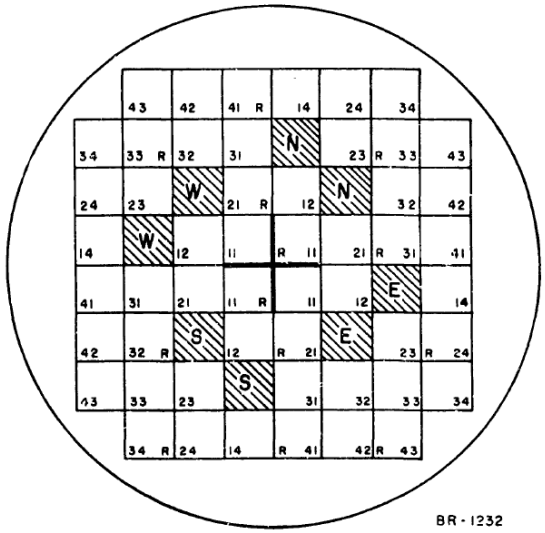

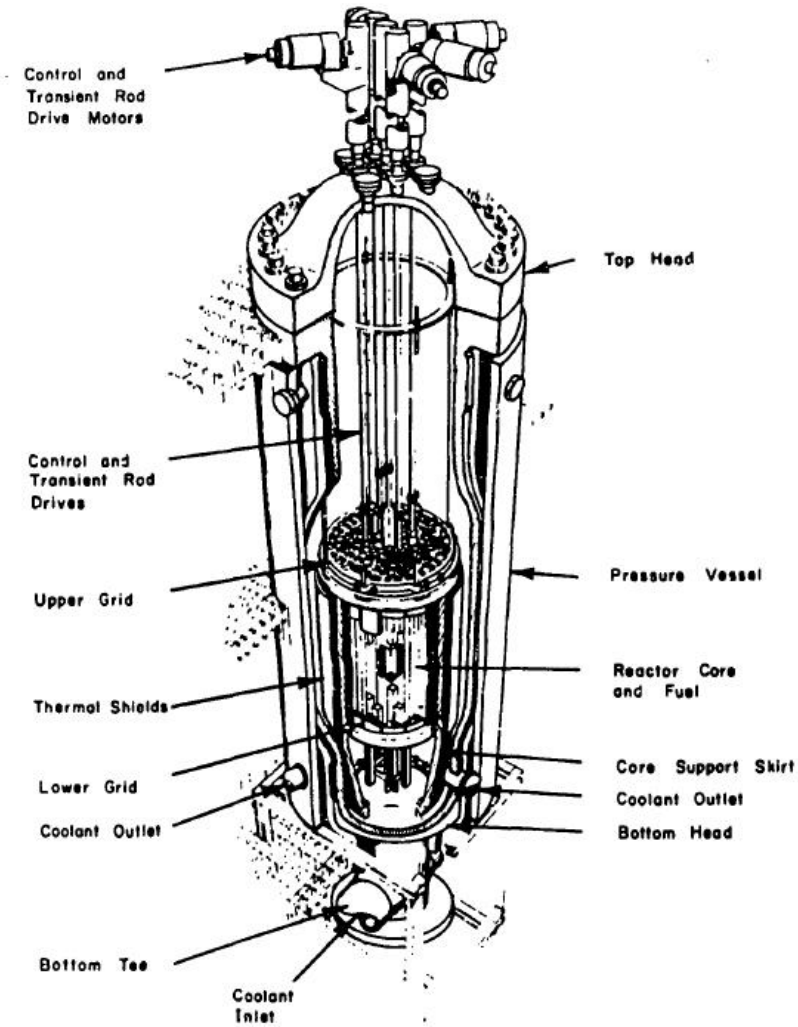

Ref. 1

MPACT Model

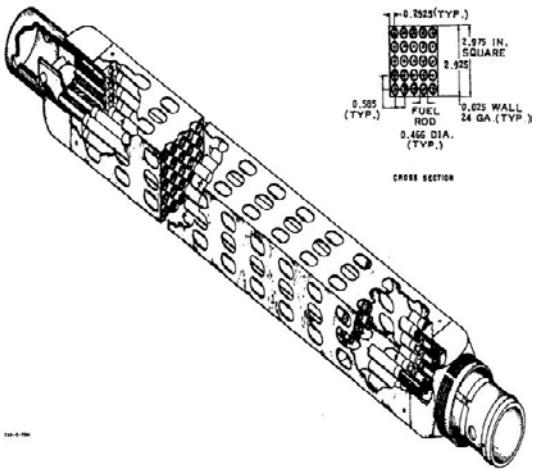

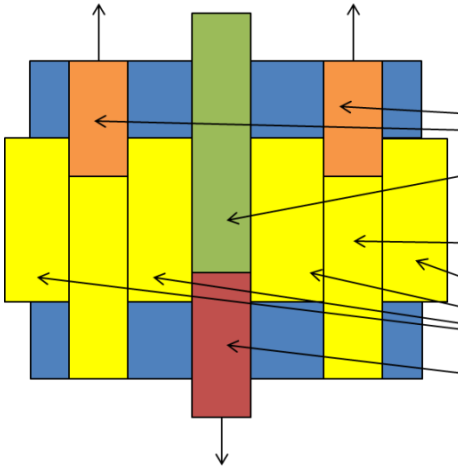

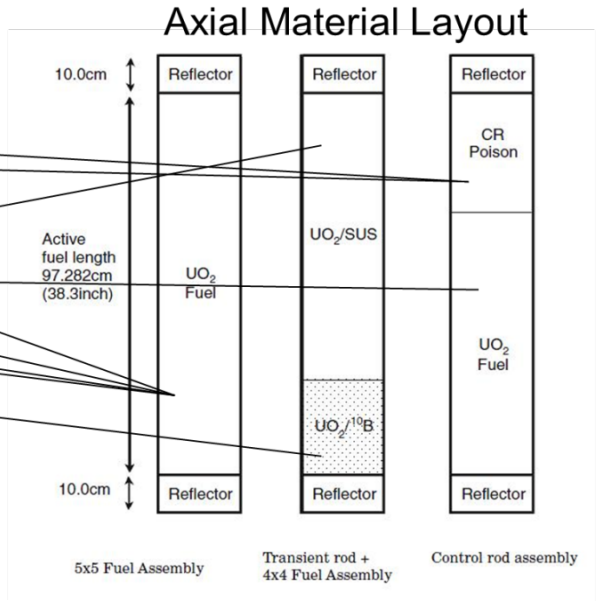

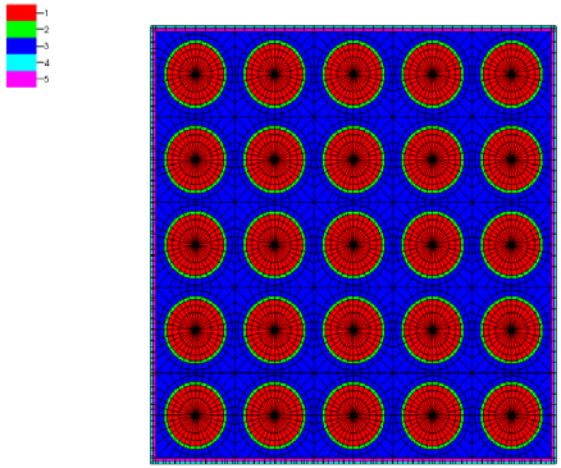

5x5 Fuel Rod Assembly

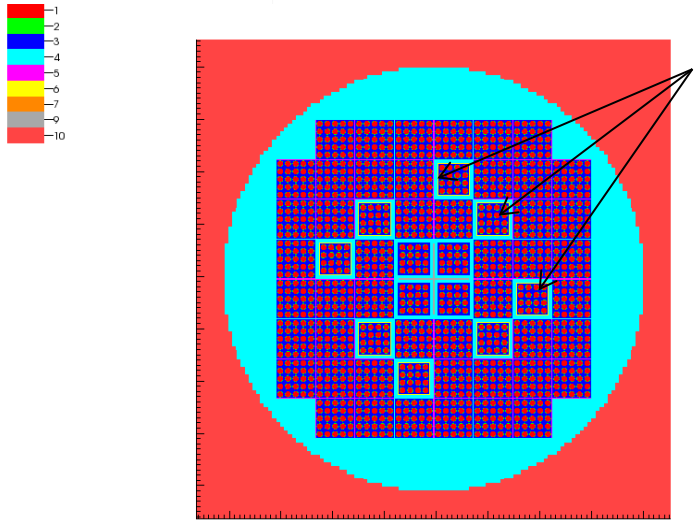

Middle of Active Core

MPACT Steady-state Results

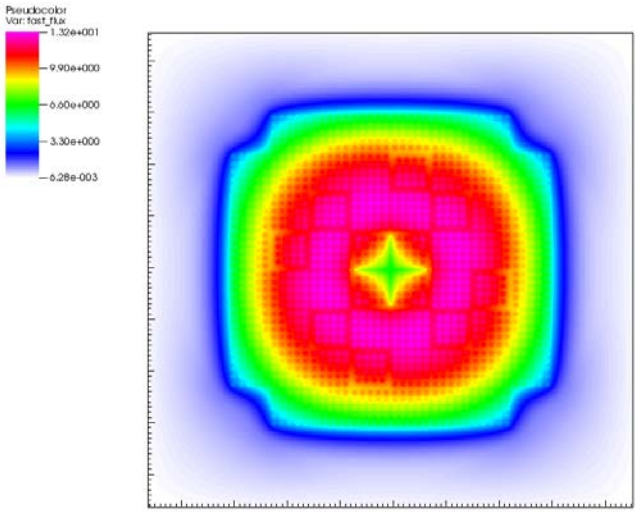

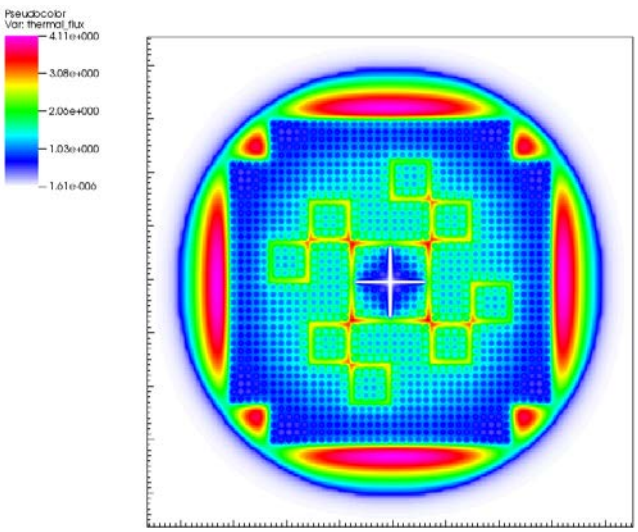

- Discretization: MOC w/ 0.05 ray spacing /16 azimuthal / 4 polar angles. 20 axial planes w/ NEM kernel
- Xsecs: ORNL 56 library (P2 scattering)
- MPACT Execution time ~ 1hour on 720 cores

Comparison of Critical Condition w/ KENO-CE

Case	Temperature (F)	C.R. Position(cm)	MPACT	KENO-CE
CZP	70	36.957	0.99411	0.99999 ±0.00082
HZP	550	71.755	0.99690	1.00242 ±0.00079

Comparison of Critical Rod Positions

Case	Temperature (F)	Experiment	MPACT	S3K	PARCS
CZP	70	36.957	38.2	30.1	31.6
HZP	550	71.755	74.4	-	46.3

Path Forward

- Complete Transient functionality (June/July/August)

- Complete SPERT Steady-State Analysis (June/July)
  - Completed S.S. SPERT KENO Models
  - Completed CZP and HZP Steady-state analysis
  - Complete HFP Steady-State Analysis

- Transient (Aug)
  - Perform Selected CZP, HZP, HFP Rod EjectionTests
  - Complete L3 milestone report

Status of VERA Progression Problem 9

- Capability to deplete a full cycle with feedback and boron search has been completed
  - P0 Scattering (to be revised with transport corrected P0)
  - 2088 cores (9 radial, 58 axial spatial decomp with 4 threads per core)
  - EOS Cray XC30 - ~20 hours

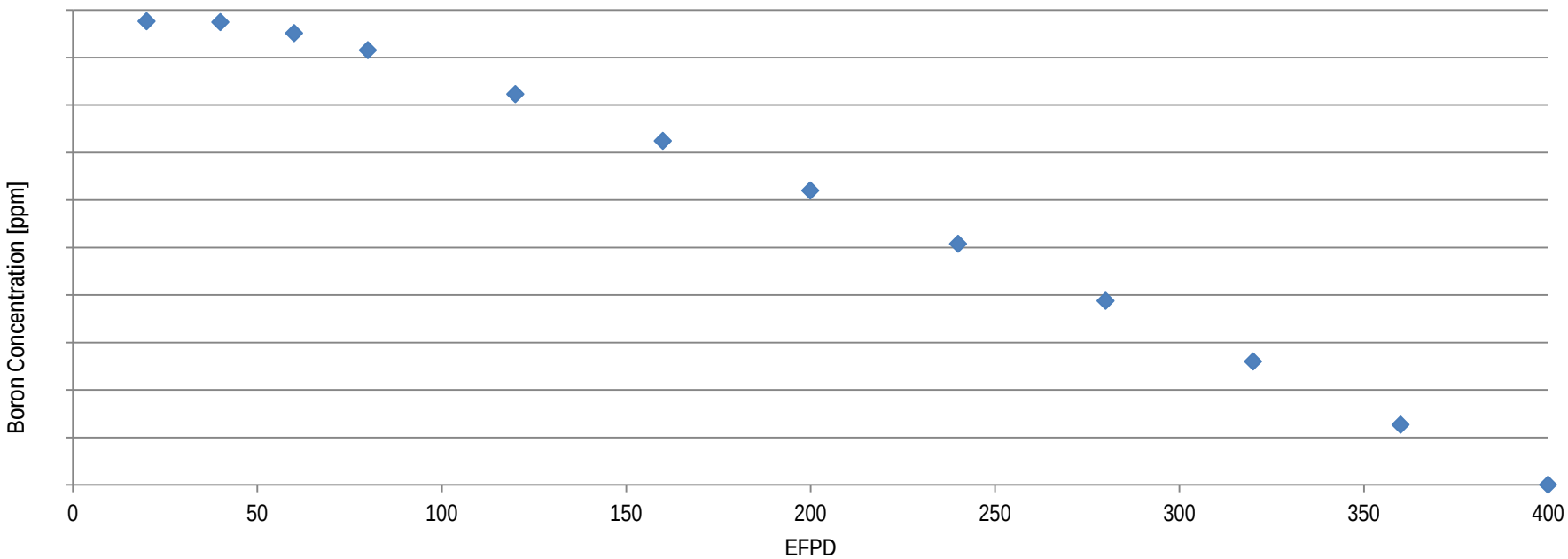

Status of VERA Progression Problem 9

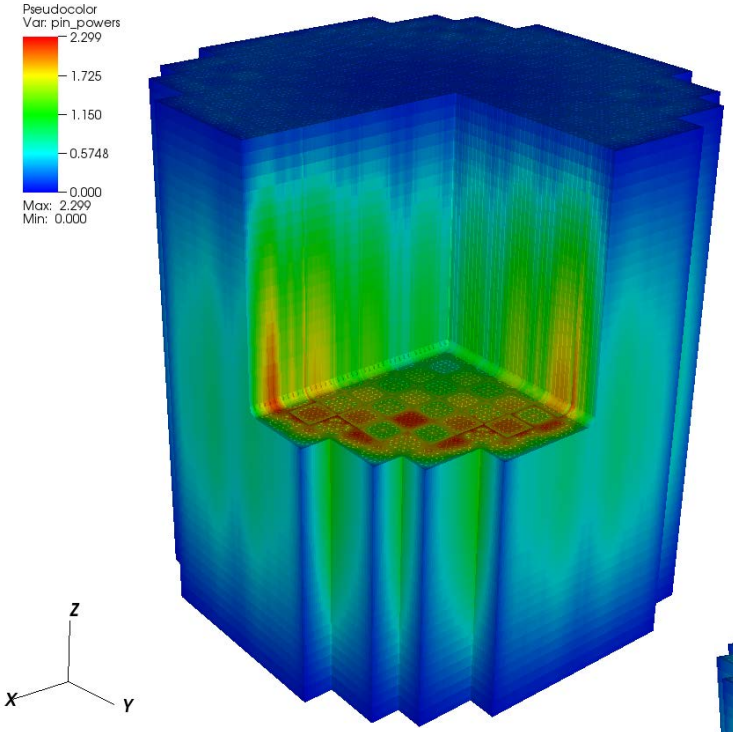

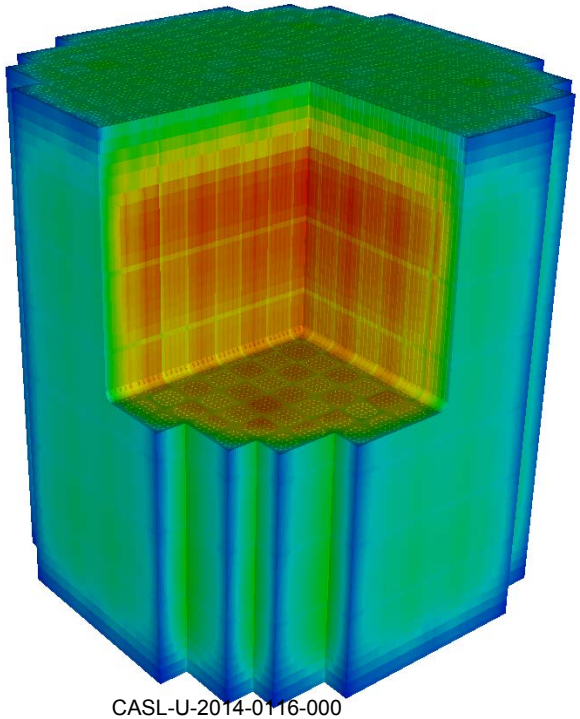

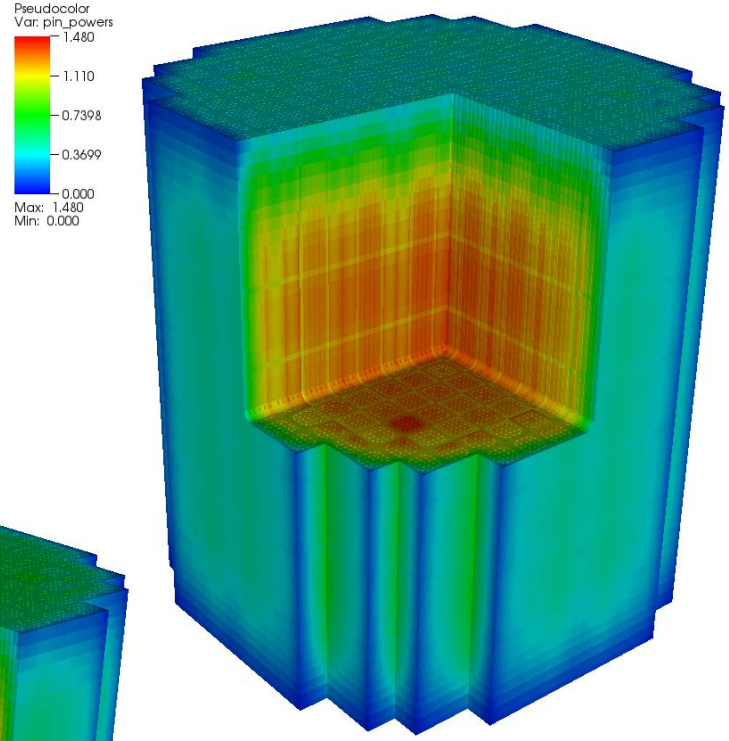

Future Work

- Capability
  - Simulation of cycle 1 depletion
  - Shuffling capability and simulation of cycle 2
  - Transient with simplified feedback
- Performance
  - Address memory usage
  - Optimize steady state iteration scheme
    - More efficient solvers
    - Runtime improvements in subgroup calculation
  - Optimize coupled TH iteration scheme

Monte Carlo Methods – Status and Plans

CASL Roundtable – RTM

July 15, 2014

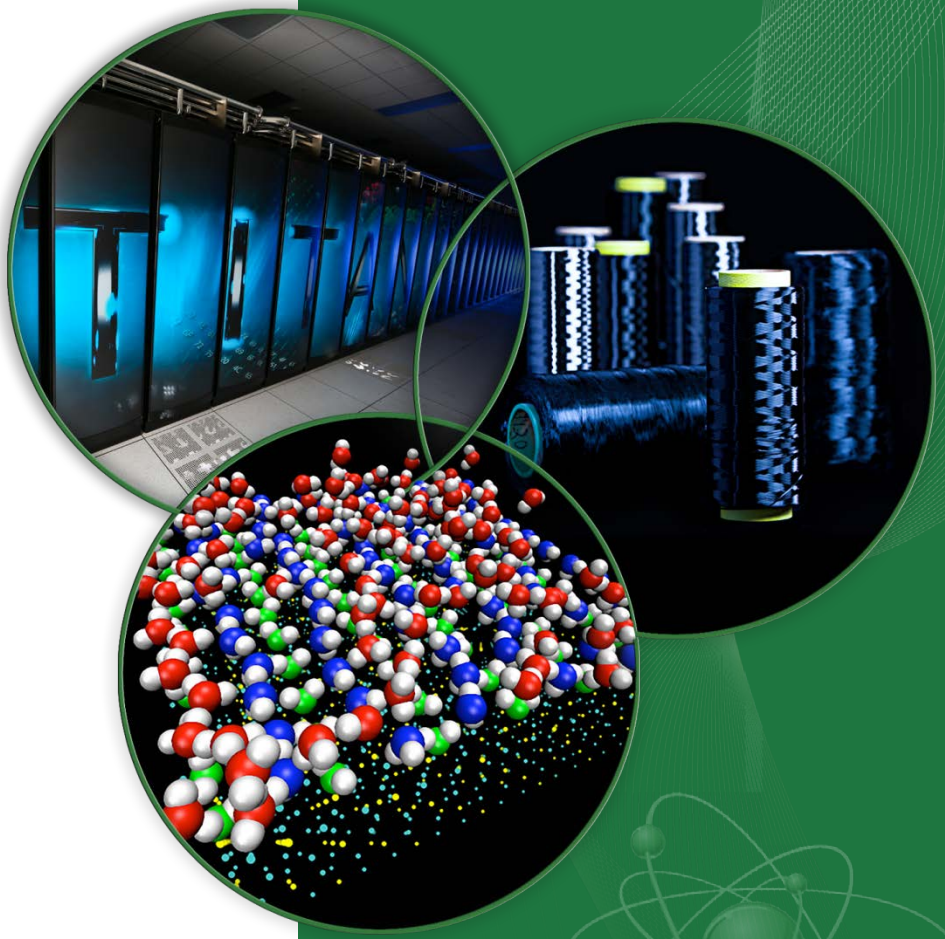

Shift/Exnihilo Team

Greg Davidson
Tom Evans
Steven Hamilton
Seth Johnson
Tara Pandya

Outline

- Current status of Monte Carlo (Shift) capabilities
- Benchmarks
- FY15 Planned Activities

RTM Monte Carlo Portfolio

- Methods and Analysis
  - Functional Monte Carlo (Michigan)
  - Doppler broadening (MIT)
- Shift Code Platform
  - Hosted at ORNL
  - CASL Monte Carlo code
  - Integrated into VERA through VERA I/O

Runtime Modes

- Fully-featured support for both fixed-source and *k*-eigenvalue modes
- Simplified set of external source definitions defined for fixed-source problems
  - Can load a fission source to use in fixed-source problems
- Three front-ends
  - Insilico – CASL neutronics (k-eigenvalue only)
  - Omnibus – XML-driven general purpose
  - Python – general purpose
- Complete set of output tools

Geometry Support

- RTK (Reactor ToolKit)
  - Tightly synced with Insilico reactor metadata model
  - Fast, optimized for PWR geometries
- Atlas
  - SCALE's new geometry package
  - Supports KENO input conventions
- Lava
  - MCNP geometry support
  - Accessible through Omnibus front-end

Physics Support

- Simple Multigroup
  - Primarily for testing and analytic benchmarking (C5G7)
  - P_0 scattering only
- SCALE Continuous Energy (SCE)
  - Completely re-engineered implementation of the SCEMPP physics package
  - Coupled neutron-gamma physics

SCE Physics Improvements

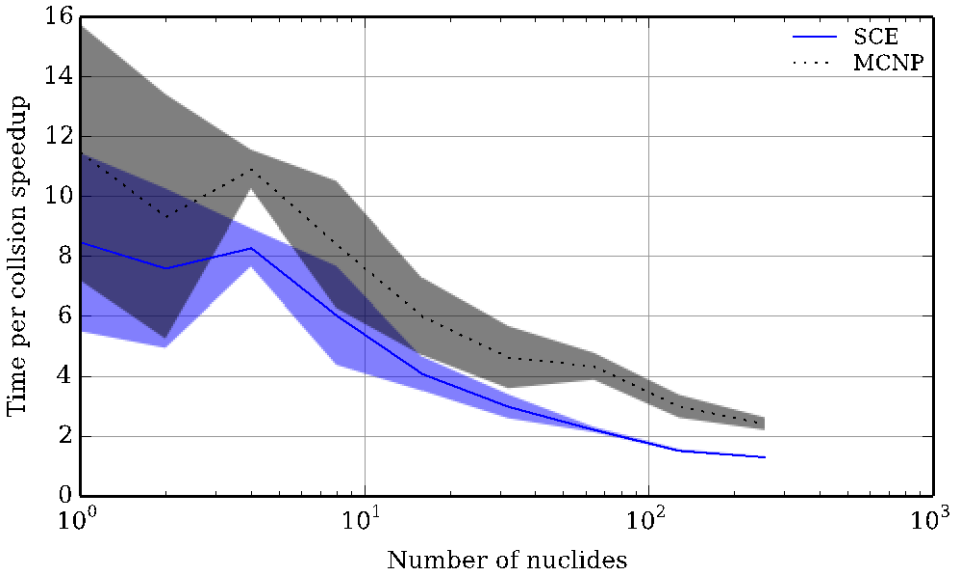

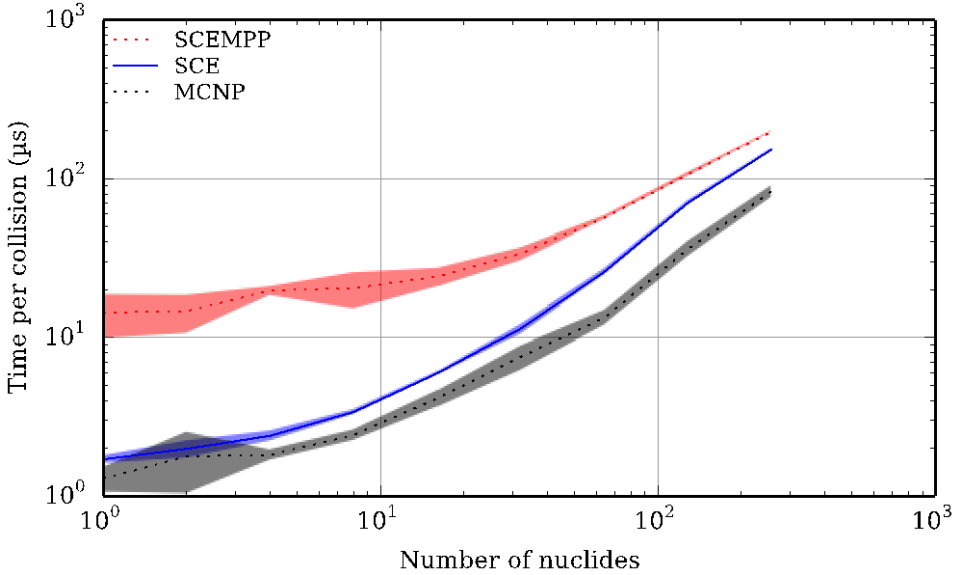

SCALE CE data optimization

- Simplified CE data API
- Reduced data storage overhead
- Reduced library load time
- Better diagnostics

SCE Diagnostics

Determining proper interpolation schemes for collisions

```
In [1]: from validate_xs import get_mt_name, get_mt_raw_name, name_to_mt, get_mt_name
        from denovo_utils import cmake_config, DB
        from mc_utils import Library, XS_Calculator
        from denovo_mpi import node
        import os
```

```
--------------------------------------------------
Exnihilo version : 5.0 (branch 'skunkworks' #e4213f99 on 2014MAR12) [debug] [DBC=7]
Python file      : -c
Build Date       : 2014MAR13
Exnihilo location: /Users/s3j/_code/_build/Exnihilo-nights/Exnihilo/packages/Transcore/pymc
--------------------------------------------------
```

```
In [2]: %matplotlib inline
        import matplotlib.pyplot as plt
        import numpy as np
```

```
In [3]: mts = range(1000)
        db = {
           'ce_lib_path': os.path.join(cmake_config("SCALE_DATA_DIR"), "ce_v7.0_endf.xml"),
           'ce_cache_path': '.scattering_cache.h5',
           'gamma_production': True,
           'reactions': mts,
           }
        library = Library(DB.from_dict(db))
```

```
In [5]: nucl = library.load_nuclide_n(8001001, 293.)
        rxn = nucl.get_reaction(name_to_mt['N_ELASTIC'])
```

Make sure the cross sections are getting interpolated correctly

```
In [8]: xs_calc = XS_Calculator()
        interp_energies = np.logspace(-3, 6, 10000)
        interp_xs = np.array([xs_calc.calc_micro(rxn, e) for e in interp_energies])
        plt.loglog(interp_energies, interp_xs)
        plt.loglog(rxn.energy, rxn.xs, linestyle='--')
```

```
Out[8]: [<matplotlib.lines.Line2D at 0x10f7e8a50>]
```

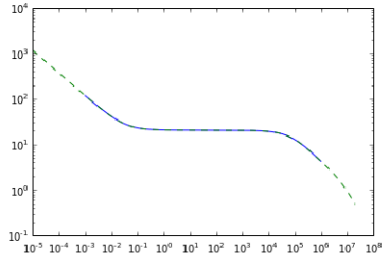

Look at collision data

```
In [9]: col = rxn.collision
        inc_energy = np.array(col.incident_energy)
```

Using python bindings to SCE classes combined with iPython notebook allows simple analysis of underlying SCALE data

Tallies

- New design implementation to meet the following goals:
  - Fast, low-overhead tallying across wide ranges of problems
  - Support for HPC scaling (domain decomposition)
  - Extensibility (adding fast and robust new tallies for customers)
- Built-in support for:
  - Multiple reaction types
  - Arbitrary *R*(E)
  - Energy binning
  - Variance calculation
- Scaling complexity:
  - Constant in number of bins
  - Linear in number of encountered bins per history

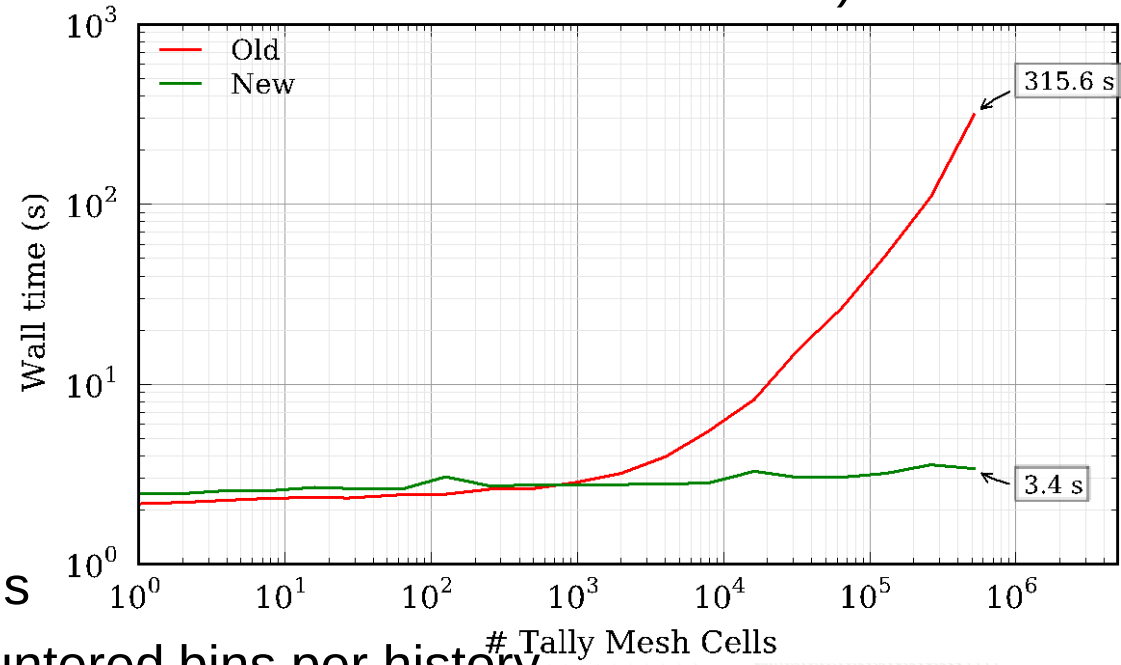

Parallelism

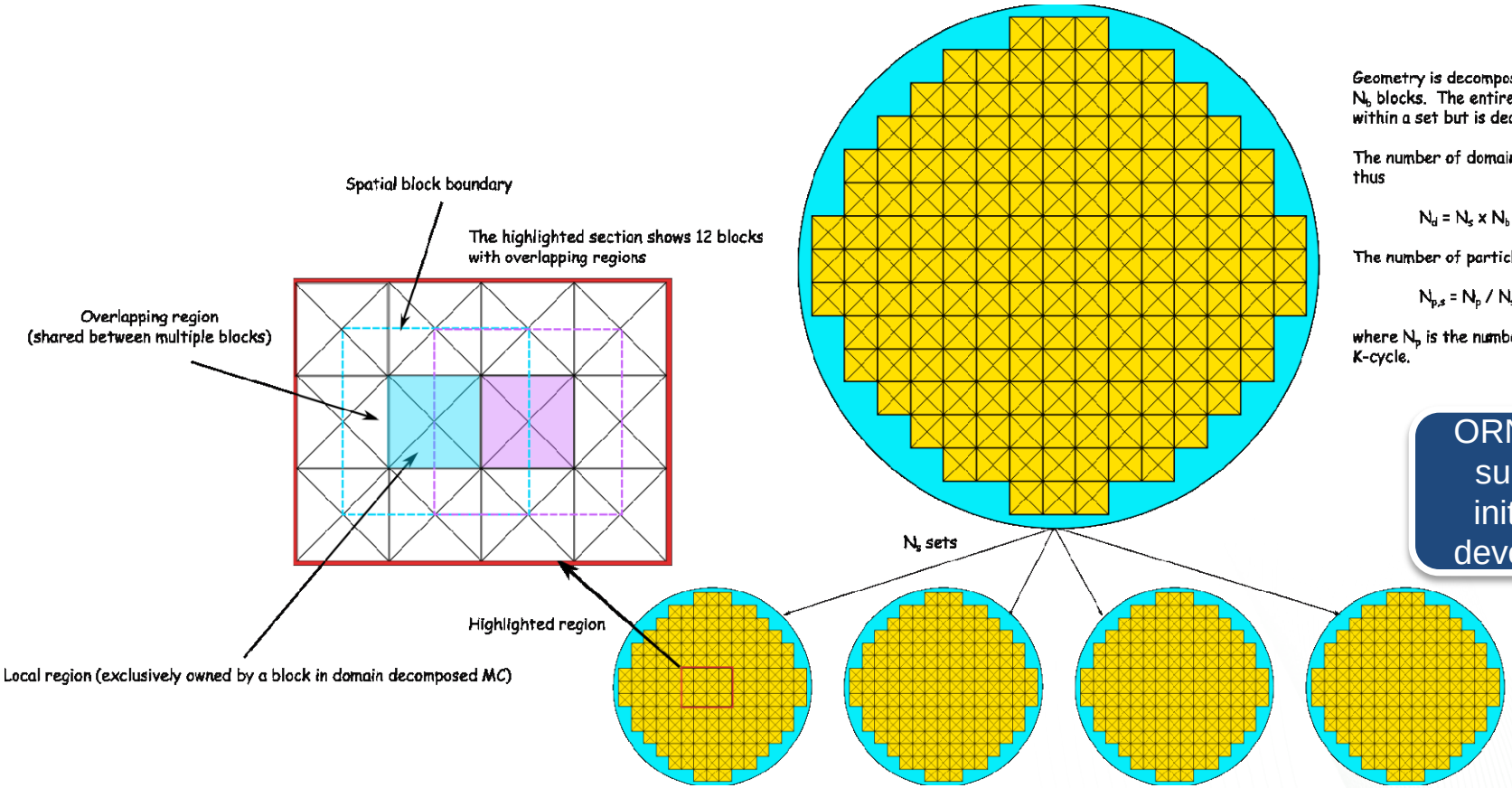

Geometry is decomposed into N_s sets, each with N_b blocks. The entire geometry is represented within a set but is decomposed across blocks.

The number of domains (processes) in a problem is thus

$$N_d = N_s \times N_b$$

The number of particles per set is

$$N_{p,s} = N_p / N_s$$

where N_p is the number of requested particles per K-cycle.

ORNL LDRD supported initial Shift development

Pictorial representation of MSOD parallel decomposition. Here the core geometry is decomposed into $N_s = 4$ sets. Each set has N_b blocks with overlapping regions such that the total number of parallel domains is $N_b \times N_s$. Particles are decomposed across sets where the number of particles per set is $N_{p,s} = N_p / N_s$. Each block can define an overlapping domain (shown in inset) to reduce block-to-block communication for particles that scatter at the interfaces between blocks.

J. C. WAGNER, S.W. MOSHER, T.M. EVANS, D.E. PEPLOW, J.A. TURNER, "Hybrid and Parallel Domain-Decomposition Methods Development to Enable Monte Carlo for Reactor Analyses," Prog. Nucl. Sci. Technol. 2, 815-820 (2011).

Tally and Data Performance

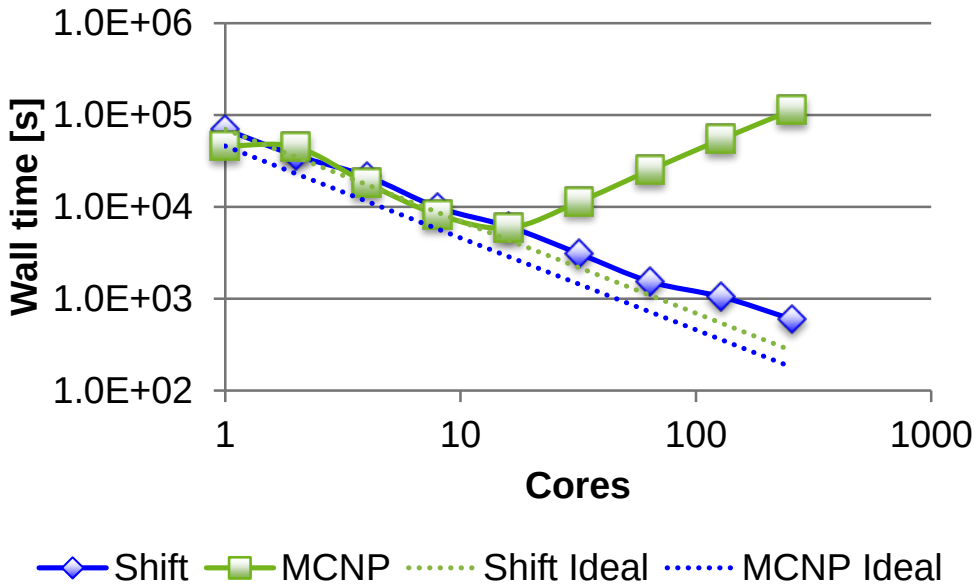

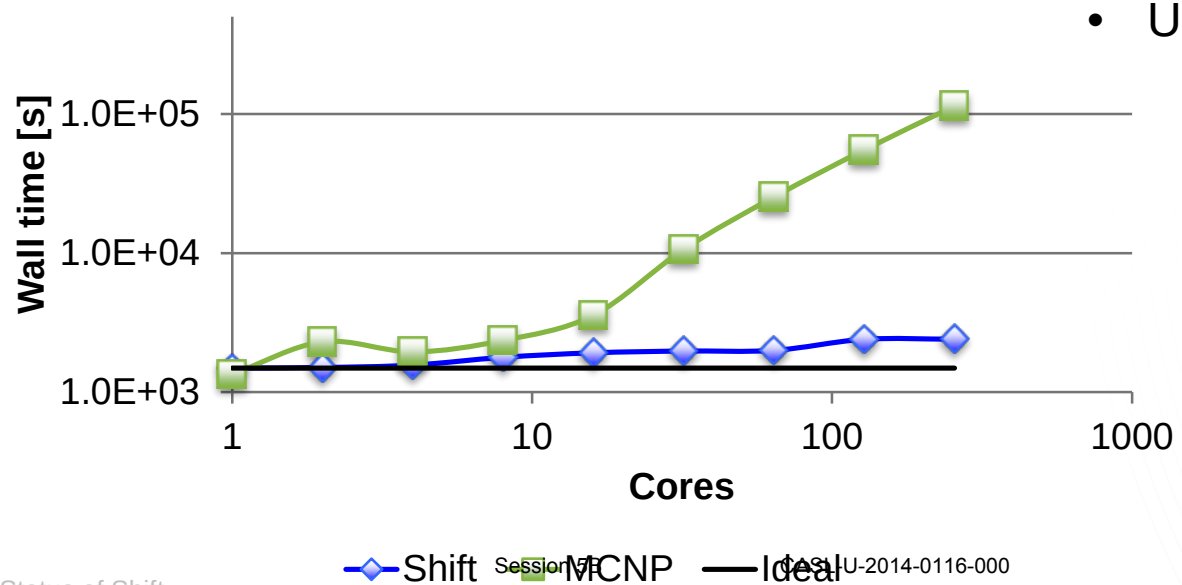

Problem setup to simulate depletion-level tallying

- 2 reactions
- 43,000 energy bins per reaction
- Union over all fuel regions

Session 73 LA-UR-2014-0116-000
OAK RIDGE National Laboratory

Depletion

- Depletion package developed to provide ORIGEN depletion capability
- Shift-ORIGEN coupling developed
  - Shift passes in materials, fluxes, and cross section library
  - Depletion produces powers and new nuclide list and updates materials for subsequent Shift calculations
- Predictor-corrector approach for coupled calculations
- Domain-decomposed and domain-replicated geometries
- Multigroup and continuous-energy physics using ORNL data libraries
- Provides complete time-dependent inventory of every nuclide in ORIGEN
- Loading of ORIGEN library HPC enabled

OAK RIDGE National Laboratory

Hybrid methods

- Parallel ray-tracer for material mixing
  - Uses same particle tracking engine as Shift (multiple geometry support)
  - Material visualization in VisIt
  - Produces Denovo mixed materials
- Biased sources and weight windows
- Denovo (SP_N/S_N) to Shift coupling
- CADIS (source-detector) implemented, FW-CADIS (global variance reduction) in progress
- Fission source acceleration in progress
  - CMFD for LWR analysis
  - Fission matrix for general criticality problems

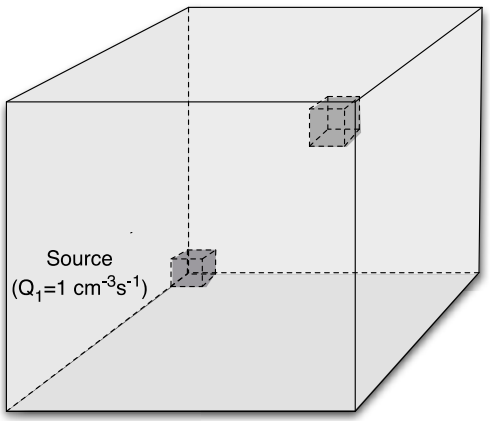

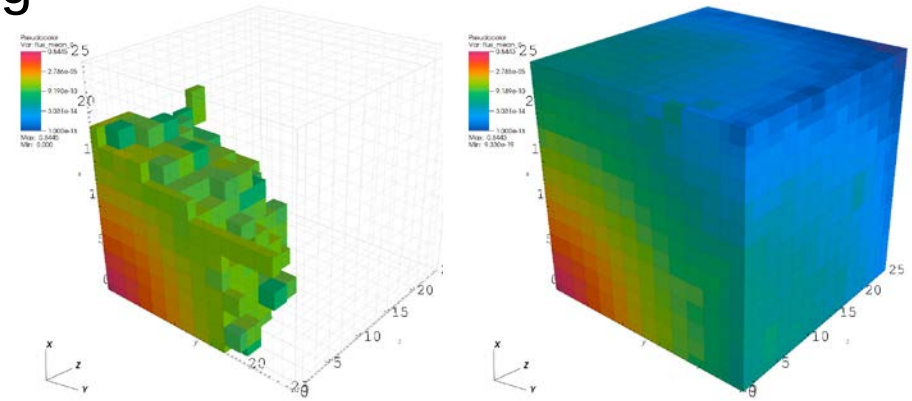

Analog FW-CADIS

Code Stats

- Exnihilo uses CMake for configuration, building, and deployment
- Version control is managed using git
- Developed using an agile KANBAN process based on *Continuous Integration*
  - We share a dashboard with the Scale software system.
  - Software verification is handled through a unit-testing framework built on Google Test
  - Each class has a uniquely compiled unit test (706 at last count)
- Acceptance tests are designed for code verification.
  - These are generally longer running

Executable Code	
C/C++ Source	226,856
C/C++ Comments	145,915
Python	15,529
FORTRAN	1,241
Test Code	
C/C++ Source	259,736
C/C++ Comments	54,007
Python	26,355
Totals	
C/C++ Source	462,221
C/C++ Comments	189,907
Python	38,820
FORTRAN	1,241

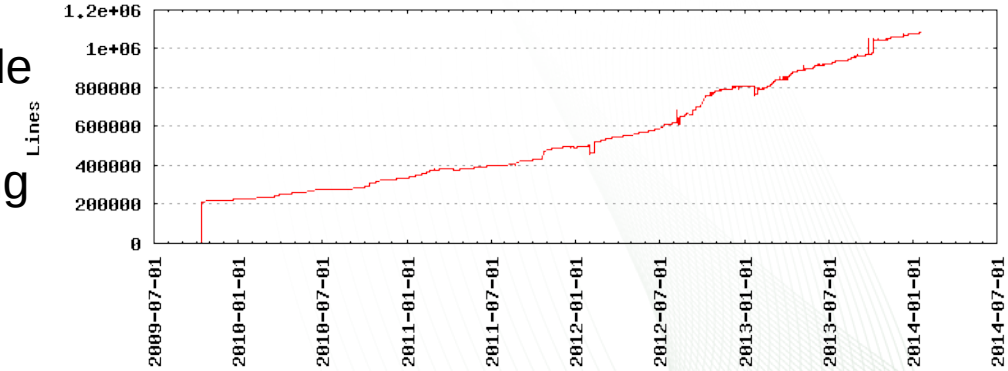

BW Core Models

- Shift
  - Using RTK geometry run through python frontend
  - Run on Remus using 64 processors
  - Did not model top grid plate
  - No vessel for BW1484 cores
  - Using AMPX processed ENDFVII.0 data
- OpenMC
  - Run on MIT machine using 128 processors
  - Using NJOY processed ENDFVII.0 data

BW1810 core 13 XY slice

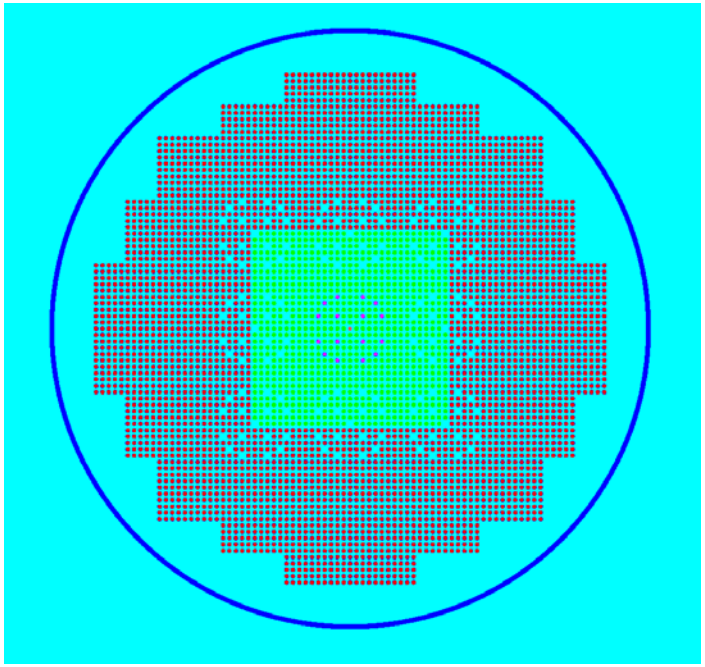

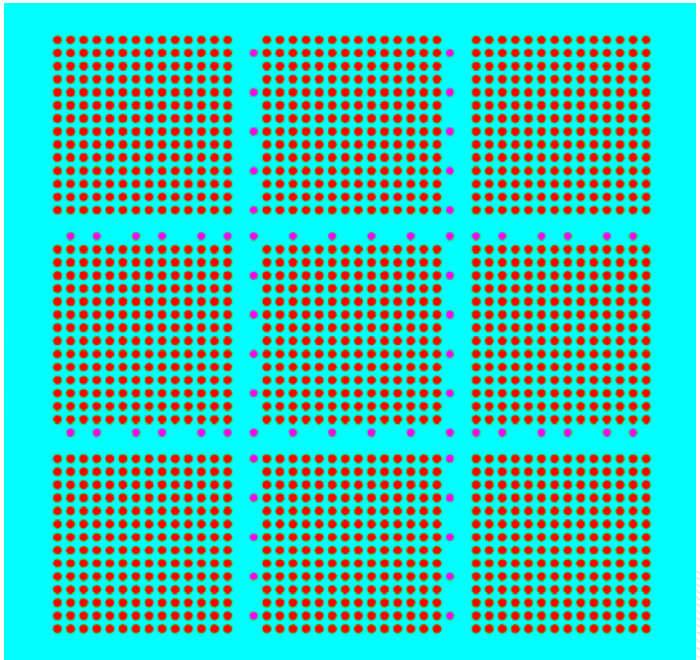

BW1484 core 5 XY slice

Current status of Shift BW V&V

- Shift k_{eff} results for these benchmarks compare well to OpenMC and experiment
- BW1810 pin power relative difference between OpenMC and Shift are all under 4.1% with majority under 2.0%
  - Comparison with experimental values is underway
- Data and model differences exist
- Further analysis of BW1484 core models is underway
- Shift is 2x slower than OpenMC in wall time

OAK RIDGE National Laboratory

CASL Early Science Results

- 1×10^{12} particles
  - 2000 cycles with 500×10^{6}/cycle
  - 500 inactive cycles
- 15000 nodes (80% of Titan)
  - 180,000 cores (12 per node)
- 4.8 hours total wall time

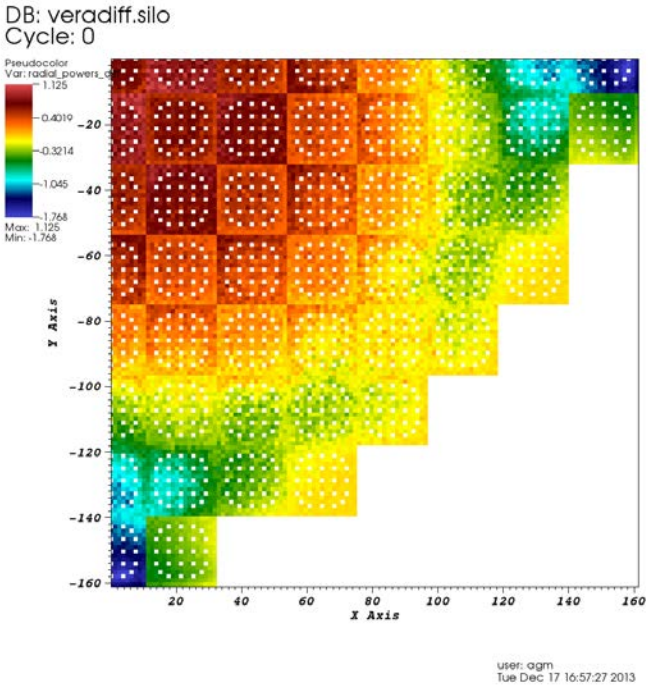

Absolute difference to CE KENO

Full core power

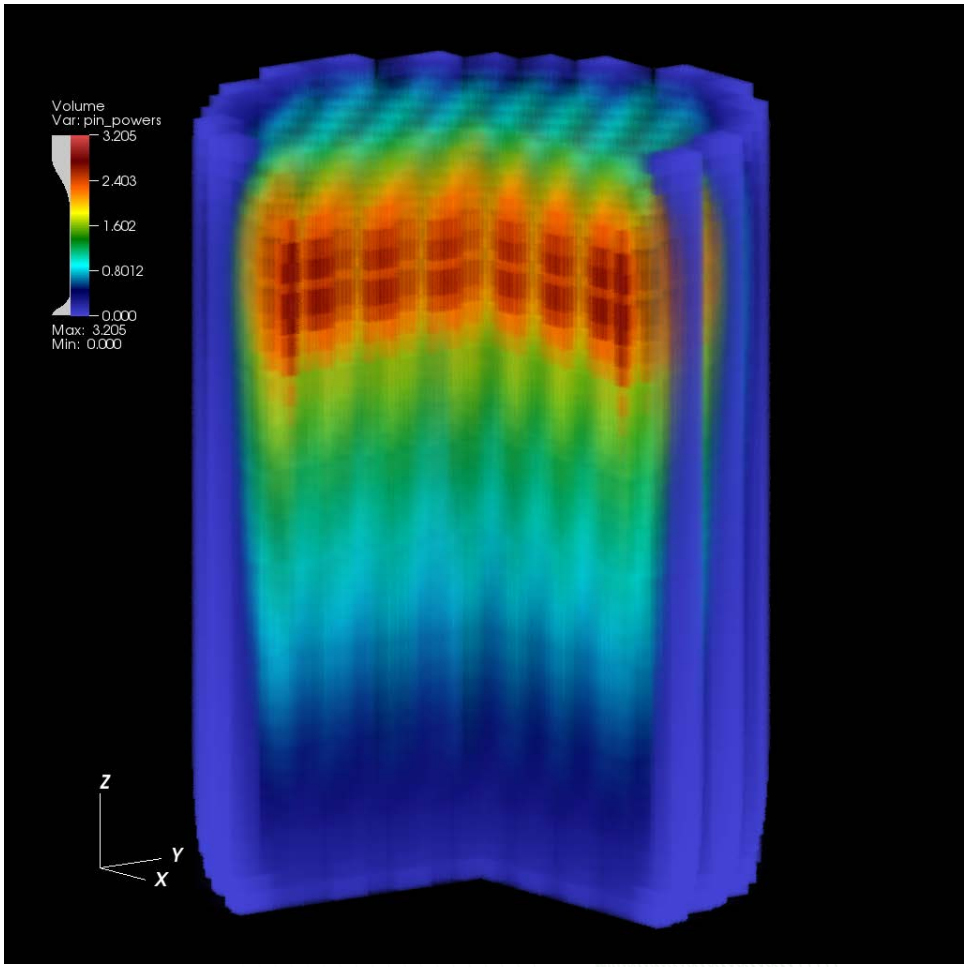

FY15 Plans

- Methods
- Capabilities
- Optimization
- V&V

Monte Carlo Methods

- Doppler Broadening
  - Multipole expansions being tested in OpenMC
  - MIT/ORNL/Michigan activity
  - Use OTF library (Michigan) to benchmark TH-coupled Monte Carlo
- Functional Monte Carlo (FMC)
  - Emphasis on testing 2 and 3-D methods
  - Thesis work at Michigan

Shift Capabilities

- Fission-source acceleration
  - Fission matrix
  - CMFD acceleration
- Hybrid methods
  - CADIS/FW-CADIS for cycle-to-cycle tallies
  - Supported by funding outside of CASL
- Depletion
  - Base capability in-place
  - Testing beginning to flesh out issues with capability
  - Supported by funding outside of CASL

Shift Capabilities

- General code features:
  - Restart
  - Rotational symmetry
  - I/O updates
  - Linking with MPACT for isotopics
  - Activate full MSOD through Insilico front-end
  - 2D buckling
- Boron/Xenon reactivity worth
  - Perturbation theory
  - Supported by funding outside of CASL

OAK RIDGE National Laboratory

Optimization

- GPU acceleration
  - Leveraging work through ASCR XPRESS project
- MSOD Testing
  - Performance and stability
  - Partially supported by ALCC allocation

V & V

- CE Data improvements
  - Some level of effort required for CE data
- Address and analyze issues that have emerged during preliminary testing
  - Verify uncertainties for K_{eff} and pin-powers
  - Examine 1% radial tilt and symmetric assembly uncertainties
  - Fix Shannon entropy on single-pin problems

CASL RTM Cross Section Development Status and Plan

Rev. 0

Kang Seog Kim
Mark L. Williams
Dorothea Wiarda
William A. Wieselquist

CASL Round Table Virtual Meeting
Oak Ridge National Laboratory
July 15, 2014

Overview

- Content
  - AMPX MG Library Improvement
    - Conventional AMPX MG library / Completed work for improvement / On-going work for improvement / Planned work for improvement
  - Burnup Library Development
    - Current status / Planned works
  - MPACT Library Development
    - Current status / On-going works
  - Cross Section Processing
    - Current status / On-going works / Future works
  - Conclusion

- Documentation
  - Kang Seog Kim, Benjamin Collins, Brendan Kochunas, “Review of the CASL Core Simulator MPACT,” CASL-X-2014-0046-000 (2014)
  - Kang Seog Kim, Yuxuan Liu, William Martin, “A Plan to Improve Resonance self-shielding methodology in the CASL core simulator MPACT,” April 30, 2014
  - William A. Wieselquist, Brendan Kochunas, Kang Seog Kim, “A plan to improve depletion capability in the CASL core simulator MPACT,” May 10, 2014

AMPX MG Library Improvement - I

- Conventional AMPX MG Library
  - Processing code package
    - AMPX-6 developed at ORNL
  - Narrow resonance approximation
    - Resolved & unresolved resonance energy groups
  - Weighting function
    - Maxwellian(thermal) + 1/E(epithermal) + Fission spectrum(fast)
  - For conventional SCALE procedure
    - BONAMI → Transport Code :: Bondarenko approach
    - BONAMI/CENTRM/PMC → Transport Code :: SCALE inherent approach
      - Includes pointwise slowing down calculation
    - Transport code :: NEWT, KENO-MG
  - Temperature independent 2-D elastic scattering matrix
    - Temperature bias for Bondarenko approach
  - Standard multigroup neutron library
    - 238-group structure
    - Reactivity bias : ~400 pcm for PWR & BWR

AMPX MG Library Improvement - II

- Completed work for improvement
  - Development of new 252-g AMPX library
    - <100 pcm bias for the conventional SCALE procedure
    - Improved energy group structure & weighting procedure by reactivity analysis
    - New weighting function
      - Typical PWR pointwise spectrum from CENTRM
  - Development of new AMPX procedure (see Figure in next slide)
    - For Bondarenko approach (and the SCALE procedure also)
    - LAMBDA
      - Intermediate resonance parameters for all nuclides
    - IRFFACTOR
      - F-factor tables : Self-shielded XS vs. background XS
      - Slowing down calculation + ESSM(Embedded Self-Shielding Method)
      - Homogeneous : Z > 39 nuclides
      - Heterogeneous models : important resonance nuclides
    - SUBGR
      - Use of F-factor tables
      - Subgroup data generation : Subgroup levels and weights
      - 45 important nuclides

AMPX MG Library Improvement - III

- Procedure to generate F-factor tables & subgroup data for Bondarenko approach

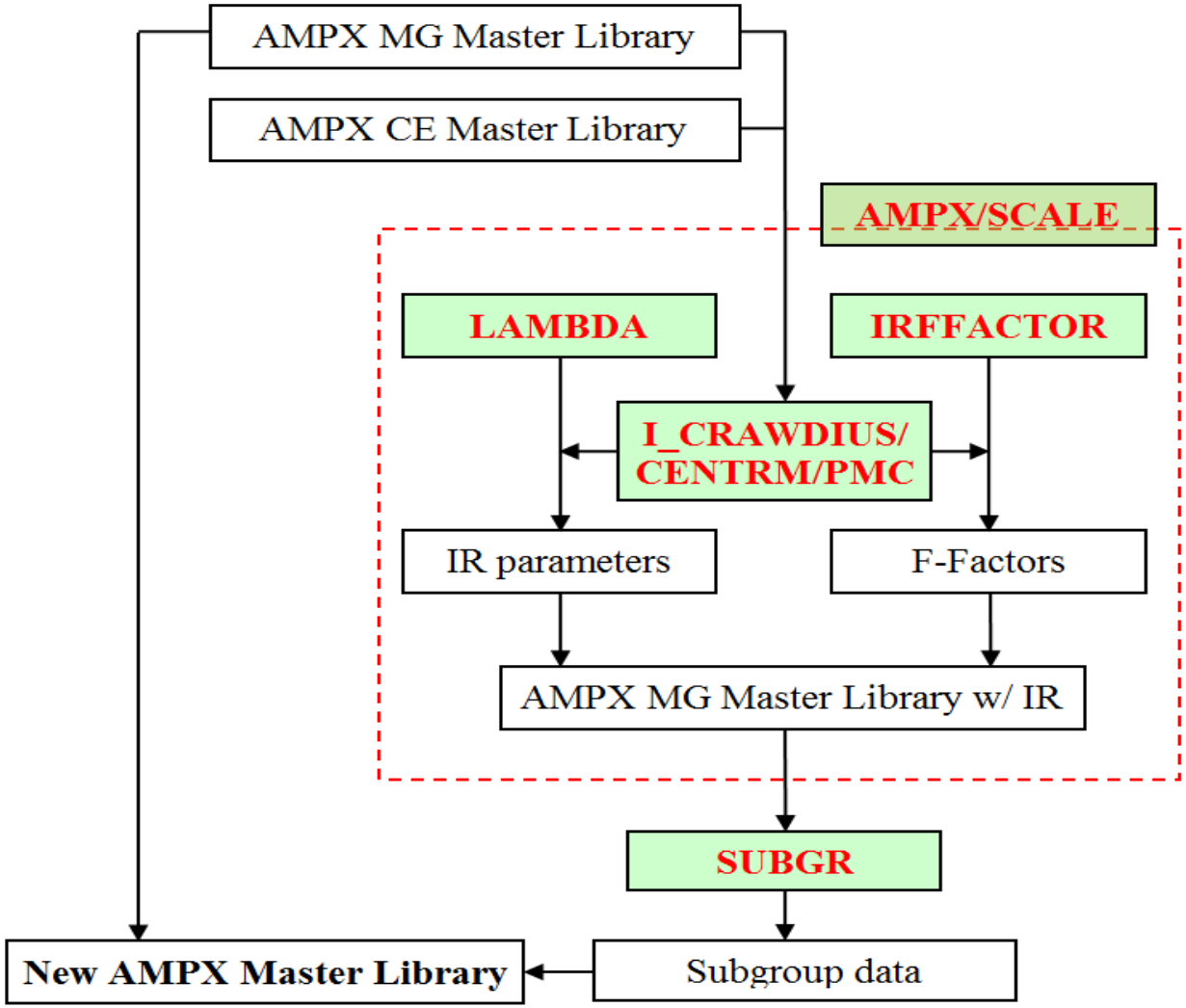

AMPX MG Library Improvement - IV

- Completed work for improvement (continued)
  - Development of coarse energy group structure
    - Develop a program called CGOP
      - Automatic optimization by reaction rate analysis
      - For both the SCALE procedure and Bondarenko approach
    - Energy group optimization
      - For both PWR and BWR
      - 56-group structure based on 252-group structure
  - New F-factor table for removal correction
    - Solved temperature bias issue
    - Only for ENDF/B-VII.1 based libraries
    - None for ENDF.B-VII.0 based libraries
  - New procedure to generate F-factors for URR groups
    - Using analytic formula with probability table
    - Small impact on PWR, but significant on BWR
      - Useful for the 2nd stage CASL

AMPX MG Library Improvement - VI

- Completed work for improvement (continued)
  - New procedure for transport corrected ^{1}H cross section
    - Leakage conservation method used in CASMO
    - Developed a new program to generate transport correction factor
      - 1-D MOC with high order scattering
      - Coupled with the simplified AMPX library
    - Working good
      - However, more tests are required
  - New AMPX libraries and subgroup data
    - ENDF/B-VII.0 252-group AMPX library
    - ENDF/B-VII.0 56-group AMPX library
    - ENDF/B-VII.0 56-group subgroup data
  - New data format of AMPX library
    - BOFF format library
      - Easily include new additional data such as subgroup & delayed neutron data
    - Resource for BOFF format library

AMPX MG Library Improvement - VII

- On-going works
  - New AMPX MG libraries subgroup data
    - ENDF/B-VII.1 based 56 & 252-group AMPX library
    - ENDF/B-VII.1 56-group subgroup data
  - Improvement of subgroup data
    - Subgroup data generation by conserving self-shielded cross sections
      - Currently conserving Resonance Integral
    - SUBGR is ready
    - Improve/modify IRFFACTOR
      - Documentation for functional requirement is ready
  - Development of the 47-group AMPX library
    - HELIOS group structure
    - ENDF/B-VII.1
    - For testing and comparison
    - For more stable transport corrected P_0 calculation
    - Since the code package and procedure are ready, it will be quite straight forward.
      - Less than 1 week

AMPX MG Library Improvement - VIII

- Planned works
  - New F-factor tables for ^{238}U
    - Consider epithermal upscattering
    - Positive impact on Fuel Temperature Coefficient
    - Candidate methods
      - A coupled procedure of KENO-CE with DBRC + ESSM
        - Improve IRFFACTOR or develop a simple procedure
        - Already a draft procedure is ready
      - Implement a new capability for epithermal upscattering into CENTRM
        - Very time consuming & require effort
  - Improvement of the AMPX MG library
    - Include more delayed neutron data
      - 6-group decay constants
      - 6-group decay fractions
    - Fission spectrum
      - Modify the definition of MT=1018 to include both prompt & delayed fission spectra
    - Gamma library
      - Fully coupled neutron + gamma library

AMPX MG Library Improvement - IX

- Planned works (continued)
  - New F-factor tables for the new ESSM + Quasi 1D slowing down methodology

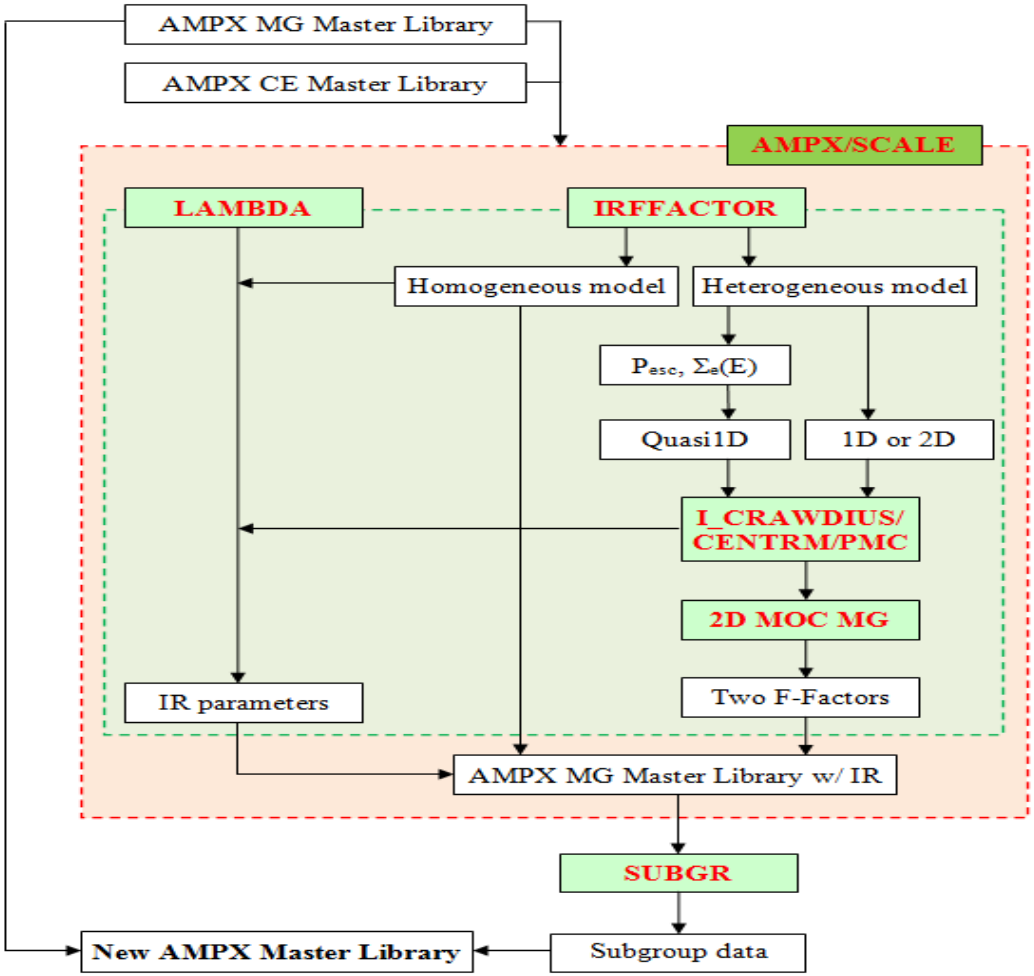

Burnup Library Development - I

- Current status
  - Two burnup solvers
    - ORIGEN based matrix exponential method
      - Simplified burnup chain including 510 nuclides
      - No Quality Assured burnup libraries
    - ORIGEN API integration
      - Completely same with the SCALE ORIGEN
      - Full burnup chain with 2237 nuclides
      - Quality Assured procedure and burnup libraries
  - Issues
    - No procedure to generate burnup libraries for simplified burnup chain
      - Consistency with full burnup chain
      - ORIGEN data format
  - Available simplified burnup chains

Chain ID	Library	Activation	Heavy	F. P.	Total
A	SCALE-ORIGEN	910	176	1151	2237
B	MPACT	196	82	232	510
C	KAERI-DeCART	62	40	142	244

Burnup Library Development - II

- Planned works
  - Develop a new program
    - Generate new burnup libraries for simplified burnup chains
    - ORIGEN data format
  - Develop new burnup libraries
    - ENDF/B-VII.1
  - Delayed gamma source data
    - Simplified burnup chain
    - Equilibrium delayed gamma
    - Method
      - ORIGEN calculation or
      - Empirical data

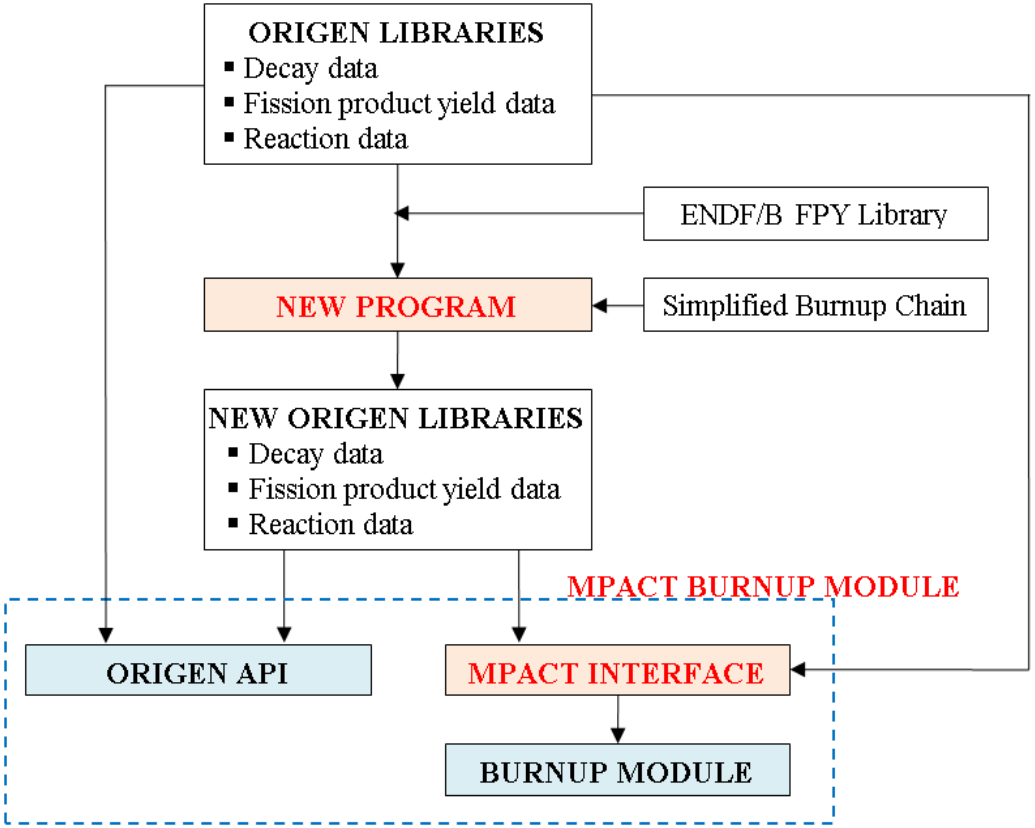

MPACT Library Development - I

- Current status
  - Library format and data structure
    - DeCART & HELIOS
  - Limitation
    - Simplified data : several categories for nuclides
      - Full : resonance data + full XS
      - Intermediate : full XS
      - Part : absorption XS
    - Subgroup data : 45 nuclides
    - Fixed resolved resonance energy groups : 26 out of 56-group
    - Limited number of nuclides
      - About 300 nuclides : ENDF/B-VII.0 393 nuclides
  - Direct use of AMPX MG library
    - Simplified AMPX data format
      - Minimize modification
      - Include all data for transport & burnup calculation
      - Full resonance data: energy & nuclides
      - Completed to develop data format and an interface program

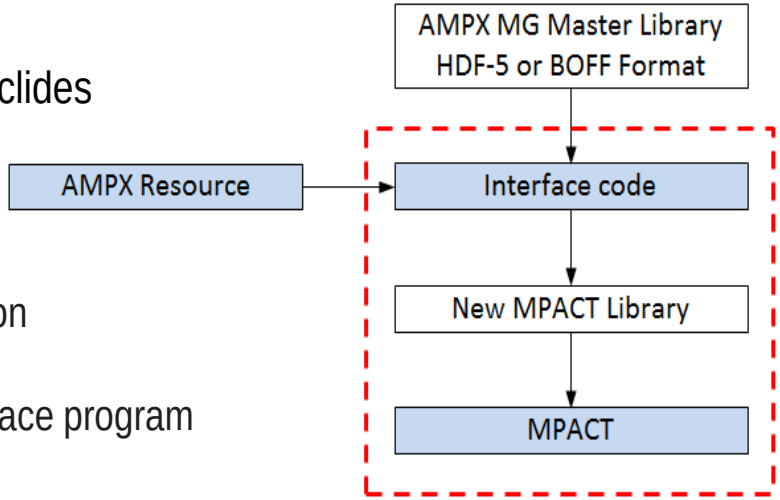

MPACT Library Development - I

- Completed works
  - Development of the MPACT library generation procedure (see Figure in next slide)
    - DECLIB
      - To generate the MPACT library based on the DeCART library format
      - Use of the AMPX MG library, ENDF/B neutron, decay & FP yield data, and subgroup data
    - DECLIBFORM
      - To convert the formatted one into the binary and vice versa
    - Library format and data structure
      - DeCART & HELIOS
  - Development of the 56-group MPACT library
    - ENDF/B-VII.0
  - Limitation of the current MPACT library
    - Simplified data : several categories for nuclides
      - Full : resonance data + full XS
      - Intermediate : full XS
      - Part : absorption XS
    - Subgroup data : 45 nuclides
    - Fixed resolved resonance energy groups : 26 out of 56-group
    - Limited number of nuclides
      - About 300 nuclides ← ENDF/B-VII.0 393 nuclides

MPACT Library Development - II

- Procedure to generate the MPACT library

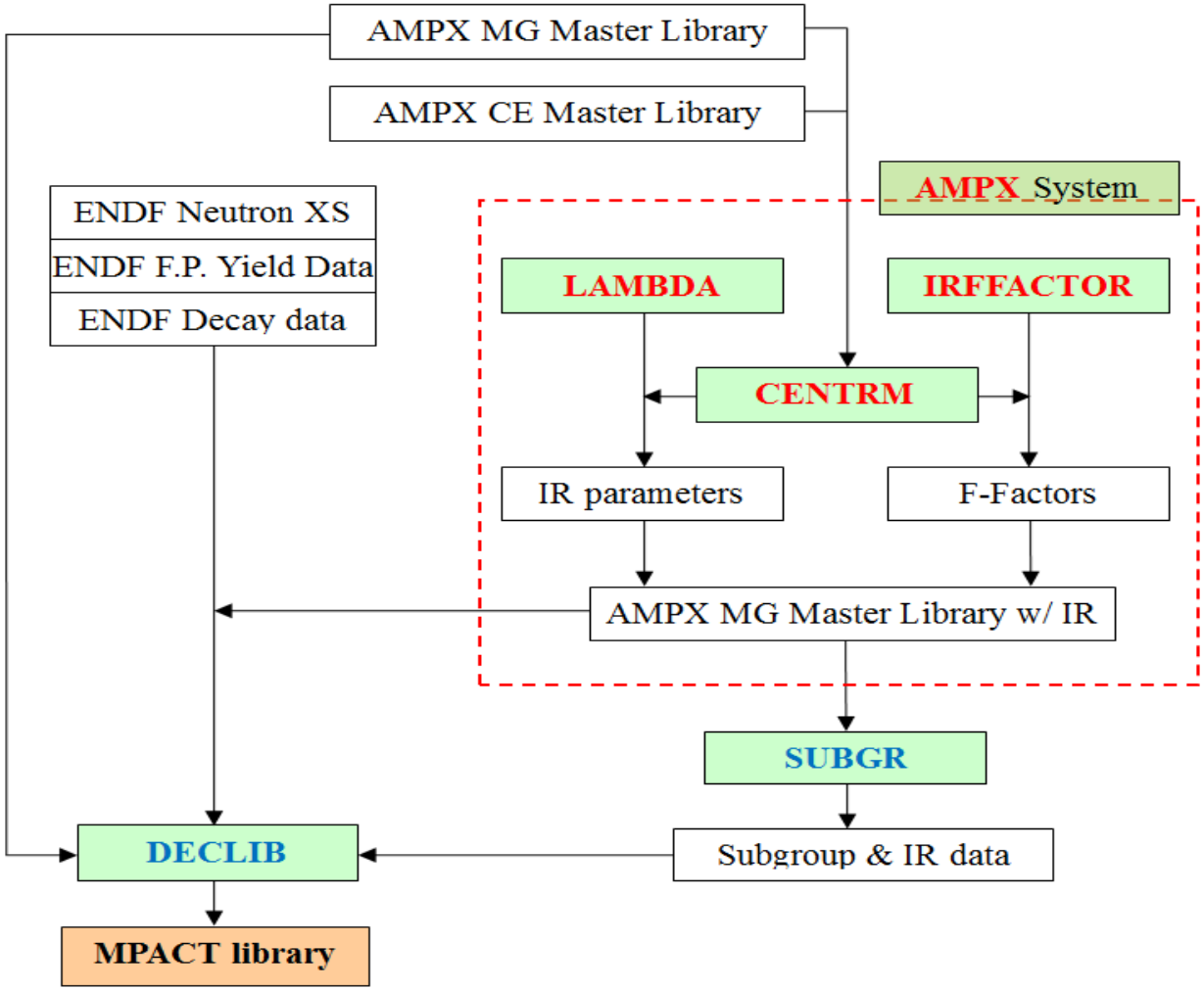

MPACT Library Development - III

- Completed works (continued)
  - Direct use of AMPX MG library
    - Simplified AMPX data format
      - Minimize modification
      - Include all data for transport & burnup calculation
      - Full resonance data: energy & nuclides
      - Completed to develop data format and an interface program

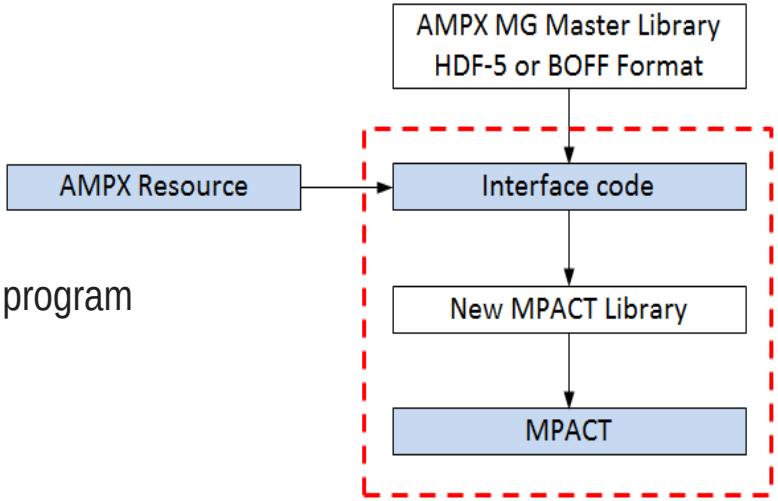

- On-going works
  - Direct use of AMPX MG library
    - Implement the capability to directly utilize the simplified AMPX MG library
      - Minimize modification
      - Include all data for transport & burnup calculation
      - Full resonance data: energy & nuclides
      - Improve resonance treatment methodology

Cross Section Processing - I

- Completed works & Current status
  - Direct use of the MPACT library
    - DeCART data format
    - 56-group library
      - AMPX code package
      - DECLIB
    - Full resonance self-shielded data : 45 nuclides
    - Resonance energy groups : 26 out of 56-group
  - Resonance self-shielding methods
    - Subgroup method
      - Similar with DeCART and HELIOS
      - Category concept : Fixed source transport calculation for each category
      - Temperature dependent resonance treatment
        - HELIOS approach
      - Resonance treatment for scattering cross sections
    - Embedded Self-Shielding Method (ESSM)
      - Developed at ORNL
      - Direct utilization of F-factor tables (Resonance integral table)
      - No category concept → Fast computing time
      - Resonance treatment for scattering cross sections

Cross Section Processing - II

- On-going works
  - Direct use of AMPX MG library
    - Implement the capability to directly utilize the simplified AMPX MG library
      - Minimize modification
      - Include all data for transport & burnup calculation
      - Full resonance data: energy & nuclides
      - Improve resonance treatment methodology
  - Improvement of resonance self-shielding methodology
    - Overall plan

      Kang Seog Kim, Yuxuan Liu, William Martin, "A Plan to Improve Resonance self-shielding methodology in the CASL core simulator MPACT," April 30, 2014
    - Subgroup + ESSM combined method
      - All energy groups
      - All nuclides
    - Subgroup method improvement
      - Non-uniform temperature distribution
    - ESSM improvement
      - Explicit radial zone dependent self-shielded XS
      - Non-uniform temperature distribution

Cross Section Processing - III

- Future work
  - New resonance self-shielding method
    - ESSM + Quasi 1D slowing down

      Yuxuan Liu, William Martin, Mark L. Williams, Kang Seog Kim, “Resonance Self-shielding Method for Fuel Annular Subdivisions Using Quasi-1D Slowing down Solutions,” (Submitted to NSE)
    - Concept &Benefit
      - Global effect by ESSM & Local by Quasi 1D
      - Explicit resonance interference
      - Explicit non-uniform temperature distribution
      - Explicit consideration of removal correction
      - Fast computing time & achievable memory
    - Works to do
      - Additional new F-factor tables
      - 1D collision probability
      - Pointwise XS data processing : Unified energy grid & temperature interpolation
      - 0D slowing down calculation
    - Research works
      - Deterministic method with probability table
      - Epithermal upscattering treatment in Quasi 1D
      - Extension to fast energy groups

Cross Section Processing - IV

- Future work (continued)
  - Common self-shielded or self-unshielded macroscopic cross section
    - Moderator cross section
      - As a function of temperature
    - Cladding cross section
      - Self-shielded XS: simple single pin model
      - As a function of temperature
    - Detector cross section
      - Self-shielded XS: simple model

Conclusion

- Current status
  - Working reasonably
    - The AMPX MG library / MPACT library generation procedures
    - Cross section processing procedure including resonance treatment
    - → Need improvement for better performance and more general applicability
- On-going works
  - Improve accuracy
    - Develop ENDF/B-VII.1 based the AMPX MG libraries
    - Direct use of the AMPX MG library
    - Improve subgroup data and self-shielding methodologies
    - → Achieve better performance and more general applicability
- Planned works
  - For best performance
    - AMPX : Epithermal upscattering, delayed neutron data, gamma data
    - Develop a procedure to generate burnup libraries for simplified burnup chain
    - Common resonance model
    - Implementation of new ESSM + Quasi 1D slowing down method
    - → Achieve high fidelity performance

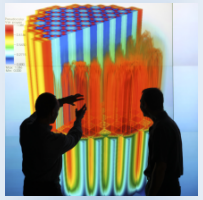

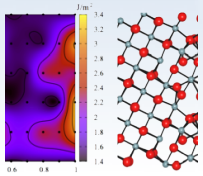

User Guidelines and Best Practices for CASL VUQ Analysis Using Dakota

Brian M. Adams (SNL), Russell W. Hooper (SNL), Ralph C. Smith (NCSU), Brian J. Williams (LANL)

Consortium for Advanced Simulation of LWRs

U.S. DEPARTMENT OF ENERGY | Nuclear Energy

CASL Round Table, July 14-16, 2014

Outline

- Overview of Dakota
  - Dakota is part of VERA
- Goals of CASL Dakota Manual
  - Support code and application PCMM
- Overview of Cobra-TF Application
  - Input parameter exposure in Cobra-TF
- Overview of VUQ methods covered
  - Sensitivity analysis, optimization and deterministic calibration, mathematical surrogate construction, UQ, Bayesian model calibration
- Cobra-TF Application
  - Solution verification, sensitivity analysis, kriging surrogate construction, Bayesian model calibration
- Conclusions

CASL Dakota manual facilitates VUQ analysis via worked applications

Dakota Supports Simulation Credibility

- Provides broader and deeper perspective for analysts and decision makers
  - *Enhances understanding of risk by quantifying margins and uncertainties (QMU)*
  - *Improves products through simulation-based design*
  - *Assesses simulation credibility through verification and validation*
- Enables QMU and design with simulations in manner analogous to experiment-based QMU and physical design/test cycles

Manages and analyzes ensembles of simulations:

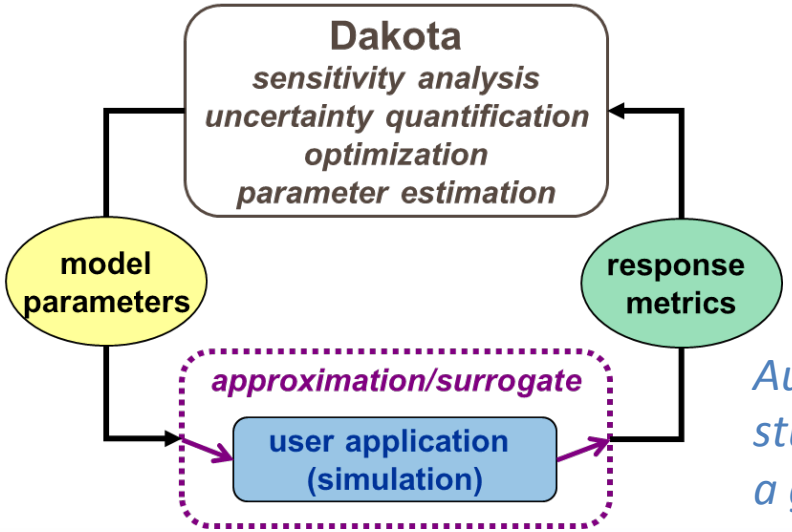

Automate typical "parameter variation" studies with various advanced methods and a generic interface to your simulation.

Dakota tailors code iterations to efficiently solve VUQ problems

Advanced Exploration of Simulations

Dakota enriches simulations to address analyst/designer questions:

- Which are crucial factors/parameters, how do they affect key metrics? *(sensitivity)*
- How safe, reliable, robust, or variable is my system?
  (quantification of margins and uncertainty: QMU, UQ)
- What is the best performing design or control? *(optimization)*
- What models and parameters best match experimental data? *(calibration)*

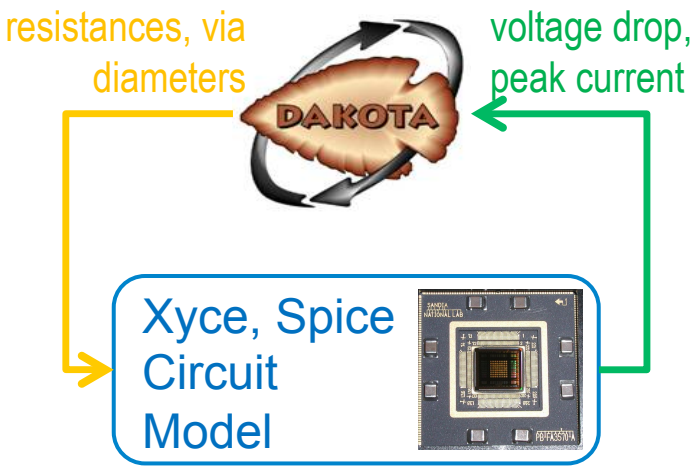

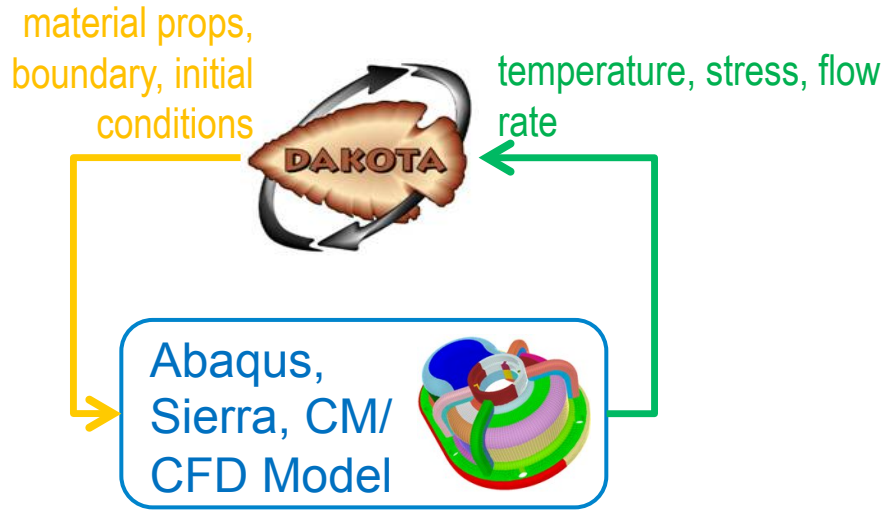

All based on iterative analysis of a computational model for phenomena of interest

- Commercial or SNL, loose-coupled/black-box or embedded/tightly integrated…

Dakota supports multiple interfaces for code interactions

Dakota Status in VERA

- Dakota synced from SNL to CASL and builds/tests in VERA to protect integration investment
- Examples in `VUQDemos` archive previous studies and test against development physics code inputs
- Focusing on loose, but validating workflows since there isn't a single coupled physics driver in VERA
- *Accumulating technical debt due to challenges adapting Dakota to VERA build infrastructure*

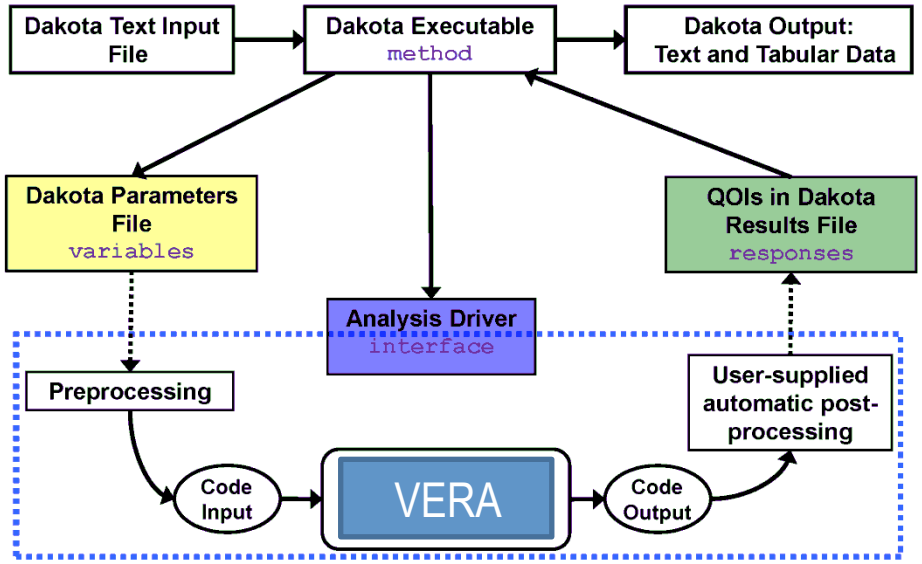

- Manipulate parameters in:
  - VERA Input
  - VUQ auxiliary data, e.g., model form
  - Offline generated input data such as meshes or cross sections
- Work in progress for better QOI extraction

Dakota enables core VUQ analyses in CASL

Summary of PCMM

MATURITY / ELEMENT	Maturity Level 0 Low Consequence, Minimal M&S Impact, e.g. Scoping Studies	Maturity Level 1 Moderate Consequence, Some M&S Impact, e.g. Design Support	Maturity Level 2 High-Consequence, High M&S Impact, e.g. Qualification Support	Maturity Level 3 High-Consequence, Decision-Making Based on M&S, e.g. Qualification or Certification
Representation and Geometric Fidelity What features are neglected because of simplifications or stylizations?	• Judgment only • Little or no representational or geometric fidelity for the system and BCs	• Significant simplification or stylization of the system and BCs • Geometry or representation of major components is defined	• Limited simplification or stylization of major components and BCs • Geometry or representation is well defined for major components and some minor components • Some peer review conducted	• Essentially no simplification or stylization of components in the system and BCs • Geometry or representation of all components is at the detail of "as built", e.g., gaps, material interfaces, fasteners • Independent peer review conducted
Physics and Material Model Fidelity How fundamental are the physics and material models and what is the level of model calibration?	• Judgment only • Model forms are either unknown or fully empirical • Few, if any, physics-informed models • No coupling of models	• Some models are physics based and are calibrated using data from related systems • Minimal or ad hoc coupling of models	• Physics-based models for all important processes • Significant calibration needed using separate effects tests (SETs) and integral effects tests (IETs) • One-way coupling of models • Some peer review conducted	• All models are physics based • Minimal need for calibration using SETs and IETs • Sound physical basis for extrapolation and coupling of models • Full, two-way coupling of models • Independent peer review conducted
Code Verification Are algorithm deficiencies, software errors, and poor SQE practices corrupting the simulation results?	• Judgment only • Minimal testing of any software elements • Little or no SQE procedures specified or followed	• Code is managed by SQE procedures • Unit and regression testing conducted • Some comparisons made with benchmarks	• Some algorithms are tested to determine the observed order of numerical convergence • Some features & capabilities (F&C) are tested with benchmark solutions • Some peer review conducted	• All important algorithms are tested to determine the observed order of numerical convergence • All important F&Cs are tested with rigorous benchmark solutions • Independent peer review conducted
Solution Verification Are numerical solution errors and human procedural errors corrupting the simulation results?	• Judgment only • Numerical errors have an unknown or large effect on simulation results	• Numerical effects on relevant SRQs are qualitatively estimated • Input/output (I/O) verified only by the analysts	• Numerical effects are quantitatively estimated to be small on some SRQs • I/O independently verified • Some peer review conducted	• Numerical effects are determined to be small on all important SRQs • Important simulations are independently reproduced • Independent peer review conducted
Model Validation How carefully is the accuracy of the simulation and experimental results assessed at various tiers in a validation hierarchy?	• Judgment only • Few, if any, comparisons with measurements from similar systems or applications	• Quantitative assessment of accuracy of SRQs not directly relevant to the application of interest • Large or unknown exper-imental uncertainties	• Quantitative assessment of predictive accuracy for some key SRQs from IETs and SETs • Experimental uncertainties are well characterized for most SETs, but poorly known for IETs • Some peer review conducted	• Quantitative assessment of predictive accuracy for all important SRQs from IETs and SETs at conditions/geometries directly relevant to the application • Experimental uncertainties are well characterized for all IETs and SETs • Independent peer review conducted
Uncertainty Quantification and Sensitivity Analysis How thoroughly are uncertainties and sensitivities characterized and propagated?	• Judgment only • Only deterministic analyses are conducted • Uncertainties and sensitivities are not addressed	• Aleatory and epistemic (A&E) uncertainties propagated, but without distinction • Informal sensitivity studies conducted • Many strong UQ/SA assumptions made	• A&E uncertainties segregated, propagated and identified in SRQs • Quantitative sensitivity analyses conducted for most parameters • Numerical propagation errors are estimated and their effect known • Some strong assumptions made • Some peer review conducted	• A&E uncertainties comprehensively treated and properly interpreted • Comprehensive sensitivity analyses conducted for parameters and models • Numerical propagation errors are demonstrated to be small • No significant UQ/SA assumptions made • Independent peer review conducted

Manual Includes Dakota Basics

- Dakota's relationship to PCMM
- Why use Dakota: key capabilities
- How to access the software, help resources, and examples
- Interacting with Dakota, at a high level
- How Dakota input files and simulation interfaces work
- *Not exhaustive: defers to core Dakota manuals for details!*
- Accessible cantilever beam example with simplified governing equations

Table 1.1: Summary of Dakota relevance for PCMM-related activities.

VUQ/PCMM Activity	Dakota relevance
select quantities of interest (QOIs)	(limited)
software quality assurance (SQA)	(limited)
code verification	conduct parameter studies as a function of mesh quality; calculate convergence rate
solution verification	conduct parameter studies over solver parameters or mesh quality; calculate convergence rate
validation	run ensemble of simulations and make (potentially uncertainty-aware) comparisons with experimental data, assess model form uncertainty
sensitivity	conduct global sensitivity analysis to rank or screen parameters; supports quantified parameter ranking table (QPRT)
uncertainty quantification	compute uncertainty in QOIs for risk-informed decision making
calibration	tune or refine models for use in particular scenarios

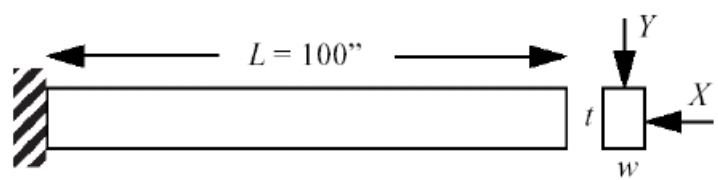

$$\texttt{area} = wt$$

$$\texttt{stress} = S - R = \frac{600}{wt^2}Y + \frac{600}{w^2t}X - R$$

$$\texttt{displacement} = D - D_0 = \frac{4L^3}{Ewt}\sqrt{\left(\frac{Y}{t^2}\right)^2 + \left(\frac{X}{w^2}\right)^2} - D_0$$

Dakota enhances code and application PCMM

VUQ Analysis of Cobra-TF for Progression Problem 6

- Simulation of a single PWR assembly
  - Hot Full Power, T/H feedback
  - Boron concentration of 1300 ppm, 100% power
  - Power supplied by neutronics held constant

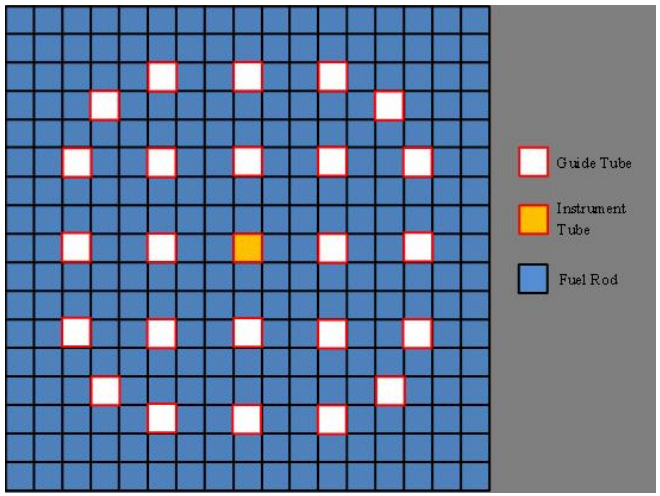

- Two CASL VUQ workflows support Cobra-TF parameter variation
  - Dakota integration with VERA common input tool suite
  - Dakota perturbation of "VUQ parameters" associated with closure laws
- Dakota studies illustrate application of VUQ methodologies described in the manual
  - 33 "VUQ parameters" exposed to Dakota for perturbation
  - Quantity of Interest: Total pressure drop through fuel rod assembly

Dakota studies illustrated with worked examples for Cobra-TF

Cobra-TF Parameter Exposure

with Noel Belcourt

For general parameter perturbations:

$$\alpha = k_\alpha \alpha_0 + s_\alpha$$

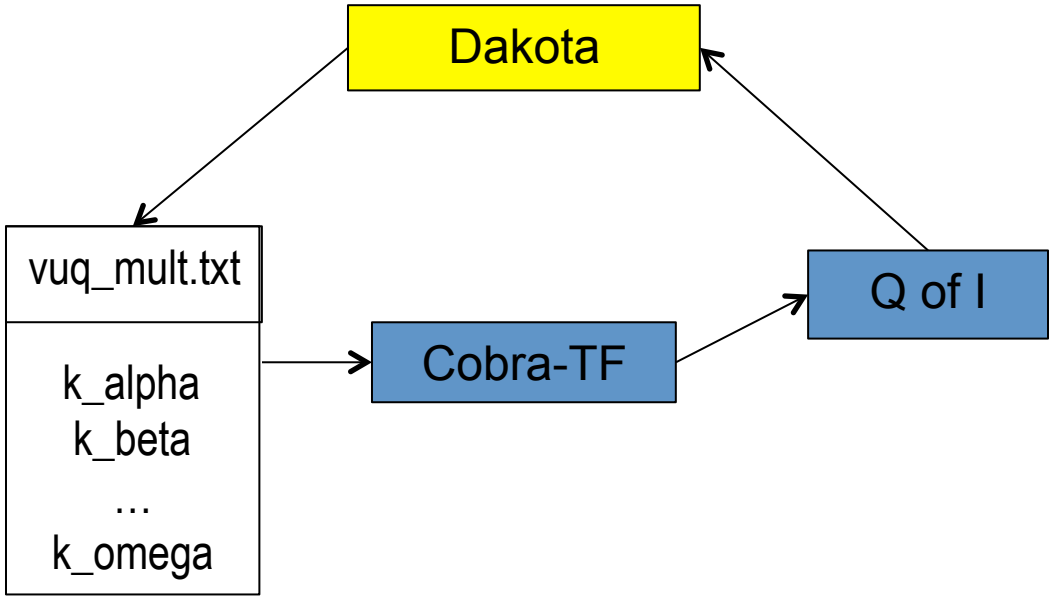

This capability enables:

- Sensitivity studies
- Uncertainty Quantification studies
- Parameter optimization and calibration

Exposure of CTF input parameters enables VUQ analysis

Dakota Sensitivity Analysis

- Overview of sensitivity analysis goals, terminology, and metrics
- Details on basic centered and tensor grid parameter studies; analysts typically conduct them anyway
- Emphasized global Latin hypercube sampling and Morris designs:
  - Sample paths around global space in coordinate directions
  - Give good measure of main (linear, first-order) and interaction / nonlinear effects for modest simulation budget

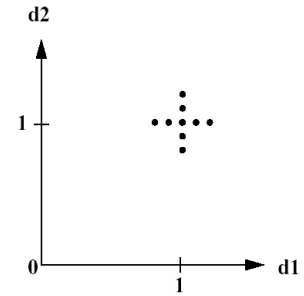

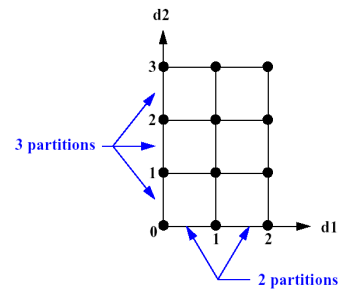

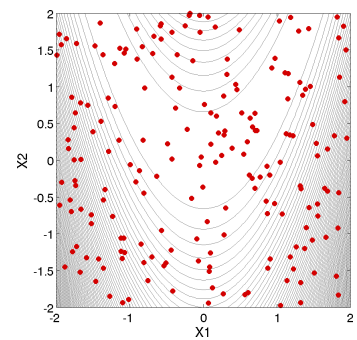

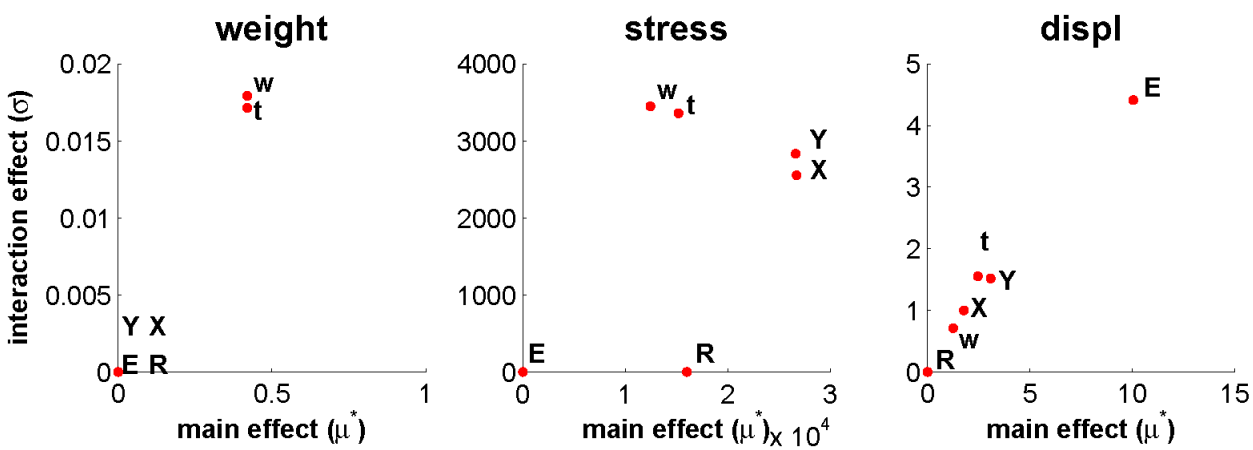

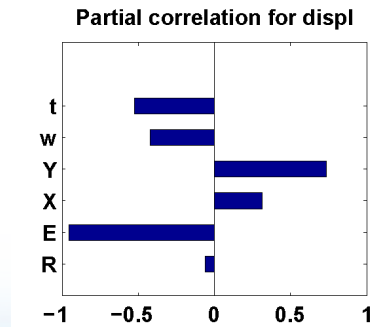

Dakota facilitates discovery of input parameter effects

Dakota Optimization and Calibration

- Survey of optimization goals and problem formulations, including considerations for calibration to experimental data
- Emphasized one each gradient-based, derivative-free local, and global algorithm and how to select from among them

$$
\begin{aligned}
\texttt{minimize} \quad & \texttt{area} = wt \\
\texttt{subject to} \quad & \texttt{stress} = S - R \leq 0 \\
& \texttt{displacement} = D - D_0 \leq 0 \\
& 1.0 \leq w \leq 4.0 \\
& 1.0 \leq t \leq 4.0
\end{aligned}
$$

```
<<<<< Function evaluation summary: 18 total (18 new, 0 duplicate)
<<<<< Best parameters          =
                     2.4000000000e+00 w
                     3.5000000000e+00 t
                     4.0000000000e+04 R
                     2.9000000000e+07 E
                     5.0000000000e+02 X
                     1.0000000000e+03 Y
<<<<< Best objective function  =
                     8.4000000000e+00
<<<<< Best constraint values   =
                    -4.7108843537e+03
                    -2.9685051703e-01
```

Table 5.1: Guidance for selecting from the top recommended Dakota optimization algorithms.

algorithm type / Dakota method	variable type	cost (samples)	goal and characteristics
gradient-based local/ OPT++ Quasi-Newton	continuous	low/ medium	single local solution/improvement, assumes smooth input/output mapping
local calibration / OPT++ Gauss Newton	continuous	low/ medium	same as previous line, but tailored to least-squares calibration
derivative-free local / Coliny Pattern Search	continuous	medium/ high	single local solution; better when can't estimate derivatives
local w/surrogate / Surrogate-based Local	continuous	medium	same as "derivative-free local," but for noisier or more expensive simulations
global / Coliny Evolutionary Algorithm	continuous or discrete	high	global optimality, with ranked family of best solutions
global w/surrogate / Efficient Global	continuous	medium	same as "global," but for more expensive simulations

Dakota offers multiple code optimization/calibration options

Guidance on Navigating All Dakota Methods

- Sensitivity Analysis

Table 3.2: Guidelines for selection of parameter study, DOE, DACE, and sampling methods.

Method Classification	Applications	Applicable Methods
parameter study	sensitivity analysis, directed parameter space investigations	centered_parameter_study, list_parameter_study, multidim_parameter_study, vector_parameter_study
classical design of experiments	physical experiments (parameters uniformly distributed)	dace (box_behnken, central_composite)
design of computer experiments	variance analysis, space filling designs (parameters uniformly distributed)	dace (grid, random, oas, lhs, oa_lhs), fsu_quasi_mc (halton, hammersley), fsu_cvt, psuade_moat
sampling	space filling designs (parameters have general probability distributions)	sampling (Monte Carlo, LHS) with optional active view override

- Optimization

Table 5.2: Detailed guidelines for selecting from among all Dakota optimization methods. Blank fields inherit the values from above.

Method Classification	Desired Problem Characteristics	Applicable Methods
Gradient-Based Local	smooth; continuous variables no constraints	optpp_cg
	smooth; continuous variables; bound constraints	dot_bfgs, dot_frcg, conmin_frcg
	smooth; continuous variables; bound constraints, linear and nonlinear constraints	npsol_sqp, nlpql_sqp, dot_mmfd, dot_slp, dot_sqp, conmin_mfd, optpp_newton, optpp_q_newton, optpp_fd_newton, weighted sums (multiobjective), pareto_set strategy (multiobjective)
Gradient-Based Global	smooth; continuous variables; bound constraints, linear and nonlinear constraints	hybrid_strategy, multi_start strategy
Derivative-Free Local	nonsmooth; continuous variables; bound constraints	optpp_pds
	nonsmooth; continuous variables; bound constraints, linear and nonlinear constraints	asynch_pattern_search, coliny_cobyla, coliny_pattern_search, coliny_solis_wets, surrogate_based_local
	nonsmooth; continuous variables; discrete variables; bound constraints, nonlinear constraints	mesh_adaptive_search
Derivative-Free Global	nonsmooth; continuous variables; bound constraints	ncsu_direct
	nonsmooth; continuous variables; bound constraints, linear and nonlinear constraints	coliny_direct, efficient_global, surrogate_based_global
	nonsmooth; continuous variables, discrete variables; bound constraints, linear and nonlinear constraints	coliny_ea, soga, moga (multiobjective)

Explicit recommendations provided for choosing covered methods

Mathematical Surrogate Construction

Steps:

1. Run a simulation experiment to collect figures of merit at designed input parameter locations.
2. Fit polynomial or kriging surrogate model to experiment results and utilize in follow-on analyses.

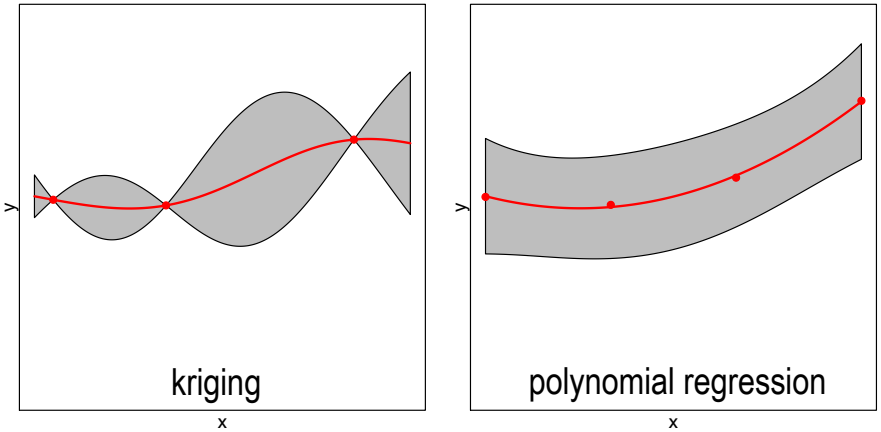

Motivation:

- Enables VUQ analyses when code calculations are time consuming and no computationally efficient physics-based surrogate is readily available.

Method	Desired Problem Characteristics	Routines
Polynomial regression	Smooth fit to physical experiment or stochastic/noisy code response	polynomial <trend>
Kriging	Interpolation of deterministic smooth code response or smooth fit to stochastic/noisy code response	gaussian_process surfpack trend <option> nugget <value> find_nugget

Surrogate model motivation and process

Uncertainty Quantification

Steps:

1. Quantify input uncertainties associated with parameters, initial and boundary conditions, or exogenous forces.
2. Propagate input uncertainties through models to construct prediction interval for quantity of interest.

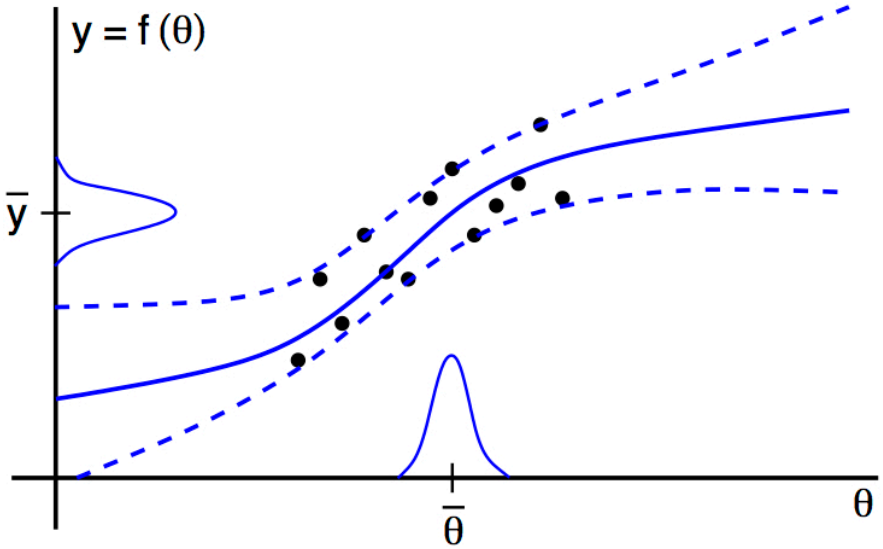

Motivation:

- Facilitate optimal design and decision making, ensure robustness, performance or safety margins.
- E.g., outputs for emergency core cooling systems include peak cladding temperatures, maximum local cladding oxidation.

Uncertainty quantification motivation and process

Uncertainty Propagation in Dakota

Method	Desired Problem Characteristics	Routines
Sampling	Nonsmooth and/or multi-modal response functions; general densities; computationally efficient models or surrogates	sampling
Stochastic Polynomial	Smooth response functions; can be combined with Dakota sparse grid routines	polynomial_chaos stoch_collocation

Representation:

$$Y(X) = \sum_{j=0}^{J} \alpha_j \Psi_j(X)$$

Example: Cantilever beam – Normally distributed input parameters, stress response

	Mean	Std. Dev.	Skewness	Kurtosis
Analytic	1.760e+04	5.787e+03	---	---
Sampling	1.735e+04	5.809e+03	-6.505e-03	7.352e-02
PCE	1.760e+04	5.787e+03	9.410e-15	6.271e-15
Collocation	1.760e+04	5.787e+03	-1.842e-14	5.773e-15

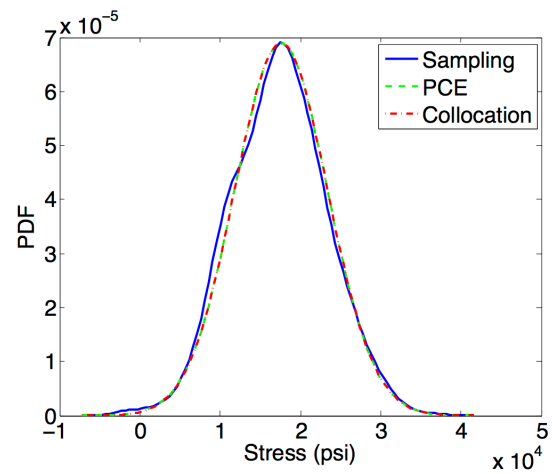

Multiple methods used to verify Dakota propagation routines

Bayesian Model Calibration

Bayes' Relation:

$$\pi(\theta|d) = \frac{\mathcal{L}(\theta;d)\pi_0(\theta)}{\int_{\Re^M} \mathcal{L}(\theta;d)\pi_0(\theta)d\theta}$$

Likelihood: Incorporates model and data

$$\mathcal{L}(\theta;d) \prod_{i=1}^{N} \frac{1}{\sigma\sqrt{2\pi}} e^{-(d_i - y_i(\theta))^2/2\sigma^2}$$

Method	Problem Characteristics
DRAM	Well-behaved posterior densities; computationally efficient models or surrogates
DREAM	Complex posteriors; inherently parallel codes
GPMSA	Employs Gaussian process emulator; can accommodate certain model discrepancies

Example: COBRA-TF parameters k_tmasl, k_tmoml, k_tnrgl, k_xkwlx, k_cd

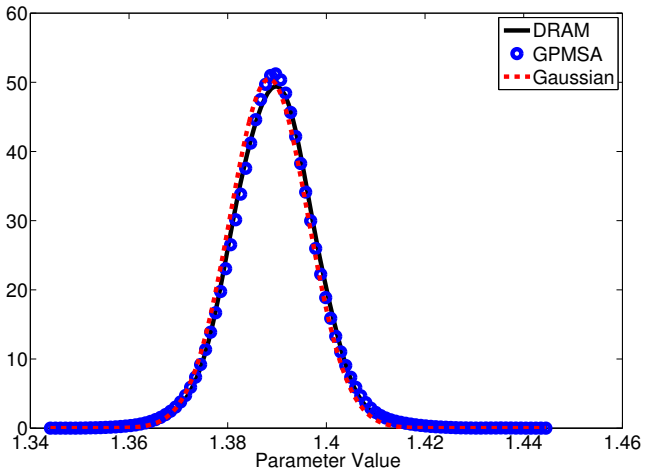

$$\eta = 0.906\,\mathtt{k_xkwlx} + 0.478\,\mathtt{k_cd}$$

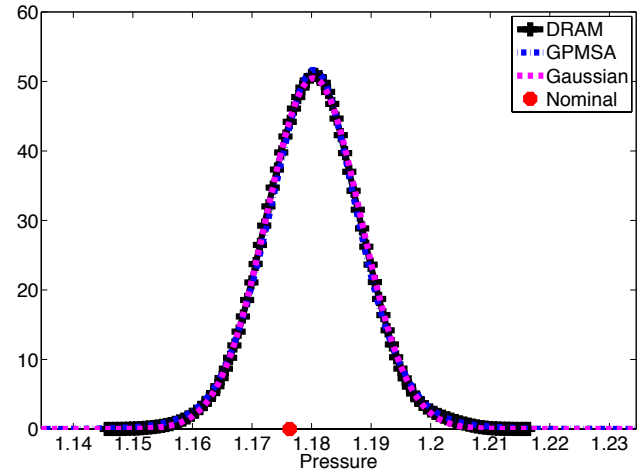

Output UQ via GP surrogate with inputs from DRAM chain

Parameter uncertainty quantified by experimental data

Linear Verification Test Suite

Objective:

- Provide hierarchy of models to test convergence of Bayesian model calibration algorithms through comparison with analytic solutions;
- Provide regime to test accuracy of uncertainty propagation algorithms since one can employ analytic relations between input and output densities;
- Facilitate the testing of algorithms for heavy-tailed distributions;
- Provide framework for analytically testing algorithms to construct Sobol global sensitivity indices.

Example: Histograms of β converging to Dirac density as number of samples N is increased.

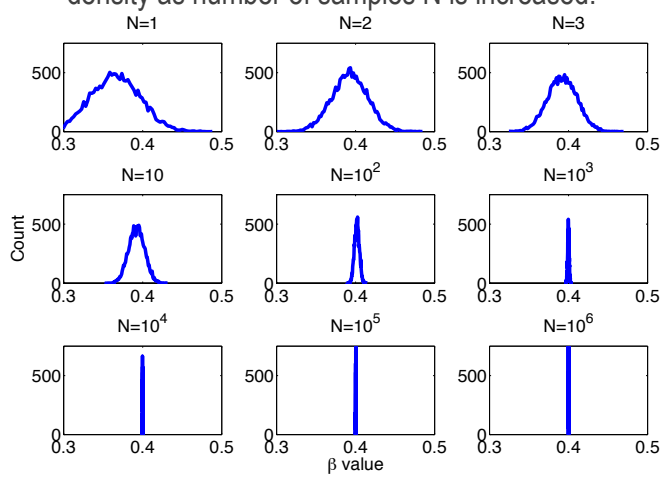

Linear Regression Model:

$$Y = G\beta + \varepsilon(\lambda, \phi)$$

Example: PDF estimates of β and λ from Bayesian calibration vs. analytical solutions.

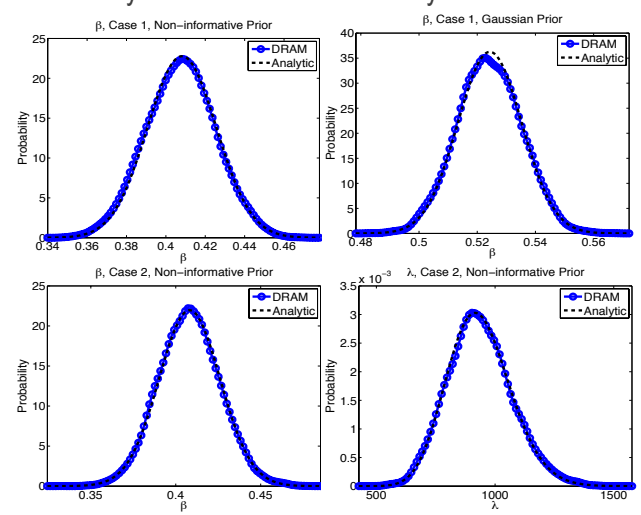

"Code"/solution verification of Bayesian calibration methods

Cobra-TF Solution Verification

Progression Problem 6 CTF-only

- Initial study produced very good agreement with theoretical expectation (b=0.946 compared to 1.0)
- Problem 6 involves spacer grids of unequal spacing (top & bottom different than interior) requiring meshes characterized by multiple Δz values
- Attempts to lump these into a singe Δz produced poor orders-of-convergence, eg ~0.7 (see report)
- A sensitivity study of total pressure drop on spacer grid locations showed low sensitivity, < 0.2%
- Spacer grid locations were shifted to produce meshes characterized by a single Δz, and the solution verification study was repeated

Axial mesh refinement convergence studies for CTF

Cobra-TF Solution Verification

Progression Problem 6 CTF-only: No Spacer Grids

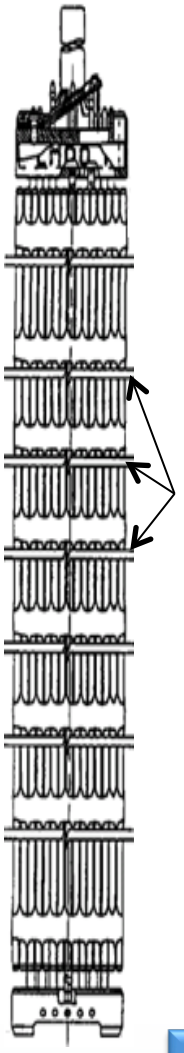

CTF-only Problem 6, No Grids			
Mesh factor, f	Δz (cm)	#Axial elements	Tot. Press. (bar)
0.5	4.160	87	0.68788
0.75	6.240	58	0.68759
1.0	8.225	44	0.68731
1.5	12.479	29	0.68673
2.0	16.450	22	0.68620

Error Model:

$$P = \bar{P} + a\,(\Delta z)^b$$

$$E = P - \bar{P} = a\,(\Delta z)^b$$

$$b = 0.946$$

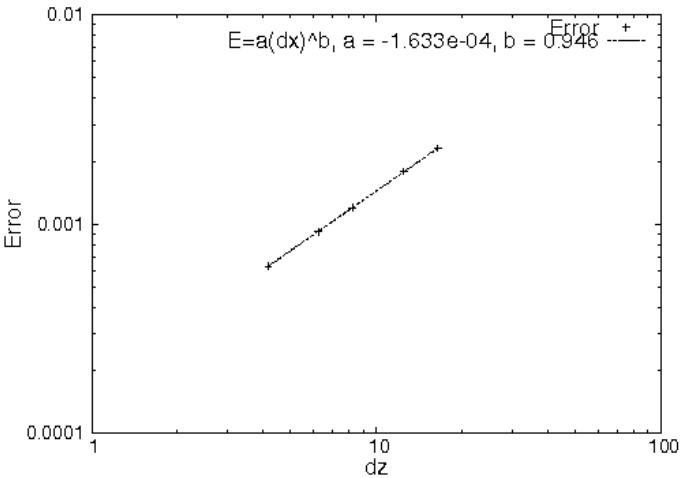

Good agreement with theoretical 1.0

Estimated and theoretical rates consistent: no spacer grids

Cobra-TF Solution Verification

Progression Problem 6 CTF-only: With Spacer Grids*

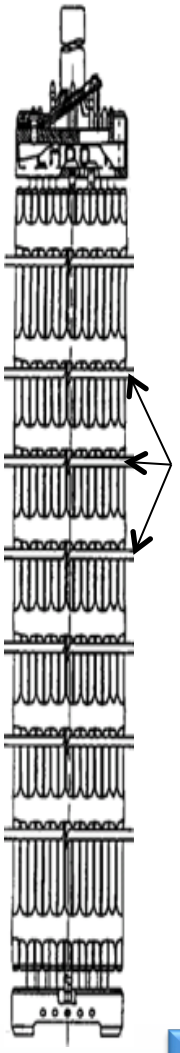

CTF-only Problem 6, With Grids*			
Mesh factor, f	Δz (cm)	#Axial elements	Tot. Press. (bar)
0.5	4.036	72	1.16843
0.75	6.054	48	1.1701
1.0	8.072	36	1.17176
1.5	12.108	24	1.17508
2.0	16.144	18	1.17845

* Grid locations were shifted to produce equal mesh spacing between all grids.

Error Model:

$$E = P - \bar{P} = a\,(\Delta z)^b$$

$$b = 1.012$$

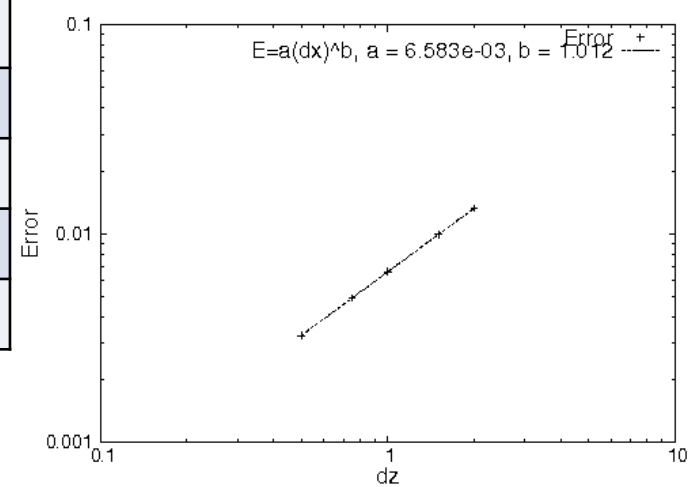

Good agreement with theoretical 1.0

Estimated and theoretical rates consistent with spacer grids

Cobra-TF Sensitivity Analysis

parameter	partial correlation	simple correlation	morris main	morris interaction	CPS variation
k_eta	0.07	0.03			
k_gama	-0.03	0.04			
k_sent	-0.03	-0.02			
k_sdent	-0.07	-0.01			
k_tmasv	-0.03	0.00			
k_tmasl	0.11	0.00	6.48E-05	2.28E-05	medium
k_tmasg	-0.19	-0.01			
k_tmomv	-0.12	-0.01			
k_tmome	0.02	0.00			
k_tmoml	0.02	-0.02	2.23E-04	1.30E-04	medium
k_xk	0.08	-0.02			
k_xkes	-0.05	0.00			
k_xkge	-0.07	0.01			
k_xkl	0.04	-0.01			
k_xkle	-0.03	0.00			
k_xkvls	0.11	-0.01			
k_xkwvw	-0.10	0.01			
k_xkwlw	0.14	0.01			
k_xkwew	-0.01	0.03			
k_qvapl	-0.09	-0.01			
k_tnrgv	-0.03	0.00			
k_tnrgl	-0.01	0.03	9.00E-06	9.49E-06	low
k_rodqq	0.02	-0.01			
k_qradd	-0.02	0.00			
k_qradv	-0.01	0.00			
k_qliht	-0.01	0.00			
k_sphts	-0.05	0.03			
k_cond	-0.04	0.00			
k_xkwvx	0.03	-0.02			
k_xkwlx	1.00	0.88	1.80E-01	7.07E-03	high
k_cd	1.00	0.46	9.59E-02	7.88E-03	high
k_cdfb	-0.02	-0.01			
k_wkr	0.02	0.02			

5 Active Inputs:

`k_cd` : Pressure loss coefficient of spacer in sub-channel

`k_xkwlx` : Vertical liquid wall drag coefficient

`k_tmasl` : Loss of liquid mass due to mixing and void drift

`k_tmoml` : Loss of liquid momentum due to mixing and void drift

`k_tnrgl` : Loss of liquid enthalpy due to mixing and void drift

33 initial VUQ parameters reduced to 5 via sensitivity analysis

Cobra-TF Mathematical Surrogate Construction

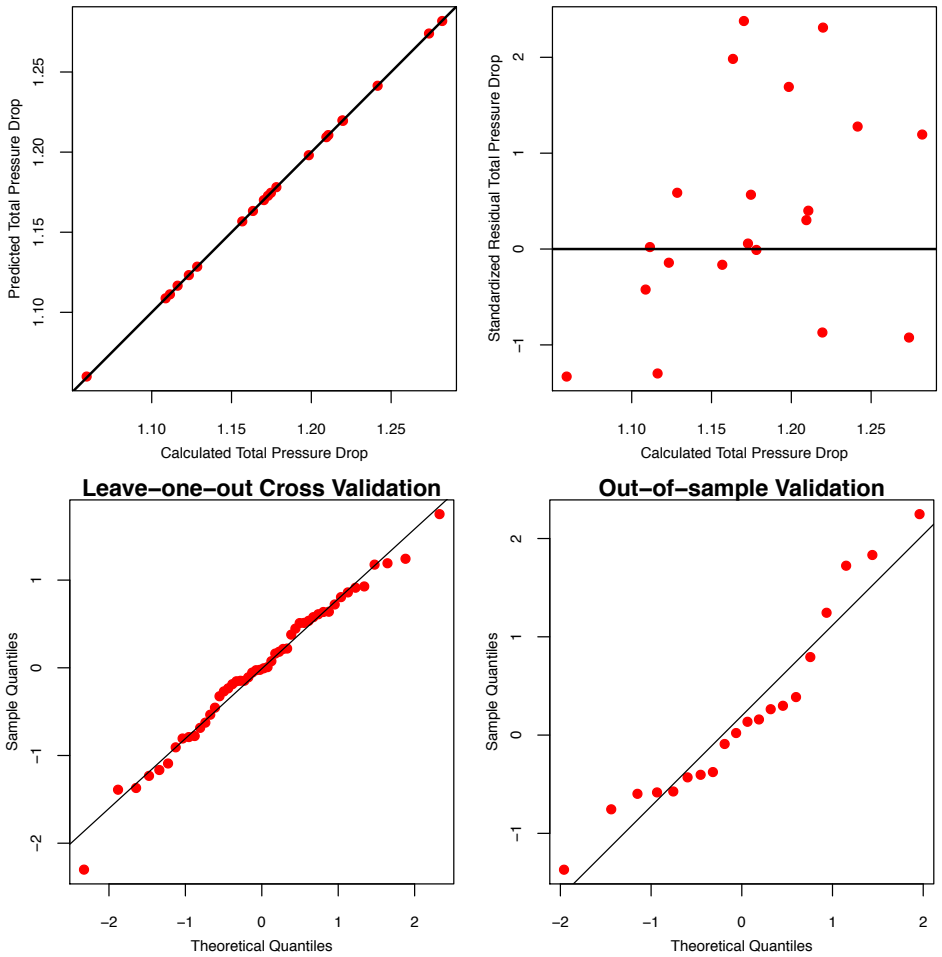

Kriging surrogate for total pressure drop using 50 Cobra-TF runs perturbing 5 active inputs

Examine the quality of surrogate fits via diagnostics post-processed from Dakota output

LOO CV RMSPE: 3.24E-4 (0.15% of observed range in pressure drop)

Validation (N_V = 20) RMSPE: 2.51E-4 (0.11% of observed range in pressure drop)

Mathematical surrogates are used for fast computation

Cobra-TF Model Calibration

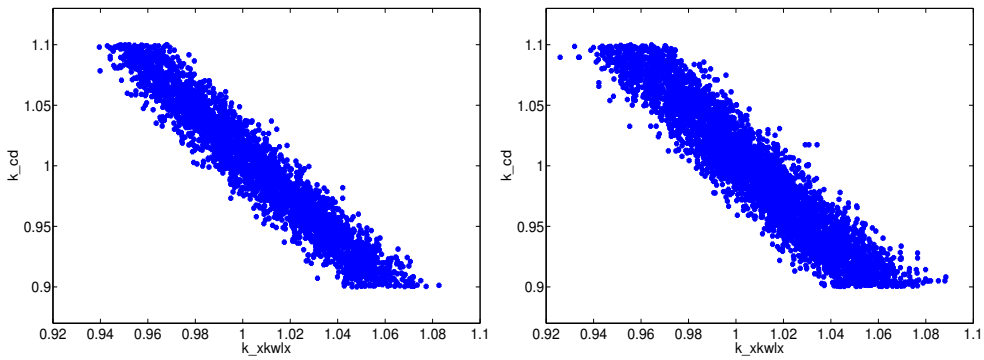

Synthetic experimental data generated by adding Gaussian noise to Cobra-TF total pressure drop value at nominal parameter setting.

Calibrated parameter samples from two calibration methods (DREAM, GPMSA) for `k_xkwlx` vs. `k_cd`.

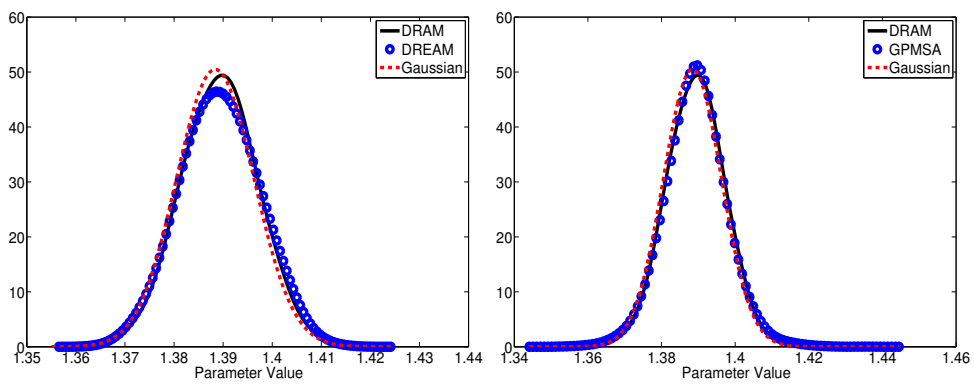

$$\eta = 0.906\,\mathtt{k_xkwlx} + 0.478\,\mathtt{k_cd}$$

Verification of three Bayesian model calibration methods (DRAM, DREAM, GPMSA) applied to kriging surrogate for Cobra-TF total pressure drop. Calibrated parameter η is approximately analytically Gaussian.

Model calibration results in input parameter UQ consistent with data

Conclusions

- Manual provides an overview of core VUQ methods expected to receive heavy use in CASL applications
- Manual provides representative Dakota input decks for the core VUQ methods with worked examples of their deployment
- Manual provides references to other Dakota manuals having more extensive discussions of methods and deployment
- Manual began development of more extensive “stochastic verification” test suite to verify performance of Bayesian model calibration methods
- Collaboration on this manual has revealed the need for targeted Dakota development projects, particularly in the areas of Bayesian model calibration and interfacing reduced order modeling techniques
- Code/solution verification methods (e.g. RMR) and validation metric computation through Percept are/will be integrated into Dakota

Continued Dakota development supports CASL-relevant VUQ analysis

Dakota Capabilities Update
2014 CASL Round Table

Brian Adams

Maria Avramova
Noel Belcourt
Mike Doster
Russell Hooper
Kostadin Ivanov
Vince Mousseau
Ralph Smith
Laura Swiler
Brian Williams

Outline

- Reminder: What is Dakota?
- Dakota capability updates in versions 5.4 and 6.0
- Dakota in CASL, current and future
- Recent Progression Problem 6 results

Dakota Supports Simulation Credibility

- Provides broader and deeper perspective for analysts and decision makers
  - *Enhances understanding of risk by quantifying margins and uncertainties (QMU)*
  - *Improves products through simulation-based design*
  - *Assesses simulation credibility through verification and validation*
- Enables QMU and design with simulations in manner analogous to experiment-based QMU and physical design/test cycles

Manages and analyzes ensembles of simulations:

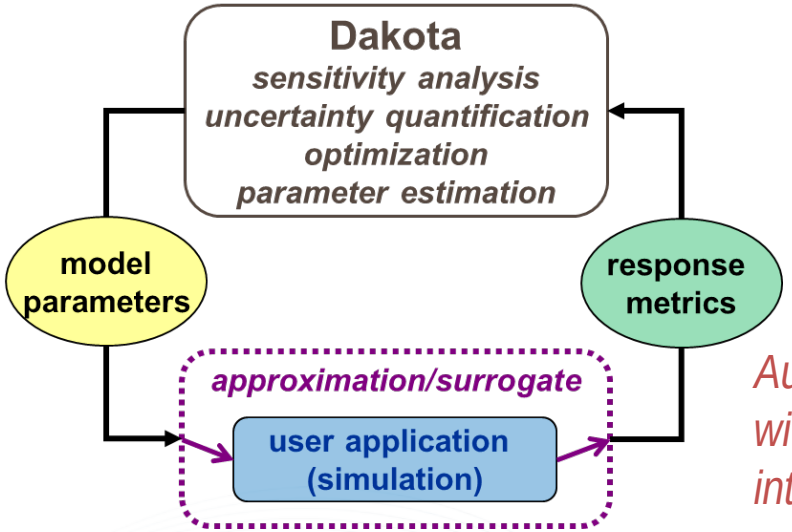

Automate typical "parameter variation" studies with various advanced methods and a generic interface to your simulation.

Dakota tailors code iterations to efficiently solve VUQ problems

Advanced Exploration of Simulations

Dakota enriches simulations to address analyst/designer questions:

- Which are crucial factors/parameters, how do they affect key metrics? *(sensitivity)*
- How safe, reliable, robust, or variable is my system? *(quantification of margins and uncertainty: QMU, UQ)*
- What is the best performing design or control? *(optimization)*
- What models and parameters best match experimental data? *(calibration)*

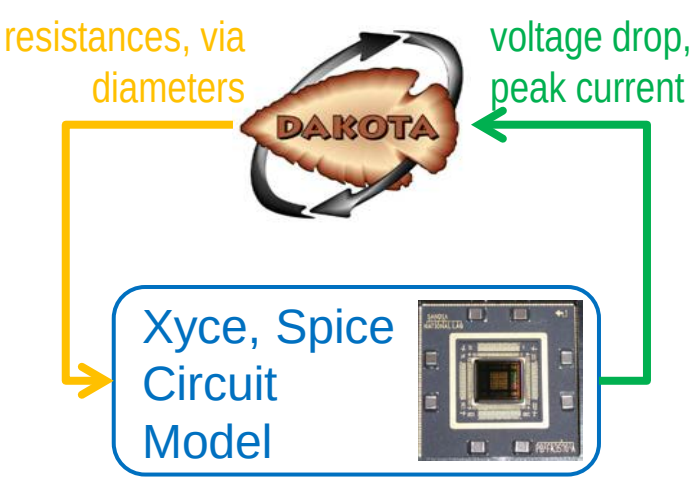

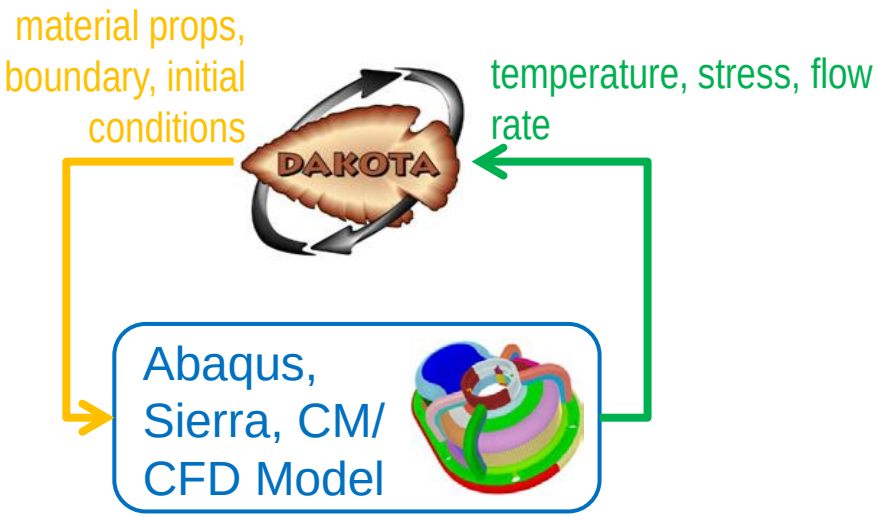

All based on iterative analysis of a computational model for phenomena of interest

- Commercial or SNL, loose-coupled/black-box or embedded/tightly integrated…

Dakota supports multiple interfaces for code interactions

Reminder of Current Dakota Capabilities
CASL: used, underutilized, unused

- Parameter studies for basic exploration
- Global sensitivity analysis for parameter ranking/screening
- Design of experiments (supporting SA and surrogate builds)
- Calibration: deterministic and Bayesian
- Optimization: local and global

- Automated surrogate (response surface model) construction
- Tailored surrogated-based versions of methods above
- Non-deterministic analysis, e.g., reliability-based design
- Epistemic uncertainty methods

Recent Algorithm Capabilities
Dakota 5.4 (Nov 2013); Dakota 6.0 (May 2014)

- Stochastic expansion UQ: improvements to multi-fidelity, compressive sensing, and orthogonal least interpolation; extension to higher dimension
- Reliability (failure detection) methods: new PoFDarts, generalization of adaptive importance sampling
- Generalization of mixed epistemic/aleatory UQ methods
- New NOMAD mixed integer and OptDARTS for optimization
- Bayesian calibration: updated QUESO method, new DREAM
- Surrogate diagnostics and cross-validation

Recent Core Capabilities

Dakota 5.4 (Nov 2013); Dakota 6.0 (May 2014)

- Data import/export improvements: surrogate models, PCE, parameter studies
- Native Windows builds
- New reference manual format
- Improved parallel configuration management
- Overhauled library API
- Performance improvements to scale UQ and surrogate methods

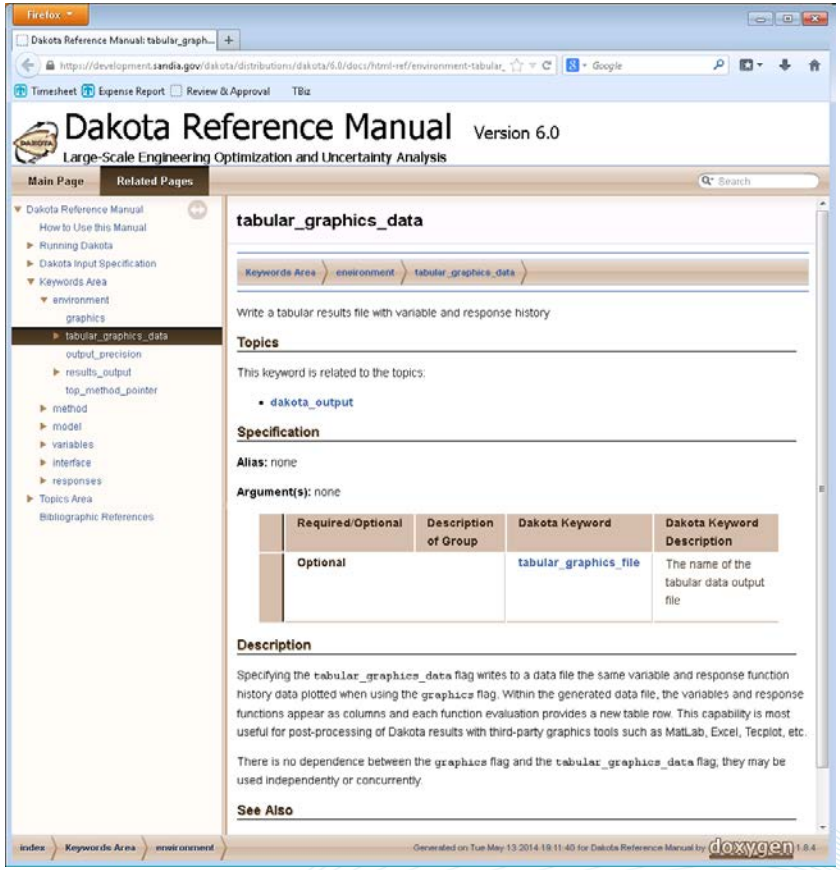

Goals for Dakota use in CASL

- Encourage broader adoption among domain experts: apply existing capabilities that are ready to go
- Automate V&V/UQ workflows to
  - Maintain V&V pedigree during code development cycles
  - Produce evidence for PCMM
- Improve Dakota tutorials, automation, and usability to lower the bar for V&V/UQ
- Improve methods in Dakota to increase rigor and accuracy, especially of verification and calibration studies

Dakota Status in VERA

- Dakota synced from SNL to CASL and builds/tests in VERA to protect integration investment
- Examples in VUQDemos archive previous milestone studies, Dakota manual examples, and test against development physics code inputs
- Focusing on automated, reproducible, validating loost coupled workflows since there isn't a single coupled physics driver in VERA
- Demonstrating more advanced methods

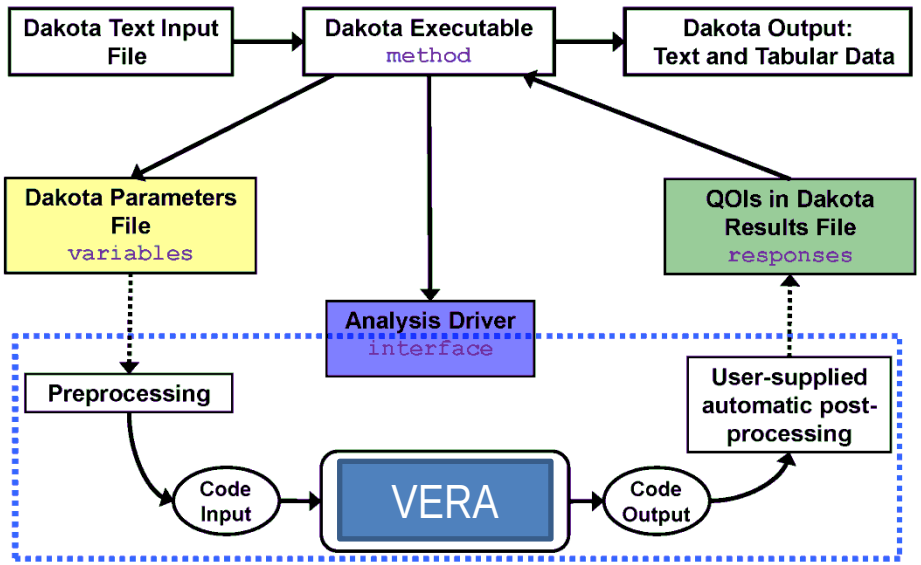

- Manipulate parameters in:
  - VERA Input
  - VUQ auxiliary data, e.g., model form
  - Offline generated input data such as meshes or cross sections
- Continual improvement of QOI extraction

Dakota enables core VUQ analyses in CASL

Recent Work Supporting Progression Problem 6

- Jointly estimated parameter distributions for Dittus-Boelter yield different uncertainty predictions
- Demonstrates use of advanced Bayesian calibration methods
- Emphasizes need for more integrated workflows across Dakota studies
- Shows effect of neutronics cross section and thermal hydraulic model parameter uncertainty on coupled physics

VUQ Analysis of Cobra-TF for Progression Problem 6

- Simulation of a single PWR assembly
  - Hot Full Power, T/H feedback
  - Boron concentration of 1300 ppm, 100% power
  - Power supplied by neutronics held constant
- CASL VUQ workflows based on Cobra-TF

  Dittus Bolter parameter variation
- Quantity of Interest is maximum fuel temperature
- Results are based on random samples of the parameter distributions.
- A 95% credible interval is calculated

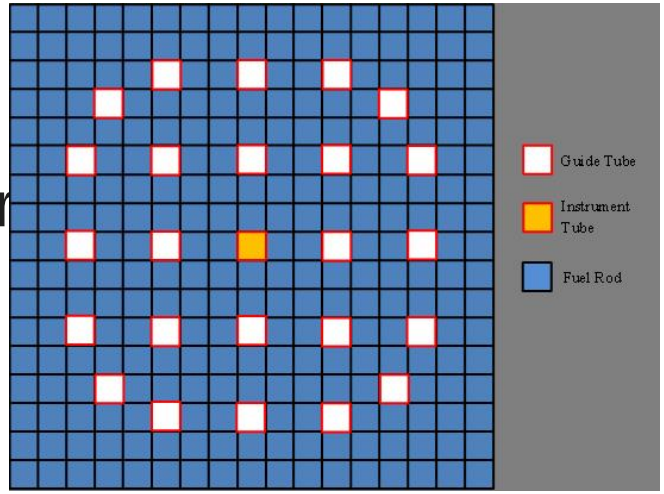

Dittus Boelter Uncertainty Quantification

$$Nu = 0.023\,\mathrm{Re}^{0.8}\,\mathrm{Pr}^{0.4} = \theta_1\,\mathrm{Re}^{\theta_2}\,\mathrm{Pr}^{\theta_3}$$

- We have three parameters, lead coefficient, θ_1, Reynolds exponent, θ_2, Prandlt exponent, θ_3.
- The challenge is to determine the parameter distribution for these three parameters.
- We will initially use "expert opinion" to say

$$\theta_1 \in [0.0, 0.046]$$

$$\theta_2 \in [0.0, 1.6]$$

$$\theta_3 \in [0.0, 0.8]$$

- We then assume a uniform distribution and do 93 samples to get a 95%-95% confidence interval from Wilks Formula.

Bayesian Calibration with One Experiment

- Morris and Whitman, "Heat Transfer for Oils and Water in Pipes," *Industrial and Engineering Chemistry*, Vol. 20, No. 3, pp.234-240, 1928. (1 of 13 Dittus-Boelter data sets)
- Use DRAM Bayesian calibration as in Dakota's QUESO
- Update from expert prior yields marginal distributions of

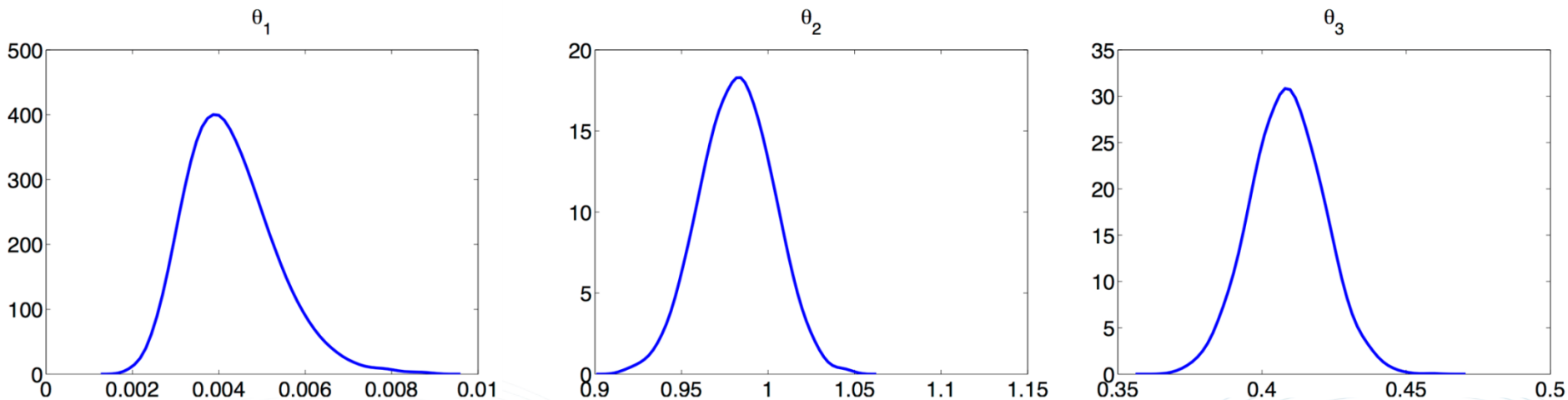

lower than 0.023 *higher than 0.8* *slightly higher than 0.4*

Bayesian Inference also Exposes Joint Distribution of Parameters

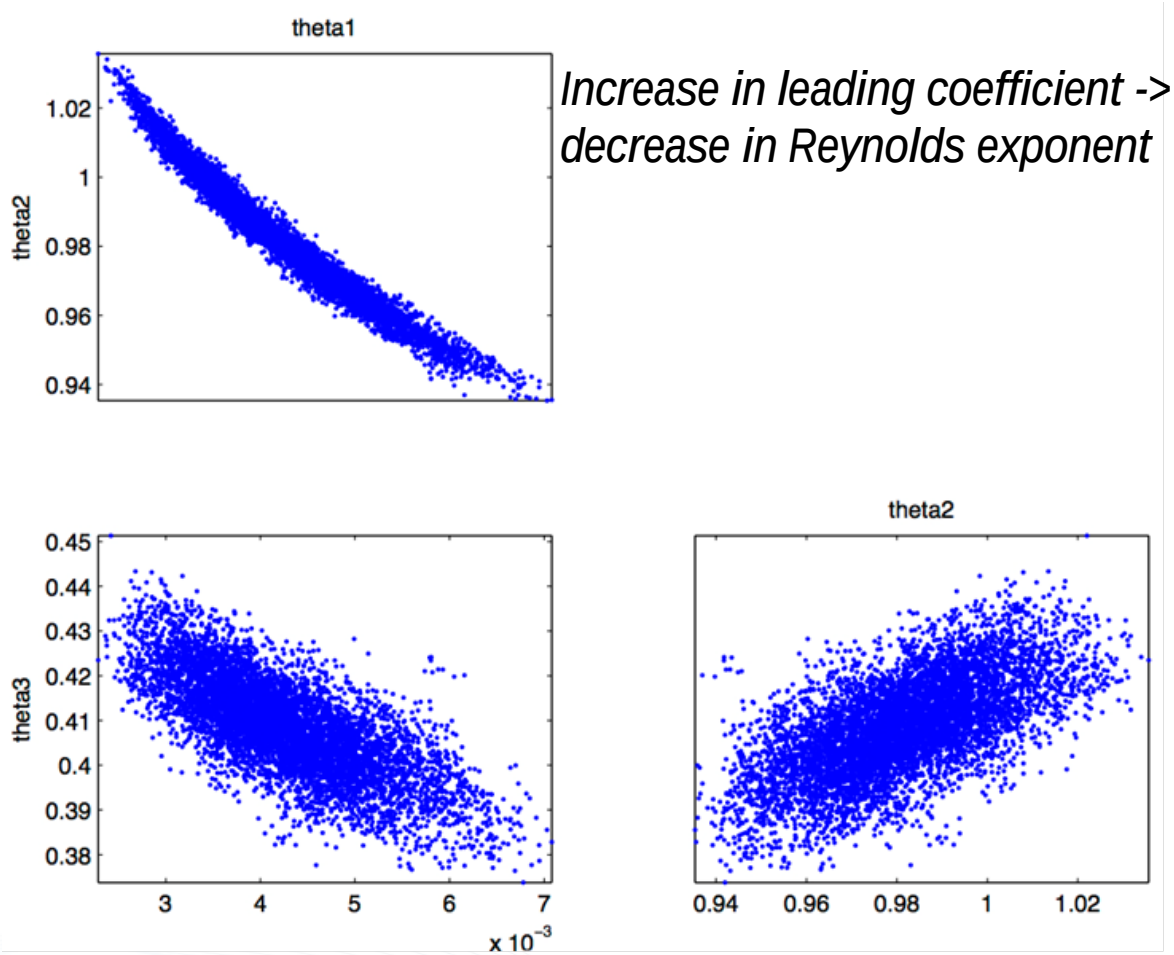

Increase in leading coefficient -> decrease in Reynolds exponent

Data-informed Joint Distributions Reduce Predicted Uncertainty

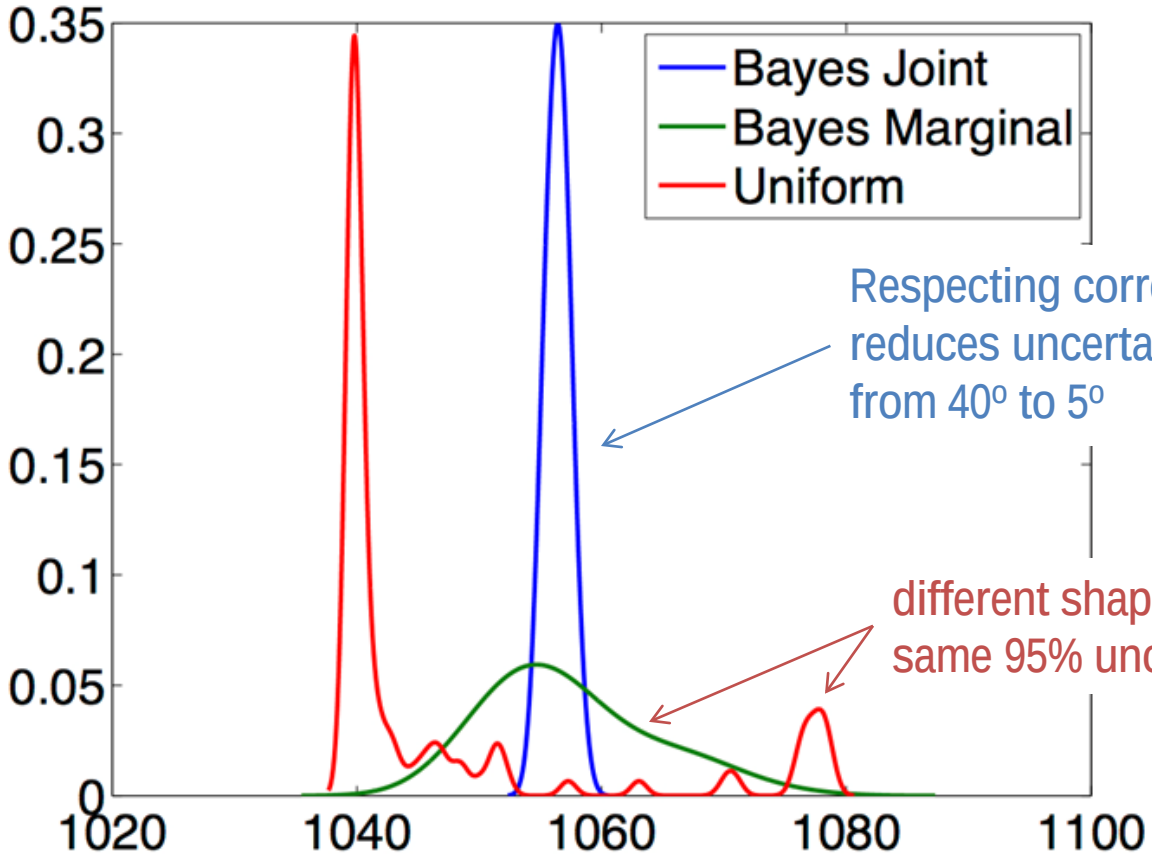

Respecting correlation reduces uncertainty from 40º to 5º

different shape; roughly same 95% uncertainty range

Preliminary Results for Coupled Neutronics/Thermal-Hydraulics Studies

- Uncertainties in Dittus-Boelter and McAdams parameters inferred from data with Bayesian calibration
- Neutronics sampled from 100 cross section libraries (courtesy Abdel-Khalik)

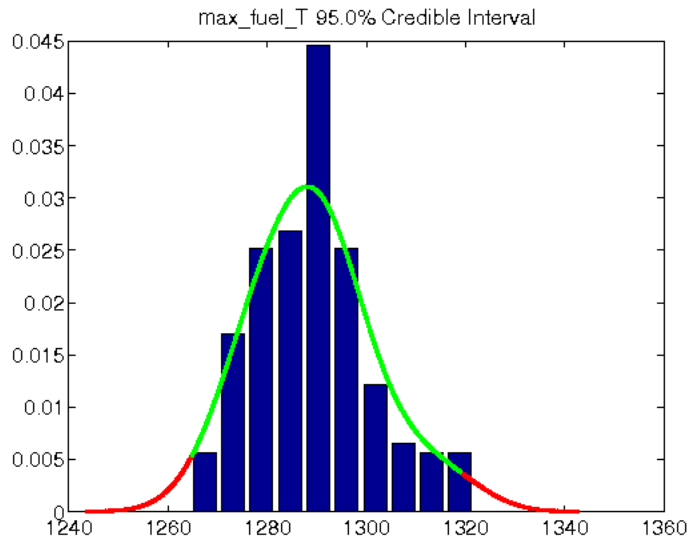

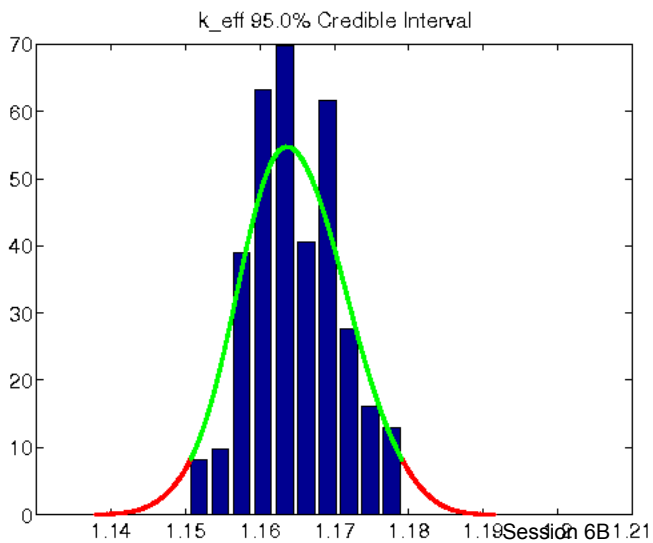

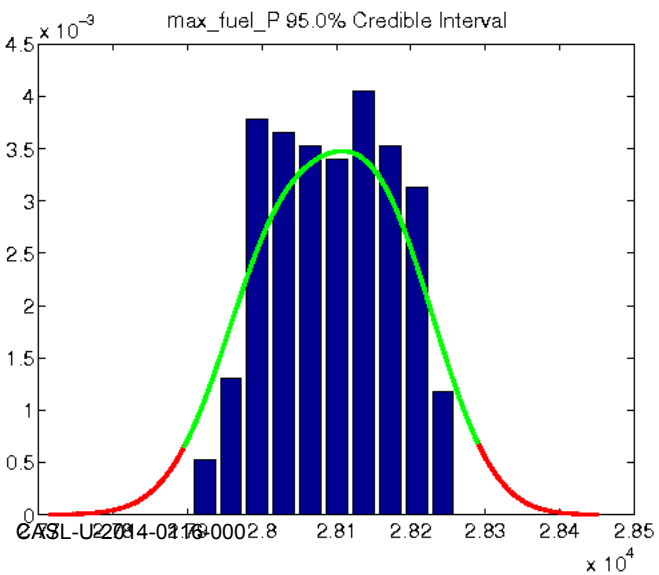

Goal: More fully utilize available Dakota features

Already some success in demonstrating:

- Sensitivity, calibration, and uncertainty studies

Progress toward:

- Use Dakota to adaptively determine where to best place code calculations; can inform physical experiments
  (Dakota may need methods for optimal experimental design)
- Integrated Dakota/Robust Method of Regression
- Calibration: use high-fidelity simulations to calibrate low
- *CASL practitioners using Dakota studies as matter of course*

Example: RMR for Dakota-automated verification

- Goal: Dakota evaluates model in batches, sampling over numerical parameters, e.g., mesh resolution, until convergence in predicted mesh-converged QOI.
- Integrate Rider robust method of regression (RMR)
  - Use ideas from compressive sensing to improve RMR (automatically select best regression bases and model forms)
  - Use optimization methods tailored to norm and basis
  - Improve estimates of uncertainty in converged solution
- Develop uncertainty methods to jointly consider parametric and numerical uncertainty factors in same study; goal: total uncertainty

Example: Why do we need automated workflows?

- Use Case: Dittus-Bolter calibration with COBRA-TF required human-in-the-loop workflow:
  - Process experimental data into right form and units
  - Setup Dakota workflow to execute simulation at all conditions needed to match data
  - Perform Dakota Bayesian calibration study to estimate joint distribution of model parameters
  - Post-process the posterior chains to get correlated and uncorrelated empirical samples for use in UQ
  - Conduct Dakota UQ studies and demonstrate reduced uncertainty when using joint distribution information

- Currently requires considerable interactive work by VUQ practitioners (e.g., Ralph, Brian, Russell)

Goal: Make Dakota more amenable to automated workflows

- Desire automated PCMM results generation: code developers can readily run V&V, UQ studies during development to improve code pedigree
- Need workflows to combine Dakota studies:
  - Well-defined input/output interfaces; flow results one to the other
  - Make Dakota more modular and scriptable to facilitate this; drive Dakota itself via a Python workflow
- Need automated post-processing of Bayesian studies and even classical Dakota studies

- Longer term: flow data to/from NE-KAMS

Goal: Make Dakota more usable in CASL

- Documentation
  - Continue to refine documentation to make best practices and workflows clear and recipe-oriented
- Worked examples
  - Increase number of CASL-relevant worked application examples
  - Protect challenge problem work with Dakota in tests
- Graphical user interface
  - Wizards/recipes to guide users through the best practices from documentation
  - Help navigate Dakota complexity
  - Provide basic visualization to help interpret Dakota results

Goal: Bayesian calibration improvements

Mature Dakota/QUESO Bayesian calibration capability

- Incorporate from UT Austin as available, including GPMSA
- Add more flexible user options for configuring studies (priors, proposal covariance, etc.)
- Output of prediction errors, intervals
- Consistent use of surrogates across Bayesian methods
- Bayesian algorithmic and interface improvements; usability and consistency of methods

Other planned Dakota developments (some CASL, some leveraged)

- Automatic surrogate quality diagnostics and prediction uncertainty
- Tolerance intervals and Wilk's methods
- Direct treatment of functional simulation and experimental data
- Improved black box simulation management
- More methods to treat discrete factors; helpful for verification studies, numerical uncertainty, model form
- Treatment of state variables for calibration: Dakota will be able to automate multiple simulation runs to match experiments at different configurations

VUQ Plans

Vince Mousseau

PCMM

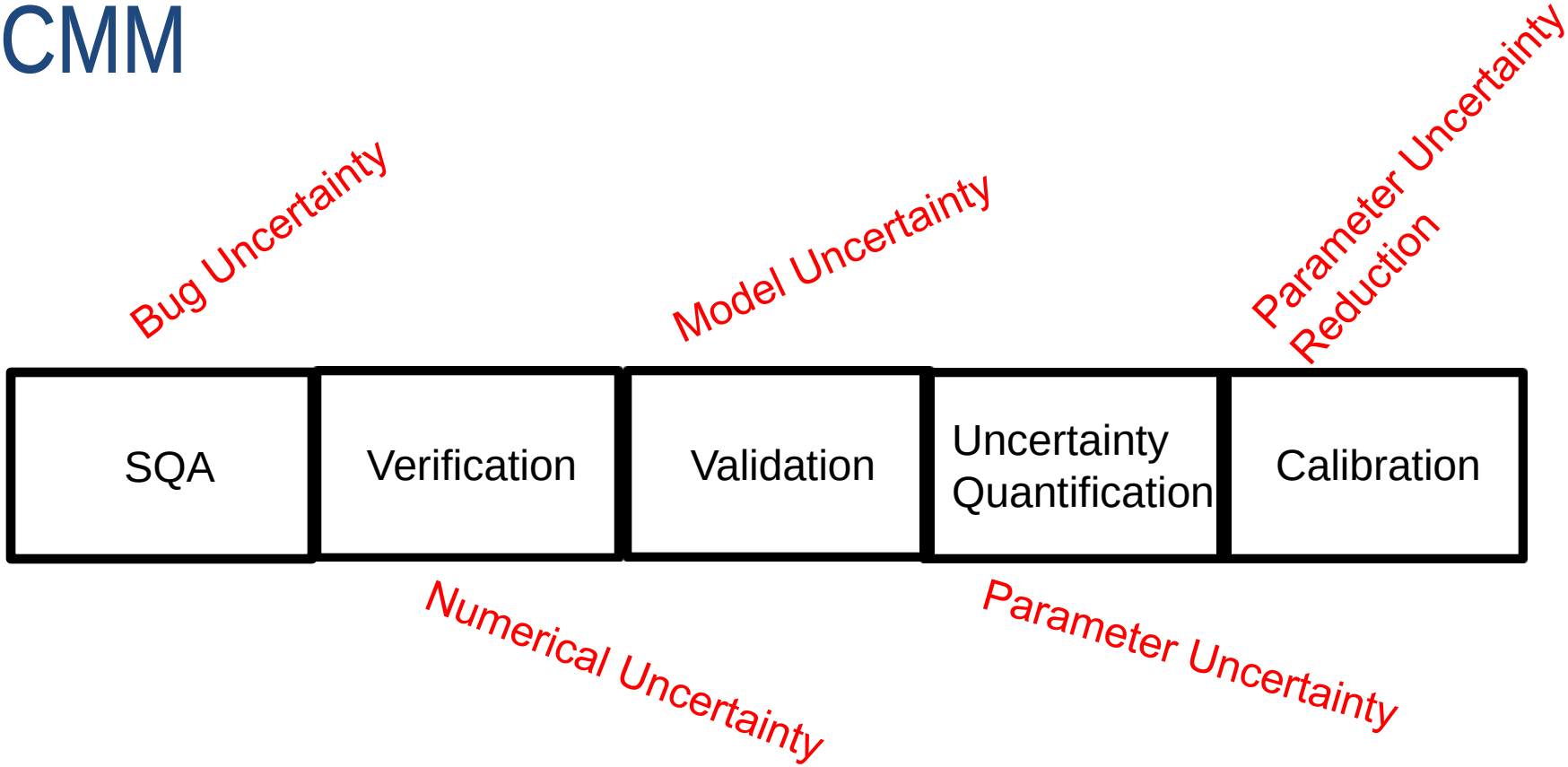

- The Predictive Code Maturity Model (PCMM) is the process being employed in CASL to measure software quality and maturity
- This is an iterative process where one continually works on the lowest score

Common Measures of Uncertainty

- Verification: $\left\| QOI_{exact} - QOI_{computed} \right\|$
- Validation: $\left\| QOI_{experimental} - QOI_{computed} \right\|$
- Uncertainty Quantification: $\left\| QOI_{perturbed} - QOI_{computed} \right\|$
- Numerical, model, and parameter uncertainty are placed on common ground to be compared

Total Uncertainty

- The real total uncertainty is a complicated nonlinear function of the different uncertainties. I will choose a simple L1 norm as my "total uncertainty model."
- Total uncertainty = numerical + model + parameter = verification + validation + uncertainty quantification
- A large uncertainty results from bad numerics, bad physical models, or large parameter uncertainties.

DAKOTA

- DAKOTA is the software package that will be used to deliver tools to improve PCMM analysis.
- Because PCMM is iterative we need to automate the collection of PCMM evidence
- DAKOTA has been strong in uncertainty quantification and calibration so we are improving its ability to do verification and validation

Key Steps

- Phenomenon Identification Ranking Table (PIRT) expert opinion and “real” physics
- Quantified Parameter Ranking Table (QPRT) measured and “code” physics
- Validation pyramid that decomposes the complex multi-scale multi-physics of the application into smaller pieces that are more easily measured.

PIRT2QPRT

- Map Physical phenomenon to correlations
- Find the correlation in the code
- Expose the parameters in that correlation
- Find the original journal paper for the correlations
- Extract the original data used to build the correlation
- Build parameter distributions from the data

Validation Pyramid

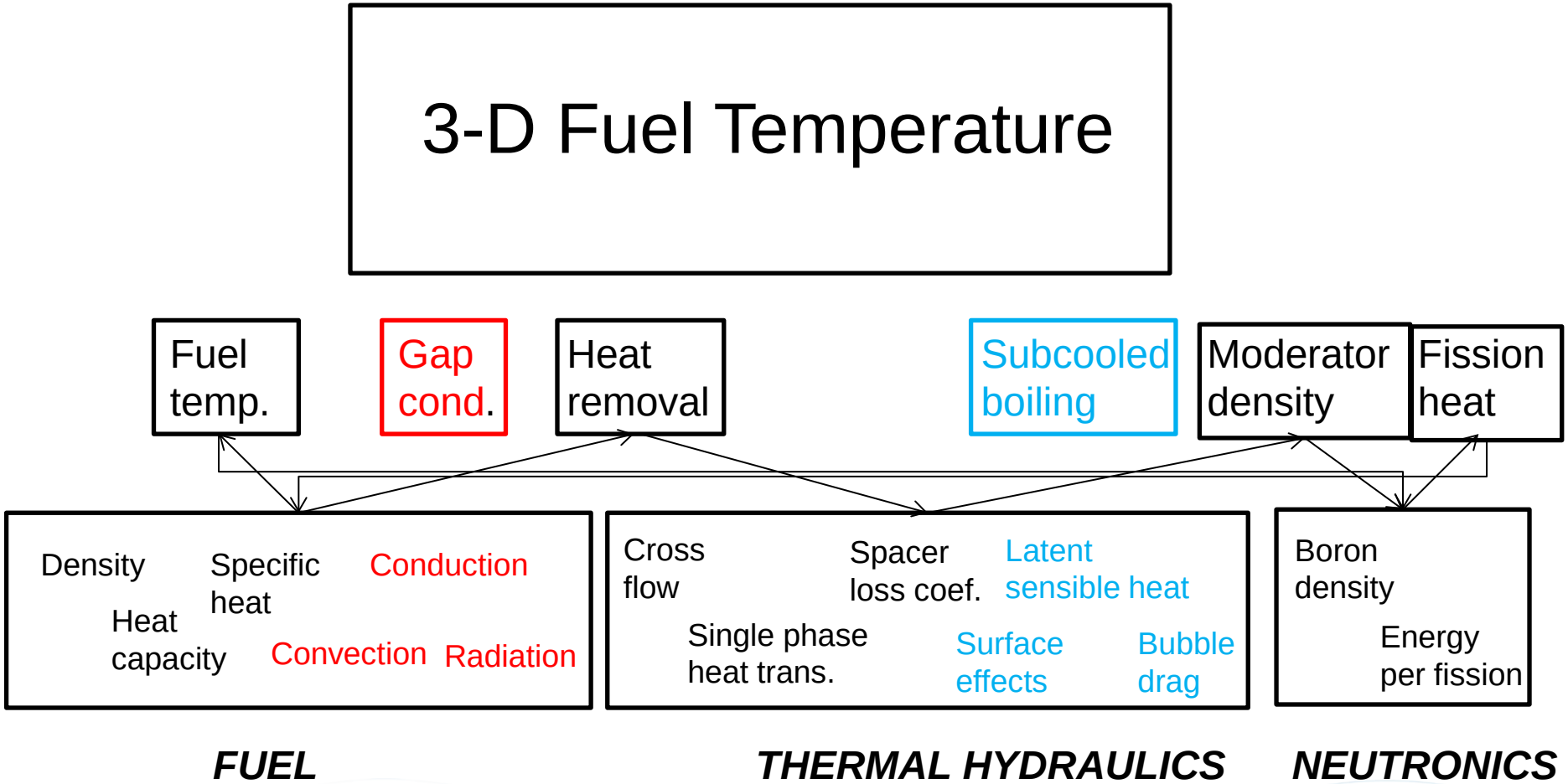

Scaling

- For nonlinear equations we rely on scaling by nondimensional numbers.
- Many of our validation data experiments are at different powers, different geometries, and different materials,
- After validation we rely on the code to scale the results up to the application.
- Note model uncertainty and numerical error do not scale.

CODE PCMM

- Code level PCMM will be done based on the lower levels of the validation pyramid.
- Does the code meet its requirements?
- Has it been documented, verified, and validated to perform basic tasks.
- Each code will have a VUQ plan to fill out the PCMM bins

Application PCMM

- Application PCMM is based on the top part of the validation pyramid.
- This is where the multi-scale, multi-physics, code coupling part of the application occurs.
- Measurements are based on the Quantity Of Interest (QOI)
- Challenge problems will have a VUQ plan that plans out how PCMM bins will be filled.

Code teams VUQ plans

- Need to address the requirements defined by the bottom of the validation pyramid.
- The code requirements is a cumulative list from each challenge problem.
- The requirements becomes the QoI (pressure drop, boiling mass transfer, conjugate heat transfer).
- The code team can define a additional requirements if they prefer.
- Need the follow steps for each requirement, documentation, code verification, SET validation, uncertainty quantification.

Challenge problem VUQ plans

- Challenge problem VUQ plans address the top of the validation pyramid.
- These are integral effects experiments.
- Many physics and a few codes coupled together to produce the solution.
- The following steps need to be done, documentation, solution verification, IET validation, uncertainty quantification.

Summary

- PIRT and QPRT are key prerequisites. These define what is important.
- Validation pyramid provides both SET and IET validation data.
- Code teams with VMA help are responsible for code PCMM.
- Challenge problem PCMM is based on code team work and is shared by PHI and VMA

A DOE Energy Innovation Hub

Round Table 2014

CASL's Phase 2 Proposal

Rose Montgomery, TVA

July 16, 2014

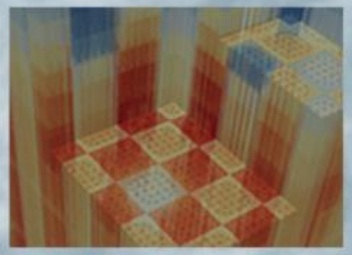

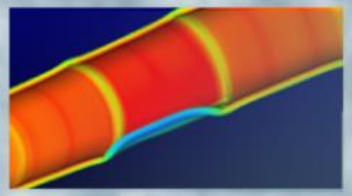

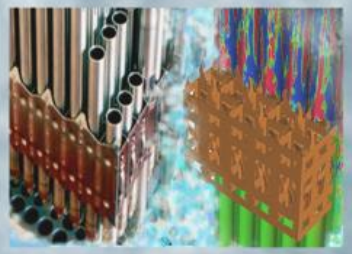

U.S. DEPARTMENT OF ENERGY | NUCLEAR ENERGY

Agenda

- Renewal status and schedule
- The proposal
  - Where is it?
  - What's in there, and how is it organized?
- Phase 2 Challenge Problems
  - How were they selected?
  - What are they?
  - How do they broaden and deepen the Phase 1 capabilities?
  - What specific R&D is being targeted?
  - What is the timing of the work?
- Phase 2 deployment - TDO

Renewal Status and Schedule

- Based on the Hub's outstanding performance in its first 5 years, CASL was invited to submit a proposal for a second 5 years of funding as an Energy Innovation Hub (Phase 2).
- The NE Hub Renewal Plan (March 2014) provides the basis for renewal applications, and establishes the renewal approach and review criteria for CASL.
  - Phase 1 R&D targets PWRs and steady state conditions to build a versatile capability.
  - In Phase 2, CASL seeks to broaden and deepen the Phase 1 technology.
  - Phase 2 will continue the successful *Challenge Problem* strategy to target simulation capability for the R&D effort.

CASL's Phase 2 Proposal was submitted on July 1

Renewal Status and Schedule

- Based on the Hub's outstanding performance in its first 5 years, CASL was invited to submit a non-competitive proposal for 5 more years of funding as an Energy Innovation Hub (Phase 2).
- The NE Hub Renewal Plan provides the basis for renewal application, the renewal approach, and review criteria for CASL.

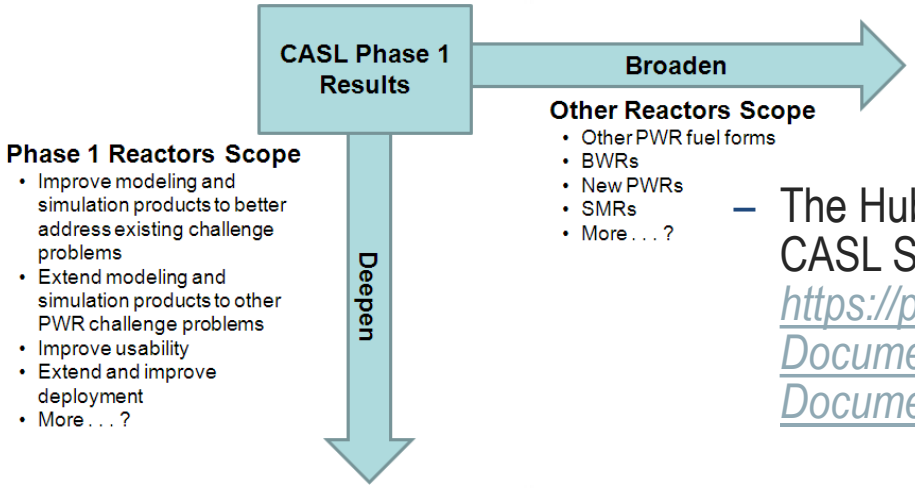

- The Hub Renewal Plan can be found on the CASL Sharepoint in the Renewal Proposal Folder *https://portal12.ornl.gov/sites/casl/Shared Documents/ Renewal Proposal/Phase 2 Proposal Document*

- The proposal was submitted on July 1 (on time); a merit review of the proposal will be completed in conjunction with the Annual Review.

If approved, CASL will transition to Phase 2 in 2015

Phase 2 Proposal

- You can find a copy of the proposal submitted on the SharePoint in the Renewal Proposal/Phase 2 Proposal Document folder.
  - Inputs, background information, and old revisions are located in this same area on SharePoint. This info will be maintained until 11/1/2014.
- The document is formatted corresponding with the review criteria:
  - Phase 1 Progress (12 pages)
    - Milestone and Project Performance
    - Successful Completion of DOE Annual Reviews
    - Publications and Innovations
    - Technology Deployment and Outreach
  - Phase 2 Objectives and Strategy (22 pages)
    - Broadening & Deepening the Phase 1 Technology
    - Extensions and Additions to VERA
    - Phase 2 Level 1 milestones
    - Technical Focus Area Roadmaps
    - Technology Deployment and Outreach
    - Education Program
    - Program Integration
  - Team Capabilities and Project Management Strategy (6 pages)
  - Summary (2 pages)

The main body target was nominally 30 pages

Phase 2 Proposal, continued

- Detailed supporting information is contained in the Appendices, which parallel the main body structure:
  - Appendix A Phase 1 Performance (67 pages)
    - A.1 Science and Technology Progress
    - A.2 Technology Deployment
    - A.3 Productivity Measures
    - A.4 Plan of Record and Milestone Performance
    - A.5 Budget and Cost Summary
    - A.6 DOE Annual Reviews
  - Appendix B Phase 2 Implementation (40 pages)
    - B.1 Challenge Problem Descriptions
    - B.2 Phase 2 Scope Selection Process
    - B.3 Detailed Focus Area Roadmaps
    - B.4 Technology Deployment Vehicles
    - B.5 Virtual One-Roof Evolution Details
    - B.6 Program Integration
  - Appendix C Team and Management Structure (54 pages)
    - C.1 Consortium Partnership
    - C.2 Changes to the Organization Structure for Phase 2
    - C.3 Biographical sketches
  - Appendix D Key Project Management Initiatives (25 pages)
    - D.1 Financial Management
    - D.2 Project Management
    - D.3 Software Engineering and Quality Assurance
    - D.4 Risk Management
    - D.5 Technology Control Plan
    - D.6 Records Management
    - D.7 Training Program
  - Appendix E Letters of Support
  - Appendix F References

No page limit on the appendices

Selection of Challenge Problems for Phase 2

(slide 1 of 5)

- CASL's overarching Phase 2 criteria:
  - Enhance the predictive fidelity of VERA to a maturity level sufficient to allow industry to incorporate and build upon CASL's capabilities for industrial usage;
  - Broaden the applicability the capabilities developed in Phase 1 so that they can be applied to a wider class of LWR types; and
  - Deepen the capabilities developed in Phase 1 and their applicability to new challenge problems.

Selection of CPs, continued (slide 2 of 5)

- To converge on an optimum scope, CASL used a 3-step process:
  1. The team suggested CPs and (where necessary) prepared "mini-charters" that described the challenge, its safety relevance, and higher fidelity path forward to ensure cross-team understanding of the scope.
     [available at https://portal12.ornl.gov/ sites/casl/Shared Documents/Renewal Proposal/Proposed Technical Scope/Potential CPs]
  2. The pool of candidate CPs (28 in total) was categorized, and a survey was created to better understand the views and priorities of stakeholders;
  3. Based on the survey results, and given CASL's overarching criteria, the SLT reduced the selections to what was believed possible given resource and time constraints. The selections were vetted through the CASL BOD.

Selection of CPs, continued (slide 3 of 5)

Step 1: Suggest Challenge Problems

- Many relevant and challenging topics of study were suggested, including both new CPs and continued research on the Phase 1 CPs. These included:

Driver	Challenge Problem or Capability		
PWR	CIPS, CILC Increased Depth	Fuel Performance (with PCI)	GTRF Increased Depth
	DNB Increased Depth	RIA Increased Depth	LOCA Increased Depth
	Boron Precip (fibrous debris)	Other NSSS and fuel arrays	Core Simulator Extension
BWR	Extend Core Simulator	Fuel Performance	CRUD/CILC
	MELLA+, ATWS	Bypass Flow	Channel Bow
	Dryout	Shadow Corrosion	Stability
SMR	Core Simulator (geometry extension only)	Extension of Phase I PWR CPs	
	Natural Convection (also applies to PWR, BWR)	Boron Precipitation (with fibrous debris)	
Structural	Fuel Assembly Distortion (PWR & SMR)	Fuel Assembly In-Core Response during Steady-State, Transient and Seismic/LOCA Events	
Accident Tolerant Fuel	Mechanical simulation of SiC ceramic matrix composite and supporting materials models	Fuel cycle impacts of proposed concepts	
	Coolant flow effects of proposed concepts	Effects of modified coolant flow and heat transfer on CRUD/chemistry for proposed concepts	

Selection of CPs, continued (slide 3 of 5)

Step 2: Survey

- The survey included a wide range of stakeholders to ensure selection of CPs that are industry-relevant, innovative science, programmatically aligned, and of interest to the investigators.
- Survey participants included:
  - CASL Partners
    - EPRI, WEC, TVA, UM, MIT, NCSU, UTK, INL, LANL, ORNL, SNL, PNNL
  - CASL Industry Council
    - ANSYS, CD-Adapco, AREVA, GNF, mPower, NuScale, TVA, EPRI, WEC, EDF, Exelon, Duke
  - INPO Driving to Zero
    - Exelon, American Electric Power, Southern, Dominion, South Carolina E&G
  - Specialists/Management
    - Constellation, WEC, DOE Accident Tolerant Fuels, AREVA, GNF
- Discussions were also held with others (e.g., NRC)

A wide range of stakeholder viewpoints

Selection of CPs, continued (slide 4 of 5)

Step 2: Survey

- Surveyed institutions ranked each proposed CP based on specific criteria:

Category		High Rating	Medium Rating	Low Rating
Programmatic	*Leverage Phase 1*	Builds directly on current works, requires incremental R&D scope	Leverages some past work, Substantive R&D work	Start from scratch
	Feasibility	Easily accomplished within planned schedule and budget	Risk associated with schedule and/or budget	Very little assurance in delivering within 5 years & suggested budget
	DOE Synergism	Fits well with other programs without being duplicative	Works moderately well with other programs; some overlap	Does not fit well and/or is duplicative
Industry Impact	*Able to Address Existing Problems*	Provides actionable insight to a current operationally-limiting issue; cost reduction likely	Provides insight to a current industry issue or parameter that is operationally limiting, cost reduction possible	Provides info on past issue, an issue that continues to occur infrequently, or a parameter that is not operationally limiting
	Likelihood of Adoption	Highly likely – in part or as a whole by industry	Moderately likely - will require modification for adoption	Low likelihood for applicability to commercial reactors
	Applicability	Many other applications & reactor designs	Few other applications & may apply to other reactor designs	Limited application & applies to few reactor designs
	Timeliness of Technology RD&D	Leads industry need	Concurrent with industry need	Lags industry need
Science & Engineering Innovation	*Predictive Capability Maturity*	Approach leads to basic understanding with little calibration needed	Approach improves scientific understanding, but some calibration still used	Approach will continue to be highly calibrated, but with some improved methods
	Gap Between R&D & Industry Practice	Game changer relative to current industry methods	Order of magnitude higher fidelity than used by industry	Parallels current industry methods
Institutional Interest	*Alignment with Interests and Competencies*	Aligned	Somewhat Aligned	Not Aligned

Selection of CPs, continued (slide 5 of 5)

- **Step 2: Survey**
- The results were evaluated using the mean score in each category
  - Because the mean can be misleading in this type of survey, the scores were re-viewed to determine if there was a majority agreement on the score (i.e., at least 50% scored it the same) and agreement was denoted with a ☺.
  - Industry participant responses were contrasted with other respondent responses in the category of Industry Impact.
  - The "programmatic" category was graphed against the "innovation" scores as an indication of the relative risk and reward associated with the various CPs.
- The full report is available on the Sharepoint *https://portal12.ornl.gov/ sites/casl/Shared Documents/Renewal Proposal/Proposed Technical Scope/Institution Perspectives]*

Survey Results on Industry Impact

Rank	CASL Partners	All Industry Participants
1	PWR Fuel Performance (with PCI) Increased Depth☺	PWR Fuel Performance (with PCI) Increased Depth
2	BWR Fuel Performance☺	Natural Convection (also applications to PWR, BWR)
3	Natural Convection (also applications to PWR, BWR)☺	DNB Increased Depth
4	BWR Extend Core Simulator☺	GTRF Increased Depth
5	DNB Increased Depth☺	SMR Core Simulator (geometry extension only)
6	PWR - Boron Precipitation (with fibrous debris)☺	BWR Extend Core Simulator
7	Fuel assembly Distortion☺	RIA Increased Depth
8	PWR CIPS, CILC Increased Depth☺	BWR Fuel Performance
9	RIA Increased Depth☺	Fuel assembly Distortion
10	LOCA Increased Depth☺	PWR - Boron Precipitation (with fibrous debris)

Survey results indicated broad agreement across stakeholders

Phase 2 Scope Recommendations

FY15-FY19

Step 3: SLT recommendations to BOD

	Phase 2 New Challenge Problems	Phase 1 CPs targeted for Phase 2 Deepening	Broadened Application Range	Additional M&S Capability / VERA Functionality
Thermal-Hydraulics	Convective Flow (thermal and solutal) iPWR CHF (DNB) BWR Flow Regimes	CHF (DNB)	PWR BWR iPWR	• Develop and incorporate in Hydra-TH Generation 2 closure models and treatment of cladding surface roughness, provide VUQ analysis. • Broaden Hydra-TH to model convective flow, including thermally-driven convection and solutal-driven convective flows relevant to flow conditions occurring during stages of certain LWR accidents and iPWR normal operations. • Expand Hydra-TH capabilities to lay foundation to model flow regimes beyond bubbly flow relevant to BWR normal operations and certain LWR accidents. • Apply Hydra-TH to DNB conditions for natural circulation flow conditions in iPWRs.
Cladding Performance	BWR PCI iPWR PCI BWR RIA BWR LOCA	PCI RIA LOCA	PWR BWR iPWR	• Enhance fidelity of Peregrine physics models (e.g., pellet cracking, fission product release, microstructure evolution, swelling, cladding stress corrosion cracking, pellet-cladding surface interaction, deformation, growth and creep), expand validation scope, and complete UQ analysis for PWRs. • Expand Peregrine capabilities to address BWRs and iPWRs, addressing BWR cladding alloy and liner, as well as accounting for the differing thermal-hydraulic conditions.
Coolant / Corrosion Chemistry	iPWR CRUD (CIPS & CILC)	CRUD (CIPS & CILC)	PWR iPWR	• Develop MAMBA corrosion product source model, improve cladding corrosion models, expand VUQ analysis for PWRs. • Show applicability of MAMBA to iPWRs.
VERA Core Simulator	Supporting: All BWR and iPWR CPs	Supporting: CRUD (CIPS & CILC) PCI DNB RIA	PWR BWR iPWR	• Increase VERA-CS computational efficiency for PWRs, expand validation scope for PWRs. • Enhance MPACT kinetics capability with reduced computational resource requirements, and if shown successful, incorporate capability into VERA-CS. • Add VERA-CS capabilities to support modeling BWR and iPWR CPs, such as applicable geometric features for MPACT, and flow regimes for CTF, and improved multi-physics solution methods.
Inter-operability		Supporting: GTRF, FAD LOCA, RIA	PWR BWR iPWR	• Add ability to support usage of ISV capabilities in conjunction with VERA, demonstrating such capabilities in the area of structural analysis. • Improve interoperability with plant systems code. • Finalize work on GTRF (e.g. cladding wear model) and validate, to enable and demonstrate interoperability with structural analysis code

Planned VERA Capability Enhancements in Phase 2

Year	Planned Capability Progression	Coupled / Interoperable Component Progression	CP Supported
1	• VERA-CS for PWR multi-cycle simulation • VERA-CS + MAMBA for PWR CIPS • MAMBA with improved CRUD source terms • VERA-CS & Shift for iPWRs • Hydra-TH for subcooled boiling & bubbly flow regime • Peregrine-3D for PCI • Shift with hybrid MC for PWR & iPWR • VERA interoperability with external CFD	Hydra-TH + MAMBA VERA-CS + MAMBA VERA + External CFD	PWR/iPWR CIPS PWR PCI PWR DNB
2	• VERA-C + Peregrine for PWR PCI • VERA-CS + MAMBA & Hydra-TH + MAMBA for PWR CILC • Peregrine + MAMBA for cladding corrosion • CTF enhancements for BWR simulation • MPACT with kinetics to support RIA • MPACT & Shift with photon transport • Hydra-TH + MAMBA advanced subgrid model for CRUD, corrosion chemistry & boron mixing/precipitation	VERA-CS + Peregrine +MAMBA Hydra-TH + MAMBA + Peregrine	PWR/iPWR CILC PWR PCI PWR RIA PWR LOCA BWR Flow Regimes
3	• Peregrine + Hydra-TH + Structural for PWR GTRF • Peregrine for PWR LOCA cladding integrity • VERA-CS for BWR subregion • Hydra-TH for onset of DNB • Hydra-TH for thermal/solutal convective flows with boron mixing • MPACT with depletion for BWR core subregion	VERA + External Structural Mechanics	PWR DNB PWR GTRF PWR LOCA Convective Flows
4	• VERA-CS + Peregrine & Hydra-TH + Peregrine for PWR RIA • VERA-C + Peregrine for BWR PCI • Optimization & integration of group & continuous nuclear data • Hydra-TH flow topology recognition for closure models for BWR-like flow regimes	VERA + External Systems Code Update as needed for new code capabilities	PWR CIPS/CILC PWR RIA BWR PCI BWR Flow Regimes
5	• Hydra-TH + Peregrine for BWR RIA • Peregrine for BWR LOCA cladding integrity • Shift with hybrid, fixed-source Monte Carlo methods for ex-core physics • Hydra-TH for low flow rate boiling in a rod bundle for iPWR	Update as needed for new code capabilities	BWR RIA BWR LOCA iPWR DNB

Phase 2 Challenge Problems – Thermal Hydraulic Category

- Develop and incorporate in Hydra-TH Generation 2 closure models and treatment of cladding surface roughness,
- Provide VUQ analysis;
- Broaden Hydra-TH to model convective flow, including thermally-driven convection and solutal-driven convective flows relevant to flow conditions occurring during stages of certain LWR accidents and iPWR normal operations;
- Expand Hydra-TH capabilities to lay foundation to model flow regimes beyond bubbly flow relevant to BWR normal operations and certain LWR accidents;
- Apply Hydra-TH to DNB conditions for natural circulation flow conditions in iPWRs.

Phase 2 Challenge Problems – Cladding Performance Category

- Enhance fidelity of Peregrine physics models (e.g., pellet cracking, fission product release, microstructure evolution, swelling, cladding stress corrosion cracking, pellet-cladding surface interaction, deformation, growth and creep),
- Expand validation scope, and complete UQ analysis for PWRs.
- Expand Peregrine capabilities to address BWRs and iPWRs, addressing BWR cladding alloy and liner, as well as accounting for the differing thermal-hydraulic conditions.

Phase 2 Challenge Problems – Coolant/Corrosion Chemistry Category

- Develop MAMBA corrosion product source model,
- Improve cladding corrosion models,
- Expand VUQ analysis for PWRs.
- Show applicability of MAMBA to iPWRs.

Phase 2 Challenge Problems – VERA Core Simulator

- Increase VERA-CS computational efficiency for PWRs.
- Expand validation scope for PWRs.
- Enhance MPACT kinetics capability with reduced computational resource requirements, and if shown successful, incorporate capability into VERA-CS.
- Add VERA-CS capabilities to support modeling BWR and iPWR CPs, such as applicable geometric features for MPACT, and flow regimes for CTF, and improved multi-physics solution methods.

Phase 2 Challenge Problems – Interoperability Category

- Add ability to support usage of ISV capabilities in conjunction with VERA,
- demonstrating such capabilities in the area of structural analysis.
- Improve interoperability with plant systems code.
- Finalize work on GTRF (e.g. cladding wear model) and validate, to enable and demonstrate interoperability with structural analysis code

A DOE Energy Innovation Hub

Roadmap for Phase 2

- The Level 1 milestones provide a roadmap of the major objectives.
- Level 2 milestones are included by focus area (proposal section 3.4).

ear	Category	CP	No.	Milestone Description
1	Coolant / Corrosion Chemistry	CIPS / CILC	1	Qualify core-wide PWR CIPS capability with corrosion product treatment: Add corrosion product source term and mass balance to MAMBA, and utilize in VERA-CS to simulate multi-cycles of a PWR that experienced CIPS.
	Core Physics	PWR CPs	2	Qualify multi-cycle PWR core simulator capability: Using VERA-CS simulate first and reload cycles of the Watts Bar Unit 1, with predictions compared to plant measurements with regard to in-core, ex-core and selected startup physics test measurements.
	Core Physics	PCI / RIA / LOCA	3	Demonstrate iPWR core simulator capability: Utilizing VERA-CS, establish an iPWR core model and simulate cycle depletion.
	Thermal-Hydraulics	CHF (DNB) Convective flow	4	Qualify multiphase CFD capability for bubbly flow regime: Hydra-TH will be used to simulate out-of-core fluid experiments targeted at providing validation data for the bubble flow regime, with predictions contrasted to measurements.
2	Cladding Performance	PCI / RIA / LOCA	5	Demonstrate core subregion & core-wide PWR PCI capability: Utilizing VERA-CS with Peregrine-2D, complete PWR multi-cycle core depletion for core maneuver to identify PCI limiting fuel rods; utilizing Peregrine-3D complete PCI analysis for limiting fuel rods.
	Coolant / Corrosion Chemistry	CIPS / CILC	6	Quality CFD-based PWR CILC capability for a subregion: Using the results of the Year 1 CIPS L1 milestone to identify CILC limiting fuel rods and associated powers, CILC analysis will be completed using Hydra-TH with embedded MAMBA coupled to Peregrine.
	Deployment	N/A	7	Create Working Group for CASL software: To support the release to external users, a Working Group will be formed, members recruited, charter written, and first meeting held in conjunction with training on selected usages of VERA.
3	Cladding Performance	GTRF	8	Demonstrate GTRF analysis methodology components: Using the fuel rod mechanical/material modeling of Peregrine, finalized rod wear model, Hydra-TH predicted turbulent pressure forces, and assumed gap opening, demonstrates interoperability capability of VERA with a structural mechanics code. Stretch goal: extend Peregrine to treat the change in spacer grid straps geometry and material properties to capture cladding-grip strap gap formation and impact on wear.
	Cladding Performance	LOCA	9	Demonstrate PWR LOCA fuel performance capability: Use Peregrine to predict the extent of clad ballooning and oxidation, as a function of initial fuel rod state (e.g. hydrogen pickup) using LOCA system transient code generated boundary conditions.
	Core Physics	All BWR	10	Establish BWR core simulator capability for core subregion: Use VERA-CS to simulate a subregion (i.e. one or more fuel assemblies) of a BWR core. Stretch goal: simulate full core.
	Thermal-Hydraulics	DNB	11	Qualify prediction of onset of DNB using M-CFD: Hydra-TH will be used to simulate out-of-core fluid experiments targeted at providing validation data for the onset of DNB, for a range of powers and coolant inlet enthalpy, flow and pressure.
	Thermal-Hydraulics	Convective flow	12	Qualify thermal/solutal convective fluid flow CFD capability: Hydra-TH will be modified via incorporation of appropriate turbulence model and boron solution/dissolution chemistry model and used to predict first thermal convective fluid flow and subsequently thermal/solutal convective fluid flow, with predictions contrasted to validation data where available.
4	Cladding Performance	RIA	13	Demonstrate core-wide PWR RIA capability to simulate ejected rod accident: VERA-CS with neutron kinetics and Peregrine-2D will be used to simulate a PWR ejected rod accident to identify RIA limiting fuel rods; utilizing Peregrine-3D complete RIA analysis for limiting fuel rod(s).
	Cladding Performance	PCI / RIA / LOCA	14	Demonstrate BWR PCI capabilities: Utilizing VERA-CS with Peregrine-2D coupled, complete BWR core subregion depletion from which a maneuver will be completed to identify PCI limiting fuel rods; utilizing Peregrine-3D complete PCI analysis for limiting fuel rod(s).
	Thermal-Hydraulics	BWR Flow Regimes	15	Demonstrate capability to simulate using M-CFD the flow regimes that exist during normal operations of a BWR. Hydra-TH will need to be modified to incorporate the appropriate closure relationships associated with each flow regime and recognize the flow topology in order to utilize the appropriate closure models, including addressing flow regime transitions.
5	Cladding Performance	RIA	16	Demonstrate BWR RIA capabilities: Utilizing Peregrine-3D complete RIA analysis for assumed limiting fuel rod(s).
	Cladding Performance	LOCA	17	Demonstrate BWR LOCA fuel performance capability: Use Peregrine to predict the extent of clad ballooning and oxidation, as a function of initial fuel rod state (e.g. hydrogen pickup) using LOCA system transient code generated boundary conditions.
	Thermal-Hydraulics	CHF (DNB)	18	Demonstrate prediction of onset of DNB using M-CFD for low flow conditions indicative of iPWRs and PWRs during post-trip loss of offsite power event.
	Deployment	N/A	19	Finalize transition of CASL-supported functions to post-CASL entity: Establish post-CASL entity and assist it to manage software release, distribution, training, and the bug fix and enhancement processes.

U.S. DEPARTMENT OF ENERGY | NUCLEAR ENERGY

Technology Deployment and Outreach (TDO)

- To facilitate CASL's terminal objective of broad technology deployment, a new focus area has been formed.
- Tasks for TDO include:
  - Ensuring sustainability of the CASL technology through the establishment of a "post-CASL entity;"
  - Creating opportunities for outreach, including training and VERA licensing;
  - Ensuring appropriate documentation exists for all of VERA;
  - Continuing to deploy and test VERA through Test Stands;
  - Expanding the VERA release and support practices established in Phase 1.
- TDO will work closely with the Education Program and Communications team.

A greater emphasis on deployment in Phase 2

In Summary….

- CASL has been invited to submit a proposal for a second five years of funding as an Energy Innovation Hub.
- A proposal has been prepared and submitted.
- The proposed scope was selected based on a robust cross-institution survey of the stakeholders.
- The primary Phase 2 objectives and milestones have been established.
- There will be a greater emphasis on deployment and supporting activities.

All information in this presentation, and oh so much more, is available on the CASL Sharepoint in the Renewal Proposal folder:
https://portal12.ornl.gov/sites/casl/Shared Documents/Renewal Proposal/

BACKUP SLIDES

THM L2 Milestones

Table 1: Phase 2 THM Level 2 milestone plan.

Year	Category	CP	L1 Milestone Supported	Description
1	Thermal-Hydraulics	CHF (DNB)	4	Demonstration of CASL M-CFD Closure Models for Subcooled Boiling and Bubbly Flow
2	Thermal-Hydraulics	CHF (DNB), CILC	11, 18	Wall Closure Models for Subcooled Boiling using DNS for Wall Conditions
	Coolant / Corrosion Chemistry	CHF (DNB), CILC, LOCA	12	Advanced Subgrid-Scale Modeling of Corrosion Chemistry and Boron Mixing/Precipitation (CFD-based CILC)
3	Thermal-Hydraulics	CHF (DNB)	18	Demonstration of Gen-II CASL M-CFD Closure Models for the onset of DNB
	Thermal / Solutal Convection	Convective Flow, LOCA	12	Demonstration of Thermal and Solutal Convection for Boron Mixing during ECCS Injection
4	Thermal-Hydraulics	Flow Regimes	15	Investigation of Flow Topology Recognition for M-CFD Closure Models for BWR-like Flow Regimes
	Coolant / Corrosion Chemistry	CHF (DNB), CILC	6, 18	Demonstration of advanced subgrid-scale chemistry model for CRUD deposition
5	Thermal / Solutal Convection	CHF (DNB)	18	Low flow rate boiling in a rod bundle
	Deployment	N/A	19	Hydra-TH User, Theory, V&V/THM Benchmarks Manuals

RTM L2 Milestones

Table 1: Phase 2 RTM Level 2 milestone plan.

Year	Category	CP	L1 Milestone Supported	Description
1	Core physics	All BWRs	10, 14, 16, 17	Deterministic neutronics for BWRs: Validation of the planar MOC methodology for BWR subregion transport requirements. (Develop mesh, data models, and geometry that can handle BWR requirements)
	Core physics	All iPWR	2, 3	Development and demonstration of hybrid Monte Carlo methods for full-core PWR and iPWR analysis.
2	Core physics	PCI, RIA	5, 13, 14, 16	Transient neutronics with feedback: Implementation of transient capability with internal TH feedback in MPACT for PWRs
	Core physics	ALL	5, 9	Implementation and validation of photon transport in Shift and MPACT.
3	Core physics	BWR	14, 16, 17	Pin-resolved deterministic neutronics for BWR subregions: Validation of deterministic methods in VERA-CS applied to BWR subregion analysis.
	Core physics	BWR	10	Develop efficient depletion methodology for BWRs including Gadolinium absorbers.
4	Core physics	All	19	Optimization and integration of state-of-the-art nuclear data for multi-group and continuous-energy.
	Core physics	PWR, BWR	19	Deploy in line, fully consistent time-dependent neutronics for VERA-CS suitable for PWRs and BWRs.
5	Core physics	All	19	Provide completed documentation for methods, users, and developers for all VERA-CS neutronics packages and methods.
	Core physics	All	19	Implementation of hybrid, fixed-source Monte Carlo methods for ex-core physics.

FMC L2 Milestones

Table 1: Phase 2 FMC Level 2 Milestone Plan.

Year	Category	CP	L1 Milestone Supported	Description
1	Coolant / Corrosion Chemistry	PWR, iPWR CIPS/CILC	1	Primary piping corrosion product source term and mass balance PWRs
	Cladding Performance	DNB, LOCA, RIA	5	3D PCI analysis using Peregrine of specific NPP with PCI failures
2	Cladding Performance	PWR PCI	5,14	Demonstration of coupled 2D/3D PCI fuel rod modeling
	Cladding performance	PWR, iPWR CIPS/CILC	5,9,13,16	Initial coupling of MAMBA and Peregrine for corrosion analysis
3	Cladding performance	LOCA	9	Benchmarking of LOCA Fuel Behavior Modeling Using Separate Effects Experiments in Halden and NSRR
	Fuel structural response	All BWR	8	Parametric evaluation of wear from turbulence excitation forces for GTRF for specified gap size. Stretch goal: predict gap growth
4	Cladding Performance	RIA	16, 13	Benchmarking of RIA Fuel Behavior Modeling Using Separate Effects Experiments from CABRI and NSRR
	Thermal-Hydraulics	PCI	15	Demonstration of coupled Peregrine/Hydra for subchannel heat transfer modeling
5	Deployment	N/A	16	Demonstration of coupled MAMBA/Peregrine for BWR LOCA
	Deployment	N/A	9	Completion of User and Theory Manual for Peregrine Usage in LOCA and RIA Analysis

PHI L2 Milestones

Table 1: Phase 2 PHI Level 2 Milestone Plan.

Year	Category	CP	L1 Milestone Supported	Description
1	Core Physics Coolant / Corrosion Chemistry	CIPS/CILC	1	VERA-CS for PWR for analysis of reactor steady-state operation including multi-cycle capability and with CIPS modeling capability
	Coolant / Corrosion Chemistry Thermal-Hydraulics Cladding Performance	DNB, GTRF, LOCA, RIA	9 11,, 12, 14, 17, 18	Demonstration of VERA interoperability with systems code/commercial CFD code
2	Core Physics	All BWR	10, 14, 16	Development and testing of CTF to support modeling of BWR operating conditions
	Thermal-Hydraulics Cladding Performance	RIA	13, 16	Development of coupled PWR transient capability to support DNB and RIA
3	Core Physics	All BWR	10, 14, 16	Document advanced solution methods research for multi-phase sub-channel flow and coupling with neutronics and implement in VERA-CS if appropriate
	Core Physics	All BWR	10, 14, 16	Develop VERA-CS for BWR for analysis of reactor steady-state operation for multiple fuel bundles
4	Cladding Performance	RIA	16	Development of BWR subregion Hydra-TH + Peregrine transient capability for RIA
	Cladding Performance	PCI	14	Update VERA_CS coupling with Peregrine to support BWR PCI challenge problem.
5	Deployment	N/A	19	Transition VERA continuous build, integration, and testing system for hand off to post-CASL entity
	Deployment	N/A	19	Finalize VERA documentation and release package for transition to post-CASL entity

VMA L2 Milestones

Table 1: Phase 2 VMA Level 2 milestone plan.

Year	Category	CP	L1 Milestone Supported	Description
1	Core physics	All PWR	2	Demonstrate the core simulator for PWRs Watts Bar Unit 1 over multiple cycles
2	Coolant / corrosion chemistry	PWR CIPS	1	Qualify the CIPS Challenge Problem for PWRs with a focus on calibration and uncertainty quantification
	Core physics	All PWR	2	Qualify the core simulator for PWRs Watts Bar Unit 1 over multiple cycles with emphasis on calibration and uncertainty quantification
	Cladding Performance	PWR PCI	5	Demonstrate the PCI Challenge Problem for PWRs
3	Coolant / corrosion chemistry	PWR CILC	6	Qualify the CILC Challenge Problem for PWRs with a focus on verification and validation
	Cladding Performance	PWR PCI	5	Qualify the PCI Challenge Problem for PWRs with emphasis on calibration and uncertainty quantification
4	Thermal Hydraulics	DNB	11	Qualify the DNB Challenge Problem for DNB with emphasis on calibration and uncertainty quantification
	Cladding performance	PWR LOCA	9	Qualify the LOCA Challenge Problem for PWRs with an emphasis on verification and validation.
5	Cladding performance	PWR RIA	13	Qualify the RIA Challenge Problem for PWRs with a focus on verification and validation.

TDO L2 Milestones

Table 1: Phase 2 TDO Level 2 milestone plan

Year	Category	Description
1	Business operations	Establish a business case, identify and evaluate options for the post-CASL entity, determine mode of recruitment, and make recommendation for post-CASL entity
2	Business operations	Select the post-CASL entity
	Working group	Establish the Advanced ModSim Working group
	Training	VERA Training Pilot
	Test stands	External Test Stand (key industry stakeholder)
3	Release	"Unlimited" VERA release only restricted by DOE regulations and US export control laws
5	Business operations	Finalize transition of CASL-supported functions to post-CASL entity (e.g., Give keys to post-CASL entity)
	Release	Final CASL VERA Release

Org Chart

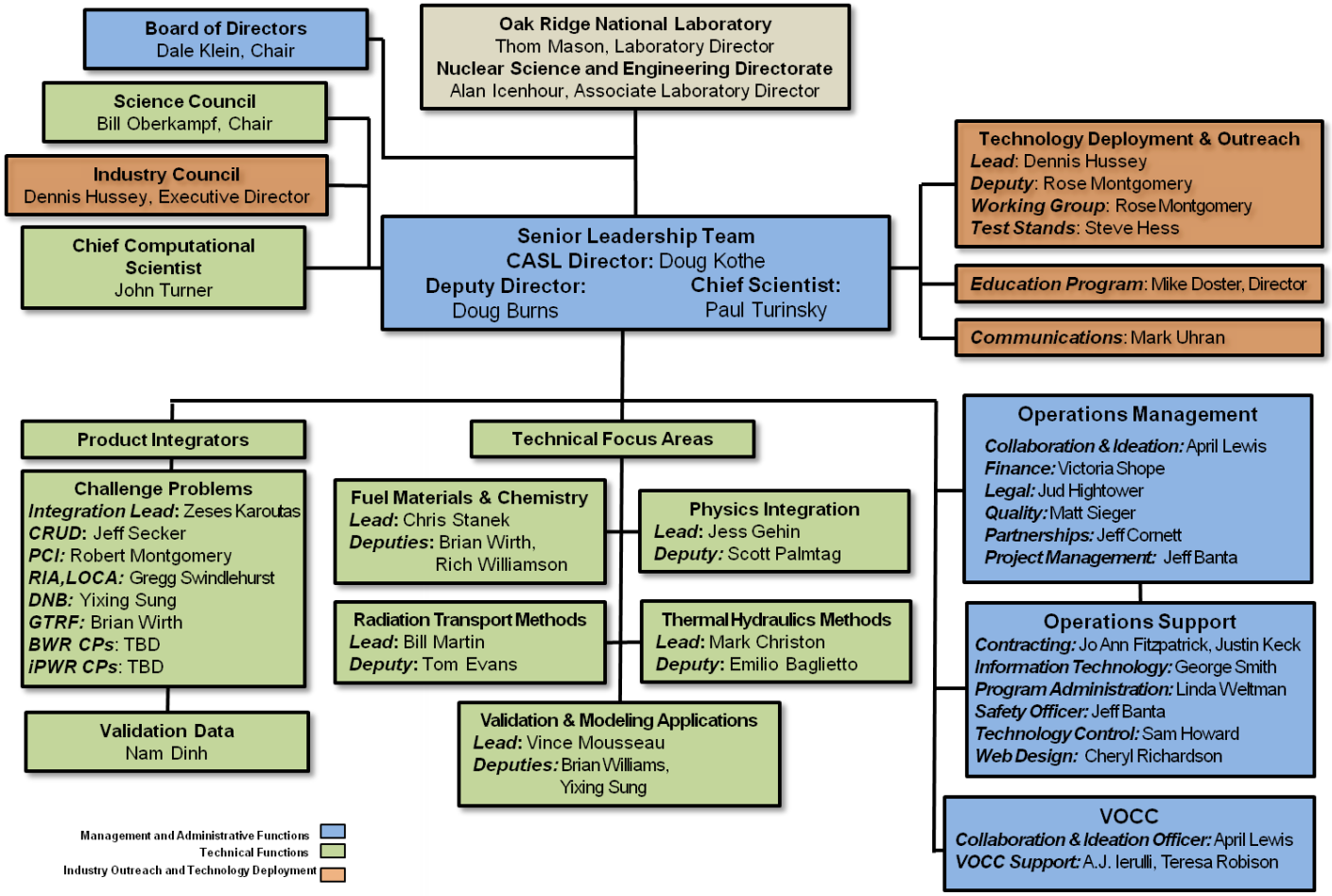
Board of Directors
Dale Klein, Chair
Oak Ridge National Laboratory
Thom Mason, Laboratory Director
Nuclear Science and Engineering Directorate
Alan Icenhour, Associate Laboratory Director
Science Council
Bill Oberkampf, Chair
Industry Council
Dennis Hussey, Executive Director
Chief Computational Scientist
John Turner
Senior Leadership Team
CASL Director: Doug Kothe
Deputy Director: Doug Burns
Chief Scientist: Paul Turinsky
Technology Deployment & Outreach
Lead: Dennis Hussey
Deputy: Rose Montgomery
Working Group: Rose Montgomery
Test Stands: Steve Hess
Education Program: Mike Doster, Director
Communications: Mark Uhran
Product Integrators
Challenge Problems
Integration Lead: Zeses Karoutas
CRUD: Jeff Secker
PCI: Robert Montgomery
RIA,LOCA: Gregg Swindlehurst
DNB: Yixing Sung
GTRF: Brian Wirth
BWR CPs: TBD
iPWR CPs: TBD
Validation Data
Nam Dinh
Technical Focus Areas
Fuel Materials & Chemistry
Lead: Chris Stanek
Deputies: Brian Wirth, Rich Williamson
Physics Integration
Lead: Jess Gehin
Deputy: Scott Palmtag
Radiation Transport Methods
Lead: Bill Martin
Deputy: Tom Evans
Thermal Hydraulics Methods
Lead: Mark Christon
Deputy: Emilio Baglietto
Validation & Modeling Applications
Lead: Vince Mousseau
Deputies: Brian Williams, Yixing Sung
Operations Management
Collaboration & Ideation: April Lewis
Finance: Victoria Shope
Legal: Jud Hightower
Quality: Matt Sieger
Partnerships: Jeff Cornett
Project Management: Jeff Banta
Operations Support
Contracting: Jo Ann Fitzpatrick, Justin Keck
Information Technology: George Smith
Program Administration: Linda Weltman
Safety Officer: Jeff Banta
Technology Control: Sam Howard
Web Design: Cheryl Richardson
VOCC
Collaboration & Ideation Officer: April Lewis
VOCC Support: A.J. Ierulli, Teresa Robison
Management and Administrative Functions
Technical Functions
Industry Outreach and Technology Deployment

SQUIRE AND KNIGHT AWARDS

Recognizing outstanding technical contributions

CASL Consortium for Advanced Simulation of LWRs
U.S. DEPARTMENT OF ENERGY Nuclear Energy

CASL SQUIRES (nominees for Knight Award)

- AMA – Fausto Franceschini & Andrew Godfrey
- MPO – Jun Qu
- RTM – Ben Collins
- PHI – Bob Salko
- THM – Lindsey Gilman
- VUQ – Brian Adams

KNIGHT SWEARING IN CEREMONY

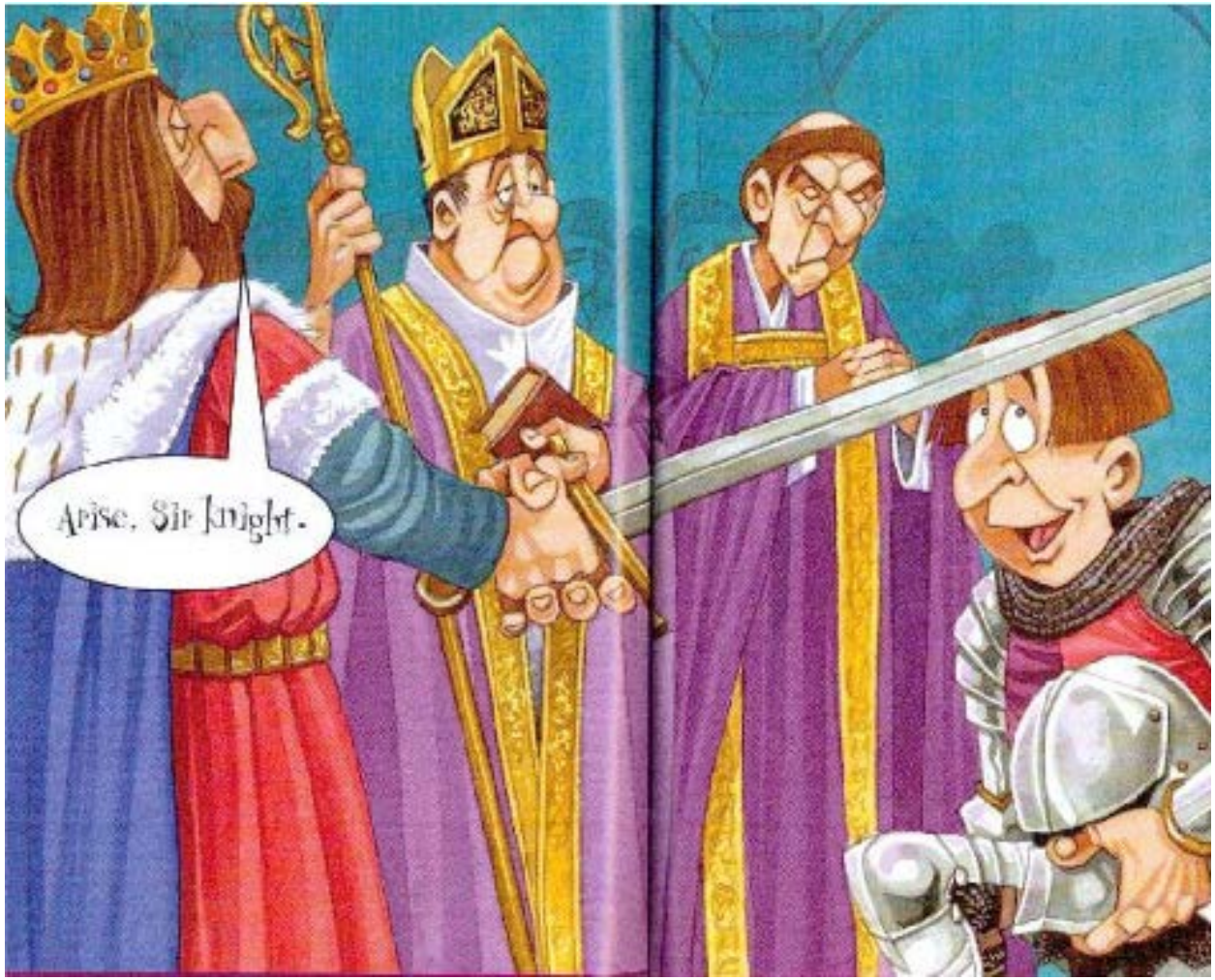

Congratulations
Bob Salko

CASL JESTER AWARD

Congratulations
Victoria Shope

© 2014 Westinghouse Electric Company LLC. All Rights Reserved.

Westinghouse Test Stand

Zero Power Physics Test Simulations for the **AP1000®** PWR

F. Franceschini[1], Andrew Godfrey[2]

[1] Westinghouse Electric Company LLC

[2] Oak Ridge National Laboratory

Presented by Jeff Secker[1]

CASL Roundtable, July 16 2014

AP1000® is a registered trademark of Westinghouse Electric Company LLC in the United States and may be registered in other countries throughout the world. All rights reserved. Unauthorized use is strictly prohibited.

© 2014 Westinghouse Electric Company LLC. All Rights Reserved.

Agenda

- Background (3 slides)
- Topics (5 slides)
- Results (9 slides)
  - Critical boron
  - Reactivity coefficients
  - Rod worth
  - Power distribution
- Usability, Benefits, Recommendations (6 slides)
- Conclusions

© 2014 Westinghouse Electric Company LLC. All Rights Reserved.

Background

© 2014 Westinghouse Electric Company LLC. All Rights Reserved.

Timeline

- Test Stand discussions (early 2013)
- Scope proposed by Westinghouse (memo April 2013)
- VERA deployment at Westinghouse (June 2013)
  - VERA built on dedicated compute cluster (Sept 2013)
  - Various VERA updates since then
- Technical analysis (July-Nov 2013)
  - Deterministic (Insilico-SP_N) plus Monte-Carlo (KENO)
- ZPPT analysis completed and documented (Jan, Rev. 1 in Mar 2014) : http://www.casl.gov/docs/CASL-U-2014-0012-001.pdf
  - Spin-off: Early Science SHIFT simulations (completed in Apr. 2014)
- Ongoing analysis with MPACT, extension to other plants

First organization to host VERA Test Stand

© 2014 Westinghouse Electric Company LLC. All Rights Reserved.

VERA Build

- VERA build at Westinghouse operational and exercised
  - 576 cores, 12 cores/ node, 96 GB/node (4.6TB total)

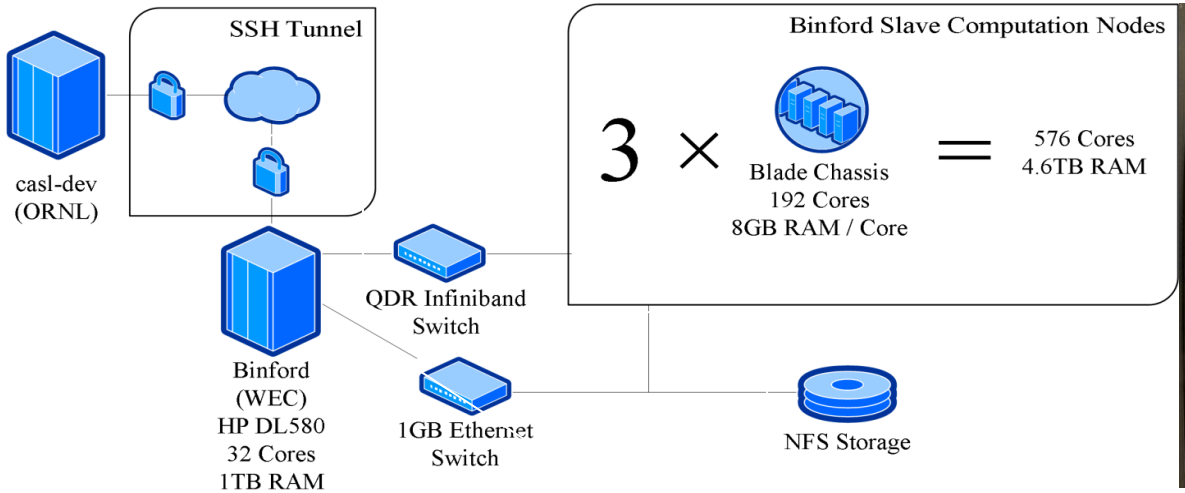

VERA ZPPT calculations performed on Westinghouse system

© 2014 Westinghouse Electric Company LLC. All Rights Reserved.

Codes Used

- INSILICO SP_N 3D flux solver
  - SP_5 with P_3 scattering in 23 energy groups
  - on-the-fly pin-homogenized XS with 1D transport calculations
  - SCALE B7.0-based 252-energy group library
- MPACT
  - 2D/1D (2D MOC, 1D Diffusion)
  - P2 scattering (waiting for TCP0)
  - 0.005 ray spacing for IFBA (apparently not required in large geometry?)
  - 56-group subgroup ORNL library
- KENO-VI Monte-Carlo
  - Reference solution for AP1000 simulations
  - Validated for WB1 and vs. MCNP (problem 5)
  - Continuous energy
  - General geometry
  - Currently only scales up to 200-300 cores
- SHIFT Monte-Carlo
  - Massively parallel (240K cores simulations performed)
  - Up to 3D core benchmark simulations (rodded configurations)
  - Early Science Award 60M core-hour allocation
  - HPC Innovation Excellence Award (June 2014)
  - Completed but need formal documentation

© 2014 Westinghouse Electric Company LLC. All Rights Reserved.

Test Stand Topics

AP1000 PWR First Core

© 2014 Westinghouse Electric Company LLC. All Rights Reserved.

Topics

- Advanced application of VERA
  - Advanced first-core
  - Radial and Axial heterogeneities
  - MSHIM™ operation
  - IFBA (ZrB_2 burnable absorber coating on pellet) vs. BP inserts in other first cores
- Licensed core – will be implemented in all units under construction
- Opportunity for state-of-the-art “replicable” measurements

MSHIM™ is a trademark of Westinghouse Electric Company LLC in the United States and may be registered in other countries throughout the world. All rights reserved. Unauthorized use is strictly prohibited.

© 2014 Westinghouse Electric Company LLC. All Rights Reserved.

AP1000 PWR First Core Design – Radial

	H	G	F	E	D	C	B	A
8	B	D 68 IFBA 12 WABA	B	D 68 IFBA 12 WABA	B	D 68 IFBA 12 WABA	E 124 IFBA	C
9	D 68 IFBA 12 WABA	B	D 68 IFBA 12 WABA	B	D 68 IFBA 12 WABA	B	E 88 IFBA 4 WABA	A
10	B	D 68 IFBA 12 WABA	B	D 68 IFBA 12 WABA	B	E 124 IFBA 8 WABA	C	
11	D 68 IFBA 12 WABA	B	D 68 IFBA 12 WABA	B	E 124 IFBA 8 WABA	C	A	
12	B	D 68 IFBA 12 WABA	B	E 124 IFBA 8 WABA	B	C		
13	D 68 IFBA 12 WABA	B	E 124 IFBA 8 WABA	C	C			
14	E 124 IFBA	E 88 IFBA 4 WABA	C	A				
15	C	A						

Region
IFBA
WABA

IT	M	M	SW	M	M	LW	M	LI
M	HI	H	M	H	H	M	M	L
M	H	HI	M	HI	HI	M	M	LI
SW	M	M	GT	M	M	GT	MI	L
M	H	HI	M	M	M	M	M	LI
M	H	HI	M	M	LW	M	M	L
LW	M	M	GT	M	M	M	M	LI
M	M	M	MI	M	M	M	MI	L
LI	L	LI	L	LI	L	LI	L	LI

High enriched fuel inboard like L^3P reload cycles.

Radial zoning in Cycle 1 to reduce spectral interface.

Mimics reload cycle to quickly establish equilibrium

© 2014 Westinghouse Electric Company LLC. All Rights Reserved.

AP1000 PWR First Core Design – Axial

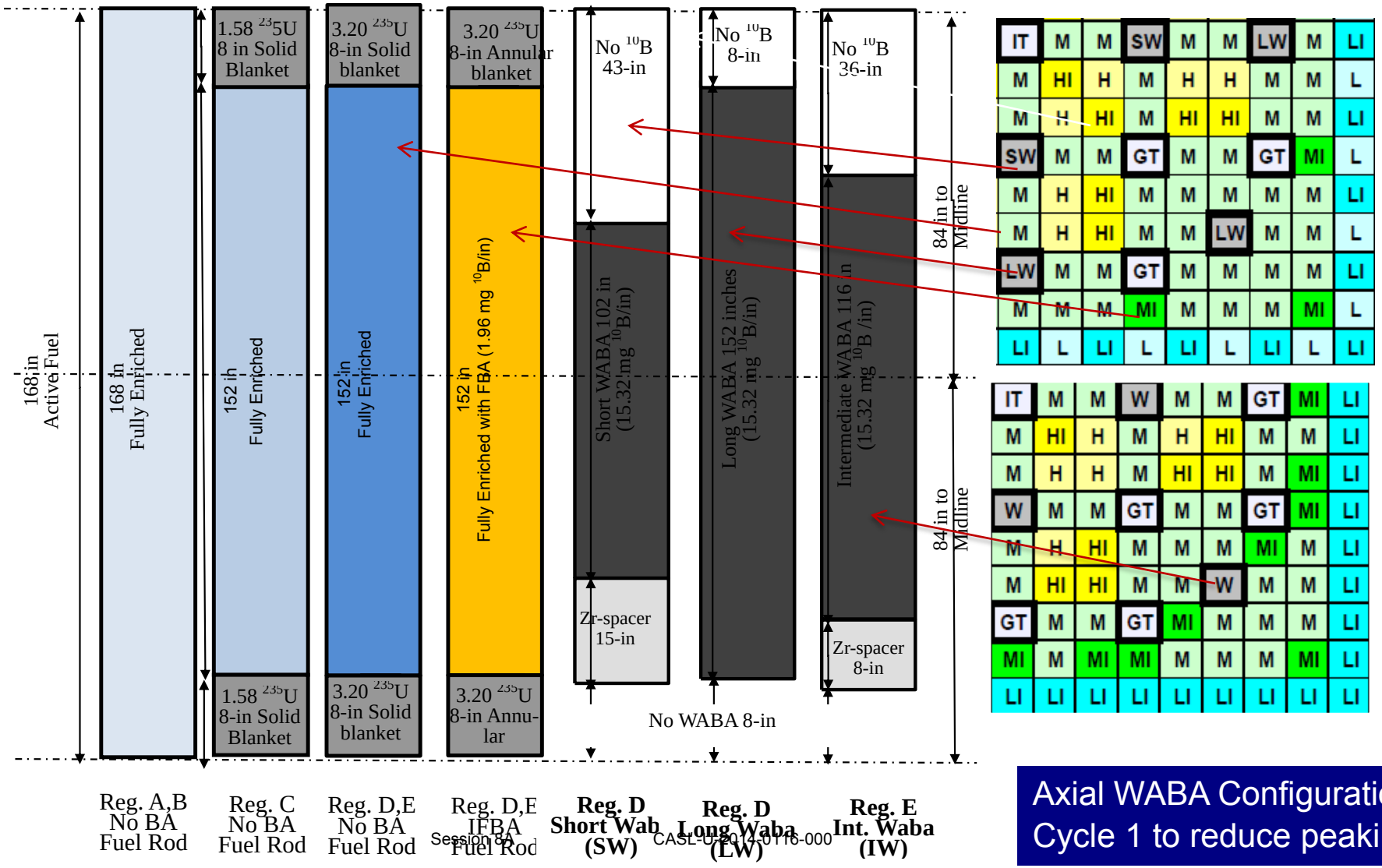

Axial WABA Configuration in Cycle 1 to reduce peaking.

© 2014 Westinghouse Electric Company LLC. All Rights Reserved.

Control Rod Layout

Shutdown:

4 Banks / 32 RCCAs (Ag-In-Cd)

- Ensures adequate shutdown margin & trip reactivity

Axial Offset:

1 Bank / 9 RCCAs (Ag-In-Cd)

- Dedicated, high impact bank provides robust axial power shaping capabilities

MSHIM:

4 Banks / 16 GRCAs (Tungsten) MA/MB/MC/MD

2 Banks / 12 RCCAs (Ag-In-Cd) M1/M2

- Provides fine reactivity control while significantly reducing changes to soluble boron

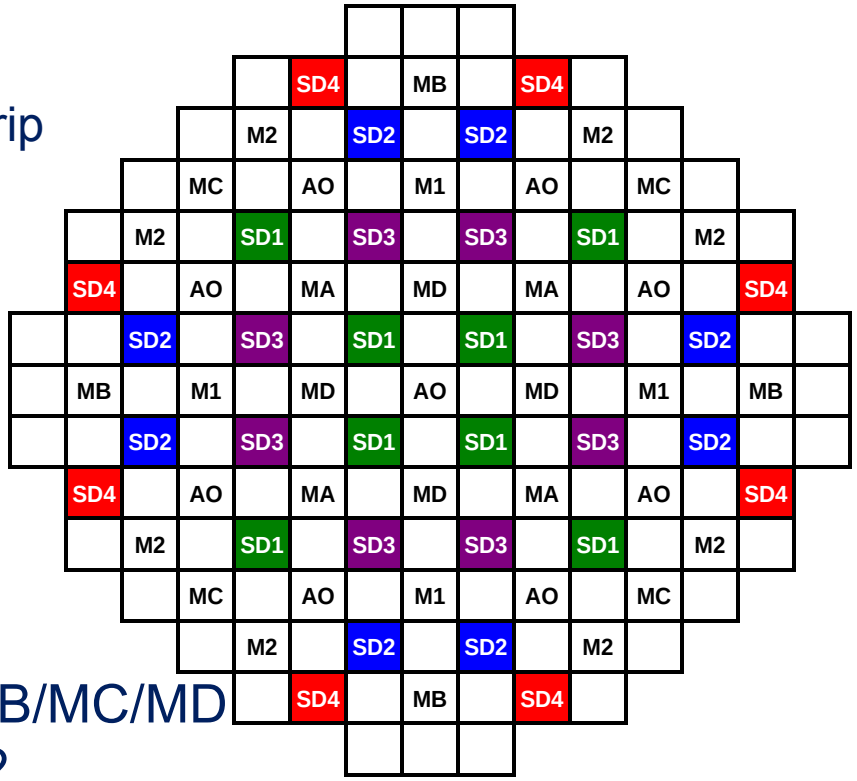

Key to MSHIM Operating Strategy

© 2014 Westinghouse Electric Company LLC. All Rights Reserved.

Test Stand Simulations Performed

2D
- **Single Lattice (20 types)**
- Multi Lattice (Unrodded and Rodded)
- **Core with Reflector** (Various Reflectors)

3D Assembly
- **Single Assembly (7 types)**
- **Multi Assembly (Partial Rod Insertion)**

3D Core
- **HZP Critical Boron**
- **Rod Worth (11 Banks)**
- **Boron Worth**
- **ITC, DTC and MTC**
- **MSHIM Maneuver Bank Configuration**

© 2014 Westinghouse Electric Company LLC. All Rights Reserved.

Results - AP1000 HZP Comparisons

Insilico SP_N vs. KENO (Completed and Documented)

SHIFT (Completed)

MPACT (Ongoing)

© 2014 Westinghouse Electric Company LLC. All Rights Reserved.

2D Lattices: Reactivity Comparison vs. KENO

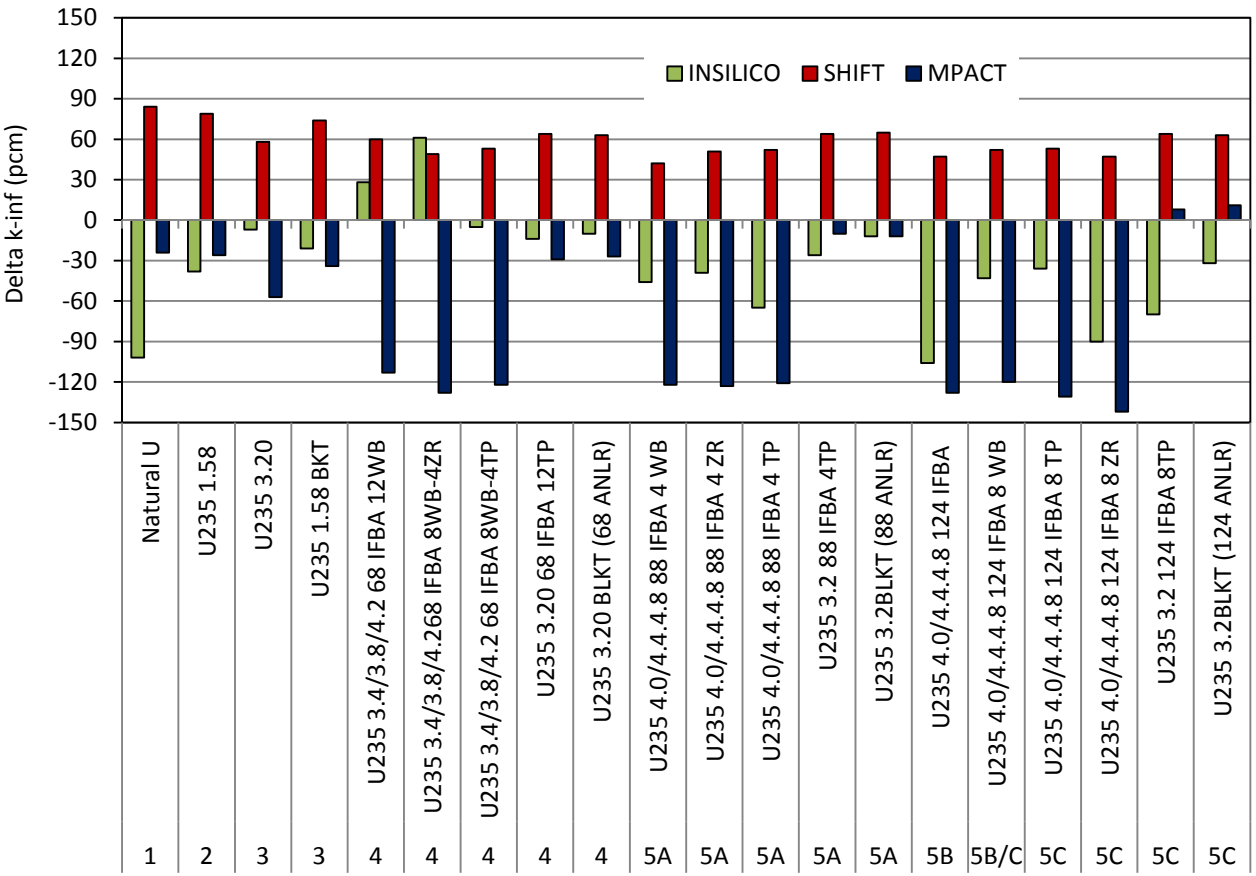

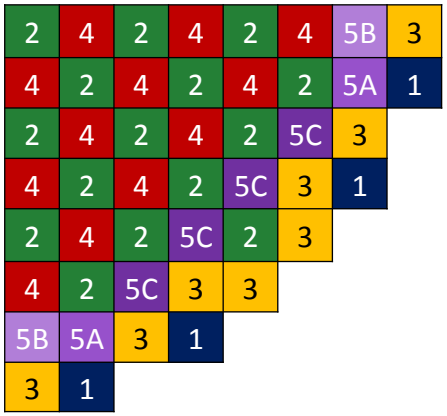

Reg #	% Core	U235 AVG	U235 BLKT	IFBA Rods	WABA Rods
1	10%	0.74	-	0	0
2	31%	1.58	-	0	0
3	18%	3.20	1.58	0	0
4	23%	3.77	3.20	68	8L+4S
5A	5%	4.34	3.20	88	4I
5B	3%	4.34	3.20	124	0
5C	10%	4.34	3.20	124	8I

MPACT appears to have a reactivity bias at high enrichments – XS library?

© 2014 Westinghouse Electric Company LLC. All Rights Reserved.

2D Lattices: Max Delta Pin Power vs. KENO

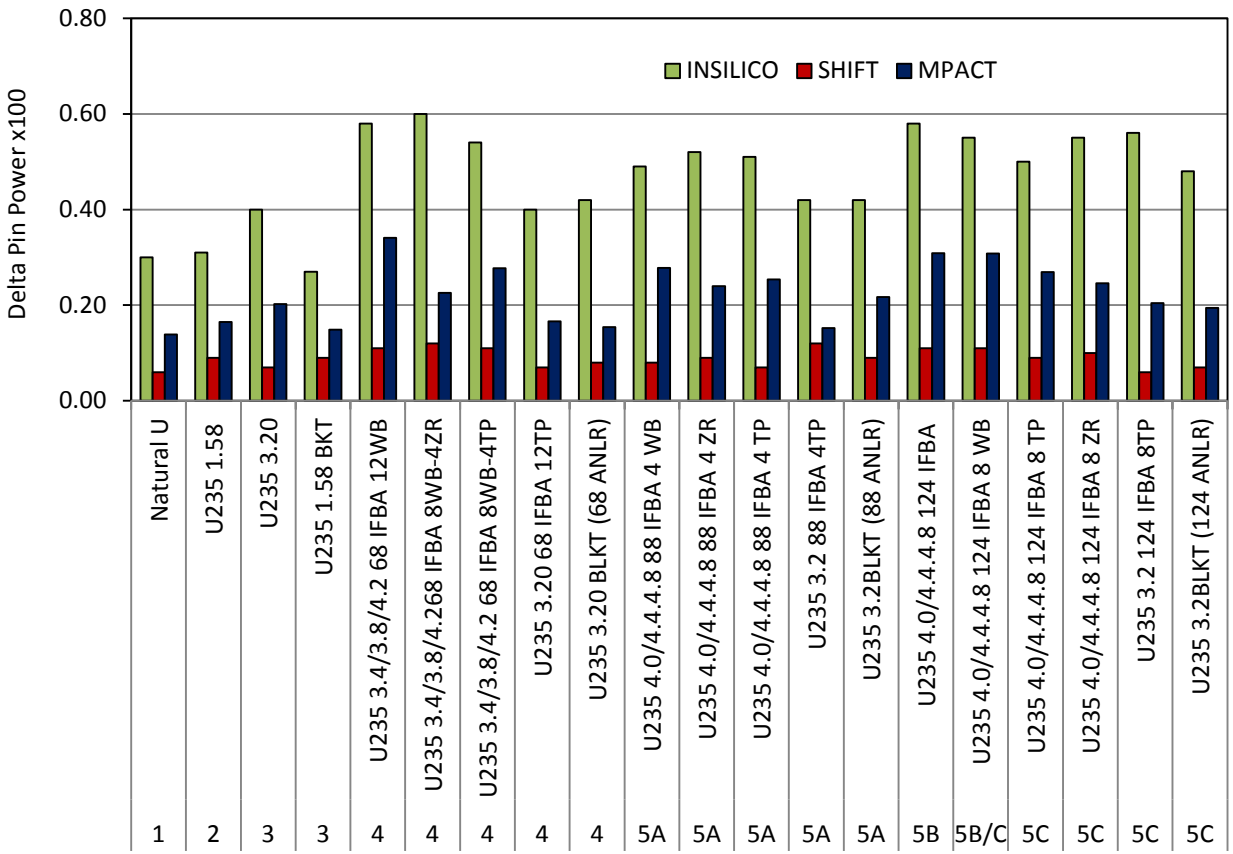

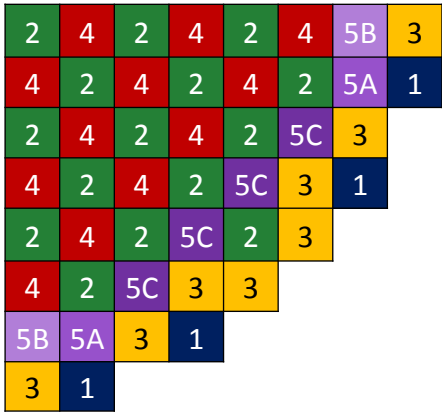

Reg #	% Core	U235 AVG	U235 BLKT	IFBA Rods	WABA Rods
1	10%	0.74	-	0	0
2	31%	1.58	-	0	0
3	18%	3.20	1.58	0	0
4	23%	3.77	3.20	68	8L+4S
5A	5%	4.34	3.20	88	4I
5B	3%	4.34	3.20	124	0
5C	10%	4.34	3.20	124	8I

© 2014 Westinghouse Electric Company LLC. All Rights Reserved.

2D Core Pin Power Comparison

INSILICO

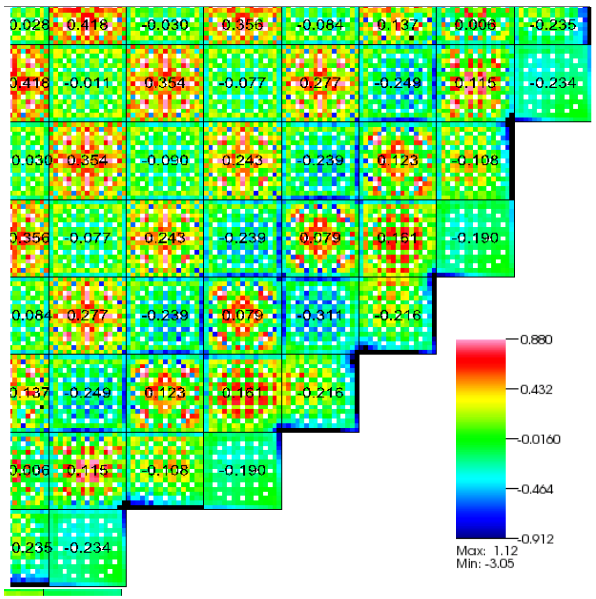

MPACT

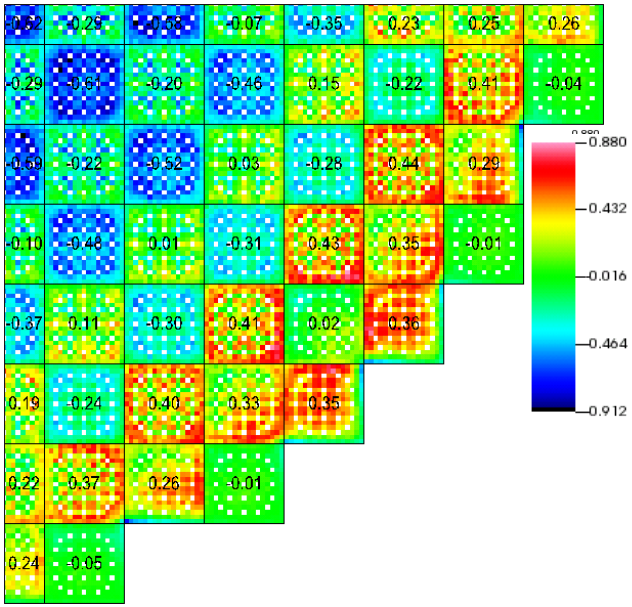

SHIFT

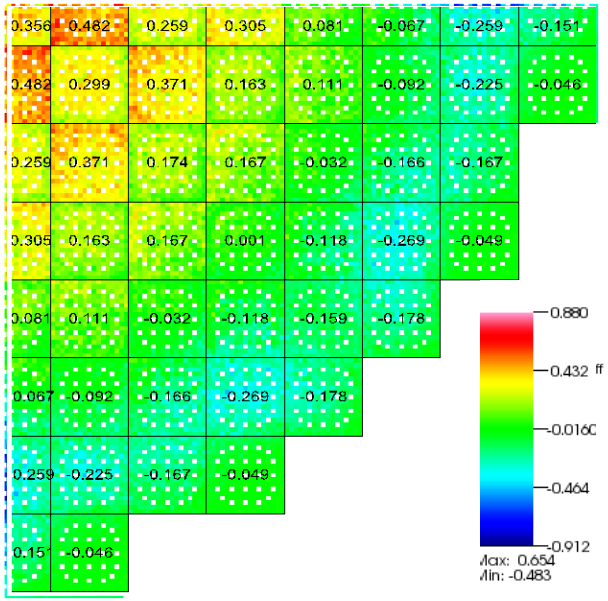

	soluble boron (ppm)	K_{inf} (+/-2 pcm)	ΔK_{inf} (pcm)	RMS ΔP Asm (%)	Max ΔP Asm (%)	RMS ΔP Pin (%)	Max ΔP Pin (%)	Hot Pin ΔP (%)
KENO	1325	1.00096	Ref	Ref	Ref	Ref	Ref	Ref
INSILICO	1325	1.00086	-10	0.2	0.4	0.4	3.0	1.0
MPACT	1325	1.00000	-96	0.3	0.4	0.4	0.9	0.6
SHIFT	1325	1.00131	+35	0.2	0.5	0.2	0.6	-0.2

© 2014 Westinghouse Electric Company LLC. All Rights Reserved.

3D Assembly – Region D (Short and Long WABAs)

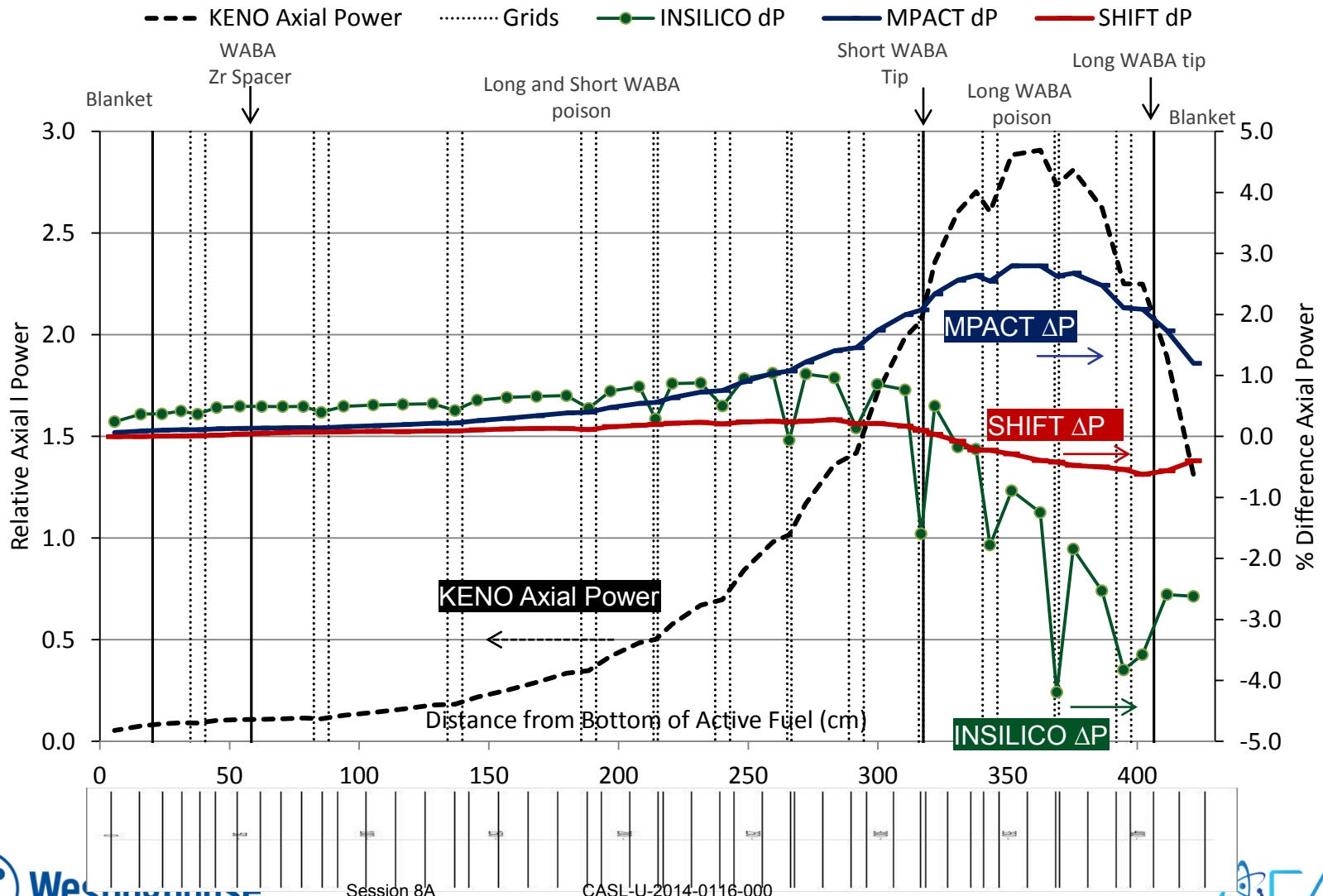

© 2014 Westinghouse Electric Company LLC. All Rights Reserved.

3x3 Assembly w/ CR: Axial Power vs. KENO

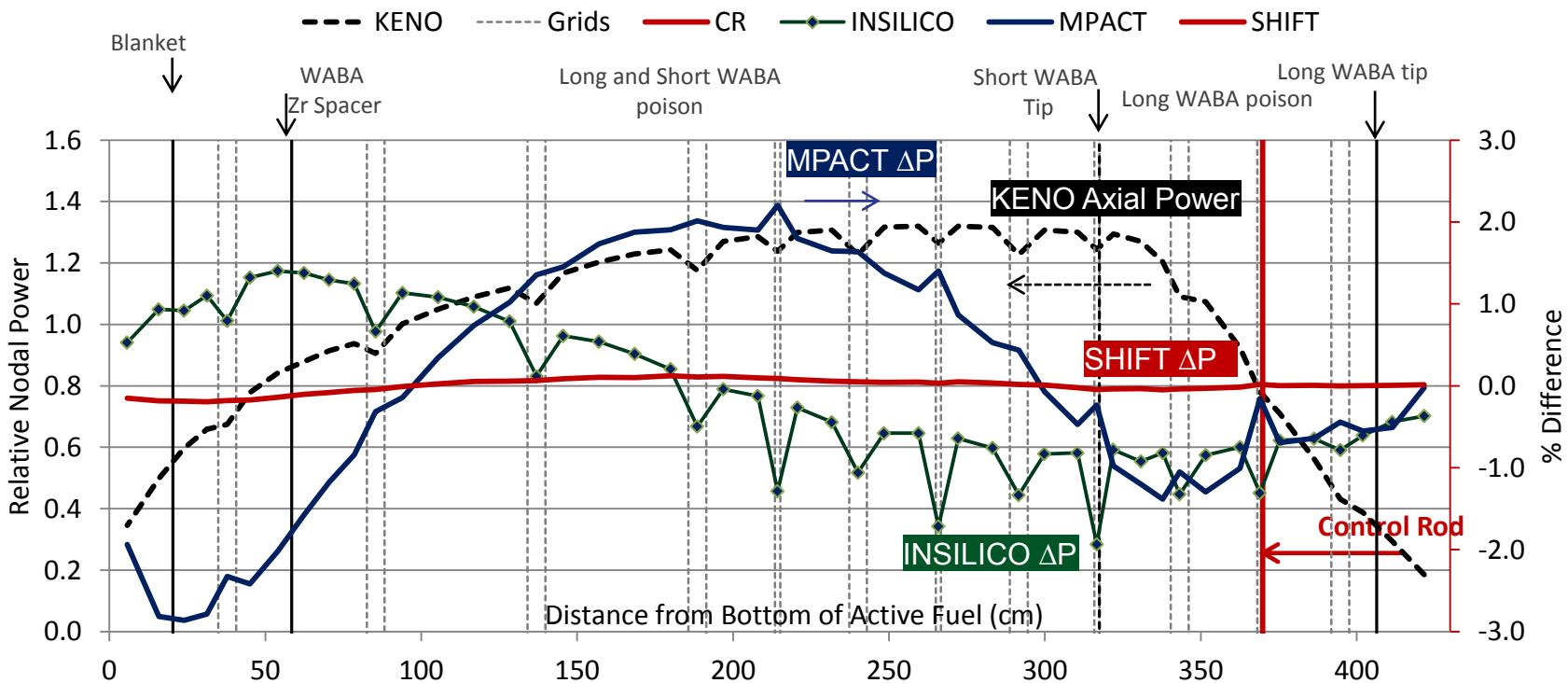

	ΔK_{eff} (pcm)	Δ AO (%)	RMS/Max ΔP Axial "Node" (%)	RMS/Max ΔP Pin (%)	RMS/Max ΔP Cell (%) →	ΔP Hot Spot (%)
INSILICO	-18	-0.7	0.9/2.1	0.3/0.8	0.9/3.1	-0.3
MPACT	-106	0.0	1.5/2.9	0.2/0.5	1.5/4.2	+1.9
SHIFT	+60	0.0	0.1/0.2	0.0/0.1	0.1/0.7	0.1

© 2014 Westinghouse Electric Company LLC. All Rights Reserved.

3D Core Rodded Configuration Results Summary

	K_{eff}	AO (%)	ΔK_{eff} (pcm)	Δ AO (%)	RMS/Max ΔP Axial "Node" (%)	RMS/Max ΔP Asm (%)	RMS/Max ΔP Pin (%)	RMS/Max ΔP Cell (%)	ΔP Hot Spot (%)
SHIFT	1.00141	-0.8	Ref	Ref	Ref	Ref	Ref	Ref	Ref
KENO	1.00090	-0.7	-50	-0.1	0.1/0.2	0.4/1.0	0.4/1.1	0.5/3.0	1.0
INSILICO	1.00078	-1.7	-63	-0.9	1.0/2.9	0.4/0.7	0.5/3.0	1.2/5.8	1.9

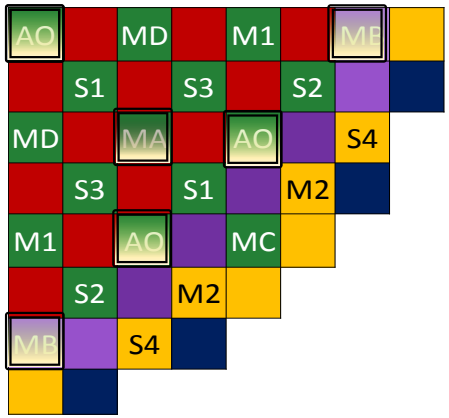

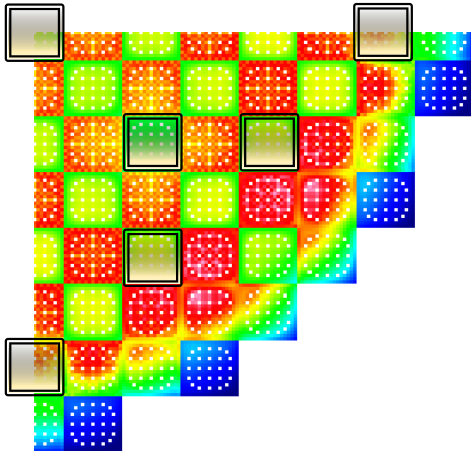

MA (Gray) Fully Inserted
MB (Gray) ~ 60% Inserted
AO (Black) ~ 15% Inserted
Boron at ~1250 ppm
HZP Temperatures

© 2014 Westinghouse Electric Company LLC. All Rights Reserved.

ZPPTs: HZP CBC and Temperature Reactivity Coefficients

	KENO	INSILICO	SHIFT
HZP Critical Boron (ppm)	1313	1310	1315
Boron Worth (pcm/ppm)	-9.6	-9.4	-9.7

	KENO	INSILICO	INSILICO-KENO
Doppler Temperature Coefficient (DTC) pcm/F	-1.54± 0.03	-1.72	-0.18
Moderator Temperature Coefficient (MTC) pcm/F	-1.12± 0.04	-1.50	-0.38
Isothermal Temperature Coefficient (ITC) pcm/F	**-2.66± 0.05**	**-3.22**	**-0.56**

Note: 3D core calculations not yet performed with MPACT
Temperature Coefficients not yet calculated with SHIFT

© 2014 Westinghouse Electric Company LLC. All Rights Reserved.

ZPPTs: Rod Worth

		KENO	INSILICO		SHIFT	
Rod Worth	**Material**	Worth (pcm)	ΔWorth (pcm)	ΔWorth (%)	ΔWorth (pcm)	ΔWorth (%)
MA	**Tungsten**	258	-1	-0.5	4	1.4
MB	**Tungsten**	217	-5	-2.1	-5	-2.3
MC	**Tungsten**	188	-2	-1.1	0	0.1
MD	**Tungsten**	234	0	0.0	5	2.0
M1	**Ag-In-Cd**	651	-4	-0.6	-1	-0.2
M2	**Ag-In-Cd**	887	3	0.4	1	0.1
AO	**Ag-In-Cd**	1635	-4	-0.3	5	0.3
S1	**Ag-In-Cd**	1079	0	0.0	9	0.8
S2	**Ag-In-Cd**	1096	-9	-0.8	-7	-0.6
S3	**Ag-In-Cd**	1124	0	0.0	10	0.9
S4	**Ag-In-Cd**	580	-3	-0.4	-5	-0.9
		RMS	4	0.8	6	1.1
		Max	9	2.1	10	2.3

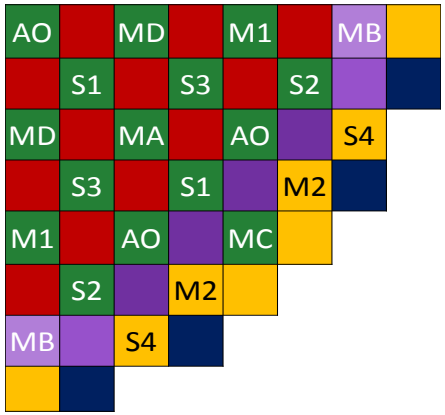

Note: All SHIFT runs are 1T particle simulations
(for power distribution comparison to deterministic)

© 2014 Westinghouse Electric Company LLC. All Rights Reserved.

Usability, Benefits, Recommendations

© 2014 Westinghouse Electric Company LLC. All Rights Reserved.

Computer Resources – AP1000 Qt. Core (MC)

	KENO							SHIFT						
	Particles (x10^9)	K Unc. (pcm)	Pin Unc. %	Cores #	Wall Time	Core Hours	Memory (TB)	Particles (x10^9)	K Unc. (pcm)	Pin Unc. %	Cores #	Wall Time	Core Hours	Memory (TB)
2D Lattice	1.1	3	0.02	312	~3.5h	1K	0.8	1.1	10	0.02	4,000	14m	1K	8.0
3x3 Lattice	3	2	0.04	300	~10h	3K	1.0	10	3.7	0.04	4,800	115m	9K	9.6
2D Core	25	0.5	0.06	300	~6d	43K	1.6	100	3.5	0.04	56.000	95m	89K	110
3D Assembly	17.5	1	0.08	240	~3d	17K	1.3	25	3.3	0.04	56,000	29m	27K	110
3D 3x3 Assembly	25	0.3	~0.1	180	~6d	26K	~1	100	2.9	0.05	56,000	131m	123K	110
3D Core (Eigenvalue)	25	1.5	0.38	180	6.5d	28K	~2	50	7	~0.6	50,000	46m	39K	100
3D Core (Pin Power)	100	0.3	0.19	240	22d	128k	~2	1,000	2.7	~0.1	240,000	3h	722K	469

Description of MC Parameters used in Test Stand report (App. A)

© 2014 Westinghouse Electric Company LLC. All Rights Reserved.

Comp. Resources – AP1000 Qt. Core (Deterministic)

	INSILICO SP_5P_3 23g					MPACT 2D/1D Diffusion 56g			
	Cores #	Cells #	Core Hours	Wall Time	Memory	Cores #	Core Hours	Wall Time	Memory
2D Lattice	12	324	0.2	~1 min	<96 GB	8	1.3	10m	< 32GB
3x3 Lattice	12	3K	0.4	~2 min	<96 GB	72	6.0	5m	< 80 GB
2D Core	144	86K	13	~5 min	<512 GB	440	477	65m	< 448 GB
3D Assembly	64	0.2M	32	30 min	<512 GB	496	91	11m	< 256 GB
3D 3x3 Assembly	144	1.5M	96	40 min	<1.2 TB	472	1.6K	200m	< 240 GB
3D Core (Eigenvalue)	320	6M	0.5K	100 min	<4 TB				
3D Core (Pin Power)	4,096	24M	2.3K	34 min	<32TB	3520	43K	740m?	<3.5 TB

P2 Scattering, Ray Spacing of 0.005 (IFBA), 8 angles and 4 rings per pellet in MPACT.
Note that memory requirements are for fresh fuel.

© 2014 Westinghouse Electric Company LLC. All Rights Reserved.

Usability

- Intuitive single-input deck
- Similar to typical core simulators
- Excessive computational time.
- Cycle depletion with coupling appears impractical
- Immature. Needs testing and bug fixing
- Some convergence issues in 3D geometry
- Mesh geometry file needed for setup is difficult and should be automated
- Very limited validation. Needs a reference (Monte-Carlo and/or measurements when available) for comparison
- Depletion under development
- No thermal expansion
- Lack of rotational symmetry
- Limited reflector options
- Limited documentation

© 2014 Westinghouse Electric Company LLC. All Rights Reserved.

Benefits

- Enhanced confidence in **AP1000** PWR start-up predictions
- Generated high-quality benchmarks for code comparison
  - KENO, SHIFT
  - Surprisingly good results from INSILICO
  - Analysis underway with MPACT and issues actively worked on
- Expanded application of VERA to an advanced core
- Provided feedback to guide future developments
- Provided framework for VERA build and update

© 2014 Westinghouse Electric Company LLC. All Rights Reserved.

Main Recommendations

- **Understand and resolve ITC predictions**
- **Understand and resolve axial power distribution challenges with axially heterogeneous fuel**
- **Mitigate computational resources**
  - **Practical calculation time and number of computer cores**
  - **Cycle depletion overnight on <~1,000 cores**
- **Multi-cycle depletion coupled analysis required**
- Expand capabilities
  - Thermal expansion
  - General reflector
  - Other fuel lattice configurations
- Expand validation basis with other plants
- Improve output
- Improve documentation

© 2014 Westinghouse Electric Company LLC. All Rights Reserved.

Reporting

- Test stand activity documented in public report
  - CASL-U-2014-0012-000

EXECUTIVE SUMMARY iii
1 INTRODUCTION 15
2 THE WESTINGHOUSE TEST STAND EXPERIENCE 17
3 VERA BUILD 20
4 ADVANCED FIRST CORE OF THE AP1000 PWR 24
5 APPROACH TO SIMULATIONS 38
6 RESULTS 48
6.1 2D Lattice Results 48
6.2 2D Multi-Lattice 51
6.3 2D Core 55
6.4 3D Single Assembly 63
6.5 3D Multi-Assemby 68
6.6 Zero Power Physics Tests 71
7 COMPUTATIONAL REQUIREMENTS 75
8 USABILITY OF VERA-CS 78
9 CONCLUSIONS 82
10 ACKNOWLEDGEMENTS 84
11 REFERENCES 85
APPENDIX A CE KENO-VI SIMULATIONS 88
APPENDIX B RADIAL REFLECTOR SENSITIVITY STUDY 103
APPENDIX C AXIAL REFLECTOR SENSITIVITY STUDY 110
APPENDIX D KENO ISOTHERMAL TEMPERATURE COEFFICIENT 114
APPENDIX E KENO VERIFICATION AGAINST MCNP 120
APPENDIX F VERA INSTALLATION GUIDE 121
APPENDIX G VERA AP1000 INPUT 125

© 2014 Westinghouse Electric Company LLC. All Rights Reserved.

Conclusions

- Relevant and engaging application of VERA to an advanced PWR first-core
- Good agreement between INSILICO and Monte-Carlo
  - Critical boron and rod worth
  - Power distribution
  - Differences in Reactivity coefficients (ITC, MTC)
- Ongoing analysis with MPACT (2D/1D) shows issues in 3D cases with tilted power shape and/or axial heterogeneities
- Serious concerns from excessive computational resources and completing methods implementation/development
- Extensive validation work is required

EPRI Test Stand

Brenden Mervin (EPRI), Project Engineer

CASL Round Table
July 15, 2014

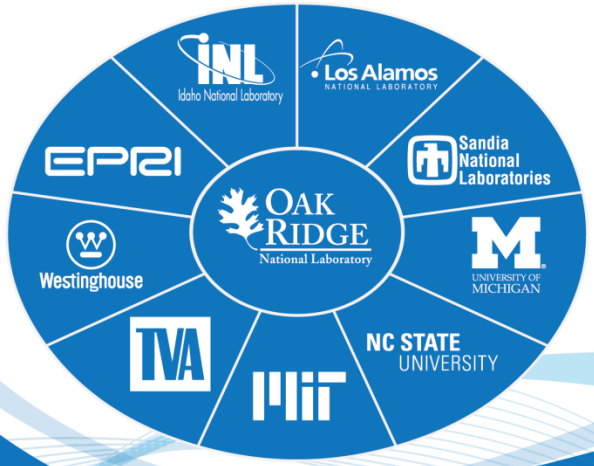

Overview

- EPRI Test Stand Deployment
- Installation and Testing
- EPRI Test Stand Results
  - Early results
  - Updated results
- Conclusions

EPRI Test Stand Deployment
Peregrine

- Built upon the MOOSE/ELK/FOX framework as an extension of the BISON code developed by Idaho National Laboratory (INL)
  - Input/output (I/O)
  - Thermal transport
  - Mechanical solutions
  - Chemical transport
- Capabilities
  - Finite element (FE) framework
  - 2D and 3D modeling capabilities
  - Swelling/densification modeling
  - Irradiation creep/growth
- Under active development
  - Fuel cracking behavior
  - Fission gas release
  - Contact modeling
  - Friction modeling
- Uses Paraview for post processing

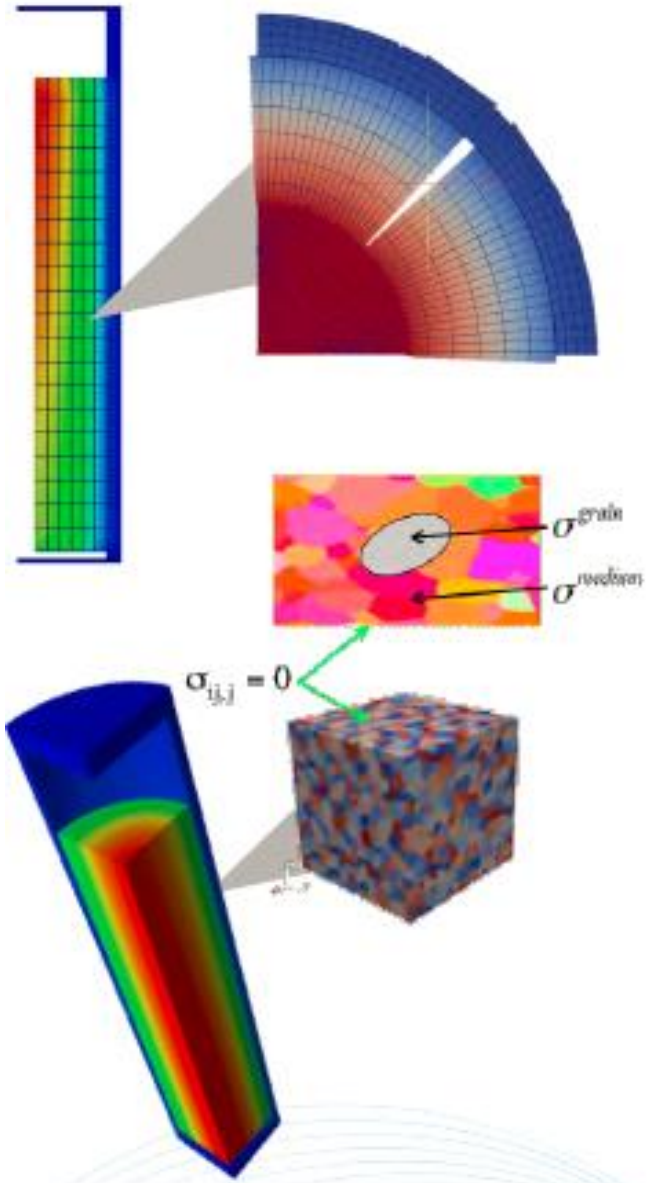

Source: Peregrine training slides

EPRI Test Stand Deployment
Phoebe – EPRI's High-Performance Computer

- Greek goddess of intellect and prophecy
- Specifications:
  - Intel® Xeon® processors
  - 31 nodes
  - 496 compute cores (~250 iPhones)
  - 100 TB storage (~1,600 iPhones)
  - 2 TB memory (~2,000 iPhones)
  - 8 teraflops (~8,700 iPhones)
  - QDR Infiniband
    - 2.5 Gbit/s (x150 faster 4G LTE)
  - Linux & Windows OS

Installation & Testing

- Updated VERA Installation (February 2014)
  - Process streamlined well as a result of the Westinghouse Test Stand
    - VERA Installation Guide
    - Installation scripts for TPLs
    - CASL Support
  - CASL support staff eager to help with architecture dependent issues
- Testing
  - Simple in most cases
  - Peregrine test suite not integrated into VERA
    - Only testing is to verify executable
    - Unit/validation tests exist in MOOSE

EPRI Test Stand Deployment
October 2013

- **Scope**
  - VERA installation & verification
  - Training
  - Assess Peregrine using Watts Bar data
- **Status**
  - VERA installed on the new EPRI industry class HPC system during October 2013
  - Training and code assessment work performed
  - Hundreds of cases analyzed
  - Test Stand report due August 1st

Component	Included	May Be Included	Not Included	Comments
Physics Components				
COBRA-TF	X			Standalone with VERAIn input
Insilico	X			Sn/Spn with Scale/XSProc and VERAIn input
Coupled Insilico + COBRA-TF	X			Single assembly
Hydra-TH			X	
MPACT	X			
MAMBA-2D			X	
Peregrine	X			Standalone
MOOSE/Bison	X			Required for Peregrine
Tiamat (CTF + Insilico + Peregrine)			X	Not ready for use.
Coupled COBRA-TF + MAMBA-2D			X	Not ready for use.
Shift			X	
Infrastructure Components and TPLs				
Trilinos	X			
TriBITS	X			
VERAIn	X			Common VERA input parser
Dakota	X			With COBRA-TF examples (VUQDemos)
LIME	X			
DataTransferKit	X			
Other Required TPLs	X			As defined in the VERA Installation Guide.

EPRI Test Stand Results

- End Goal: evaluate hoop stress results using Watts Bar Unit 1 data provided by TVA and Westinghouse
- Challenges
  - Full length fuel rod (meshing)
  - Complex power profile including both down power and second cycle startup
- Risks
  - Significant development of Peregrine still underway throughout Test Stand
  - Moderate risk of not achieving end goal due to complexity of modeling PWR fuel rods
    - Full-length fuel rods (not documented/well-validated)
    - Heat-up and cool-down power histories (significant power changes introduce solution instabilities)

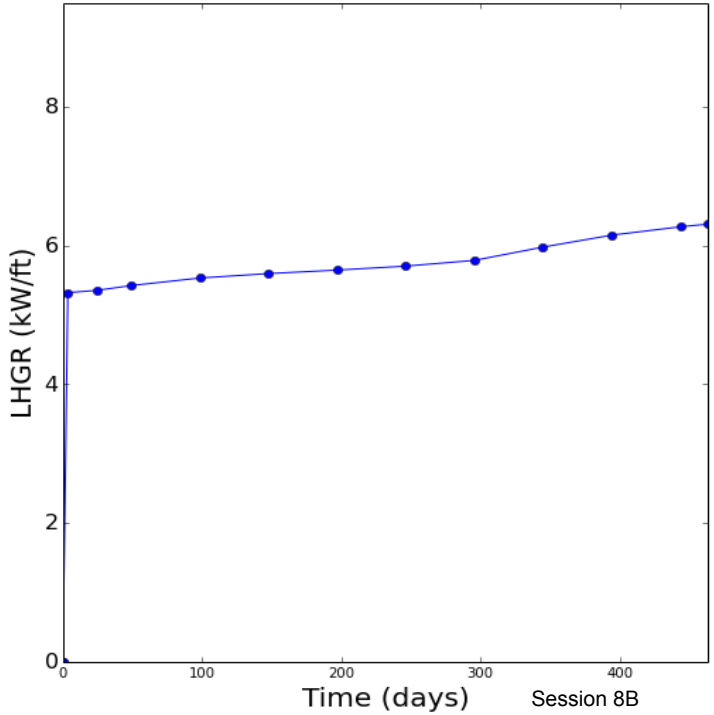

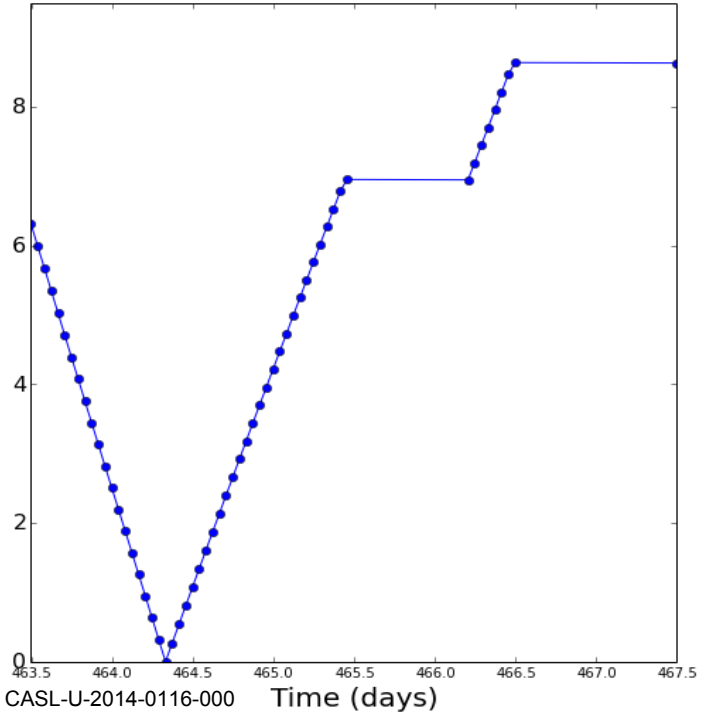

EPRI Test Stand Results

Thermal results: fuel centerline temperature

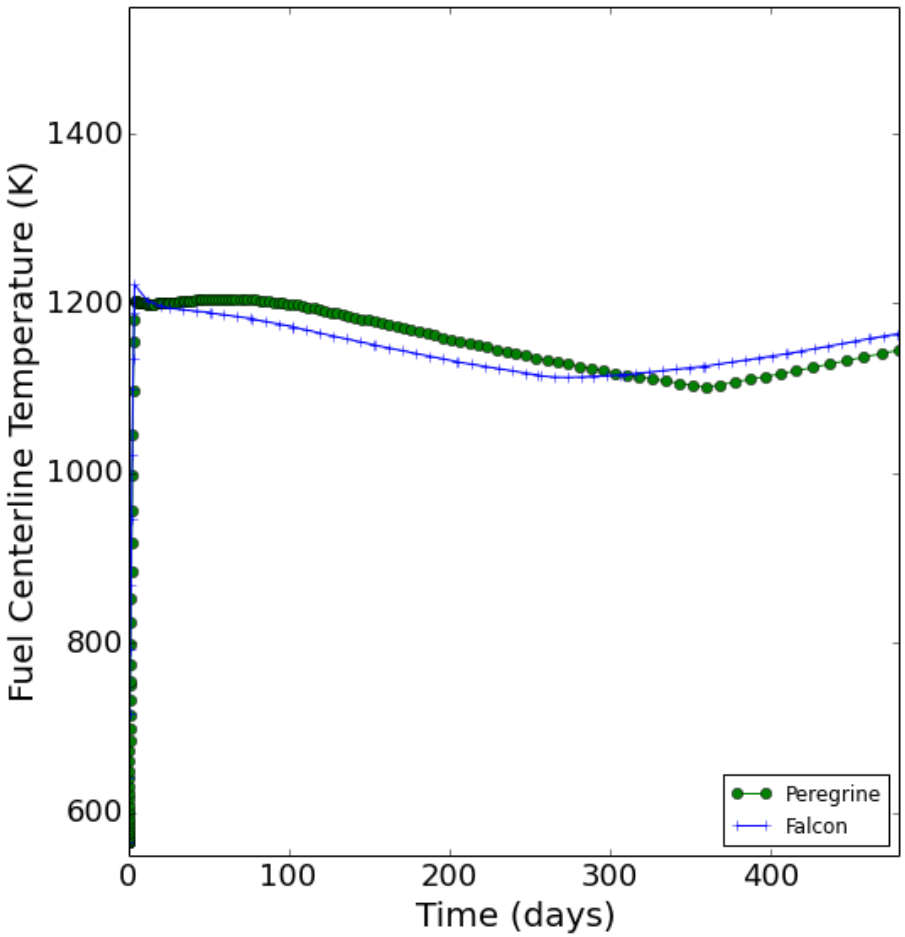

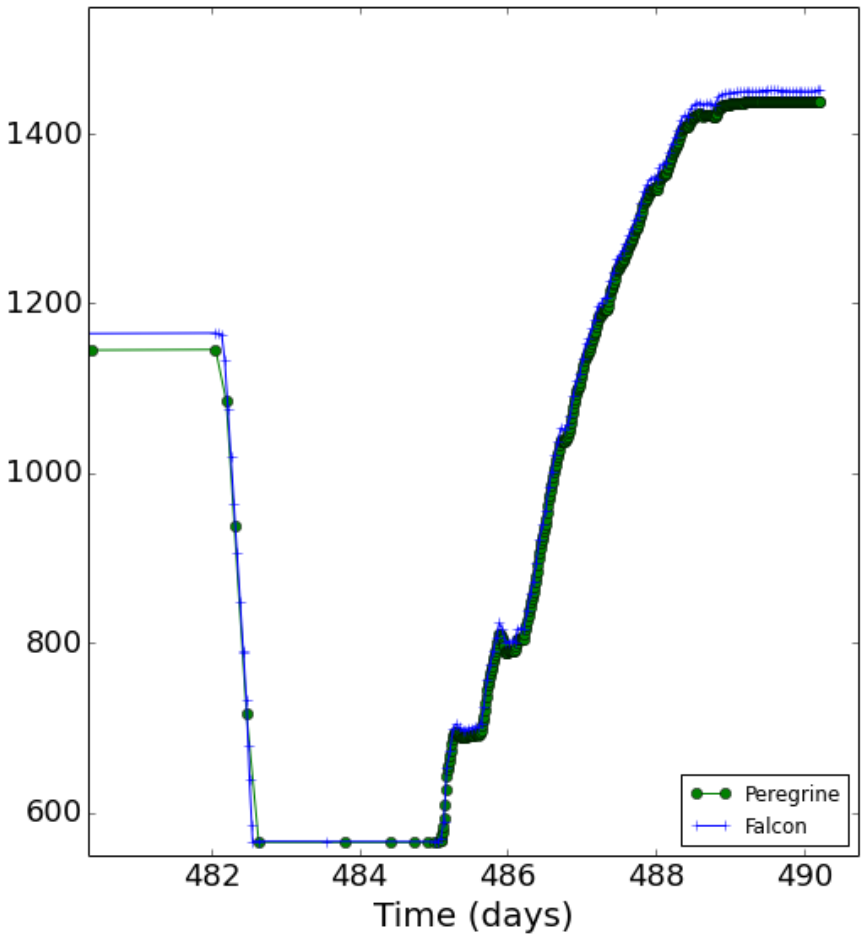

Good agreement in fuel centerline temperature between Falcon and Peregrine (March 2014)

EPRI Test Stand Results

Mechanical results: gap closure behavior

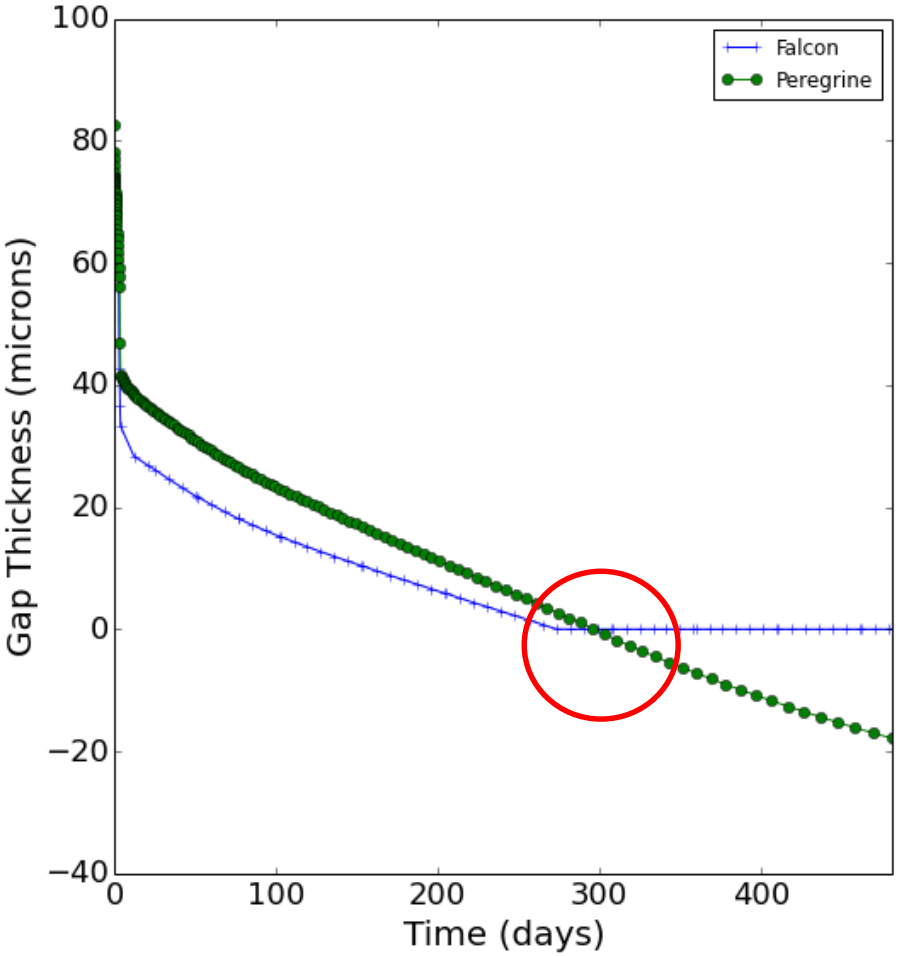

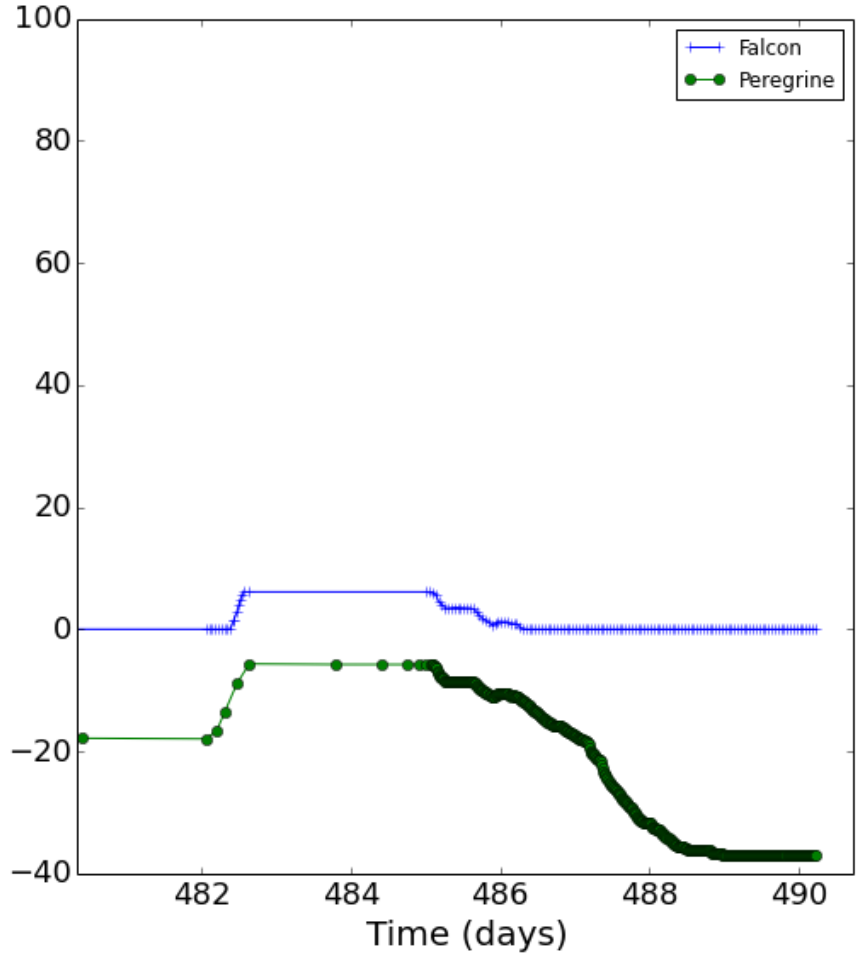

Gap closure predictions within approximately 30 days of each other

EPRI Test Stand Results

Mechanical results: hoop stress comparison

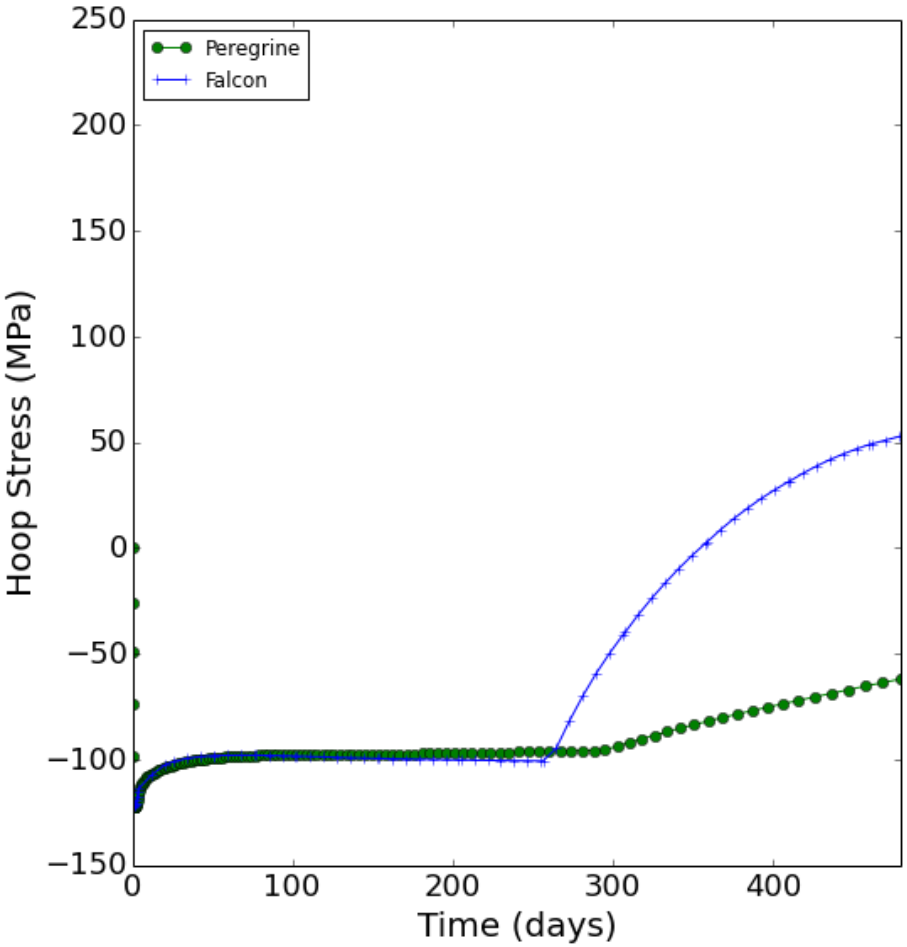

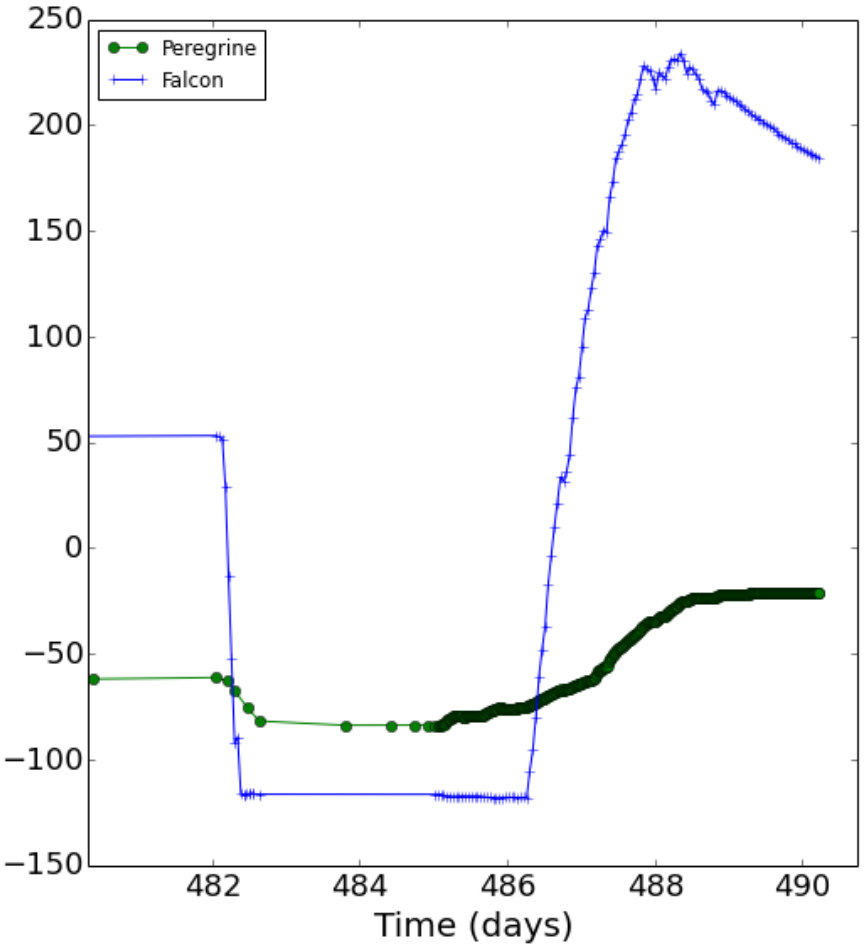

Hoop stresses not being generated due to mechanical contact formulation

EPRI Test Stand Results
Analysis of Results (April-May 2014)

- Pellet-cladding contact and friction modeling still undergoing significant development activities
  - ☑ Kinematic contact formulation instead of penalty (April)
  - ☑ SIFGRS fission gas release model much more stable than Forsberg-Massih in Peregrine (April)
  - ☑ Frictionless contact model with release (May)
  - ☑ Constraint-based contact system (July)
- Mesh refinement required
- Time stepping strategy needed additional attention

EPRI Test Stand Results

Gap width using kinematic formulation (April 2014)

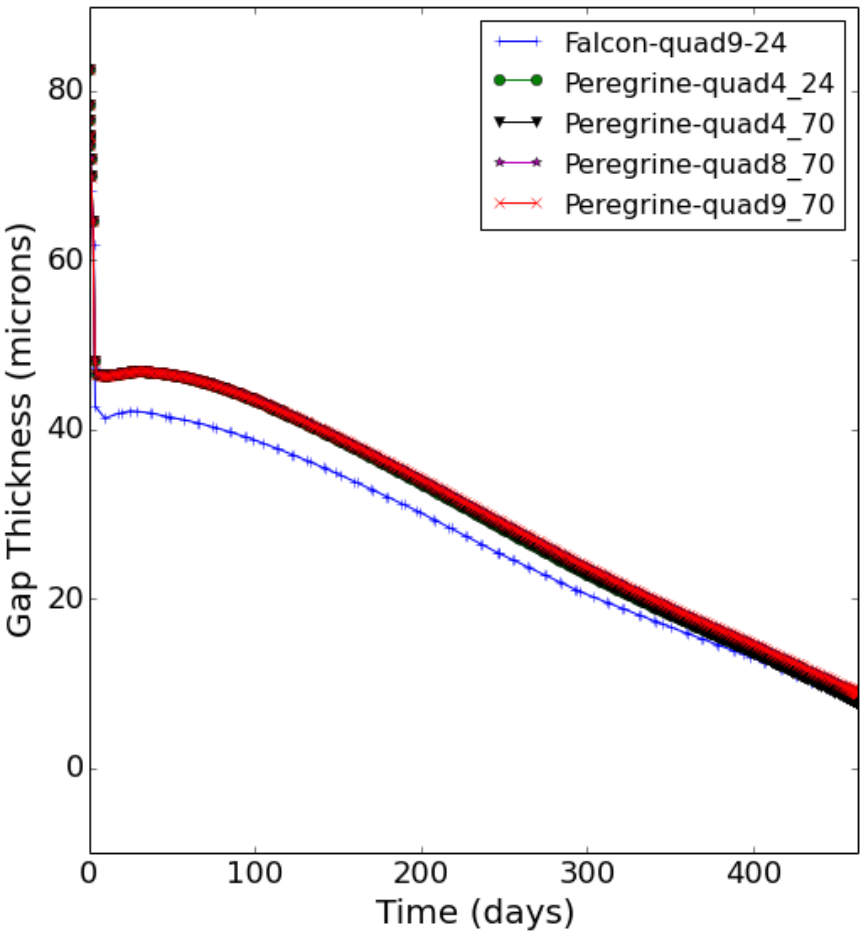

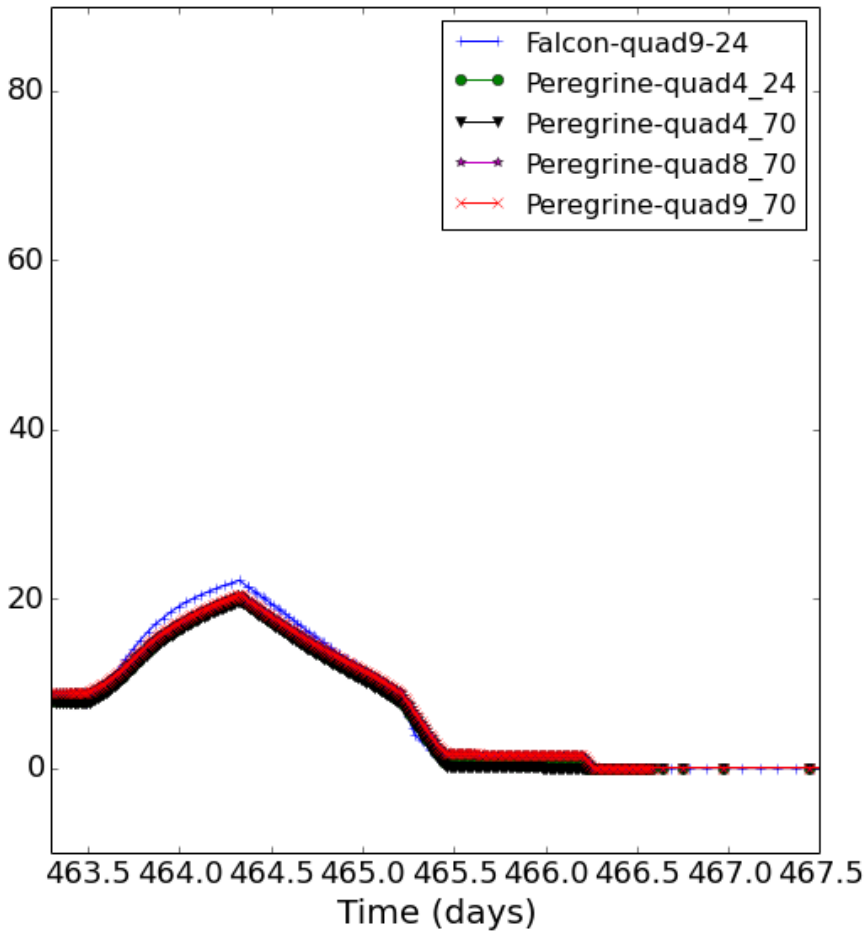

Gap thickness agreement is significantly improved

EPRI Test Stand Results

Gap closure with increased power history (April 2014)

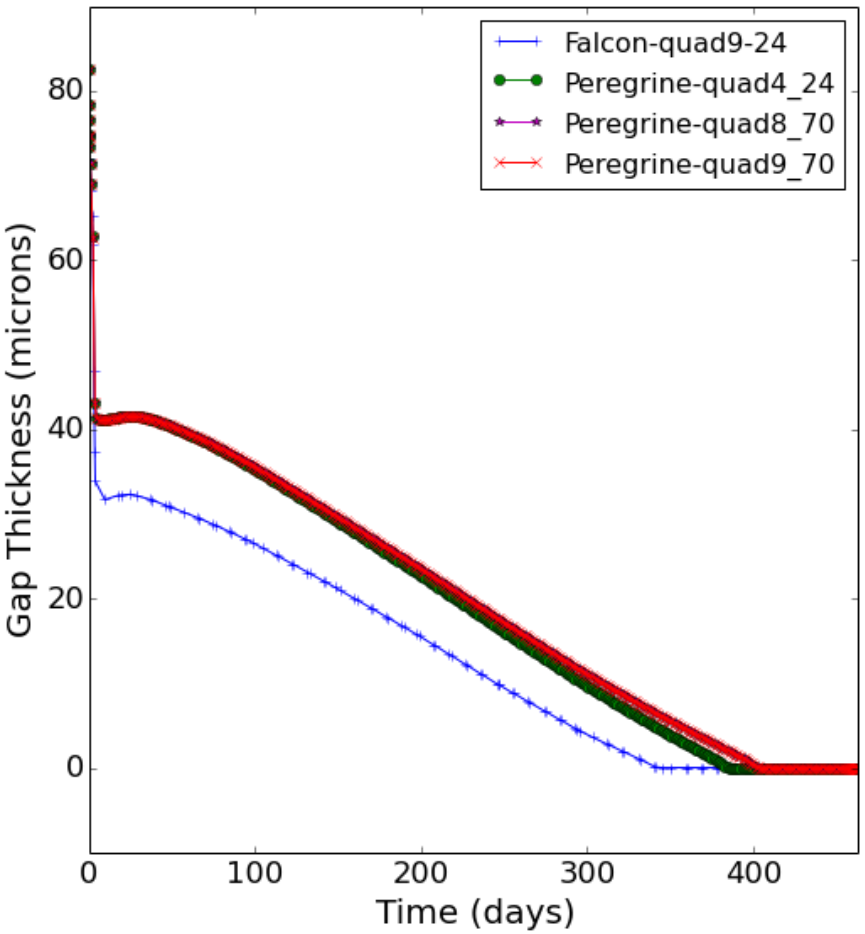

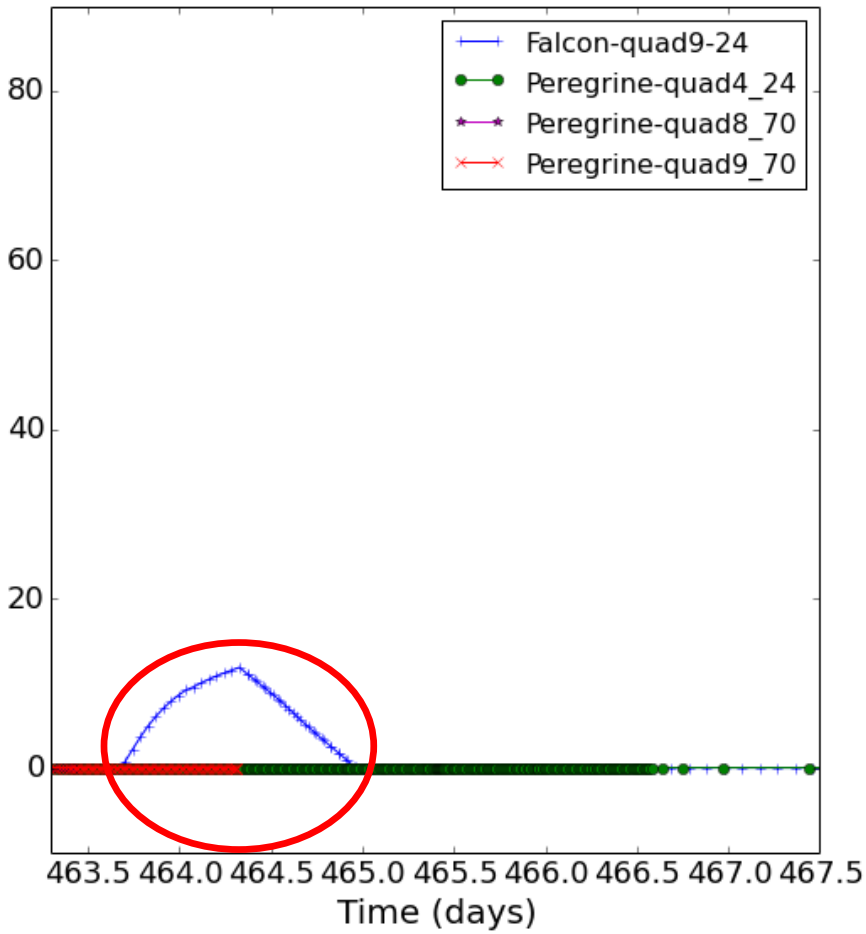

Fuel-cladding glued together.

EPRI Test Stand Results

Gap closure using contact model w/ release (June 2014)

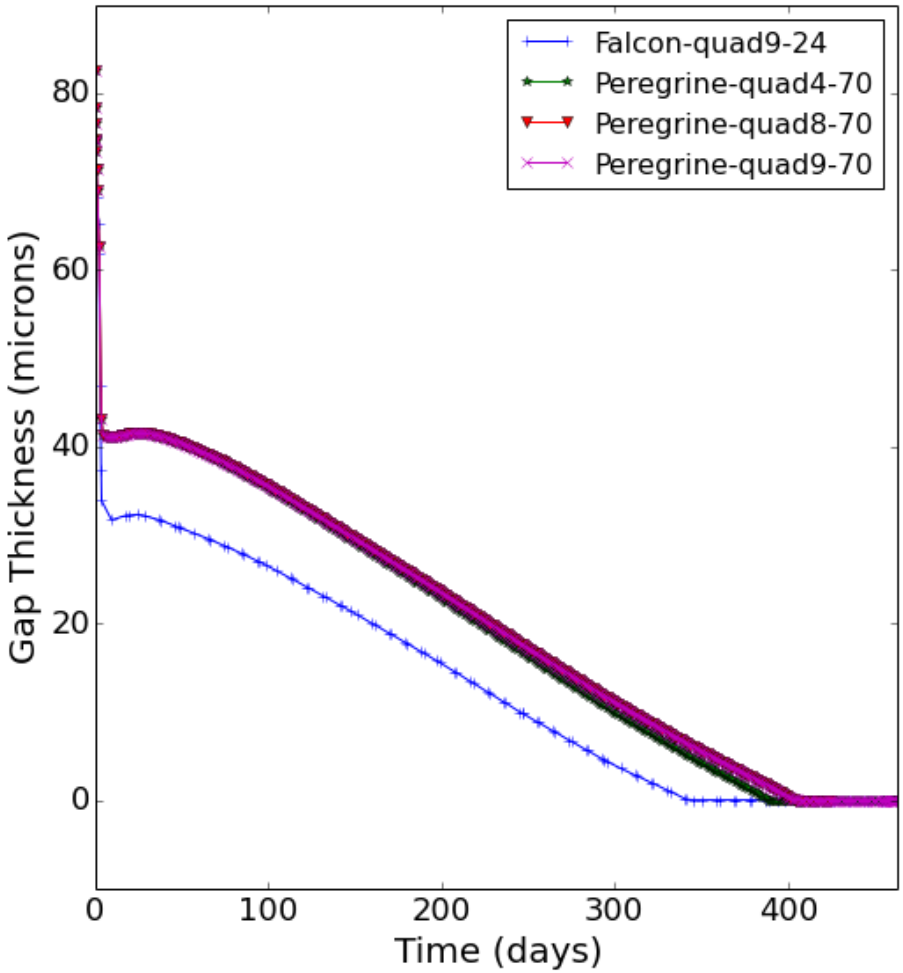

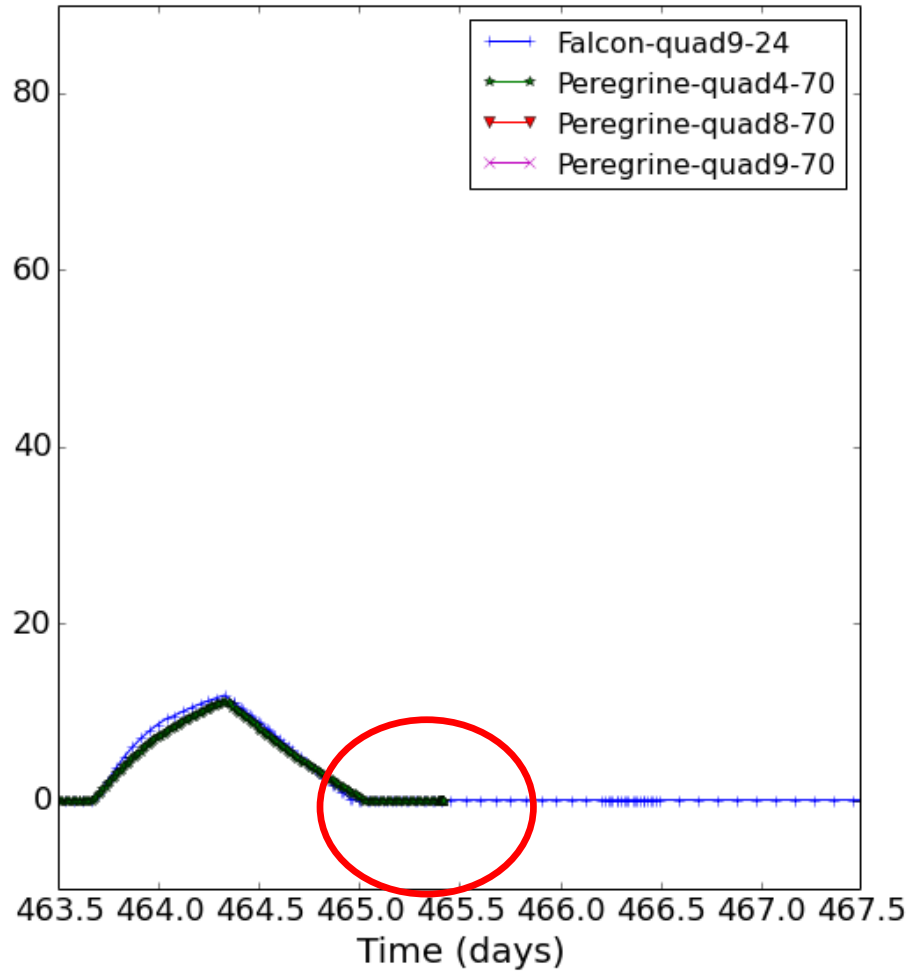

Stability issues observed when power ramps after gap is closed

Progression Problem Strategy (June-July 2014)

1. Thermal analysis of shortened rod with a flat axial profile
2. Single-cycle thermo-mechanical analysis of a full-length PWR fuel rod
3. Scale up power history to force gap closure
4. Append period of down power to single-cycle simulation
5. Append additional ramp to single-cycle simulation (no down power)
6. Thermo-mechanical analysis with down power and 2nd cycle ramp
7. Thermo-mechanical analysis using proprietary reactor data

EPRI Test Stand Results
Gap thickness results

Falcon

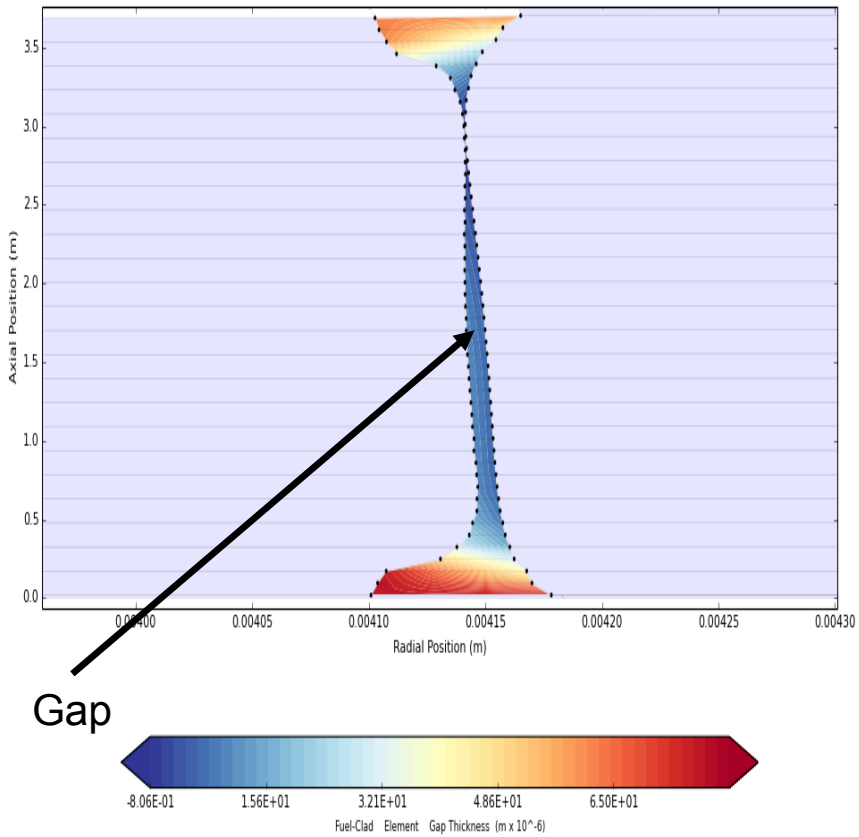

Peregrine

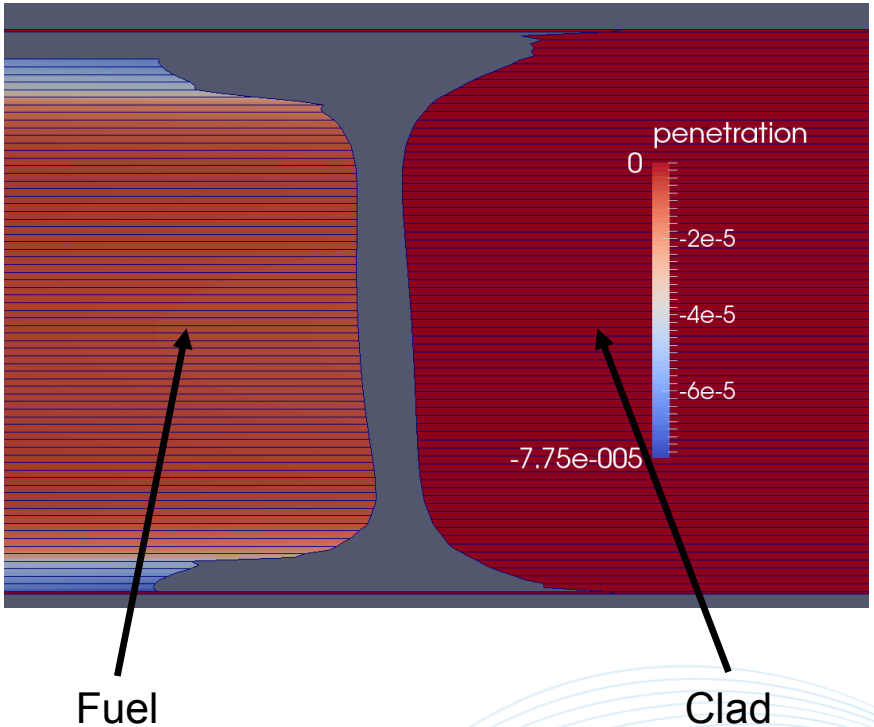

EPRI Test Stand Results
Fuel/clad temperature/displacement

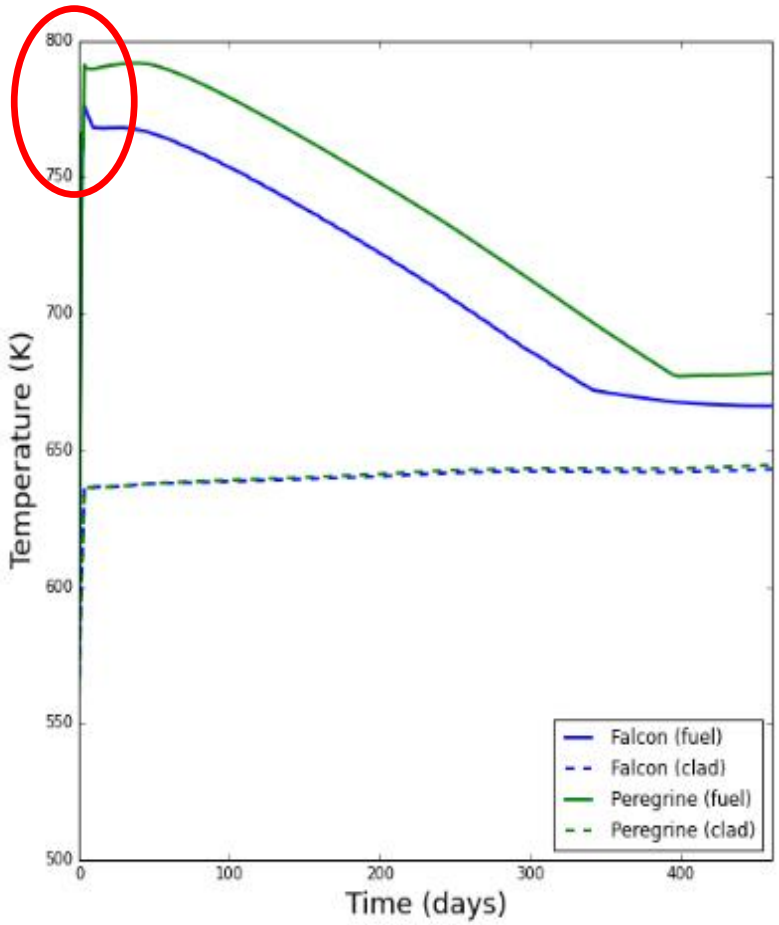

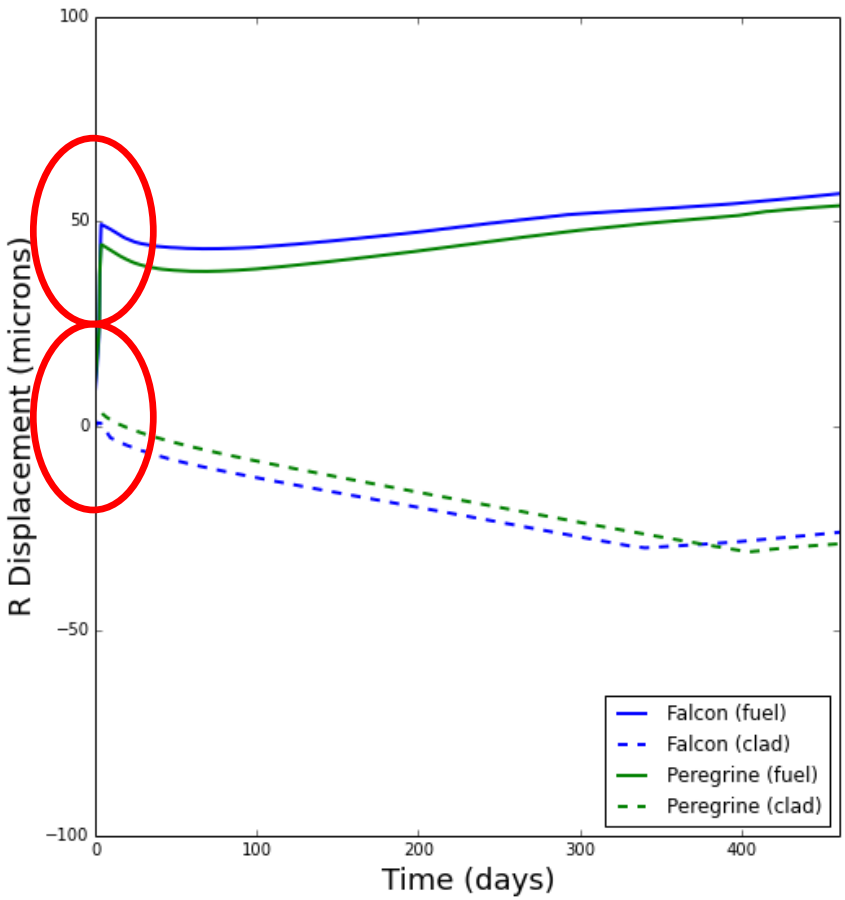

Significant difference in estimates produced during power ramp

EPRI Test Stand Results

Fuel/clad temperature/displacement

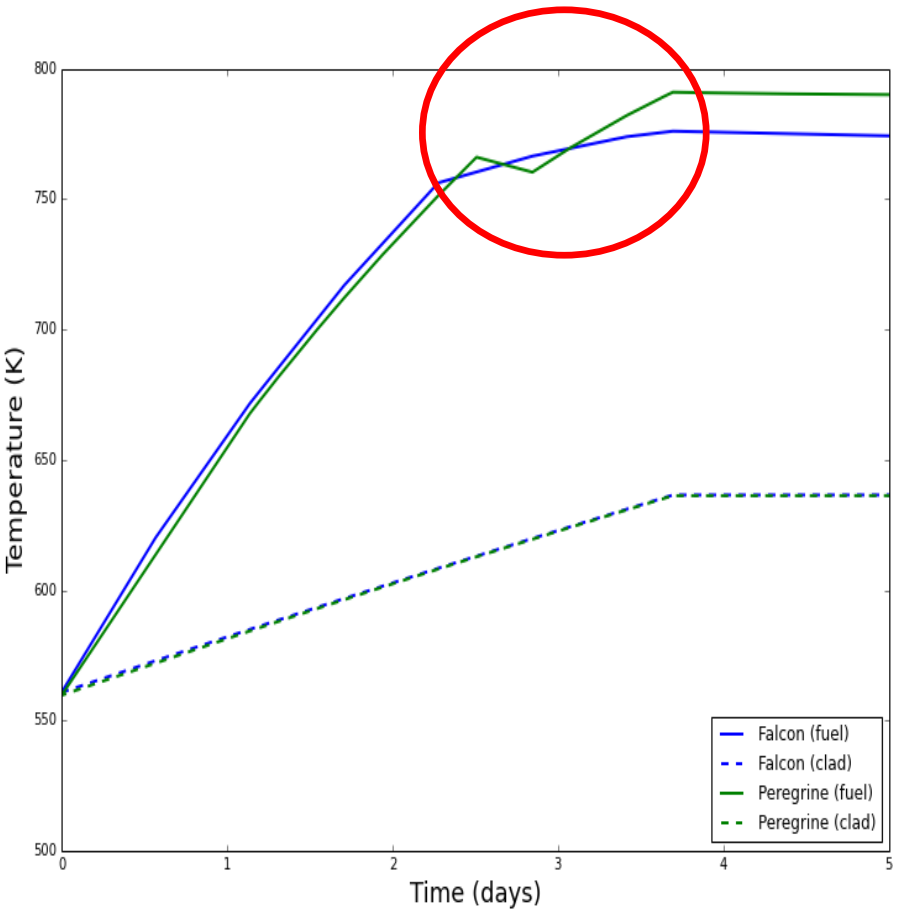

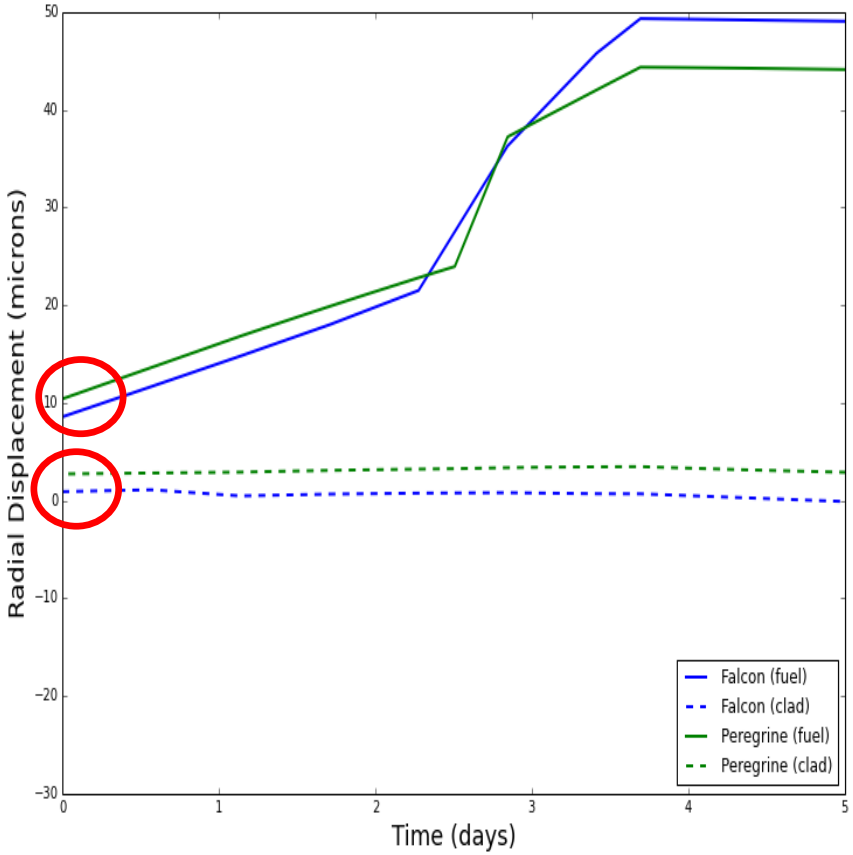

Interesting differences observed during the initial ramp period

EPRI Test Stand Results

Hoop stress trends are the same

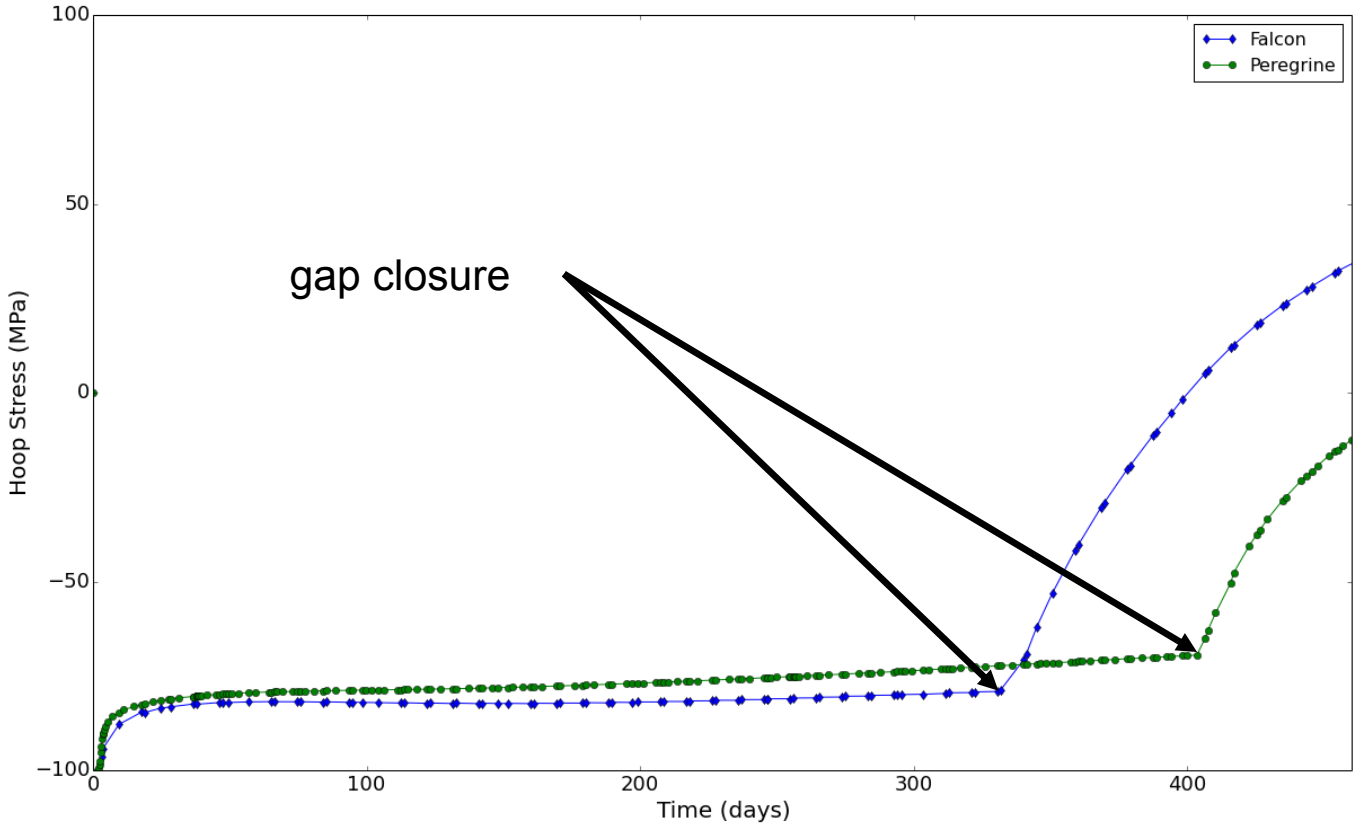

Conclusions

- Technical Evaluation
  - Impressive potential to solve multi-physics simulations in 2D and 3D space
  - Native Peregrine input is cumbersome
  - Significant work on guidance and documentation is required in order to integrate Peregrine into VERA and release these capabilities to the user community
  - Comparisons with other fuel performance codes are difficult and important so that the general behavior of Peregrine can be verified
  - **Deriving definitive assessments/conclusions is inappropriate: authoritative comparisons between codes should never supplant data validation of individual codes**
- Administrative Evaluation
  - Repository updates taxing too everyone involved
  - Technical issues being documented and tracked in CSICAT
  - Testing/verification needs to be integrated into VERA test suite
  - Continuous validation required as development progresses (requires appropriate PIE data)
  - Technical/administrative meetings essential to Test Stand success
  - INL support available through user's groups
  - **Support is key to maximizing Test Stand efficiency and success**

Supplemental Slides

EPRI Test Stand Results
Difference in mesh formulation

Falcon

Peregrine

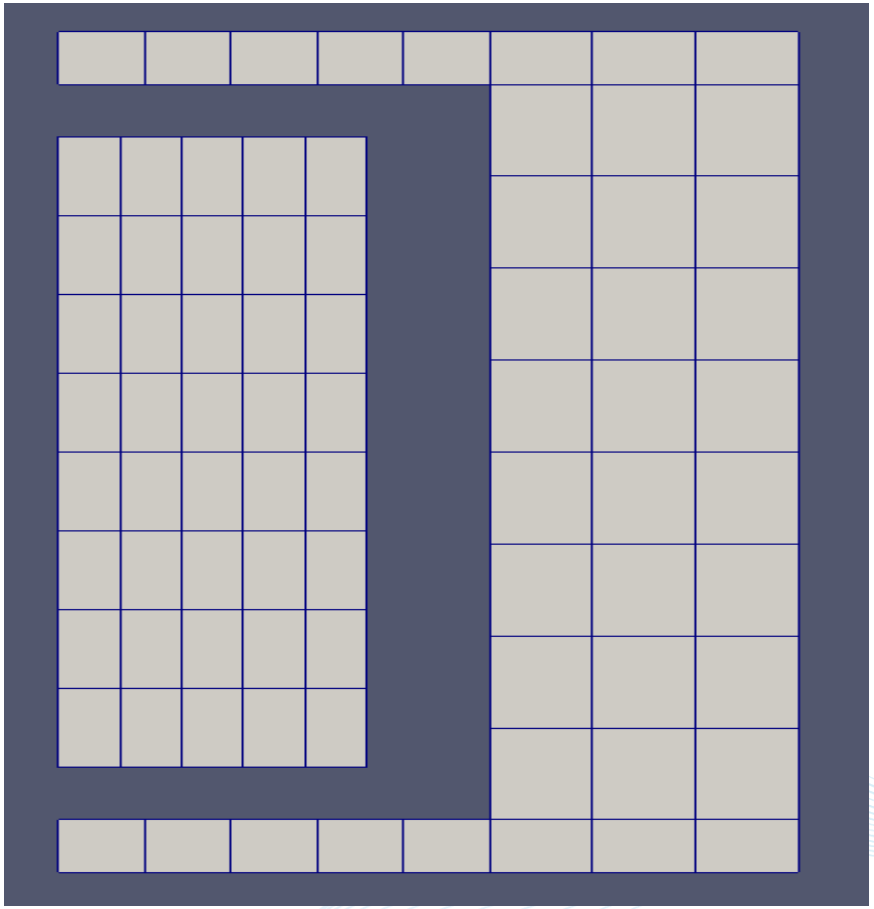

Mesh Study

- Mesh
  - # Axial: 24, 48, 96, 144
  - # Fuel Radial: 3, 5, 10, 20
  - # Clad Radial: 2, 3, 6, 12

- Parameters:
  - Temperature
  - Displacement
  - Gap thickness
  - Hoop stress

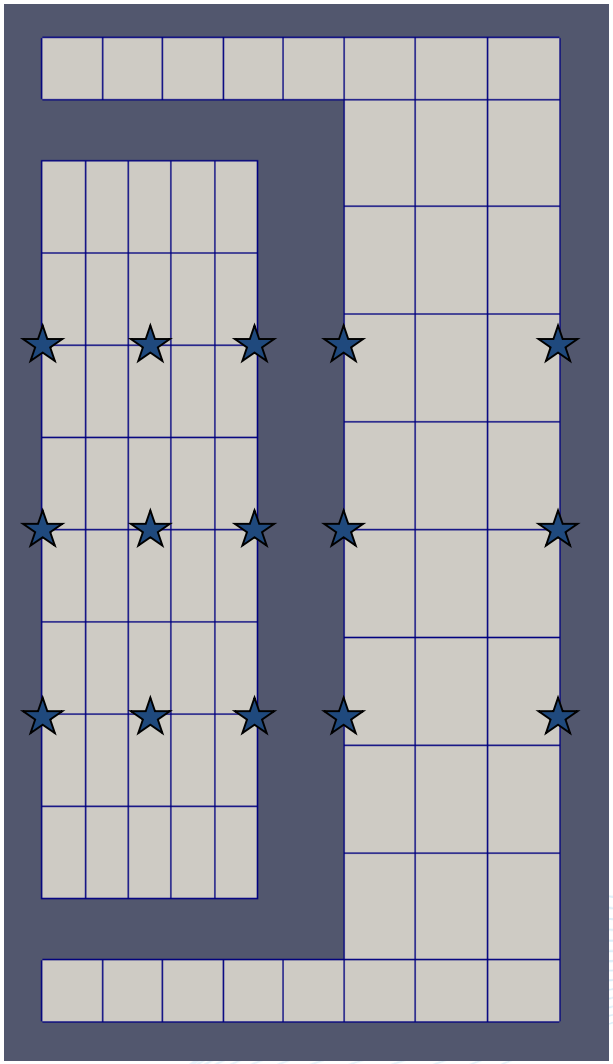

EPRI Test Stand Results

Hoop stress using kinematic formulation (April 2014)

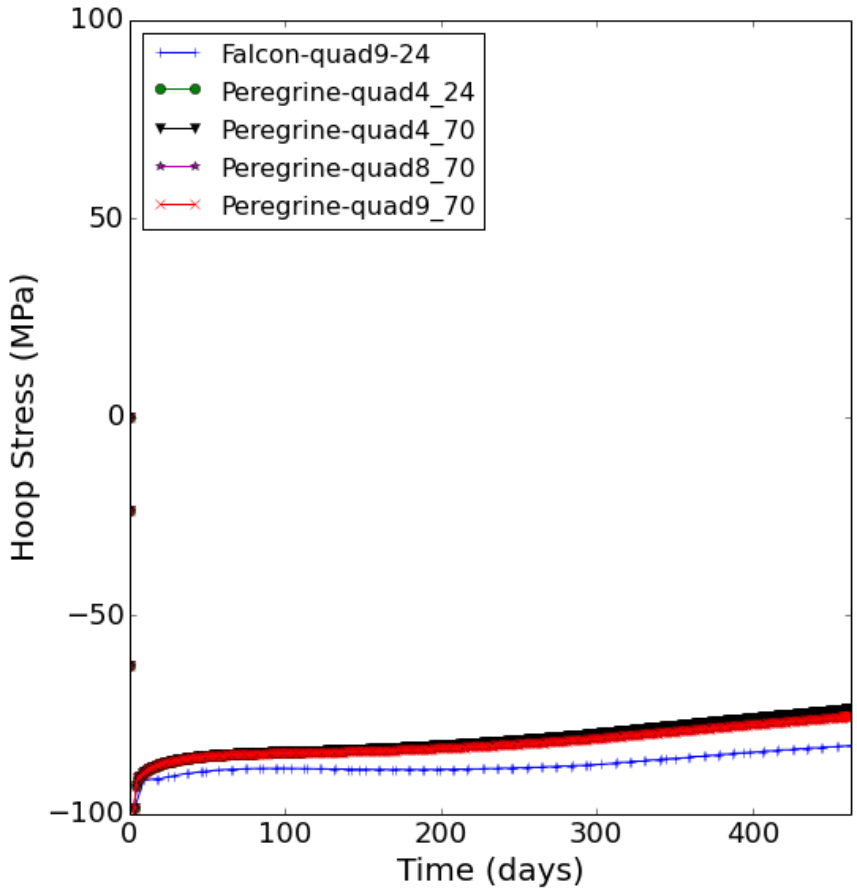

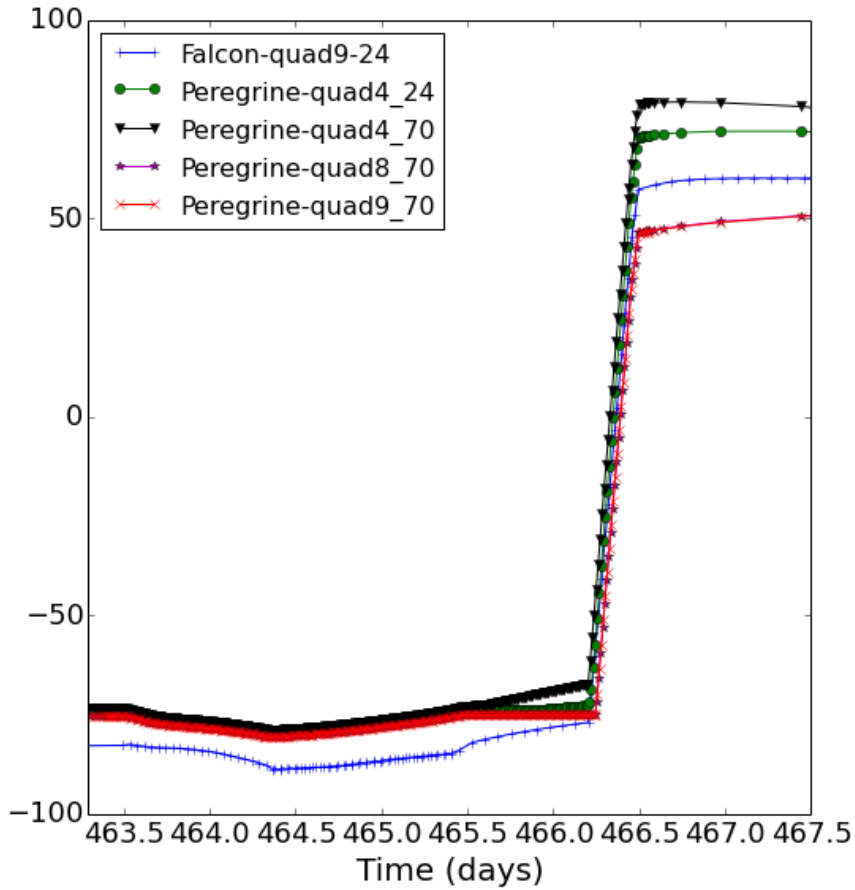

Hoop stress results are much improved after update

CASL: The Consortium for Advanced Simulation of Light Water Reactors

A DOE Energy Innovation Hub for Modeling and Simulation of Nuclear Reactors

TVA Test Stand
Lower Plenum Flow Anomaly Modeling Using VERA
July 16, 2014

Bill Bird – TVA
Rose Montgomery - TVA

Lower Plenum Flow Anomaly (LPFA)

- Many plants (10+) have reported observations associated with LPFA
- Power, flow and temperature measurements deviate from predictions
  - Pattern repeated over many operating cycles
- Postulated root causes
  - Flow vortices within the reactor vessel during operation
    - Standing vortices or periodic
  - Susceptible design and/or as-built geometry, including asymmetry in lower internals and loop inlet/outlet placement
  - Loop flow differentials, including geometric differences in loop geometry
- Possible influencing parameters
  - Reactor Coolant Pump impeller replacement
  - Pump startup sequence

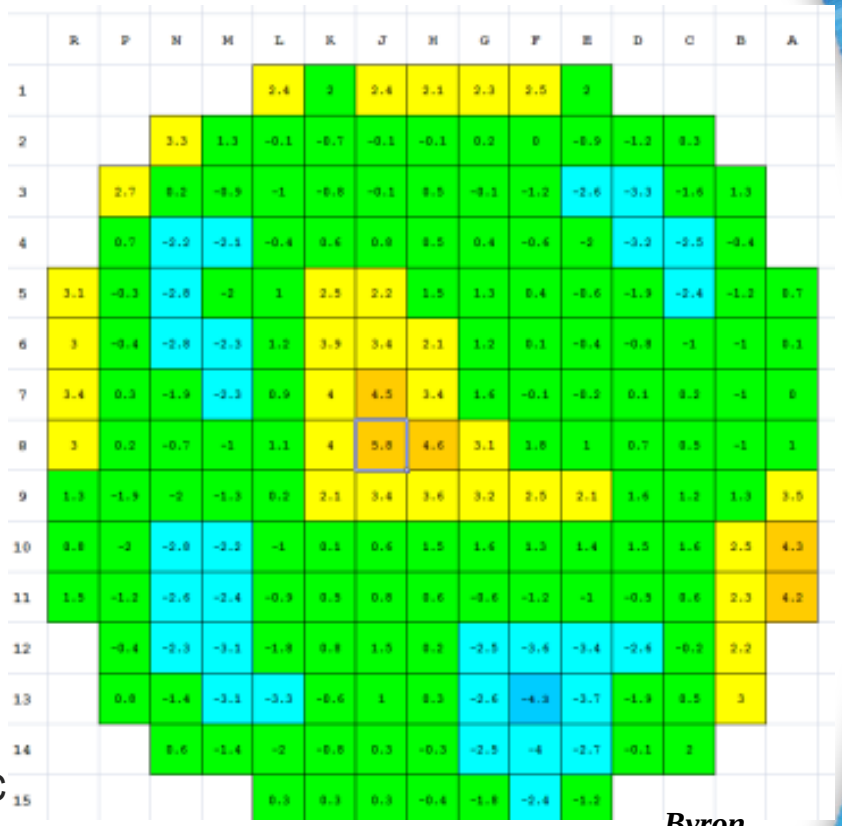

Byron Station, cycle 18

LPFA – Watts Bar specific

- Watts Bar Nuclear (WBN) Unit 1 has historically experienced core power distributions that differ from design predictions
- The magnitude of the difference of measured versus predicted (M-P) has been as high as 12% in the past at individual core locations
- The pattern persists through the cycle
  - Changes in power don't appear to change the pattern
  - Burnup does appear to change the pattern slightly
  - Steam generator change-out didn't appear to affect the phenomenon
- TVA investigations have evaluated
  - Errors in prediction
  - Measurement errors
  - Core mis-loading
  - Fresh fuel fabrication issue
  - Dropped RCCA or RCCA rodlet
  - Core design input error

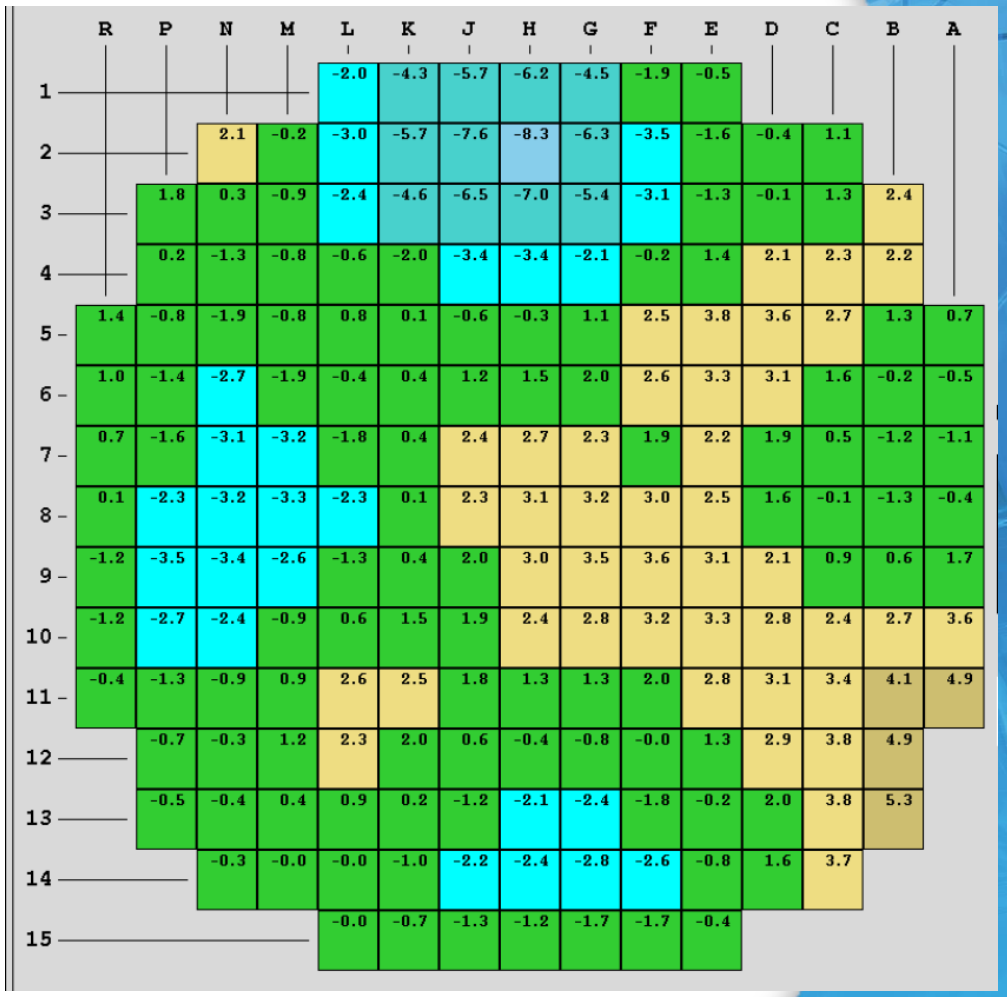

LPFA – instrumentation indications

- Square wave pattern in ex-core detector signals correlated with:
  - Other ex-core channels
  - Reactor coolant system (RCS) loop flow
  - RCS loop ΔT
  - Core exit thermocouples (CETC)
  - In-core detectors
- Perturbations in reactivity computer traces

WBN-1 power range voltage signals and several Core Exit Thermocouple signals observed during postulated LPFA event

Operational Impacts of LPFA

- Consequences
  - WBN-1 is assessed a 3.3% generic DNBR penalty in its safety analysis
  - Reduced FQ & FDH margins.
  - CRUD susceptibility

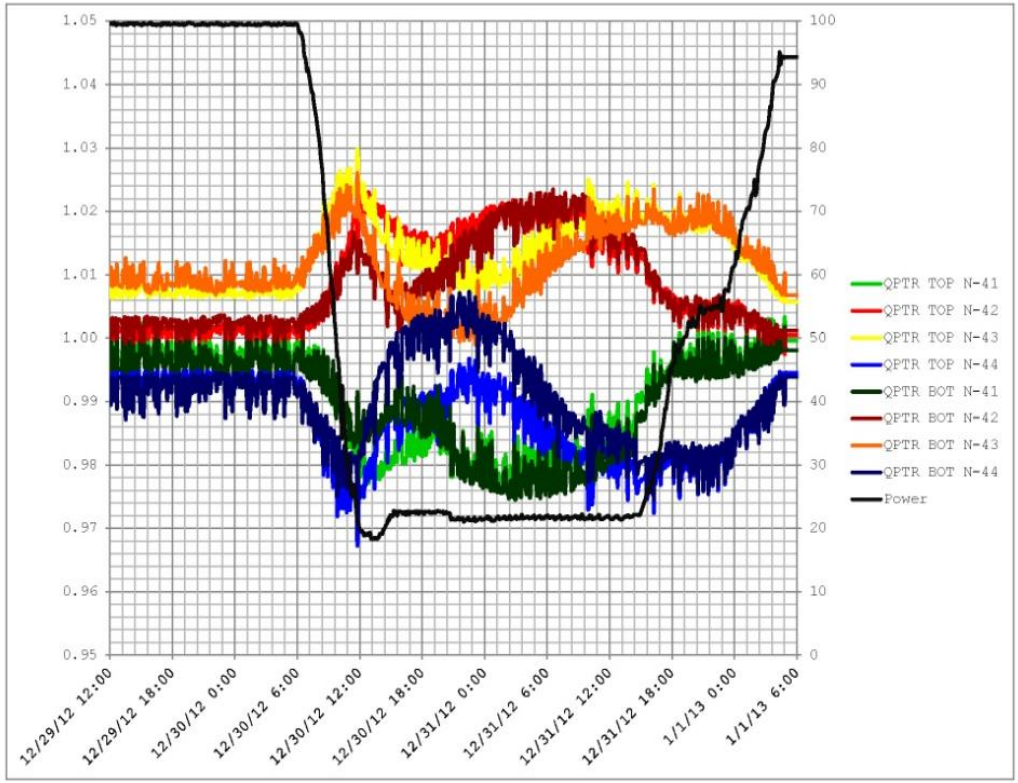

Close up of a single WBN fluctuation (approximately 24-hour duration)

TVA is exploring the flow distribution in Watts Bar unit 1 using VERA's Hydra-TH

- Using simplified boundary conditions
  - Intent is to show scalability of Hydra-TH to reactor scale
  - BC's: vessel inlet pressure, flow velocity, temperature/density
  - Currently using k-ε turbulence model with implementation of renormalization group theory (RNG k-ε)
    - Shear Stress Transport (SST) k-ω model not yet available in Hydra-TH
- Perform mesh density study
  - Evaluate 3-4 mesh densities to determine density required for calculation fidelity
- Perform steady flow calculation to look for standing flow vortices in lower plenum and downcomer regions
  - Determine impact of identified flow vortices on core inlet flow distributions

Example of current mesh size being used

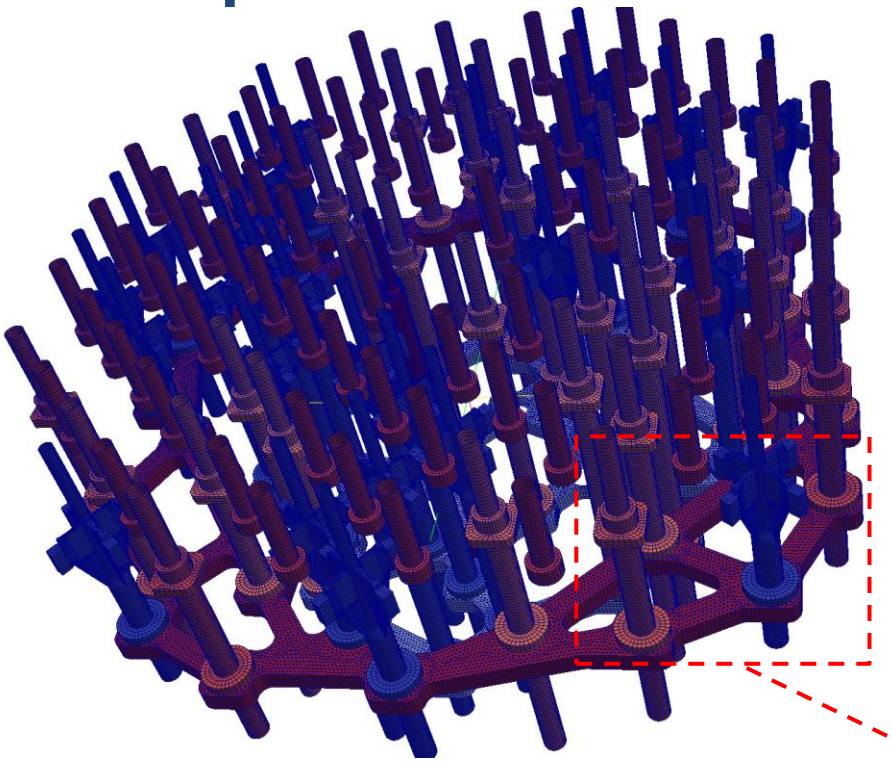

Mesh created by UT-C SimCenter

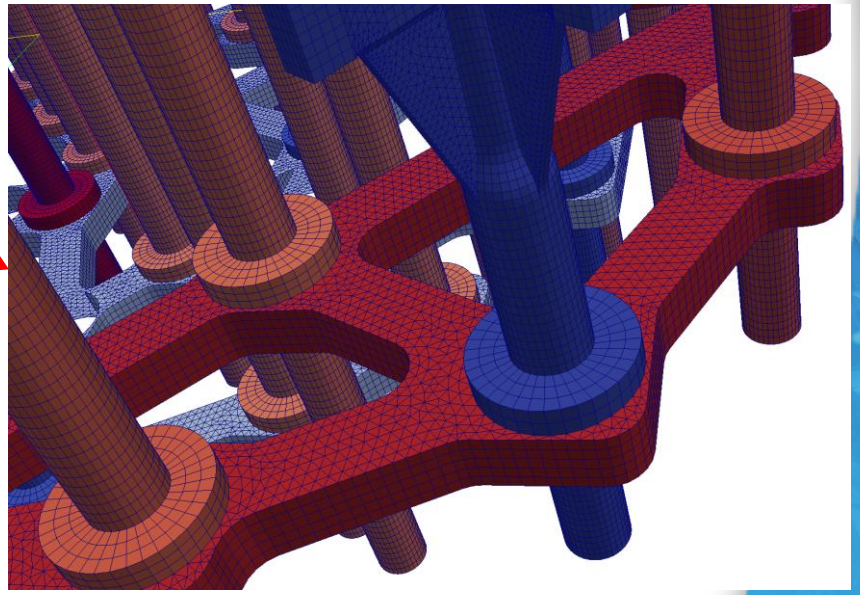

View of reactor lower internal structures

LPFA Expected output and demonstration of capability

- Local flow in downcomer, lower plenum, fuel inlet and exit
- Local coolant temperature at fuel inlet, exit, hot loop, etc.
- Local coolant density within the core region
- Identification of standing vortices
- Indication of influence of pump startup sequence (contingent on use of new turbulence model)
- Later, with transient simulation, identification of periodic vortices

TVA Application for Titan Resources

- Size/Complexity of WBN model requires HPC resources
- TVA does not have sufficient engineering computing resources
- Application submitted for Director's Discretion allocation on Titan
  - ~1 million core-hours to run full case matrix
  - Preliminary work on Titan proceeding under CASL's allocation
  - Application approved pending export control review
- Anticipate a similar process for other utilities when running large problems in VERA/Hydra-TH

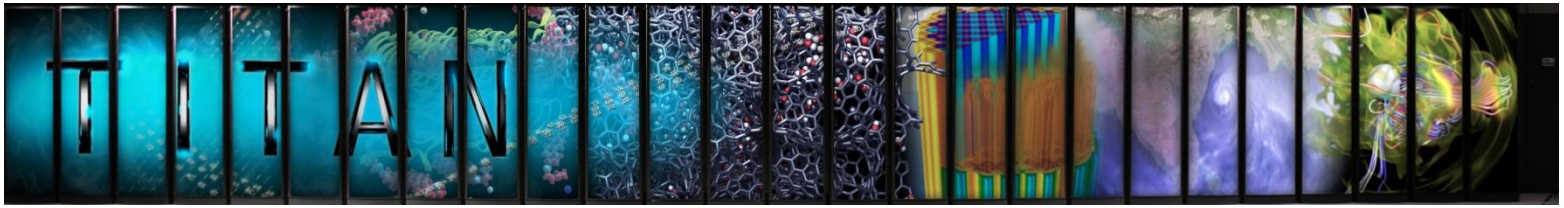

TVA application for Titan resources approved

Challenges Identified

- Mesh
  - No tools within VERA for generation of large meshes (Cubit was not capable of resolving intricacy of lower internals)
  - Reliant on UT-C SimCenter for meshing support
  - Exodus-II is the only supported format
- Hydra-TH
  - Implicit solver not available; even SS calculations require transient approach (i.e., large number of time steps)
  - Error messages are not explicit
  - Errors following restart from dump file
    - Hydra-TH exits with an error when writing Exodus-II plot file after restarting from a previous run
  - Manuals not comprehensive
- Visualization of mesh and results
  - Large amount of data generated overwhelms ParaView when running locally
  - Entire result (each transient time step and full geometry) must be read in
  - Resolved by running in client/server mode using Titan

Challenges to success

Future Work

- Mesh size study is first priority to gain experience with Hydra-TH with smaller models
- Get steady flow model to run
- Evaluate sensitivity to variations in reactor coolant loop flows
- Evaluate sensitivity to pump startup sequence
  - Will likely require transient modeling to identify

Watts Bar Unit 2
Open Vessel Testing

Acknowledgements

- TVA Watts Bar
  - *Kevin Elam*
- UT-C SimCenter
  - *Steve Karman, Ethan Hereth, and Bruce Hilbert*
- Westinghouse
- ORNL

Thank you!

THE UNIVERSITY of TENNESSEE UT KNOXVILLE

iPWR Modeling with VERA

Kelly Kenner, UTK

07/16/2014

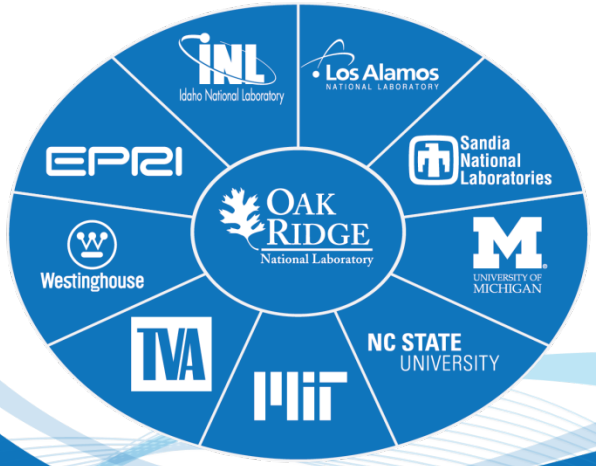

U.S. DEPARTMENT OF ENERGY
Nuclear Energy

CASL
Consortium for Advanced Simulation of LWRs

Acknowledgements

Many thanks and much gratitude to:

- Rose Montgomery, Dan Stout, Gary Adkins, TVA, and CASL
- Dr. Maldonado, Andrew Godfrey, Andy Worrall, Mark Baird, Jess Gehin, AJ Ierulli, Cole Gentry, Ben Collins and the MPACT developers
- This research used resources of the Oak Ridge Leadership Computing Facility at the Oak Ridge National Laboratory, which is supported by the Office of Science of the U.S. Department of Energy under Contract No. DE-AC05-00OR22725.

Introduction

- The objective of this study involved using VERA tools to perform a core cycle design for a typical iPWR SMR

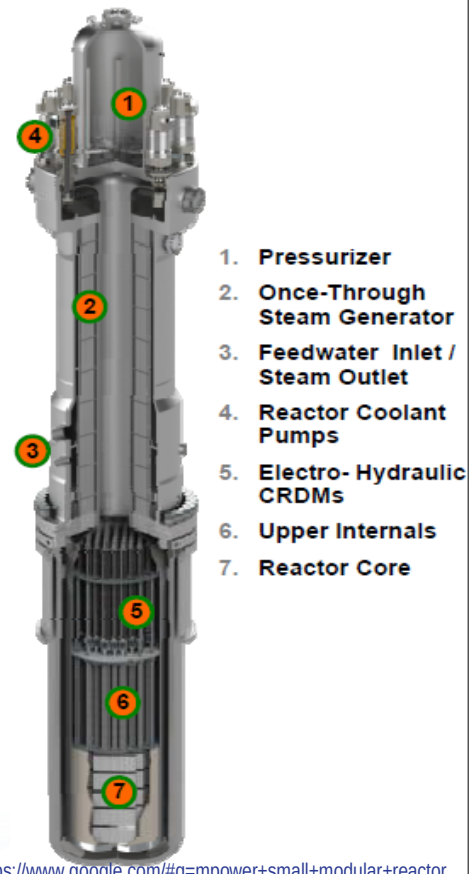

https://www.google.com/#q=mpower+small+modular+reactor+pressurizer+once-through+steam

- 69 17x17 fuel assemblies
- No soluble boron
- Active fuel height of 241.3 cm
- Core power of 530 MWt and 180 MWe
- ~4 kW/ft average linear power density
- 4.95% standard fuel enrichment
- Fixed BPRs and gad rods

Introduction

- No soluble boron is used for reactivity control of the SMR
- Each fuel assembly type has varying number of BPRs of B_4C-Al_2O_3
- BPR pins do not include fuel, and are in fixed locations in each assembly (not inserts in guide tubes)
- Additionally, some assembly types include fuel rods of UO_2 mixed with gadolinia

CASL Tools Used in This Study

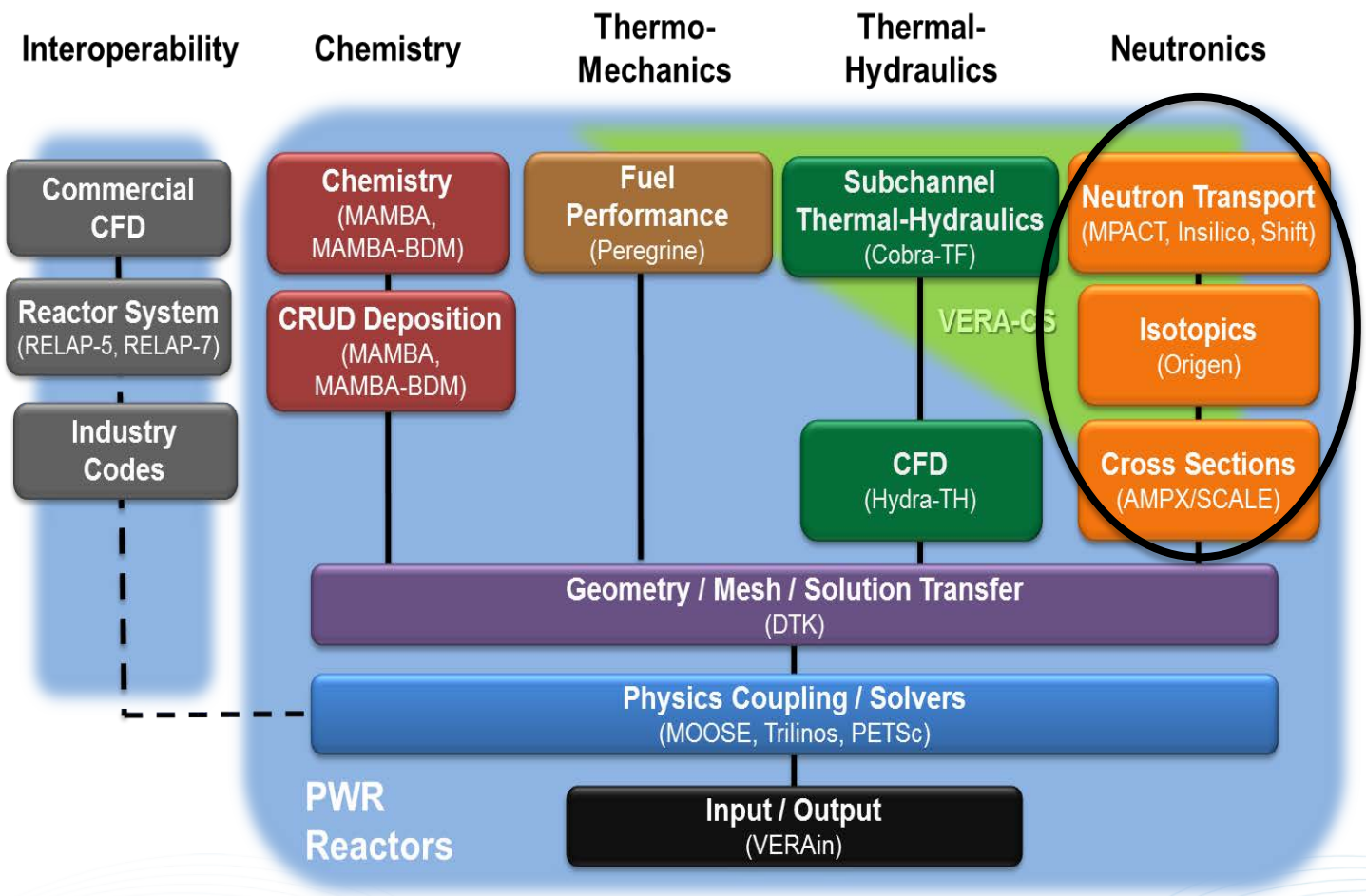

2D Single Assembly Lattice Models (1 of 2)

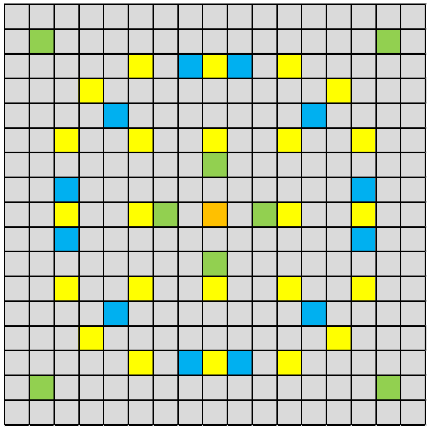

Type A: 12-BPR

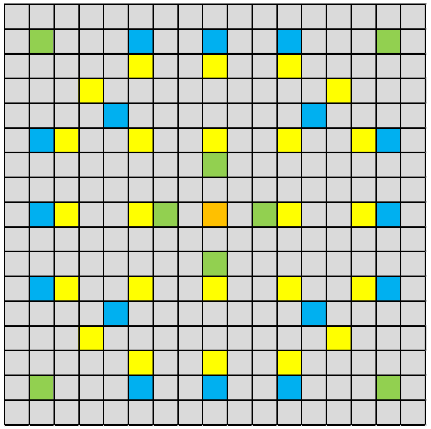

Type B: 16-BPR

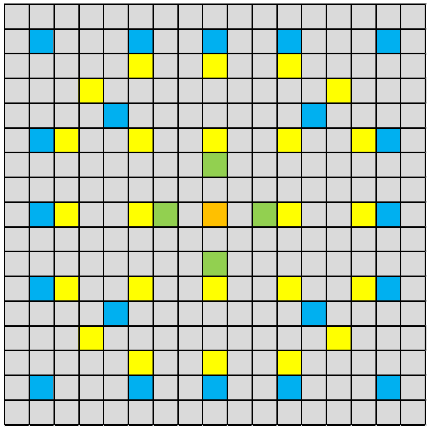

Type C: 20-BPR

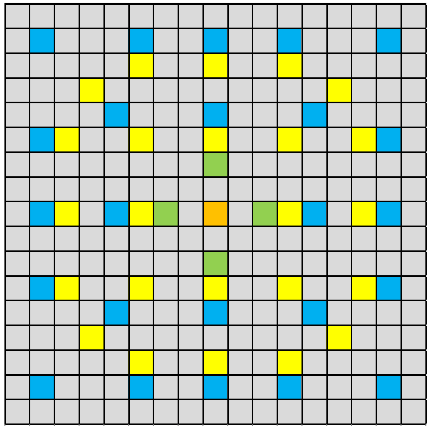

Type D: 24-BPR

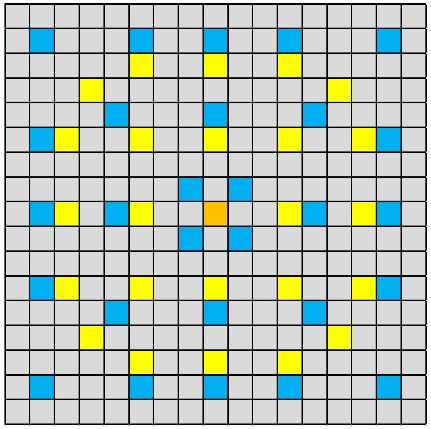

Type E: 28-BPR

	Standard Fuel Pin
	Control Rod
	Gd Fuel Pin
	BPR
	Instrument Tube

- Several lattices were evaluated for eigenvalue and peak pin power
- The initial core loading plan was selected based on the results from this 2D study

Example 2D Lattice Calculation

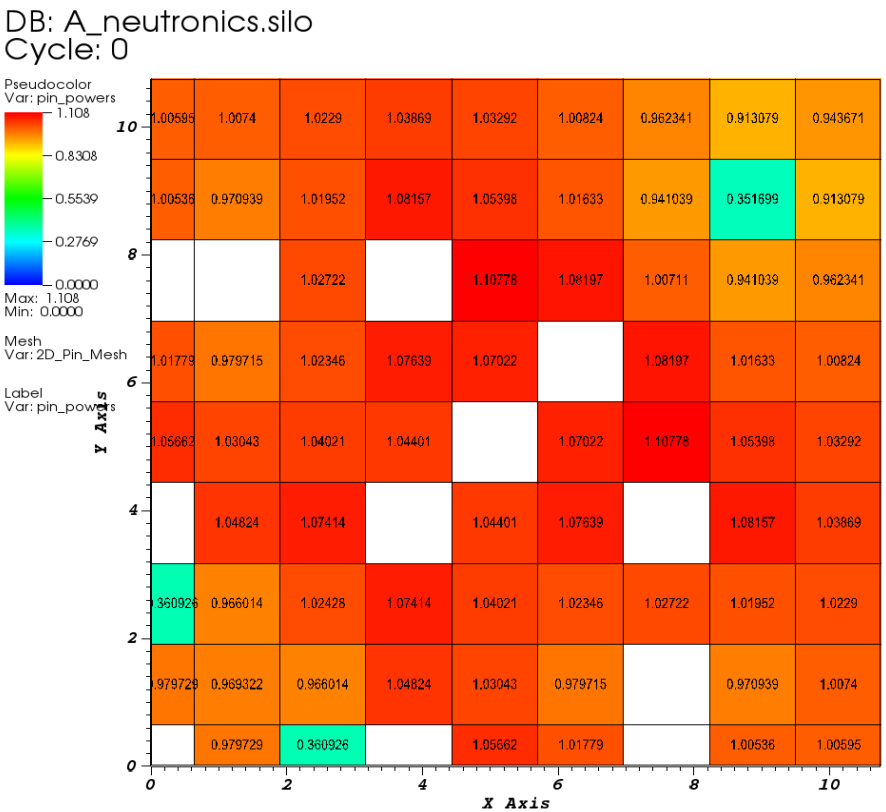

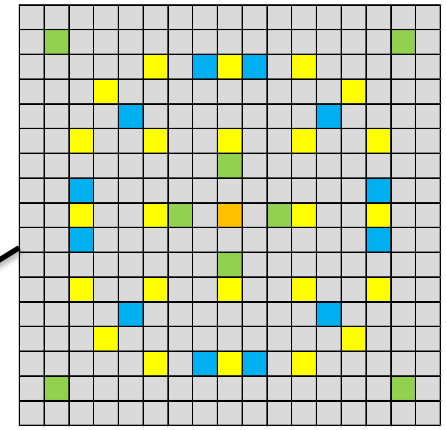

Example of the relative pin power distribution across the top right quadrant of the lattice (type “A” assembly, 12-BPR).

Assembly	Peak Relative Pin Power	Minimum Relative Pin Power	k-inf
Type A	1.1078	0.3517	1.2152
Type B	1.1120	0.3545	1.1739
Type C	1.1010	0.3699	1.1686
Type D	1.1281	0.3686	1.0823
Type E	1.1241	0.9239	1.0717

Final Core Loading Plan

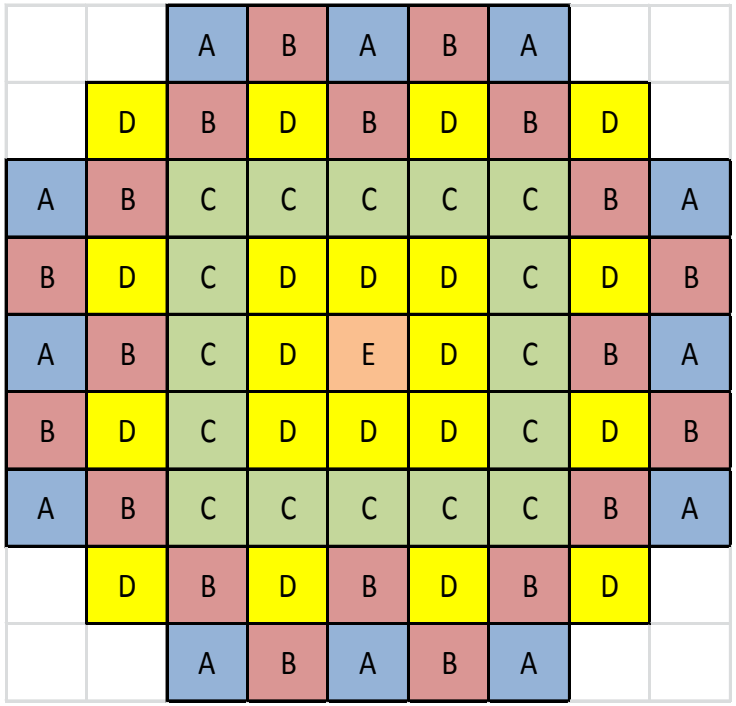

1.352 1.447	1.379 1.480	1.424 1.566	1.274 1.520	0.791 1.077
1.379 1.480	1.334 1.469	1.325 1.522	1.055 1.318	0.697 0.957
1.424 1.566	1.325 1.522	1.194 1.402	0.935 1.185	0.553 0.803
1.274 1.520	1.055 1.318	0.935 1.185	0.593 0.862	
0.791 1.077	0.697 0.957	0.553 0.803		

Avg Pwr
FΔH

- Several configurations were tested
- The final configuration was selected based on power peaking
- The reference limit used for this study was for a typical PWR
  - Average relative assembly power of ~1.45

[Ref. *Sequoyah HTP Fuel Transition*. Attachment 8, Rev 2. AREVA NP Inc. June 2011. Print.]

Assembly Type	# Standard Fuel Pins	Standard Fuel Pin Enrichment	# Gd Fuel Pins	Wt% Gd	Enrichment of Gd Pins	# BPR Pins
A	248	4.95	4	3	3.95	12
B	244	4.95	4	3	3.95	16
C	240	4.95	4	3	3.95	20
D	236	4.95	4	3	3.95	24
E	236	4.95	0	3	3.95	28

Final Core Loading Plan, Hot Full Power, Beginning of Cycle

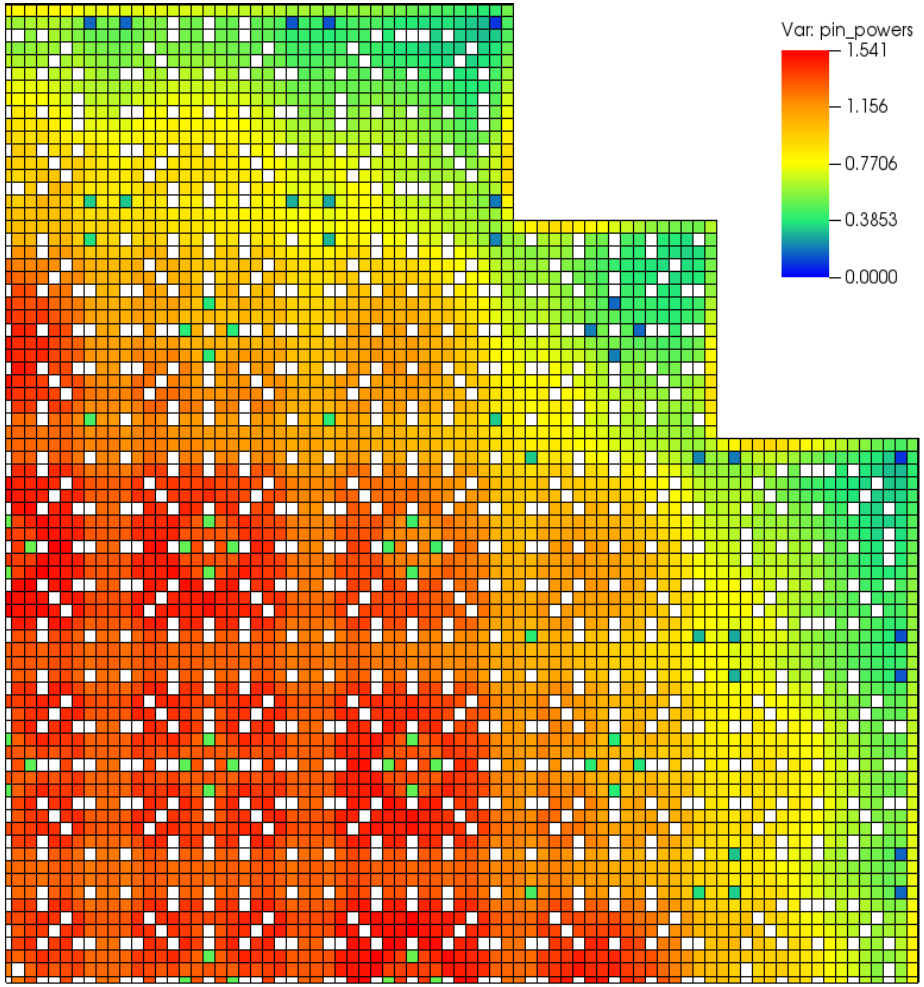

- Eigenvalue: 1.1287
- Max Relative Pin Power: 1.541
- Runtime: ~2.5 minutes for up to 49 cores on the Fissile-4 machines with Insilico
  - SP_5 angular approximation
  - PN order of 3
  - 252-group cross sections
  - 2-by-2 pin mesh

Reference Limit: FΔH < 1.55 for a typical PWR

[Ref. *Watts Bar Nuclear Reactor FSAR.* Tennessee Valley Authority. Print.]

3D Study with Insilico, HFP, BOL

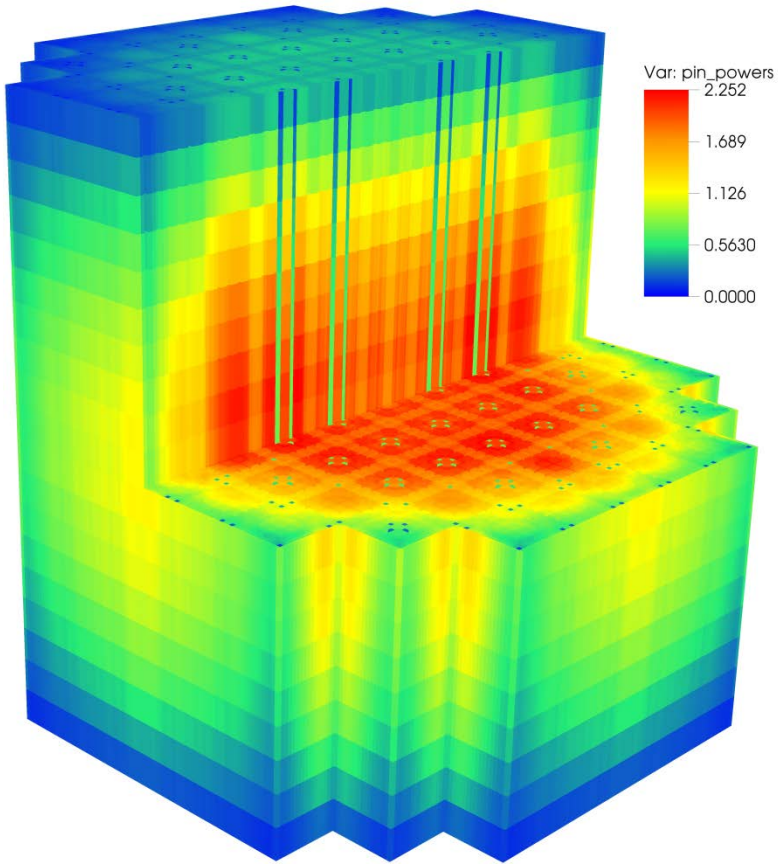

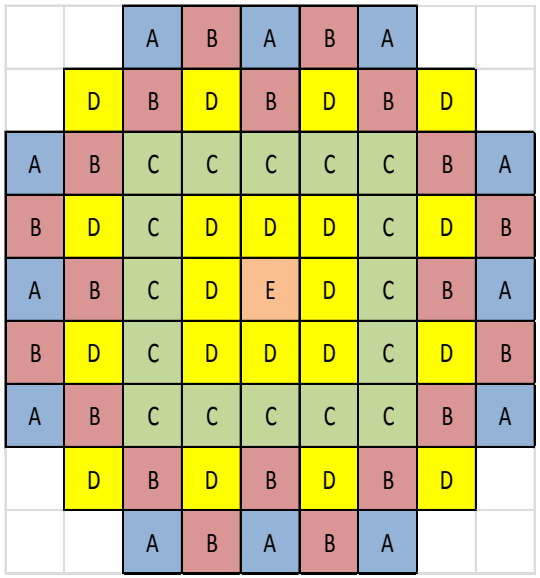

Number of Cores	400
Runtime	~20 minutes
Eigenvalue	1.1049
Peak relative pin power	2.252

Reference Limit: FQ < 2.4

[Ref. *Watts Bar Nuclear Reactor FSAR.* Tennessee Valley Authority. Print.]

3D Modeling with MPACT (no depletion)

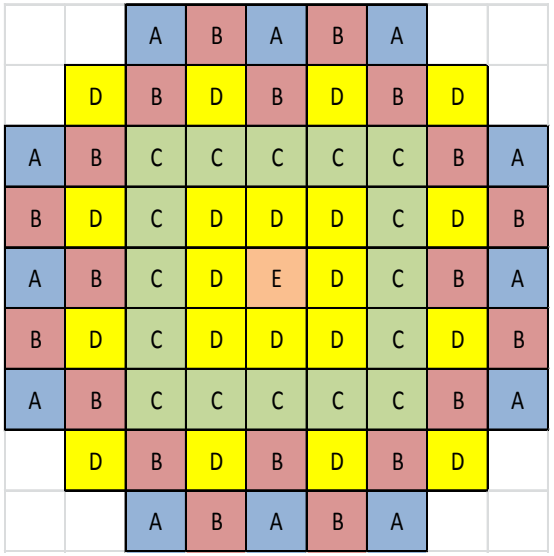

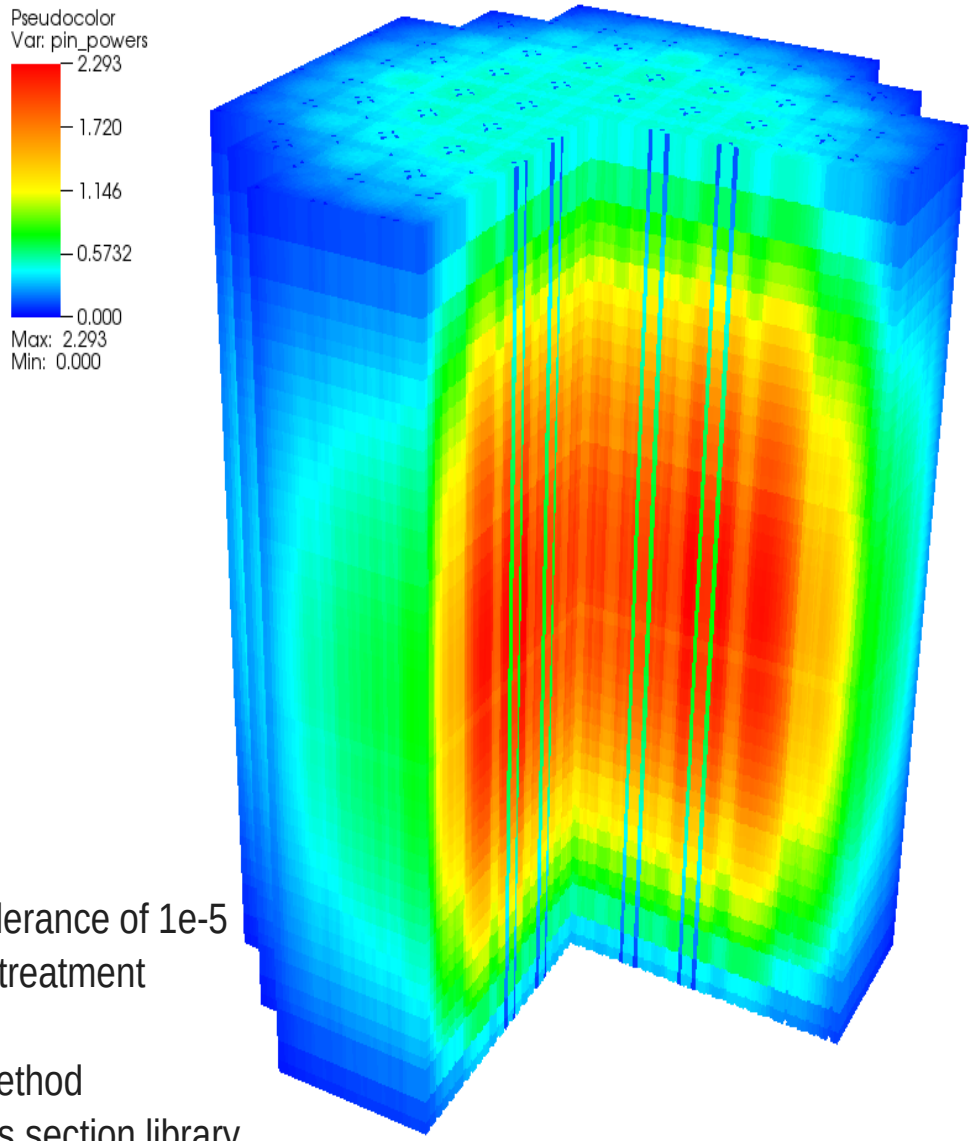

Number of Cores	1155
Runtime	~1 hour
Eigenvalue	1.1184
Peak relative pin power	2.293

- 0.1 cm ray spacing
- 8 azimuthal angles/octant
- 2 polar angles/octant
- Chebyshev-Yamamoto quadrature set
- Flux tolerance of 1e-4
- Eigenvalue tolerance of 1e-5
- P2 scattering treatment
- CMFD solver
- NEM nodal method
- 56 group cross section library

Determination of a Target Eigenvalue for Depletion Studies

- The desired cycle length for this iPWR is 1400 EFPD.
- 3D depletion was not available, so the depletion study was performed in 2D using MPACT.
- Because the 2D analysis does not account for all leakage, a target eigenvalue for the 2D study was calculated based on undepleted 2D and 3D MPACT models.
  - Using MPACT, the initial core design was modeled in 2D and 3D to determine the target eigenvalue for the end of cycle in 2D depletion.
  - The eigenvalue in 2D was subtracted by the eigenvalue in 3D, and the difference was added to 1.0 to give the target eigenvalue.
    - 1.1392 - 1.1184 = 0.028 + 1 = 1.028

MPACT Depletion of the 2D Core

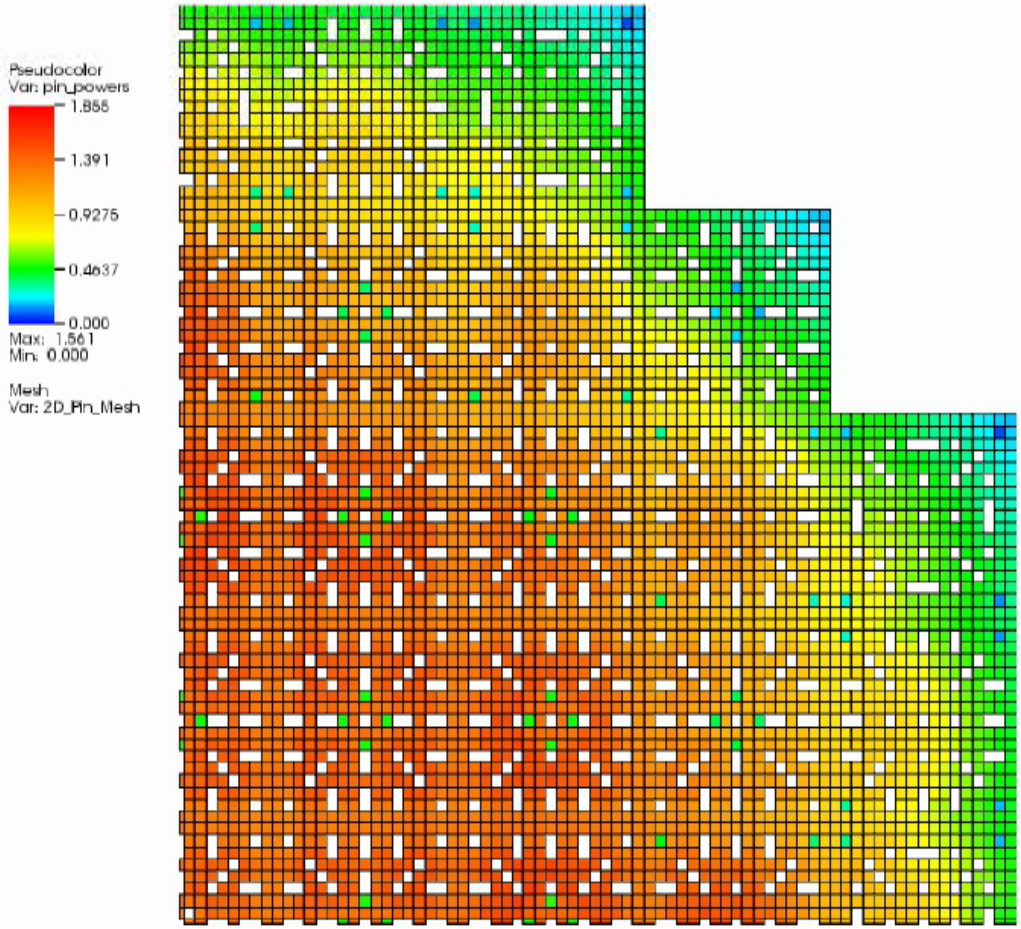

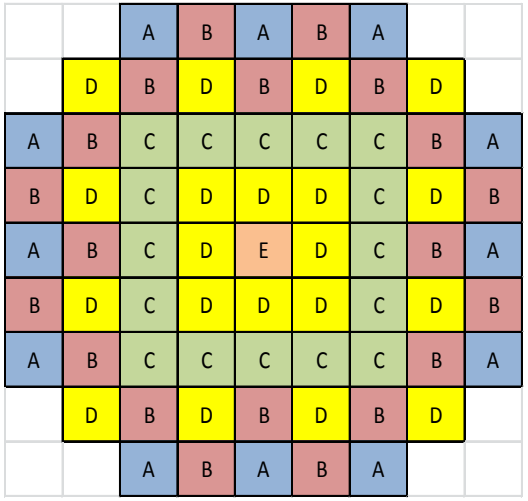

- This core produces the rated power for 1210 EFPD.
- Video shows depletion of the 2D core in EFPD time steps to 1300 EFPD.
  - Maximum relative pin power of 1.855

Cycle Length Not Achieved with the Selected Core Loading Plan

- This core did not reach 1400 EFPD (the goal lifespan of the core) and went subcritical between 1300 and 1400 EFPD.

MWD/kgHM	EFPD	k-effective
0.0797	3	1.1103
1.3287	50	1.1099
2.6574	100	1.1152
3.9861	150	1.1207
5.3148	200	1.1266
6.6435	250	1.1318
7.9722	300	1.1352
9.3009	350	1.1370
10.6296	400	1.1378
11.9583	450	1.1372
13.287	500	1.1352
15.9444	600	1.1264
18.6018	700	1.1137
21.2592	800	1.0983
23.9166	900	1.0814
26.574	1000	1.0635
29.2313	1100	1.0449
31.8887	1200	1.0260
34.5461	1300	1.0069
35.8748	1350	0.9977

- A 2D study using MPACT was performed to try to find a core design that would allow the reactor to remain critical to 1400 EFPD.
  - Only in extreme cases did the iPWR core reach 1400 EFPD.
- This study did not include control rod management
  - iPWRs are expected to operate their control components similar to a BWR, and this is expected to increase the cycle length.

Below target eigenvalue of 1.028

Using Substepping in MPACT

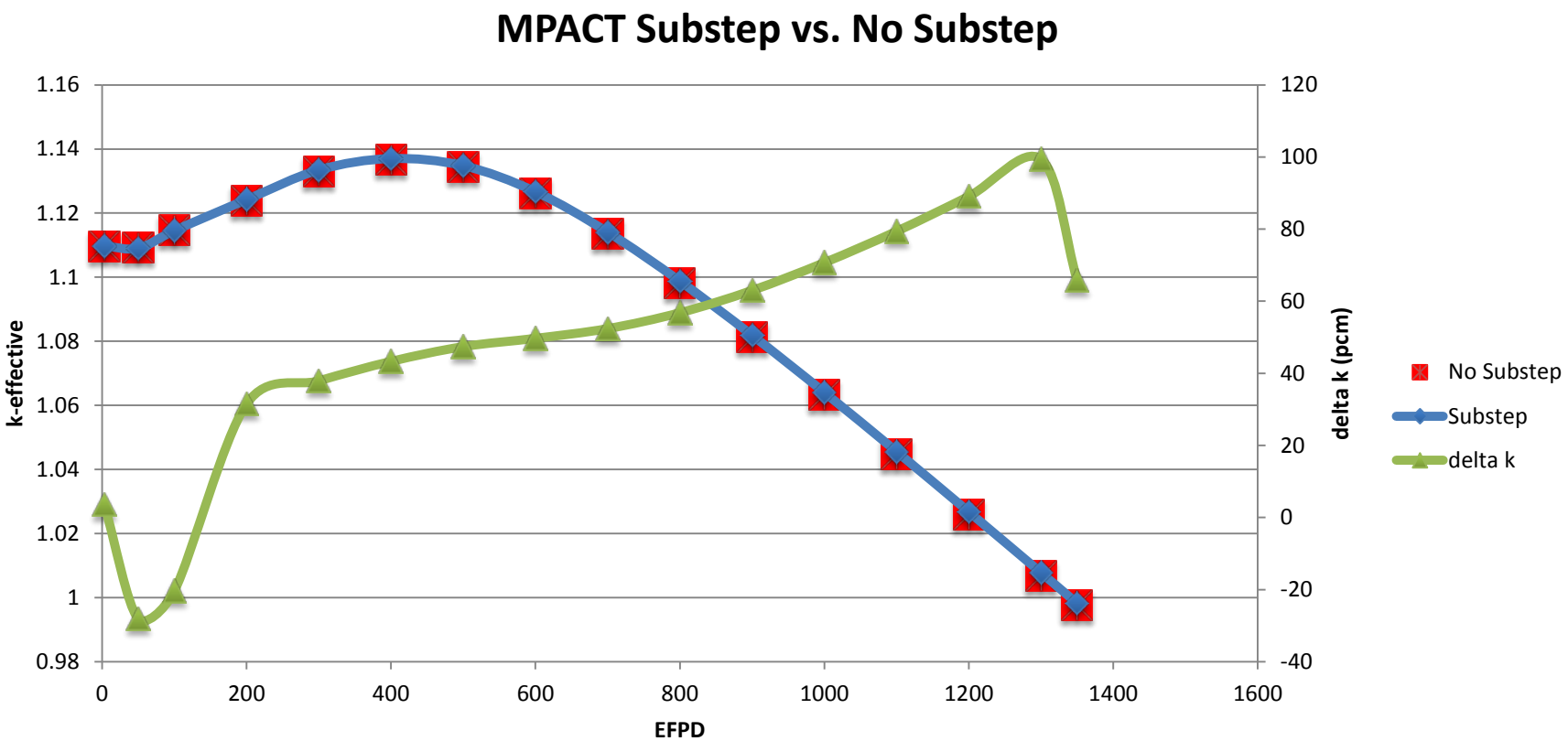

- The graph above shows a comparison between using the substepping option in MPACT
  - Substepping is advertised as a more accurate solution without increasing calculations of flux
- Runtime of ~30 minutes (coarse settings, few time steps) to ~1.5 hours (finer settings, many time steps).
- Longer runtime, same answer!

3D Model with Axial Blankets

Fuel Rods		Gd Rods		BPR Pins	
Natural U	4"	Natural U	4"	Zirc/Moderator	4"
4.95% Fuel	87"	3.95% Fuel	4"	BPR Pins	87"
		3.95% Fuel with 3wt% Gd	79"		
		3.95% Fuel	4"		
Natural U	4"	Natural U	4"	Zirc/Moderator	4"

MPACT Depletion of 3D Core

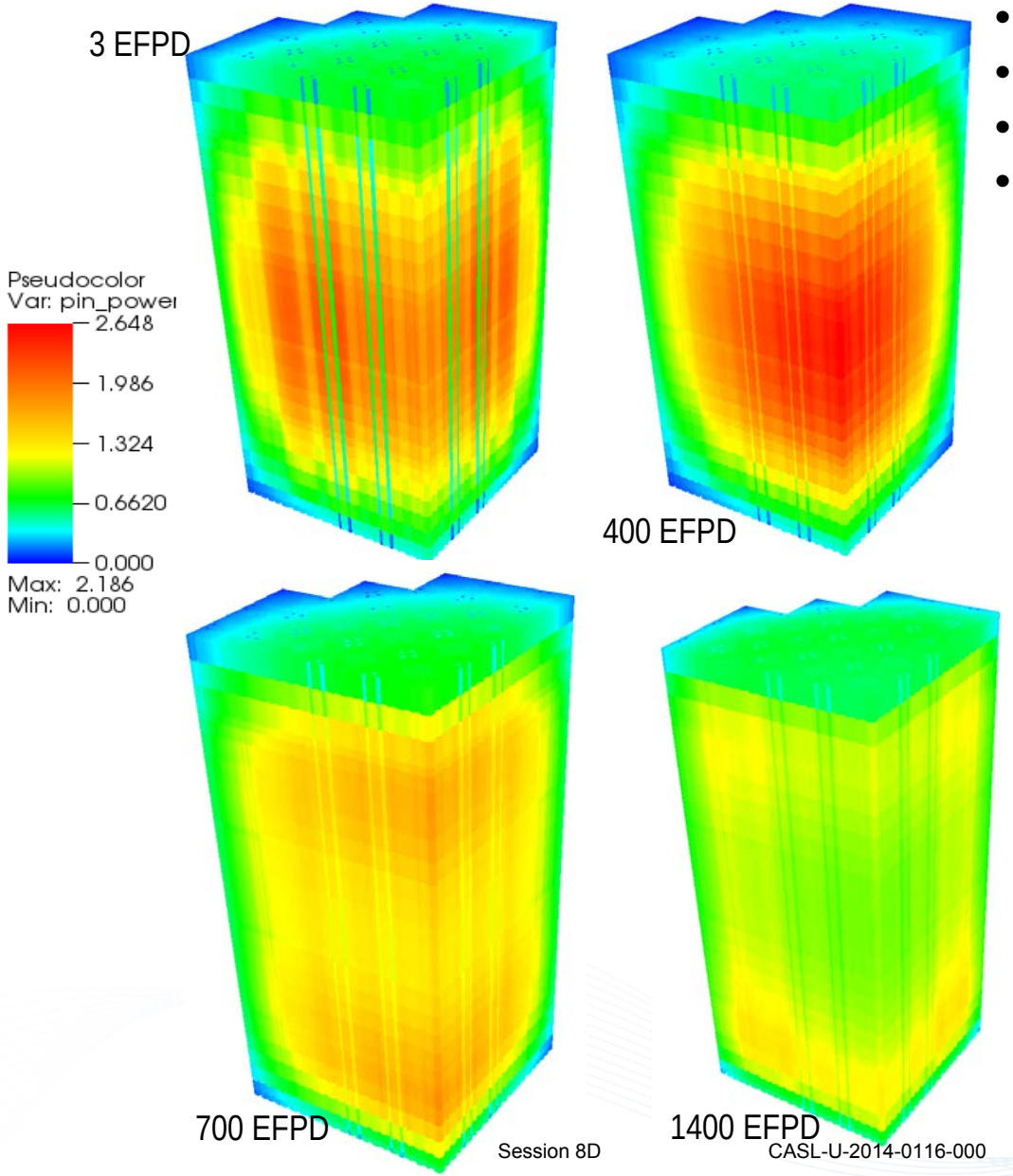

- Runtime of ~ 8 hours
- Coarse settings
- 18 time steps in EFPD
- Max Relative Power of 2.648

MWD/kgHM	EFPD	k-effective	Adjusted 2D (for comparison)
0.0797	3	1.0893	1.0823
0.6643	25	1.0870	
1.3286	50	1.0901	1.0819
2.6572	100	1.0964	1.0872
5.3144	200	1.1067	1.0986
7.9716	300	1.1131	1.1072
10.6289	400	1.1113	1.1098
13.2861	500	1.1027	1.1072
15.9433	600	1.0904	1.0984
18.6005	700	1.0759	1.0857
21.2577	800	1.0599	1.0703
23.9149	900	1.0430	1.0534
26.5721	1000	1.0252	1.0355
29.2294	1100	1.0071	1.0169
31.8866	1200	0.9887	0.9980
34.5438	1300	0.9703	0.9789
37.201	1400	0.9520	

2D Calculations with Shift for Comparison with MOC Results

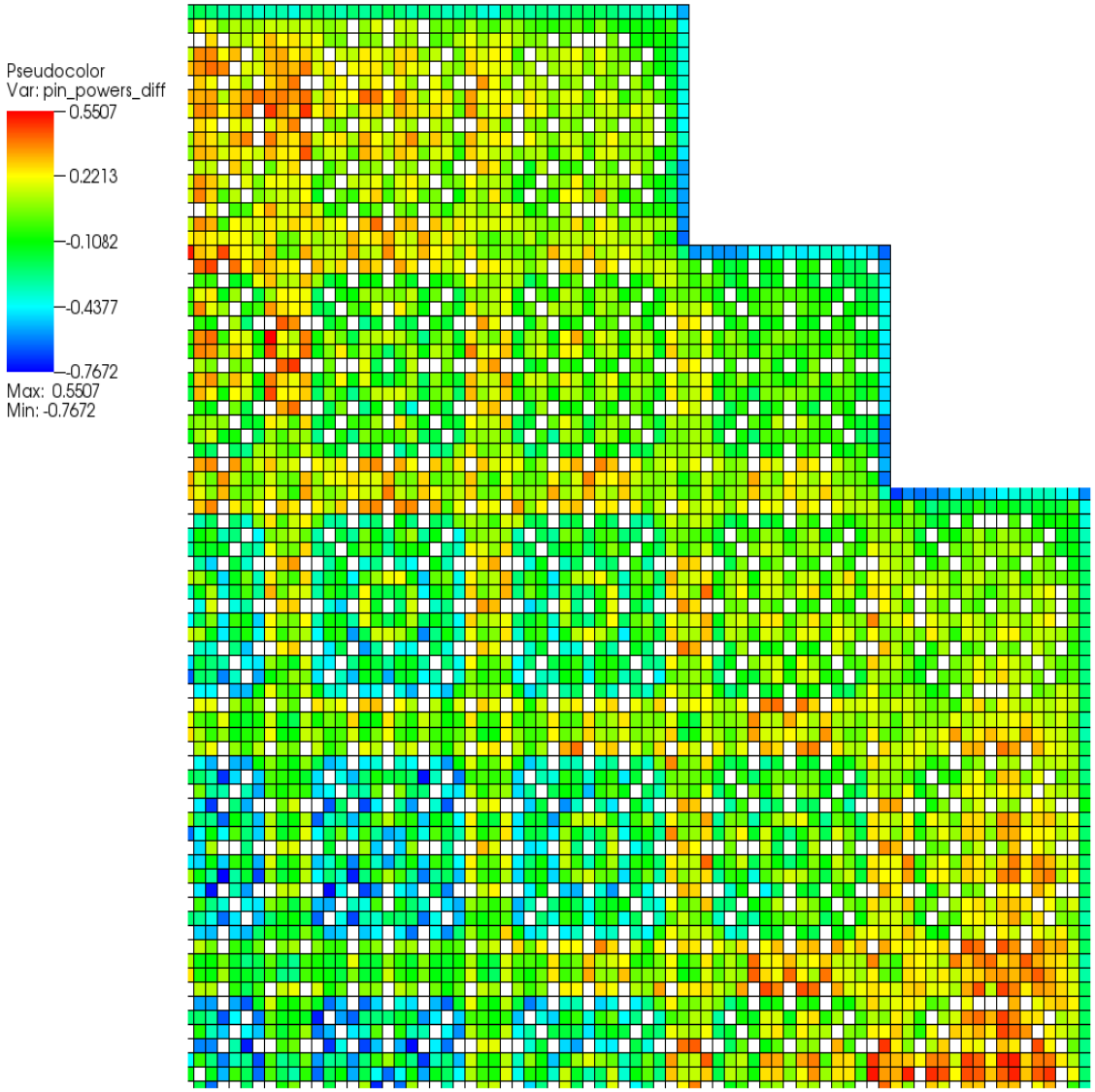

- An average -327 pcm difference exists between the k-effective for the 2D Shift case and the 2D MPACT case.

2D Calculations with Shift for Comparison with SP_N Results

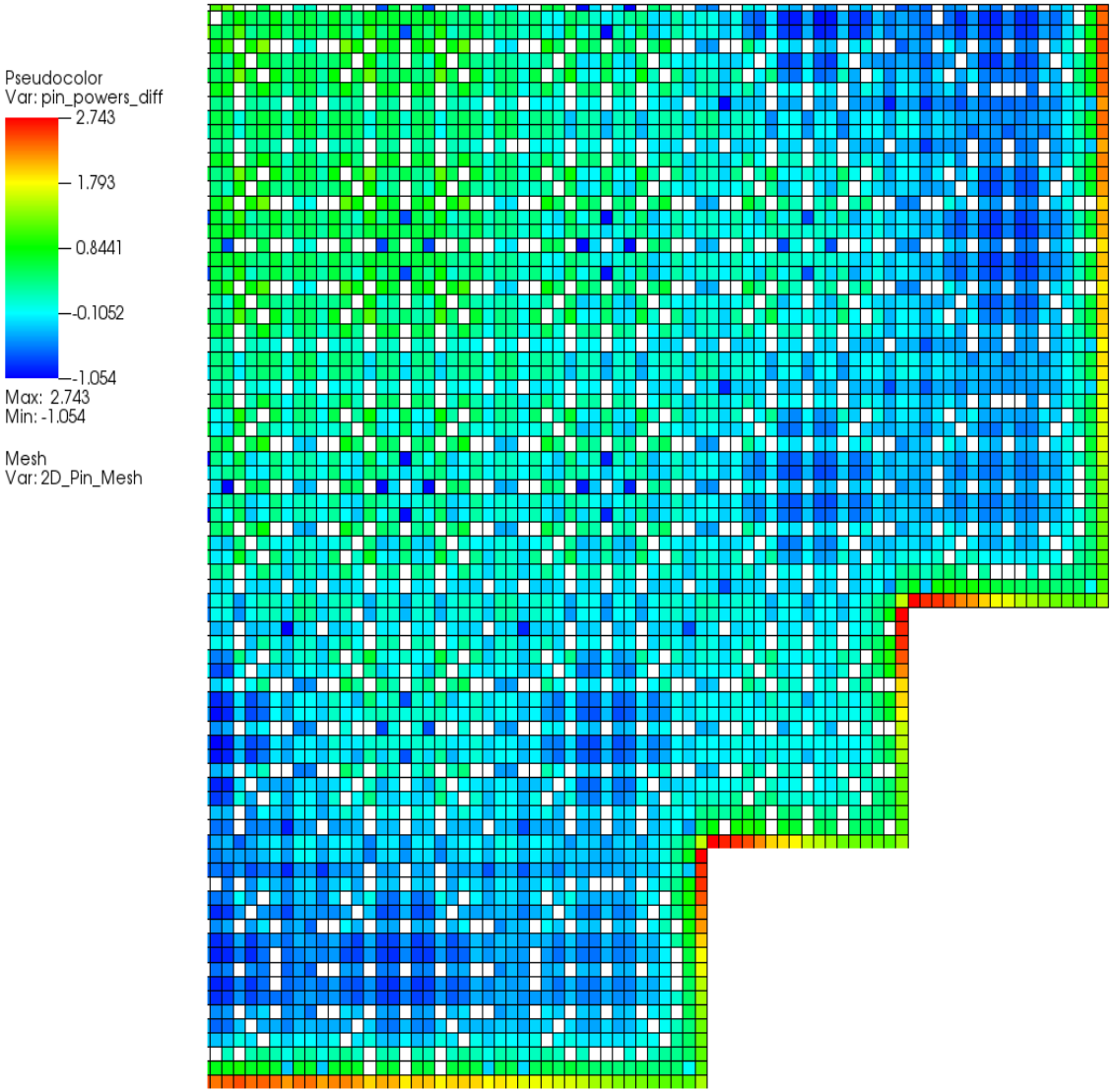

- An average -163 pcm difference exists between the k-effective for the 2D Shift case and the 2D Insilico case.

Experience Using CASL Tools (1 of 2)

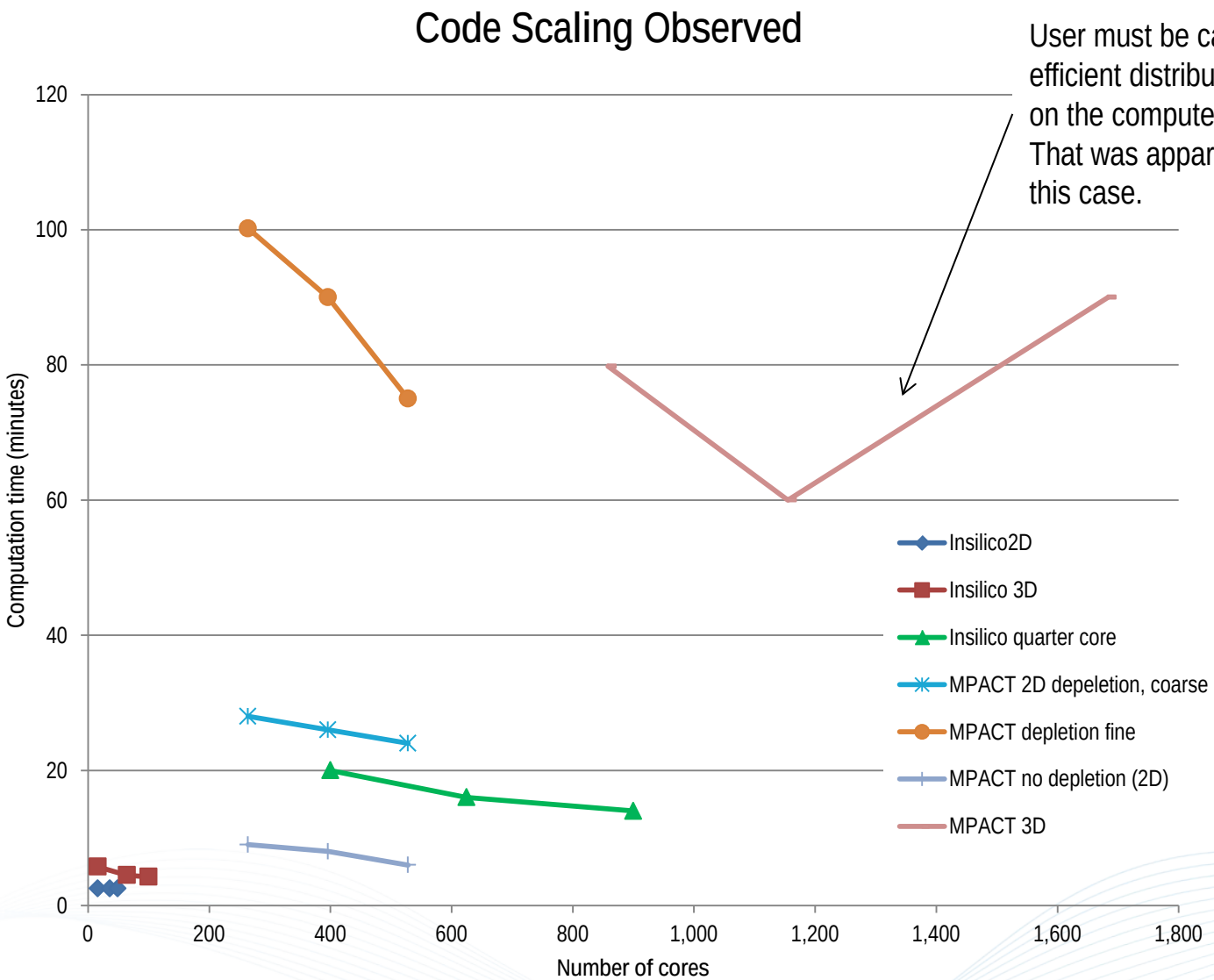

User must be careful to select an efficient distribution of the problem on the computer nodes specified. That was apparently not done in this case.

Experience Using CASL Tools (2 of 2)

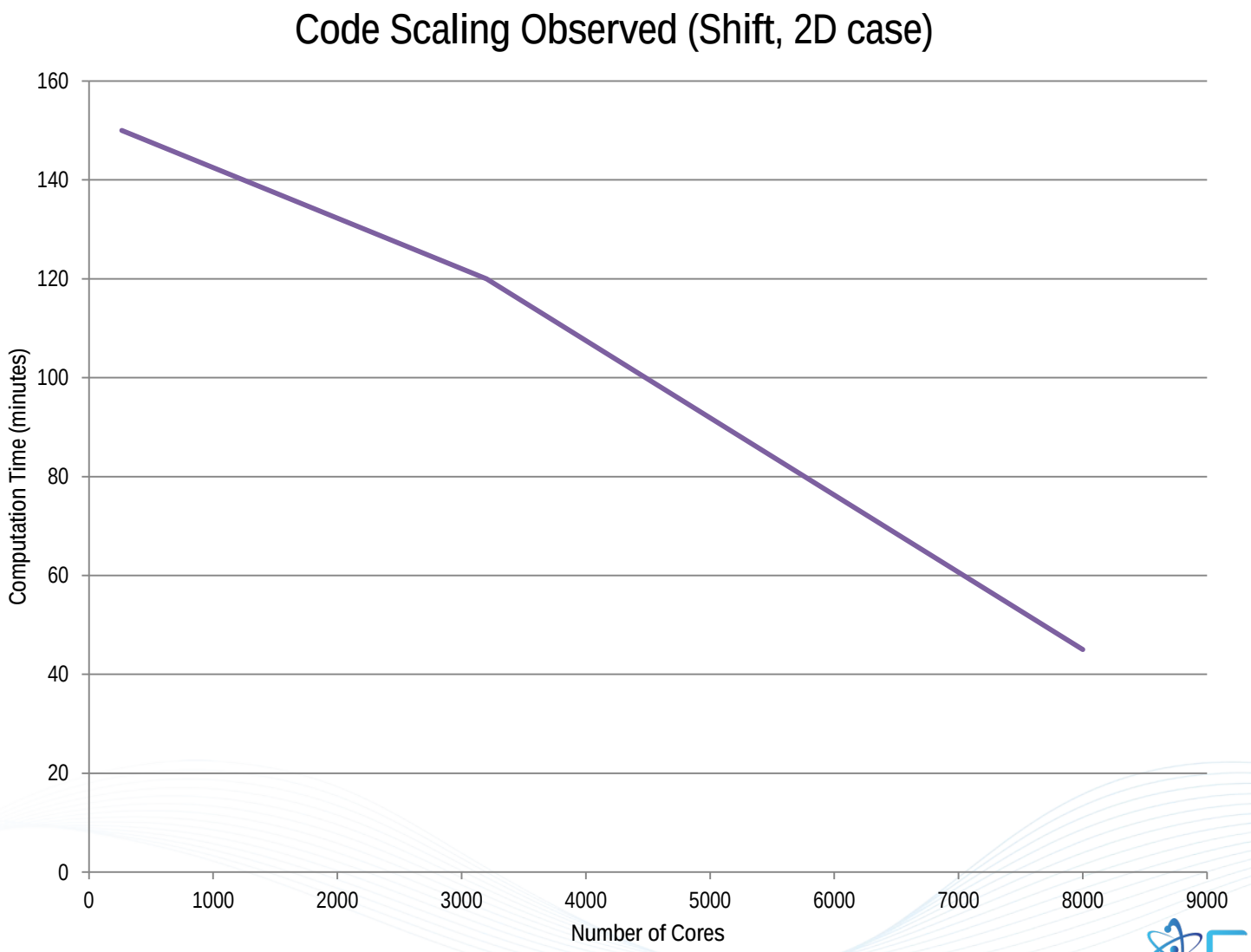

Challenges

- VERA is not fast enough for core design from scratch
  - Core design selected was optimum design that could be created in the available time
  - Faster codes should be used to zero in on a few arrangement and VERA used to optimize.
- 3D depletion capability was not available at the time of this study
  - Target eigenvalue assumption had to be made for 2D depletion studies
  - Control rod management could not be studied
- Identified Insilico limitations for core cycle analysis
  - Could not handle the larger baffle size needed to reduce radial leakage in iPWR

Conclusions

- VERA successfully modeled the iPWR SMR
- MPACT pin power and Insilico eigenvalue results agree well with Shift; MPACT and Shift eigenvalue difference is higher than expected
- Scalability appears to be good for all three neutronics codes
  - Coupled T/H was not studied
  - Longest runtime for 3D cases was ~1.5 hours using MPACT on 1683 cores
  - Longest runtime for 2D cases was ~2.5 hours using Shift on 264 cores
  - User will need to be cautioned on selecting number of cores and distribution. Recommendations are needed in the User documentation.
- Insilico did not have the capability to handle a larger baffle size
- MPACT substepping did not appear to have a significant affect on the solution
- There was difficulty reaching the goal cycle length of 1400 EFPD
  - It appears that meeting the advertised SMR cycle length will rely very heavily on the control rod management. For this study, the core designed reached a cycle length of 1210 EFPD. Extreme modifications are required to reach the target cycle length of 1400 EFPD without control rods.

Interface Tracking, Direct Numerical Simulation and Experimental capabilities in THM

Presented by: Igor A. Bolotnov (NCSU)

with contributions from:

Bren Phillips, Alex Guion, Carolyn Coyle, Jacopo Buongiorno (MIT)

Jun Fang (NCSU)

Carlos Estrada, Yassin Hassan (Texas A&M)

Jiacai Lu, Gretar Tryggvason (UND)

Outline

- Experimental work:
  - Subcooled flow boiling database (MIT)
  - Gas-Liquid Two-phase flow experiments (Texas A&M)
  - Effects of CRUD on boiling (MIT)
- Interface tracking / DNS:
  - Lift force on a single bubble (UND, NCSU)
  - Phase change (MIT)
- Large scale ITM / data analysis:
  - Transient motion of large number of bubbles (UND)
  - Simulations and analysis of two-phase flow in a subchannel (NCSU)
  - DNS of single-phase flow through 2x2 mixing vanes / spacer grid geometry (NCSU)

ITM/DNS and Experimental capabilities in THM

Subcooled Flow Boiling Database Completed (MIT)

- Boiling curve and heat transfer coefficient
- Bubble departure diameter
- Bubble departure frequency
- Wait and growth times
- Bubble nucleation site density
- Sliding bubble velocity and local cooling

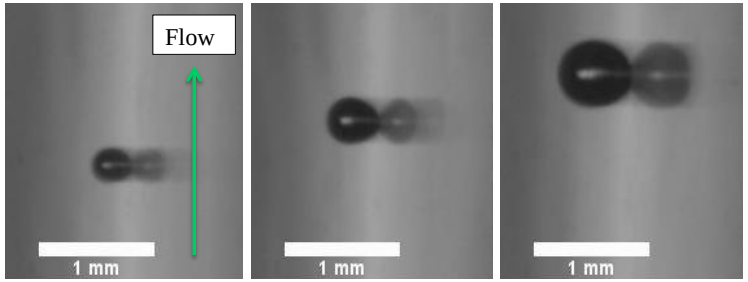

Simultaneous PIV/HSV/IR images taken for single bubble conditions

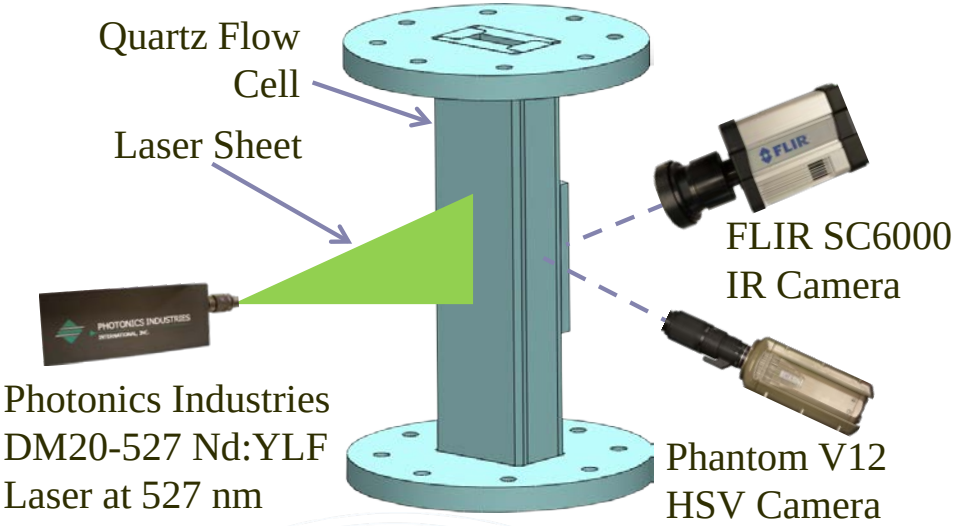

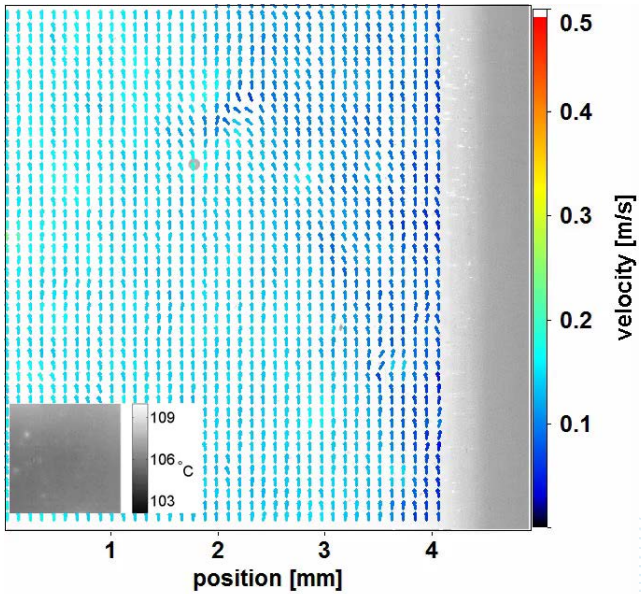

Test matrix includes >700 combinations of heat fluxes, mass fluxes, subcoolings and pressures

Two-Phase Flow Experimental Contributions (TAMU)

- Gas-Liquid Two-phase flow experiments.
- Subcooled flow boiling experiments.

Test facility capabilities

- Simultaneous PTV and Shadowgraphy experiments
- Local measurements of instantaneous and average two-phase flow parameters
- Multi-scale capabilities

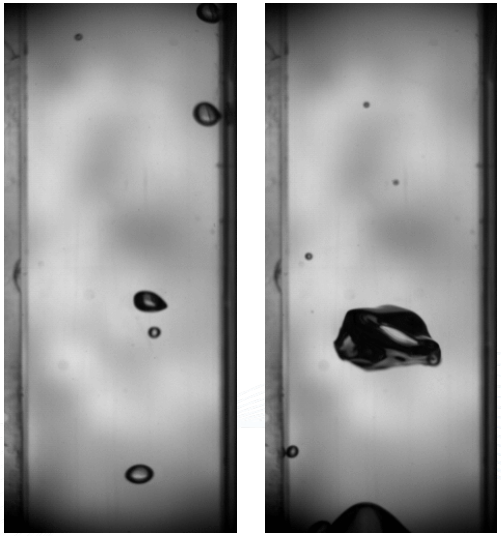

•Bubbly Flow (low void fraction)
•Slug Flow (High void fraction)

•Focus on the bubbly flow regime.

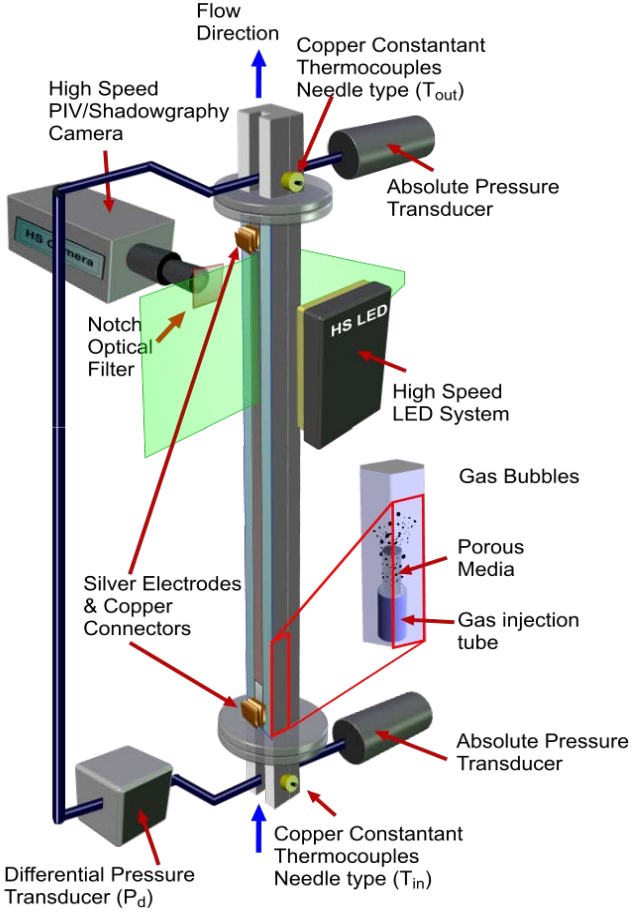

Gas-Liquid Bubbly Flow Experiments (TAMU)

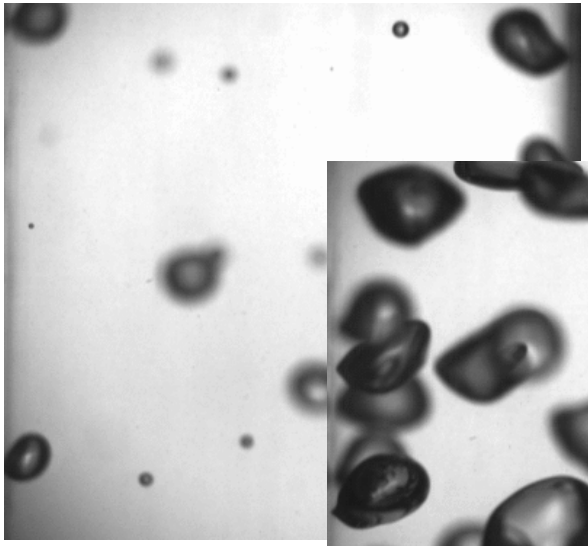

J_g = 0.82 mm/s
J_f = 0.38 m/s

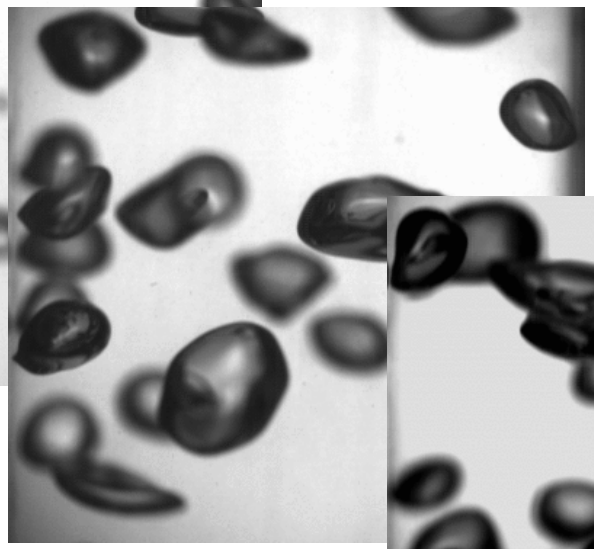

J_g = 5.5 mm/s
J_f = 0.38 m/s

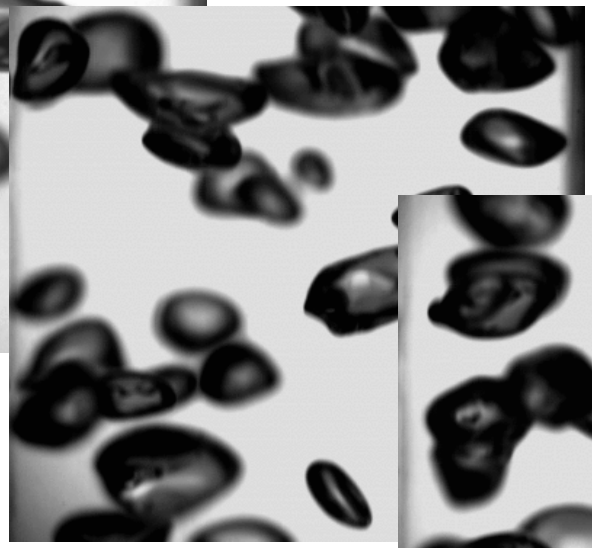

J_g = 9.17 mm/s
J_f = 0.38 m/s

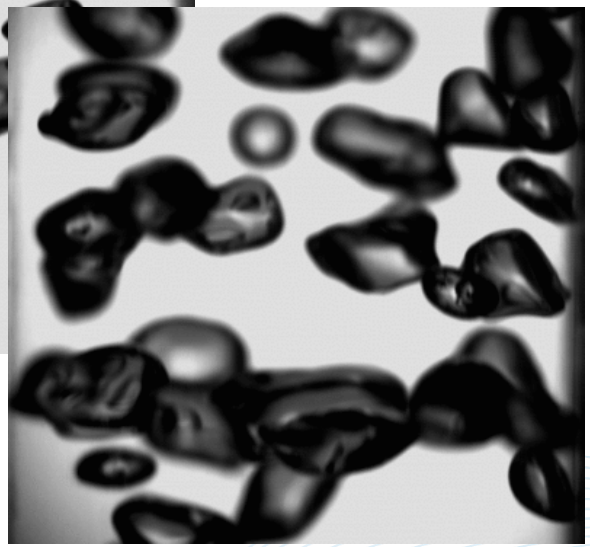

J_g = 16.5 mm/s
J_f = 0.38 m/s

Focus on bubbly flow regime with

- Different gases (Nitrogen, Helium)
- Different gas velocities
- Different liquid Reynolds numbers

Simultaneous Measurements of Liquid Velocities and Bubble Dynamics (TAMU)

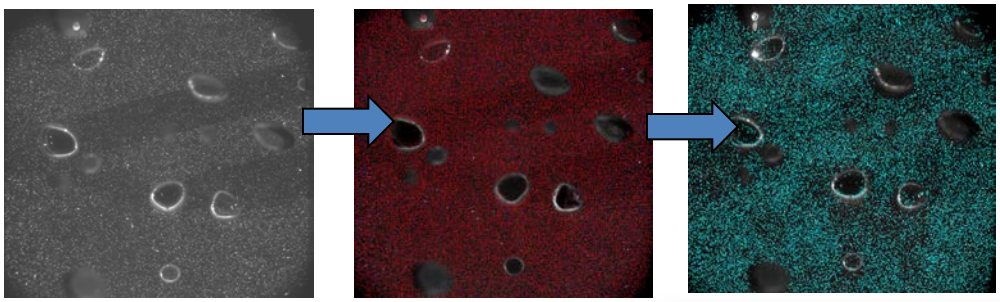

Bubble dynamics from visualization techniques validation by means of optical sensor

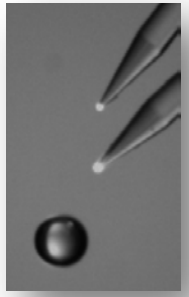

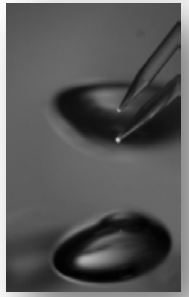

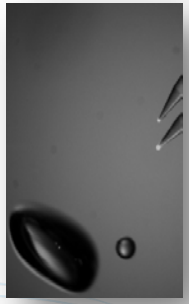

Simultaneous Implementation of Visualization Techniques:

- **Particle Tracking Velocimetry**
  - for liquid velocity measurements
- **High Speed Shadowgraphy**
  - for bubble dynamics estimations

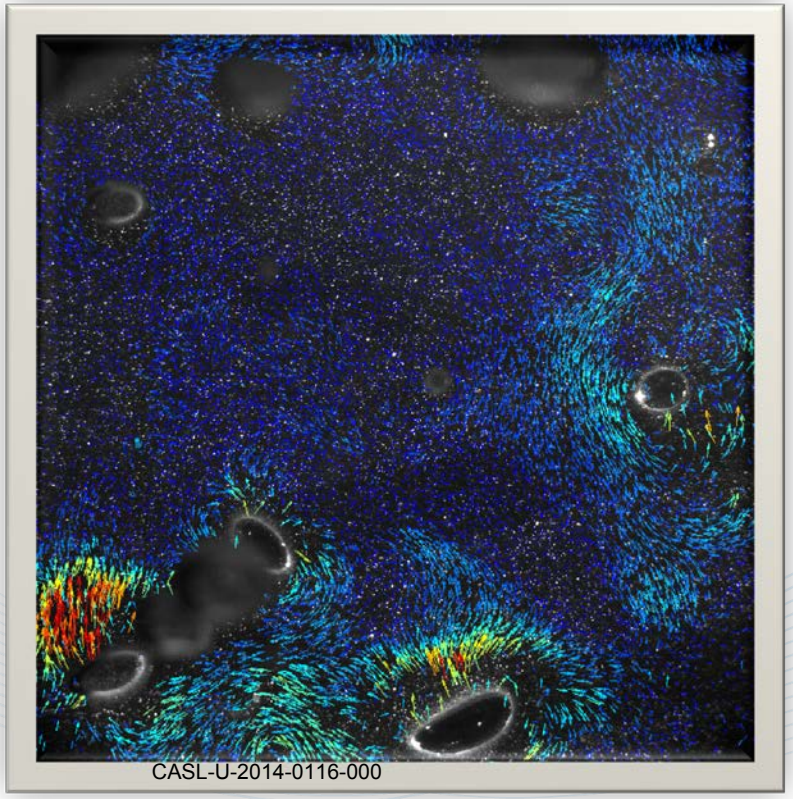

CASL-U-2014-0116-000

Results Example: Modification of Liquid Turbulence Due to The Influence of Void Fraction (TAMU)

Gas= Helium
J_f = 0.38 m/s

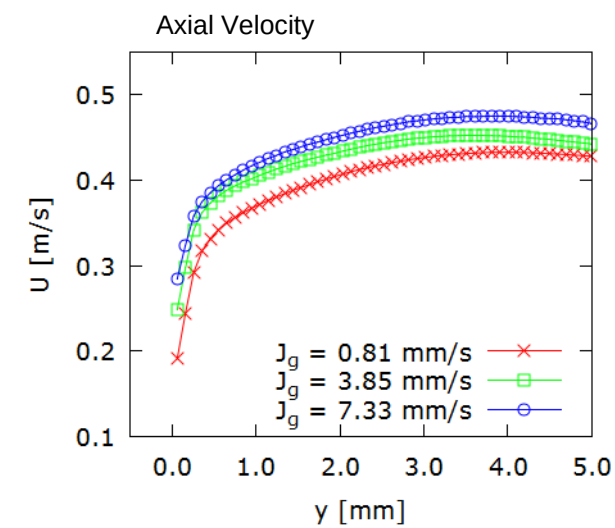

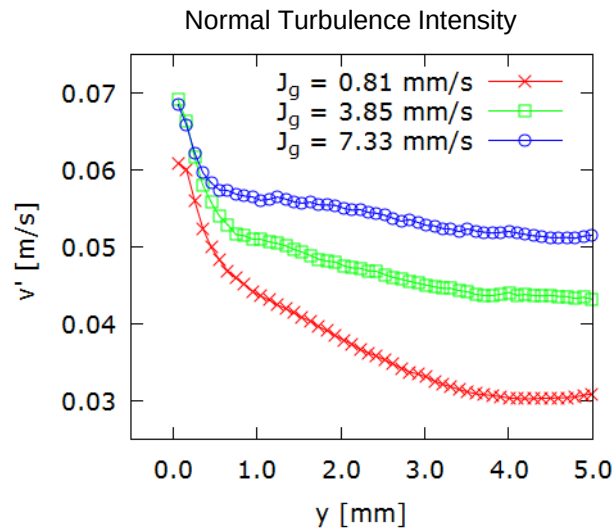

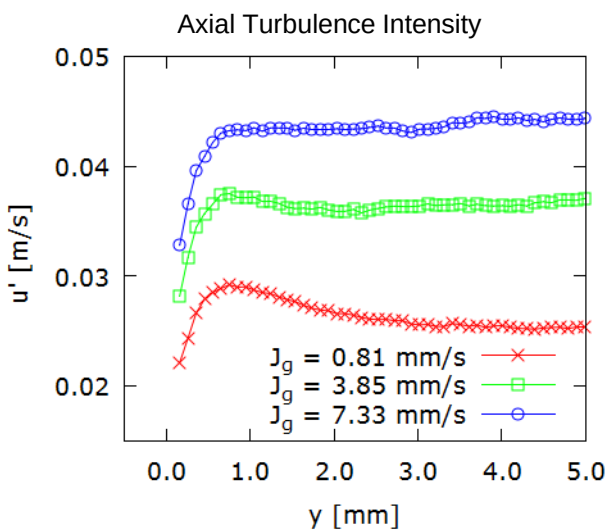

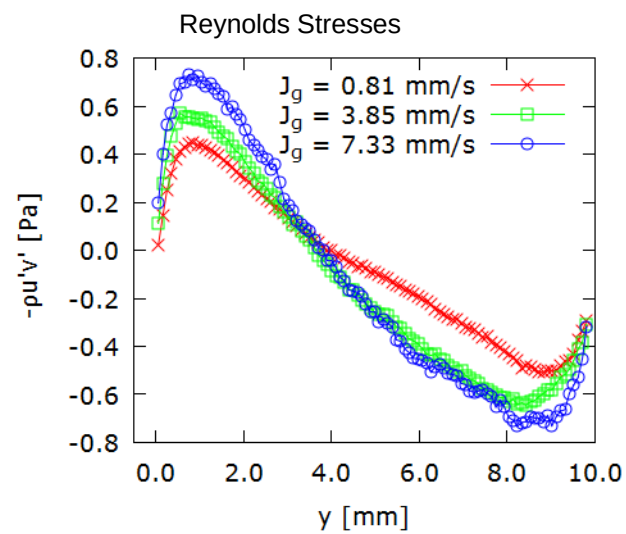

Effects of CRUD on Boiling (MIT)

Synthetic CRUD: iron-oxide nanoparticles deposited with layer-by-layer technique, chimney array created by photolithography; laid on sapphire-ITO heaters

Reactor CRUD

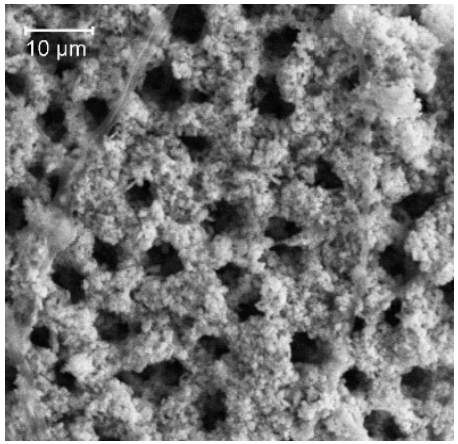

Synthetic CRUD

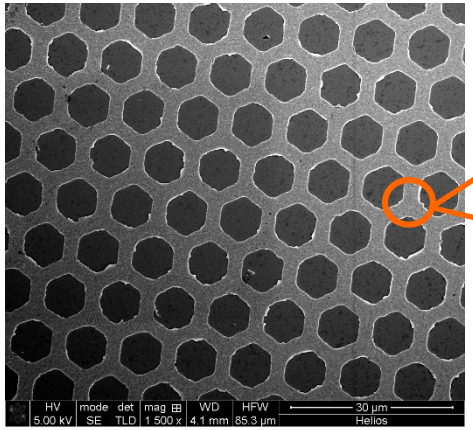

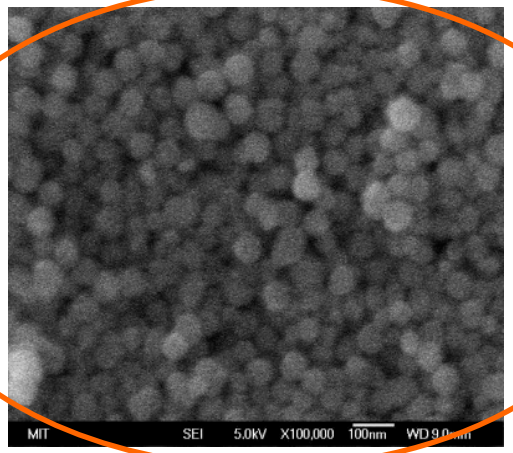

	Reactor CRUD	Synthetic CRUD
Composition	NiO, Fe_3O_4, $NiFe_2O_4$, ZrO_2	Fe_3O_4
Thickness	10-100 µm	5-15 µm
Roughness	$R_a \sim$ 0.5-3.0 µm	$R_a <$ 0.5 µm
Wettability (contact angle)	10-30°	20-40°
Porosity (not including chimneys)	40-50%	40-60%
Pore size	0.1-1.0 µm	0.02-0.2 µm
Chimney size	2-10 µm	5-10 µm
Chimney spacing	5-20 µm	10-100 µm

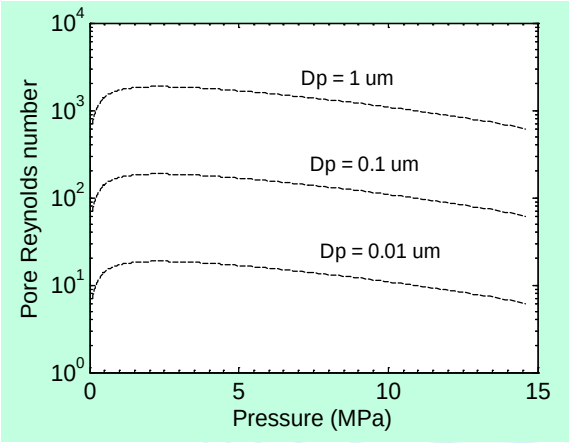

favorable scaling from atmospheric to PWR pressure

Next, heaters with synthetic CRUD coating will be tested in MIT boiling facility and compared to FY12-13 results for clean surface

Using Direct Numerical Simulations to Generate Data for Modeling (UND, NCSU)

- Simulations of single bubbles to quantify the effect of fluid shear, the presence of walls, and bubble deformability on the lift and drag on the bubbles
- Large-scale simulations of many bubbles in turbulent flows to examine the structure of the flow at steady state; the transient motion of bubbles and the turbulent modification by the bubbles
- Current focus is mostly on large scale simulations and efforts to connect the DNS data to modeling, including exploring the use of data mining techniques
- Simulations on the TITAN of the transient evolution in a vertical channel with Re_τ = 500 and over 500 bubbles of different sizes

Forces on a single bubble (UND)

- The lift on a single bubble depends strongly on the fluid shear, proximity to walls, and bubble deformability
- The lift induced lateral motion of bubbles determines the large scale structure of the flow and thus the void fraction distribution and pressure drop

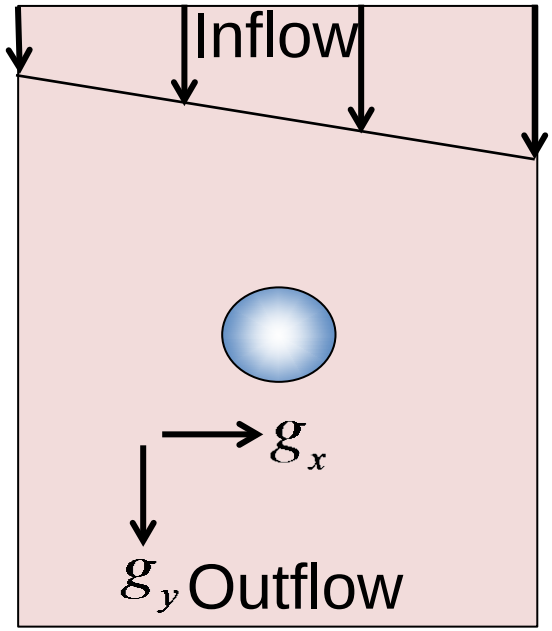

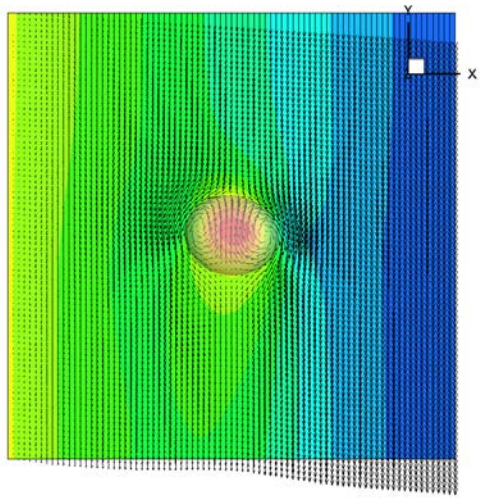

The velocity field around a single bubble in shear

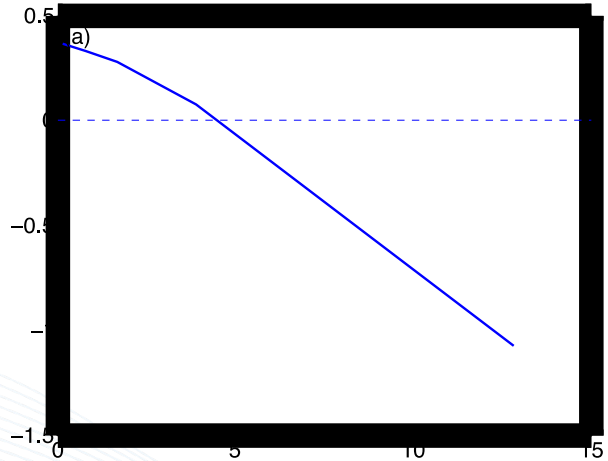

The lift coefficient versus the deformability of the bubbles (Eo)

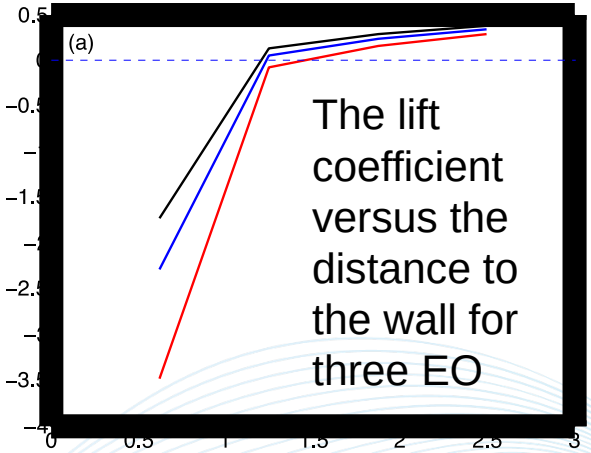

The lift coefficient versus the distance to the wall for three EO

Forces on a single bubble (NCSU)

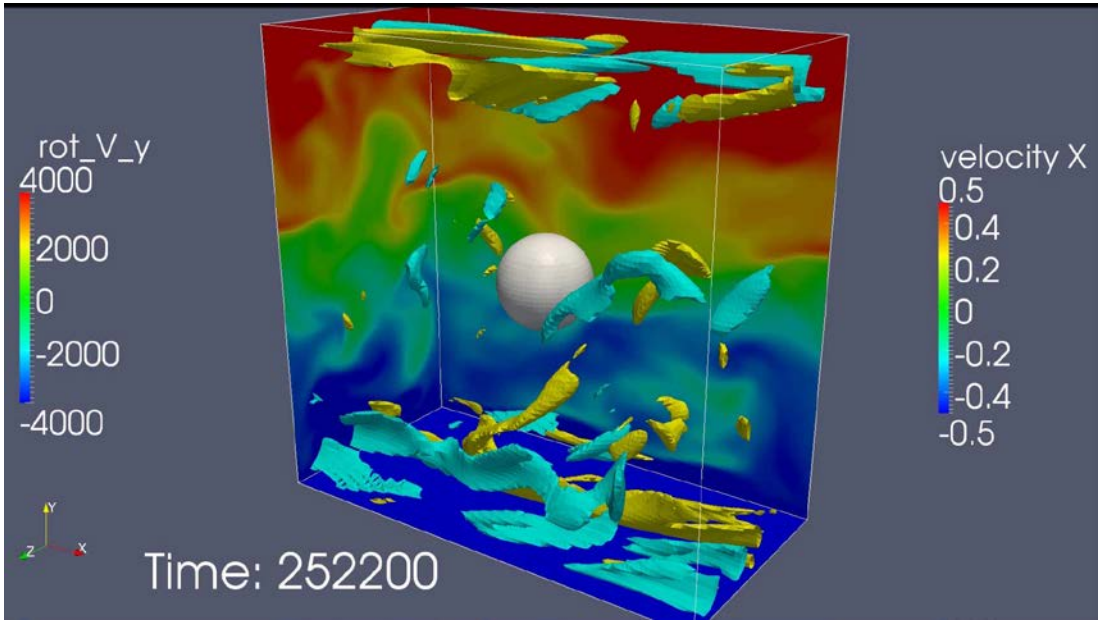

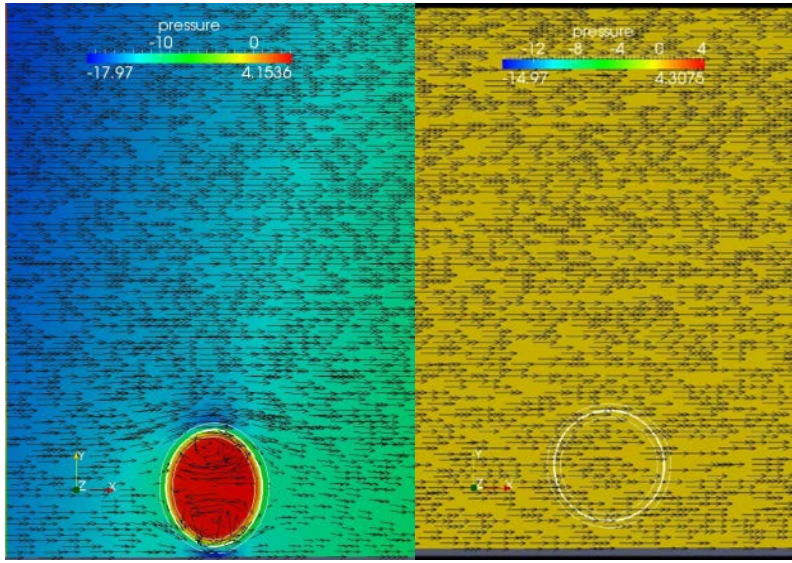

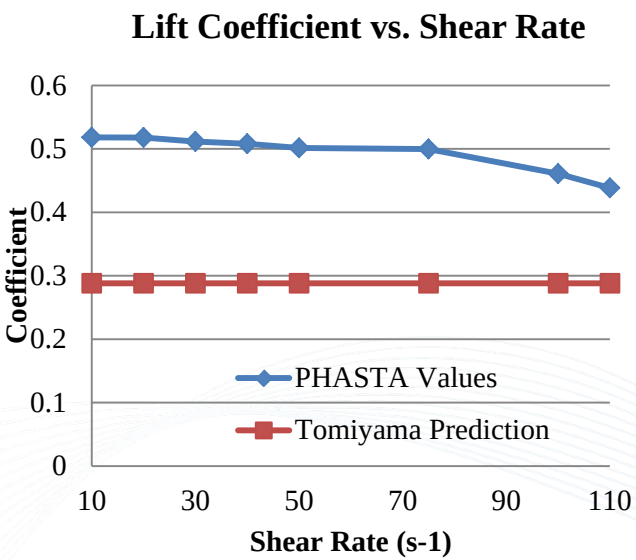

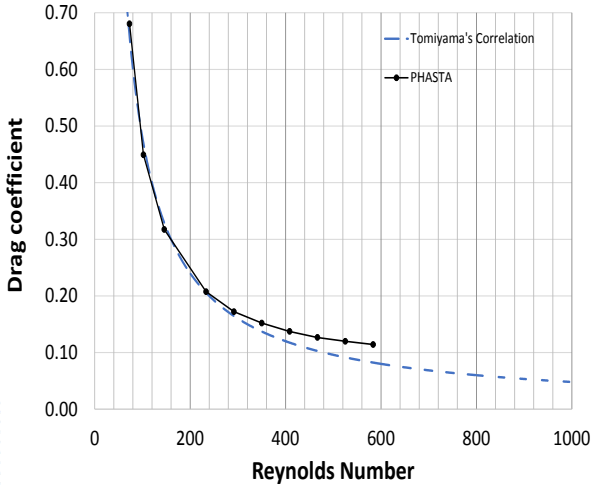

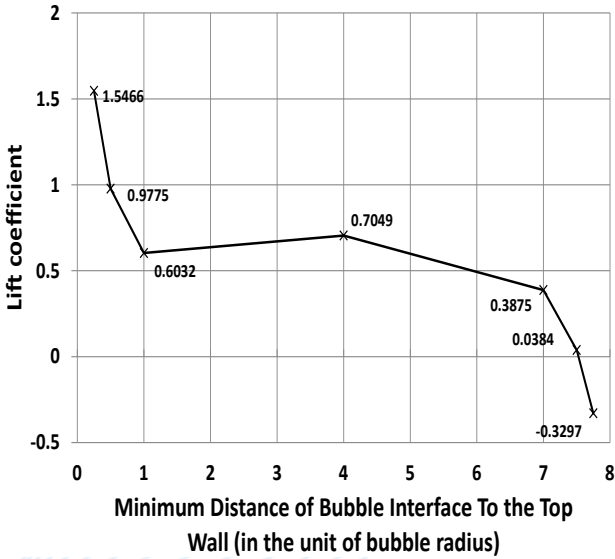

Simulations of phase change using ITMs (MIT)

1D and 2D simulations for challenging water/steam properties

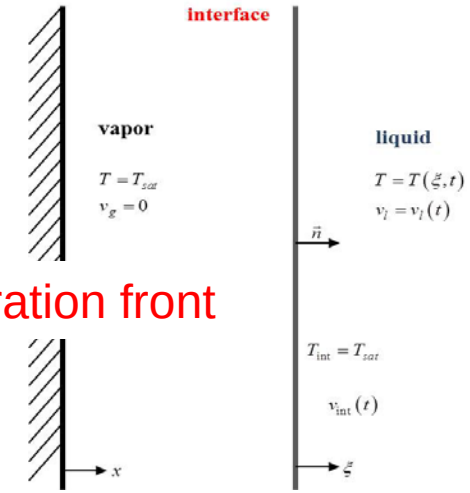

1D evaporation front

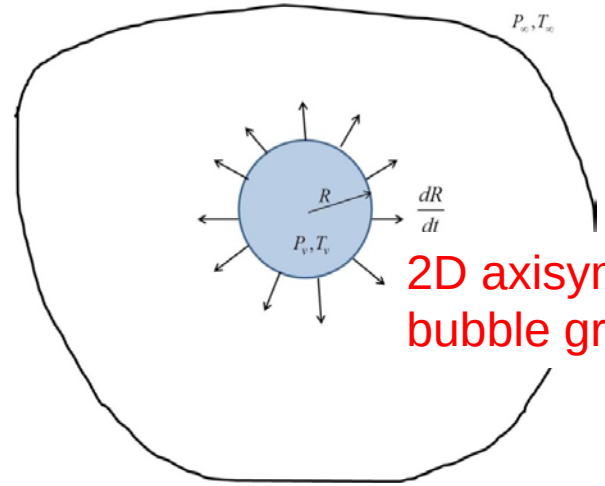

2D axisymmetric bubble growth

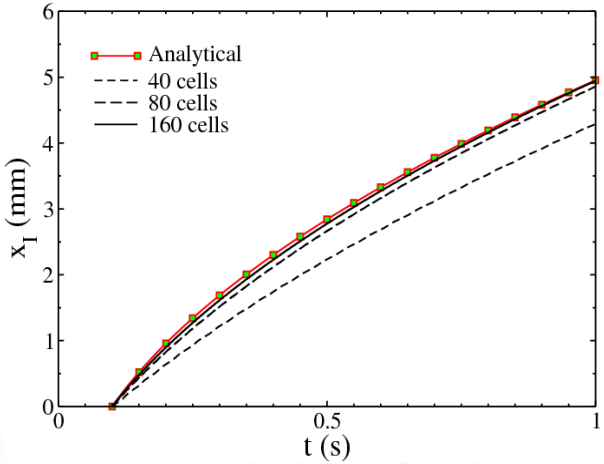

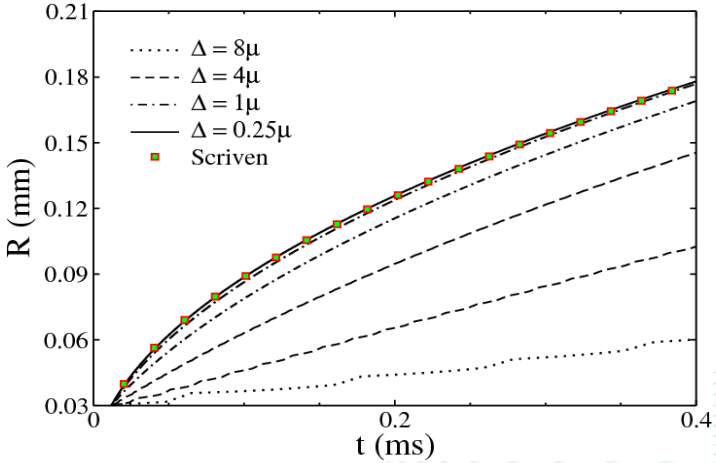

Sharp-interface level-set approach (implemented in TransAT) converges to analytical solutions

Simulations of phase change using ITMs (MIT)

3D simulations of nucleate boiling (ITM test Case 3b)

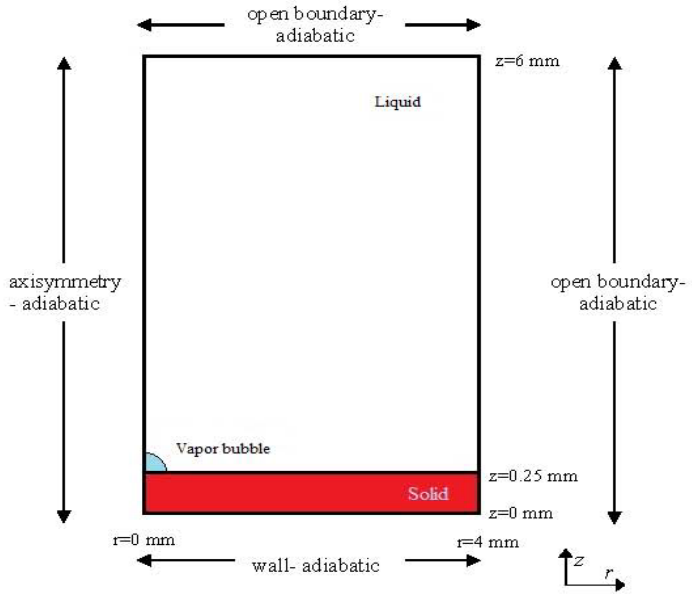

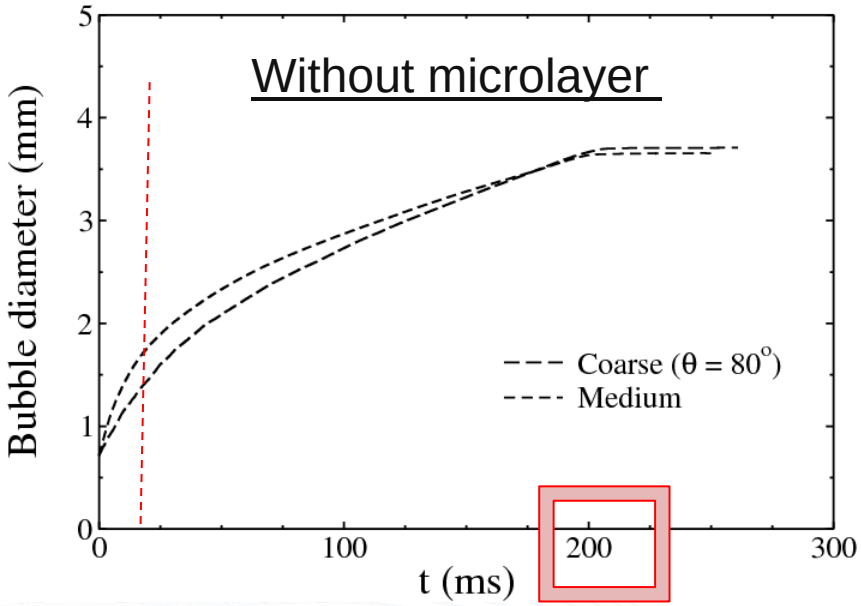

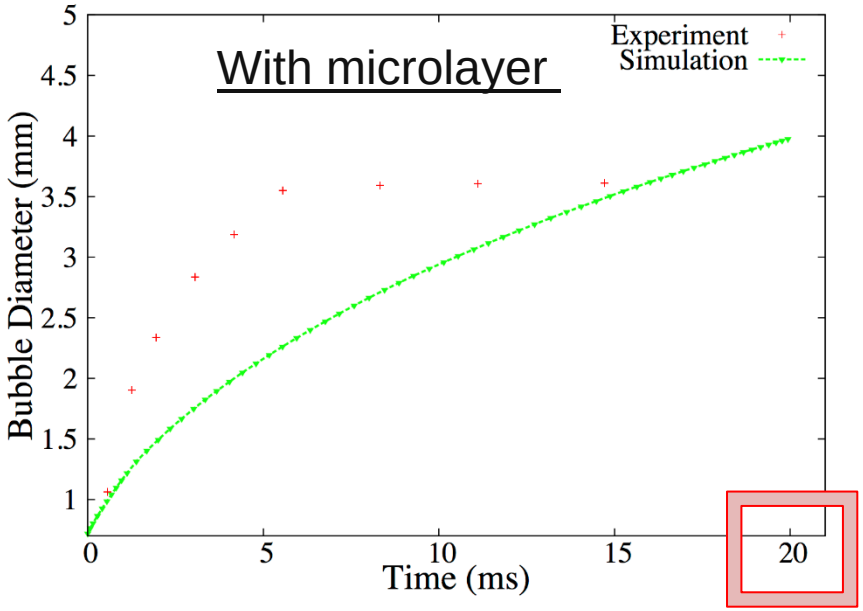

Inclusion of microlayer evaporation model is key to capturing correct growth curve and departure time

Transient Motion of a Large Number of Bubbles (UND)

The transient evolution of bubbly flow in vertical channels takes very long, making it important to capture it accurately. We are currently running a large simulation with bubbles of many different sizes to produce a database that can be mined for data needed in closure modeling for both two-fluid and LES-like computations

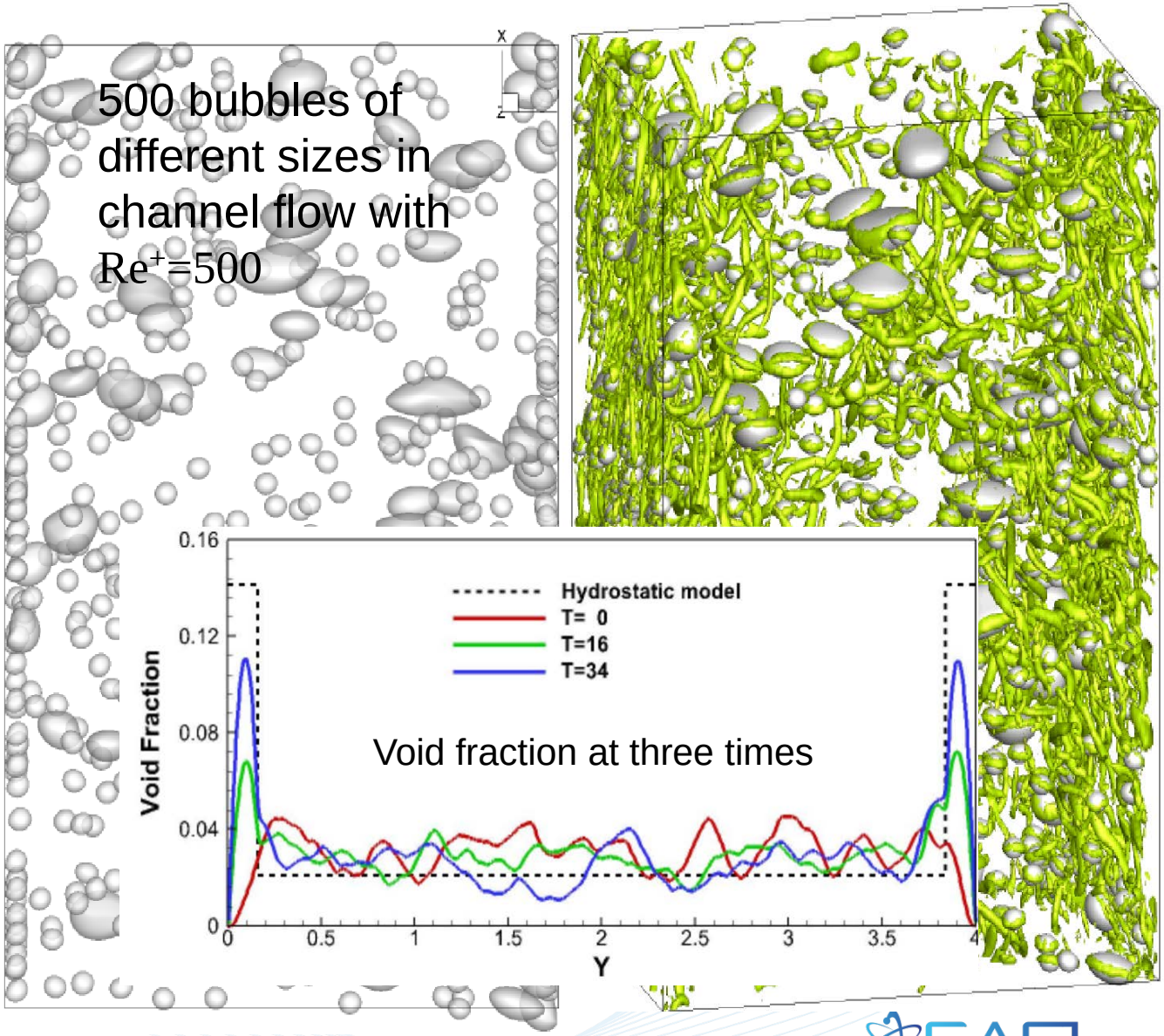

Transient Motion of a Large Number of Bubble (UND)

Correlating closure terms using a Neural Network

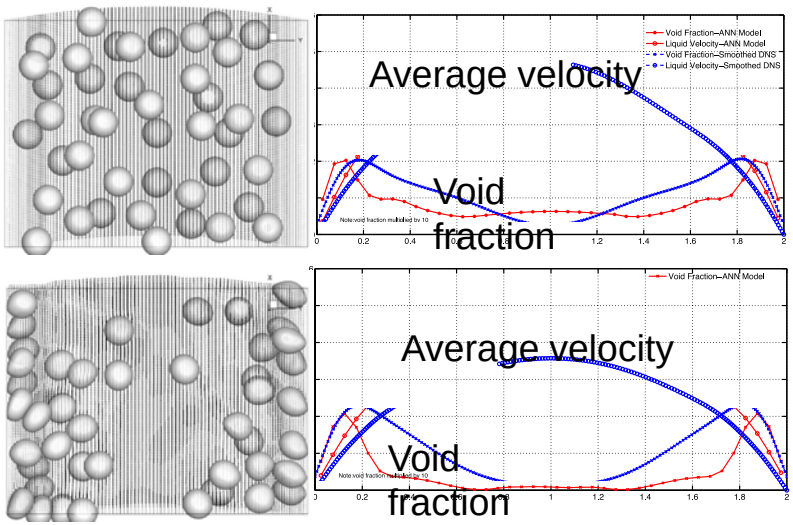

Preliminary comparison of a prediction of a two-fluid model using closure terms correlated using a Neural Network (blue), with DNS data (red). The average velocity and void fraction are shown at two times.

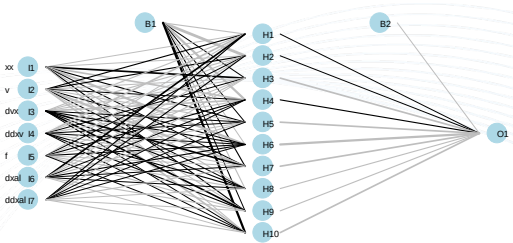

The Neural Network

"LES-like" filtering

The effect of applying a top hat filter with a size slightly larger than the diameter of the smallest bubbles to both the velocity and the interface. Large bubbles and vortical structures are smoothed and small bubbles become point particles

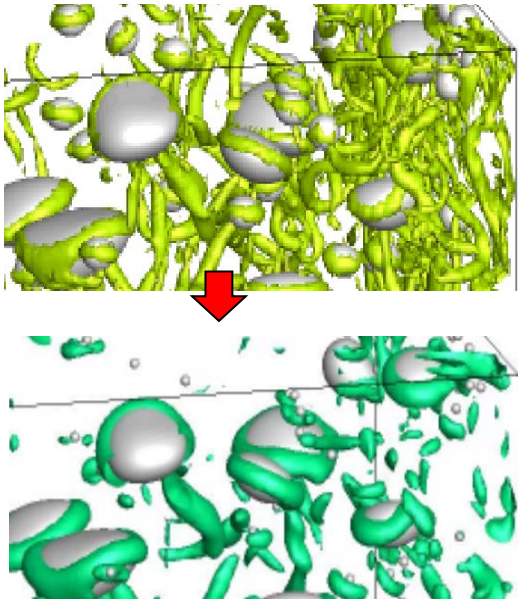

$$\overline{\mathbf{u}}(\mathbf{x}) = \int G_\Delta(\mathbf{x}-\mathbf{x}')\mathbf{u}(\mathbf{x}')d\mathbf{x}'$$

$$\overline{\mathbf{X}}(s) = \int G_\Delta(\mathbf{X}(s)-\mathbf{X}(s'))\mathbf{X}(s')ds'$$

$$G_\Delta(\mathbf{x}) = \begin{cases} 1 & \text{if} \quad |\mathbf{x}| < \Delta; \\ 0 & \text{if} \quad |\mathbf{x}| > \Delta. \end{cases}$$

Simulations and analysis of two-phase flow in a subchannel (NCSU)

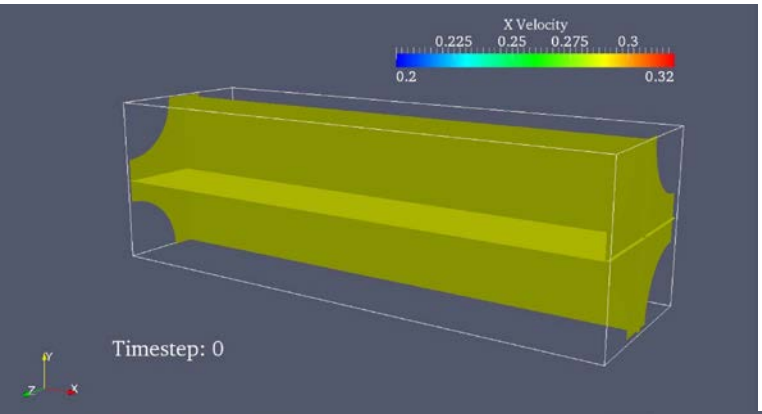

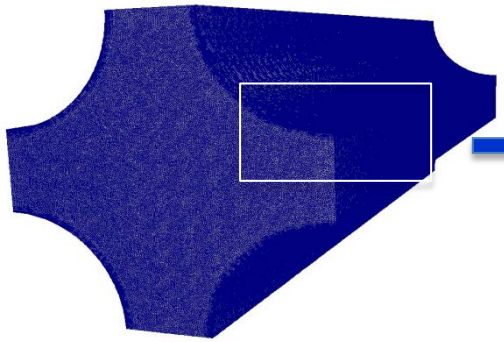

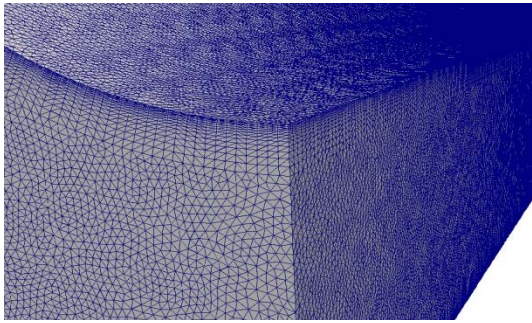

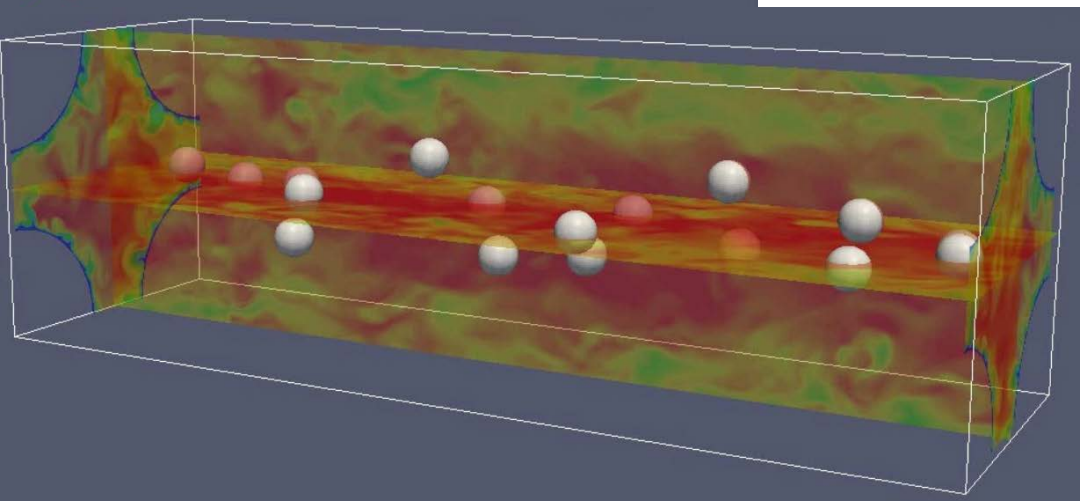

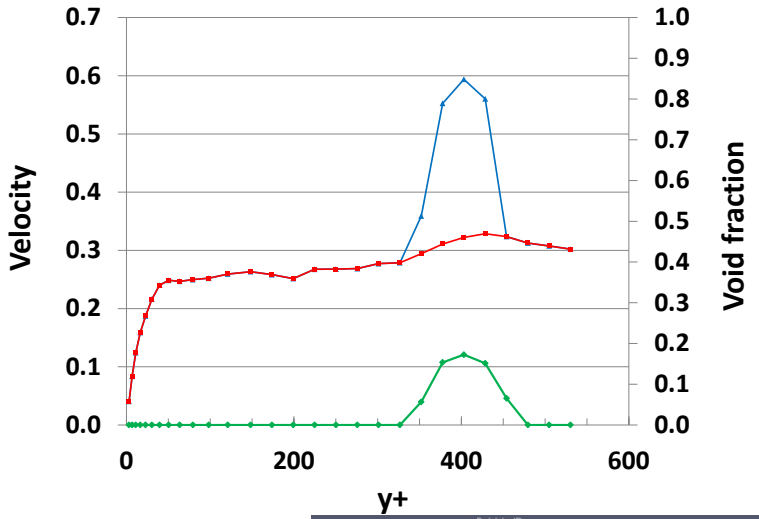

Single-subchannel with 17 bubbles at Re_τ = 400 (7% of normal PWR Re_τ), 1% void fraction
52M elements, 4,000 core run

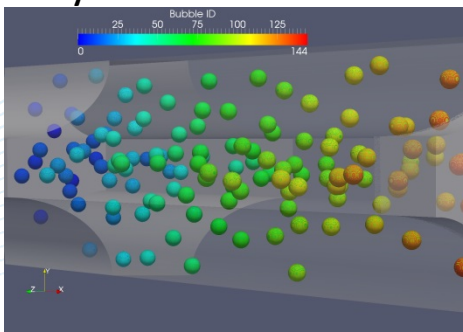

Next: 144 bubble run at Re_τ = 900

DNS of single-phase flow through 2x2 mixing vanes / spacer grid geometry (NCSU)

192M Elements mesh, 18,600 cores on Titan, in-situ visualization capabilities

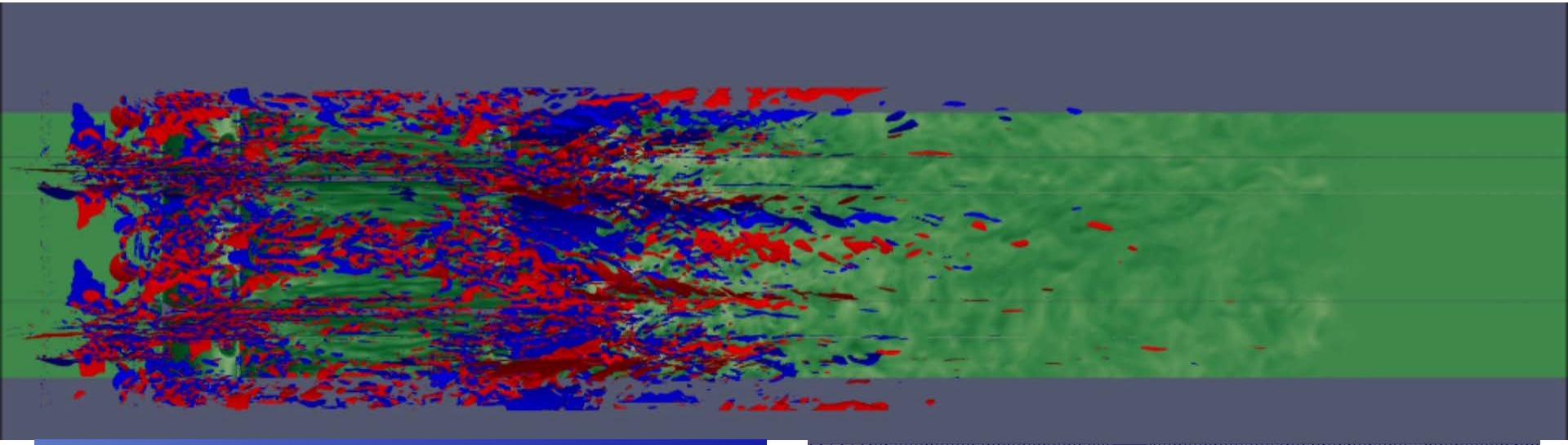

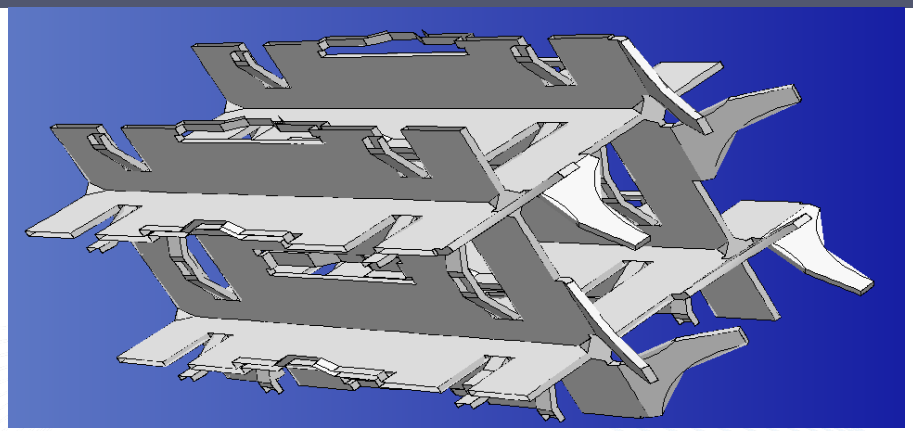

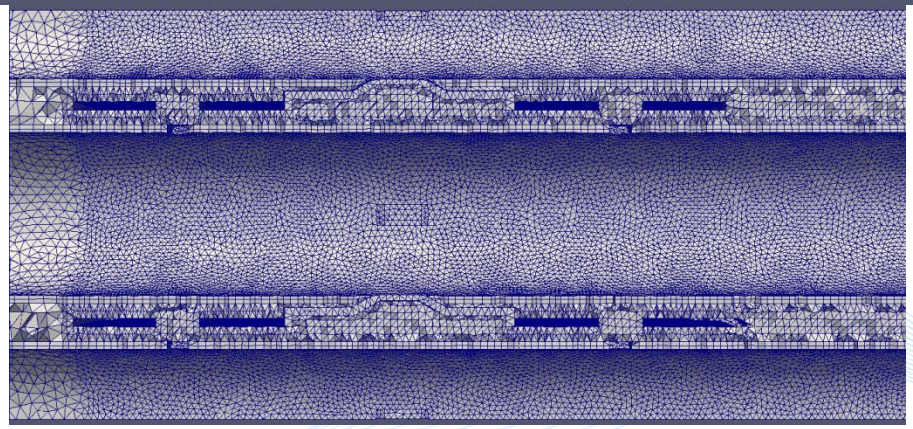

Summary

- We reviewed experimental and DNS/ITM capabilities and contributions to thermal-hydraulics methods focus area
- These capabilities represent state-of-the-art high fidelity experimental and simulation techniques applied to the problems relevant to CASL
- The focus of the work has been to provide essential data for closure model development necessary to address CASL Challenge Problems in THM area

New Capabilities in Hydra-TH

Mark A. Christon
Computational Physics Group
Los Alamos National Laboratory

2014 CASL RoundTable
July 14-16, 2014

LA-UR-14-25361

THM FY2014 Hydra-TH Centric L3 Milestones & ISV Collaboration

DOE Reportable:

- L2:THM.CFD.P9.01: Single Phase Validation of Hydra-TH for Fuel Applications

Development and Distribution Environment:

- L3:THM.CFD.P9.09: Hydra-TH release, bug/issue tracking and feature enhancement

New Features, Performance Enhancement:

- L3:THM.CFD.P8.02: Expose porous drag capabilities for DNB single-phase “mixing” calculations
- L3:THM.CFD.P9.02: Expose native CHT in Hydra-TH for stand-alone rod-bundle calculations
- L3:THM.CFD.P9.11: Hydra-Mamba coupling, i.e., Mamba as a sub-grid scale model
- L3:THM.CFD.P9.03: Hydra-TH linear algebra improvements and performance optimization

Turbulence Modeling:

- L3:THM.CFD.P9.06: Enhanced turbulence model capabilities in Hydra-TH
- L3:THM.CFD.P9.07: Advanced turbulence models for multiphase flow (BHR, cascade, etc.)
- L3:THM.CFD.P9.13: EARSM turbulence modeling for fuel assembly applications

V&V and Assessment

- L3:THM.CFD.P9.01: CFD hexahedral mesh generation for selected problems and Hydra-TH verification
- L3:THM.CFD.P9.05: Single/Multiphase CFD assessment, verification and validation

Multiphase

- L3:THM.CFD.P9.12: Demonstration of multiphase boiling flow with Hydra-TH in realistic subchannels with mixing vanes

Kitware Collaboration

Staffing, Dropped & Delayed Milestones, …

- Signficant staff turnover: ~12 staff over past 36 months across CASL THM
  - We are re-training developers every 3 months on average
  - Lack of technical continuity, continually "re-trenching" the same ground
  - Unlikely to be able to sustain any significant development or technical advances

- Delayed and/or Dropped Milestones
  - L3:THM.CFD.P8.02: Expose porous drag capabilities for DNB single-phase "mixing" calculations (delayed, but now complete)
  - L3:THM.CFD.P8.01: Demonstration of Multiphase in Hydra-TH (dropped, insufficient staff)
  - L3:THM.CFD.P9.02: Expose native CHT in Hydra-TH for stand-alone rod-bundle calculations (delayed, more invasive than expected)
  - L3:THM.CFD.P10: Nonlinear Krylov Acceleration for Fully-Implicit Solution Algorithms (delayed, probably drop, or absorb in other milestones)
  - L3:THM.CFD.P9.11: Hydra-Mamba coupling, i.e., Mamba as a sub-grid scale model (in-progress, concerns)
  - L3:THM.CFD.P9.12: Demonstration of multiphase boiling flow with Hydra-TH in realistic subchannels with mixing vanes (delayed to December, 2014)
  - L3:THM.CFD.P7.04: General-purpose library for steam property evaluation for multiphase CFD (working code never delivered)

Development Environment and Deployment

Jozsef Bakosi, Mark A. Christon
LANL

Milestones Supported:
L3:THM.CFD.P9.09: Hydra-TH release, bug/issue tracking and feature enhancement

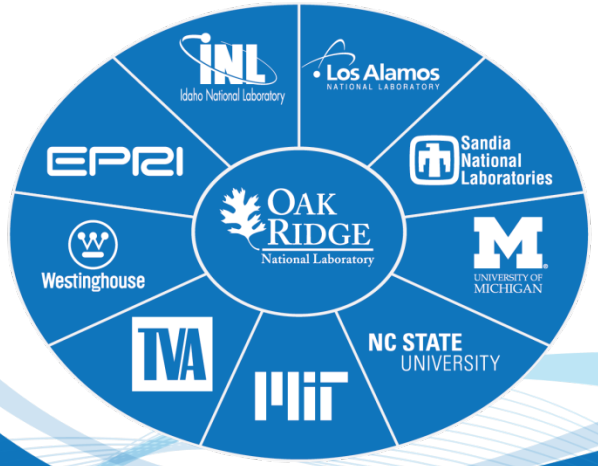

Revamped Development Environment – based on methods/practices used by Kitware, DS SIMULIA

- FY14 saw a rapid expansion in Hydra developers outside LANL
  - Typical LANL process was extremely long (~3 months), required use of VPN which typically doesn't work for non-LANL computers, and resulted in many project delays
- Desirable to have "open-access" to project tracking, repositories, documentation while preserving export controls
  - Model based on environment used by Kitware, and practices by Kitware/DS SIMULIA
  - Using ccs-green machine at LANL on "open" network
  - git for code repositories, Redmine for development process, gerrit for code-reviews, migrating to CTest/CDash
  - New time for adding a developer ~ 3-4 days for Tech Transfer licensing
  - 12 new developers added over the past 6 months

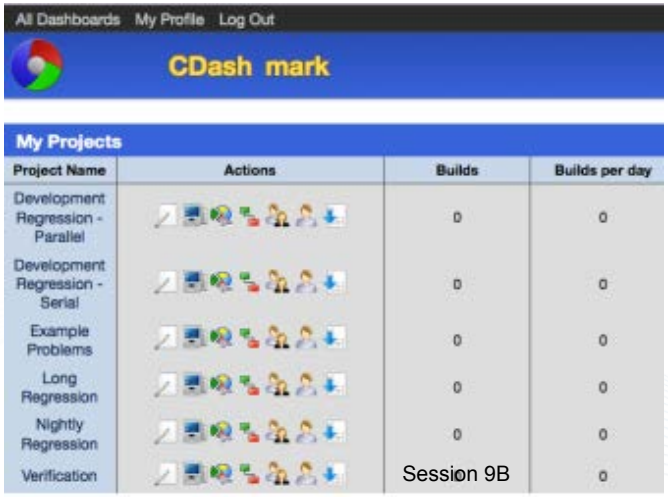

Mapping issues by milestones and other tasks such as bug fixes, features

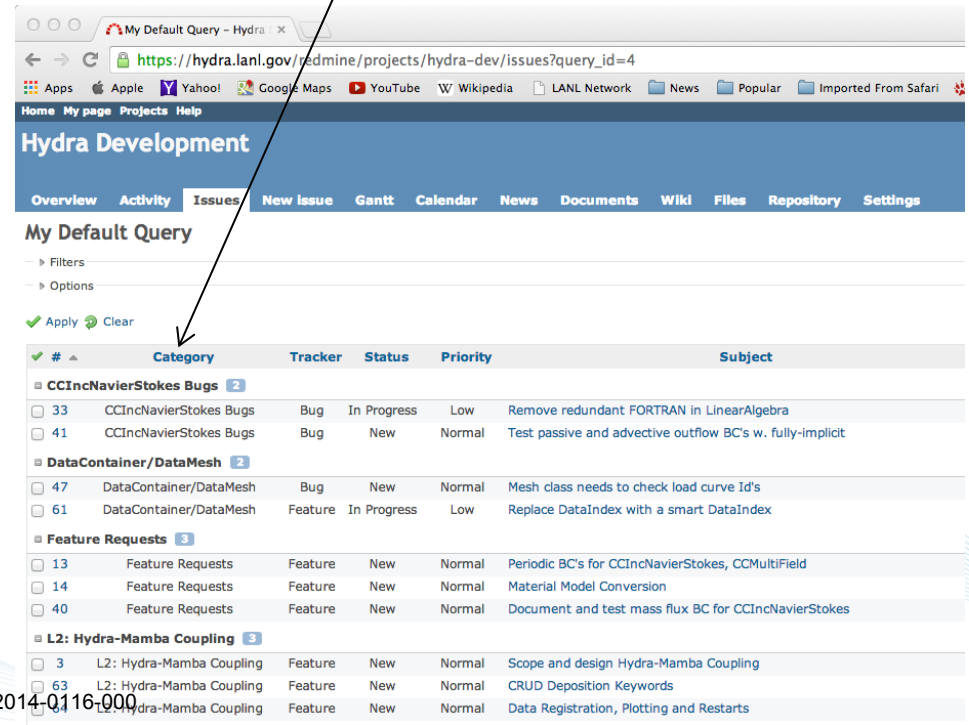

Hydra-TH Deployment, Support & Impact

- Early deployment of Hydra-TH was requested by a number of users, e.g., Jin Yan at Westinghouse, AMA, Dec., 2012
- Hydra-TH Licenses since January 2013
- User support, code distribution, porting issues have diluted Hydra-TH development efforts in FY13/FY14
- E-mail support: hydra-th-users@lanl.gov
- Downloads: get-hydra.lanl.gov
- Pursuing code distribution via Kitware…

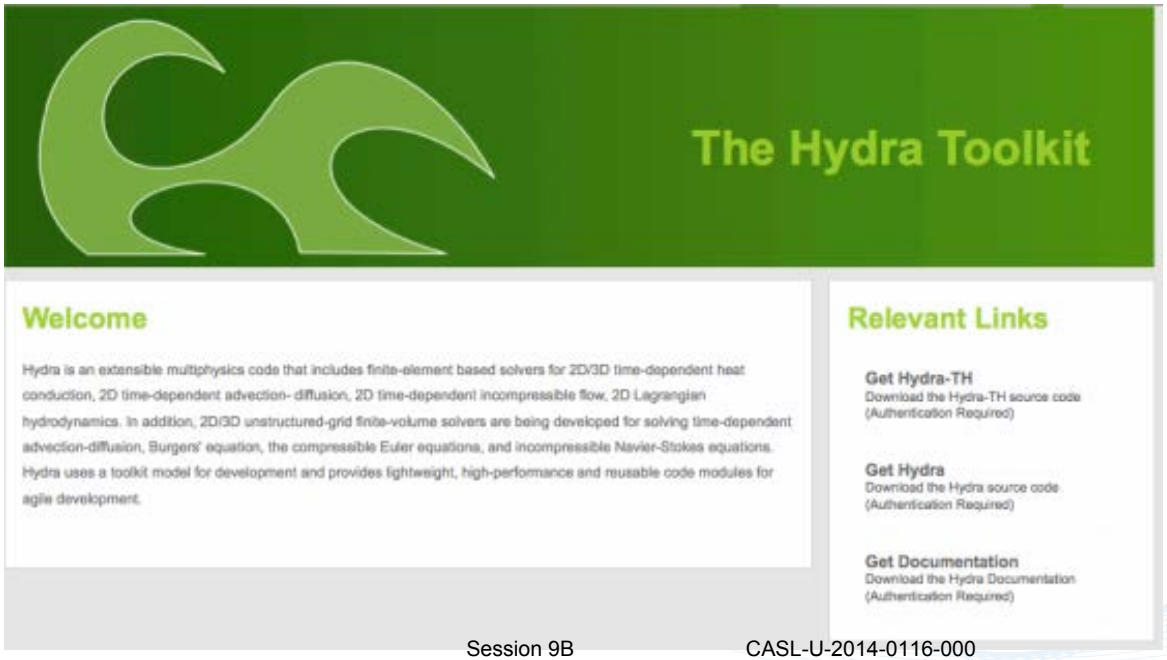

Institution	Seats
AECL (Canada)	3
Aston University (UK)	2
Carnegie-Mellon	2
INL	1
Kitware	5
MIT	8
NASA -- Houston	1
NCSU	7
ORNL	2
Penn State	2
Sandia	3
Texas A&M	2
TVA	2
U. Michigan	3
U. Texas	2
WEC	7
Total	52

Porous Drag, CHT, Hydra-Mamba Coupling, and Performance Enhancement

Jozsef Bakosi, Markus Berndt,
Mark Christon, Balu Nadiga, LANL

Alan Stagg, ORNL

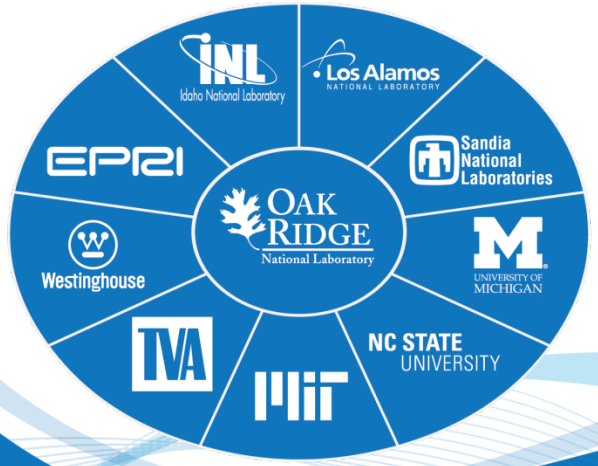

Milestones supported:

L3:THM.CFD.P8.02: Expose porous drag capabilities for DNB single-phase "mixing" calculations

L3:THM.CFD.P9.02: Expose native CHT in Hydra-TH for stand-alone rod-bundle calculations

L3:THM.CFD.P9.11: Hydra-Mamba coupling, i.e., Mamba as a sub-grid scale model

L3:THM.CFD.P9.03: Hydra-TH linear algebra improvements and performance optimization

L1:CASL.P9.02: Application of Multi-Scale Thermal Hydraulic Models to DNB Analysis

L2:CASL.P9.02: Demonstration of Coupled CFD and CRUD/Corrosion Chemistry for a Fuel Sub-Region

TVA Test Stand

Porous Drag Capability in Hydra-TH

Will be used to Simulate Core Region

Replace Spacer Grid/Support Structure With Porous Medium

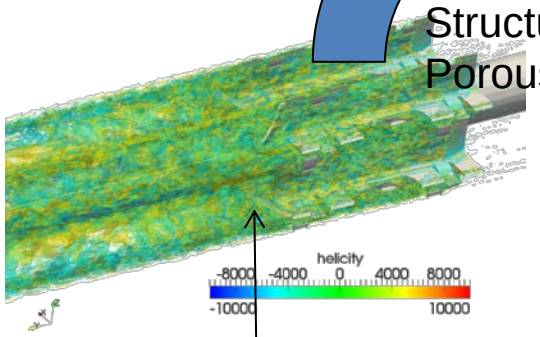

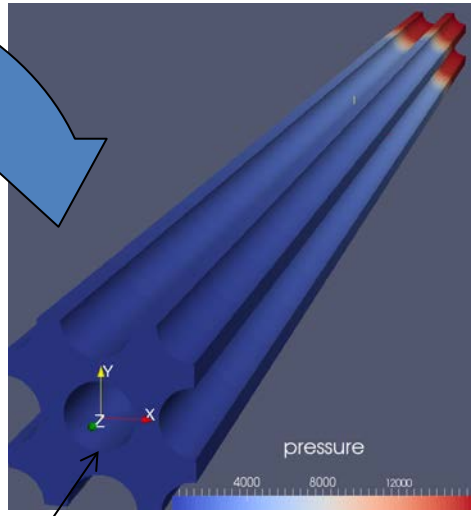

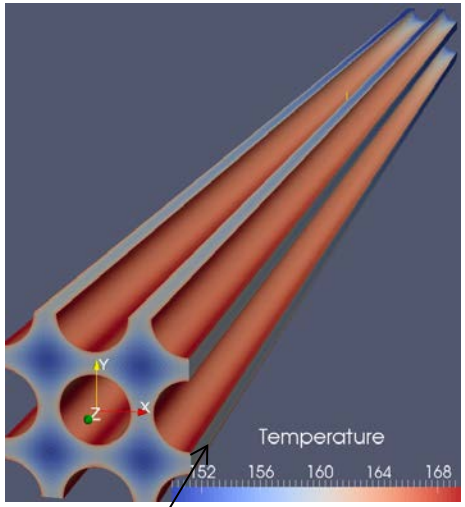

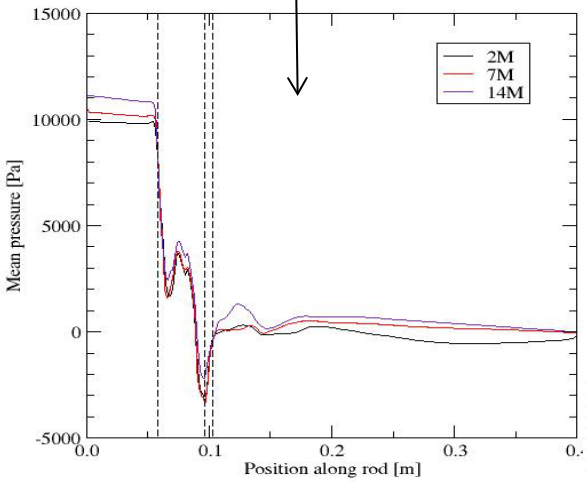

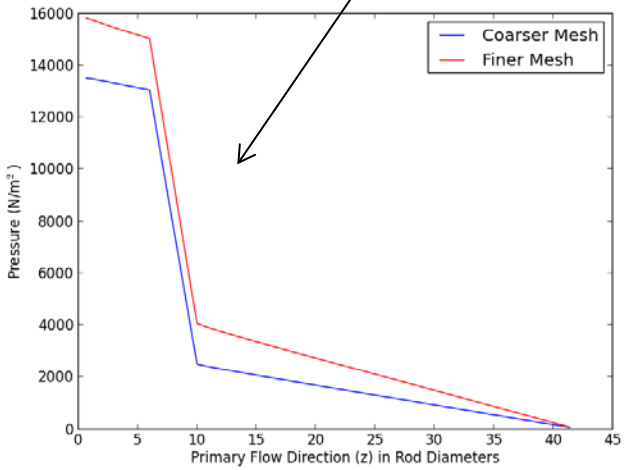

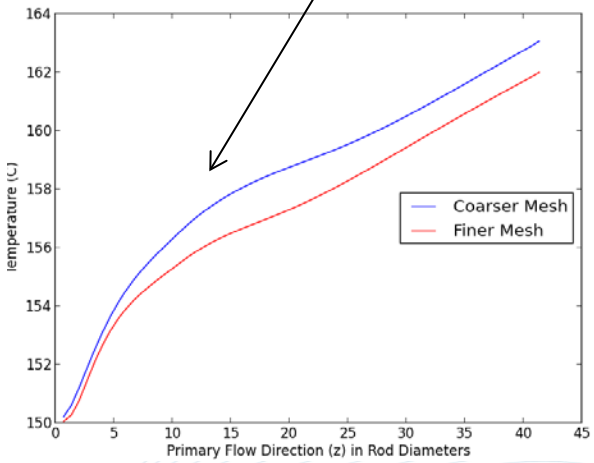

Beavers-Joseph Verification Problem

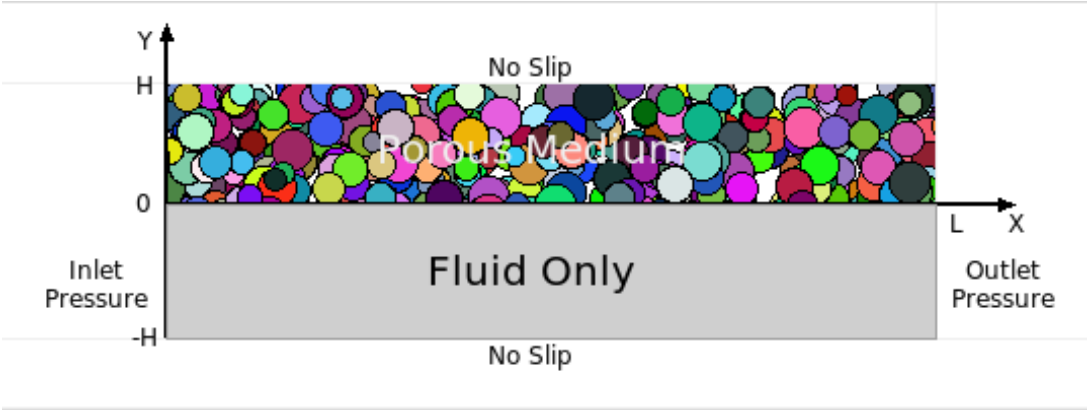

Anaytic solution based on Vaifai and Kim, Int. J. Heat and Fluid Flow, 1990

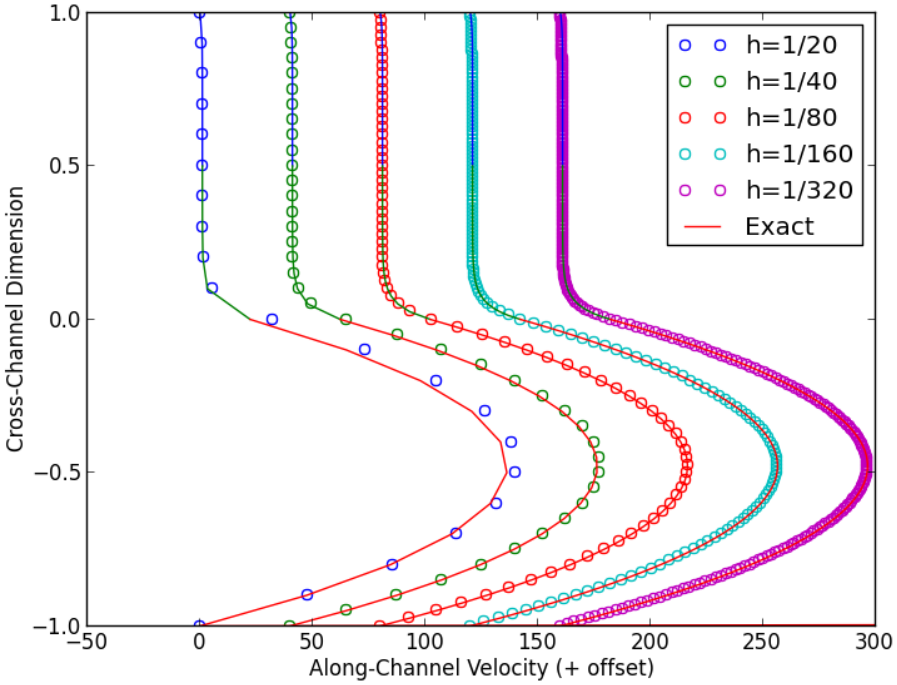

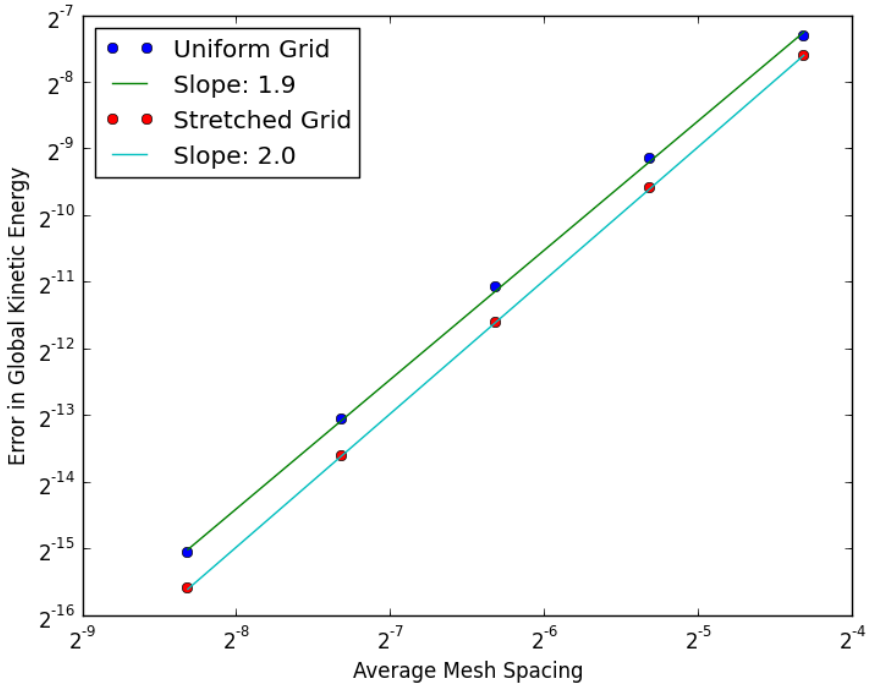

Native Conjugate Heat Transfer Uses Automated Interface Detection for Complex Reactor Geometries

- Automated interface detection segregates solid materials from fluid materials
  - Automatic specification of no-slip/no-penetration BC's, turbulence quantities, etc.
  - Preserves heat flux continuity at the fluid-solid interface
  - Avoids time-consuming, error-prone user identification of fluid-solid interface for CHT
- Hexpress/Hybrid permits meshing multiple volumes, e.g., fluid and solid, in one step with coincident interfaces

Automated interface detection can be applied to arbitrarily complex geometries

Hydra Native Conjugate Heat Transfer Verification

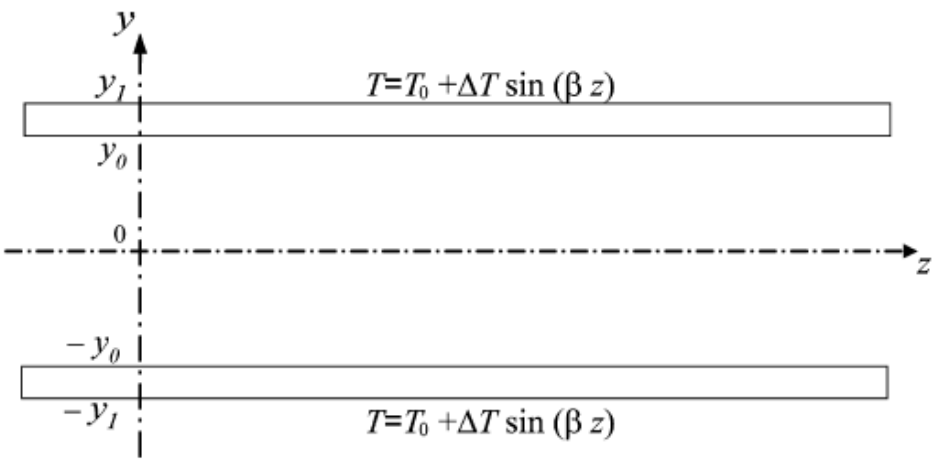

Figure 2: Longitudinal section of channel with boundary conditions

- Heat conducting through solid walls into fully developed fluid flow
- Automatic construction of internal fluid/solid interfaces and associated boundary conditions for complex reactor geometries.
- Preliminary Hydra CHT results with comparison to analytic solution
  - ✧ *Conjugate forced convection heat transfer in a plane channel: Longitudinal periodic regime (A. Barletta et al., International J. Thermal Sciences 47, 42-51, 2008).*

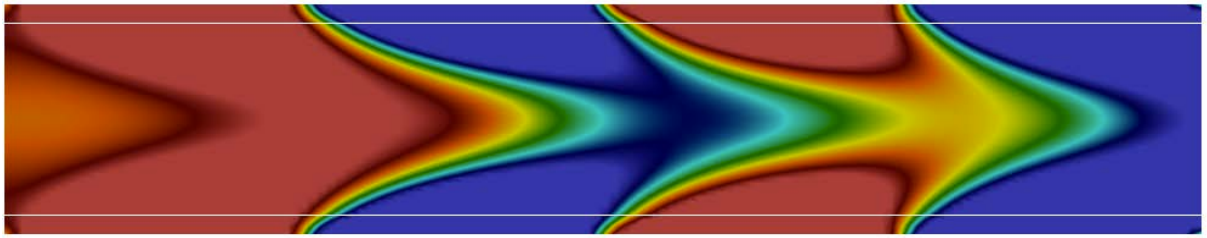

Figure 1: Non-dimensional Temperature

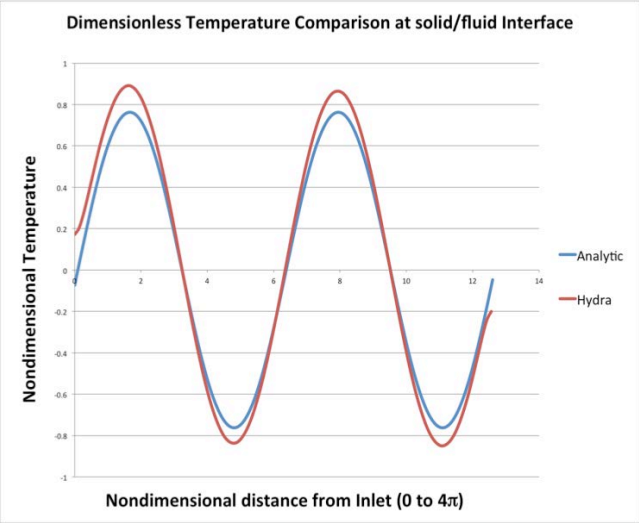

Conjugate heat transfer through wall into fluid.
Temperature distribution at fluid/solid interface.

A. Stagg: Oak Ridge National Laboratory
K. Frick: North Carolina State University

Integration of Surface Chemistry Capability into Hydra-TH

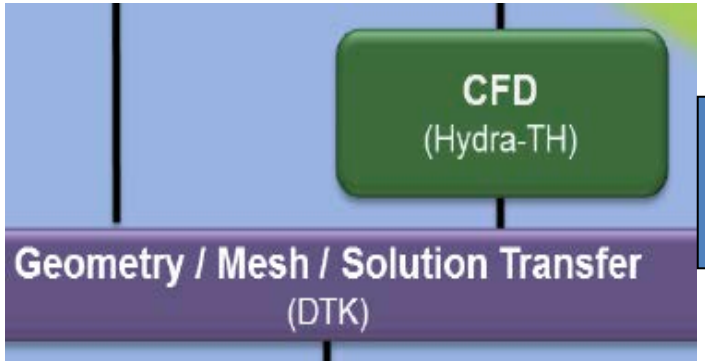

Evolution of Hydra-TH in VERA From End of Phase 1 to Phase 2

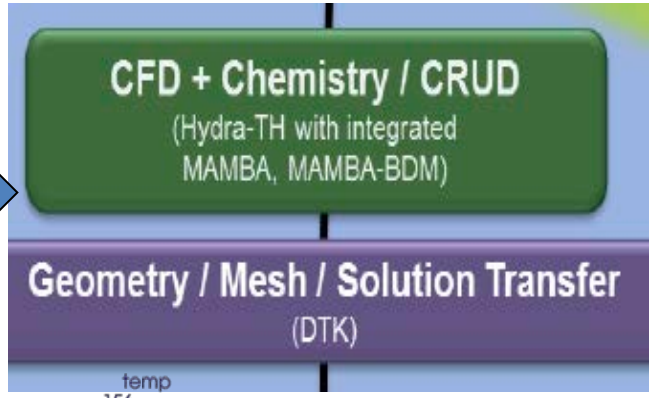

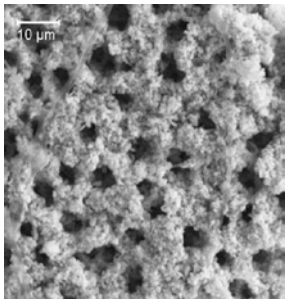

- Local CRUD Chemistry
- Boiling, chimney formation
- CRUD deposition
- Thermal resistance

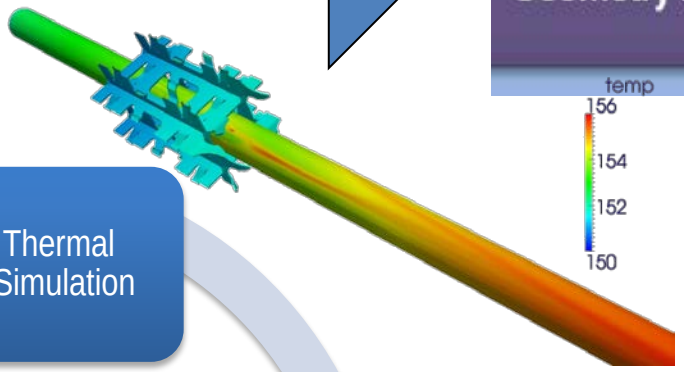

Hydra-TH Thermal Hydraulics Simulation

- **CRUD Induced Power Shift**
- **CRUD Induced Localized Corrosion**
- **Difficult to Predict**
- **Drive to Zero Fuel Failure**

MAMBA Sub-Grid Scale Model

Wall-Shear, Temperature, Heat Flux

Fully-Implicit Projection

- RNG k-ε model
- Re ~ 4.0×10^5
- $q_w = 10^6$ W/m^2
- 2.4M elements, ~18M DoF
- ~ 4.75 hours on 16-core Intel Xeon desktop

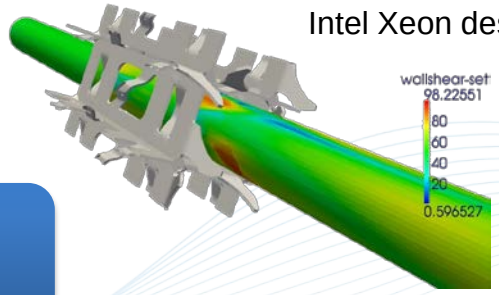

Performance Assessment and Improvements

Assessed computational performance of Hydra-TH using existing MPI-parallelism on Titan and LANL Turquoise HPC clusters using V5H GTRF problem, *Status: 100% completed*

- Hydra-TH scales well as long as work load per core is sufficiently large.
- There is no consistent benefit from running Hydra-TH in full stream mode on Titan.

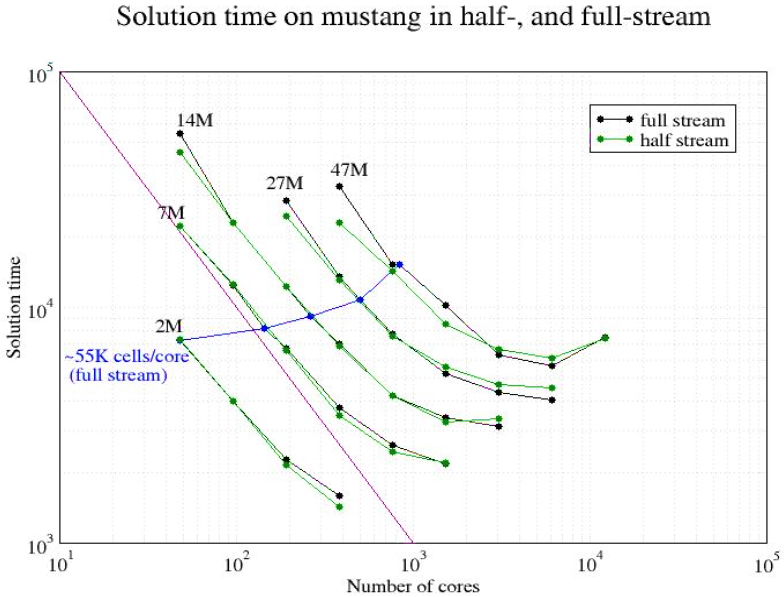

Per element HYDRA memory footprint

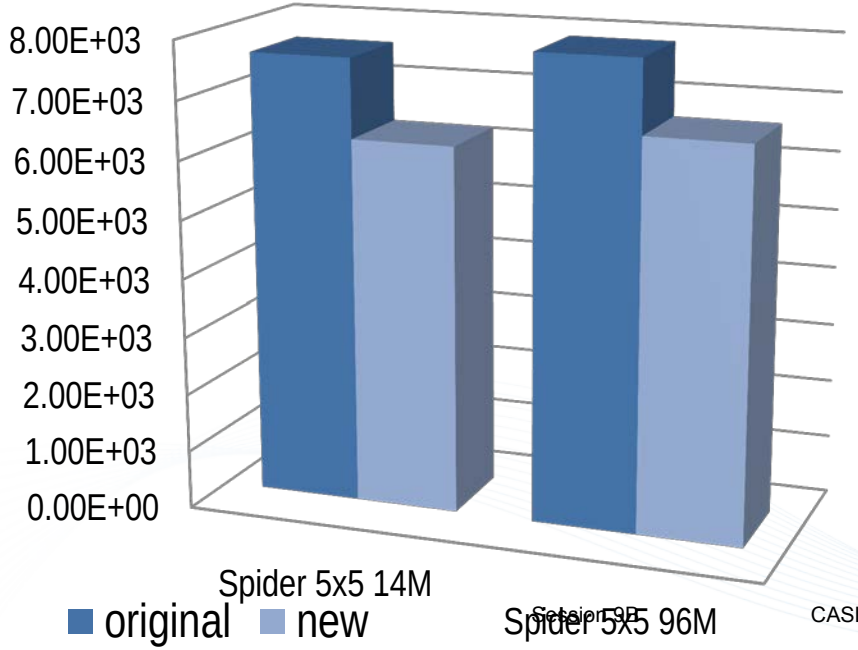

New matrix pre-allocation algorithms for Hydra's PETSc linear solvers:

- Small additional communication cost during the setup phase for conduction physics.
- No additional communication cost for momentum and transport.
- The new pre-allocation algorithm results in memory allocation much closer to what is actually needed to store the matrices.

NVIDIA AmgX Solver Library Integration

NVIDIA's "AmgX library offers optimized methods for massive parallelism"

Completed Tasks:

- AmgX is available as an optional TPL (users need license from NVIDIA for use).
- Hydra's interface for the PPE solver to AmgX is code complete on a branch.
- Selecting AmgX solver for PPE via an option through standard Hydra input.
- Preliminary testing at workstation scale with an NVIDIA supplied Tesla K20 card.

Remaining Tasks:

- Performance assessment of AmgX as PPE solver in Hydra.
- Performance tuning of Hydra interface to AmgX.
- Identify recommended set of parameters to AmgX library (eg. Krylov solver setup, and specific setup for unsmoothed aggregation preconditioner)

```
AMG Grid:
        Number of Levels: 3
           LVL          ROWS                NNZ     SPRSTY        Mem (GB)
        ------------------------------------------------------------------
          0(D)          9261             226981   0.00265         0.00276
          1(D)          1143              37429    0.0286        0.000881
          2(D)           144               3684     0.178        8.67e-05
        ------------------------------------------------------------------
        Grid Complexity: 1.13897
        Operator Complexity: 1.18113
        Total Memory Usage: 0.00372878 GB
        ------------------------------------------------------------------
          iter      Mem Usage (GB)       residual           rate
        ------------------------------------------------------------------
           Ini            0.373898   8.363096e-07
             0            0.373898   6.208815e-08         0.0742
             1              0.3739   2.929195e-08         0.4718
             2              0.3739   9.269233e-09         0.3164
             3              0.3739   2.841682e-09         0.3066
             4              0.3739   1.942728e-09         0.6837
             5              0.3739   1.709682e-09         0.8800
             6              0.3739   1.582546e-09         0.9256
             7              0.3739   1.385003e-09         0.8752
             8              0.3739   1.009331e-09         0.7288
             9              0.3739   4.618366e-10         0.4576
            10              0.3739   1.717884e-10         0.3720
            11              0.3739   6.590460e-11         0.3836
            12              0.3739   2.014400e-11         0.3057
            13              0.3739   6.651266e-12         0.3302
        ------------------------------------------------------------------
        Total Iterations: 14
        Avg Convergence Rate:                   0.4323
        Final Residual:                    6.651266e-12
        Total Reduction in Residual:       7.953115e-06
        Maximum Memory Usage:                   0.374 GB
        ------------------------------------------------------------------
Total Time: 0.034682
    setup: 0.0151521 s
    solve: 0.0195299 s
    solve(per iteration): 0.00139499 s
```

Sample AmgX output from a Hydra run.

Hydra-TH Conversion to Trilinos/ML from PETSc/ML

- **Required by VERA for Multiphysics Coupling:** Multi-Level (ML) Algebraic Preconditioner for Pressure-Poisson Eq. (PPE) currently used with PETSc, being switched to use Trilinos
- **Avoid library incompatibilities in VERA integration**
- **Follow new releases of ML:** maintained under Trilinos
- **Implement with:** Epetra/Trilinos vector and matrix and Belos/Trilinos solver packages
- **Easy-to-use generic wrappers in Hydra linear algebra classes:** Minimal change to client code

PETSc → Trilinos

Turbulence Modeling Efforts

Tom Smith, SNL
Emilio Baglietto, Ben Magolan, MIT
Igor Bolotnov, Cameron Brown, NCSU

Milestones supported:

L3:THM.CFD.P9.06: Enhanced turbulence model capabilities in Hydra-TH

L3:THM.CFD.P9.07: Advanced turbulence models for multiphase flow (BHR, cascade, etc.)

L3:THM.CFD.P9.13: EARSM turbulence modeling for fuel assembly applications

L2:THM.P9.02: Single Phase Validation of Hydra-TH for Fuel Applications

Spalart-Allmaras Rotation and Curvature Correction: U-Channel

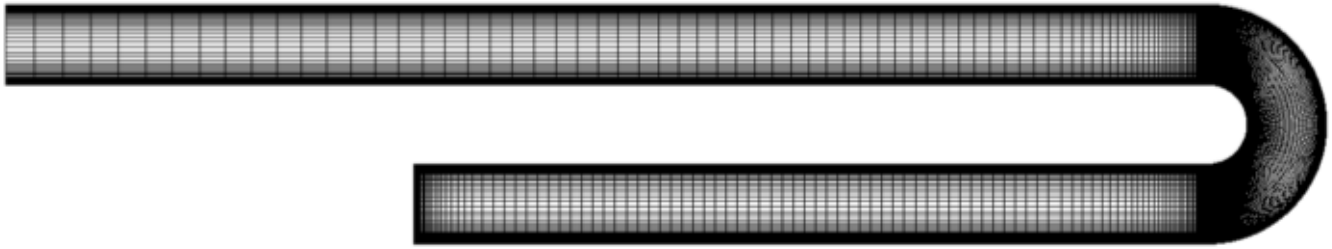

2D U-Channel
mesh: 421x112x2
Re=1.0E6
Uniform inflow profile
Rumsey, et al., AIAA, 2000

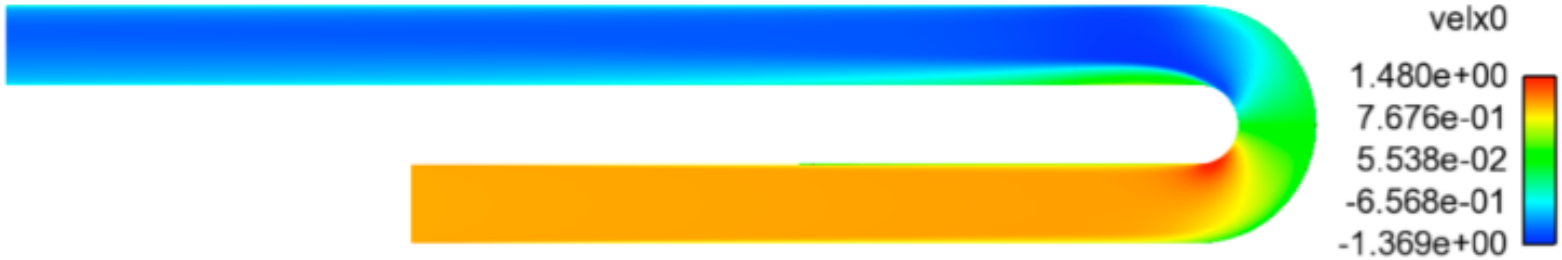

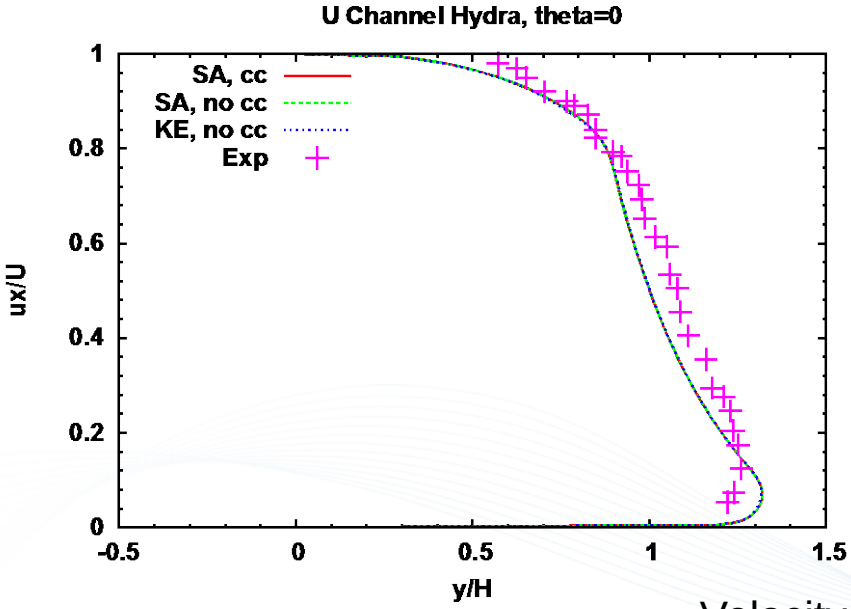

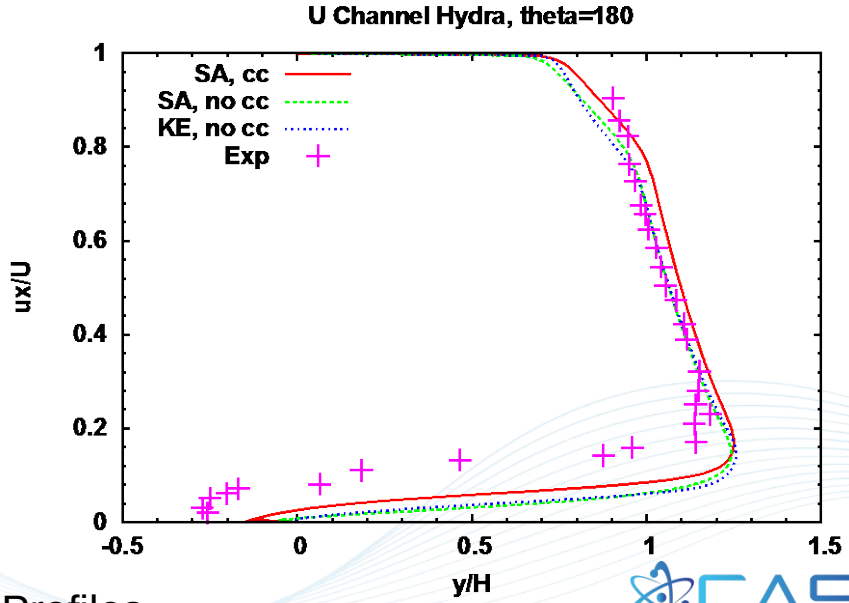

Velocity Profiles

New k-ε models in Hydra-TH

Restructuring permits addition of multiple variants of the k-ε model

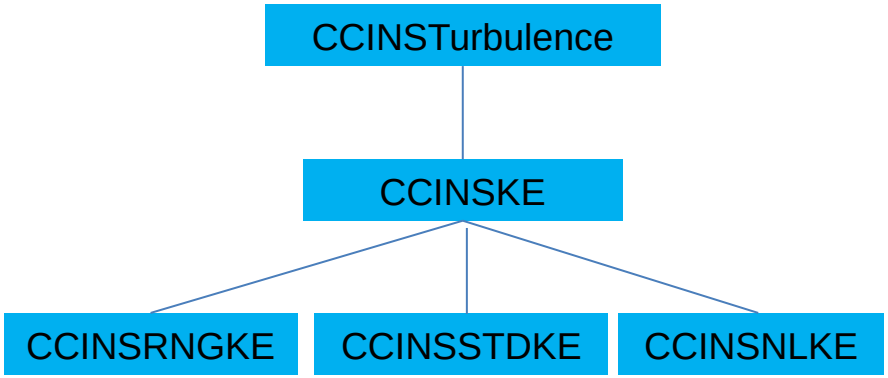

- Standard model
- RNG model
- Non-linear model (anisotropic viscosity model)
  - Captures secondary rotational flows damped by other k-ε models

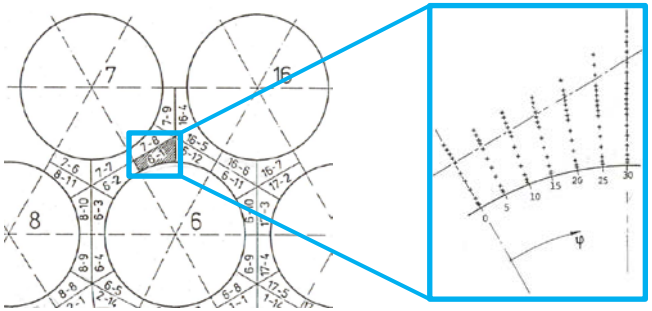

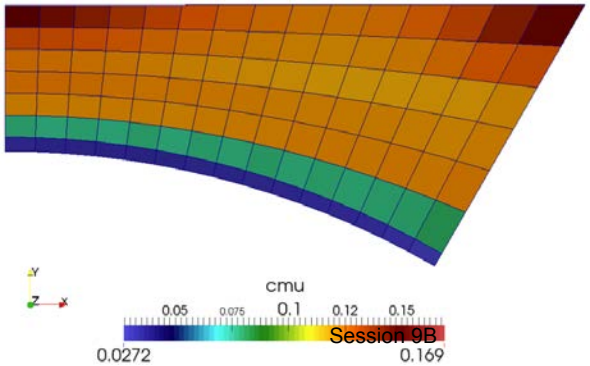

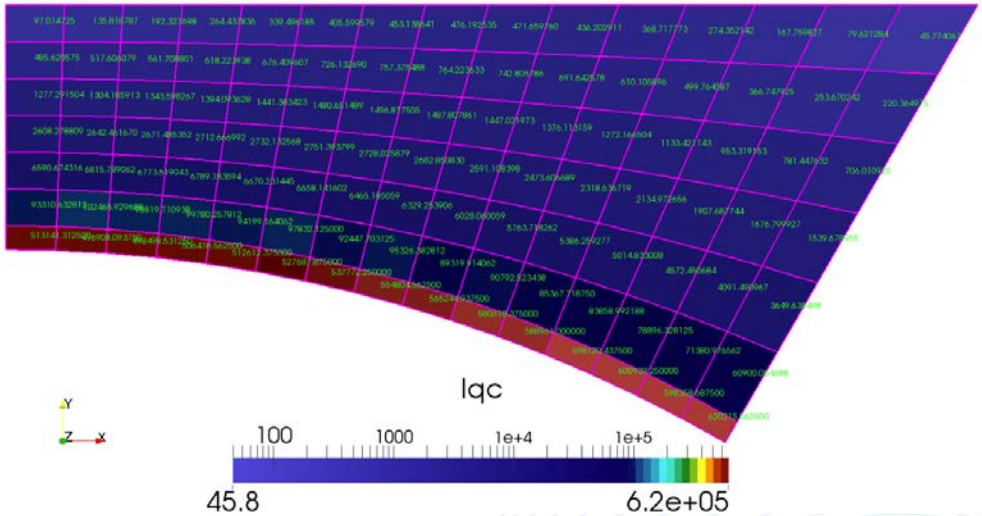

Ratio of Linear to Quadratic Stresses

Exploratory Work on Advanced Turbulence Models for Multiphase Flows

- The literature survey found:
  - Current turbulence modeling for bubbly two-phase flows still relies on two-equation turbulence models providing the turbulent viscosity for closure.
  - The often used k-ε model can be extended to bubbly two-phase flows with added terms in both the turbulent kinetic energy and dissipation equations that account for the turbulent interactions between phases.
  - The current state-of-the-art is to solve the k-ε equations for the continuous liquid phase only and then relate the dispersed vapor phase turbulence viscosity to the known continuous phase turbulent viscosity.
- The RNG k-ε equations have been formulated for bubbly two-phase flow based off of Lahey (2005) consistent with the Hydra-TH discretization.
- Cascade model may be viable, but expensive, and risky at this point in time… more Hydra-TH development required
- Follow-on work to consider “BHR” model, Besnard, et al., LANL, 1987

V&V and Assessment

Hong Luo, Xia (Tim) Yidong, Aditya Pandare, Chuanjin Wang, NCSU
Victor Petrov, Annalisa Manera, U. Michigan

Milestones supported:

L3:THM.CFD.P9.01: CFD hexahedral mesh generation for selected problems and Hydra-TH verification

L3:THM.CFD.P9.02: Expose native CHT in Hydra-TH for stand-alone rod-bundle calculations

L3:THM.CFD.P9.05: Single/Multiphase CFD assessment, verification and validation

Hexahedral meshes for single pin and 5x5 assembly problems including spacer grids and mixing vanes

L3:THM.CFD.P9.01

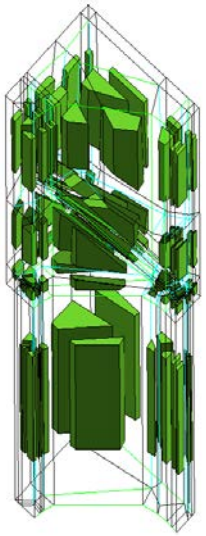

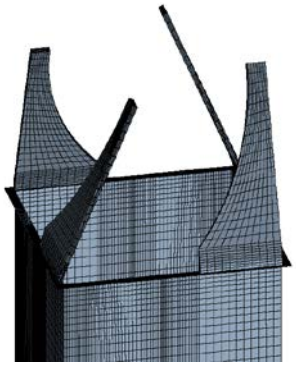

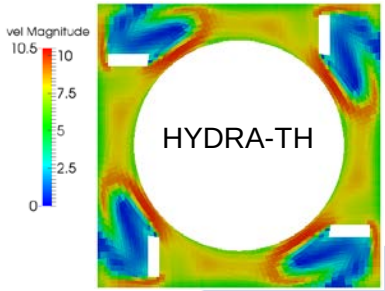

Simulation

Mesh

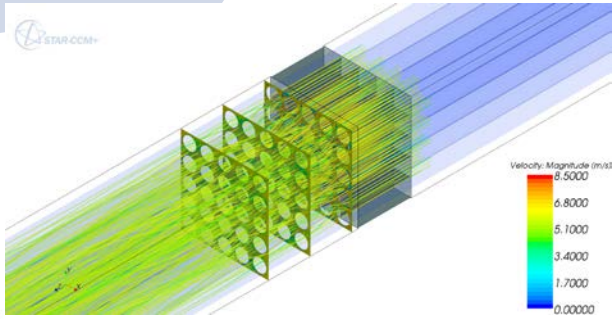

Block structure

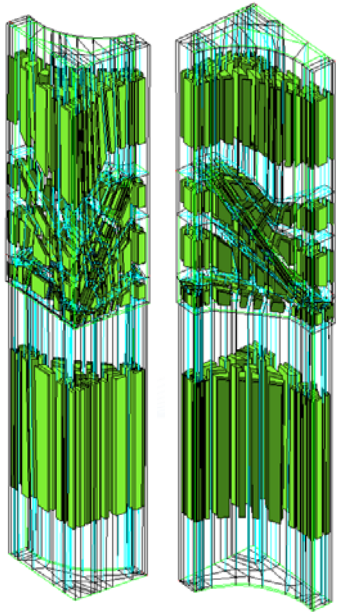

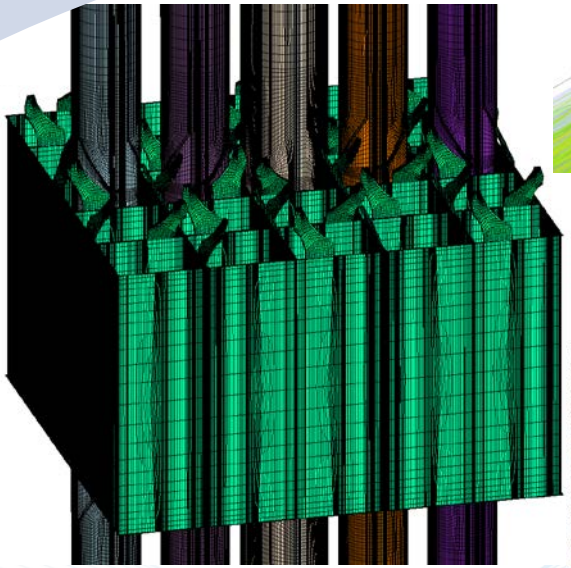

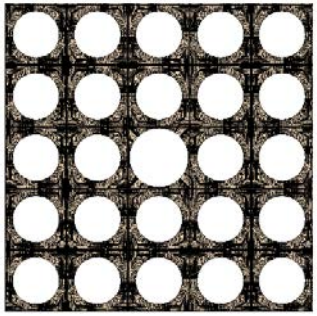

Development of user-defined initial / boundary conditions

- Objective
  - Provide support for user-defined BC's and IC's for velocity, temperature, and pressure in single/multifield flow solvers
  - Serve the CHT development, verification and validation
- Design
  - Integrated with existing keyword input to provide a simple way to extend the input (control) file
  - Present the minimum interface to a user that can be programmed
- Example of usage
  - User-defined velocity BC: Poiseuille flow with an inlet velocity profile
  - User-defined temperature BC: differentially heated box with oscillating temperature boundary
  - User-defined velocity IC: Taylor-Green vortex test with Dirichlet boundary
  - User-defined temperature IC: differentially heated box with oscillating temperature boundary

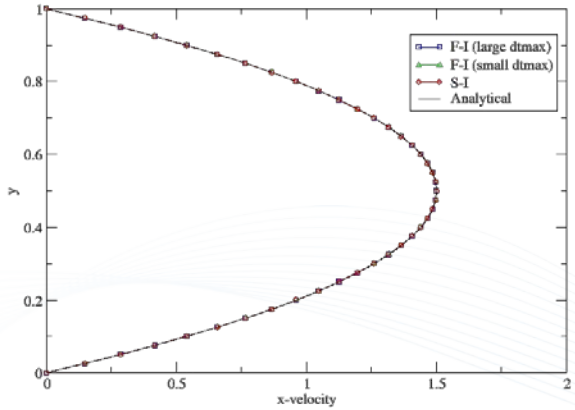

X-velocity profiles, Level 4 grid

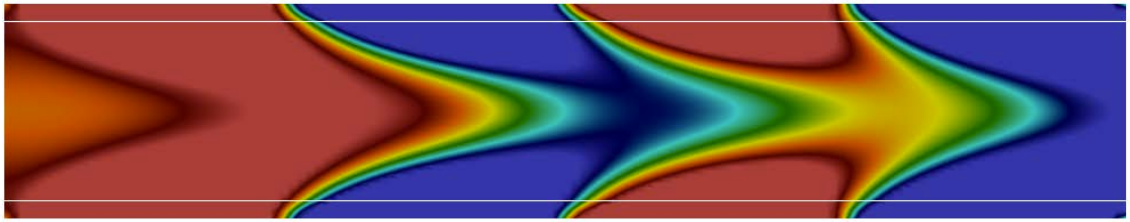

Hydra-TH Verification & Validation

- Grid turbulence
  - Turbulence model
    - RNG *k-ε*
  - Solution method
    - P2 semi-implicit method (baseline solution)
    - P2 fully-implicit method (with one inner iteration) Equivalent to P2-SI

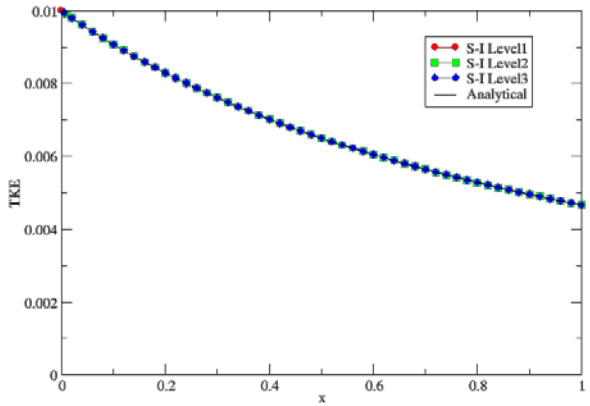

TKE profiles by P2-SI

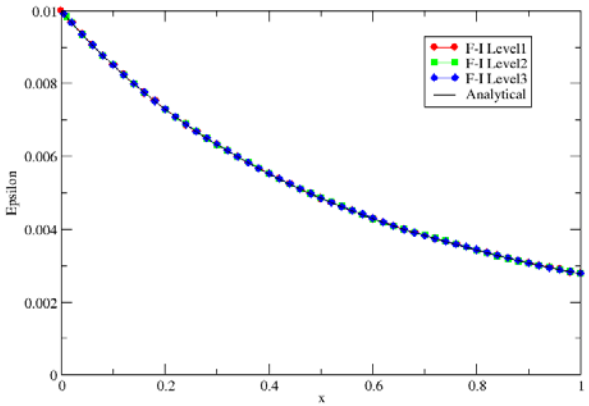

Epsilon profiles by P2-SI

- Turbulent channel flow at $Re_\tau = 590$
  - Turbulence model: RNG *k-ε*
  - Solution method: P2 semi-implicit, and P2 fully-implicit
  - Grid points: 50x81x2, 50x161x2, and 50x321x2
    - P2 fully-implicit method (with one inner iteration) Equivalent to P2-SI
    - P2 fully-implicit method (with multiple inner iterations)

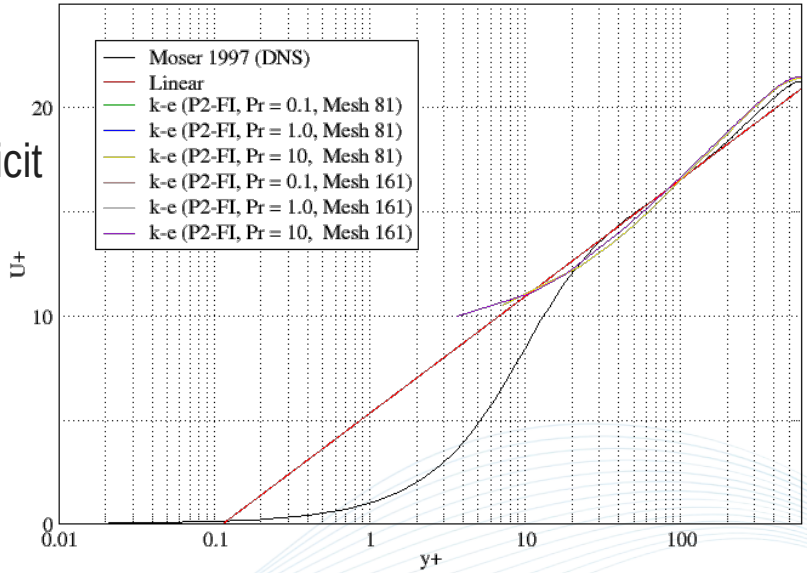

CMB Evaluation

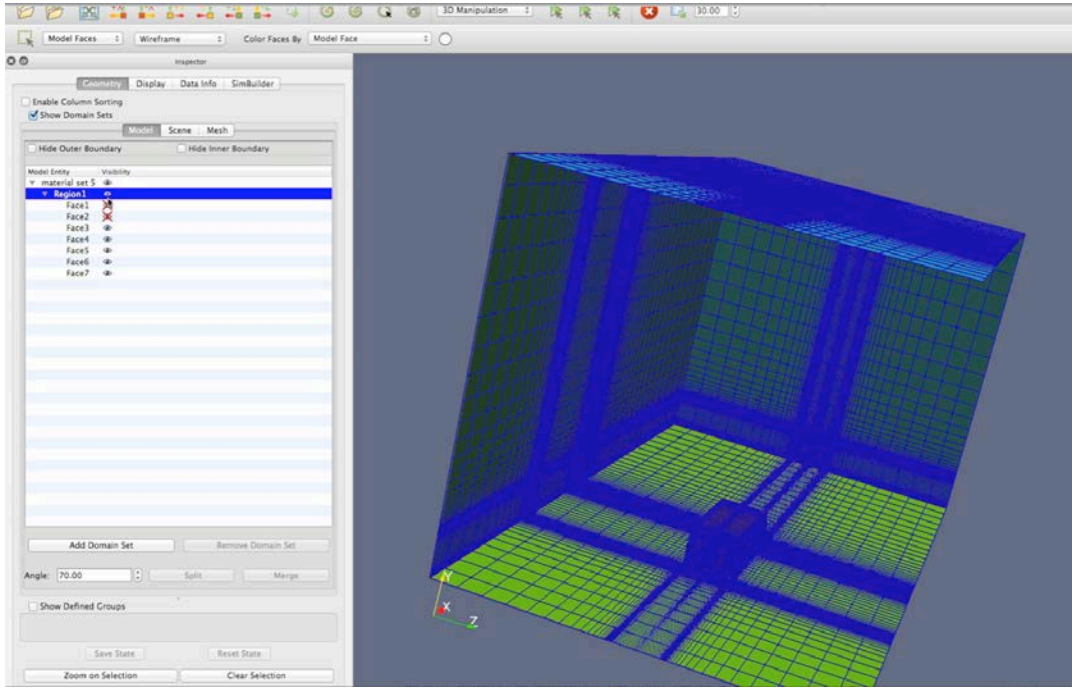

- Goals :
  - Using CMB to generate correct control files for Hydra-TH
- Procedure:
  - Build CMB on Linux OS (Ubuntu 13.10)
  - Select a problem from the “Examples”/ “Regression” suites
  - Load mesh of selected problem on CMB
  - Use the Hydra template file to get SimBuilder tab
  - Set up the simulation parameters for the problem in the SimBuilder tab
  - Export Simulation File using the Hydra Exporter file
  - Compare the resulting output control-file with the example control file in the “Examples”/ “Regression” suite
  - Report bugs in this procedure / inconsistencies in the Control file to Kitware.

Assessment of time-accuracy & projection methods

- Objective: To develop and implement a projection method that achieves a fully second-order-in-time convergence in both velocity and pressure for general domains and boundary conditions.
- The following three methods of updating pressure are considered to study their effect on the order of convergence in time for projection methods.

$$\text{PMI:} \quad p^{n+\frac{1}{2}} = q + \phi^{n+1},$$

$$\text{PMII:} \quad p^{n+\frac{1}{2}} = q + \phi^{n+1} - \frac{\nu \Delta t}{2} \Delta \varphi^{n+1},$$

$$\text{PMIII:} \quad p^{n+\frac{1}{2}} = 2q - p^{n-\frac{1}{2}} + \phi^{n+1} - \frac{\nu \Delta t}{2} \Delta \varphi^{n+1}$$

- Our preliminary results indicate that only the PMIII is able to achieve second order of accuracy in time for the pressure, and will be implemented and tested in Hydra-TH.

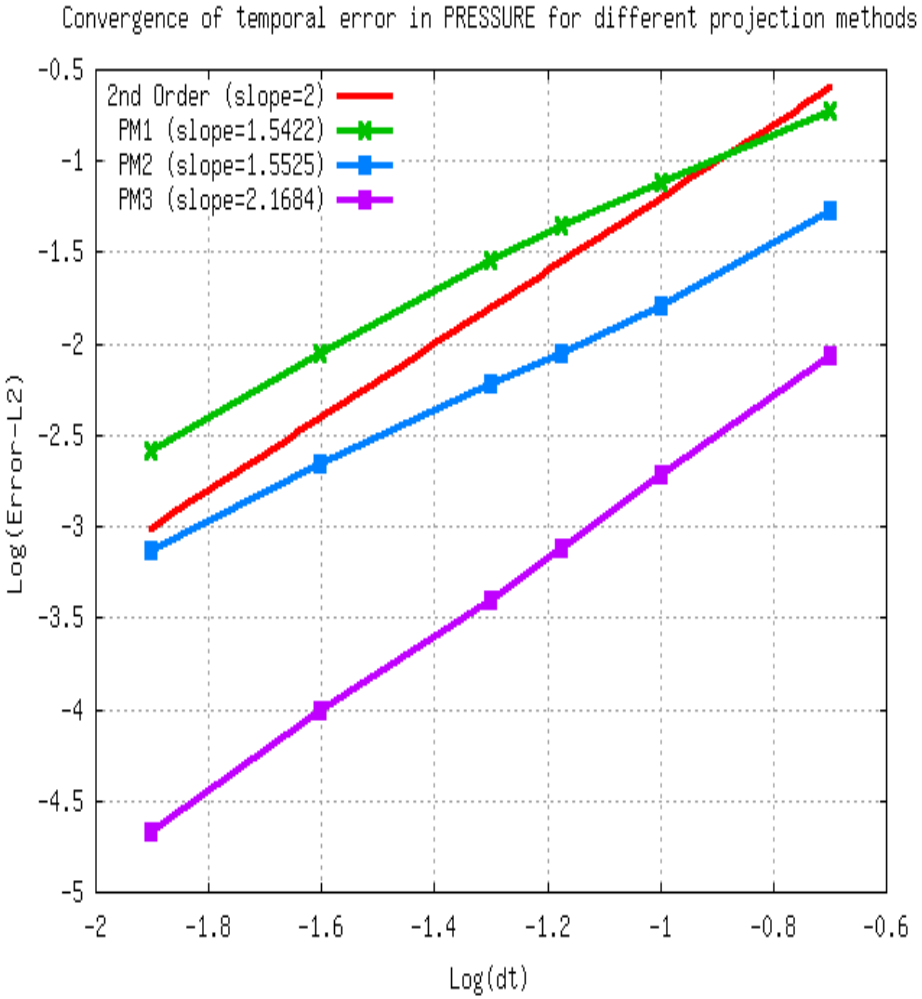

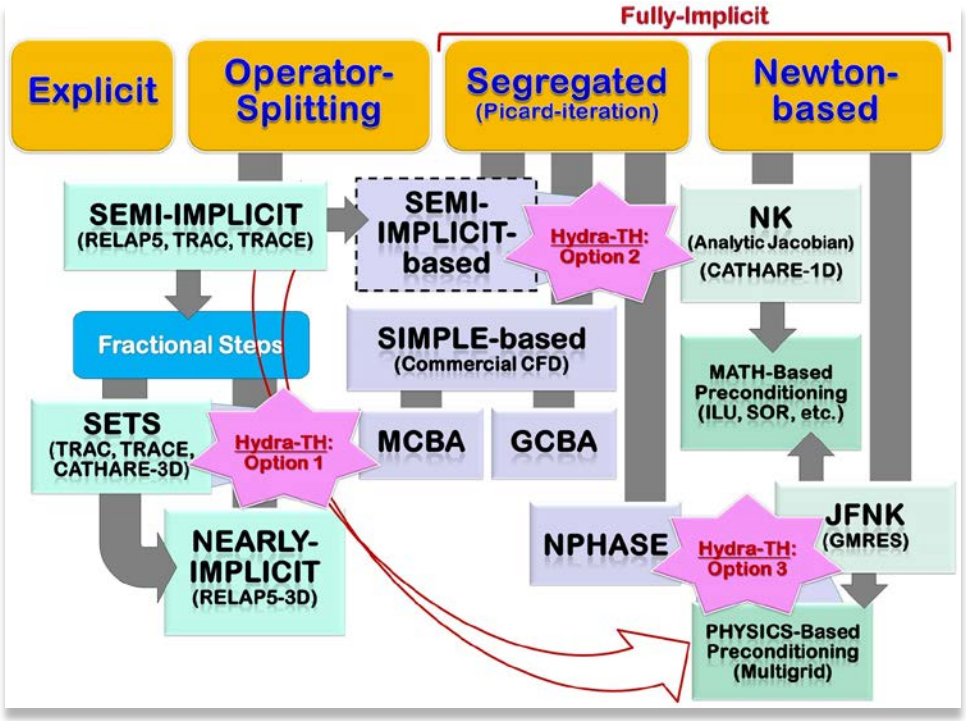

Multiphase Flow & Fully-Implicit Methods

Mark A. Christon, Jozsef Bakosi, Markus Berndt, Duan Zhang, LANL

Igor Bolotnov, Cameron Brown, NCSU

Milestones supported:

L3:THM.CFD.P9.12: Demonstration of multiphase boiling flow with Hydra-TH in realistic subchannels with mixing vanes

L3:THM.CFD.P9.07: Advanced turbulence models for multiphase flow (BHR, cascade, etc.)

Fully-Implicit Algorithms based on Projection Methods

- Projection method acts a physically-based preconditioner providing an approximate factorization of the discrete Navier-Stokes Equations
- Nonlinear Krylov acceleration (NKA) for fully-implicit algorithms implemented for single/multiphase

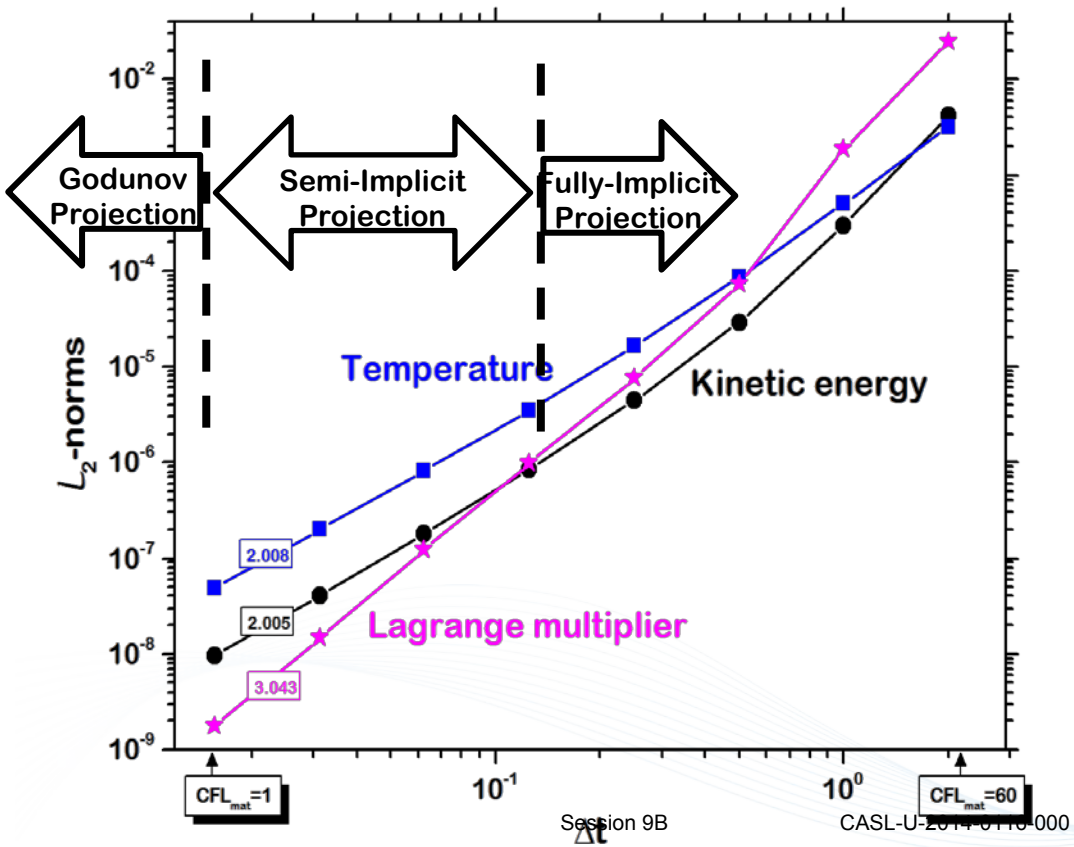

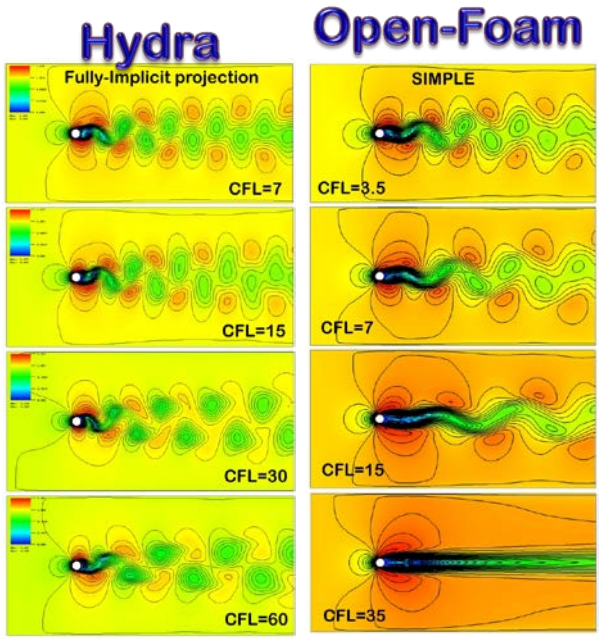

Comparison of NKA with other solvers on the C5G7-MOX benchmark

- ✓ NKA was significantly more efficient and robust than other methods, including JFNK
- ✓ J. Comput. Physics 238 (2013) 188-209.
- ✓ SIAM J. Sci. Comput. 19 (1998) 728-765.

Multiphase Flow in Hydra-TH

- **Generic *N*-field algorithm:** fully coupled, semi-implicit, skew-symmetry preserving, predictor-corrector, documented in theory manual
- **Expert-user multiphase algorithm:** User can specify different closure for any field-pair
- **Scales:** Tested on Titan with 35K CPU cores
- **Momentum exchange:**
  - drag, lift machinery implemented, verified (more closures to come)
  - mass and energy exchange (e.g., vetted THM sub-cooled boiling model) to come

$$D^n_{kj} = \left[\begin{array}{ccc|ccc|ccc} \cdot & \cdot & \cdot & D^x_{12} & \cdot & \cdot & D^x_{13} & \cdot & \cdot \\ \cdot & \cdot & \cdot & \cdot & D^y_{12} & \cdot & \cdot & D^y_{13} & \cdot \\ \cdot & \cdot & \cdot & \cdot & \cdot & D^z_{12} & \cdot & \cdot & D^z_{13} \\ \hline D^x_{21} & \cdot & \cdot & \cdot & \cdot & \cdot & D^x_{23} & \cdot & \cdot \\ \cdot & D^y_{21} & \cdot & \cdot & \cdot & \cdot & \cdot & D^y_{23} & \cdot \\ \cdot & \cdot & D^z_{21} & \cdot & \cdot & \cdot & \cdot & \cdot & D^z_{23} \\ \hline D^x_{31} & \cdot & \cdot & D^x_{32} & \cdot & \cdot & \cdot & \cdot & \cdot \\ \cdot & D^y_{31} & \cdot & \cdot & D^y_{32} & \cdot & \cdot & \cdot & \cdot \\ \cdot & \cdot & D^z_{31} & \cdot & \cdot & D^z_{32} & \cdot & \cdot & \cdot \end{array}\right]$$

Example calculation

- Two-phase calculation with drag
- V5H 5x5 Spacer – 14M Cells
- Re=28,000 (TAMU Exp. Cond.)
- 100:1 water/air density ratio

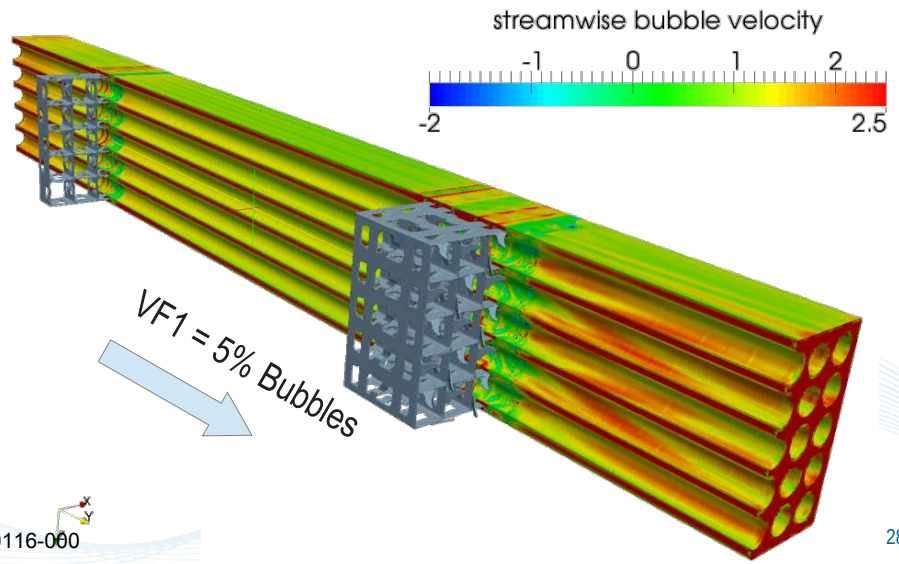

Momentum Exchange Terms

- Fully-coupled for all phasic eq.'s
- Skew-symmetry-preserving, i.e., locally conservative
- One dense linear solve per cell
- Applied after momentum prediction in the projection method
- Momentum exchange uses a predictor-corrector

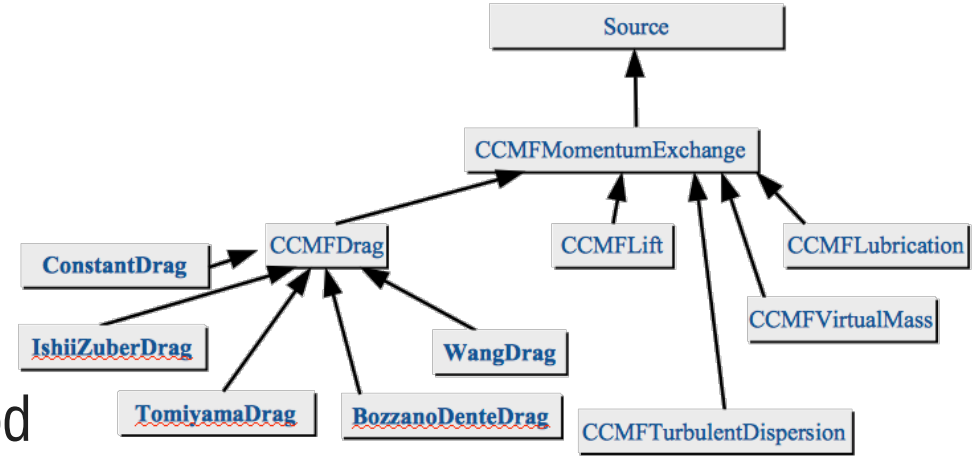

$$
D^n_{kj} = \left[\begin{array}{ccc|ccc|ccc}
\cdot & \cdot & \cdot & D^x_{12} & \cdot & \cdot & D^x_{13} & \cdot & \cdot \\
\cdot & \cdot & \cdot & \cdot & D^y_{12} & \cdot & \cdot & D^y_{13} & \cdot \\
\cdot & \cdot & \cdot & \cdot & \cdot & D^z_{12} & \cdot & \cdot & D^z_{13} \\
\hline
D^x_{21} & \cdot & \cdot & \cdot & \cdot & \cdot & D^x_{23} & \cdot & \cdot \\
\cdot & D^y_{21} & \cdot & \cdot & \cdot & \cdot & \cdot & D^y_{23} & \cdot \\
\cdot & \cdot & D^z_{21} & \cdot & \cdot & \cdot & \cdot & \cdot & D^z_{23} \\
\hline
D^x_{31} & \cdot & \cdot & D^x_{32} & \cdot & \cdot & \cdot & \cdot & \cdot \\
\cdot & D^y_{31} & \cdot & \cdot & D^y_{32} & \cdot & \cdot & \cdot & \cdot \\
\cdot & \cdot & D^z_{31} & \cdot & \cdot & D^z_{32} & \cdot & \cdot & \cdot
\end{array}\right]
$$

$$
L^n_{kj} = \left[\begin{array}{ccc|ccc|ccc}
\cdot & L^{\omega_z}_{11} & -L^{\omega_y}_{11} & \cdot & L^{\omega_z}_{12} & -L^{\omega_y}_{12} & \cdot & L^{\omega_z}_{13} & -L^{\omega_y}_{13} \\
-L^{\omega_z}_{11} & \cdot & L^{\omega_x}_{11} & -L^{\omega_z}_{12} & \cdot & L^{\omega_x}_{12} & -L^{\omega_z}_{13} & \cdot & L^{\omega_x}_{13} \\
L^{\omega_y}_{11} & -L^{\omega_x}_{11} & \cdot & L^{\omega_y}_{12} & -L^{\omega_x}_{12} & \cdot & L^{\omega_y}_{13} & -L^{\omega_x}_{13} & \cdot \\
\hline
\cdot & L^{\omega_z}_{21} & -L^{\omega_y}_{21} & \cdot & L^{\omega_z}_{22} & -L^{\omega_y}_{22} & \cdot & L^{\omega_z}_{23} & -L^{\omega_y}_{23} \\
-L^{\omega_z}_{21} & \cdot & L^{\omega_x}_{21} & -L^{\omega_z}_{22} & \cdot & L^{\omega_x}_{22} & -L^{\omega_z}_{23} & \cdot & L^{\omega_x}_{23} \\
L^{\omega_y}_{21} & -L^{\omega_x}_{21} & \cdot & L^{\omega_y}_{22} & -L^{\omega_x}_{22} & \cdot & L^{\omega_y}_{23} & -L^{\omega_x}_{23} & \cdot \\
\hline
\cdot & L^{\omega_z}_{31} & -L^{\omega_y}_{31} & \cdot & L^{\omega_z}_{32} & -L^{\omega_y}_{32} & \cdot & L^{\omega_z}_{33} & -L^{\omega_y}_{33} \\
-L^{\omega_z}_{31} & \cdot & L^{\omega_x}_{31} & -L^{\omega_z}_{32} & \cdot & L^{\omega_x}_{32} & -L^{\omega_z}_{33} & \cdot & L^{\omega_x}_{33} \\
L^{\omega_y}_{31} & -L^{\omega_x}_{31} & \cdot & L^{\omega_y}_{32} & -L^{\omega_x}_{32} & \cdot & L^{\omega_y}_{33} & -L^{\omega_x}_{33} & \cdot
\end{array}\right]
$$

$$
\mathcal{M}_k = M_k + \theta \Delta t \textstyle\sum_l D_{kl}(\,\cdot\,)
$$

$$
\mathcal{D}_{kj} = -\theta \Delta t D_{kj}(\,\cdot\,)
$$

$$
\mathcal{L}_{kj} = \begin{cases} \theta \Delta t \sum_l L_{kl}(\,\cdot\,) & \text{for} \quad k = j, \\ -\theta \Delta t L_{kj}(\,\cdot\,) & \text{for} \quad k \neq j, \end{cases}
$$

$$
\mathcal{F}_k = M_k \mathbf{v}_k - (1-\theta)\Delta t \Big[\textstyle\sum_l D_{kl}(\mathbf{v}_k - \mathbf{v}_l) + \sum_l L_{kl}(\mathbf{v}_k - \mathbf{v}_l) \Big]
$$

$$
\left[\begin{array}{ccc|ccc|ccc}
\mathcal{M}^x_1 & \mathcal{L}^{\omega_z}_{11} & -\mathcal{L}^{\omega_y}_{11} & \mathcal{D}^x_{12} & \mathcal{L}^{\omega_z}_{12} & -\mathcal{L}^{\omega_y}_{12} & \mathcal{D}^x_{13} & \mathcal{L}^{\omega_z}_{13} & -\mathcal{L}^{\omega_y}_{13} \\
-\mathcal{L}^{\omega_z}_{11} & \mathcal{M}^y_1 & \mathcal{L}^{\omega_x}_{11} & -\mathcal{L}^{\omega_z}_{12} & \mathcal{D}^y_{12} & \mathcal{L}^{\omega_x}_{12} & -\mathcal{L}^{\omega_z}_{13} & \mathcal{D}^y_{13} & \mathcal{L}^{\omega_x}_{13} \\
\mathcal{L}^{\omega_y}_{11} & -\mathcal{L}^{\omega_x}_{11} & \mathcal{M}^z_1 & \mathcal{L}^{\omega_y}_{12} & -\mathcal{L}^{\omega_x}_{12} & \mathcal{D}^z_{12} & \mathcal{L}^{\omega_y}_{13} & -\mathcal{L}^{\omega_x}_{13} & \mathcal{D}^z_{13} \\
\hline
\mathcal{D}^x_{21} & \mathcal{L}^{\omega_z}_{21} & -\mathcal{L}^{\omega_y}_{21} & \mathcal{M}^x_2 & \mathcal{L}^{\omega_z}_{22} & -\mathcal{L}^{\omega_y}_{22} & \mathcal{D}^x_{23} & \mathcal{L}^{\omega_z}_{23} & -\mathcal{L}^{\omega_y}_{23} \\
-\mathcal{L}^{\omega_z}_{21} & \mathcal{D}^y_{21} & \mathcal{L}^{\omega_x}_{21} & -\mathcal{L}^{\omega_z}_{22} & \mathcal{M}^y_2 & \mathcal{L}^{\omega_x}_{22} & -\mathcal{L}^{\omega_z}_{23} & \mathcal{D}^y_{23} & \mathcal{L}^{\omega_x}_{23} \\
\mathcal{L}^{\omega_y}_{21} & -\mathcal{L}^{\omega_x}_{21} & \mathcal{D}^z_{21} & \mathcal{L}^{\omega_y}_{22} & -\mathcal{L}^{\omega_x}_{22} & \mathcal{M}^z_2 & \mathcal{L}^{\omega_y}_{23} & -\mathcal{L}^{\omega_x}_{23} & \mathcal{D}^z_{23} \\
\hline
\mathcal{D}^x_{31} & \mathcal{L}^{\omega_z}_{31} & -\mathcal{L}^{\omega_y}_{31} & \mathcal{D}^x_{32} & \mathcal{L}^{\omega_z}_{32} & -\mathcal{L}^{\omega_y}_{32} & \mathcal{M}^x_3 & \mathcal{L}^{\omega_z}_{33} & -\mathcal{L}^{\omega_y}_{33} \\
-\mathcal{L}^{\omega_z}_{31} & \mathcal{D}^y_{31} & \mathcal{L}^{\omega_x}_{31} & -\mathcal{L}^{\omega_z}_{32} & \mathcal{D}^y_{32} & \mathcal{L}^{\omega_x}_{32} & -\mathcal{L}^{\omega_z}_{33} & \mathcal{M}^y_3 & \mathcal{L}^{\omega_x}_{33} \\
\mathcal{L}^{\omega_y}_{31} & -\mathcal{L}^{\omega_x}_{31} & \mathcal{D}^z_{31} & \mathcal{L}^{\omega_y}_{32} & -\mathcal{L}^{\omega_x}_{32} & \mathcal{D}^z_{32} & \mathcal{L}^{\omega_y}_{33} & -\mathcal{L}^{\omega_x}_{33} & \mathcal{M}^z_3
\end{array}\right]
\left\{\begin{array}{c} v^x_1 \\ v^y_1 \\ v^z_1 \\ \hline v^x_2 \\ v^y_2 \\ v^z_2 \\ \hline v^x_3 \\ v^y_3 \\ v^z_3 \end{array}\right\}
=
\left\{\begin{array}{c} \mathcal{F}^x_1 \\ \mathcal{F}^y_1 \\ \mathcal{F}^z_1 \\ \hline \mathcal{F}^x_2 \\ \mathcal{F}^y_2 \\ \mathcal{F}^z_2 \\ \hline \mathcal{F}^x_3 \\ \mathcal{F}^y_3 \\ \mathcal{F}^z_3 \end{array}\right\}
$$

Multiphase Flow in Hydra-TH – Verification

- Verify drag force anti-symmetry and momentum-conservation to machine precision
- Drag verification

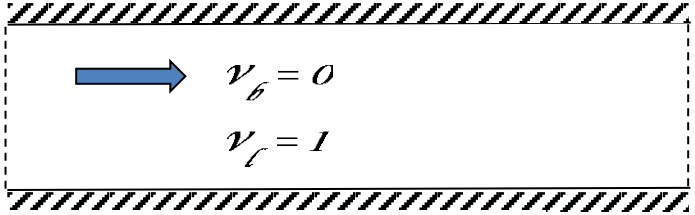

$$\mathbf{F}_d^D = -\frac{3}{8r_d} C_D \alpha_d \rho_c \left|\mathbf{v}_r\right| \mathbf{v}_r$$

- Lift verification

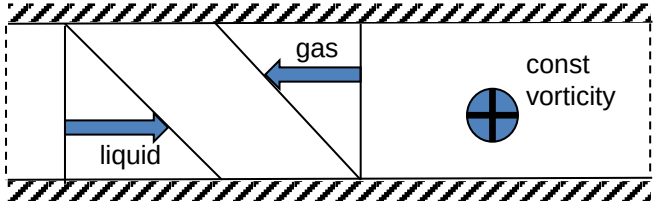

$$\mathbf{F}_d^L = -C_L \alpha_d \rho_c \mathbf{v}_r \times (\nabla \times \mathbf{v}_c)$$

- More complex cases testing lift from:
  - Emilio Baglietto, Star-CCM+
  - Gretar Tryggvason's interface tracking code

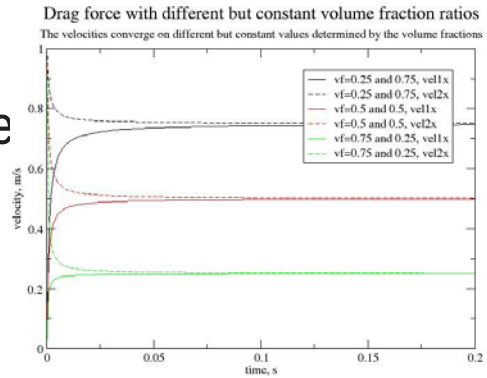

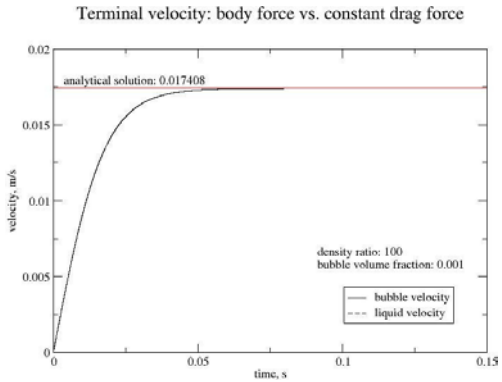

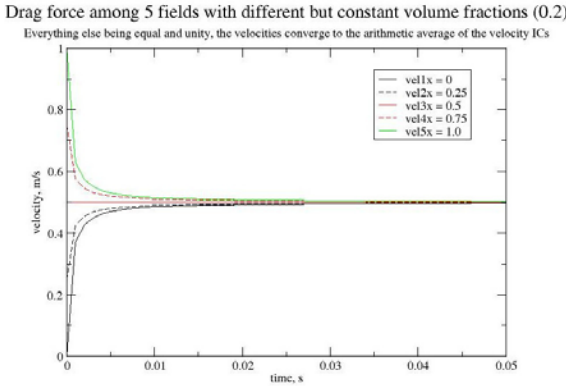

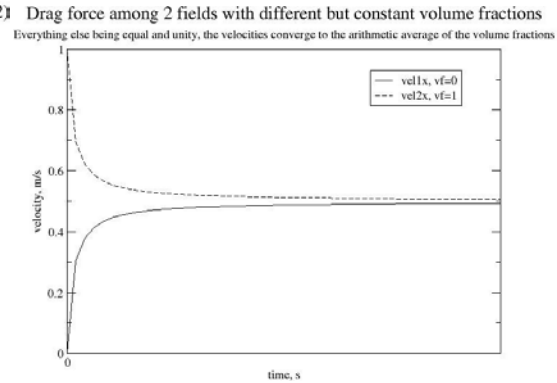

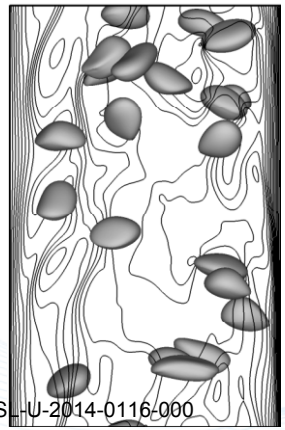

- Vary bubble diameter
- Vary spatial directions
- Vary volume fractions
- Vary number of fields
- Validation: balance of drag and body force results in terminal velocity with analytical solution

Development of Verification Problems for Hydra-TH

- Hydra-TH multiphase capabilities will be tested using analytic solutions, NPHASE, and available DNS resources at NCSU.
- A single-phase, single subchannel geometry has been run in Hydra-TH for comparison to DNS data.
  - The DNS data also exists for two-phase and will be used for Hydra-TH multiphase validation. (Right: Single-phase x-direction velocity in the subchannel.)

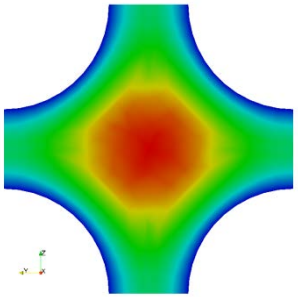

- A simple channel domain with constant inlet mass flux has been tested with NPHASE and compared to analytic solutions for correct advection of void fractions and implementation of the drag force.
  - Hydra-TH provides correct phasic velocities
  - Advection of void fraction is under development with multiphase turbulence modeling
  - Results are prepared for direct Hydra-TH comparison

Parameter	Analytic	NPHASE	%Error
Total inlet mass flux	948.2548	948.2548	N/A
Total outlet mass flux	948.2548	948.2617	≈ 0.00 %
u_l	0.992296	0.992168	0.01 %
u_g	1.173034	1.176431	0.29 %
α_l	0.957375	0.957506	0.01 %
α_g	0.042625	0.042494	0.31 %
u_{rel}	0.180738	0.184263	1.91 %

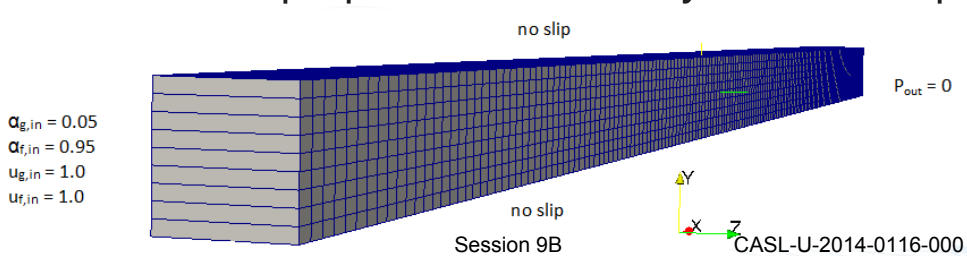

Some MultiField Flow Calculations

- Manifold flow
- 2 fields, same densities
- Coupled through single pressure via projection algorithm
- IC: VF1: 50%, VF2:50% (both fluids present)
- BC: VF1 at inlet = 90V%

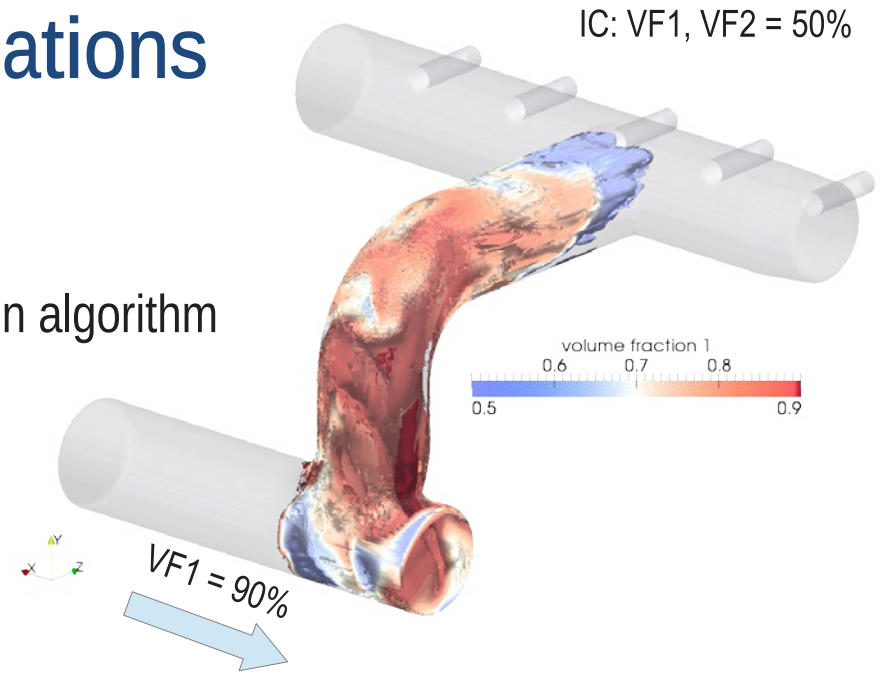

- V5H GTRF 3x3
- Same conditions as previous pipe flow
- Titan (400 CPU cores)

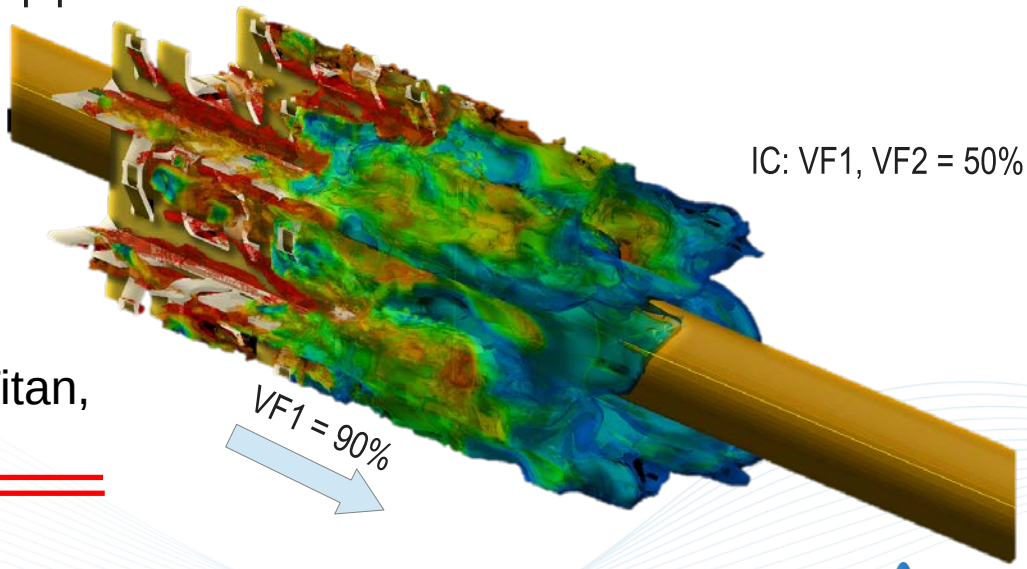

Scaled to 36,000 cores on Titan,
192 Million element mesh

Kitware Interactions

Patrick O'Leary,
Bill Hoffman,
Andy Bauer,
Kitware

Kitware

Hydra-Catalyst Integration

Andrew Bauer

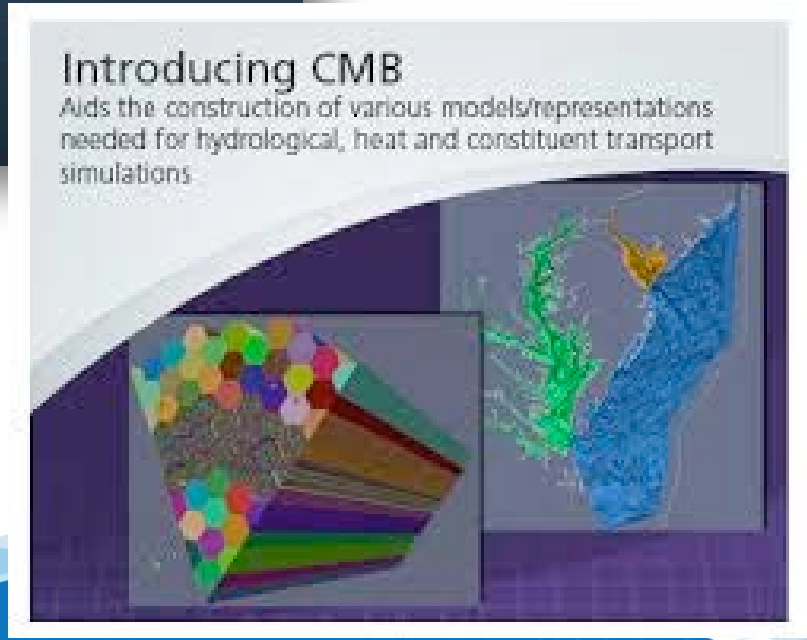

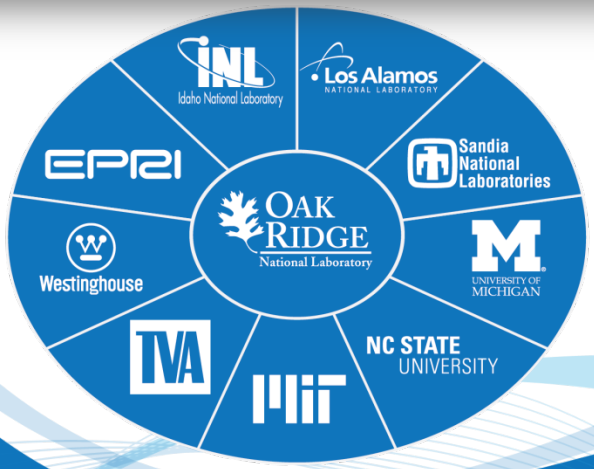

Computational Model Builder (CMB)

CMB Movie at: http://get-hydra.lanl.gov

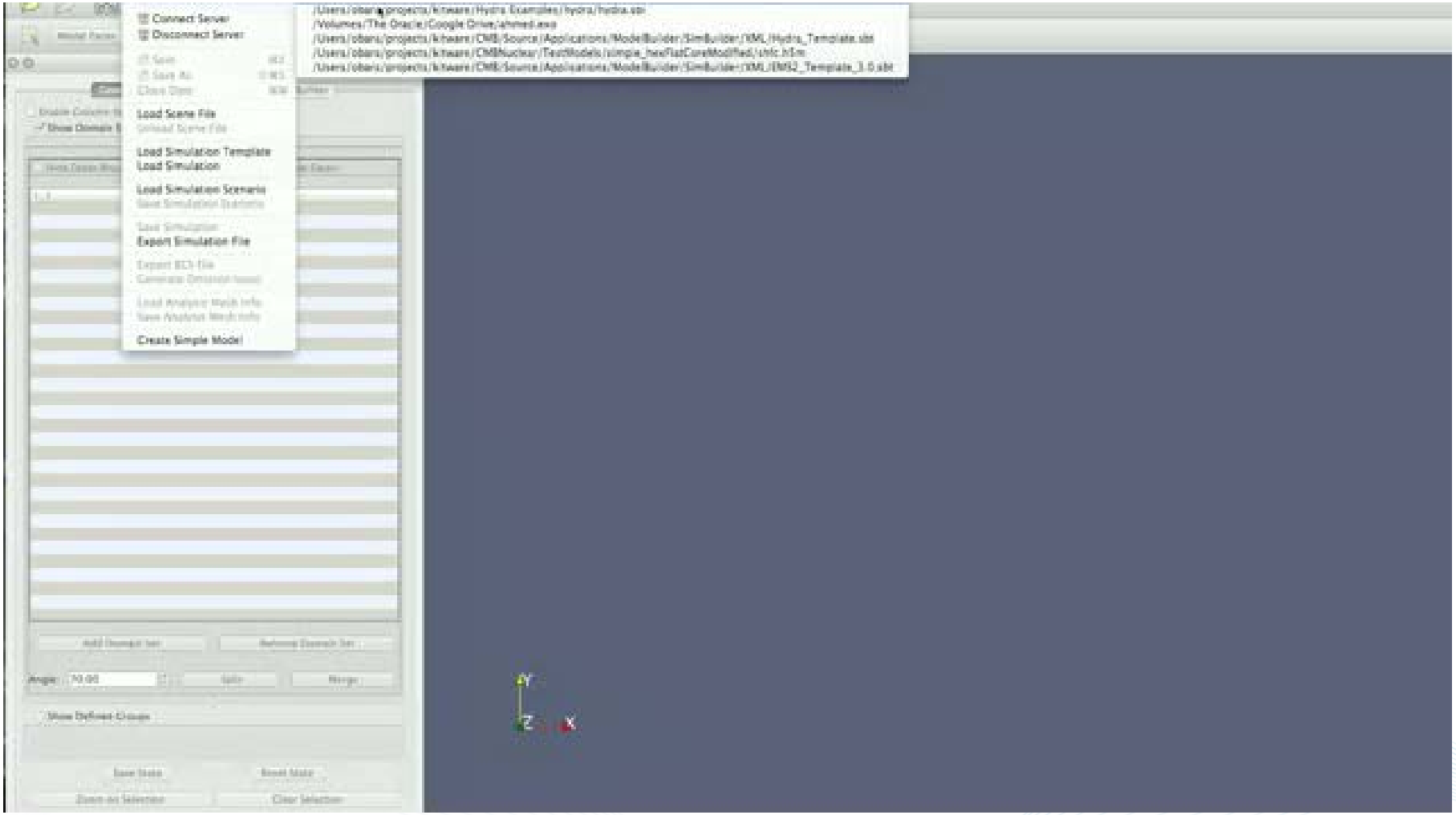

Catalyst – an *in situ* Analysis and Visualization tool

Need a supercomputer to analyze results from a Hydra-TH run

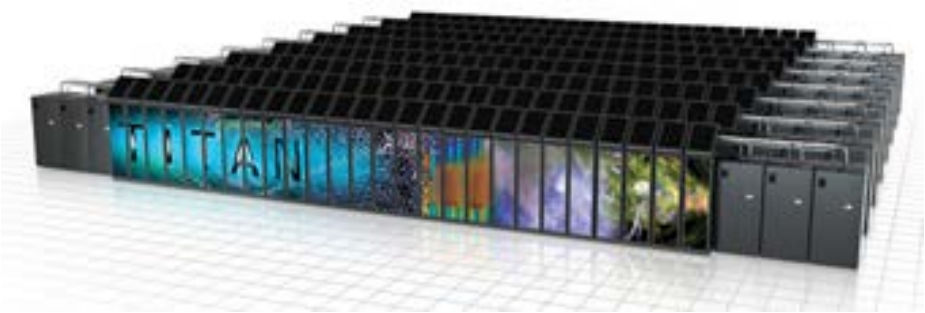

RHEA

2 orders of magnitude difference in capacity between each level

Workflow with Outputs

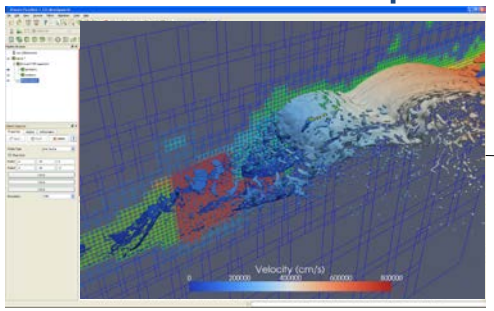

Script Export

```
# Create the reader and set the filename.
reader = servermanager.sources.Reader(FileNames=path)
view = servermanager.CreateRenderView()
repr = servermanager.CreateRepresentation(reader, view)
reader.UpdatePipeline()
dataInfo = reader.GetDataInformation()
pDinfo = dataInfo.GetPointDataInformation()
arrayInfo = pDInfo.GetArrayInformation("displacement9")
if arrayInfo:
  # get the range for the magnitude of displacement9
  range = arrayInfo.GetComponentRange(-1)
  lut = servermanager.rendering.PVLookupTable()
  lut.RGBPoints  = [range[0], 0.0, 0.0, 1.0,
                    range[1], 1.0, 0.0, 0.0]
  lut.VectorMode = "Magnitude"
  repr.LookupTable = lut
  repr.ColorArrayName = "displacement9"
  repr.ColorAttributeType = "POINT_DATA"
```

Augmented script in input deck.

Hydra-TH

Catalyst

Output Processed Data

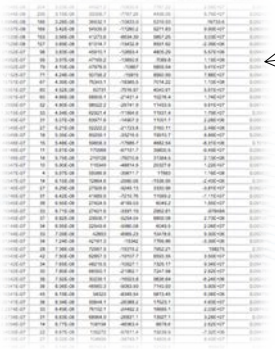

Statistics

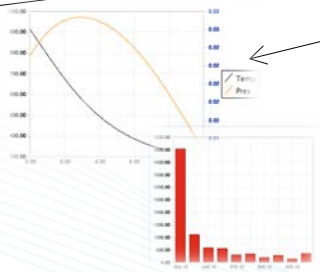

Series Data

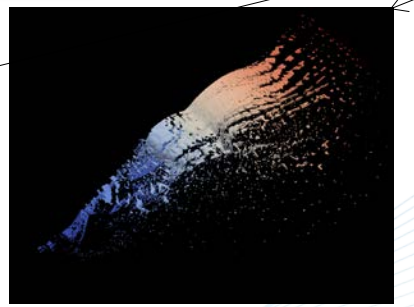

Polygonal Output with Field Data

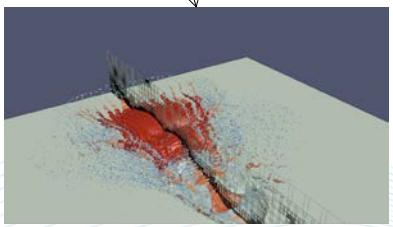

Rendered Images

Phase-2 L2 THM Milestones

- Supporting L3 Milestones for PoR10 have not been defined yet

Table 14: Phase 2 THM Level 2 milestone plan.

Year	Category	CP	L1 Milestone Supported	Description
1	Thermal-Hydraulics	CHF (DNB)	4	Demonstration of CASL M-CFD Closure Models for Subcooled Boiling and Bubbly Flow
2	Thermal-Hydraulics	CHF (DNB), CILC	11, 18	Wall Closure Models for Subcooled Boiling using DNS for Wall Conditions
	Coolant / Corrosion Chemistry	CHF (DNB), CILC, LOCA	12	Advanced Subgrid-Scale Modeling of Corrosion Chemistry and Boron Mixing/Precipitation (CFD-based CILC)
3	Thermal-Hydraulics	CHF (DNB)	18	Demonstration of Gen-II CASL M-CFD Closure Models for the onset of DNB
	Thermal / Solutal Convection	Convective Flow, LOCA	12	Demonstration of Thermal and Solutal Convection for Boron Mixing during ECCS Injection
4	Thermal-Hydraulics	Flow Regimes	15	Investigation of Flow Topology Recognition for M-CFD Closure Models for BWR-like Flow Regimes
	Coolant / Corrosion Chemistry	CHF (DNB), CILC	6, 18	Demonstration of advanced subgrid-scale chemistry model for CRUD deposition
5	Thermal / Solutal Convection	CHF (DNB)	18	Low flow rate boiling in a rod bundle
	Deployment	N/A	19	Hydra-TH User, Theory, V&V/THM Benchmarks Manuals

Advances in Multiphase Closure Modelling

Emilio Baglietto
Assistant Professor of Nuclear Science and Engineering
Massachusetts Institute of Technology

with contributions from:
Igor Bolotnov (NCSU)
Gretar Tryggvason (ND)
Jacopo Buongiorno (MIT)
Yassin Hassan (TAMU)
Nam Dinh (NCSU)
Mike Podowski (RPI)

2014 CASL RoundTable
July 14-16, 2014

U.S. DEPARTMENT OF ENERGY
Nuclear Energy

1. The goal: develop novel and predictive capability for DNB Analysis

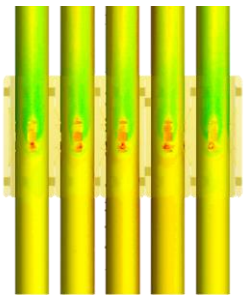
boiling heat transfer

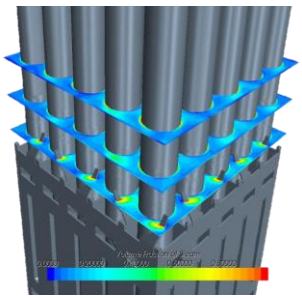
void fraction

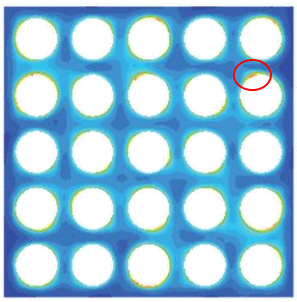
DNB

- **L1:CASL.P9.02**

Application of Multi-Scale Thermal Hydraulic Models to DNB Analysis

2

2. The milestones: physics based, robust, assessable

ITM/DNS (Physical understanding/Closure parameters)

- **L3:THM.CLS.P8.01**: Perform limited time simulations of single subchannel geometry and 2x2 realistic geometry with spacer grids and mixing vanes
- **L3:THM.CLS.P9.02**: Transient evolution and dispersion of bubbles in a channel and data mining

Experiments (Physical understanding/Closure parameters)

- **L3:THM.CLS.P9.01**: Experimental Determination of the Effects of (Synthetic) CRUD on Subcooled Boiling
- **L3:THM.CLS.P9.05**: High Resolution (PTV)/ Shadowgraphy of near wall bubbly flow

Closure Modeling

- **L3:THM.CLS.P9.06**: Assessment and improvement of heated surface effects treatment for subcooled flow boiling models
- **L3:THM.CLS.P9.04**: Development of a mechanistic subcooled boiling model for PWR assemblies
- **L3:THM.CLS.P9.07**: Novel Robust Momentum Closure Approach for Multiphase CFD
- **L3:THM.CLS.P9.08**: Advanced Subcooled Flow Boiling Models

3

3. The approach: physics based, robust, assessable

In order to provide advanced modeling capability for multiphase flow with subcooled boiling to the industry:

- *From Experience*
  - Leverage lesson learned in previous attempts (method)
  - State-of-the-art as baseline (reference solution)
  - Focus on hardened simulation capability (industrial relevance)
- *New Approach*
  - Separation of Framework and Modeling
  - Builds on existing strengths, models and code testing
  - Built-in minimal redundancy
  - Piece-by-piece approach
  - Targeted Work on critical components

4

3. The approach: physics based, robust, assessable

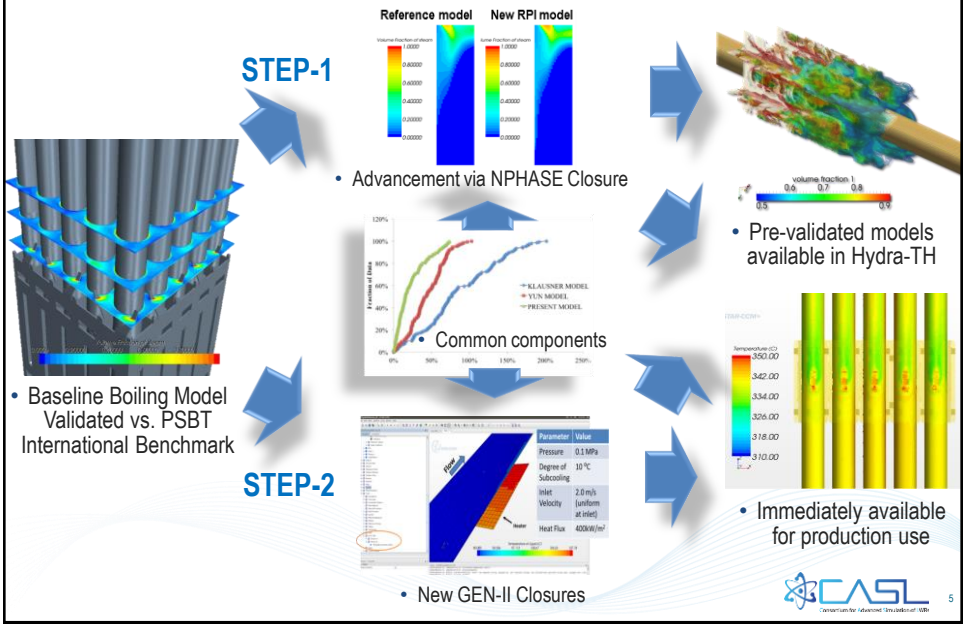

4. Closure Modeling Status and Plans

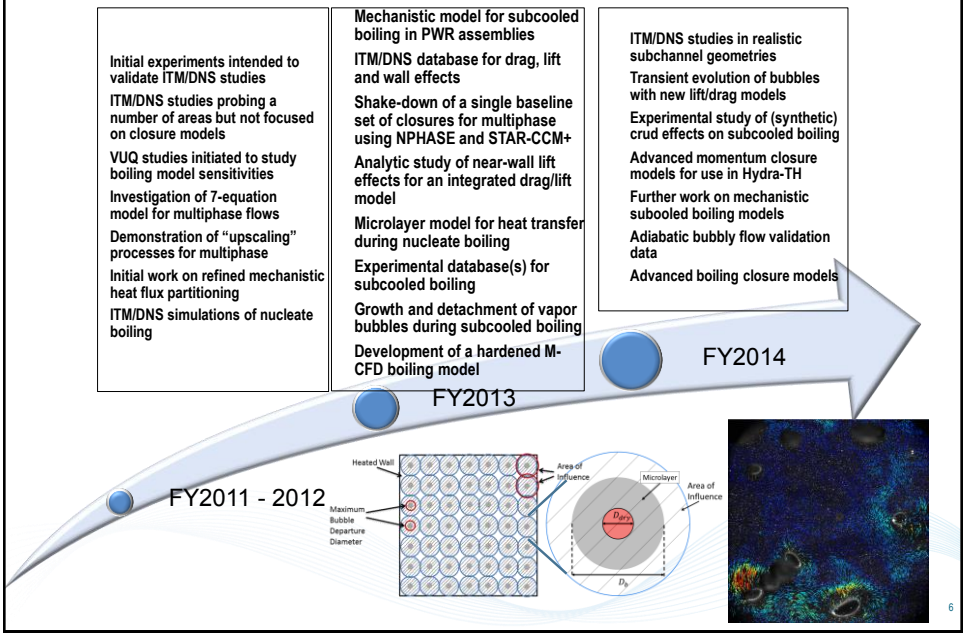

2013 Deliverable: GEN-I Robust Baseline Closure

- Confirms the findings from PoR-3 V&V Study (Fidkowski)
- Bubble departure diameter and Nucleation Site density correlations drive the Wall temperature effect
- Hydrodynamic closure has limited effect on wall temperatures, but more understanding necessary for regions of void accumulation

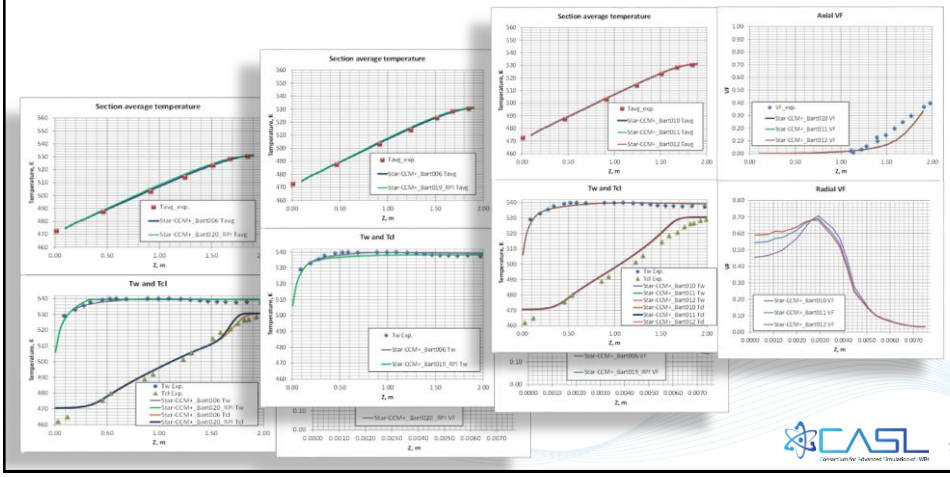

7

2014 : GEN-I Continuing Testing and Validation

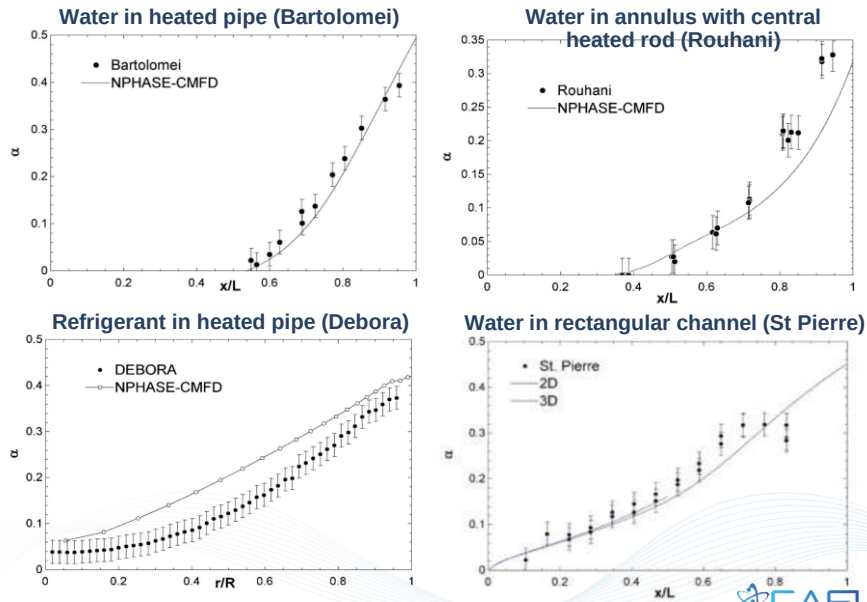

8

2014 Focus – GEN-II Boiling → towards DNB

Robust Baseline Closure

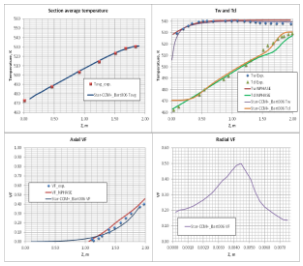

- First Generation Closure in Hydra-TH should leverage existing experience
- Implementation of baseline closure in STAR-CCM+ allows direct comparison to CD-adapco baseline closure results (platform independent)
- Sensitivity of model parameters should confirm PoR-3 studies

Innovative GEN-II Closure

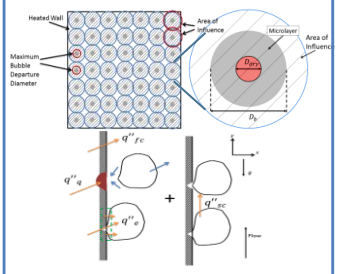

- Second Generation Closure should incorporate new physical understanding
- Increased synergy with experimental "micro" measurements
- Extended applicability (lower/ higher vapor generation)
- Include modeling toward limiting behavior (CHF)

New M-CFD Platform

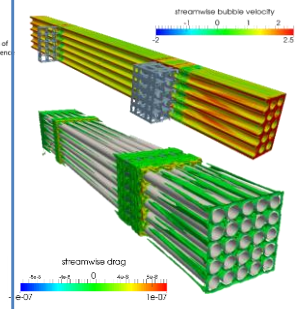

- Hydra-TH baseline multiphase capabilities first shakedown
- Hydra-TH Mupltiphase implementation should target enhanced applicability towards transient simulations (including fast transients)

9

The fundamental role of Experiments / DNS

- Extension to DNB requires physical representation of heater surface
- Includes bubbles interaction

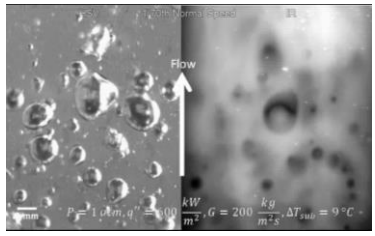

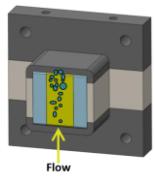

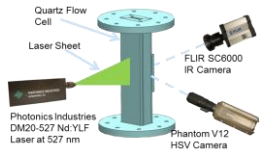

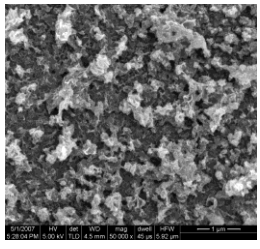

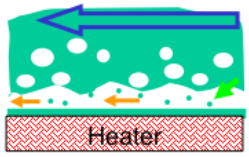

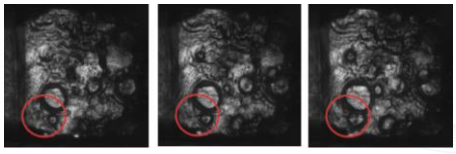

- Platform must include the modeling capabilities
- Experiments/DNS are used for continuing improvement of physical understanding
- Understand/agreement on boiling microhydrodynamics

10

GEN-II Heat Partitioning: Improved Physical Understanding

GEN-I

$$q''_{tot} = q''_{fc} + q''_q + q''_e$$

Convective Quenching Evaporation

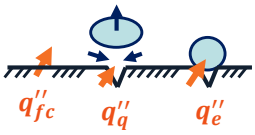

- Mechanistic model proposed by Judd and Hwang (1976)
- Adapted by Kurul and Podowski (1990) for wall heat flux partitioning during pool nucleate boiling.
- While limited it is de-facto the only model in M-CFD

GEN-II

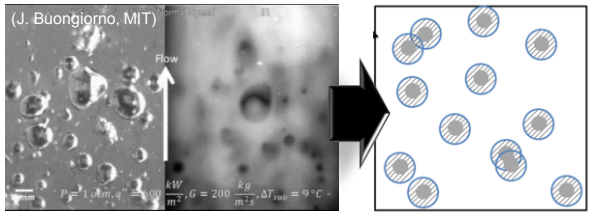

Subgrid Representation of Surface (flow boiling)

Challenge:

- Extremely complex model, cannot be represented by first principle
- What local characteristic in the CFD solution can be used to drive the SGS Model
- Incomplete understanding / open discussion
- Generality – e.g. surface characteristics

11

GEN-II Heat Partitioning: Quick Overview

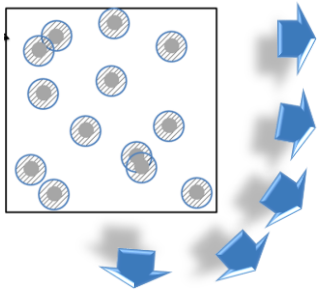

1. Mechanistic Representation of Bubble Lift off and Departure Diameters

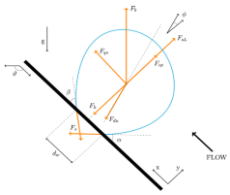

2. Accurate evaluation of evaporation heat flux by modeling effective microlayer

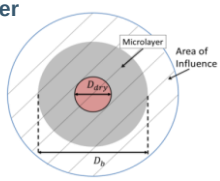

3. Account for sliding bubble effect on heat transfer and nucleation sites

5. Account for bubble interaction on surface

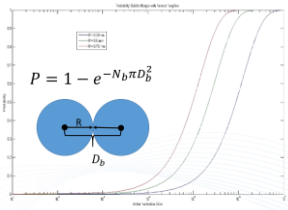

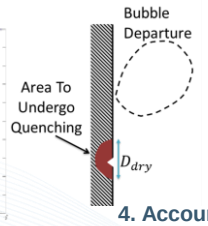

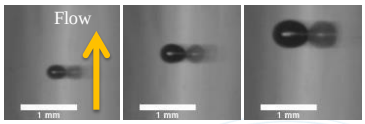

4. Account surface quenching after bubble departure

12

GEN-II Heat Partitioning: Evaporative Component

Evaporative Heat Transfer q''_e

- *Kurul-Podowski is "a posteriori" concept*
- *D_d^3 behavior*
- *e.g. → q''_e = 0 until OSV*
- *New model targets capturing the real evaporative q''_e*
- *Builds in tracking of physical limits →*
- *Naturally extends to limit behavior without need for new empirical model*

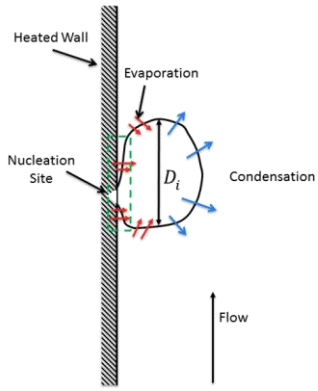

1) **Initial bubble growth**

$$q''_{e,init} = \frac{4}{3}\pi\left(\frac{D_m}{2}\right)^3 \rho_v h_{fg} f N''$$

2) **Evaporation of the micro-layer**

$$q''_{e,mL} = V_{mL}\rho_f h_{fg} f N''$$

Need to model the microlayer
leverage ITM-DNS
+ experiments

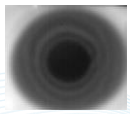

Kim 2011 (NURETH-14)

13

GEN-II Heat Partitioning: Sliding Bubbles Component

- Requires D_m and D_l predictions
- Bubble grows while sliding

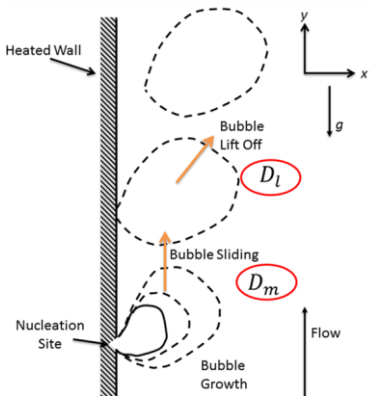

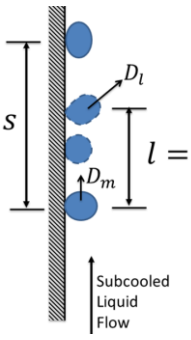

$$s = \frac{1}{\sqrt{N''}}$$

$$t_{sl} = \frac{s}{v_l}$$

$$\frac{(D_{sl}^2 - D_{in}^2)}{t_{sl}\alpha_l Ja_{sup}} = \frac{1}{15(0.015 + 0.0023 Re_b^{0.5})(0.04 + 0.023 Ja_{sub}^{0.5})}$$

14

GEN-II Heat Partitioning: Sliding Conduction Component (q''_{sc})

- Determination of sliding distance (l) and area (a_{sl})

$$a_{sl} = D_{avg} l \qquad l = N_{merged} s + l_{D_n - D_l}$$

  - Deactivation of nucleation sites (R_f)

$$R_f = \frac{1}{1 + l/s} \rightarrow N^{*\prime\prime} = R_f N''$$

$$q''_{sc} = \frac{k_l (T_w - T_l)}{\sqrt{\pi \alpha_l}} a_{sl} \sqrt{t^*} f N^{*\prime\prime}$$

$$t^* = \left(\frac{k_l}{h_{fc}}\right)^2 \frac{1}{\pi \alpha_l}$$

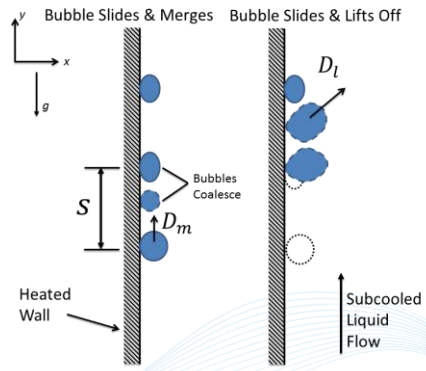

15

Force Balance Model for Bubble Size Prediction

- Sugrue et al. (2013) modified force balance model
- Predicts both D_m and D_l

$$\sum F_x = F_{sx} + F_{qs} - F_b sin\vartheta + F_{du} sin\emptyset$$

$$\sum F_y = F_{sy} + F_{sL} - F_b cos\vartheta - F_h + F_{cp} + F_{du} cos\emptyset$$

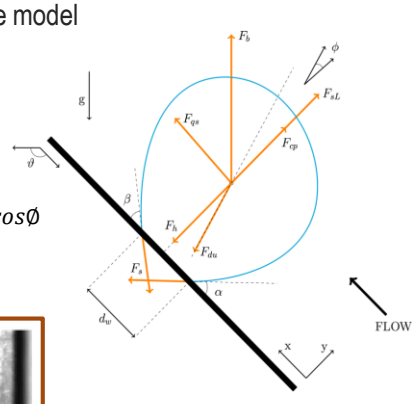

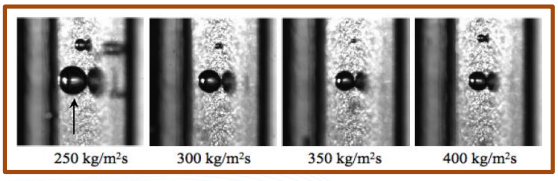

Pictures provided by Rosemary Sugrue

16

GEN-II Heat Partitioning: components

Effects of bubble crowding

- *Current models are strongly sensitive to active nucleation site density (require the use of experienced based limiters)*
- *Built in crowding effect eliminates need for limiters*
- *Prediction of dry surface can be directly verified against experimental measurements*
- ***DNB can be expressed as the limit of this behavior***
- ***Potentially local/scalable model for DNB***

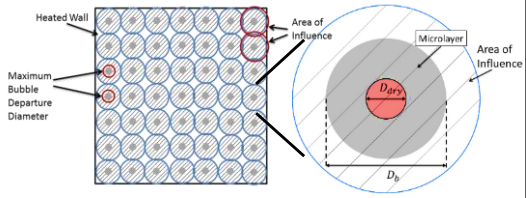

- ***Allows tracking physical limits***

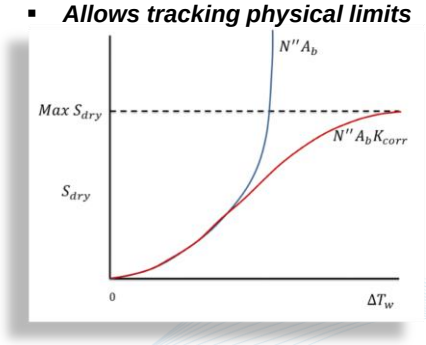

17

Bubble Merging on the Heater

- Bubbles merge on heater surface prior to departure
  - Indicates size of dry surface patches
- Fraction of nucleation sites ACTIVE at a point in time

$$N_b'' = f t_g N''$$

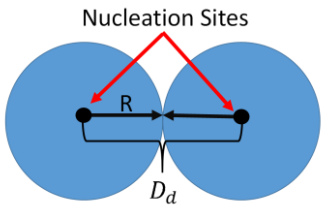

$$P = 1 - e^{-N_b'' \pi D_d^2}$$

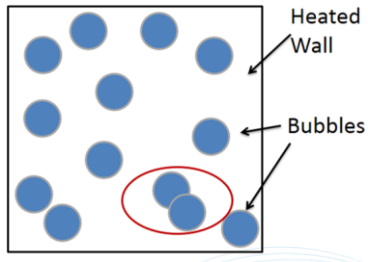

18

Nucleation Site Density Models

Nucleation Site Density is the "Boundary" Condition

- *Current models are strongly sensitive to active nucleation site density (require the use of experienced based limiters)*

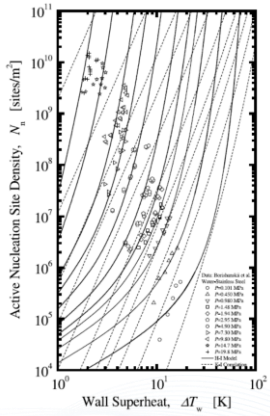

T. Hibiki and M. Ishii, "Active nucleation site density in boiling systems," International Journal of Heat and Mass Transfer, vol. 46, no. 14, pp. 2587 – 2601, 2003.

- ***At higher pressure 1k means orders of magnitude change in N"***

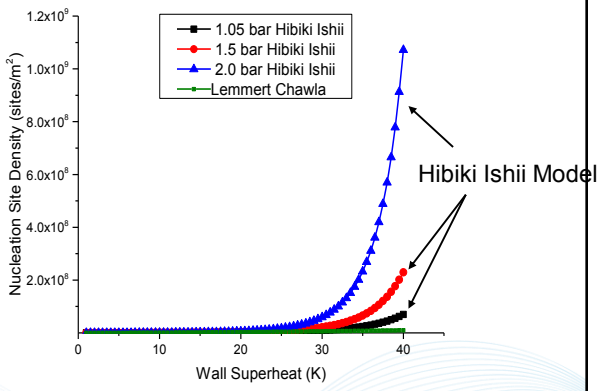

Nucleation Site Density Models

Nucleation Site Density is the "Boundary" Condition

- *Current models are strongly sensitive to active nucleation site density (require the use of experienced based limiters)*

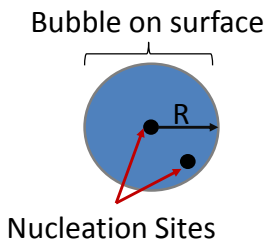

$$N_b'' = f t_g N''$$

$$P = 1 - e^{-N_b'' \pi (D_d/2)^2}$$

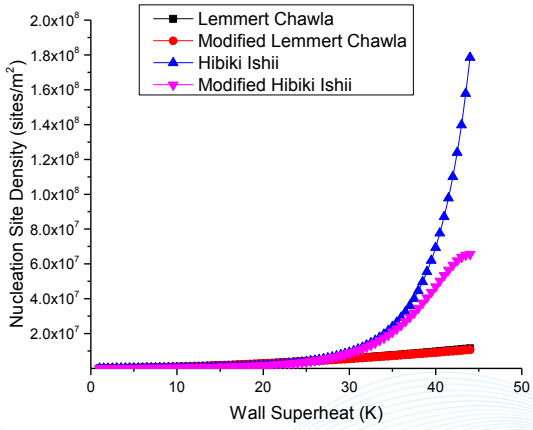

GEN-II Heat Partitioning: components

Quenching of "walls"

- *Currently related to fluid properties (can be combined into evaporative)*

Influence of heater material

- *Semi-analytical representation of the influence area of the bubble on the heater back to the wall superheat and temperature distribution prior to bubble departure*

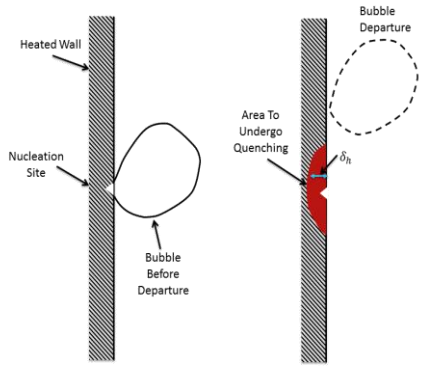

$$V_q = \frac{2}{3}\pi\left(\frac{D_{dry}}{2}\right)^3$$

$$q_q'' = \rho_h c_{p,h} \Delta T V_q f N^{*''}$$

21

Novel Mechanistic Flow Boiling Model

Law of the "boiling" wall

- *Forced convection should be modified to account for presence of bubbles (growing, sliding, departing)*
- *Introduced equivalent sand roughness to represent bubbles*

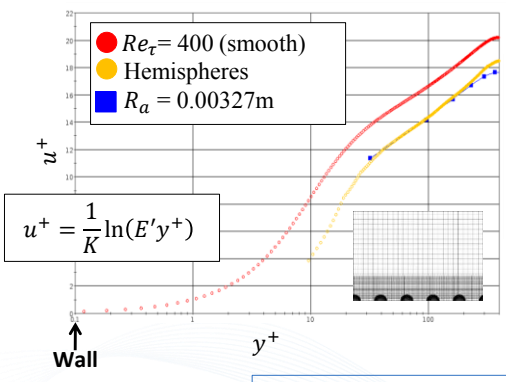

$$u^+ = \frac{1}{K}\ln(E' y^+)$$

$$E' = E/f$$

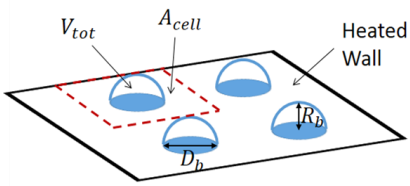

$$q_{fc}'' = h_{fc}(T_w - T_b)$$

22

Demonstration of Wall Function correction DNS/LES data for hemispherical obstacles (ITM-1 results)

22

Targeting generality

- *Microlayer Evaporation* → *DNS Simulations*
- *Active Nucleation Site Density* → *Experimental Meas.*
- *Departure diameter (D_d)* → *Sugrue et. al*
- *Departure frequency* → *Consistent with Sugrue et al.*
- *Sliding (and coalesc.) Bubbles* → *Dedicated measurements*
- *Quenching* → *… working on it*

Robust Boiling Model

- So let's look at some "tuning-free" results

23

MIT Flow Boiling Facility

- Subcooled flow boiling experiments
- Captures multiple parameters simultaneously
- 2D surface temperature distribution of heater

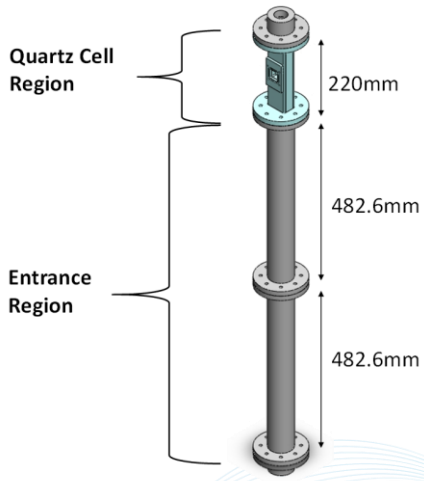

Atmospheric Pressure and 10°C Subcooling

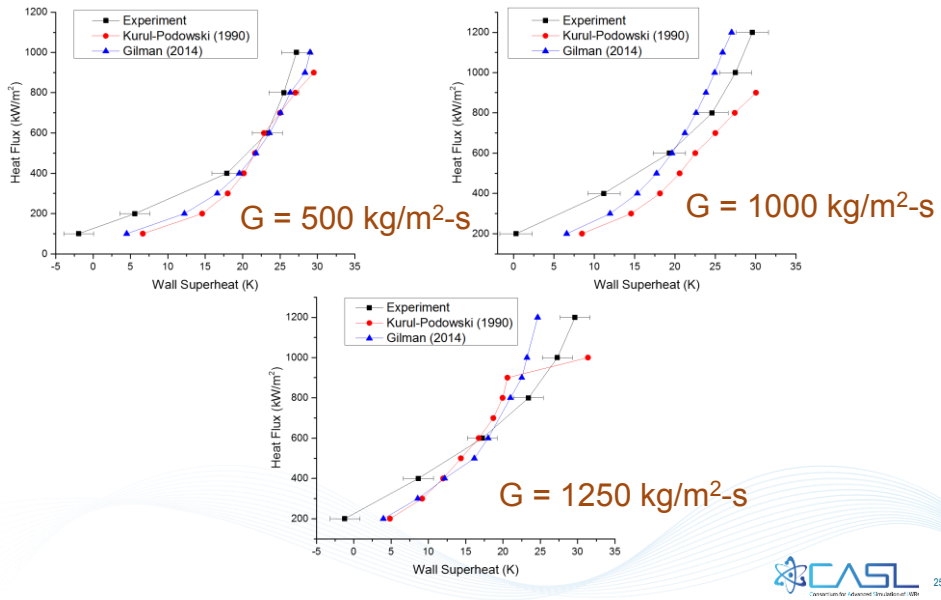

25

Pressure = 2.0 bar and 10°C Subcooling

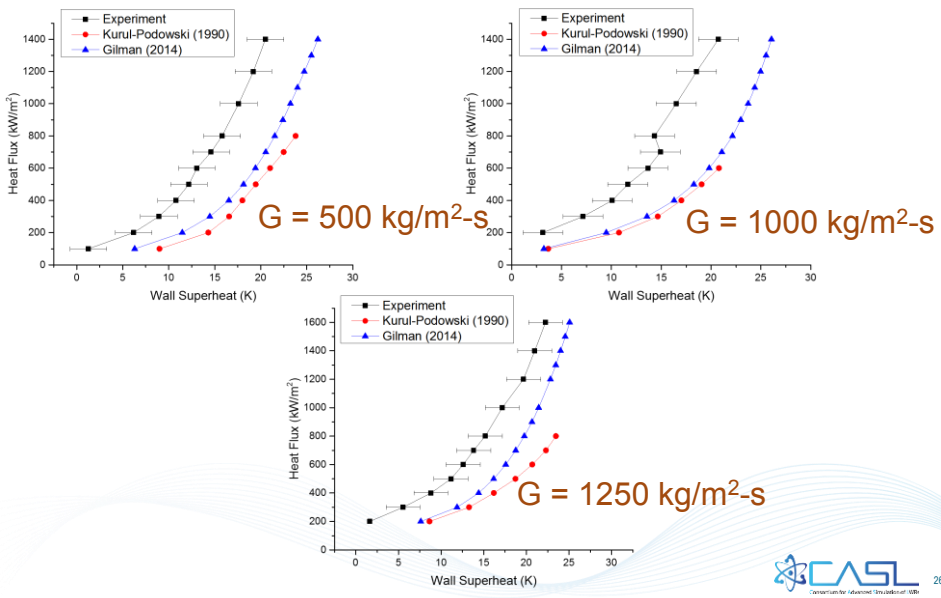

26

Pressure = 2.0 bar and 10°C Subcooling

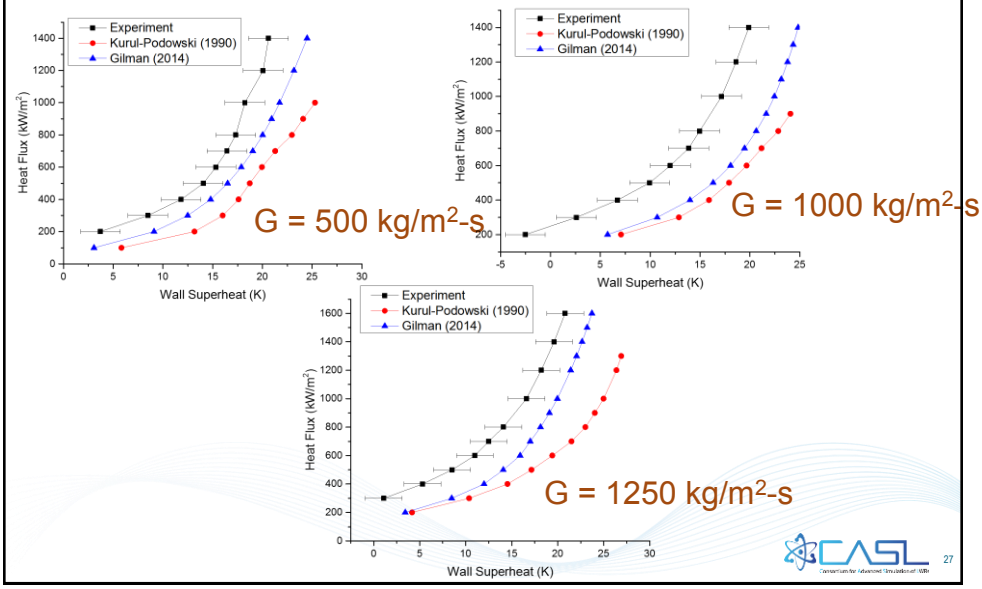

27

Pressure = 2.0 bar and 15°C Subcooling

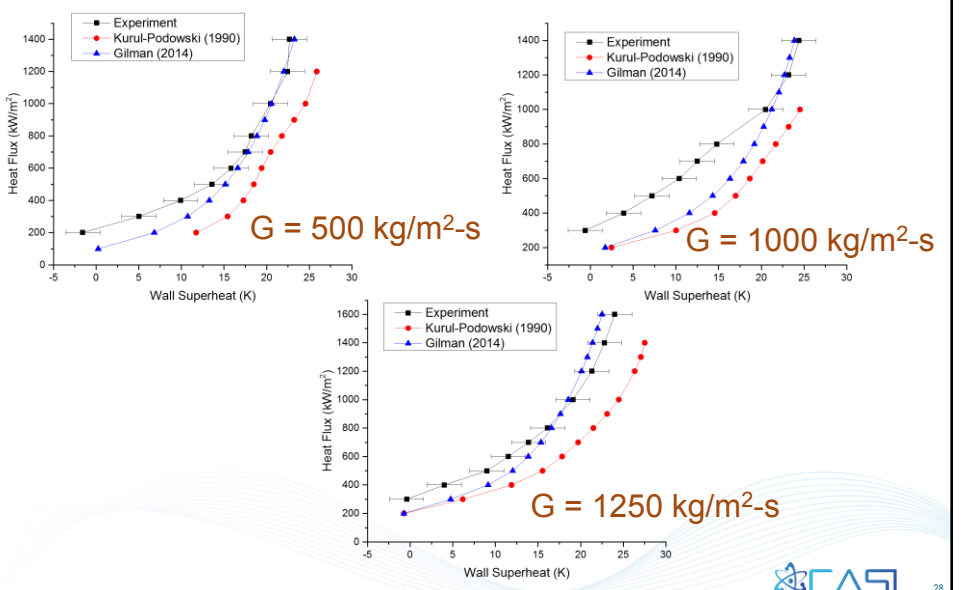

28

Rohsenow High Pressure Experiments

- P = 2000 psi (137.9 bar)
- Nickel tube 9.4 inches long
- Inner diameter of 0.1805 inches
- Outer wall temperature measurements at 7 locations
- Vertical upflow

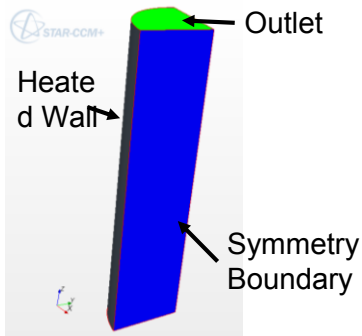

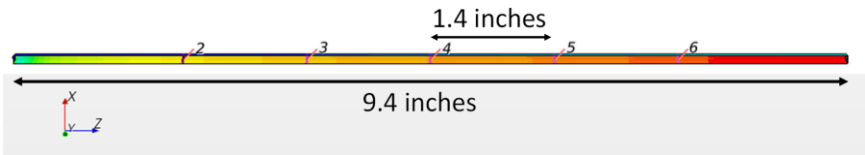

29

P = 2000 psi Results

Heat Flux [MW/m2]	Inlet ΔT_{sub} [K]	Thermocouple Positions	Experiment ΔT_{sup} [K]	Experiment Error [K]	Gilman (2014) ΔT_{sup} [K]

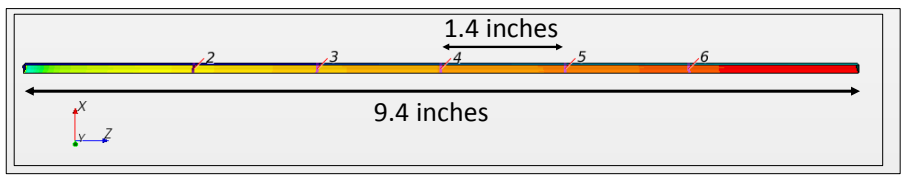

New Model Heat Partitioning Components

MIT Test Case
v = 0.52 m/s, Pressure = 1.0 bar, 10°C Subcooling

Rohsenow Test Case
v = 3.05 m/s, Pressure = 2000 psi, 136.4°C Subcooling
q" = 5.11 MW/m^2

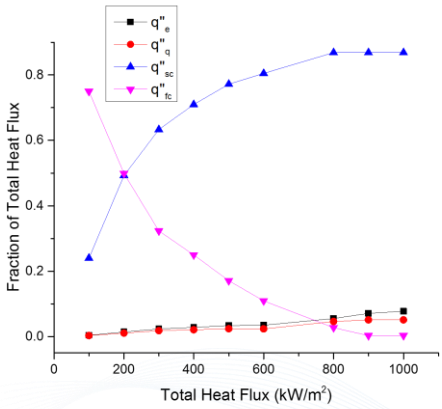

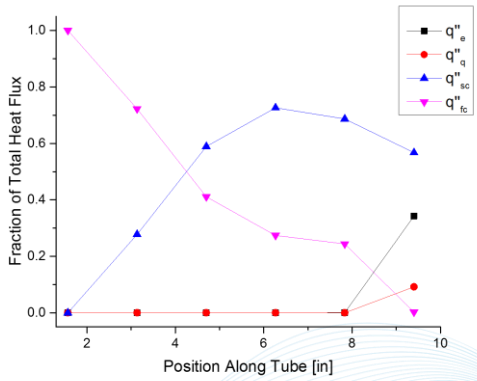

31

Next Step: Evaluating Applicability to 5x5 DNB Tests

- Evaluate Robustness of Closures
- Evaluate computational cost of GEN-I vs. GEN-II
- Provide Platform for DNB methods testing

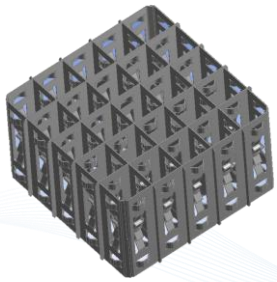

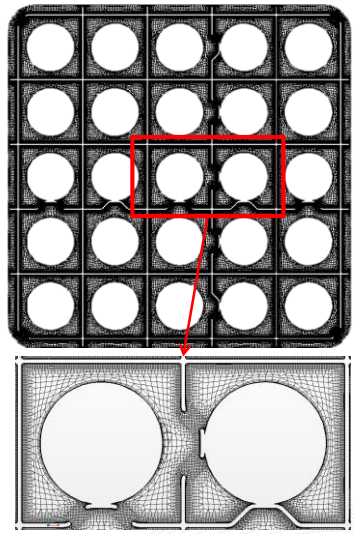

- Hexpress Mesh (244M cells) provided by Westinghouse

32